

BUDKER INSTITUTE OF NUCLEAR PHYSICS
of Siberian Branch of Russian Academy of Sciences

ANNUAL REPORT

2012

NOVOSIBIRSK 2013

Contents

Introduction	7
1. Particle physics	11
1.1. CMD-3	13
1.2. The SND detector	15
1.2.1 Experiments at VEPP-2000	15
1.2.2 Detector status	15
1.2.3 Software status	15
1.2.4 Data analysis	16
1.2.5 Energy calibration	20
1.3. KEDR detector	21
1.3.1 Repair and upgrade of detector	21
1.3.2 FARICH technique	22
1.4. Results of KEDR detector operation on the VEPP-4M collider in 2012	23
1.5. Detectors for HEP	24
1.6. X-ray detectors	24
1.7. Other works	24
1.8. Micro-pattern gas detectors	25
1.8.1 THGEMs-based two-phase cryogenic avalanche detectors (CRADs).....	25
1.8.2 Upgrade of the scattered electron system in the KEDR experiment.....	28
1.8.3 Participation in collaborations.....	29
1.9. BELLE experiment	30
1.9.1 Main results.....	30
1.9.2 Data analysis	30
1.9.3 Upgrade of the detector	36
1.10. BABAR experiment	40
1.11. Participation in the atlas experiment at the large hadron collider (LHC)	41
1.12. LHCb experiment	42
1.12.1 Technical support forthe LHCb detector	42
1.12.2 Physical results	42
1.12.3 Review of the LHCb results and planned upgrade.....	43
1.12.4 Modeling radiation environment in the detector area	43
2. Electro – and photonuclear physics	47
2.1. Experiments with internal targets	49
3. Theoretical physics	53
3.1. CP nonconservation	55
3.2. Gravity	55
3.3. QCD	55
3.4. QED.....	59
3.5. Gravitation and astrophysics	60
3.6. Chaos	61
4. Plasma physics and controlled thermonuclear fusion	63
4.1. Research on the GDT device	65
4.1.1 Study of kinetic instabilities	65

4.1.2 State of work on additional ECR plasma heating in the GDT device	67
4.1.3 The status of work on preparation of experiment with the injection of the electron beam in GDT.....	68
4.1.4 Experiments with offset of atomic beams axial lines relative to the axis of plasma symmetry	68
4.1.5 Measurements of the heat flux density at the mirror plane	69
4.2. GOL-3 facility	70
4.2.1 Description and main operation modes of the facility.....	70
4.2.2 Terahertz radiation at relaxation of relativistic electron beam	71
4.2.3 Motivation for injection of long-pulse electron beam into multiple-mirror trap.....	71
4.2.4 Source of long-pulse electron beam with plasma emitter	72
4.2.5 Injection of long-pulse electron beam into GOL-3.....	73
4.2.6 Plasma heating	74
4.2.7 Microwave radiation at relaxation of weakly relativistic electron beam	74
4.2.8 Summary of the GOL-3 results	75
4.3. Plasma theory	76
4.3.1 Alfvén ion-cyclotron instability	76
4.3.2 Development of the theory of electron cyclotron heating	76
4.3.3 Theory of electromagnetic emission generated in a turbulent plasma	76
4.3.4 Two-dimensional simulations of nonlinear beam-plasma	76
4.3.5 Optimization of the reactor based on the open trap	77
4.4. Beam Injectors of Hydrogen Atoms and Ions	77
4.4.1 Beam Injectors of Hydrogen Atoms	77
4.4.2 Development of powerful continuous injector of beam of fast hydrogen atoms	77
4.5. Installation GDMT-T	78
4.5.1 Conceptual design of the GDMT-T facility	78
4.5.2 Superconducting magnetic system	78
4.5.3 Production of steady-state plasma flow	79
4.5.4 Electron beam generator	80
4.5.5 Conclusion.....	80
4.6. Research on generation of millimeter wave radiation on the ELMI installation	80
4.6.1 Introduction.....	80
4.6.2 Arrangement of the experiment	81
4.6.3 Results of research	82
4.6.4 Preparation of experiments on two-step generation of terahertz radiation	83
5. Electron-Positron Colliders	85
5.1. VEPP-2000 complex: work with round beams and plans on upgrade	87
5.1.1 Round beams on VEPP-2000	87
5.1.2 Modernization of booster ring BEP and channel K-500	90
5.1.3 Resonance depolarization on VEPP-2000	91
5.2. VEPP-4 accelerator complex	92
5.2.1 Distribution of working time	92
5.2.2 DEUTRON experiment at VEPP-3	92
5.2.3 The output beam at VEPP-4M	92
5.2.4 Scattered electron registration system	93
5.2.5 7-pole wiggler with a 3T field	93
5.2.6 Experiment on CPT-invariance check	93
5.3. Injection complex VEPP-5	94
5.3.1 Activity in 2012	94
5.3.2 Studies of wakefield acceleration	94
5.4. Electron-beam welding	94
5.4.1 Works carried out in 2012	94
5.4.2 Design of vacuum system and technology for its production for high-intensity colliders.....	95
5.5. Technical project of linear induction accelerator LIA - 20R	95
5.6. Quadrupoles for NSLS II	96
5.7. Switched power supply for NSLS II booster injection/extraction system	99
5.8. Connection module for the european XFEL (Desy)	101

5.9. Electron cooling facility	102
5.9.1 Electron cooling facility for the German Synchrotron COSY	102
5.9.2 Compass for measurement of straightness of line of force.....	102
5.9.3 Electron beam profiler.....	103
5.9.4 Collector with Wien filter	103
5.10. Accelerator mass spectrometer	104
5.11. Vacuum systems	105
5.11.1 Electron clouds	105
5.11.2 Vacuum system of the NSLS-II booster	108
5.11.3 Study of activation and gas-absorbing characteristics of WM cartridge based on St'707 getter.....	108
6. Synchrotron Radiation Sources and Free Electron Lasers	111
6.1. Introduction	113
6.2. Work on SR beams from VEPP-3	113
6.2.1 Station "Extreme state of matter"	113
6.2.2 Station "LIGA technology and X-ray lithography"	115
6.2.3 Station "Anomalous Scattering" and "Precision Diffractometry"	116
6.2.4 Station "X-ray fluorescence analysis"	119
6.2.5 Station "Hard X-ray diffraction"	122
6.2.6 Station "X-ray microscopy and tomography"	123
6.2.7 Station "Diffraction movie"	124
6.2.8 Station "EXAFS spectroscopy"	125
6.3. Works on SR beams from VEPP-4M	128
6.3.1 Metrological Station "Space"	128
6.3.2 Outcoupling of radiation from 7-pole wiggler into SR bunker on VEPP-4	129
6.4. Work with terahertz radiation beams	131
6.4.1 Novosibirsk terahertz free electron laser	131
6.4.2 Experiments on THz beams	131
6.4.3 Upgrade of the FEL and commissioning of the third stage of the energy recovery linac	132
6.4.4 Assembling undulators for the third stage of the FEL and correcting field in them	132
6.4.5. Results of 2012 and plans for 2013	133
6.5. Development and creation of specialized SR generators – superconducting wigglers	134
7. Radiophysics and electronics	137
7.1. Power supplies for electrophysical installations	139
7.1.1 Stabilized current sources	139
7.2. Sources of stabilized high direct voltage	140
7.2.1 High-voltage power supplies for atom injectors for diagnostics and plasma heating	140
7.2.2 High-voltage power supplies for accelerating tubes.....	140
7.2.3 Switching Power Supplies for electromagnets of accelerator complexes.....	141
7.3. Development of measurement systems and devices for automation of physical experiments	141
7.4. Development of tailor-made and special electronics	144
7.5. Research related to modeling and solving electrostatic and electrodynamic problems of acc. physics.....	144
7.6. New 174 MHz rf system for the bep storage ring	145
7.7. 816 MHz passive single-mode rf cavity	145
7.8. Works with the rf system of the VEEP-4 storage ring	145
7.9. Development of rf systems for high-power injectors of beams of neutral atoms for plasma facilities	146
7.9.1 RF system of the diagnostic injector of neutral beams of RUDI-X for the "Wandelstein" stellarator..	146
7.9.2 RF system for high-power continuous injector of beams of fast hydrogen atoms	146
7.10. CCDTL accelerating structures for Linac4, CERN	147
7.11. accelerating rf stations of ion booster of NICA-MPD collider	148
7.12. Reconstruction of rf systems of the electron accelerator of the research center KAERI.....	151
7.13. RF injector of microtron-recuperator	151
7.14. RF gun for accelerator of VNIIEF.....	151
7.15. upgrade of the RF system of the FEL microtron	151

8. Powerful Electron Accelerators and Beam Technologies	153
8.1. Accelerator supplies	155
8.2. Development of new powerful electron accelerators	155
8.2.1 Development of the beam scanning system with independent power supply	155
8.2.2 Development of the control system for ILU machines powerful pulse modulators	156
8.3. New radiation technologies development	156
9. Physics for medicine	159
9.1. The current status on BNCT	161
9.1.1 Introduction	161
9.1.2 Dark currents	161
9.1.3 Beam injection	161
9.1.4 Charge-exchange target	162
9.1.5 Modification of the insulator	162
9.1.6 Dark matter	162
9.1.7 Results and prospects	163
9.2. X-ray detectors for medicine and examination of people	164
9.2.1 Low Dose digital Radiographic Device (LDRD) "Siberia"	164
9.2.2 System for Radiographic Control (SRC) "Sibscan" for people examination	164
Bibliography	165
List of publications	165
Conference presentations	191
Preprints	208
Theses reviews	211
Participation in conferences	212
List of Collaboration Agreements	214
Research Personnel	217
Members of Russian Academy of Science	217
Director board	217
Scientific council	217
Specialized sections of scientific council	218
Research staff and publications	221

Introduction

In May 1958, the USSR Council of Ministers declared creation of the Institute of Nuclear Physics of the Siberian Branch of the USSR Academy of Sciences. The new institute was created on the basis of the Laboratory of new acceleration methods, headed by G.I. Budker, of the Nuclear Energy Institute, directed by I.V. Kurchatov. Since 1977, the Institute of Nuclear Physics has been directed by academy member A.N. Skrinsky.

Currently, BINP SB RAS with over 2,800 employees is the largest academic institute of Russia. The Institute research staff of 417 members includes 11 members and corresponding members of the Russian Academy of Sciences (as by the end of 2012), 60 Doctors of Sciences and 170 Candidates of Sciences. BINP has a large experimental production department (with about 1,000 employees) with high-level engineering and technology equipment.

The Institute is doing much for training of scientific and technical personnel of high qualification. BINP is a base institution for seven subdepartments of the Physics Department of Novosibirsk State University (NSU) and the Physicotechnical Department of Novosibirsk State Technical University (NSTU) (in total about 200 students). 65 post-graduate students are pursuing post-graduate studies at BINP, NSU and NSTU.

BINP is one of the world's leading centers in a number of areas of high energy physics, accelerator physics, plasma physics and controlled fusion physics. The Institute conducts large-scale elementary particle physics experiments on electron-positron colliders and a unique complex of open plasma traps and develops up-to-date accelerators, high-power sources of synchrotron radiation and free electron lasers. In most of these areas, the Institute is the only one research institution in Russia.

Below are listed the main BINP achievements in science and technology.

In the field of elementary particle physics and nuclear physics:

- pioneering works on the development of the colliding beam technique, which is now the leading one in the high energy physics:
 - first experiments on the electron-electron interaction (simultaneously with the Princeton/Stanford works) (1965),
 - world's first experiments on the electron-positron interaction (1967),
 - world's first observation of the process of double bremsstrahlung (1967),
 - pioneering works in the two-photon physics (1970);
- research on the characteristics of vector mesons on the installations with colliding electron-positron beams VEPP-2, VEPP-2M and VEPP-4 (since 1967);
- discovery of the phenomenon of multiple production of hadrons in electron-positron annihilation (1970);
- precision measurement of the contribution of hadronic vacuum polarization to the value of muon

anomalous magnetic moment for one of the most sensitive tests of the Standard Model, which is conducted in cooperation with the Brookhaven National Laboratory (1984 - 2005);

- development of the resonance depolarization method for precision measurement of the masses of elementary particles and achievement of a record accuracy in measurements of the masses of K, rho, omega, phi and psi mesons and upsilon mesons (1975 - 2004);
- discovery of parity violation effects in atomic transitions and confirmation to the unified theory of electroweak interactions (1978);
- development of experiments on hyperfine internal targets in storage rings (since 1967) and investigation into the electromagnetic structure of deuteron in polarization experiments (since 1984);
- development of a technique for production of intense fluxes of labeled high-energy gamma quanta through the use of inverse Compton scattering (1980 - 1982); experimental observation of photon splitting in the Coulomb field of nucleus (1997);
- development of new methods for detection of high-energy charged and neutral particles and creation of unique detectors for installations with colliding beams (OLYA, CMD-1, MD-1, CMD-2, CMD-3, ND, SND, and KEDR) (since 1974);
- development of X-ray detectors for medical applications and creation of a low-dose digital radiographic installation on their basis, with an ultra-low level of patient exposure, and the X-ray system "Sibscan" for inspection of people (since 1981).

In the field of theoretical physics:

- development of the resonance theory of dynamical chaos and pseudo-chaos in the classical and quantum mechanics (since 1959);
- the first-time computation of charge renormalization in the Yang-Mills theory (1969);
- development of the method of the QCD sum rules (1979 - 1984);
- prediction of large enhancement of the parity violation effects in neutron resonances in heavy nuclei (1980 - 1985);
- development of the theory of hard exclusive reactions in the QCD (1977 - 1984);
- development of an operator approach to quantum electrodynamics in external fields (1974 - 1976);
- development of quantum electrodynamics in periodic structures, including a laser wave (1972 - 1997);
- development of the theory of radiation effects in passage of high-energy charged particles and photons through orientated single crystals (since 1978);
- derivation of evolution equation in the QCD for energy distribution of partons (the BFKL equation) (1975 - 1997);
- prediction of the coherence effect in the emission of gluons in the QCD and investigation into its influence on hadron distribution (1981 - 1982).

In the field of accelerator physics and technology:

- successful long-term experience in creation of storage rings and installations with colliding beams;
- invention, development and experimental verification of the "electron cooling" method for heavy-particle beams, which is currently used at laboratories around the world; delivery of efficient "coolers" to accelerator heavy-ion complexes in Germany, China and CERN (1965 - 2005);
- invention and development of new types of high-power RF generators (gyrocon, relativistic klystron and Magnicon) (since 1967);
- suggestion of a technique of linear electron-positron colliding beams for production of super-high energies (1968) and presentation of a physically self-consistent project (1978);
- development of elements of intense-field pulsed magnetic optics (X lenses and lithium lenses), which are currently used at different laboratories (since 1962);
- invention and experimental verification of the method of charge-exchange injection, which is currently applied at all the major proton accelerators (1960 - 1964);
- theoretical and experimental investigation into generation of polarized beams and spin dynamics in accelerators and colliders and conceptual designing and creation of highly efficient spin rotators and "Siberian snakes" for a number of accelerator complexes, (1966 - 1995);
- theoretical and experimental research on stochastic instability and "collision effects" that impose limitations on the luminosity of colliding-beam installations (since 1966);
- development of the physical concept of a new generation of electron-positron colliders of very high luminosity, so-called electron-positron factories (since 1987);
- suggestion and development of a method of ionization cooling of muons for creation of muon colliders and neutrino factories (1969 -1981 - 2002);
- development and creation of high-power low-energy electron accelerators for a variety of technological applications, including environment protection (accelerators ELV-12 with a power of 500 kW and an energy of 1 MeV and ILU-10 with a power of up to 50 kW and an energy of 5 MeV) (since 1963);
- suggestion and implementation of a scheme of recuperator accelerator for high-gain free electron lasers (1979 - 2003).

In the field of plasma physics and thermonuclear synthesis:

- invention (1954) and creation (1959) of the "classical" open magnetic trap (magnetic bottle) for hot plasma confinement;
- invention and development of new schemes of open traps (multiple-mirror, rotating-plasma, ambipolar, and gas-dynamical ones); experimental realization of

multiple-mirror confinement of plasma with sub-fusion parameters in the trap GOL-3; experimental implementation of MHD instability stabilization in an axially symmetric gas-dynamic trap (on the installation GDT) (since 1971);

- discovery of collisionless shock waves in plasma (1961);
- development of a technique of plasma heating with relativistic electron beams (since 1971);
- development of high-intensity surface-plasma sources of negative ions, now widespread in the world (1969 - 1981);
- suggestion and development of a concept of a high-power open-trap source of fusion neutrons for materials science (since 1987).
- theoretical prediction of the Langmuir collapse (1972) and experimental discovery of strong Langmuir turbulence and collapse of Langmuir waves in a magnetic field (1989 - 1997);
- creation of a series of unique high-power precision sources of hydrogen atoms for high-temperature plasma investigation for a number of large installations (since 1997).

In the field of synchrotron radiation and free electron lasers:

- application of synchrotron radiation of the BINP storage rings to science and technology and establishment of the international Siberian Synchrotron Radiation Center based on VEPP-2M, VEPP-3 and VEPP-4 (1973);
- theoretical and experimental research on particle emission in periodic structures (undulators, wigglers, and crystals) (since 1972);
- development and creation of specialized sources of synchrotron radiation (since 1983);
- development and creation of one- and two-coordinate detectors for experiments with synchrotron radiation (since 1975);
- invention and development of the optical klystron (1977) and generation of coherent radiation in the infrared to the ultraviolet spectrum (since 1980);
- development and creation of a high-power free electron laser (for photochemical research and technological applications as well as for energy transfer from the Earth to a satellite) on the basis of the most promising scheme, which uses a recuperator microtron; generation of high-power (400 W) laser radiation in the terahertz range (since 1987);
- creation of a series of intense-field superconducting magnetic devices for SR sources and electron storage rings (wigglers and bending magnets with fields of up to 10 T and solenoids with fields of up to 13 T) (since 1996).

Applied works performed by BINP SB RAS rely entirely on the results of the basic research performed by the Institute and are focused on the following main areas:

- industrial high-power electron accelerators for modification of polymers, treatment of industrial and domestic waste, production of powders of pure metals, silica, oxides, carbides and nitrides of metals, radiation processing of food, sterilization of medical equipment, disposable instruments and garments and other technological applications;
- low-dose scanning-type digital radiographic installations with ultra-low patient exposure for medical and security systems;
- development of nuclear medicine facilities for proton-, ion- and boron-neutron-capture therapy of malignant tumors;
- installations for electron beam welding;
- radiographic equipment for defense research.

During the past 20 years, BINP was financing basic and applied research from assets received from contract works. The cost of high-tech products developed, manufactured and supplied annually by BINP to customers in Europe, Asia, and North and South Americas (20 countries), as well as in Russia, makes over 500,000,000 rubles. The so earned money was used for completion and commissioning of the accelerator complex VEPP-4M with the unique detector KEDR, designing and construction of large unique installations (the electron-positron collider VEPP-2000, free electron laser and a new injection system for the existing and future BINP facilities. Throughout the post-Soviet period, these funds have been maintaining the continuous work of BINP facilities and related infrastructure.

BINP excels in long-term international cooperation with most major foreign and international research centers. A striking example is the BINP participation in the largest international project - the Large Hadron Collider at the European Organization for Nuclear Research (Geneva). Within this framework, BINP has developed, manufactured and delivered to CERN unique hi-tech equipment for an amount of over 100 million Swiss francs. Other cases of BINP international cooperation include participation of the Institute in the projects of B-factories in the U.S. and Japan and implementation of the following large European projects: the synchrotron-radiation source PETRA-III, X-ray free electron laser (DESY, Hamburg), heavy-ion accelerator facility (GSI, Darmstadt), and some others.

BINP has played a key role in several major Russian projects, including the following: the Center for Synchrotron Radiation at the Research Center 'Kurchatov Institute', the synchrotron radiation source in Zelenograd, the neutron source for the JINR in Dubna, and radiographic equipment for defense research at VNIITF in Snezhinsk.

The Institute is deeply integrated into the work of the Russian Academy of Sciences and its Siberian Branch, implementing 18 projects under programs of the Presidium of the Russian Academy of Sciences and its branches

and 24 projects under SB RAS integration programs. The Institute is executing 27 state contracts and agreements under the Federal Target Programs 'Research and development in priority directions of the science-and-technology complex of Russia for 2007 – 2013' and 'Scientific and pedagogical staff of innovative Russia for the years 2009 – 2013' and over 60 RFBR projects, including 22 projects within a new competition of the Fund 'My first grant'.

Every year, members of the Institute make about 200 reports at international and Russian conferences, publish about 500 articles in leading Russian and foreign scientific journals and issue monographs and textbooks. According to data published in the review 'Bibliometric indicators of the Russian Science and Russian Academy of Sciences' (RAS Bulletin, June 2009, Volume 79, № 6), the number of links to papers by BINP members that are accounted in the authoritative international database ESI was 28,267 in 1997-2007. In accordance with the survey data, this is a maximum value among all the institutions of the Russian Academy of Sciences. Four members of the Institute are winners of the Elsevier special premium as the most cited authors in the post-Soviet area in the field of natural sciences.

Below are listed works recognized as the best in 2012 by the BINP Scientific Council.

In the field of **nuclear physics, elementary particle physics and physics of basic interactions:**

- 1) on the VEPP-3 storage ring, the first-time determination of the two-photon exchange contribution to the elastic scattering of electrons on protons and positrons;
- 2) within the ATLAS collaboration, the first-time observation of the Higgs boson at the Large Hadron Collider;
- 3) the first-time model-independent measurement of the angle φ_3 of the unitarity triangle in the decays of B mesons in the Belle and LHCb experiments;
- 4) attainment of a record high level of separation of muons and pions in the joint work of the Institute of Catalysis and BINP on the creation of a Cherenkov ring detector based on focusing aerogel;
- 5) the first-time demonstration of the fact that the hypothesis of existence of gravitational four-fermion interaction results in a contradiction to the Friedmann-Robertson-Walker cosmology;
- 6) determination of the kernel of the Bartels-Kwiecinski-Praszalowicz equation in the odderon channel in the QCD and supersymmetric Yang-Mills theory with $N = 4$ in the next-to-leading approximation;
- 7) determination of the eigenvalues of the kernel of the BFKL equation in the supersymmetric Yang-Mills theory with $N = 4$ in the next-to-leading order for the adjoint representation of the gauge group;

- 8) exact (in atomic field strength) derivation of charge asymmetry in electron-positron pair production by a high-energy photon in the field of a heavy atom;
- 9) prediction of the existence of superconducting and isolating states for electrons in a one-dimensional undulator nanochannel.

In the field of **plasma physics:**

1) attainment of plasma pressure in relation to magnetic field pressure, $\beta = 0.6$, at the gas dynamic trap (GDT) facility, which is a record value for axially symmetric open magnetic traps;

2) the world's first experiments at the multiple-mirror trap GOL-3 on plasma heating and generation of subterahertz radiation while an electron beam with a density of 10^{19} – 10^{20} m⁻³, a power of up to 10 MW, energy of 100 keV and a duration of up to 300 microseconds is being injected into the plasma;

3) the world's first suggestion and successful implementation in experiments at the GDT facility of the method of vortex plasma confinement in axially symmetric magnetic traps;

4) the first-time creation of a planar free-electron maser with a strip relativistic electron beam and a combined cavity containing two-dimensional Bragg mirrors (in cooperation with the Institute of Applied Physics and Novosibirsk State University);

5) the first-time demonstration of effective plasma heating and stabilization of MHD pinch instabilities with a reversed field during powerful atom injection (in joint experiments with the University of Wisconsin, USA).

In the field of **the physics and technology of charged particle accelerators, SR sources and FELs:**

1) the first-time experimental observation of interference of MeV-range γ quanta in inverse Compton scattering of laser radiation on an electron beam in a magnetic field (on the VEPP-2000 collider);

2) fabrication and mounting on the BEPC II collider (China) of a unique system for measuring the energy of electron and positron beams from inverse Compton scattering, which allows significant improvement in the accuracy of determination of the tau lepton mass;

3) designing, manufacturing and delivery to the Brookhaven National Laboratory (USA) of a booster synchrotron for an energy of 3 GeV and a beam intensity that is record high in this facility class;

4) construction and commissioning of the world's first 4-track recuperator accelerator;

5) development of a unique method of ultrafast high-resolution spectral measurements in the terahertz range;

6) development of a method of manufacture of diffractive and refractive intraocular lenses using the LIGA technology on a synchrotron radiation beam.

RAS member N.S. Dikansky was awarded the Order of Friendship for his contribution to the development of science and many years of fruitful activity,

Wechsler award of the Russian Academy of Sciences in 2012 was conferred on a team of I.A. Koop, E.A. Pervedentsev and Y.M. Shatunov for their work 'Facility with circular colliding electron-positron beams for precision measurement of hadron cross sections at energies of up to 2 GeV'.

Budker award of the Siberian Branch of the Russian Academy of Sciences was conferred on I.V. Timofeev for his work 'On the evolution of plasma turbulence under the influence of high-power electron beam'.

Seven young researchers of the Institute – A.Yu. Barnyakov, V.V. Prikhodko, A.L. Romanov, E.I. Soldatkina, A.L. Solomakhin, I.V. Timofeev, and D.A. Stohl – received the Russian Federation President scholarship for young scientists in 2012.

22 staff members of the Institute were awarded the commemorative medal 'For contribution to the development of the Novosibirsk region' in connection with the 75th anniversary of the Novosibirsk region.

The three Thesis Boards of the Institute, which are entitled to accept Doctor of Sciences (Candidate of Sciences) theses, continued their work in 2012. 11 meetings of the Boards took place, at which 2 Doctor of Sciences and 11 Candidate of Sciences theses were defended.

50 tours of the BINP facilities were conducted for school pupils, students, school and university teachers, members of other organizations and guests of the Institute, in total about 2,000 people. Lectures were delivered at Novosibirsk schools.

1.1 CMD-3 DETECTOR

Fig. 1.1.1 shows the CMD-3 detector in the VEPP-2000 experimental hall.

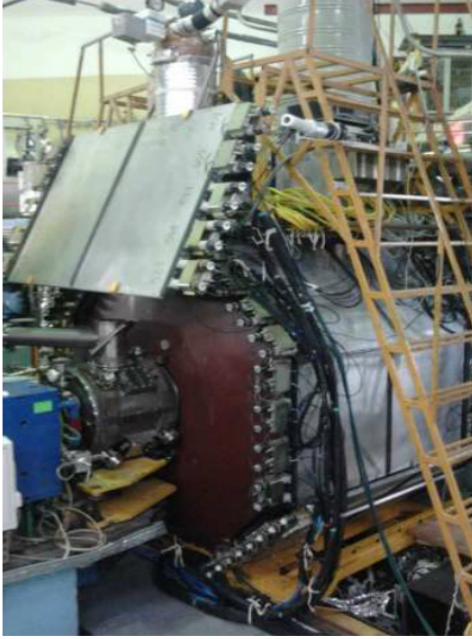


Fig. 1.1.1 CMD-3 detector in the VEPP-2000 experimental hall .

During 2012, four sessions of data acquisition were carried out with the CMD-3 detector. Fig. 1.1.2 shows the timetable of the data acquisition.

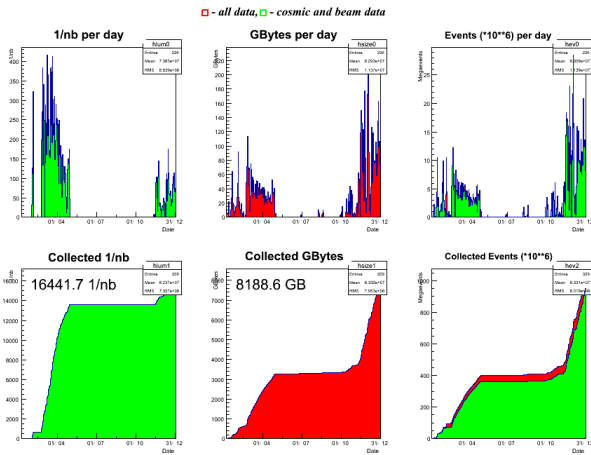


Fig. 1.1.2 Timetable of the data acquisition with the CMD-3 detector in 2012.

The first session began in late January 2012 and traditionally included scanning of the energy region of ϕ meson for calibration of the energy scale of the VEPP-2000 collider. An integral luminosity of 240 nb^{-1} was acquired at 6 points with beam energies of 508 - 513 MeV, which corresponds to 12 million recorded physical events.

The second session of data acquisition was carried out in February-May 2012 with energies of 1.28 - 1.98 GeV in the center of mass system with a beam energy step of 40 MeV. The measurements were made at 16 energy points. The integral luminosity recorded was about 13 pb^{-1} , which corresponds to 350 million physical events, or 3 TB data written to a disc.

Combining these data with those acquired in 2011 in the energy range of 1.05 - 2.0 GeV enabled completion of the analysis of the $e^+e^- \rightarrow 3(\pi^+\pi^-)$ process.

The cross section of the production of six charged pions was measured in the energy range of 1.5 - 2.0 GeV with a systematic error of 6% or less.

Fig. 1.1.3 shows measured cross section of $e^+e^- \rightarrow 3(\pi^+\pi^-)$ vs. energy in the center of mass system.

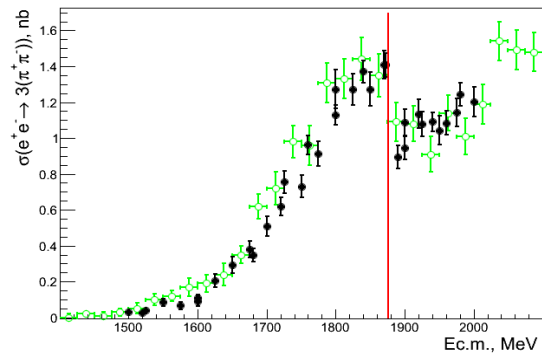


Fig. 1.1.3 Cross section of the $e^+e^- \rightarrow 3(\pi^+\pi^-)$ process vs. energy. Black circles: results of the CMD-3 experiment; open circles: results of the BaBar experiment. The vertical line indicates the threshold of production of proton-antiproton pair.

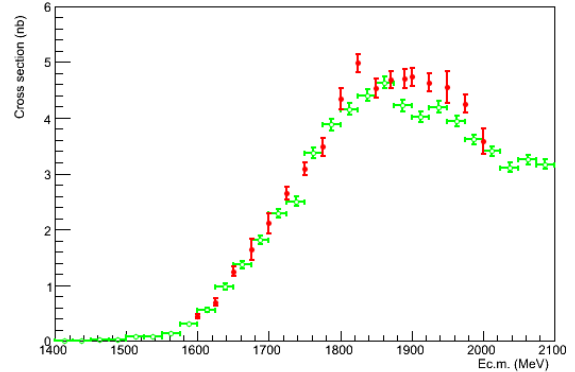


Fig. 1.1.4. Cross section of the $e^+e^- \rightarrow K^+K^-\pi^+\pi^-$ process vs. energy. Black dots: results of the CMD-3 experiment; open circles: data from the BaBar detector.

Further, a preliminary research on the dynamics of the production of the final state $3(\pi^+\pi^-)$ was carried out. Results of this work have been prepared for publishing.

In 2012, the CMD-3 detector was still engaged in the study of the process of e^+e^- annihilation into a proton-antiproton pair. Fig. 1.1.5 shows cross section of the

process vs. energy. The black dots show the preliminary results of the CMD-3 experiment, and the open circles show present data from the BaBar experiment.

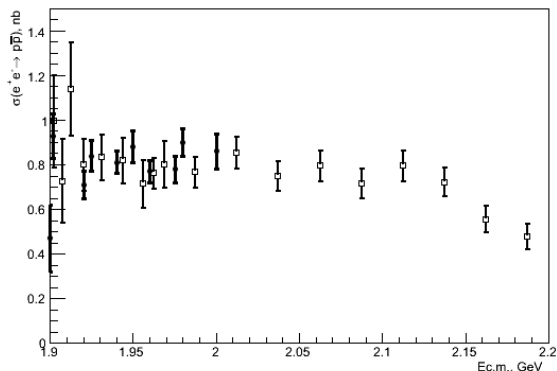


Fig. 1.1.5. Cross section of the e^+e^- annihilation into a proton-antiproton pair vs. energy. Black dots: preliminary result from the CMD-3 detector; open circles: result from the BaBar detector.

From analysis of angular distributions we determined the ratio of the electric and magnetic form factors of proton. Fig. 1.1.6 shows the results of this study. The black dots show the form factor ratio as obtained with the CMD-3 detector, and the open circles correspond to the measurement carried out on BaBar.

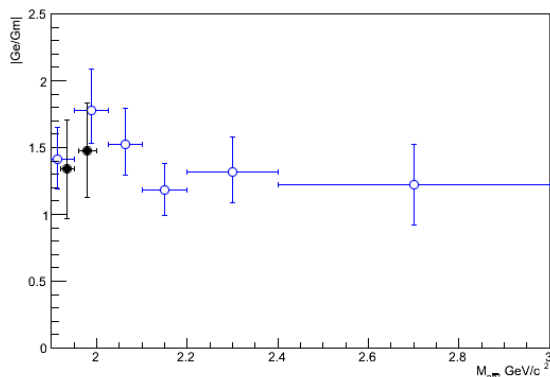


Fig.1.1.6. Ratio of the electric and magnetic form factors of proton as measured in the CMD-3 experiment (black dots) and with the BaBar detector (open circles).

A system for beam energy measurement using the inverse Compton scattering of laser light on a beam of electrons in the storage ring started operation at VEPP-2000 in September 2012. For tuning of the system, the energy region of ϕ meson was scanned once again. In this third session, data were acquired at 10 points in the range of beam energies of 507 - 525 MeV. The luminosity integral was 683 nb^{-1} , which corresponds to 130 million physical events recorded on discs. In this session, the VEPP-2000 beam energy was controlled by the system for energy measurement from the inverse Compton scattering. Analysis of these data resulted in the measurement of curves of excitation of the ϕ resonance in K^+K^- , $K_L K_S$,

$\pi^+\pi^-\pi^0$ decay channels. The obtained parameters of the ϕ meson are in good agreement with each other and with the world average values.

At the very end of the year, data acquisition in the region of the ρ - ω resonances was launched for measuring the form factor of charged pion. The energy region of 0.77 - 0.788 GeV was scanned in November and December 2012 in the center of mass with a beam energy step of 1 MeV. The total luminosity integral acquired at 8 energy points was about 340 nb^{-1} . The curve of excitation of ω meson in the $\omega \rightarrow \pi^+\pi^-\pi$ decay channel was obtained from analysis of these data. In the session, beam energy was also controlled with the system for energy measurement by inverse Compton scattering. That revealed some instabilities in the system and allowed finding ways to fix them. Currently, the CMD-3 detector is still engaged in data acquisition in the area of ρ resonance. Physical analysis is being done simultaneously, which enables prompt monitoring of the quality of data from the detector and performance of its systems.

1.2. THE SND DETECTOR

1.2.1. Experiments at VEPP-2000

Experimental season in 2012 started in February. The main part of the experimental program in 2012 was the scanning of the center of mass energy range $2E = \sqrt{s}$ from 1280 to 2000 MeV. Before the scan, collider energy calibration was performed. For this goal a short scan of the energy region near the ϕ -meson resonance was performed and the ϕ -meson mass was measured. This measurement confirmed the correctness of the collider energy setting. By the end of April, about 13 pb^{-1} experimental statistics was accumulated, about half of the announced program. Average luminosity in the runs varied from 2 to $10 \times 10^{30} \text{ cm}^{-2}\text{c}^{-1}$. Since the fall of 2012, experiments were continued in the ω -meson energy region, below $2E = 1000$ MeV. Average luminosity was $2 \times 10^{30} \text{ cm}^{-2}\text{c}^{-1}$. By the end of the year, about 1.5 pb^{-1} integrated luminosity was accumulated.

1.2.2. Detector status

Simultaneously with the experiment, modernization of the SND detector was continued in 2012. The modernization was required to ensure successful data taking over the entire energy range of VEPP-2000 collider.

Using the charge division method, a procedure was developed for the absolute calibration of the z -coordinate measurement. Coordinates of the cathode strip clusters served as a reference in the procedure. $e^+e^- \rightarrow e^+e^-$ events were used for the calibration. As a result, the accuracy of the z -coordinate determination of the emission points of charged particles was improved by 25% and amounted to $\simeq 2$ mm.

In 2012, the energy dependence of the average signal amplitudes of the Cherenkov counters from kaons, muons and pions were measured. These data are used to create parameters of particle identification.

97 % counters are operational in the SND calorimeter. In 2012, the replacement of the electronics of the first layer was completed. During this replacement, all vacuum phototriodes have been removed, their parameters have been verified and devices with a weak signal were replaced. New electronics for the second and third layers was tested on prototypes and is currently in production. The energy resolution of the calorimeter for photons with an energy of 0.7 – 1 GeV is almost the same and is about 5.4%.

Using experimental data collected in 2011, the efficiency of detection of muons with energies above 600 MeV from the process $e^+e^- \rightarrow \mu^+\mu^-$ by the muon system was measured. It amounted to more than 96%. In determining the efficiency, it was required that both proportional tubes and scintillation counters trigger on a track registered by both drift chamber and the calorimeter. Reasons why the effectiveness is less than 100% are studied.

Tests of the new shaper - flash ADC cards for the calorimeter electronics channel were carried out at the special stand. The new channel will allow in addition of

the signal amplitude to determine the response time of the calorimeter counters, which is especially necessary for the measurement of the $e^+e^- \rightarrow n\bar{n}$ process cross section. Temporal resolution, measured with cosmic muons and the generator was 1.5 ns. The amplitude resolution, measured by the generator was 0.5%, which corresponds to 1.25 MeV. Now it is planned to install several new cards directly into the crates of the SND electronics for further inspection.

1.2.3. Software status

Over the past period the number of users of the software (SW) of data processing and MC simulation was significantly increased. This led to a painstaking analysis of its performance and correction of many errors and inefficiencies. Some new software features were realized. Two software releases (4.2 and 5.1) were produced and a new major release is being prepared.

In a general part of the software changes have been made aimed to simplify and standardize its use. These changes include: the organization of a hierarchy of sets of identical modules; standardized setting units for various applications of software; the possibility of creating inherited and combined objects; expanding the storage space for PAWC; realization of possibility of cloning of modules and sequences, adding of modules and sequences; assembly management in order to reduce the number of unnecessary or even harmful dependencies; modification of modules of control by events and tertiary trigger modules so that they can be used in a standard data processing and MC simulation too.

Changes in the MC simulation include: creation of new primary generators of e^+e^- annihilation into different final states such as: 3γ , $\mu^+\mu^-$, $\omega\pi^+\pi^-$, $e^+e^-2\gamma$, $\eta\omega$, $2\pi^0\pi^+\pi^-$, incorporation of the BHWIDE generator of the electron-positron scattering and existing UNIMOD primary generators; upgrade to Geant4 9.5; Modeling of additional features of calorimeter counters and cathode strips in the proportional and drift chambers; interaction point parameters setting from the database of calibrations; development and implementation of the software part of the procedure of mixing (overlays) of random hits of detector channels to the simulated events.

Calibration and reconstruction procedures are also well advanced: accuracy of particles reconstruction parameters was improved thanks to corrections to the calorimeter clusters energies and angles; a new algorithm providing better efficiency was created based on the segmented histogram method (by D. A. Bukin) using pairs of hits; cathode strips clusters were integrated into the object "particles"; calculation of the interaction point mean position and its dispersion was realized; a method was developed to account for jumps in the measured drift time associated with the incorrect determination of the beams interaction instant; a software package was developed to work with the stored sets of particles parameters (HBOOK n-tuples) implementing the so-called kinematic reconstruction of events; and so on.

Massive reconstruction and preselection of events

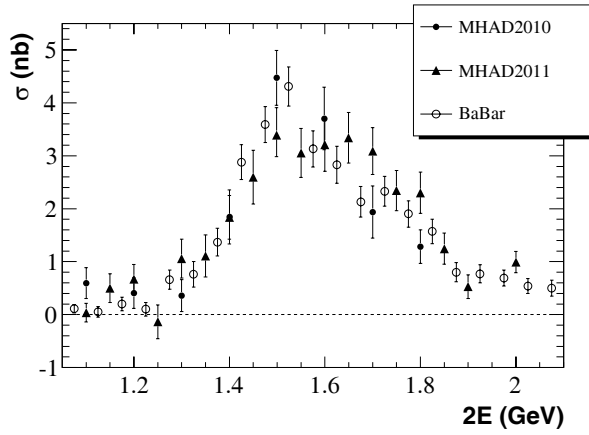


Figure 1.2.1: Cross section of the process $e^+e^- \rightarrow \eta\pi^+\pi^-$ measured by SND using 2010 and 2011 data. For comparison, the results of BABAR detector are also shown.

from the 2009-2010 and 2010-2011 scans (the so-called "perekachka" was carried out. For this purpose access to the NSU supercomputer cluster was used.

Realization of the access was based on the virtualization system with a two-level batch processing: job manager starts virtual machines on the supercomputer cluster and, in turn, they are registered in the system of batch processing of custom jobs. The same scheme was used to produce quite a significant amount of MC simulation events.

1.2.4. Data analysis

The process $e^+e^- \rightarrow \eta\pi^+\pi^-$ was investigated in the decay mode $\eta \rightarrow \gamma\gamma$ based on the experimental statistics collected in 2010 and partly in 2011. Events with two charged particles and with two or three photons were selected. For the charged particles it was required that they have central tracks. To suppress the beam related background, it was required that the total energy deposition in the calorimeter is within $(0,6 \div 1,8)E$.

Charged tracks are fitted to a common vertex under the assumption that, in the plane perpendicular to the beam axis, the vertex coincides with the position of the beam interaction point. Fairly mild condition $\chi_r^2 < 100$ was then required for the χ^2 of the fit. The obtained z -coordinate of the fitted vertex was used for recalculation of the polar angles of the photons.

Then a kinematic reconstruction of the final state in the hypothesis $\pi^+\pi^-\gamma\gamma$ was performed. In the presence of several photons in the event, reconstruction was carried out for all two-photon combinations and then the combination with the smallest χ^2 was selected. On the final χ^2 of the reconstruction, the condition $\chi_{\pi^+\pi^-\gamma\gamma}^2 < 60$ was imposed.

For determination of the number of $e^+e^- \rightarrow \eta\pi^+\pi^-$ events, the distribution of the invariant mass of photon pairs was approximated by the sum of distributions for the effect and background. The effect (the η -meson peak) was described by the sum of two Gaussian distributions, and the

background was approximated by a second degree polynomial.

The measured $e^+e^- \rightarrow \eta\pi^+\pi^-$ cross section is shown in Fig. 1.2.1 together with the results of BABAR detector. It is clear that the results of SND 2010, 2011 scans and the BABAR data do not contradict each other.

The process $e^+e^- \rightarrow \pi^+\pi^-\pi^0$ was studied in the energy region $2E$ from 1.05 to 2.00 GeV. The analysis used experimental data recorded in the 2011 experiment. The process $e^+e^- \rightarrow \pi^+\pi^-\pi^0\pi^0$ constitutes the main background for the process being studied in the energy region of interest.

The analysis used the events with two photons and two or three charged particles with central tracks. To suppress the background from the process $e^+e^+ \rightarrow e^+e^-$, it was required that tracks acollinearity angle in the plane perpendicular to the beams was more than 10° ($|\Delta\phi| > 10^\circ$). Against the beam related and electrodynamic backgrounds, the following conditions were required on the energy deposition in the calorimeter: the total energy in the event should be in the range of $0.6E$ to $1.6E$, and the energy deposition of the charged particles must be less than E .

Kinematic reconstruction procedure was applied to the events selected in such a way. At first step, common vertex was searched for tracks and compared to the interaction point obtained from the calibration. When there are three tracks in the event, two tracks with the smallest value of χ_r^2 are selected. The event was considered good if it satisfied the condition $\chi_r^2 < 100$. For good events, kinematic reconstruction was performed in the hypothesis that the event comes from the process $e^+e^- \rightarrow \pi^+\pi^-2\gamma$ and satisfies the laws of energy and momentum conservation. On the χ^2 of the reconstruction, the imposed condition was $\chi^2 < 80$.

For the selected events, two photon invariant mass spectrum was formed and approximated by the sum of the distributions for the effect and the background obtained from the MC simulation of processes $e^+e^- \rightarrow \pi^+\pi^-\pi^0$ and $e^+e^- \rightarrow \pi^+\pi^-\pi^0\pi^0$, respectively. Number of background events was 10–25% of the selected events. Fig.1.2.2 shows the resulting cross section along with the BABAR results and SND measurements at VEPP-2M for energies $2E < 1.4$ GeV.

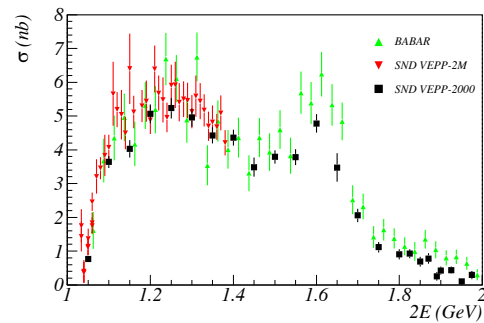


Figure 1.2.2: A comparison of the measured cross section $e^+e^- \rightarrow \pi^+\pi^-\pi^0$ to the previous measurement of SND at VEPP-2M ($2E < 1.4$ GeV) and to the results of the detector BABAR.

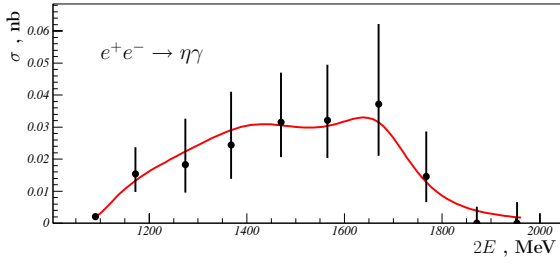


Figure 1.2.3: Cross section of the process $e^+e^- \rightarrow \eta\gamma$.

The process $e^+e^- \rightarrow \eta\gamma$ was investigated in the decay mode $\eta \rightarrow 3\pi^0$ based on the experimental statistics collected from 2010 to 2012. For the process under study, in the energy range $530 \text{ MeV} < E \leq 1000 \text{ MeV}$, the main background is associated with the processes $e^+e^- \rightarrow K_S K_L$, $e^+e^- \rightarrow \pi^0\pi^0\gamma$ and $e^+e^- \rightarrow \omega\pi^0\pi^0$ with decay $\omega \rightarrow \pi^0\gamma$. To select the events of the required process and suppress the contribution of background processes, events without charged particles were selected under the following selection criteria: the number of neutral particles $N_\gamma \geq 7$; total energy deposition (E_{tot}) in the calorimeter is from $1.4E$ to $2.4E$; the total normalized momentum of the photons $p_{tot} \cdot c/2E$ is less than 0.3; the condition $(E_{tot} - p_{tot} \cdot c)/2E > 0,7$ is satisfied to suppress the background with charged particles; kinematic reconstruction supports the hypothesis $e^+e^- \rightarrow n\gamma$ ($\chi_{n\gamma}^2 < 30$) and the hypothesis $e^+e^- \rightarrow 3\pi^0\gamma$ ($\chi_{3\pi^0\gamma}^2 < 50$); invariant recoil mass of the most energetic photon in the event lies in the range $400 \text{ MeV} < M_{rec\gamma} < 600 \text{ MeV}$. To suppress the background from the process $e^+e^- \rightarrow \pi^0\pi^0\gamma$, an additional constraint $\chi_{\pi^0\pi^0\gamma}^2 > 20$ was used.

In the energy range from 530 to 1000 MeV, 60 events were selected. The following decay parameters of the light vector mesons into $\eta\gamma$ final state were measured in the channel $\eta \rightarrow 3\pi^0$:

$$\sigma_{\rho'} = (55, 7^{+11,2}_{-9,7} \text{ } ^{+7,1}_{-1,8} \pm 1, 6) pb,$$

$$\sigma_{\rho''} = (47, 4^{+72,1}_{-21,6} \text{ } ^{+4,8}_{-18,1} \pm 1, 3) pb,$$

where the first error is statistical, the second and the third - systematic, the second error being the contribution from the model dependence. Cross section of the process is shown in Fig.1.2.3. Currently, we are working to refine our understandings of the luminosity determination and of the systematic errors estimation.

A particular interest to the processes of e^+e^- annihilation into six pions is caused by the interference structure observed in the cross sections of $e^+e^- \rightarrow 3(\pi^+\pi^-)$ and $e^+e^- \rightarrow 2(\pi^+\pi^-\pi^0)$ processes at energy of about 1.9 GeV, that is near the threshold of the nucleon-antinucleon pair production. This structure was first observed in the DM2(1988) experiment. Its presence was confirmed in BABAR (2006) experiment where the cross sections of these two processes were measured by using radiative return method. The BABAR data are virtually the

only published experimental data on the cross sections of $e^+e^- \rightarrow 3(\pi^+\pi^-)$ and $e^+e^- \rightarrow 2(\pi^+\pi^-\pi^0)$. The process $e^+e^- \rightarrow \pi^+\pi^-4\pi^0$ has not been yet studied experimentally.

A preliminary analysis of the processes of e^+e^- annihilation into six pions was based on 2011 data.

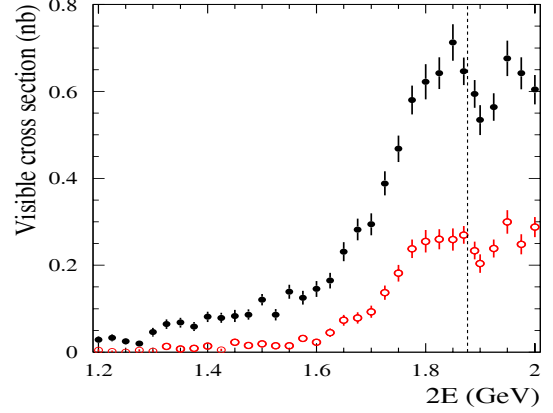


Figure 1.2.4: The visible cross section for selected five track (filled circles) and six track (empty circles) candidates of the $e^+e^- \rightarrow 3(\pi^+\pi^-)$ process events. The vertical dashed line shows the position of the nucleon-antinucleon pair production threshold.

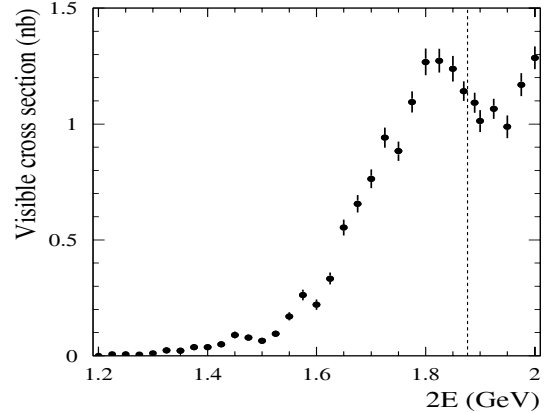


Figure 1.2.5: The visible cross section for selected candidates of the $e^+e^- \rightarrow 2(\pi^+\pi^-\pi^0)$ process events. The vertical dashed line shows the position of the nucleon-antinucleon pair production threshold.

To study the process $e^+e^- \rightarrow 3(\pi^+\pi^-)$, events with five or more tracks in the drift chamber were selected. It was required that at least five tracks are fitted to a common vertex which in the plane perpendicular to the beam axis coincides with the interaction point. The visible cross section for selected in such a way events is shown in Fig. 1.2.4 (filled

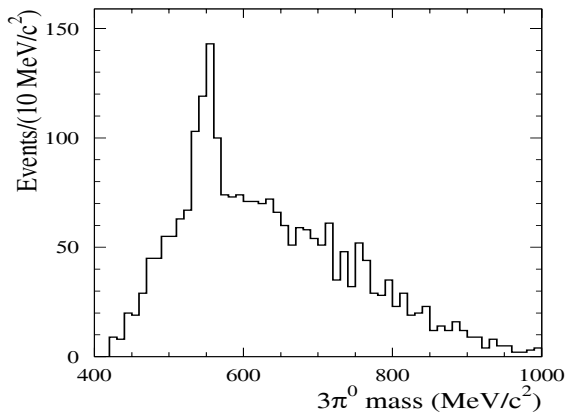


Figure 1.2.6: Distribution of the invariant mass of the three less energetic π^0 mesons for selected candidates of the $e^+e^- \rightarrow \pi^+\pi^-4\pi^0$ process events.

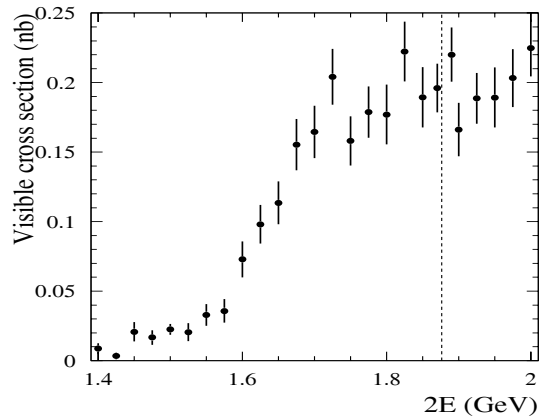


Figure 1.2.7: The visible cross section for selected candidates of the $e^+e^- \rightarrow \pi^+\pi^-4\pi^0$ process events. The vertical dashed line shows the position of the nucleon-antinucleon pair production threshold.

circles). The vertical dashed line shows the position of the nucleon-antinucleon pair production threshold. A resonant structure at energies of about 1.9 GeV is clearly visible in the measured cross section. Below 1.6 GeV, five track events are contaminated by background events from the process $e^+e^- \rightarrow 2(\pi^+\pi^-)$ with one additional superfluous track, for example due to delta-electron. If one requires that the sixth track is also registered in the event, this background is suppressed, but at the cost of twofold decrease in statistics. The visible cross section of selected events with six tracks is shown in Fig. 1.2.4 (empty circles). In future, the background from the process $e^+e^- \rightarrow 2(\pi^+\pi^-)$ is assumed to be subtracted by using MC simulation.

In the analysis of the $e^+e^- \rightarrow 2(\pi^+\pi^-\pi^0)$ process, events were selected with four tracks in the drift chamber which can be fitted to a common vertex as was described above, and at least with four photons. For these events, a kinematic reconstruction was performed with six conditions: four laws of energy and momentum conservation, and two more conditions that the invariant masses of photon pairs are equal to the π^0 -meson mass. χ^2 of the kinematic reconstruction was used as a selection parameter. The visible cross section for the selected events is shown in Fig. 1.2.5. An interference pattern at an energy of about 1.9 GeV is also visible in it.

In the analysis of the $e^+e^- \rightarrow \pi^+\pi^-4\pi^0$ process, events were selected with two tracks in the drift chamber, which can be fitted to a common vertex, and at least with eight photons found in the calorimeter. Then a kinematic reconstruction was performed with eight conditions: four laws of energy and momentum conservation and 4 conditions on the invariant masses of photon pairs. On the χ^2 of the reconstruction, $\chi^2 < 50$ condition was imposed. For this channel, a significant part of the registered events comes from the background process $e^+e^- \rightarrow \pi^+\pi^-\pi^0\eta$ followed by the decay $\eta \rightarrow 3\pi^0$. These events are easily seen in

the distribution of the invariant mass of three π^0 -mesons, shown in Fig. 1.2.6. In the distribution only one of the four possible combinations of the three π^0 -mesons with least energetic particles was included. The condition on this invariant mass $0, 51 < M_{3\pi^0} < 0.59$ GeV/ c^2 suppresses the background from the process $e^+e^- \rightarrow \pi^+\pi^-\pi^0\eta$. The visible cross section for selected events is shown in Fig. 1.2.7. In this case, at current level of statistics, a resonance structure is not visible.

To continue the analysis, the development of event generators for the MC simulation of the e^+e^- annihilation into six pions is required. This work was commenced. MC simulation of the background processes $e^+e^- \rightarrow 2(\pi^+\pi^-)$, $e^+e^- \rightarrow \pi^+\pi^-2\pi^0$, $e^+e^- \rightarrow \pi^+\pi^-3\pi^0$ and some others will be also performed.

Results on the $e^+e^- \rightarrow \omega\pi^0 \rightarrow \pi^0\pi^0\gamma$ cross section, obtained by using SND 2010 statistics, were published in 2012. Here we present preliminary results based on the unified 2010 and 2011 data sample for energy range $2E = 1.05 \div 2.00$ GeV.

Fig. 1.2.8 shows the measured cross section of the process being studied and the results of previous measurements at detectors SND(2000), CMD-2(2003), CLEO(2000) and DM2(1991). The DM2 cross section was measured in the channel $\pi^+\pi^-\pi^0\pi^0$ and it was recalculated using relative probabilities of the ω meson decays taken from the PDG table. CLEO measured the spectral function in the decay $\tau \rightarrow \omega\pi\nu_\tau$. The cross section of the process under study can be obtained from this spectral function assuming conservation of the vector current. Interestingly, a naive application of the relation based on the vector current conservation hypothesis gives the result shifted by 7-10 %. Fig. 1.2.8 also shows the result of a joint approximation of the SND data used in this work and of the published SND(2000) data. The approximation used

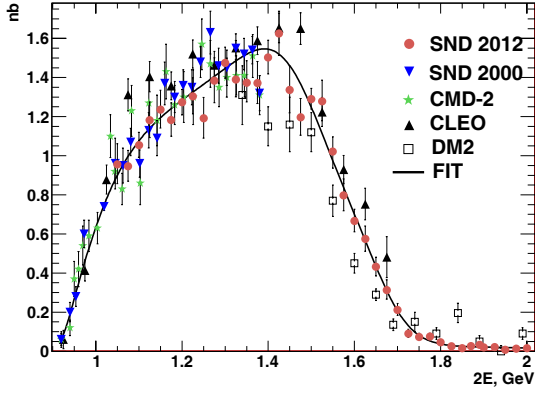


Figure 1.2.8: Cross section of the process $e^+e^- \rightarrow \omega\pi^0 \rightarrow \pi^0\pi^0\gamma$. The figure shows the results of the SND(2012) experiment (this work) along with the SND(2000), CMD-2, CLEO and DM2 results. The curve represents the result of the joint approximation of the SND(2012) and SND(2000) data.

vector meson dominance model with $\rho(770)$, $\rho(1450)$ and $\rho(1700)$ in the intermediate state.

The cross section of the process $e^+e^- \rightarrow p\bar{p}$ was measured using 2011 statistics. To study the effect, we use statistics at six energy points above the threshold of the proton-antiproton pair production, and to measure the background cross section — at two energy points below the threshold. In the region from the threshold to 1.91 GeV, the ionization mean free path of secondary charged nucleons is less than the VEPP-2000 vacuum chamber thickness. Therefore, the proton is not registered by the tracking system, and the antiproton annihilation generates secondary charged particles whose tracks have a common vertex on the vacuum chamber wall. At energies above 1.92 GeV, proton and antiproton tracks are registered by the tracking system as two collinear tracks with a high density of ionization.

The main condition for the selection of events in the two energy points near the threshold was the presence of three or more charged tracks emerging from a common vertex on the wall of the vacuum chamber. Two tracks with the greatest energy deposition in the calorimeter should have $R > 0.3$ cm, $|\Delta\phi| > 5^\circ$ and $|\Delta\theta| > 10^\circ$. The total energy deposition in the calorimeter should be in the range from 650 to 1400 MeV. The detection efficiency for these selection criteria obtained from the MC simulation is 21%.

For four energy points from 1.925 to 2 GeV, two collinear central tracks were required with the ionization energy losses dE/dx 1.3 times greater than the average value of this quantity for the tracks of the elastic e^+e^- scattering. It was required that no additional central tracks were registered in the drift chamber. The total energy deposition in the calorimeter was required to be more than 650 MeV, and the energy deposition in the calorimeter for one of the

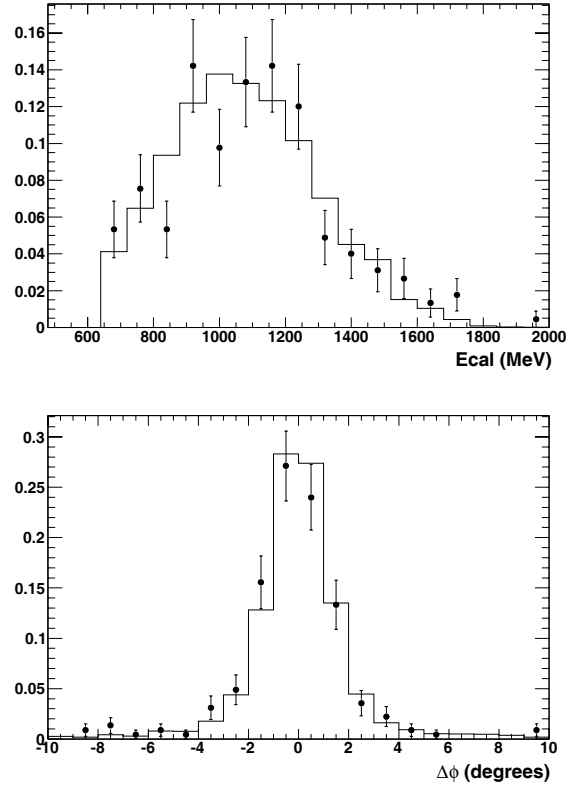


Figure 1.2.9: A comparison of experimental distributions of selected events of the process $e^+e^- \rightarrow p\bar{p}$ (points) with the MC simulation results (histogram) for $2E = 2$ GeV. Distributions of the total energy deposition in the calorimeter (top) and of the acollinearity angle in the plane perpendicular to the beam (bottom) are shown.

selected collinear particles should be less than 300 MeV. The use of the low threshold for the dE/dx in comparison with the actual ratio of the ionization density on the proton and electron tracks, more than 10 in the studied energy range, is related to the operation of the SND tracking system in the reduced proportionality regime. The detection efficiency for these selection criteria calculated using MC simulation is in the range from 45% to 58% for energies from 1.925 to 2 GeV.

Fig. 1.2.9 shows a comparison of the experimental distributions for selected events of the total energy deposition in the calorimeter and of the acollinearity angle in the plane perpendicular to the beam with the corresponding distributions for the MC simulated events of the process $e^+e^- \rightarrow p\bar{p}$. It is seen that the experimentally observed distributions are in a good agreement with the MC simulated ones.

Preliminary SND results on the Born cross section of the $e^+e^- \rightarrow p\bar{p}$ process are shown in Fig.1.2.10. Only the statistical errors are shown. analysis of the systematic errors isn't finished yet .

Analysis of the $e^+e^- \rightarrow n\bar{n}$ process was continued us-

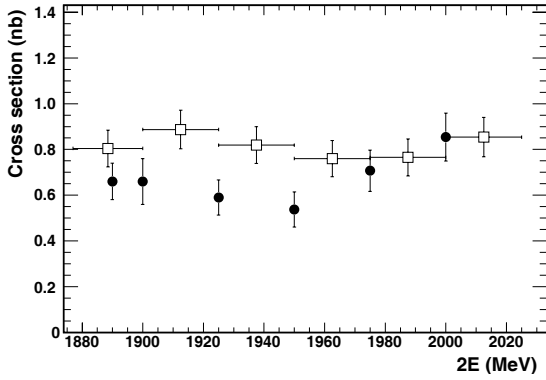


Figure 1.2.10: Energy dependence of the cross section of the $e^+e^- \rightarrow p\bar{p}$ process. Circles — preliminary SND results, squares — BABAR (2006) results.

ing 2011 data. Selection criteria generally remained the same (see the INP Annual Report for the year 2011). We added only a new selection parameter “shcosm” to suppress the extensive air showers in the calorimeter which are not discriminated by the anticoincidence system. Time distribution of the $n\bar{n}$ candidate events indicates the presence of a time delay at the expected level. Angular and energy distributions were also obtained and analyzed. To estimate systematic errors in the $e^+e^- \rightarrow n\bar{n}$ cross section determination, selection criteria were varied (Fig. 1.2.11). The systematic error was estimated to be about 40%. The mean cross section for the energy range from the threshold to 2 GeV is $0,44 \pm 0,18$ nb (the error is statistical).

1.2.5. Energy calibration

In 2012, the creation and installation of VEPP-2000 beam energy measurement system via inverse Compton scattering of CO laser radiation was completed thanks to efforts of the staff of several laboratories. In the experiments with the system, the interference effect was observed for the first time in the energy spectrum of back-scattered MeV range gamma rays caused by influence of the magnetic field on the Compton scattering process. Quantitative description of the shape of the spectrum (Fig.1.2.12) was developed which allows to carry out an absolute calibration of the collider energy. In parallel with the data taking process, testing of the system had began. According to the preliminary results, the accuracy of the VEPP-2000 energy setting at $E \approx 1$ GeV was not worse than 1 MeV.

This work was financially supported by the Ministry of Education and Science of the Russian Federation, by basic projects BINP 13.1.1. and 13.3.1., by a project of the Division of Physical Sciences OFN.I.1.2., as well as by RFBR grants RFBR 12-02-00065-a, RFBR 12-02-01250-a, RFBR 11-02-00276-a and by Russian Federation President Grant for the support of scientific schools NSh 5320.2012. 2.

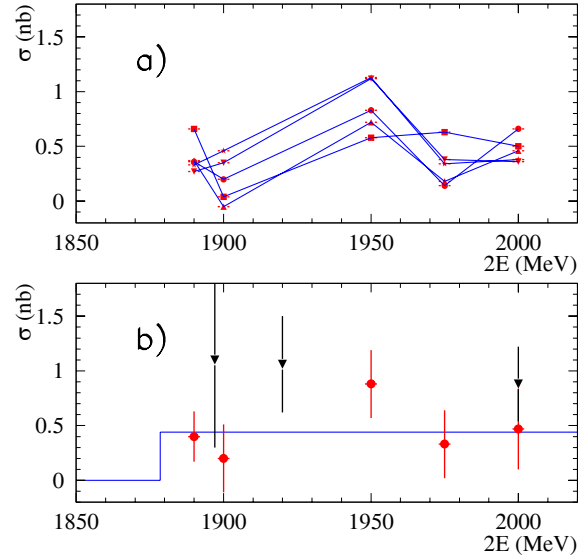


Figure 1.2.11: a) Change in the measured $e^+e^- \rightarrow n\bar{n}$ cross section upon variation of the selection criteria. The lines connect points with the same conditions of selection; b) $e^+e^- \rightarrow n\bar{n}$ process cross section averaged over several variants of the selection criteria (circles). FENICE(1998) data are also shown (triangles).

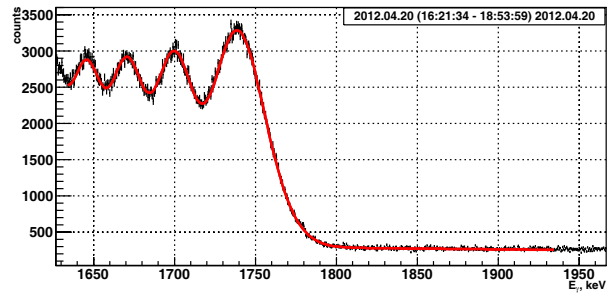


Figure 1.2.12: End of the spectrum of the scattered photons. Solid line – approximation with the theoretical shape of the spectrum.

1.3. KEDR DETECTOR

KEDR is a universal magnetic detector, which is used in experiments on the e^+e^- collider VEPP-4M at energies of 2 to 11 GeV in the center of mass system.

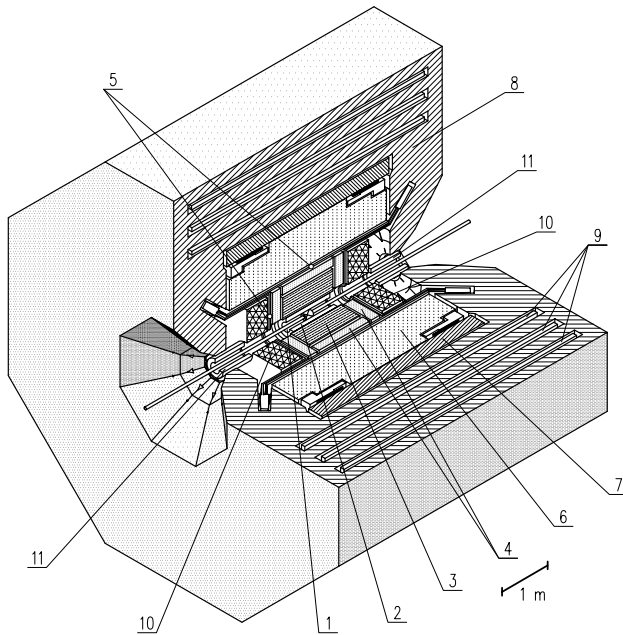


Figure 1.3.1: KEDR detector. 1 – vacuum chamber of the accelerator, 2 – vertex detector, 3 – drift chamber, 4 – aerogel threshold counters, 5 – time-of-flight counters, 6 – liquid-crypton barrel calorimeter, 7 – superconducting coil, 8 – yoke, 9 – muon chambers, 10 – end-cap CsI calorimeter, 11 – compensating coil.

Main systems of the KEDR detector are shown in Fig. 1.3.1. Besides that, the detector includes a system for registration of scattered electrons for $\gamma\gamma$ physics studies and luminosity monitor. Parameters of the detector are comparable with those of the best world detectors operating in this energy range; the detector is described in detail in preprint INP 2010-40.

In 2012, magnetic systems of the KEDR detector were subjected to tests. For this end, all the parts of the magnetic circuit and cryogenic system that provides superconductivity of the detector magnet were assembled in a regular way on the VEPP-4M ring. The magnetic tests showed that the actual design of the magnetic and cryogenic systems allows stable operation at fields of up to 6kG. Then the implementation of some changes in the cryogenic system design was started for improvement of operation stability and increasing the working field in the detector. When the magnetic circuit of the detector had been assembled, the ring of the

VEPP-4M accelerator was closed, and methodological and engineering works were being conducted with beams but without the KEDR detector practically throughout the year 2012.

1.3.1. Repair and upgrade of the detector. Preparation for experimental run with the KEDR detector on VEPP-4M.

The repair and upgrade of the KEDR detector were started in 2011 and completed almost entirely in 2012. Assembly of the detector and beginning of experiments on the VEPP-4M collider at the energy $W = 3 - 8$ GeV are planned for 2013. Below is described the status of the systems as by the end of 2012.

- The vertex detector has been reconditioned and prepared for installation in the detector; more screens for the electronics were mounted inside the detector; reconnection of signal channels in the digitizing modules is underway.
- The drift chamber (DC) has been reconditioned and prepared for installation in the detector; some electronics were fabricated for reconstruction of the longitudinal coordinate in the inner layer of the chamber by the charge division method. The DC has passed tests with cosmic particles.
- The ASHIF system of Cherenkov aerogel counters has been reconditioned and improved. The system is now ready for full-scale (160 counters) installation in the detector.
- The time-of-flight counters have been reconditioned and can be installed in the detector; additional magnetic screens for the barrel counters have been designed; their production has been started at the BINP workshop.
- The electronics of the liquid-rypton barrel calorimeter have been repaired and tested on stands; the mounting of the new system for cryton purification is underway. The entire gas volume (22 tons) will be cleaned before the start of statistics collection using the detector.
- Mechanical alterations to the end thallium-activated CsI-crystal calorimeter have been made in full scale (8 calorimeter modules have been combined into four; thus the position of each crystal will be known with an accuracy better than 1 mm); the electronics have been reconditioned; phototriodes in the modules of one end have been replaced; the Ekran plant is now producing phototriodes for the modules of second end, which are then tested and accepted at BINP.
- Electronics in all the muon chambers (88 units) have been reconditioned and replaced; half of the units have been installed in the detector; their performance has been checked.

- All the elements of the detector yoke have been completed.
- The "old"-configuration magnetic system of the detector is ready for use. A new power supply for the main solenoid has been designed and manufactured. Development tests and adjustment of the control systems and interfaces are underway. A remake of the cryoguide, from the superconducting transformer to the main solenoid and cryostat for superconducting switches and transformer, has been designed; manufacturing of corresponding parts is underway at the BINP workshop.
- A calibration system for the scattered electron detection system (SEDS) was created. It is based on precision electromagnetic BGO-monocrystal calorimeter and two lasers with wavelengths of 532 nm and 1064 nm. The system allows calibration of the dependence of track coordinate on scattered electron energy and measurement of energy resolution. The automation of SEDS calibration on the electron arm is underway.

1.3.2. FARICH technique

FARICH (Focusing Aerogel RICH) is a promising detector for identification of charged particles in a wide momentum range. It is a detector of Cherenkov rings with a radiator made of a multilayer "focusing" aerogel. The aerogel group of the KEDR detector together with a group of the Institute of Catalysis has carried out this work since 2004.

In 2009-2010, BINP created the installation "Extracted electron beam on the VEPP-4M accelerator" to study prototypes of new detectors of elementary particles on beams of electrons and gamma rays in the energy range from 100 to 4000 MeV. The installation is described in more detail in the BINP report for the year 2011.

In 2012, the following works were carried out within the development of the FARICH technique:

- The system of coordinate chambers for extracted beam was upgraded. One-coordinate drift chambers with a coordinate resolution of 500 microns were replaced with two-coordinate detectors based on gas electron multipliers. The detectors were mounted on the beam line; an experiment on electrons with an energy of 1 GeV was carried out. A designed coordinate resolution of 80 microns was attained.
- A simulation was performed and the optimal thickness of the converter was found, which equals 35% of the radiation length.
- The efficiency of photon detection with silicon detectors produced by CPTA (Moscow) (CPTA 151-30 and CPTA 149-35) was studied. It was shown that at wavelengths of 400 to 650 nm, the detection efficiency varies from 5 to 20%, which is about two times lower

than data in the manufacturer's catalog. These studies will be continued.

- Prototype 2 was prepared for experiment on extracted beam. The main part of the prototype is a photon detector consisting of 60 silicon photomultipliers of the CPTA 151-30 type with a sensitive area diameter of 1.28 mm. Prototype 2 applies new amplifier-discriminator boards based on NINO chips. The efficiency of the electronics has been tested with photon detectors CPTA 151-30 at illumination from a picosecond laser. The time resolution was measured at detection of single photons; it equals 300 ps. Properties of focusing "aerogels" that are being developed at the Institute of Catalysis SB RAS will be studied in detail in experiments with prototype 2 with the upgraded coordinate system. As compared with prototype 1, the precision of Cherenkov radiation angle measurement is about 2 times better.
- In June 2012, on a beam of pions and protons in CERN, our group together with physicists from INR RAS (Moscow) and engineers of Philips Digital Photon Counting (Germany) used digital silicon photomultipliers for recording for the first time a full ring of Cherenkov radiation from "focusing" aerogel radiator. A photo of the FARICH prototype based on a matrix of digital silicon photomultipliers of 20x20 cm² in size is shown in 1.3.2.



Figure 1.3.2: FARICH prototype on beam at CERN.

The matrix has 2,304 pixels. For prototype operation in a single-photon regime, the matrix was cooled to -40° . A four-layer "focusing" aerogel radiator has been tested on a beam with a momentum of 2 to 6 GeV/c. Pion and proton distribution over the radius of the Cherenkov ring is shown in 1.3.3. The average number of detected photons was 14 for pions with a momentum of 6 GeV/c. The radius resolution is 0.7 mm for pions and 1.1 mm for protons. These results confirm the possibility of separation of pions and kaons at a significance level of 3σ up to a momentum of 7 GeV/c and separation of muons and pions up

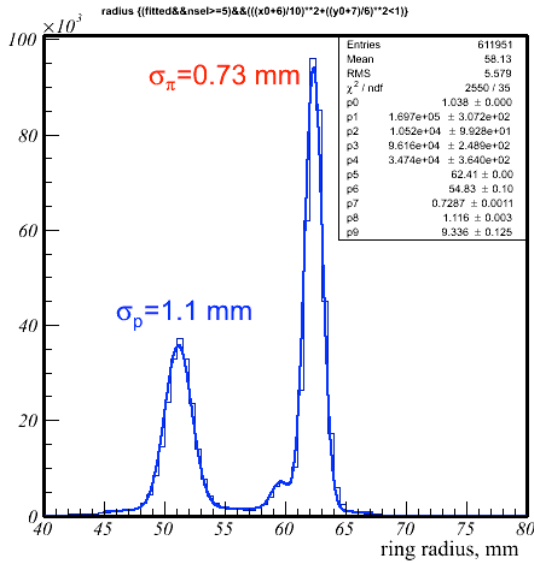


Figure 1.3.3: Distribution over the measured radius of the Cherenkov ring for pions and protons.

to a momentum of 1.3 GeV/c. A record high level of separation of muons and pions has been attained. Such detection efficiency is required for creation of an identification system for the detector for the Super Charm-Tau Factory.

1.3.3. Results of KEDR detector operation on the VEPP-4M collider in 2012.

Processing of the VEPP-4M statistics collected in the KEDR experiment in 2012 yielded the following main results.

- The results of experiments on the measurement of the main parameters of the $\psi(2S)$ and $\psi(3770)$ mesons were published.
- The mass of the J/ψ and $\psi(2S)$ mesons is being measured using the statistics collected throughout the experiment.
- Lepton universality in decays of the J/ψ meson was checked.

Below is given a more detailed description of these analyzes.

1.3.4. Measuring parameters of the $\psi(2S)$ and $\psi(3770)$ mesons.

Works on the measurement of parameters of the $\psi(2S)$ and $\psi(3770)$ mesons were published in 2012. The main results of the experiment are as follows.

- The $\psi(2S)$ meson mass was measured with a precision of about 15 keV, which is half as better as that of the best of the previous measurements.
- The product of the e^- -width by the probability of decay into hadrons was measured for the $\psi(2S)$ meson

with a precision of 2%, which may yield twice as precise value of the e^- -width.

- Measurement of main parameters of the $\psi(3770)$ meson with due account of the interference of resonant and non-resonant production of $D\bar{D}$ pairs. The $\psi(3770)$ mass was measured with a precision equal to that of the BaBar experiment, which is the best to date. The e^- -width was measured for the first time with due account of interference effects.

1.3.5. Precision measurement of the masses of the J/ψ and $\psi(2S)$ mesons.

Application of the method of resonant depolarization in the KEDR experiment made it possible to attain a fundamentally new level of precision in measuring masses of narrow resonances. However, finding ways to further increase the precision to the level of a few keV is an important task for the KEDR collaboration.

During the experiment with the KEDR detector we performed 6 scans of the J/ψ resonance and 7 scans of the $\psi(2S)$ resonance. The statistics collected is 0.75 pb^{-1} and 1 pb^{-1} , respectively.

Preliminary results on the new precision measurement of the masses of J/ψ and $\psi(2S)$ resonances are as follows:

$$M_{J/\psi} = 3096.900 \pm 0.002 \pm 0.006 \text{ MeV},$$

$$M_{\psi(2S)} = 3686.100 \pm 0.003 \pm 0.009 \text{ MeV}.$$

KEDR results in the measurement of the masses of the J/ψ and $\psi(2S)$ mesons remain unsurpassed in precision.

1.3.6. Checking lepton universality in decays of the J/ψ meson.

One of HEP topical tasks is the search for deviations from the Standard Model; increasing the precision of experiments on checking the conservation laws is one of the main focuses of the current research.

In 2012, the KEDR collaboration performed an experiment on checking lepton universality in decays of the J/ψ meson. The ratio of the partial widths of the decays $J/\psi \rightarrow e^+e^-$ and $J/\psi \rightarrow \mu^+\mu^-$ was measured; the following preliminary result was obtained:

$$\Gamma_{e^+e^-}(J/\psi)/\Gamma_{\mu^+\mu^-}(J/\psi) = 0.9964 \pm 0.0048 \pm 0.0060$$

The precision of the preliminary results of the KEDR experiment is twice as high as that of the current most precise measurement performed by the CLEO collaboration.

The works were partially supported by RFBR grants 10-02-00871-a, 10-02-00904-, 11-02-00558-a, 11-02-01064-a, 11-02-01422-a, 12-02-00023-a, 12-02-01076-a, 12-02-31523 mol_a, Grant of the RF President for State Support of Leading Scientific Schools NSh-5320.2012.2, and SB RAS integration project 103 (2012–2014), as well as financially supported by the RF Ministry of Education and Science.

1.5. DETECTORS FOR HEP

Below are listed works done in 2012 as a part of upgrade of electronics of the detectors.

In 2012, as part of the modernization of the detector electronics were the following work:

1.5.1. *KEDR*.

1. In the muon system of the detector full replacement of discriminators is made, all blocks are tested. Thus, modernization of the muon system of the detector is completely executed.

2. The module of a calorimeter on crystal BGO is developed and entered into work.

3. Repair of chamber electronics of calorimeters of the detector – the CsI and krypton ones, with partial replacement of amplifiers was continued.

1.5.2. *SND*.

1. Upgrade of the electronics for the first layer of the calorimeter was completed.

2. New electronics (preamplifiers and motherboards (1,120 channels)) were manufactured for the second and third layers of the calorimeter; under testing.

3. A new version of the F12 module was made.

1.6. X-RAY DETECTORS

1. In the framework of works on creation of the multiline coordinate detector in which as registering elements it is planned to use silicon microstrip structures, the technical project on their manufacturing is made.

Discussions with potential manufacturers were held. All technical issues have been agreed on with HAMAMATSU company; the contract will be signed in February 2013. Under the contract, three modifications of coordinate structures for testing and selection of optimal parameters will be made.

2. In 2012, the workshop of BINP fabricated five housings for the detectors OD-3M and an appropriate amount of ceramic electrodes for proportional wire chambers, which form the basis of the coordinate structure of the detectors. The detectors will be used in diffractometers to be produced under a program of the SB RAS instrument committee.

3. Development of the topology of the motherboard of the detector OD-4, designed for experiments on SR wide-angle scattering, was almost completed in 2012. In OD-4, a wire structure, such as in OD-3M, for example, is replaced with a multistage gas electron multiplier (GEM). This allows, in addition to high gas gain (over 10,000), to make a detector in the arc form with arbitrary angular aperture.

1.7. OTHER WORKS

In the framework of international projects, the sector staff continued to actively participate in works associated with the development of new data acquisition system for the BELLE-II detector (KEK, Japan).

In 2012:

1. The equipment for check of counters of a cylindrical calorimeter is created. With its help all counters and the cables connected to them have been checked up.

2. The new version of the collector module, providing high-speed data exchange is developed.

3. Mechanical and electrical specifications for the new VME crate were developed.

Among the staff there are co-authors of more than 25 publications by the results of processing of the BELLE experiment (KEK, Japan).

1.8. MICRO-PATTERN GAS DETECTORS

In 2012, the staff of Institute continued the development of detectors based on Gas Electron Multipliers (GEMs) in the following directions:

1) development of two-phase cryogenic avalanche detectors (CRADs) based on thick GEMs (THGEMs) for low-background experiments for dark matter search and registration of coherent neutrino scattering on nuclei and for medical imaging;

2) modernization of the scattered electron system in the KEDR experiment;

3) participation in the collaborations RD51 at CERN for the development of micro-pattern gas detectors and the TPC for the International Linear Collider.

1.8.1. THGEMs-based two-phase cryogenic avalanche detectors (CRADs).

Introduction.

Fig. 1.8.1 shows a schematic of two-phase Ar CRAD for search for dark matter and coherent scattering of neutrinos.

The ultimate goal of this project is the development of new methods for dark matter detection using two-phase GEM-based CRADs of ultimate sensitivity, in Ar and Xe. The method is based on the amplification of ultimately weak signals from recoil nuclei produced in a cryogenic liquid due to scattering of dark matter particles. The signals are amplified in the gas phase by an electron multiplier on cascaded GEMs. The uniqueness of the two-phase CRAD is that it should be able to operate in the mode of counting of single primary-ionization electrons, which means very little energy released in the liquid (less than 1 keV), and with a sufficiently high spatial resolution (less than 1 cm) and very low noise. The ultimate sensitivity of the detector is attained due to an original idea of using a combined multiplier consisting of THGEMs and Geiger avalanche photodiodes (G-APDs), which perform optical reading from THGEMs in the near infrared (IR) spectral region. Such a detector would have sensitivity that significantly (several times) exceeds that of the available detectors for dark matter due to its ability to work in the single-electron counting mode with improved (less than 1 cm) spatial resolution

For this project, two unique installations are to be created – a smaller CRAD and a larger one, with the cryogenic chamber volume of 9 l and 160 liters, respectively (installation 1 and installation 2). The first installation will be used in measurements for obtaining planned results on the two-phase CRAD with combined multiplier (GEM/G-APD matrix) and on the two-phase CRAD response to neutron scattering. As concerns the second installation, its basic elements will be refined on with a view of creation of a draft designing documentation for a practical two-phase CRAD.

Besides that, the plasma staff of BINP will be engaged in the designing and creation of metrological neutron beams for calibration of dark matter detectors. A prospective result of this work may be creation of a BINP-based international metrological neutron center for calibration of dark matter and low-energy neutrino detectors.

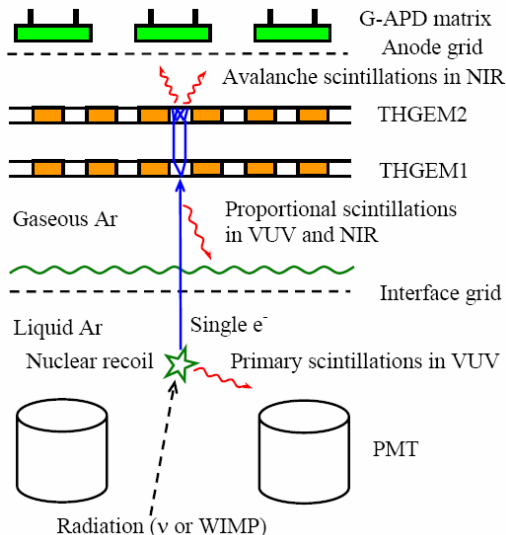


Fig. 1.8.1. Schematic diagram of the experimental model of two-phase Ar CRAD with a combined multiplier (THGEM/G-APD matrix).

Study of two-phase Ar CRAD with a practical active volume and two-stage and three-stage hybrid multiplier THGEM/GEM.

Measurements were performed in a two-phase Ar CRAD with a two-stage thick GEM assembled with a practical active volume with an active area of $10 \times 10 \text{ cm}^2$ and liquid layer thickness of 1 and 5 cm. Fig. 1.8.2 shows the amplification characteristics of this detector for single-stage and two-stage THGEMs in comparison with a detector with a smaller active area ($2.5 \times 2.5 \text{ cm}^2$). One can see that the characteristics are similar in both the working voltages and the maximum gain, which was as high as 1,000. Even larger gains were attained with the three-stage hybrid multiplier THGEM/GEM/PCB, up to 5000 (see Fig. 1.8.3). These results prove successful operation of thick GEMs with a practical active area, namely $10 \times 10 \text{ cm}^2$, under conditions of a practical two-phase Ar CRAD, with relatively high gains.

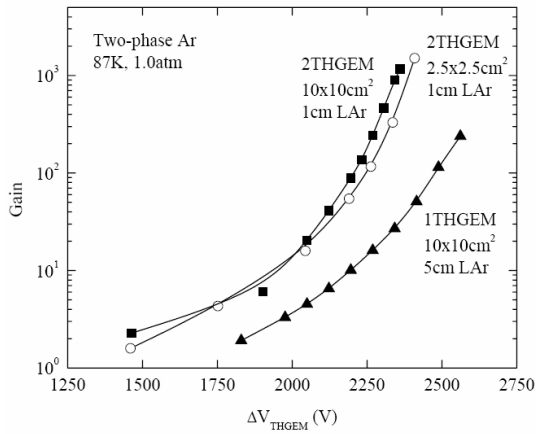


Fig. 1.8.2. Gain characteristics of the two- and one-stage thick GEMs with an active area of $10 \times 10 \text{ cm}^2$, obtained in a two-phase Ar CRAD with the liquid layer 5 cm and 1 cm thick.

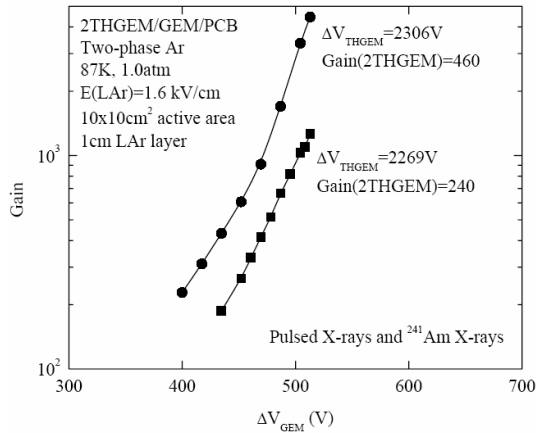


Fig. 1.8.3. Gain characteristics a three-stage hybrid multiplier 2THGEM/GEM/PCB with an active area of $10 \times 10 \text{ cm}^2$, obtained in a two-phase Ar CRAD.

Study of a two-phase Ar CRAD with combined multiplier (THGEM /G-APD matrix).

A two-phase CRAD with a 9l cryogenic chamber and a combined multiplier (THGEM/G-APD matrix) was successfully studied in 2012. Its schematic diagram is presented in Fig. 1.8.1, and Fig. 1.8.4 shows mounting of the two-phase CRAD in the G-APD. Optical reading of signals from the two-stage coordinate-resolution THGEM was executed with the use of a matrix of 9 G-APDs arranged as a square lattice with 1 cm spacing at a distance of 7 mm from the last of the THGEMs. The multi-channel data acquisition system was based on the VME-standard electronic module FADC CAEN 1720 (8 channels); reading and writing of data was performed with the newly-created software within the package Labview.

Fig. 1.8.5 shows a photograph of the first stage of unique experimental installation 1 (of smaller size), including an experimental two-phase CRAD with a 9l

cryogenic chamber, part of cryogenic and vacuum systems, and electronics of the high-voltage and data acquisition systems.

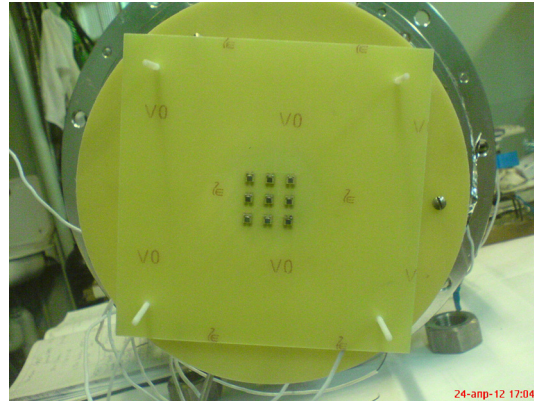


Fig. 1.8.4. Photo of assembling of the G-APD matrix at the stage of mounting of the two-phase CRAD.

In accordance with the activity plan for 2012, we measured the amplitude and coordinate characteristics of the combined multiplier (THGEM/G-APD matrix) in the two-phase Ar CRAD. For this end, over 10 cryogenic sessions were carried out in the period from June to December 2012. The detector was irradiated with soft X-ray photons with an average energy of 15-40 keV from a pulsed X-ray tube. For the purpose of measurement of the coordinate characteristics of the detector, in particular its spatial resolution, the detector was irradiated through a cylindrical steel collimator of 2 mm in diameter.

Fig. 1.8.6 shows a typical optical signal from the G-APD in the two-phase Ar CRAD with the combined multiplier (THGEM/G-APD matrix). The relatively long signal duration (over $15 \mu\text{s}$) is due to the physics of electron emission across the phase interface in two-phase Ar, namely, the presence of slow component of emission.

During the measurements we revealed particularities of operation of the G-APDs (made by CPTA, Moscow) at cryogenic temperatures. They turned out to fail when the detector was under a load of X-ray photons in excess of 100 Hz. This effect is under study now, a tentative explanation being the large constant of the time for charging of G-APD pixel after the "Geiger" breakdown due to a significant increase in the damping resistance of pixel at cryogenic temperatures.



Fig. 1.8.5. Photo of the first stage of experimental installation 1. Prototype of the two-phase CRAD with a 9l cryogenic chamber, part of the cryogenic and vacuum systems, and electronics of the high-voltage and data-collection systems.

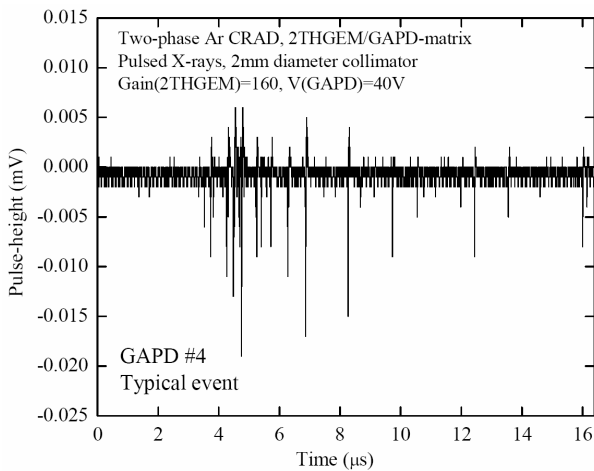


Fig. 1.8.6. Typical optical signal from G-APD in a two-phase Ar CRAD with a combined multiplier (THGEM/G-APD matrix); the THGEM gain is $G = 160$ at irradiation with 20 keV X-ray photons through a collimator of 2 mm in diameter.

Fig. 1.8.7 shows the amplitude distribution of the sum optical signal of the matrix from all active G-APDs (7 of 9) in the two-phase CRAD, from which one can estimate the light yield of the combined multiplier (THGEM/G-APD) and therefore the threshold sensitivity of the two-phase CRAD. One can see that even with such a modest gain ($G = 160$) a signal from a 20 keV X-ray photon yields a substantial optical signal on the G-APD matrix – of about 100 photoelectrons.

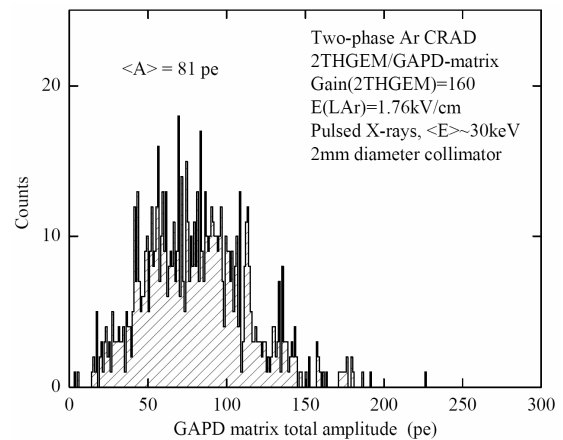


Fig. 1.8.7. Amplitude distribution of the sum optical signal from all active G-APDs of the matrix (right) in the two-phase Ar CRAD, the THGEM gain $G = 160$, under irradiation with 20 keV X-ray photons through a collimator of 2 mm in diameter.

This means that even for rather low energies—about 1 keV—released in liquid Ar, a two-phase CRAD may have a sufficient optical signal—with an amplitude of 10 photoelectrons at a quite operational THGEM gain $G = 500$. This is enough to attain to a record (sub-cm) spatial resolution using a G-APD matrix, even at such low energies. It should be noted that energy of 1 keV is half the detection threshold of the dark matter detector DAMA/LIBRA, which is the most sensitive detector at the present time.

Fig. 1.8.8 illustrates the spatial resolution of the two-phase Ar CRAD with combined multiplier (THGEM/G-

APD matrix). In the two-dimensional distribution of reconstructed events one can clearly see an "image" of the hole in the collimator. From this image one can assess the spatial resolution of the detector, subtracting the squared contribution of the hole size (2 mm). For the Y coordinate, the evaluation yields FWHM = 3.2 mm. Hence, the contribution of the G-APD matrix into the measurement accuracy is 2.5 mm (FWHM) or 1.1 mm (standard deviation).

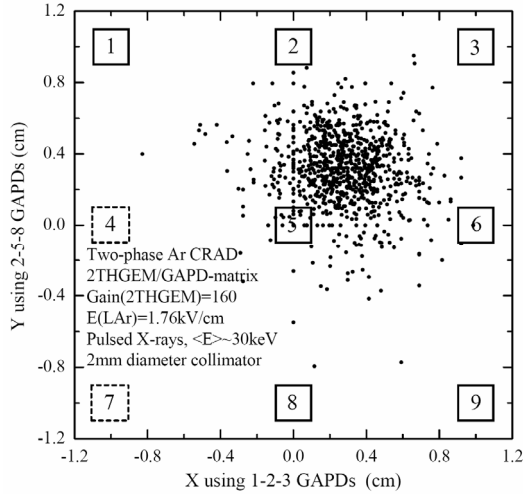


Fig. 1.8.8. Two-dimensional distribution of events in the two-phase Ar CRAD as reconstructed from the amplitude of signals from the G-APD matrix (G-APDs #1-2-3 and #2-5-8 for the X and Y coordinates, respectively), the THGEM gain $G = 160$, under irradiation with 20 keV X-ray photons through a collimator of 2 mm in diameter.

Thus, with the help of a unique system for signal reading, namely the combined multiplier (THGEM/G-APD matrix), and with optical reading in the NIR, we received a record spatial resolution for two-phase dark matter detectors. Considering that the resolution decreases with the number of photoelectrons as $1/\sqrt{N_{pe}}$, one can make an estimate for the above ultimate-sensitivity case, i.e. for release of an energy of 1 keV and a THGEM gain $G = 500$. In this case, the coordinate resolution will be 8 mm (FWHM) or 3 mm (sigma), which is still at the sub-cm level, i.e. without a rival among two-phase detectors.

1.8.2. Upgrade of the scattered electron system in the KEDR experiment.

The system for registration of scattered electrons is an essential part of the KEDR experiment and allows detection of electrons scattered at small angles from the place of collision. Such electrons are a typical sign of photon-photon interaction, and their detection and accurate measurement of pulse are an important physical problem.

For attainment of ultimate scattered electron pulse resolution, which is defined by parameters of beam in the accelerator, and improvement of the signal/background separation, each of the eight stations of the system was

equipped with a detector based on a triple GEM with two-coordinate readout. The detectors allow coordinate measurement in the orbital plane with a resolution of ~ 0.1 mm. In the direction perpendicular to the orbital plane, the spatial resolution will be ~ 0.25 mm within ± 1 cm from the orbit and ~ 1 mm at a larger distance. We developed a special reading plane design with variable angle of the stereo strips. The size of the detectors is 125×100 mm to 250×100 mm, depending on the station type.

The KEDR detector was stopped in 2012 for repair, and GEM-based detectors were removed from the scattered electron detection system for a purpose of systematic study of their parameters on beam extracted from VEPP-4M. For these experiments, a system of 4 detectors was assembled. Its schematic is shown in Fig. 1.8.9.

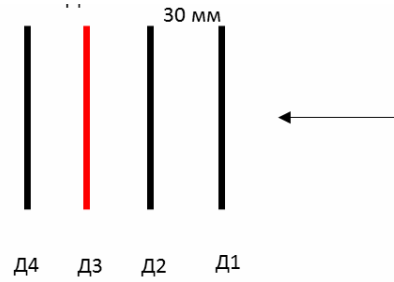


Fig. 1.8.9. System of the 4 GEM-based detectors installed on beam extracted from VEPP-4M.

There were installed four identical detectors with a spacing of 30 mm. Three of them were used for the tracking, while detector D3 was under investigation. About 200,000 events were collected on a 1 GeV electron beam. The main parameters studied on the extracted beam were the efficiency and spatial resolution in dependence on the gas gain.

Fig. 1.8.10 shows detector efficiency vs gas gain. It is seen that the efficiency reaches a plateau at a gain of about 20,000, and efficiency on the plateau is close to 98%.

Research into the inefficiency in $\sim 2\%$ has shown that the underlying cause is associated with the gaps between the segments of the GEM coating plates, where some events are lost. This is illustrated in Fig. 1.8.11, which shows coordinates of tracks in detector D2 that failed to be registered in test detector D3. It is evident that such tracks are concentrated along the vertical lines spaced by 10 channels (5 mm). There are two kinds of such lines, with a larger and a smaller number of lost events. Indeed, the gaps between the segments have a spacing of 10 mm on the top and bottom coatings, the gaps on the lower coatings shifted by 5 mm relative to the top ones. Therefore, an efficient step of inefficient areas in the detector should be 5 mm, as shown in Fig. 1.8.11. In addition, since ionization is differently lost on the top and bottom gaps, we should expect different values of inefficiency, which is also seen in Fig. 1.8.11. Efficiency in the spacing between the gaps was 99.1% at a gain of $\sim 20,000$.

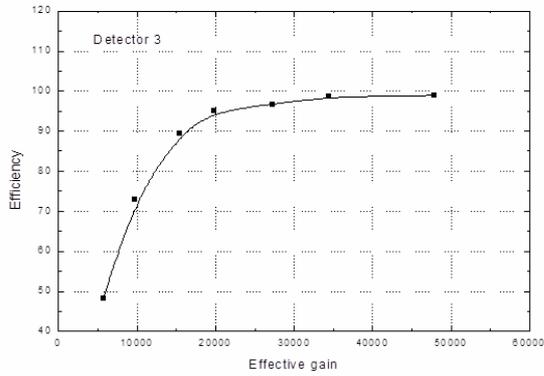


Fig. 1.8.10. Efficiency of GEM-based detector for the scattered electron detection system vs. gas gain.

The measured spatial resolution was ~ 57 microns. The result is shown in Fig. 1.8.12, which illustrates the distribution of differences between measured track coordinates and those calculated from three detectors. Multiplying the standard deviation of this distribution, 70 microns, by ~ 1.22 , one can obtain the resolution of one detector.

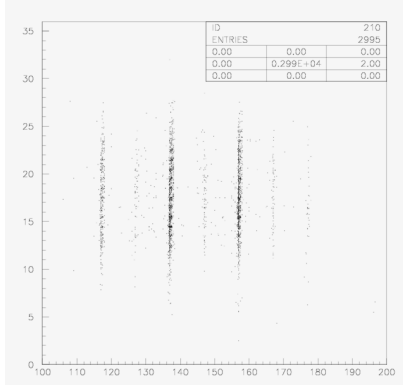


Fig. 1.8.11. Two-dimensional distribution of coordinates of tracks in detector D2 that fail to be recorded in detector D3.

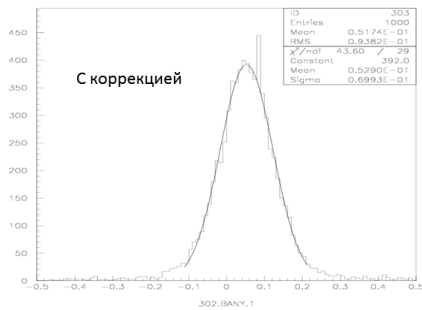


Fig. 1.8.12. Distribution of differences between measured track coordinates and those calculated from readings of the three detectors. The standard deviation of this distribution, 70 μm , should be multiplied by ~ 1.22 (square root of $3/2$), because the track detectors were identical to that under study.

1.8.3. Participation in collaborations.

The BINP group for micro-pattern gas detectors participates in the CERN international collaboration RD51 for development micro-pattern gas detectors. RD51 was formed in 2008. In 2012, the group continued its participation in this collaboration.

In 2012, members of the BINP group for micro-pattern gas detectors continued their participation in developing a TPC for the International Linear Collider (ILC). Currently, a cascaded GEM is seen as the most likely candidate for the end tracker of the TPC.

The works on cryogenic avalanche detectors were supported by the following grants: in 2009-2012, the federal target program "Scientific and scientific-pedagogical personnel of innovative Russia" 2009-2013 (Ministry of Education and Science contracts P682 and P980); in 2011-2013, RF Government Grant 11.G34.31.0047.

1.9. BELLE EXPERIMENT

1.9.1. Main results.

- The main activity of this working group is cooperation in the field of physics of elementary particles with the High Energy Accelerator Research Organization (KEK), Tsukuba, Japan, which is one of the largest and fastest growing HEP laboratories worldwide. In recent years KEK has been rapidly expanding its international cooperation to become an international centre in this field of physics. At the present time, one of the main experiments in Japan in the physics of elementary particles is the study of CP violation in B meson decays using the Belle detector on an electron-positron storage ring with very high luminosity (the so-called B factory).

BINP members have contributed a lot to the creation of the electromagnetic calorimeter of the Belle detector, including the designing, manufacture, assembling and adjustment of elements of this world's largest calorimeter based on cesium iodide monocrystals.

In 2010, the Belle detector was stopped for upgrade. The integral luminosity accumulated so far exceeds 1040 inverse femtobarn. These experimental data are being processed now. The detector and accelerator are being upgraded with the aim of increasing the luminosity of the facility and preparation of experiments for improvement of the accuracy of CP violation parameter measurement by an order of value and, possibly, observation of manifestation of physical phenomena beyond the Standard Model.

BINP members take an active part in the upgrade of the detector and processing of the acquired experimental data.

Below are given the main results of the year 2012.

- The unitarity triangle parameter φ_3 was measured by a model-independent method.
- Search for exotic X state decays into various modes with η_c participation ($\eta_c\pi^+\pi^-$, $\eta_c\omega$, $\eta_c\eta$, and $\eta_c\pi^0$) has started.
- The spin and P parity of the earlier discovered exotic $Z_b(10610)$ and $Z_b(10650)$ states have been determined.
- The relative probabilities of the decays $Y(5S)\rightarrow Y(1S)\eta$ and $Y(5S)\rightarrow Y(2S)\eta$ have been measured; the upper limit for the relative probability of the decay $Y(5S)\rightarrow Y(1S)\eta'$ has been determined.
- A reliable indication of the existence of the neutral exotic state $Z^0(10610)$ has been obtained.
- The Dalitz analysis of the decay $B\rightarrow D^*\omega\pi$ was performed. A procedure of signal reconstruction was carried out; the full decay width has been measured; estimates for parameters of the decay model have been obtained.
- The search for lepton flavor violation decays $\tau^-\rightarrow l^-hh'$, where $l = e, \mu$ and $h = \pi, K$, was completed.

- Measurement of the relative probabilities and mass spectra in τ^- decays involving the K_s^0 meson is close to completion.
- Measurement of the probability of the decay $\Lambda_c^+\rightarrow pK^-\pi^+$ by a model-independent method is underway.
- Measurement of neutral D meson mixing parameters is going on.
- A VME-standard shaper-digitizer module for the end part of the calorimeter of the Belle-II detector has been designed. An order for 100 modules has been placed.
- Software for various tests and inspection of shaper-digitizers has been developed.
- A stand for inspection of the counters of the cylindrical calorimeter has been built. All the counters and cables to them have been tested on this stand.
- A new version of the collector has been developed; its logic allows operation with high-speed data exchange.
- New mechanical and electrical specifications for the VME crate have been developed.
- Measurements of the radiation resistance of counters based on CsI crystals and made by the Institute for Scintillation Materials in Kharkov were carried out.

1.9.2. Data analysis.

Model-independent measurement of the unitarity triangle angle φ_3

Measurements of parameters of the so-called unitarity triangle in decays of B mesons are important for the search of processes that go beyond the Standard Model of low-energy electroweak interactions. Such research is the main point in the activity of B factories. Investigation into various decays of B mesons allows independent measurement of parameters of the triangle, effects of the New Physics manifesting themselves in mismatch of these measurements (e.g. the sum of the angles of the triangle may turn out to differ from 180°). The angle φ_3 , which manifests itself in decays of B meson into a neutral D meson and kaon, is among the most poorly measured parameters. The theoretical uncertainty in the measurement of this parameter is very small, and the current measurement accuracy is fully determined by the amount of decays $B\rightarrow D^0K$ available in experiments.

The most sensitive method of φ_3 measurement uses the decay $B^\pm\rightarrow D^0K^\pm$, where D^0 is reconstructed in the three-particle decay $D^0\rightarrow K_s\pi^+\pi^-$. In this case, parameters of the D^0 decay amplitude are different for the decays of B^+ and B^- (i.e. CP violation is observed). Fitting the event distribution over the phase space of the decay of D^0 into B^+ and B^- , one can measure the φ_3 parameter. It should be noted that the traditional analysis uses a model description of the D decay amplitude, which leads to an additional measurement error, which becomes comparable with the statistical accuracy. A group of BINP members has developed a modified method for φ_3 measurement in which the

phase volume of decay is divided into areas (bins), and the missing information on the amplitude is obtained from experiment on the study of quantum correlations of D mesons in the process $e^+e^- \rightarrow \psi(3770) \rightarrow DD$. A study of DD correlations was performed in 2010 in the CLEO experiment, and in 2012 a BINP group performed analysis of the data and published the first model-independent measurement of the ϕ_3 angle in *Physical Review D*. This analysis revealed CP violation with a statistical significance larger than 99% (see Fig. 1.9.1). The resulting $\phi_3 = [77 \pm 15(\text{stat}) \pm 4(\text{syst}) \pm 4(\text{CLEO})]^\circ$ is only slightly inferior to the model method in accuracy, but instead of a hard-to-interpret model error, which is estimated to be as high as 9° , it has a purely statistical additional uncertainty of 4° , which can be improved significantly in future.

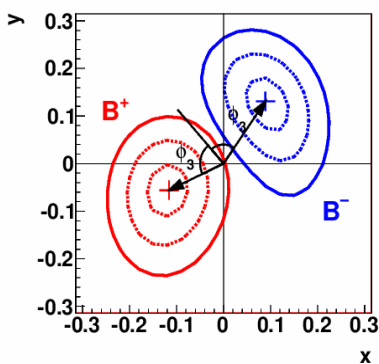


Fig. 1.9.1. Results of measurements of the (x,y) parameters of the amplitude D and the angle ϕ_3 from the decay $B \rightarrow DK$.

Search for X decays into modes with participation of η_c meson

The exotic state X(3872) was first discovered by the Belle collaboration in 2002 in exclusive decays $B^+ \rightarrow K^+ \pi^+ \pi^- J/\psi$. The mass of this state is close to the threshold $M(D^0) + M(\bar{D}^{*0})$, which led to a conjecture that X(3872) might be a $D^0 \bar{D}^{*0}$ molecule. So, it was suggested that there may be other similar particles which are also bound states of $D^{(*)}$ mesons. If these states exist, their quantum numbers differ from that of X(3872) and can be found in decays with participation of η_c meson. A group of BINP researchers were searching for decays of an exotic X-like state into various modes with participation of η_c : $\eta_c \pi^+ \pi^-$, $\eta_c \omega$, $\eta_c \eta$, and $\eta_c \pi^0$. An algorithm was developed for extraction of events of the decay $B^\pm \rightarrow K^\pm X$ with subsequent decay into the above-mentioned modes. On the basis of events of the signal modeling, optimal conditions for extraction were selected and detection efficiencies were determined for each of the four decays. For verification of correctness of the algorithm, a study of the test decay $B^\pm \rightarrow K^\pm \psi(2S) \rightarrow K^\pm (J/\psi \pi^+ \pi^-)$ was carried out. No signal has been detected so far in any of the studied X decay channels (see Fig. 1.9.2), and thus the upper limits for the corresponding products of branchings of X production and decay H were determined. The work is close to completion and will be published after discussion within the collaboration.

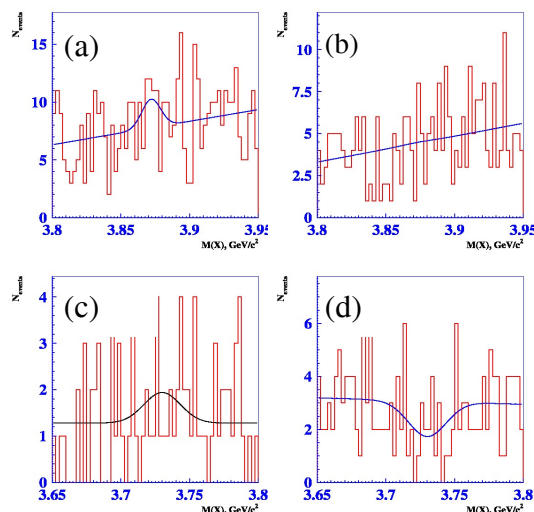


Fig. 1.9.2. Distributions of invariant masses of $\eta_c \pi^+ \pi^-$ (a), $\eta_c \omega$ (b), $\eta_c \eta$ (c) and $\eta_c \pi^0$ (d) in the corresponding decays $B^\pm \rightarrow K^\pm X$.

Study of the exotic states Z(10610) and Z(10650)

In 2010-2011, the BINP group in the Belle collaboration performed analysis of data on e^+e^- annihilation to final states of the form $Y(nS)\pi^+\pi^-$, where $n = 1, 2$, and 3. The most important result was the first observation of charged bottomonium-like states $Z_b(10610)$ and $Z_b(10650)$. The analysis, however, used a simplifying assumption that contributions in which pions are in an S wave are dominant in the observed transitions $Y(5S) \rightarrow Y(nS)\pi^+\pi^-$. Further development of the amplitude analysis method allowed the BINP group to do without the simplifying assumptions and carry out full amplitude analysis of six-dimensional phase space.

The analysis involves completely reconstructed events of $Y(5S) \rightarrow Y(nS)\pi^+\pi^-$, where $Y(nS)$ is reconstructed in the channel of the decay $Y(nS) \rightarrow \mu^+\mu^-$. For suppression of the background, the KLM system of the Belle detector should identify muons reliably. Fig. 1.9.3. presents two-dimensional $M^2(Y(nS)\pi)_{\text{max}}$ distributions vs. $M^2(\pi^+\pi^-)$ for background and signal events in the decay $Y(5S) \rightarrow Y(nS)\pi^+\pi^-$.

A substantial contribution to the background of the processes under study are events $Y(5S) \rightarrow \mu^+\mu^-\gamma$, in which the photon is then converted into an e^+e^- pair. In view of the smallness of pulses of the tracks, the electron identification with the Belle detector has low efficiency in this case. Such events however can be easily dropped with the requirement $M(\pi^+\pi^-) > 0.4 \text{ GeV}/c^2$. The distribution of background events for the remaining part of the phase space is well approximated with a smooth polynomial function. One-dimensional distributions by two-particle invariant masses are shown in Fig. 1.9.4.

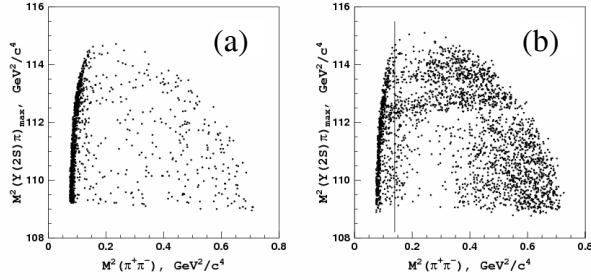


Fig. 1.9.3. Dalitz distribution for background events (a) and events from the signal area (b) for the decay $Y(5S) \rightarrow Y(2S)\pi^+\pi^-$.

The distribution of signal events over the phase space for all the three final states is parametrized by the following general model:

$$A_\pi = A_{Z1} + A_{Z2} + A_{f_0} + A_{f_2} + A_{NR},$$

where A_{Z1} and A_{Z2} are the amplitudes of the $Y(5S)$ decay with appearance of intermediate Z states; A_{f_0} and A_{f_2} are the amplitudes of the decays $Y(5S) \rightarrow Y(nS)f_0(980)$ and $Y(5S) \rightarrow Y(nS)f_2(1270)$, respectively; A_{NR} is the non-resonant decay amplitude. In the course of approximation of the experimental data with a combination of signal and background distributions, the relative phases and contributions of individual quasi-two-particle amplitudes are determined, as well as the masses and widths of the Z_b states. Each final state is fitted in four different model versions corresponding to the quantum numbers of Z_b resonances: $J^P = 1^+, 1^-, 2^+$ and 2^- (the 0^- and 0^+ combinations are forbidden).

The most important result of this work was the determination of the spin and P parity of previously discovered exotic states $Z_b(10610)$ and $Z_b(10650)$ directly from the data. The best description of the observed distributions of signal events over the phase space was obtained with the $J^P = 1^+$ model. Because of decays of the $Y(5S) \rightarrow Y(nS)\pi^+\pi^-$ form, Z_b cannot be classified as two-quark systems. So, there must be four quarks at least. The authors of this work have suggested considering the new states as a weakly coupled system of B and B^* mesons for the state $Z_b(10610)$ and a system of B^*B^* mesons in for the state $Z_b(10650)$. Being in good agreement with all the known properties of Z_b states, this model also predicts new characteristics, some of which can be verified with the statistics already accumulated. The results of the work were published in *Physical Review Letters*.

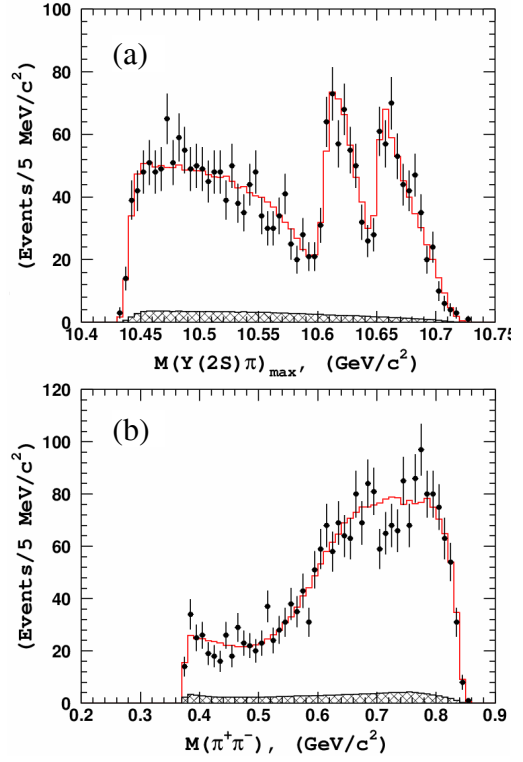


Fig. 1.9.4. Invariant mass distribution of the $Y(2S)\pi^\pm$ (a) and $\pi^+\pi^-$ (b) systems for events from the signal area for the decay $Y(5S) \rightarrow Y(2S)\pi^+\pi^-$. Points: experimental data; histogram: result of the fit; crosshatched histogram: predicted level of background events.

Study of the $Y(5S) \rightarrow Y(1,2S)\eta$ decays

Transitions between bottomonia with η meson are poorly described theoretically. In particular, the measured width of the transition $Y(4S) \rightarrow Y(1S)\eta$ is two orders higher than the estimated one. So, measurement of the probabilities of the $Y(5S) \rightarrow Y(1,2S)\eta$ decays is of undoubted scientific interest. Record statistics of 120 fb^{-1} were collected for e^+e^- annihilation at the $Y(5S)$ resonance energy in the Belle experiment.

Completely reconstructed $Y(5S) \rightarrow Y(nS)\eta$ events are used in the analysis; $Y(nS)$ is reconstructed in the $Y(1,2S) \rightarrow \mu^+\mu^-$ and $Y(2S) \rightarrow Y(1S)\pi^+\pi^-$ decay channel. The η meson is reconstructed in the final $\gamma\gamma$ and $\pi^+\pi^-\pi^0$ states. Suppression of background requires reliable identification of muons with the KLM system of the Belle detector. The signal is extracted using the distribution by the difference between the total energy of a candidate and the collision energy in the center-of-mass system. The distributions by the invariant mass of candidates for η mesons are also used. The corresponding distributions are shown in Fig.1.9.5.

As a result, the following decay probabilities were measured:

$$\begin{aligned} \text{Br}[Y(5S) \rightarrow Y(1S)\eta] &= (7,3 \pm 1,6 \pm 0,8) \cdot 10^{-4}, \\ \text{Br}[Y(5S) \rightarrow Y(2S)\eta] &= (38 \pm 4 \pm 5) \cdot 10^{-4}, \text{ and} \\ \text{Br}[Y(5S) \rightarrow Y(1S)\eta'] &< 1,2 \cdot 10^{-4} \text{ (90\% CL)}. \end{aligned}$$

These results were presented at international scientific conferences and are being prepared for publications in a peer-reviewed journal.

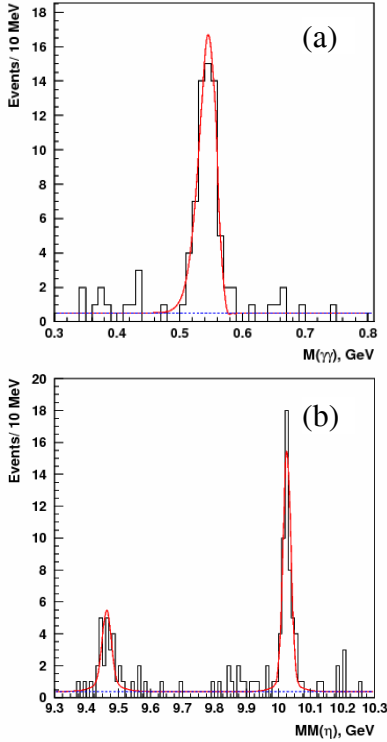


Fig. 1.9.5: (a) $\eta \rightarrow \pi^+\pi^0$ candidate missing mass distribution. (b) $\eta \rightarrow \gamma\gamma$ candidate invariant mass distribution. Histogram: data; solid curves: result of approximation; dotted lines: contribution of background events.

Discovery of the exotic state $Z^0(10650)$

In 2011, in the course of analysis of $Y(5S) \rightarrow Y(nS)\pi^+\pi^-$ decays, BINP members discovered two exotic charged states: $Z^+(10610)$ and $Z^+(10650)$, which decay into $Y(nS)\pi^+$. A model was proposed that describes the new states as a bound system of BB^* и B^*B^* mesons for $Z(10610)$ and $Z(10650)$, respectively. This model describes well the observed properties of the Z states.

To verify this model, BINP members carried out a search for and amplitude analysis of the $Y(5S) \rightarrow Y(nS)\pi^0\pi^0$ decays. $Y(nS)$ is reconstructed in the $Y(1,2S) \rightarrow \mu^+\mu^-, e^+e^-$ and $Y(2S) \rightarrow Y(1S)\pi^+\pi^-$ decay channel. The π^0 mesons are reconstructed from a pair of photons. Muons are identified with the KLM system of the Belle detector; photons are reconstructed and electrons are identified using an electromagnetic calorimeter. Events that meet the energy-momentum conservation laws are selected. The quantity of signal events is determined from fitting of missing mass distribution to two π^0 (see Fig.1.9.6).

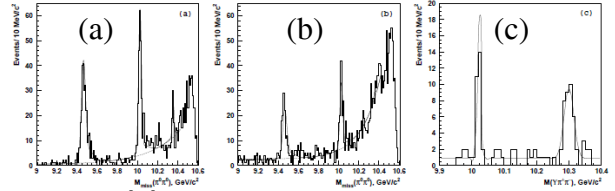


Fig. 1.9.6: $\pi^0\pi^0$ system missing mass distributions for $Y(nS)\pi^0\pi^0$ candidates, (a) $Y(nS) \rightarrow \mu^+\mu^-$, (b) $Y(nS) \rightarrow e^+e^-$. (c) $Y(1S)\pi^+\pi^-$ invariant mass distribution. Histograms: experimental data; solid curves: result of approximation; dotted lines: contribution of background events.

Thus the following decay probabilities were measured: $\text{Br}[Y(5S) \rightarrow Y(1S)\pi^0\pi^0] = (2,25 \pm 0,11 \pm 0,20) 10^{-3}$ and $\text{Br}[Y(5S) \rightarrow Y(2S)\pi^0\pi^0] = (3,66 \pm 0,22 \pm 0,48) 10^{-3}$.

Search for possible intermediate states was performed via amplitude analysis of the three-particle states of $Y(nS)\pi^0\pi^0$. For both final states, distribution of events over the Dalitz plot is described by the following general model:

$$A = A_{Z1} + A_{Z2} + A_{f0} + A_{f2} + A_{NR},$$

where A_{Z1} and A_{Z2} are the amplitudes of the $Y(5S)$ decay with formation of intermediate Z states; A_{f0} and A_{f2} are the amplitudes of the $Y(5S) \rightarrow Y(nS)f_0(980)$ и $Y(5S) \rightarrow Y(nS)f_2(1270)$ decays, respectively; A_{NR} is the amplitude of non-resonant decay. In the course of approximation of experimental data with a combination of signal and background distributions, the relative phases and contributions of individual quasi-two-particle amplitudes are determined. The masses and widths of the Z states are fixed at the $Z^+(10610)$ and $Z^+(10650)$ values. Possible model and systematic errors were studied. As a result, in the $Y(2S)\pi^0\pi^0$ final state, a reliable indication of the existence of neutral exotic state $Z^0(10610)$ was obtained. The $Z^0(10650)$ signal was found to be statistically insignificant because of scanty available statistics, about 10 times less than in $Y(nS)\pi^+\pi^-$, which, however, does not contradict its existence. Fig.1.9.7 shows $Y(2S)\pi^0$ invariant mass projections. The results obtained were reported at an international scientific conference and published in [arXiv:1207.4345](https://arxiv.org/abs/1207.4345). A publication in a peer-reviewed journal is being prepared.

Dalitz analysis of the $B \rightarrow D^*\omega\pi$ decay

BINP researchers have performed the Dalitz analysis of the $B \rightarrow D^*\omega\pi$ decay, which is interesting from the point of view of both D^{**} spectroscopy and study of the dynamics of production of light $\omega\pi$ states. Study of the properties of orbitally excited states of D mesons (the so-called D^{**}) allows verification of the heavy quark effective theory (HQET) and QCD sum rules. Currently, there are some discrepancies between the theory and experiments in decays of B mesons into D^{**} states. In addition to intermediate D^{**} states, there are produced light $\omega\pi$ resonances in this decay mode. The virtual $\rho(770)$ and its excitations $\rho(1450)$ and $\rho(1700)$ are of particular interest. In this mode, the $\rho(1450)$ state was observed in B meson de-

cays only once, by the CLEO collaboration, however, with no account of the contribution of the virtual $\rho(770)$. No $\rho(1700)$ state was observed in B meson decays at all. Thus, both D^{**} and light $\omega\pi$ resonances are taken into account in the full signal amplitude of the decay.

At this stage, a parametrization of the matrix element for the $B \rightarrow D^* \omega \pi$ decay was proposed; the angular distributions of the final particles of the decay were investigated. The results of this study have been published in *Journal of High Energy Physics*. In addition, the signal reconstruction procedure was completed; the total decay width has been measured; estimates of parameters of the decay model were obtained. For extraction of the signal model parameters, an unbinned fitting to experimental data has been performed. Fig. 1.9.8. presents the results of the fitting for the invariant masses of the $D^* \pi$ pair and the $\omega \pi$ pair. This work is close to completion, and will be published after discussion within the collaboration.

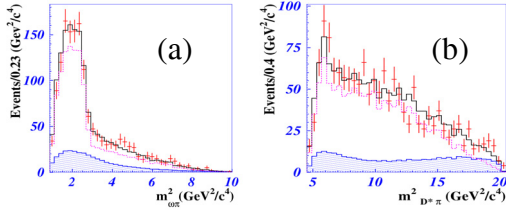


Fig. 1.9.8. Results of signal area fitting in the Dalitz plot. (a) $D^* \pi$ mass distribution, (b) $\omega \pi$ mass distribution. Dots: experimental data; shadowed histogram: background contribution to the signal area; dotted histogram: signal component of the fitting; black histogram: complete result of the fitting.

Studies of τ -lepton decays

The search for $\tau^- \rightarrow l^- hh'$ decays violating the lepton flavor was completed. Here $l = e, \mu$ and $h = \pi, K$ (in total, 14 different decay modes). This analysis was carried out with statistics corresponding to 854 fb^{-1} , or 782×10^6 pairs of τ -leptons produced. In all but two modes, the desired signal does not exceed the predicted background, which allows setting upper limits for the relative probabilities of corresponding decays – $B(\tau^- \rightarrow e^- hh') < (2,0 - 3,7) \times 10^{-8}$, $B(\tau^- \rightarrow \mu^- hh') < (2,1 - 8,6) \times 10^{-8}$ – at a 90% confidence level. These limits are 1.8 times higher than the previous results of Belle and more powerful than those obtained by BaBar. This improvement was achieved due to larger statistics, stronger suppression of background processes and more efficient selection of events. The results are shown in Table (1.9).1. Preliminary results of this work have been published in *Nuclear Physics B*. The final results have been presented in *Nuclear Physics B*.

The measurement of relative probabilities of decays and mass spectra in τ^- decays involving the K_S^0 meson is close to completion. In this case, the analysis used statistics corresponding to 669 fb^{-1} , or 616×10^6 pairs of τ -leptons produced. As a result, on the basis of the effec-

tiveness matrix, the relative probabilities of the inclusive $\tau^- \rightarrow K_S^0 X \nu_\tau$ decay and six exclusive decays – $\tau^- \rightarrow K_S^0 \pi^- \nu_\tau$, $\tau^- \rightarrow K_S^0 K^- \nu_\tau$, $\tau^- \rightarrow \pi^0 K_S^0 \pi^- \nu_\tau$, $\tau^- \rightarrow \pi^0 K_S^0 K^- \nu_\tau$, $\tau^- \rightarrow K_S^0 K^0 \pi^- \nu_\tau$, and $\tau^- \rightarrow K_S^0 K^0 \pi^0 \pi^- \nu_\tau$ – were determined. Finally, with the use of the procedure of elimination of detector effects, the invariant mass spectra for the $\tau^- \rightarrow \pi^0 K_S^0 \pi^- \nu_\tau$ and $\tau^- \rightarrow \pi^0 K_S^0 K^- \nu_\tau$ decays were found (see Fig. (1.9).9). Preliminary results of this work can be found in *Nuclear Physics B*. The final results will also be published in the very near future.

Table 1.9.1. Upper limits for each of the modes studied. The table presents the signal efficiency (ϵ), number of expected background events (N_{BG}), total systematic uncertainty (σ_{syst}), number of events observed in the signal area (N_{obs}), upper limit at a 90 % confidence level for the number of signal events including systematic uncertainties (S_{90}) and upper limit at a 90% confidence level for the relative probabilities of decays (B) for each decay mode.

Decay mode	ϵ (%)	N_{BG}	σ_{syst} (%)	N_{obs}	S_{90}	B (10^{-8})
$\tau^- \rightarrow \mu^- \pi^+ \pi^-$	5,83	$0,63 \pm 0,23$	5,7	0	1,87	2,1
$\tau^- \rightarrow \mu^+ \pi^- \pi^-$	6,55	$0,33 \pm 0,16$	5,6	1	4,01	3,9
$\tau^- \rightarrow e^- \pi^+ \pi^-$	5,45	$0,55 \pm 0,23$	5,7	0	1,94	2,3
$\tau^- \rightarrow e^+ \pi^- \pi^-$	6,56	$0,37 \pm 0,19$	5,5	0	2,10	2,0
$\tau^- \rightarrow \mu^- K^+ K^-$	2,85	$0,51 \pm 0,19$	6,1	0	1,97	4,4
$\tau^- \rightarrow \mu^+ K^- K^-$	2,98	$0,25 \pm 0,13$	6,2	0	2,21	4,7
$\tau^- \rightarrow e^- K^+ K^-$	4,29	$0,17 \pm 0,10$	6,7	0	2,29	3,4
$\tau^- \rightarrow e^+ K^- K^-$	4,64	$0,06 \pm 0,06$	6,5	0	2,39	3,3
$\tau^- \rightarrow \mu^- \pi^+ K^-$	2,72	$0,72 \pm 0,28$	6,2	1	3,65	8,6
$\tau^- \rightarrow e^- \pi^+ K^-$	3,97	$0,18 \pm 0,13$	6,4	0	2,27	3,7
$\tau^- \rightarrow \mu^- K^+ \pi^-$	2,62	$0,64 \pm 0,23$	5,7	0	1,86	4,5
$\tau^- \rightarrow e^- K^+ \pi^-$	4,07	$0,55 \pm 0,31$	6,2	0	1,97	3,1
$\tau^- \rightarrow \mu^+ K^- \pi^-$	2,55	$0,56 \pm 0,21$	6,1	0	1,93	4,8
$\tau^- \rightarrow e^+ K^- \pi^-$	4,00	$0,46 \pm 0,21$	6,2	0	2,03	3,2

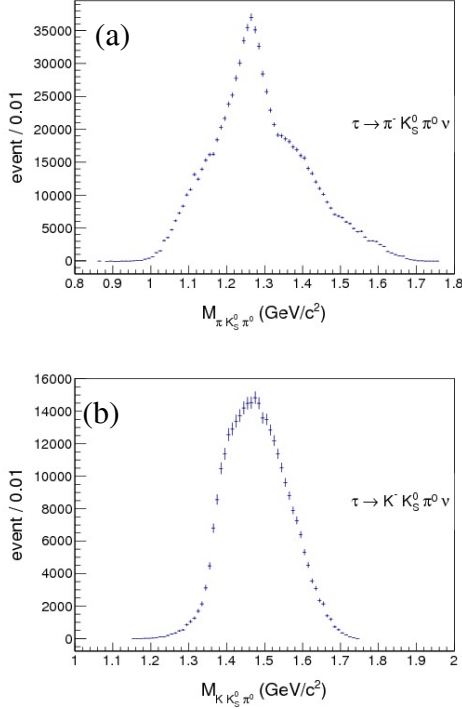


Fig. 1.9.9. $\pi^0 K_S^0 \pi^-$ (a) and $\pi^0 K_S^0 K^-$ (b) invariant mass spectra in τ -lepton decays.

Model-independent measurement of the relative probability of the $\Lambda_c^+ \rightarrow p K^- \pi^+$ decay

The absolute value of the relative probability of the $\Lambda_c^+ \rightarrow p K^- \pi^+$ decay is an important factor for the theory of physics of heavy quarks because the probabilities of most other Λ_c^+ baryon decays were experimentally measured relative to this mode. The absolute probability of the $\Lambda_c^+ \rightarrow p K^- \pi^+$ decay (5.0 ± 1.3)% has a large uncertainty (26%), mainly because of the dependence of the measurements on theoretical models. BINP members have developed a model-independent method of measurement of the probability of the $\Lambda_c^+ \rightarrow p K^- \pi^+$ decay. This method is based on the following two ways of extraction of exclusive $e^+e^- \rightarrow \Lambda_c^+ \bar{p} \bar{D}^0$ and $\Lambda_c^+ \bar{p} \pi^+ D^{(*)-}$ processes: (1) reconstruction of Λ_c^+ in the recoil mass (Fig. 1.9.10 (a)) and (2) full reconstruction of the desired process with Λ_c^+ detection in the invariant mass of $p K^- \pi^+$ from a peak at a zero in the recoil energy (Fig. 1.9.10 (b)). The ratio of signal events in (2) to those in (1) gives the desired result with an error of about 10% (with due account of systematic uncertainties). This work is close to completion and will be published after discussion within the collaboration.

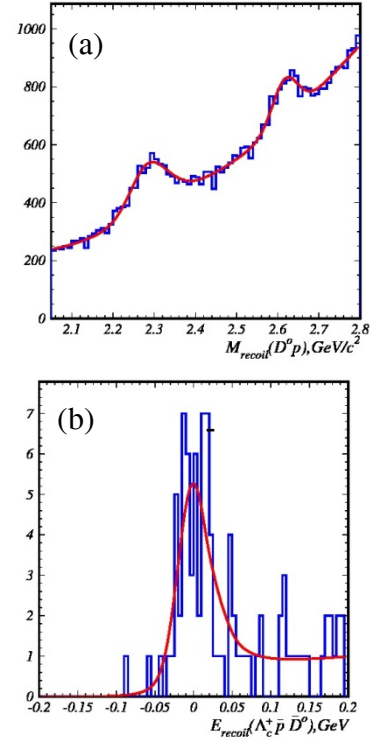


Fig. 1.9.10. (a) Recoil mass ($D^0 p$) in GeV/c^2 for the $e^+e^- \rightarrow \Lambda_c^+ \bar{p} \bar{D}^0$, $\bar{D}^0 \rightarrow K^+ \pi^-$ process. (b) Recoil energy ($\Lambda_c^+ \bar{p} D^0$) in GeV for the $e^+e^- \rightarrow \Lambda_c^+ \bar{p} D^0$, $\Lambda_c^+ \rightarrow p K^- \pi^+$ process.

Model-independent measurement of D meson mixing

The measurement of parameters of neutral D meson mixing is going on. Parameters of mixing and characteristics of CP symmetry violation in the mixing are obtained via a model-independent approach proposed by the authors in *Phys. Rev. D* 82, 034033 (2010). This method uses the three-particle final state, being, however, independent of the model of D meson decay into this state and thus allowing getting rid of the model error. Parameters of the mixing are very important for charmed quark physics. Measurement of parameters of CP violation in the mixing will provide validation of the Standard Model, for these parameters are tantalizingly constrained in it. In addition, precise measurement of parameters of the mixing will reduce the theoretical uncertainty in other dimensions, in particular, in the measurement of the unitarity triangle angle γ . The distribution of kinematic parameters for signal and background events has been studied; the strategy of extraction of parameters of the mixing from the time distribution of D meson decay is being refined (see Fig. 1.9.11). Preliminary results are expected next year.

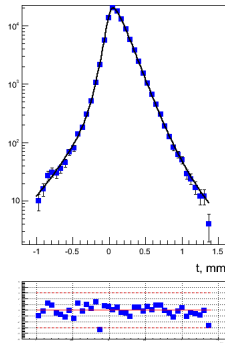


Fig. 1.9.11. Example of time distribution for D meson decay. This distribution is sensitive to parameters of D meson mixing.

1.9.3. Upgrade of the detector

The upgrade of the detector (Belle II) and the collider is underway. The goal is to increase the facility luminosity up to $8 \times 10^{35} \text{ cm}^{-2} \text{ s}^{-1}$. The new experiment will allow measuring all the angles of the unitarity triangle with accuracy of up to a few percent, and perhaps going beyond the Standard Model. Besides the study of the CP violation mechanism, the huge amount of data obtained in this experiment will yield new results on the physics of decays of B and D mesons and τ -lepton.

The increase in the luminosity and background load on collider imposes new requirements on the detector systems. The calorimeter also needs an upgrade. A BINP group engaged in the development of methods for upgrade of the calorimetric system of the detector has developed and proposed a relevant scheme.

The electronics of the cylindrical part of the calorimeter is assumed to be replaced with a new one, which will ensure continuous digitization of signals from counters and subsequent fitting with a response of a known shape. Such a procedure would allow determining both the energy of signal and the time of arrival. Use of the time information will enable manifold suppression of occurrence of false clusters.

For the end part, where the background conditions are the most strict, first the electronics will be upgraded, and then the scintillation CsI(Tl) crystals will be replaced with pure CsI crystals, which have shorter decay time. This will improve 30 times the time resolution of the counters and, subject to the fitting of the signal shape, ensure over 150-fold suppression of background.

In 2012, BINP completed the development of a VME-standard shaper-digitizer and placed an order for 100 such modules (see Fig. 1.9.12). This module is the basic unit of the new electronics system. It is used for shaping signals from counters, digitizing of the signal shape every $0.5 \mu\text{s}$ and subsequent digital processing with reconstruction of the amplitude and time of arrival of signal. In addition, the module generates a fast analog signal for use in the neutral trigger system. Testing of the modules proved their functionality and compliance of measured param-

eters with the expected ones. In 2012, an order for mass production of shaper-digitizer modules was placed. 100 such boards will be made by April 2013.



Fig. 1.9.12. Electronic module of the 16-channel VME-standard shaper-digitizer.

- For check of the efficiency of the modules produced and measurement of their parameters, a stand was built (see Fig. 1.9.13). The stand allows checking 16-channel shaper-amplifiers, amplitude-to-digital converters, programmable logic integrated circuits, and fast trigger signal shapers. The inputs of a module to measure are connected to 16 preamps, and information is read into the computer via units of the collector. A trigger signal is delivered to the unit of fast digitizing of trigger information (FAM), developed by our colleagues from Hanyang University (Korea). Software for the following tests was developed:
 - check of operation of all ADC bits;
 - check of the programmable logic integrated circuit;
 - identification of signal shape in 16 spectrometer channels and retrieving of parameters of a function that describes this shape;
 - identification of the shape of fast trigger channel and retrieving of parameters of a function that describes this shape;
 - measurement of coherent and incoherent noise;
 - measurement of the conversion factor and nonlinearity of the spectrometric channel and the trigger ones;
 - serviceability testing and measurement of the range of adjustment of attenuators of the trigger channel.

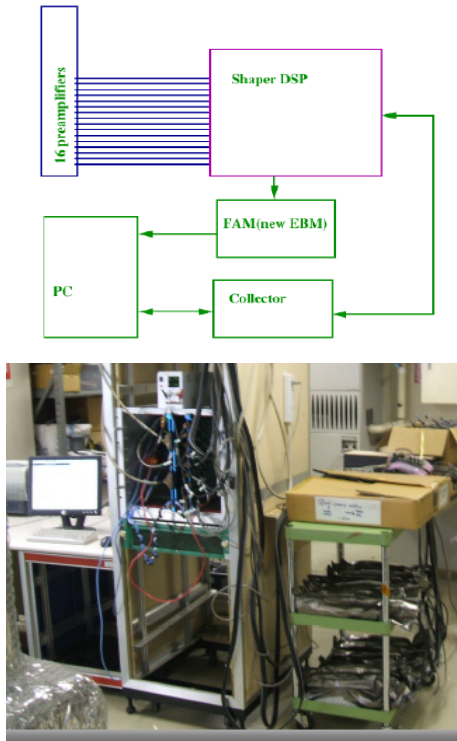


Fig. 1.9.13. Scheme and appearance of the stand for testing of modules of the shaper-digitizers.

Checking one module takes about twenty minutes, after which a graphical representation of the measured data is output (see Fig. 1.9.14), as well as a list of parameters that failed to meet the specifications.

Based on 12 modules, a stand was created for checking the counters of the cylindrical calorimeter (see Fig.1.9.15). The stand allows measuring 184 counters of the calorimeter. We measured the noise level, response to calibration signal and position of a peak corresponding to the maximum possible energy release of minimum ionizing cosmic particles. Sequentially switching the stand to the 36 stations of the cylindrical calorimeter over a period of three months, we have tested all the counters. As a result, 10 damaged cables were revealed. The cables were repaired. All the counters turned out to be serviceable. Measurement results are shown in Fig. 1.9.16.

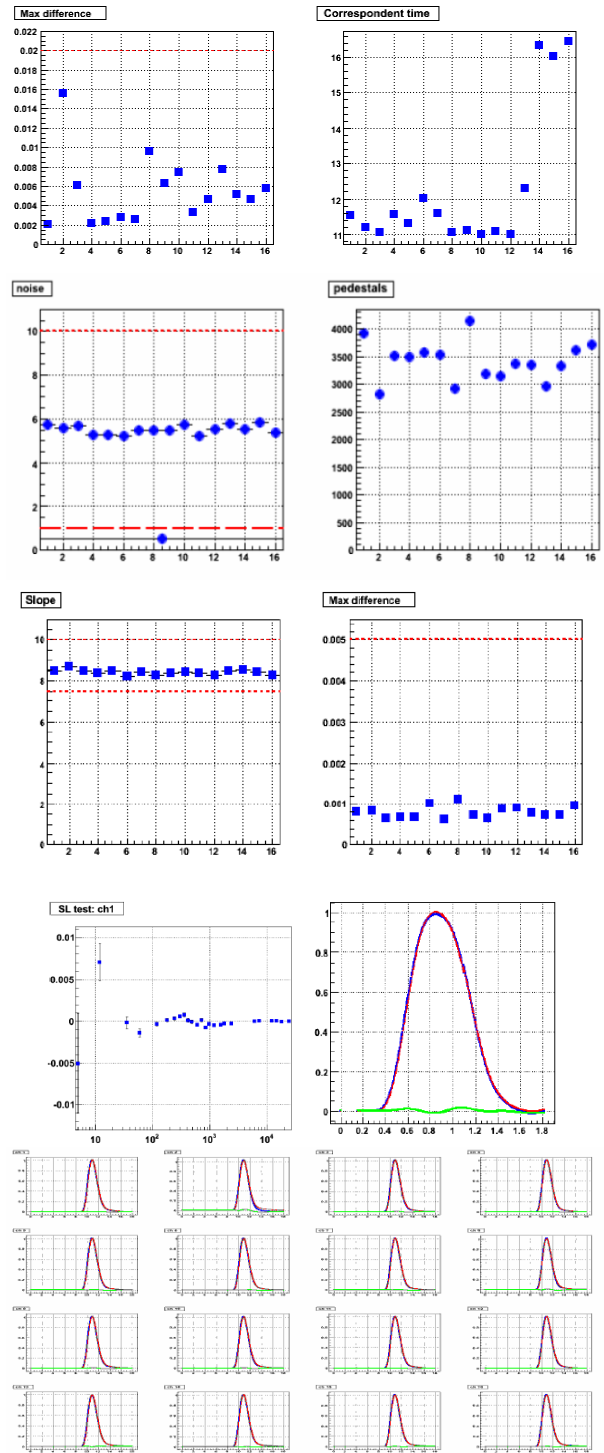


Fig.1.9.14. Example of graphical representation of information from the stand for testing shaper-digitizer modules.

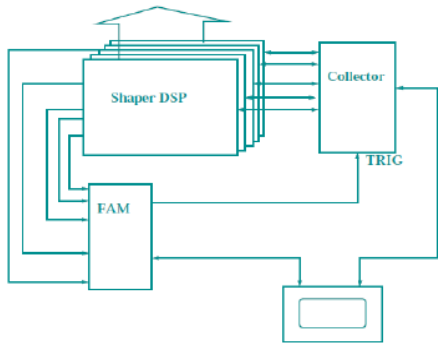


Fig.1.9.15. Scheme and appearance of the stand for testing of the counters of the cylindrical calorimeter.

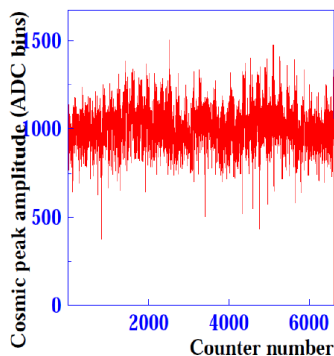
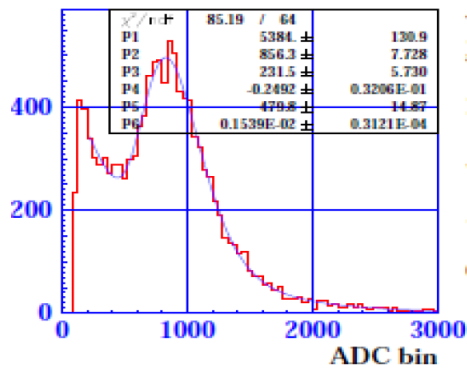


Fig. 1.9.16. Energy release spectrum of minimum ionizing particles (above). Position of the peak of the spectrum in dependence on the counter number (below).

Besides the designing of the shaper-digitizer module, a team of BINP experts in electronics has developed a new version of the collector module with logic allowing work

with high-speed (gigabits per second) data exchange. The new module has been fabricated and is under testing now.

BINP members have developed mechanical and electrical specifications for the new VME crate (see Fig.1.9.17) for operation of 12 shaper-digitizer modules with no increase in noise. One crate has been manufactured and tested. Measurements performed with this crate have made a basis for improvements in the design. An order for mass production of such crates is being prepared now.



Fig. 1.9.17. Appearance of the VME crate for calorimetry electronics.

The next stage of the upgrade will be the placement of pure CsI crystals on the end part of the calorimeter. The crystals may be supplied by Kharkov Institute of Scintillation Materials. In 2011, an order for an experimental batch of 50 crystals was made. 15 crystals from this batch were passed to BINP, where the radiation resistance of counters on their basis was measured

A scheme of the irradiation setup is shown in Fig.1.9.18 (a). The crystals were irradiated with bremsstrahlung photons produced on a lead converter by 1.4 MeV electron beam from the first industrial accelerator ELV-6, built and working at BINP. The average photon energy was about 0.4 MeV (see Fig.1.9.18 (b)). Crystals irradiated with such photons from both sides, the dose heterogeneity does not exceed 20%. The absorbed dose was measured with a counter on a small ($2 \times 2 \times 1$ cm) CsI (Tl) crystal.

The total dose to be received by the counters during the operation of the detector is expected to be about 10 krad.

A few irradiation series with a dose of 0.3, 1, 3, and 10 krad were carried out. Fig. 1.9.19 shows the distribution of light yield decrease at different doses and correlation of light yield decrease for the maximum and minimum doses. For most crystals, the light yield decrease is 20% or less, which is acceptable for calorimeter operation. For three of the counters, the light yield decrease was about 30%. Information on radiation resistance will be used for improvement of the technology for crystal growth. Due to the correlation of the light yield decrease for high and low

doses, crystals may be rejected by results of irradiation with a dose of 300 rads.

100 shaper-digitizer modules are to be tested and 330 such units are to be produced in 2013. There are plans to complete the development and proceed to mass production of the modules of the collector. In addition, it is necessary to dismount and upgrade the preamplifiers of the end cap calorimeter and inspect its counters.

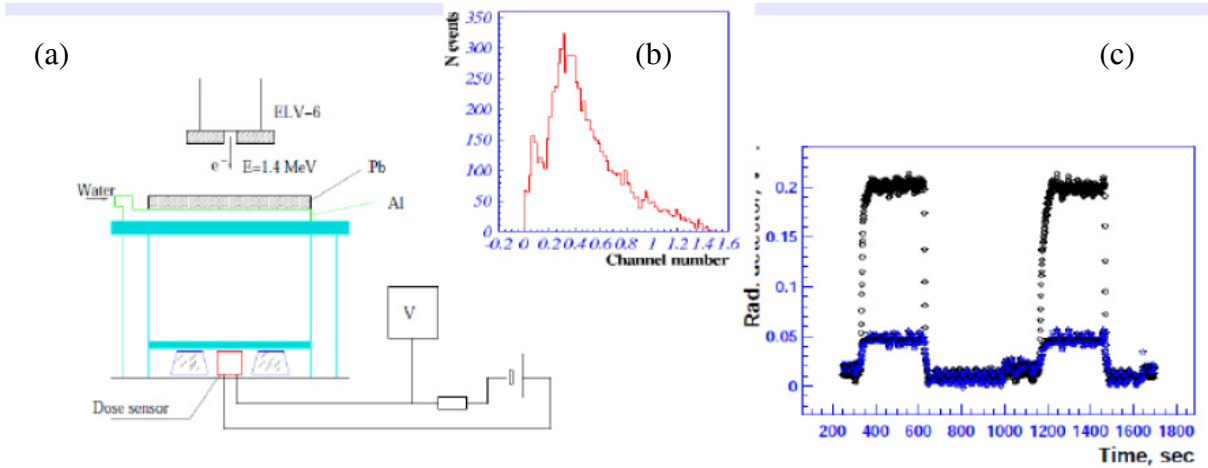


Fig. 1.9.18. (a) Experimental setup for irradiation of crystals. (b) Spectrum of photons after the converter. (c) Signal from irradiation dose counter.

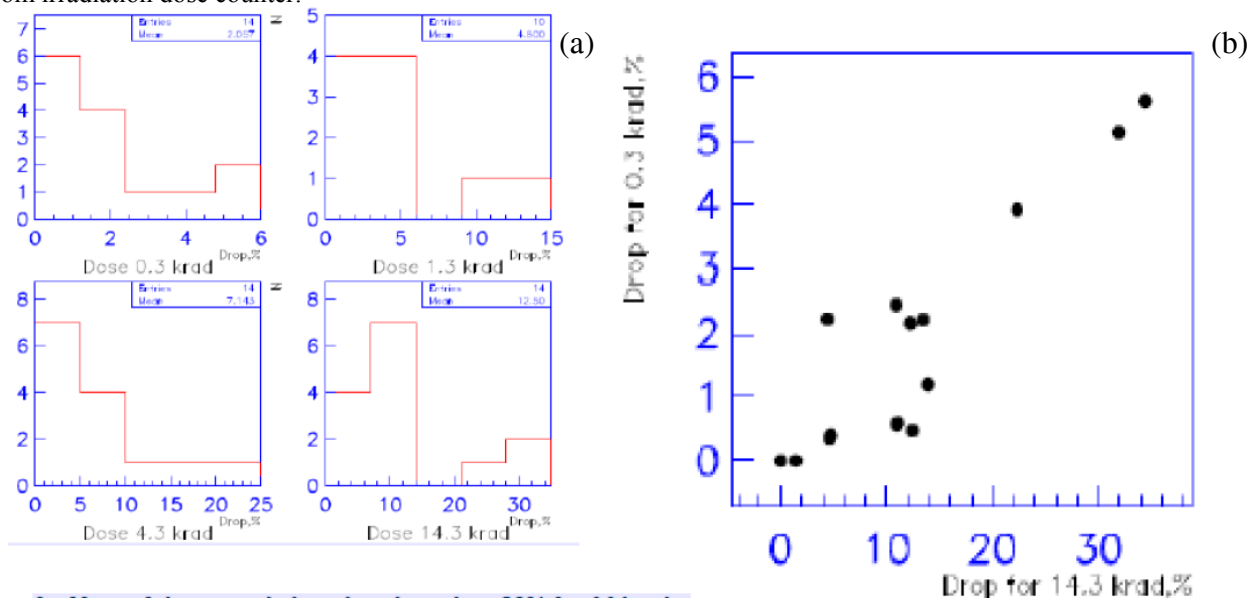


Fig. 1.9.19(a) Light yield decrease at different irradiation doses. (b) Correlation of light yield decrease at high and low doses.

1.10. BABAR EXPERIMENT

Experiments with the BABAR detector were conducted on the e^+e^- collider PEP-II at SLAC (USA) from 1999 to 2008. Data collected in the experiment are being processed now. The BABAR collaboration consists of about 300 physicists, representing 72 institutions of 12 countries, BINP members among them. In 2012, the collaboration published 32 articles (30 papers in 2011). The total number of publications is 504.

The main objectives of the BABAR experiment are the research on CP violation in decays of B mesons, precise measurement of decays of B and D mesons and τ leptons and search for their rare decays. Though the detector and collider have been optimized for research on CP asymmetry, the potential of investigation into other processes was not reduced.

BINP participants of the collaboration are engaged in the analysis of measurements of the V_{ub} element of the CKM matrix, measurements of the cross sections of the e^+e^- annihilation into hadrons by the radiative return method and research on two-photon processes with registration of scattered electrons.

The radiative return method was developed by BINP members. It consists in the registration of processes with hard photon emission from initial particles and the residual energy thus being spent on production of hadrons at lower energies, to the production threshold. This allows one to study the exclusive processes of e^+e^- annihilation into hadrons in the hadron mass range from the threshold to 6.5 GeV/c^2 .

Analysis of the $e^+e^- \rightarrow p \bar{p}$ process from the complete statistic (about 500 fb^{-1}) that was acquired in the BABAR experiment was completed in 2012. The analysis was performed by the radiative return method. The cross section was measured from the reaction threshold to 4.5 GeV. Below 3 GeV, this is today's most accurate measurement. The effective electromagnetic form factor of proton was derived from the measured cross section. The measured dependence of the form factor on the invariant mass of the $p \bar{p}$ pair is shown Fig.1.10.1 in comparison with data of previous experiments. The form factor growth near the threshold of the reaction, which was discovered earlier in the experiment PS170 at the facility LEAR (CERN), was confirmed. At higher energies, the energy behavior of the form factor is complicated. In three areas – near 2.2 GeV, 2.55 GeV, and 3 GeV – there was revealed a stepwise decrease in the form factor and cross section with energy growth. No theoretical explanation to such behavior has been found yet.

In the analysis of the angular distribution of proton, the ratio of the electric and magnetic form factors was measured. The dependence of the forms factors on the invariant mass of the $p \bar{p}$ pair is presented in Fig.1.10.2. Near the threshold, below 2.1 GeV, this ratio turned out to exceed 1 by far, which contradicts the measurement of the PS170 experiment. The asymmetry of angular distribution of proton was also measured. It was found to be small,

-0.025 ± 0.014 , and compatible with the zero value with the available level of accuracy.

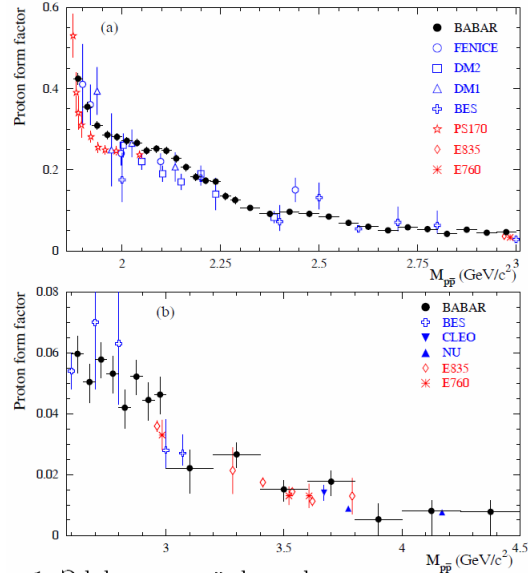


Fig. 1.10.1. Effective form factor of proton as measured in the BABAR experiment and other e^+e^- and $p \bar{p}$ experiments for $p \bar{p}$ invariant masses from the threshold to 3.01 GeV/c^2 (a) and for masses of 2.58 to 4.50 GeV/c^2 (b).

Currently, BINP physicists are analyzing the higher-accuracy measurement of the V_{ub} parameter. Works on the measurement of the cross sections by the radiative return method are going on.

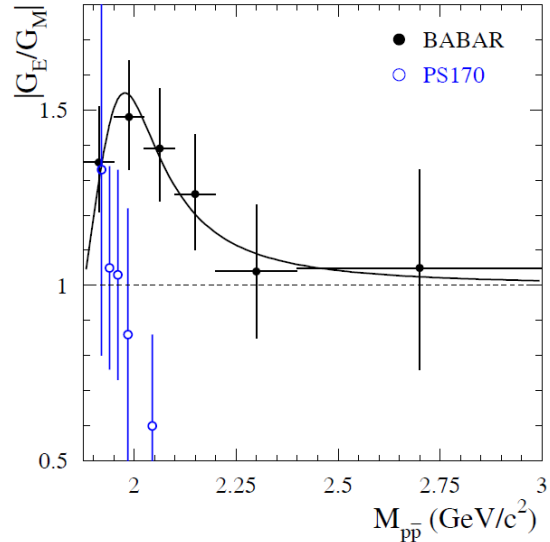


Fig. 1.10.2. Ratio $|G_E/G_M|$ as measured in the BABAR experiment (black circles) vs. invariant mass of the $p \bar{p}$ pair. The empty circles show results of a previous measurement in the experiment PS170 at the facility LEAR (CERN).

1.11. PARTICIPATION IN THE ATLAS EXPERIMENT AT THE LARGE HADRON COLLIDER (LHC)

In 2012 the detectors ATLAS and CMS collected statistics at world highest energy of colliding protons, 8 tera-electron-volt (TeV) in center of mass system. By begin of July, 6 inverse femtobarn (fb^{-1}) were acquired, a little bit more than in full 2011 year at energy of 7 TeV. In total 20 fb^{-1} were accumulated in 2012.

The most important result is reliable observation of a new particle, properties of which came out to be similar to those expected for the Higgs boson. This discovery was announced at special seminar, held at CERN 4th July 2012 as a curtain-raiser of the major particle physics conference ICHEP2012. This discovery is a culmination of tenacious searches, conducted over decades at most powerful particle physics installations. It is important to note that physicists and engineers from Budker INP have made significant contribution to common success, starting with design and fabrication of many accelerator and detectors elements (the total cost of the supplied equipment exceeds 140 millions Swiss francs), continuing by works on commissioning, calibration, tuning of simulation and reconstruction and finishing by participation in data taking and data analysis (in particular, for Higgs boson decay into four leptons).

The Higgs boson was proposed by theorists for simplest realization of the electroweak symmetry breaking as far back as in 1960s. The strength of interaction of the Higgs boson with other fundamental particles depends on the Higgs boson mass. Unfortunately, both theoretical considerations and results of previous experiments imposed quite weak constraints on its value, and it was necessary to perform a search in a wide mass region (see Fig. 1.11.1).

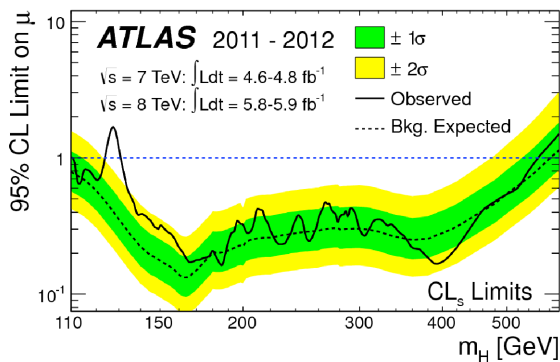


Fig. 1.11.1. Combined (over three Higgs boson decay channels, $H \rightarrow \gamma\gamma$, $H \rightarrow ZZ^* \rightarrow 4l$ и $H \rightarrow WW^* \rightarrow l\nu l\nu$) upper limit (at 95% confidence level) on μ value (the ratio of measured cross section to expected in the Standard Model). The mass interval 111-559 GeV is excluded, except the region 122-131 GeV, where significant excess of the signal over expected background is observed.

Two factors, hampering the search for the Higgs boson (in addition to small production cross section), are large background for highly probable decay modes (e.g. in two photons, Fig. 1.11.2) and small branching ratio for more “clean” channels (e.g. with four leptons in the final state, Fig. 1.11.3).

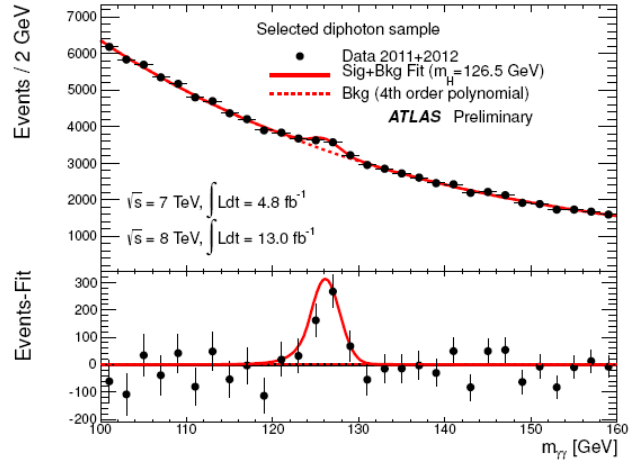


Fig. 1.11.2. The distribution over the two-photon invariant mass $m_{\gamma\gamma}$. In bottom inset the fit of the signal after subtraction of the background (which was approximated by fourth order polynomial) is shown.

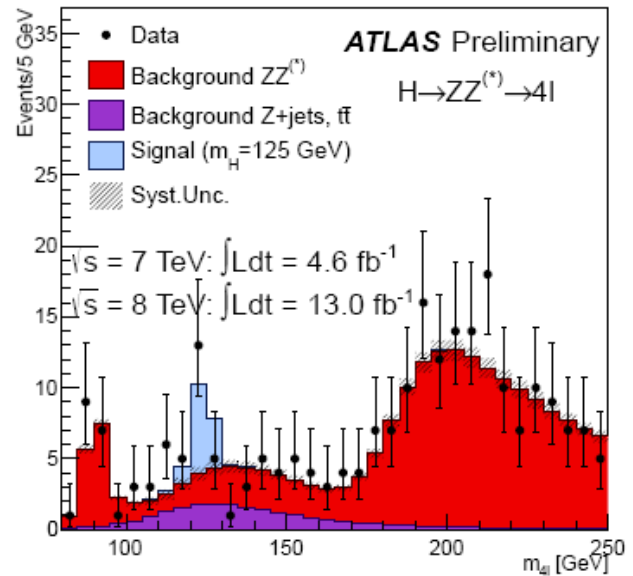


Fig. 1.11.3. The distribution over the four-lepton invariant mass m_{4l} for selected events-candidates. Blue histogram shows expected signal for the Standard Model Higgs boson with a mass of $m_H=125 \text{ GeV}$.

By the end of 2012, the existence of the new boson should be considered as firmly established. The probability of background fluctuation is estimated as $2.8 \cdot 10^{-8}$ for decay into two photons ($2.1 \cdot 10^{-5}$ for decay into four lep-

tons), corresponding to 5.4 (4.1) standard deviations. The mass of the new boson (according to last ATLAS results) is $125.2 \pm 0.3 \pm 0.6$ GeV. But one should clearly realize, that it is by far not necessarily that the new particle is just the Standard Model Higgs boson (though present data do not contradict this hypothesis so far). Similar particles appear in many “new physics” theories. For example, in minimal supersymmetric model there are 5 Higgs bosons (2 charged and 3 neutrals, one of them should have negative parity). It is clear, that to study in detail the properties of the new particle (spin, parity, decay branching ratios, coupling constants) a long dedicated work and much larger statistics is required. It may be collected not earlier than 2015-17, since for 2013-14 the shutdown is planned to prepare the accelerator and detectors for work at the design energy (14 TeV in center of mass system).

The search for new physics is not at all exhausted by Higgs bosons. In particular, BINP physicists continued to search for heavy neutrino in the channel with leptons and hadronic jets in the final state. Two theoretic models were examined – Left-Right Symmetric Model, in which the neutrino is generated by hypothetic right vector boson W_R , and the model with virtual W boson Standard Model. The world best upper limits are set on masses (up to the level of 1.5 TeV), production cross sections and coupling constants of heavy neutrinos. Based on these results, K. Skovpen has defended the PhD thesis. The analysis of 8 TeV data is continuing. But further significant improvement is possible only after the increase of the energy of colliding protons in the LHC (as mentioned above, it is planned in 2015).

In total, the ATLAS collaboration with participation of BINP authors has published 227 papers, based on collisions data (2010-2012), including 128 papers in 2012.

The work on support and development of the computing infrastructure and software is constantly under way. Thanks to 10-gigabit network, BINP physicists are able to run jobs in NSU and SB RAS computing centers (the virtualization technology based on KVM platform is used).

Since 2007 BINP experts continuously participate in activities of the Trigger and Data Acquisition Sysadmins group, dealing with maintenance and development of the hardware and software for High Level Trigger (HLT), Event Builder and other parts of the Data Acquisition System. The equipment includes about 2300 network booted servers (in total, about 17000 CPU cores), 50 servers supporting the ATLAS control room, and many other units of the experiment’s IT infrastructure.

Of great importance is the work on the support and administration of the ATLAS central computers (~300 units), located in CERN main computer building. They ensure smooth uninterrupted operation of critical services – numerous components of ATLAS distributed computing system, data bases, detector’s electronic logbook, data quality monitor, event display etc.

Since 2008 BINP programmers have made and continue to make significant contributions into creation and advancing of important services and applets to manage the ATLAS Distributed Computing system (ATLAS GRID): Data Replication Monitoring and ATLAS GRID Information System (AGIS).

At present time the upgrade project for the LHC collider is developed in order to increase the luminosity by an order of magnitude, up to 10^{35} cm⁻²s⁻¹. In this connection, the work on corresponding upgrade of the ATLAS detector is started. The BINP group takes part in the experiment on study of the operation of ATLAS liquid argon calorimeters at high rates. In April 2012 the new data taking run was carried out at the U-70 accelerator in Protvino with new front-end electronics, much better adapted for high rate environment. The BINP team has supplied the new secondary emission chamber for more precise proton beam profile measurement close to the calorimeter min-modules. Special electronics developed in Lab. 6, allowed to perform several (~10) measurements of the beam profile during the spill (of duration about 1.5 s). As a result, significant movement of the beam during the spill was observed (up to 18 mm in horizontal direction for beam size of 15 mm). The correction, significantly reducing the systematic error for the integral of the beam intensity, was introduced.

1.12. LHCb EXPERIMENT

1.12.1. Technical support for the LHCb detector.

The data flow from the LHCb detector, which is recorded for subsequent storage and processing, consists of about 50 kB of events, which pass through the high-level trigger (HLT2) with a frequency of about 4 kHz. Thus, the flow of data to store is about 200 MB/s or 2000-3000 TB per year of operation. This volume is too large to process in each specific analysis. Instead of it, centralized preliminary offline selection of events (the so-called "stripping") is applied in the LHCb experiment. Around 10% of events are selected from the total data volume and then recorded in a few (5-8) flows. Thus, each flow has a much smaller amount of similar events (e.g. one flow can group all channels with muons in the final state or events from D meson decays), which can be really processed in the GRID system in a relatively short time. In addition, after the "stripping", data already contain information about candidate particles and their combinations, which significantly reduces the time for processing and obtaining a physical result. This approach has a disadvantage of certain pre-selection to perform already at the data collection stage. The problem is partially solved via inclusive selections (for example, of muons with large transverse momentum, "topological" selections, and so on).

The BINP group is responsible for developing and supporting the software environment which provides pre-selection of events ("stripping") following the selection criteria description specified by developers of physical analysis. Environment for "stripping" allows simultaneous operation of several hundreds of physical event selection processes, sends events for recording into multiple data streams, and contains modules for adjustment of selection criteria and monitoring of results. In addition, the BINP group participates in the support for pre-selection for analysis of angle γ measurement in tree-level decays of B mesons. These selections cover channels of decay of b mesons and b baryons into open-charm states.

The BINP team is also directly engaged in the provision of the experiment, its members working as shift supervisors and experts responsible for the quality of data collected.

1.12.2. Physical results.

The research program of the BINP group in the LHCb experiment is focused on the observation of effects beyond the Standard Model of electroweak interactions. A particular task within this general project is precision measurement of parameters that are sensitive to CP violation—unitarity triangle angle γ and parameters of D meson mixing. Spectroscopy of heavy hadrons is a separate task.

At present, the data volume for the year 2011 with an integrated luminosity of 1 fb^{-1} is available for analysis. The corresponding number of detected B meson decays in the main channel exceeds the statistics collected in experiments on the Tevatron collider, and for many decay channels exceeds the B meson statistics acquired on the electron-positron B factories.

CP violation

CP violation defines the asymmetry of matter and anti-matter in the Universe. In the Standard Model, CP violation is described by the Cabibbo-Kobayashi-Maskawa (CKM) matrix, which characterizes transitions between different generations of quarks through weak interaction. One of the CKM matrix representations is the so-called unitarity triangle (UT). There are various processes sensitive to the lengths of the sides and values of angles of this triangle. Effects beyond the Standard Model manifest themselves in disagreement of UT measurements (for example, in the deviation of the sum of the triangle angles from 180 degrees). Thus, precision measurements of UT parameters complement direct searches for the "New Physics" effects at high energies on plants such as ATLAS and CMS.

Many CP-violation processes, which are most sensitive to the UT parameters, are observed in decays of B mesons. Only one of the UT angles (often referred to as β) has been measured so far with an accuracy of about 1 degree (the Belle and BaBar experiments). The LHCb will greatly clarify many other parameters of CP violation. In particular, the γ angle can be measured to within a few degrees.

In 2012, the LHCb experiment yielded a few results relating to the measurement of the γ angle. The BINP contribution was, first of all, the traditional analysis of the $B \rightarrow DK$ decay, where D is reconstructed in the two-particle $D \rightarrow K\pi$, KK or $\pi\pi$ state (the so called GLW and ADS techniques of γ measurement). In this decay, parameters and the value of the suppressed channel $D \rightarrow K\pi$ were measured. CP violation in the decays $B \rightarrow DK$ and $D \rightarrow hh$ with significance over 5 standard deviations was observed for the first time.

Another way of γ measuring involves the process $B \rightarrow DK$, where D decays into the three-particle state $K_s\pi^+\pi^-$ or $K_sK^+K^-$. In this case a model-independent modification of this method was applied, in which the theoretical uncertainty associated with the amplitude of the D decay is completely eliminated due to the use of the CLEO experiment data on the threshold of production of DD pairs. This method was developed and first used in analysis of the Belle experiment data. Now it is applied to the LHCb experiment with significant contribution of the BINP group. γ angle restrictions resulting from analysis of $D \rightarrow hh$ and $D \rightarrow KShh$ in the LHCb experiment are shown in Fig. (1.12).1. Combination of all the measurements in the $B \rightarrow DK$ decays yields $\gamma = (71^{+17}_{-16})^\circ$ (see Fig. (1.12).2), which is comparable in accuracy with the final results of experiments on the B factories.

Another process that is potentially sensitive to the γ angle is the process $B_s \rightarrow D^0 K^+ K^-$, which was recently discovered in the LHCb experiment.

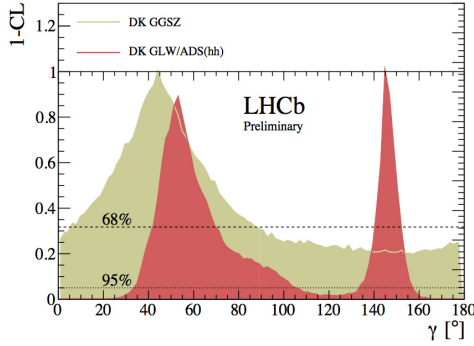


Fig.1.12.1. Results of γ measurement in the decays $B \rightarrow DK$ with $D \rightarrow hh$ (ADS and GLW) and $D \rightarrow K_{shh}$ (GGSZ).

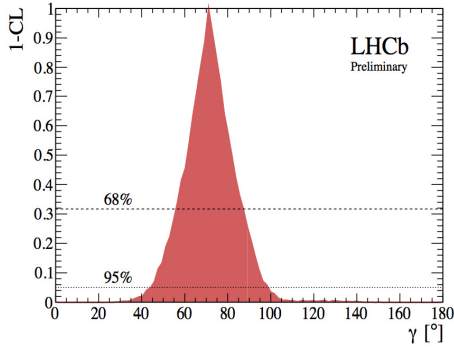


Fig.1.12.1. Results of γ measurements in the LHCb experiment (combination of all measurements in the process $B \rightarrow DK$).

Spectroscopy of heavy hadrons

Today the LHCb detector provides an opportunity to study a large number of decays of Λ_b baryons, which can be used for analysis of spectroscopy of heavy baryons containing the b quark. BINP members completed analysis of the $\Lambda_b \pi^+ \pi^-$ spectrum, which resulted in discovery of two excited Λ_b baryon states, $\Lambda_b^*(5912)$ and $\Lambda_b^*(5920)$. According to the quark model predictions, these states are radial excitations of Λ_b with spin 1/2 and 3/2, respectively. The significance of the observation of the new states is 5.2 and 10.2 standard deviations for $\Lambda_b^*(5912)$ and $\Lambda_b^*(5920)$, respectively. Masses of the discovered particles have been measured: $M[\Lambda_b^*(5912)] = 5911.97 \pm 0.12(\text{stat.}) \pm 0.02(\text{syst.}) \pm 0.66(\Lambda_b \text{ mass}) \text{ MeV}/c^2$, $M[\Lambda_b^*(5920)] = 5919.77 \pm 0.08(\text{stat.}) \pm 0.02(\text{syst.}) \pm 0.66(\Lambda_b \text{ mass}) \text{ MeV}/c^2$.

1.12.3. Review of the LHCb results and planned upgrade.

In 2012, the LHCb collaboration with participation of theorists published a review of the LHCb results on the study of rare decays of mesons and CP violation in the system of B and D mesons. In addition to discussion of the most significant LHCb results and their theoretical interpretation, that review presented plans for upgrade of the detector, which is scheduled for 2018, and the expected physical results.

1.12.4. Modeling radiation environment in the detector area

This work was carried out in the following three directions:

1. porting of the existing simulation in the FLUKA environment from the local machine to the GRID computing system, using the GANGA framework (hereafter referred to as FLUKA, GRID and GANGA),
2. visualization of simulation results with a special web-based application, and
3. creation of documentation.

Porting of simulation in the FLUKA system to GRID

Based on the existing scripts, new ones have been developed, which are adapted to the specific simulation (magnetic field maps have been added) and easier to use.

In the previous system, for simulation on GRID, it was necessary to cut a source FLUKA file into two parts: the first part was to contain the geometry, material specification and scoring, and the second part only included command to start the simulation. On the target host of GRID, these two parts were glued together into one, a random seed directive inserted between them.

Naturally, this was associated with some inconvenience; the file had to be prepared in such a special way at each iteration. In the new system, there is no necessity to cut the file. Immediately after a test on the local machine, the source file from FLUKA can be routed to GRID using the UNIX utility SED (stream editor), which allows in-place editing of files. The SED command receives a special regular expression, which specifies search for the command RANDOMIZE and replacement of the found string with a new one with a random seed unique for each grid node.

Besides, in the old system, random seeds were part of a sequence (a random seed was taken as the number of task in the GANGA system). As a result, there may be intersections of sequences of random numbers, which reduces the efficiency of simulation.

In the new system, random seeds are taken from a file, which allows fine tuning of the behavior and elimination of possible intersections of sequences of random numbers. If there is no file of seeds, a rollback to the previous scheme occurs.

Besides that, the FLUKA distributive that is used on GRID was updated to the new version (FLUKA has a feature of older versions turning off in a few years).

Table 1.12.1: Test passes on the grid.

Total number of sent jobs	Duration of one job (hours)	Number of failed jobs	Number of hung jobs by the time of completion of the first one	Percentage of incom-pleted jobs
20	3	0	1	0 %
40	80	23	23	58 %
80	48	1	3	1 %

After passes of test simulation on the grid (see Table 1.12.1), it became clear that jobs taking more than two days are under a significant risk of total loss. Jobs lasting less than 48 hours result in too much output data, and there is a risk to exceed the DIRAC storage quota. A large amount of output data is associated with difficulties in summing. Each job generates 150 Mb of uncompressed data, the packet with results compressed on a node to a more manageable 30 Mb. Each file contains text and numbers. A special script has been developed that calculates the average of numbers over all the files and does not change the text. The output file is of the same format as the initial ones.

Visualization of results

Although the tools for visualization and analysis of results were ready, their preparation, assembly and adjustment would be a challenge for an average user. Thus it was decided that a web-based application on a special web page would be the easiest way to provide users with simulation results, which do not require any special skills or special settings.

The web page for visualization of simulation results was designed with the use of the library BOOST (www.boost.org), framework ROOT (root.cern.ch) and web framework WT (www.webtoolkit.eu). ROOT was used for data analysis, loading data from a file and generation of pictures for the web page. We used various services from the library BOOST for work with the file system, smart pointer templates, BOOST_FOREACH etc.

The framework WT is worth a special mentioning. This framework allows writing web applications in C++ using the signal-slot paradigm and a set of web widgets, similar to how this is done in the framework QT. The framework WT performs all the work on generation of a valid HTML and Javascript code for the page to be shown to the user. The resulting executable module can contain a simple

embedded web server or be connected to popular web servers (Apache or Lighttpd) via the FastCGI interface (the current project used the latter scheme).

With connection through FastCGI, operation is possible in two modes: shared (a new stream is set for each session) and dedicated (a separate process is set for each session). Naturally, the shared mode gives higher performance and rapid response to new connections, while the dedicated one provides high reliability. Since each session is executed in a separate process, it is isolated from the others and a fail of one session does not cause fall of all other sessions on this computer, as it occurs in the shared scheme.

The source data for the page are three-dimensional histograms (ROOT TH3), downloaded from root files.

The requirements list included the following:

- a cross-section of histogram on one of the XYZ axes at a given point and visualization of the resulting two-dimensional histogram in a color scale mode.
- superposition of schematic detector geometry in a given cross-section ('Overlap schematics');
- calculation of the minimum, maximum, and mean values in a selected area;
- retention of image's proportions ('Keep aspect ratio');
- possibility of setting a multiplier ('Number of collisions');
- catalogue of histograms with the possibility of selection from it ('Choose map').

A result of job completed is shown in Fig. 1.12.3. In addition to the requirements list, the following several useful features were implemented:

- clicking any bin of visualized histogram invokes a small message about the value of the selected bin;
- one can increase any area via giving its boundaries in numerical form or just selecting it in the picture with the mouse and typing the 'zoom' command in the appearing context menu;
- the axes can be inverted ('Invert axes');
- the statistics panel can display the minimum, average, and maximum values over a two-dimensional cross section ('2D-plane'), as well as on a selected volume ('3D-box');
- when the schematic image is superimposed over the histogram, a cross-section in the library of pictures that is closest to a given point is selected; one, however, can manually set the superimposed image.

The web server had been configured on a separate workstation of CERN, and the prototype system was started for final testing and collection of requirements for the next, mass, version. A separate version of web-based visualization of radiation dose maps of old format was realized as a bonus job.

In fact, the web-based application can be used for visualization of other two-dimensional and three-dimensional histograms, which are not locked to this experiment and simulation.

Creation of documentation

All source codes of the web-based application and GRID simulation scripts have been laid out in the system for control of versions

/afs/cern.ch/lhcb/software/GIT/curie_git/. This system is accessible for all the CERN staff.

The knowledge base twiki.cern.ch has two pages describing the rules for the use of scripts for FLUKA simulate on GRID:

<https://twiki.cern.ch/twiki/bin/view/LHCb/LHCbFlukaGanga/>
as well as the assembling and setting up the web-based visualization of simulation results:
<https://twiki.cern.ch/twiki/bin/view/LHCb/LHCbFlukaResults/>

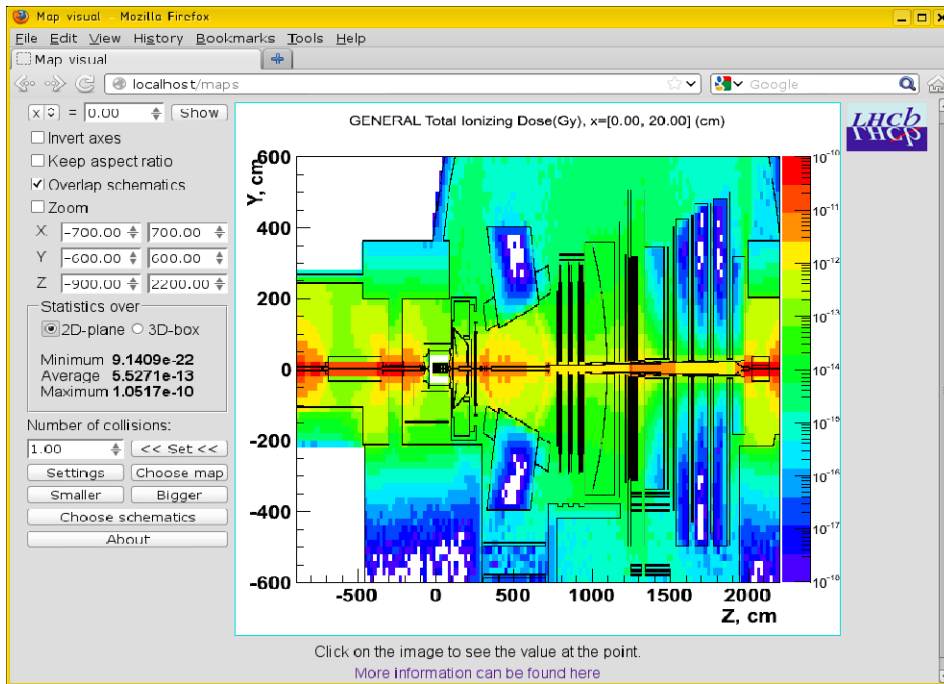


Fig. 1.12.3. View of the web application in operation.

2.1. EXPERIMENTS WITH INTERNAL TARGETS

I. The experiment on a new measurement of R ratio of cross sections of elastic scattering of electrons/positrons on proton was continued in 2012:

$$R = \sigma_{e^+p}/\sigma_{e^-p}$$

It is well known that measurement of R makes it possible to determine the contribution of the two-photon exchange (TPE) into this process. The revival of interest in the two-photon exchange is associated with the fact that information on TPE may explain the dramatic difference in the results of recent experiments on the proton form factors that were carried out in TJNAF (the U.S.) by the polarization method with the results of earlier, non-polarization measurements, in which the proton form factors were determined via analysis of differential cross sections of the reaction under the assumption of validity of single-photon approximation.

The allowance for TPE corrections, however, faces both theoretical difficulties (there are no generally accepted correct calculations because of the complexity of taking into account of excited states of proton in the intermediate state) and experimental ones. Attempts to determine the TPE contribution into the scattering cross section were made in the 70s, but either the statistic and systematic accuracies were bad or the angles of scattering of electrons/positrons were small (the TPE contribution should be very little in this case).

In 2009, R measurements were carried on VEPP-3 at an positron/electron beam energy of 1.6 GeV in two areas of the angle of e^+e^- scattering: 16-23 and 56-75 degrees.

To extend the kinematic range of measurements it was suggested to perform data acquisition at a lower electron/positron energy with simultaneous increase in the angle of particle scattering.

In this case, the R value was expected to be close to that in the experiment in 2009. The statistical accuracy of the new measurement, however, was expected to be much higher.

Statistics gathering in the new kinematic region – at a beam energy of 1 GeV and electron/positron scattering angles of 67-105 degrees began in late September 2011 and ended in March 2012. Fig.2.1.1 presents the course of data gathering in time. The integral of the electron/positron beam current on VEPP-3 reached almost 100 kC, and the integral luminosity was up to 600 pb^{-1} .

Table 2.1.1 shows the main stages of the experiments on R measurement on VEPP-3, and Fig.2.1.2 demonstrates their preliminary results. The figure also presents the known world data and results of some theoretical calculations

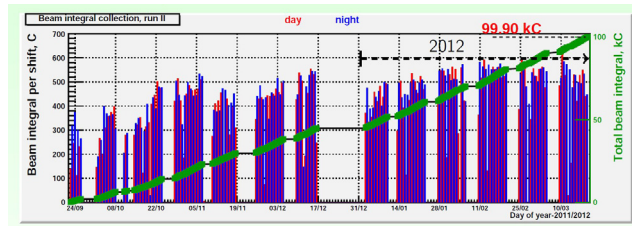


Fig. 2.1.1. Beam current integrals accumulated over a shift (histogram) and total beam current integral vs. time (solid line).

Then statistics gathering was started at a beam energy of 0.6 GeV. It was, however, interrupted.

Table 2.1.1. Stages of the experiment on R measurement on VEPP-3.

Milestones of the Novosibirsk experiment				
• The proposal was published (Aug 2004): nucl-ex/0408020				
Two-photon exchange and elastic scattering of electrons/positrons on the proton. (Proposal for an experiment at VEPP-3). J. Aronson, V.F. Dmitriev, R.J. Holt, D.M. Nikoloski, I.A. Rachev, Yu.V. Shestakov, V.N. Solunov, D.R. Toporkov, H. de Vries, Aug 2004 13sp. e-Print: nucl-ex/0408020 [inSPIRE] [PDF]				
References BibTeX LaTeX/EU Harlow Endnote Detailed record - Cited by 45 records				
• Data taking:				
Run	Duration	E_{beam} , GeV	Number of e^+e^- cycles	\int luminosity, pb^{-1}
Engineering run	May–Jul 2007	1.6	90	12
Run I	Sep–Dec 2009	1.6	1100	324
Run II	Sep 2011 – Mar 2012	1.0	2350	600
Run III	Apr 2012	0.6	220	18
• Some preliminary results were published (Dec 2011): arXiv:1112.5369				

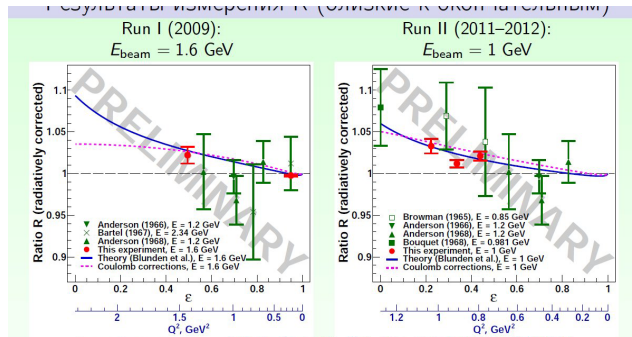


Fig.2.1.2. Preliminary results of the R measurements on VEPP-3 (red circles), known world data (green squares, triangles and crosses), and results of some theoretical calculations (curves).

We note that the accuracy of our results is much better as compared with the world-famous data: experimentally-determined TPE contribution to the elastic (ep) scattering is rather large; calculations made by P.G. Blunden, et al, 2005 (which are recognized as the most correct so far) are in agreement with our data. As a result, the known contradiction in the measurements of proton form factors by different techniques may be eliminated.

Completion of the data analysis is planned for 2013.

It should be noted that two similar experiments have already been conducted in the world. Those are measurements on the CLAS detector, TJNAF (U.S.) and the storage ring DORIS, Germany, OLYMPUS collaboration. No information on results of these experiments is available yet.

II. During the summer stop of the acceleration complex, the detector and the target of the experiment on R measurement were dismantled and the mounting of equipment for research on coherent photoproduction of neutral pion on tensor-polarized deuteron was started (Fig. 2.1.4).

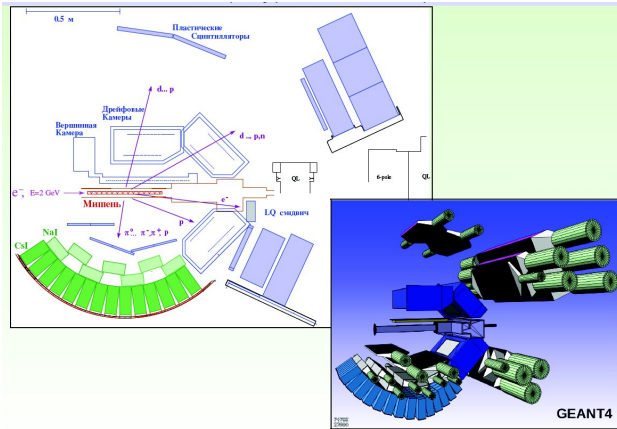


Fig. 2.1.4. Scheme of the detector for the experiment on coherent photoproduction of neutral pion on tensor-polarized deuteron on VEPP-3.

This is one of the most important processes in nuclear physics; it provides valuable information about the structure of the pion-nucleon and nucleon-nucleon interaction.

Although theoretical studies of this reaction, with predictions for the differential cross sections and various polarization observables, have been carried out for a long time with the use of diverse approaches to description of the process, detailed experimental data on the cross sections appeared only in recent years.

As concerns polarization observables, there are some measurements of Σ asymmetry. There were no data at all on T_{2i} (tensor analyzing power in the reaction) before our data appeared (JETP Letters, 89 (2009) 518).

The upcoming experiment will significantly improve the measurement accuracy as compared with the previous data, which will enable assessment of correctness of the theoretical predictions (Fig. 2.1.5).

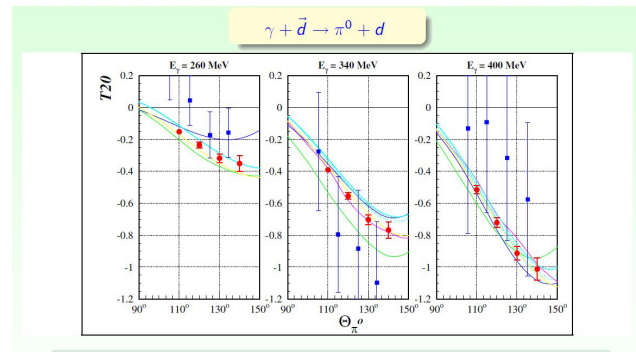


Fig. 2.1.5. Expected accuracy of measurements of the tensor analyzing power T_{20} in the reaction of coherent photoproduction of neutral pion on deuteron (red circles), results of previous measurements (blue squares), and some theoretical predictions (curves).

III. Works on the creation of a system for quasi-real photon tagging (SPT) on VEPP-3 continued. The SPT will significantly enhance the research on photoreactions on VEPP-3 and attaining a photon energy of 1.5 GeV. Furthermore, it will be possible to determine the transverse polarization of a substantial portion of photons and thus to carry out experiments with double polarization. It should be noted that, apart from obtaining new data on deuteron, it will be possible to expand these measurements on neutron.

All first-stage orders have been executed. As for the SPT detectors, the first version of a GEM-based detector and its electronics were successfully tested. It is planned to prepare the SPT for the first test on VEPP-3 and then to carry out this test in autumn 2013.

Creation of detectors for an experiment on the photo-disintegration of deuteron with the use of SPT at photon energies of up to 1.5 GeV was started.

IV. During intervals between the experiments, some works were carried out on improvement of the target. For instance, a stand was constructed for investigation into the effects that reduce polarization of the target and search for ways to suppress them.

It was suggested to change the procedure of application of coating on the cell for protection of atoms from de-polarization. A stand was made for fixation (heating in vacuum) of coating on the storage cell. It was made all-metal (with metal seals) for prevention of contamination of the coating with gassing from rubber seals. An ion pump with nitrogen trap pumps out the volume. Measurements have shown that with such coating the portion of recombining atoms on the surface of the cell (an atom in the cell experiences on average about 200 collisions with the walls) was 0.29 - 0.08, which is close to the known data.

The source of polarized deuterium atoms was upgraded, i.e. a stage of intermediate pumping out was added between the skimmer and the wall of the superconducting sextupole magnet. The superconducting sextupole magnet has a temperature of 4.2 K and therefore is a

cryopump. A TMN-1500 turbomolecular pump was used. Creation of this system made it possible to investigate an interesting and little-studied phenomenon - formation of a free-molecule regime from a transition gas flow (between a continuum flow and a free-molecule one). As for the impact of the additional pumping on increase in the intensity of the atom stream from the source of polarized atoms (SPA), it was ineffective.

The stray flux of molecules from the SPA into the storage cell, which decreases polarization of target, was measured. It was quite small - less than 3% of the intensity of focused atom beam.

It is now generally recognized that the intensity of SPA is limited to $\sim 10^{17}$ atoms/sec, which is insufficient for many experiments with polarized targets. Production of polarized orthohydrogen via spatial separation of hydrogen molecular beam due to interaction of nuclear moments with inhomogeneous magnetic field is being examined. It is suggested to demonstrate the capabilities of this method using an existing SPA with superconducting sextupole magnets with a magnetic field of about 4 T.

The experiments with internal targets are carried in collaboration with groups from Tomsk, St. Petersburg, NIKHEF (Netherlands) and ANL (USA).

3.1. CP NONCONSERVATION

Difference between radiative transition rates in atoms and antiatoms

A.D. Dolgov, I.B. Khriplovich, A.S. Rudenko
JETP Letters 96, No. 7, 421-423 (2012)

We demonstrate that CP -violation results in a difference of the partial decay rates of atoms and antiatoms. The magnitude of this difference is estimated.

3.2. GRAVITY

Gravitational four-fermion interaction on the Planck scale
I.B. Khriplovich
Phys. Lett. B 709, Iss. 3, 111-113 (2012)

The four-fermion gravitational interaction is induced by torsion, and gets essential on the Planck scale. On this scale, the axial-axial contribution dominates strongly the discussed interaction. The energy-momentum tensor, generated by this contribution, is analyzed, as well as stability of the problem with respect to compression. The trace of this energy-momentum tensor can be negative.

Cosmology constrains gravitational four-fermion interaction

I.B. Khriplovich and A.S. Rudenko
JCAP11 (2012) 040

If torsion exists, it generates gravitational four-fermion interaction (GFFI). This interaction gets dominating on the Planck scale. If one confines to the regular, axial-axial part of this interaction, the results do not comply with the Friedmann-Robertson-Walker (FRW) cosmology for the spatial flat or closed Universe. In principle, the anomalous, vector-vector interaction could restore the agreement.

3.3. QCD

Check of the gluon-reggeization condition in the next-to-leading order: Gluon part

M.G. Kozlov, A.V. Reznichenko, V.S. Fadin
Physics of Atomic Nuclei, Volume 75, Issue 4, pp 493-506, April 2012

The last bootstrap condition whose validity has not been verified to date is considered. This condition is an indispensable element in the unitarity-relation-based proof of the multi-Regge form of high energy gluon-exchange QCD amplitudes in the next-to-leading-logarithm approximation. The approach used here relies on the s-channel unitarity and makes it possible to reproduce successively, in all orders of perturbation theory, the multi-Regge form of the amplitude, provided that specific nonlinear relations, called bootstrap conditions, hold. All of them were derived, and all, with the exception of one, were tested. An explicit verification of fulfillment of the last condition (the bootstrap condition for the inelastic amplitude of the production of one gluon in multi-Regge kinematics) is

performed. In our preceding study, we performed such a verification for purely fermion contributions, while, in the present study, we complete it for one-loop gluon corrections to the components of the condition being considered.

Impact factor for gluon production in multi-Regge kinematics in the next-to-leading order

M.G. Kozlov, A.V. Reznichenko, V.S. Fadin
Physics of Atomic Nuclei, Volume 75, Issue 7, pp 850-865, July 2012

The one-loop correction to the impact factor for gluon production upon the transition of a one-Reggeon state in the t channel to a two-Reggeon state is found. This impact factor is an element of multiparticle amplitudes in multi-Regge kinematics. The correction in question is necessary for developing the theory of Regge and multi-Regge processes. In particular, it is necessary for proving the multi-Regge form of the amplitude in the next-to-leading-logarithm approximation. This correction also makes it possible to complete the verification of the last of the unproven bootstrap conditions for gluon Reggeization and to prove, in this approximation, the validity of the multi-Regge form of the amplitude. All necessary calculations are presented, and an explicit expression for the impact factor in front of all possible color states in the t channel is given.

Colour-octet bound states, induced by Higgs mechanism,
S. Bladwell, V. F. Dmitriev, V. V. Flambaum, A. Kozlov
arXiv:1212.5416.

The current limits for fourth generation quarks allows to expect their mass of the order of 500 GeV. In this mass region for quark-anti-quark pair the additional Yukawa-type attraction due to Higgs mechanism is expected to emerge. This Higgs induced attraction greatly exceeds strong interaction between quarks and leads to the formation of bound states in both colour octet $S(8)$ and singlet $S(1)$ states. In the key of recent works on significance of colour octet channel for production of colour singlet state of fourth generation $q\bar{q}$ we calculated the binding energies for both octet and singlet states. Such attraction localizes quarks in extremely small area. Hence colour octet pair of fourth generation quarks can form the "nucleus" and together with colour neutralizing light particle that is captured by strong interaction in orbit around the nucleus, create particle, similar by its structure to Deuterium.

Decays of Fourth Generation Bound States

V. F. Dmitriev, V. V. Flambaum
International Journal of Modern Physics A Vol. 27 (2012)
1250179.

We consider the decay modes of the heavy $q'\bar{q}'$ bound states originating from Higgs boson exchange between

quark – anti-quark pair. In case of a small coupling between the fourth and lower generation the main decay mode is $q'q'$ annihilation. We show that for a vector state the dominant decay modes are Higgs-gamma and Higgs-Z decays, while for a pseudoscalar state the strong two-gluon decay mode dominates. The bound states are very narrow. The ratio of the total width to the binding energy is less than 1% if we are not extremely close to the critical quark mass where the binding energy is very small. The discussed decay modes exist for any fermion-antifermion bound states including heavy leptons and heavy neutrinos if their masses are high enough to form a bound state due to attractive Higgs boson exchange potential.

Evolution equation for 3-quark Wilson loop operator.
R.E. Gerasimov, A.V. Grabovsky.
arXiv:1212.1681 [hep-th]

The evolution equation for the 3 quark Wilson loop operator has been derived in the leading logarithm approximation within Balitsky high energy operator expansion.

BFKL equation for the adjoint representation of the gauge group in the next-to-leading approximation at N=4 SUSY
V.S. Fadin and L. N. Lipatov
Phys. Lett. B **706** (2012) 470-476.

We calculate the eigenvalues of the next-to-leading kernel for the BFKL equation in the adjoint representation of the gauge group $SU(N_c)$ in the N=4 supersymmetric Yang-Mills model. These eigenvalues are used to obtain the high energy behavior of the remainder function for the 6-point scattering amplitude with the maximal helicity violation in the kinematical regions containing the Mandelstam cut contribution. The leading and next-to-leading singularities of the corresponding collinear anomalous dimension are calculated in all orders of perturbation theory. We compare our result with the known collinear limit and with the recently suggested ansatz for the remainder function in three loops and obtain the full agreement providing that the numerical parameters in this ansatz are chosen in an appropriate way.

Connection between complete and Möbius forms of gauge invariant operators
V.S. Fadin, R. Fiore, A.V. Grabovsky and A. Papa
Nucl. Phys. B **856** (2012) 111-124.

We study the connection between complete representations of gauge invariant operators and their Möbius representations acting in a limited space of functions. The possibility to restore the complete representations from Möbius forms in the coordinate space is proven and a method of restoration is worked out. The operators for transition from the standard BFKL kernel to the quasi-conformal one are found both in Möbius and total representations.

NLO impact-factor for one-gluon production in the multi-Regge kinematics

M. G. Kozlov, A. V. Reznichenko and V. S. Fadin
I, **75** (2012) 905-920; Phys. Atom. Nucl. **75** (2012) 850-865.

The one-loop correction to the impact-factor for one-gluon production at one-reggeon state transition into two-reggeon t -channel state. This impact-factor is a part of multi-particle production amplitudes in the multi-Regge kinematics. The correction under consideration is required for development of the theory of Regge and multi-Regge processes. In particular, it is necessary for the proof of the multi-Regge form of production amplitudes in the next-to-leading logarithmic approximation. It permits one to complete verification of the last unproved bootstrap condition for the gluon reggeization and to prove in this approximation validity of the multi-Regge form. All necessary calculations are described and explicit expressions for the impact-factors at all possible colour states in the t -channel are presented.

Check of the gluon reggeization condition in the next-to-leading order: Gluon part
M. G. Kozlov, A. V. Reznichenko and V. S. Fadin
I, **75** (2012) 529-542; Phys. Atom. Nucl. **75** (2012) 493-506.

The last bootstrap condition which fulfillment was not checked till now is considered. This condition is a necessary part of the proof of the multi-Regge form of the high energy QCD amplitudes with gluon exchanges in the next-to-leading logarithmic approximation. The proof is based on the s -channel unitarity and permits to reproduce sequentially the multi-Regge form of the amplitudes in all orders of perturbation theory provided that definite nonlinear relations between the reggeon vertices and the gluon Regge trajectory, which are called bootstrap conditions, are fulfilled. All these conditions were obtained and fulfillment of all but one of them was proved before. In this paper verification of the last unproved condition – bootstrap condition for one-gluon production in the multi-Regge kinematics – is performed in the next to leading order. In our previous paper this verification was done for the fermion contributions; here the gluon contributions are considered and the proof of validity of the last bootstrap condition is completed.

Difference between standard and quasi-conformal BFKL kernels
V.S. Fadin, R. Fiore and A. Papa
Nucl. Phys. B **865** (2012) 67-82.

As it was recently shown, the colour singlet BFKL kernel, taken in Möbius representation in the space of impact parameters, can be written in quasi-conformal shape, which is unbelievably simple compared with the conventional form of the BFKL kernel in momentum space. It was also proved that the total kernel is completely defined by its Möbius representation. In this paper we calculated the difference between standard and quasi-conformal BFKL kernels in momentum space and discovered that it is rather simple.

Therefore we come to the conclusion that the simplicity of the quasi-conformal kernel is caused mainly by using the impact parameter space.

NLO Corrections to the kernel of the BKP-equations
J. Bartels, V.S. Fadin, L.N. Lipatov and G.P. Vacca
arXiv:1210.0797 [hep-ph]; to be published in Nucl. Phys.
B 867 (2013) 827-854.

The NLO kernel of the Bartels-Kwiecinski-Praszalowicz equation for composite states of three reggeized gluons in the Odderon channel was calculated both in QCD and in N=4 supersymmetric Yang-Mills model (SYM). The NLO kernel consists of the NLO BFKL kernel in the adjoint representation of the colour group and the connected 3 to 3 kernel, computed in the tree approximation.

Presenting LiteRed: a tool for the Loop InTEgrals
REDuction
R. N. Lee
arXiv: 1212.2685

Mathematica package LiteRed is described. It performs the heuristic search of the symbolic IBP reduction rules for loop integrals. It implements also several convenient tools for the search of the symmetry relations, construction of the differential equations and dimensional recurrence relations.

DRA method: Powerful tool for the calculation of the loop integrals
R. N. Lee
Journal of Physics: Conference Series **368** (2012) 012050

We review the method of the calculation of multiloop integrals based in the recurrence relations and analyticity of the integrals as functions of space-time dimensionality.

Master Integrals for Four-Loop Massless Propagators up to Transcendentality Weight Twelve
R. N. Lee, A. V. Smirnov and V. A. Smirnov
Nucl.Phys. **B856** (2012) 95-110
arXiv: 1108.0732

We evaluate a Laurent expansion in dimensional regularization parameter $\epsilon = (4 - d)/2$ of all the master integrals for four-loop massless propagators up to transcendentality weight twelve, using a recently developed method of one of the present coauthors (R.L.) and extending thereby results by Baikov and Chetyrkin obtained at transcendentality weight seven. We observe only multiple zeta values in our results. Therefore, we conclude that all the four-loop massless propagator integrals, with any integer powers of numerators and propagators, have only multiple zeta values in their epsilon expansions up to transcendentality weight twelve.

The Dimensional Recurrence and Analyticity Method for Multicomponent Master Integrals: Using Unitarity Cuts to Construct Homogeneous Solutions
R. N. Lee and V. A. Smirnov
JHEP **1212** (2012) 104
arXiv: 1209.0339

We consider the application of the DRA method to the case of several master integrals in a given sector. We establish a connection between the homogeneous part of dimensional recurrence and maximal unitarity cuts of the corresponding integrals: a maximally cut master integral appears to be a solution of the homogeneous part of the dimensional recurrence relation. This observation allows us to make a necessary step of the DRA method, the construction of the general solution of the homogeneous equation, which, in this case, is a coupled system of difference equations.

Spin-dependent part of $\bar{p}d$ interaction cross section and Nijmegen potential
S. G. Salnikov
Nuclear Physics A 874 (2012),98–107.

Low energy $\bar{p}d$ interaction is considered taking into account the polarization of both particles. The corresponding cross sections are obtained using the Nijmegen nucleon-antinucleon optical potential with shadowing effects taken into account. Double-scattering effects are calculated within the Glauber approach and found to be about 10 ÷ 20%. The cross sections are applied to the analysis of the polarization buildup which is due to the interaction of stored antiprotons with a polarized target. It is shown that, at realistic parameters of a storage ring and a target, the filtering mechanism may provide a noticeable polarization in a time comparable with the beam lifetime. The energy dependence of the polarization rate for deuterium target is similar to that for hydrogen one. However, the time of polarization for deuterium is much smaller than that for hydrogen.

Massless two-loop self-energy diagram: Historical review
A.G.Grozin,
Int. J. Mod. Phys. A 27 (2012) 1230018 (22 p.)
[arXiv:1206.2572v3 [hep-ph]]

This class of diagrams has numerous applications. Many interesting results have been obtained for it.

Simultaneous decoupling of bottom and charm quarks
A.G.Grozin, M.Höschele, J.Hoff, M.Steinhauser,
Proceedings of Science (LL2012) 032 (10 p.)
(<http://pos.sissa.it/cgi-bin/reader/conf.cgi?confid=151>)
[arXiv:1205.6001 [hep-ph]]

Parameters and light fields of the QCD Lagrangian with two heavy flavours, b and c, are related to those in the low-energy effective theory without these flavours, to

three-loop accuracy taking into account the exact dependence on m_c/m_b . Similar relations for bilinear quark currents are also considered.

Decoupling in QED and QCD
A.G.Grozin

Int. J. Mod. Phys. A (2013), in print
[arXiv:1212.5144[hep-ph]]

Decoupling of a heavy flavour in QCD is discussed in a pedagogical way. First we consider a simpler case: decoupling of muons in QED. All calculations are done up to 2 loops.

Quantum Chromodynamics
A.G.Grozin
arXiv:1205.1815 [hep-ph]

The classical Lagrangian of chromodynamics, its quantization in the perturbation theory framework, and renormalization form the subject of these lectures. Symmetries of the theory are discussed. The dependence of the coupling constant α_s on the renormalization scale μ is considered in detail.

Reduce interface
A.G.Grozin
arXiv:1204.3020 [cs.MS]

This tutorial (based on the talk at the macs workshop in Faro, Portugal, February 26 – March 2, 2012) describes the new and improved Reduce plugin in GNU with Reduce.

Mass Spectrum in SQCD and Problems with the Seiberg Duality. Another Scenario
V.L. Chernyak
JETP, **114** (2012) pp. 61-79

The $\mathcal{N} = 1$ SQCD with $SU(N_c)$ colors and N_F flavors of light quarks is considered within the dynamical scenario that assumes that quarks can be in the two different phases only: the HQ (heavy quark) phase where they are confined, or they are higgsed, at the appropriate values of the lagrangian parameters. The mass spectra of this (direct) theory and its Seiberg's dual are obtained and compared for quarks of small equal or unequal masses. It is shown that in those regions of the parameter space where an additional small parameter exists (it is $0 < (3N_c - N_F)/N_F \ll 1$ at the right end of the conformal window where the direct theory is weakly coupled in the vicinity of its IR-fixed point, or its dual analog $0 < (2N_F - 3N_c)/N_F \ll 1$ for the dual theory at the left end of the conformal window), the mass spectra of the direct and dual theories are parametrically different. A number of other regimes are also considered.

Mass spectrum in SQCD with additional fields. I,
V.L. Chernyak
arXiv : 1205.0410 [hep-th], 2012, pp. 1-54

Considered is the $\mathcal{N} = 1$ SQCD-like theory with $SU(N_c)$ colors and $0 < N_F < 2N_c$ flavors of light quarks Q_i, \bar{Q}_j and with the additional N_F^2 colorless flavored fields Φ_{ij} with the large mass parameter $\mu_\Phi \gg \Lambda_Q$. The mass spectra of this Φ - theory (and its dual variant, the $d\Phi$ - theory) are calculated at different values of $\mu_\Phi/\Lambda_Q \gg 1$ within the dynamical scenario which implies the (quasi)spontaneous breaking of chiral symmetry. It is shown that, under appropriate conditions, the seemingly heavy and dynamically irrelevant fields Φ 'return back' and there appear two additional generations of light Φ - particles with small masses $\mu(\Phi) \ll \Lambda_Q$. Also considered is the X - theory which is the $\mathcal{N} = 2$ SQCD with $SU(N_c)$ colors and $0 < N_F < 2N_c$ flavors of light quarks, broken down to $\mathcal{N} = 1$ by the large mass parameter of the adjoint scalar field X , $\mu_X \gg \Lambda_2$. The tight interrelations between these X and Φ - theories are described, in particular, the conditions under which they are equivalent.

Mass spectrum in SQCD with additional fields. II,
V.L. Chernyak
arXiv : 1211.1487 [hep-th], 2012, pp. 1-27

This article continues arXiv:1205.0410 [hep-th]. Considered is the $\mathcal{N} = 1$ SQCD-like theory with $SU(N_c)$ colors and $3N_c/2 < N_F < 2N_c$ flavors of light quarks Q_i, \bar{Q}_j , and with the additional N_F^2 colorless flavored fields Φ_{ij} with the large mass parameter $\mu_\Phi \gg \Lambda_Q$. The mass spectra of this Φ - theory (and its dual variant, the $d\Phi$ - theory) are calculated at different values of $\mu_\Phi/\Lambda_Q \gg 1$ within the dynamical scenario which implies that quarks can be in two different phases only: either this is the HQ (heavy quark) phase where they are confined, or they are higgsed at appropriate values of the lagrangian parameters. It is shown that at the left end of the conformal window, i.e. at $0 < (2N_F - 3N_c)/N_F \ll 1$, the mass spectra of the direct and dual theories are parametrically different.

Hard two photon processes $\gamma\gamma \rightarrow M_2 M_1$ in QCD,
V.L. Chernyak

Invited talk given at the Taipei International Workshop "QCD in two photon processes", 2 - 4 October 2012, Taipei, Taiwan, arXiv : 1212.1304 [hep-ph], 2012, pp. 1-19 (will be published in proceedings of the Workshop).

A review of leading term QCD predictions vs those of the handbag model for large angle cross sections $\gamma\gamma \rightarrow \bar{P}_2 P_1$ (P is the pseudoscalar meson $\pi^{\pm,0}, K^{\pm,0}, \eta$), and for $\gamma\gamma \rightarrow \bar{V}_2 V_1$ (V is the neutral vector meson ρ^0, ω, ϕ), in comparison with Belle Collaboration measurements.

3.4. QED

Charge asymmetry in the differential cross section of high-energy e+e- photoproduction in the field of a heavy atom

R.N. Lee, A.I. Milstein, V.M. Strakhovenko
Phys. Rev. A 85, 042104 (2012).

Quasiclassical correction to the differential cross section of high-energy electron-positron photoproduction in the electric field of a heavy atom is obtained with the exact account of the field. This correction is responsible for the charge asymmetry A in this process. When the transverse momentum of at least one of the produced particles is much larger than the electron mass m , the charge asymmetry can be as large as tens percent. We also estimate the contribution A_1 to the charge asymmetry coming from the Compton-type diagram. For heavy nuclei, this contribution is negligible. For light nuclei, A_1 is noticeable only when the angle between the momenta of the electron and positron is of order of m/ω (ω is the photon energy) while the transverse momenta of both particles are much larger than m .

Angular distribution of high-energy e+e- photoproduction close to the end of the spectrum at large momentum transfer

A. Di Piazza, A. I. Milstein
Phys. Rev. A 85, 042107 (2012).

We consider the differential cross section of electron-positron pair production by a high-energy photon in a strong Coulomb field close to the end of the electron or positron spectrum. When the momentum transfer Q largely exceeds the electron mass, the cross section is obtained analytically in a compact form, and it is proportional to $1/Q^4$. Coulomb corrections essentially modify the cross section even for moderate values of the nuclear charge number Z . In the same kinematical region, the angular distribution for bound-free pair production, bremsstrahlung, and photorecombination is also obtained.

Quasilocalized states in a model of electron-electron interaction in graphene

R.N. Lee, A.I. Milstein, I.S. Terekhov
Phys. Rev. B 86, 035425 (2012).

A quantum mechanical model of two interacting electrons in graphene is considered. We concentrate on the case of zero total momentum of the pair. We show that the dynamics of the system is very unusual. Both stationary and time-dependent problems are considered. It is shown that the complete set of wave functions with definite energy includes new functions that were previously overlooked. The time evolution of the wave packet, corresponding to the scattering problem setup, leads to the appearance of a localized state at large time. The asymptotics of this state is found analytically. We obtain the lower bound

of the lifetime of this state, which is connected with the breakdown of the continuous model on the lattice scale. The estimate of this bound gives one hope to observe the localized states experimentally

Quasiclassical approach to high-energy QED processes in strong laser and atomic fields

A. Di Piazza, A. I. Milstein
Physics Letters B 717, 224 (2012).

An approach, based on the use of the quasiclassical Green's function, is developed for investigating high-energy quantum electrodynamical processes in combined strong laser and atomic fields. Employing an operator technique, we derive the Green's function of the Dirac equation in an arbitrary plane wave and a localized potential. Then, we calculate the total cross section of high-energy electron-positron photoproduction in an atomic field of arbitrary charge number (Bethe-Heitler process) in the presence of a strong laser field. It is shown that the laser field substantially modifies the cross section at already available incoming photon energies and laser parameters. This makes it feasible in principle to observe with present technology the analogous effect in a laser field of the Landau-Pomeranchuk-Migdal effect for the Bethe-Heitler process.

Production of a Pair by a Polarized Photon in a Uniform Constant Electromagnetic Field

V.M. Katkov

Journal of Experimental and Theoretical Physics, 2012,
Vol. 114, No. 2, pp. 226-233.

The total probability of production of an electron-positron pair by a polarized photon in a constant uniform electromagnetic field of an arbitrary configuration is determined using the imaginary part of the diagonalized polarization operator. Approximate expressions are derived for this probability in four ranges of photon energy. In the high-energy range, the corrections to the standard semiclassical approximation are calculated. In the range of intermediate energies, in which this approximation is inapplicable, the probability of the process is calculated using the steepest descent method. It is shown that in the range of photon energies higher than the pair production threshold in a magnetic field, a weak electric field removes root divergences in the probability of production of the particles at the Landau levels. For relatively low photon energies, a low energy approximation is developed. At such energies, the effect of the electric field on the process is decisive, while the effect of the magnetic field is associated with its interaction with the magnetic moment of the particles being produced. Such an interaction is manifested, in particular, in the difference in the probabilities of production of a pair by an external field for scalar and spinor particles.

3.5. GRAVITATION AND ASTROPHYSICS

First order representation of the Faddeev formulation of gravity

V. M. Khatsymovsky

arXiv:1201.0806[gr-qc], pp. 1-9, (2012).

We study Faddeev formulation of gravity where metric is composed of the ten four-dimensional vector fields, that is, of the tetrad 4×10 . One can speak of the new vector index corresponding to the ten-dimensional vector space with the flat Euclidean or Minkowsky metric. By using equations of motion, we can reduce Faddeev gravity to the Einstein one. We propose representation of the Faddeev gravity in terms of independent connection variable, an analog of the known connection representation of the usual Einstein gravity. Now we introduce the $SO(10)$ connection. Excluding this connection via the equations of motion leads to the Faddeev action. Further, we consider some one-parametric generalization of the Faddeev action which still results in the Hilbert-Einstein action on the equations of motion. We propose connection representation for this action as well. The parameter on which the action depends is a fundamental constant, an analog of the Barbero-Immirzi parameter in the Einstein gravity.

On some feature and application of the Faddeev formulation of gravity

V. M. Khatsymovsky

Thesis of Conference "Quantum Field Theory and Gravity 2012", July 31 - August 4 2012, Tomsk, Russia - TSPU Bulletin, No. 13(128), pp. 76-80, (2012); arXiv:1212.0978 (2012).

Faddeev formulation of gravity considers metric as composite field bilinear in the $d = 10$ four-vector fields. Its unique property is that the discontinuous fields are possible on quantum theory. On the discrete level, when the space-time is constructed of elementary 4-tetrahedra, this means that the 4-tetrahedra are allowed to mismatch on their common faces, that is, to be independent. We apply this to the particular problem of the quantization of surface considered as that composed of the virtually independent elementary areas (triangles). We find that the spectrum of surface area is proportional to the Barbero-Immirzi parameter in the Faddeev gravity and is described as the sum of spectra of independent elementary areas. According to the known in the literature approach, we find that the Barbero-Immirzi parameter exists ensuring the Bekenstein-Hawking relation for the statistical entropy of the black hole for the arbitrary d , in particular, being 0.39... for the genuine $d = 10$.

Faddeev formulation of gravity in discrete form

V. M. Khatsymovsky

arXiv:1201.0808[gr-qc], pp. 1-18, (2012).

We study Faddeev formulation of gravity which considers metric as a field composed of the vector fields. We regard

these fields as constant inside the 4-tetrahedra constituting the space in the discrete framework. The action depends not only on the fields inside the 4-tetrahedra, but also on the details of the (regularized) jump of the fields between the 4-tetrahedra. Though, if the fields vary arbitrarily slowly from the 4-tetrahedron to the 4-tetrahedron, this dependence is negligible (it is of the next-to-leading order of magnitude). We rewrite the earlier proposed in our work first order representation (in terms of connection) of the Faddeev action in the discrete form. We show that upon excluding the connection it agrees with the above mentioned Faddeev action on the piecewise constant fields in the leading order. Thus, using the discrete form of the connection representation of the Faddeev action can serve as the method to fix the action on the piecewise constant fields on the 4-tetrahedra.

On area spectrum in the Faddeev gravity

V. M. Khatsymovsky

arXiv:1206.5509[gr-qc], pp. 1-17, (2012).

We consider the Faddeev formulation of gravity in which metric is bilinear in $d = 10$ 4-vector fields. A unique feature of this formulation is that the action is finite on the discontinuous fields (although continuity is recovered on the equations of motion). This means that space-time is decomposed in the discrete approach into the 4-tetrahedra virtually not coinciding on their common faces, that is, independent 4-tetrahedra. This allows to consider a surface as composed of a set of the virtually independent elementary areas (triangles). Then area spectrum is the sum of independent elementary area spectra. We use connection representation for the Faddeev action on the manifold composed of the 4-tetrahedra earlier proposed in our paper. Elementary area tensors (bilinear in the tetrad fields) are canonically conjugated to the orthogonal rotation matrices (connection). These are quantized in the same manner as the angular moment in quantum mechanics conjugated to the rotation angle is. We find that the spectrum of the elementary area is proportional to the Barbero-Immirzi parameter in the Faddeev gravity and is similar to the angular moment spectrum in the space of dimensionality $d - 2$. Knowing this spectrum allows to evaluate the statistical black hole entropy. Requiring that this entropy be coincident with the Bekenstein-Hawking one gives the equation which is known in the literature. This equation allows one to find the Barbero-Immirzi parameter for arbitrary d , in particular, the value 0.39... for it for the genuine $d = 10$.

Charged black rings in supergravity with a single non-zero gauge field.

A. Feldman, A.A. Pomeransky

JHEP 1207 (2012) 141

General charged black ring solution of the 5D Einstein-Maxwell-dilaton theory with Kaluza-Klein dilaton is

found by the inverse scattering method. The metric has two independent angular momenta, a charge and a dipole charge. The solution is presented in a relatively concise form in which its symmetries are manifest. The regularity conditions are found and the physical characteristics of the regular solution are expressed via its parameters.

3.6. CHAOS

Wigner crystal in snaked nanochannels: outlook

O.V. Zhirov, D.L. Shepelyansky
Physica B407(2012) p.1909-1911.

We study properties of Wigner crystal in snaked nanochannels and show that they are characterized by a conducting sliding phase at low charge densities and an insulating pinned phase emerging above a certain critical charge density. We trace parallels between this model problem and the Little suggestion for electron transport in organic molecules. We also show that in presence of periodic potential inside the snaked channel the sliding (conducting) phase exists only inside a certain window of electron densities that has similarities with experimentally observed pressure dependence of conductivity in organic conductors. Our studies show emergence of dynamical glassy phase in a purely periodic potential in absence of any disorder that can explain enormously slow variations of resistivity in organic conductors. Finally we discuss the KAM concept of superfluidity induced by repulsive Coulomb interaction between electrons. We argue that the transition from the sliding KAM phase to the pinned Aubry phase corresponds to the superfluid-insulator transition.

Elastic enhancement factor as a quantum chaos probe

Ya.A. Kharkov, Valentin.V. Sokolov
arXiv:1211.1773v2 [quant-ph] 8 Nov 2012; published in
Phys. Lett. B **718** (2013) 1562-1565.

Recent development of the resonance scattering theory with a transient from the regular to chaotic internal dynamics inspires renewed interest to the problem of the elastic enhancement phenomenon. We reexamine the question what the experimentally observed value of the elastic enhancement factor can tell us about the character of dynamics of the intermediate system. Noting first a remarkable connection of this factor with the time delays variance in the case of the standard Gaussian ensembles we then prove the universal nature of such a relation. This reduces our problem to that of calculation of the Dyson's binary form factor in the whole transition region. By the example of systems with no time-reversal symmetry we then demonstrate that the enhancement can serve as a measure of the degree of internal chaos.

Chaotic interference versus decoherence: external noise,
state mixing and quantum-classical correspondence

V.V. Sokolov

Proceedings of the Chaos2012 International conference,
Athens, Greece, pp. 2-5, (2012).

Possible mechanisms are discussed of suppression of the quantum interference ("decoherence"). Being, in essence, of quite general nature, this question takes on special significance for understanding the quantum-classical correspondence in the non-trivial case of non-linear classically chaotic quantum systems. Because of exponential instability of such a dynamics, an arbitrarily weak interaction with a disordered environment crucially influences the motion and turns it into an irreversible random process. Quite opposite, the quantum dynamics of the same systems manifest, because of quantization of the phase space, a considerable degree of stability against external perturbations. The resulting crucial difference lies in the fact that though the rapid decay of phase correlations is an underlying feature of the classical dynamical chaos, so called "quantum chaos" is not, by itself, capable of destroying the quantum phase coherence. Basically, formation of incoherent mixed states is necessary for decoherence to appear. For this reason, interaction with a disordered environment plays a primary role in the both, classical as well as quantum cases. We illustrate the ways the decoherence takes place by a number of examples including a systems driven by a periodic multimode external force and a stationary electron quantum transport through a 2D mesoscopic structure.

4.1. RESEARCH ON THE GDT DEVICE

GDT (Gas Dynamic Trap) in the Budker Institute of Nuclear Physics SB RAS is designed for experimental research on basic plasma physics problems that should be solved for controlled nuclear fusion in axially symmetric magnetic open traps.

Table 4.1. The main parameters of GDT device.

Parameter	Value
Distance between mirrors	7 m
Magnetic field in the central plane	up to 0.35 T
Mirror ratio	33
Power of atomic beams	5.5 MW
Energy of the injected deuterium atoms	25 keV
Average energy of hot ions	≈ 10 keV
Duration of atomic injection	5 ms
Inclination angle of atomic beams	45°
Warm ions density in the central plane	$2 \cdot 10^{19} \text{ m}^{-3}$
Maximum density of hot ions	$5 \cdot 10^{19} \text{ m}^{-3}$
Electron temperature	до 250 eV
Plasma radius in the central plane	14 cm
Relative pressure of plasma	up to $\beta = 0.6$

Plasma confined in the GDT contains two ions components with very different energies. The main component is the hot ions formed as a result of oblique injection of atomic beams. This component is characterized by adiabatic confinement regime, and it is responsible for the fusion reactions in the reactor systems designed on the basis of the GDT device. Ions of another component are isotropic in velocity space with Maxwell distribution function. Such a distribution is realized when the length of the device exceeds the characteristic length L of ion scattering by an angle equals to the angle at the vertex of the loss cone:

$$L \gg \lambda_{ii} \ln(R)/R,$$

where λ_{ii} - the mean free path of the ions relative to the scattering by angle of the order of unity, R - mirror ratio, which is supposed to be large for GDT ($R \gg 1$). The temperature of the warm ion component is close to the electron temperature and has a value of few percent relative to the energy of the atomic beams particles. It should be noted that the presence of warm plasma in the GDT is necessary as it can help solve fundamental problems of plasma confinement: the suppression of drift-cone cyclotron instability and suppression of transverse losses associated with magnetohydrodynamic instabilities.

As a first application GDL offers a powerful 14 MeV neutron generator of DT reaction for solution of thermonuclear material science problems and for the management of subcritical nuclear reactors for various purposes,

including apparatus for consuming of long-lived radioactive waste. The record for axially symmetric magnetic traps value of relative plasma pressure $\beta = 0.6$, reached in recent experiments on the GDT, as well as a simple and well-studied physics of longitudinal confinement are reliable basis for the construction of fusion reactors with the essential parameters for fusion applications.

However, for a more complete and in-depth study of reactor applications of GDT, an additional number of problems should be solved. Some of them were the subject of research in 2012:

1) The study of kinetic instabilities (or microinstabilities), which are a consequence of the non-equilibrium distribution function of the main component of the plasma - hot ions with energy of fusion range (≈ 10 keV) and formed as a result of oblique injection of neutral beams with energies of deuterium particles 25 keV and a total power of more than 5 MW;

2) The study of additional heating of the plasma electron component by microwave radiation at a frequency of electron cyclotron resonance, as well as injection of an electron beam through a magnetic mirror along the axis of the GDT device.

In addition, experiments with small displacement of axial lines of atomic beams relative to the axis of symmetry of the plasma in order to transmit an additional momentum of different signs to the plasma column depending on beams aiming geometry. In this mode, the maximum has been achieved to date, the temperature of electrons $T_e > 250$ eV.

And finally, there were direct measurements of the heat flux density on a section of one of the GDT mirrors. Showed that this parameter had a maximum value of $Q = 0.25 \text{ GW/m}^2$ at the end of the atomic injection pulse. This result is of interest for specialists in the study of the interaction effects "plasma - surface" for large values of the heat flux delivered by the plasma to the elements of construction of future fusion reactors.

The results of the preparation or conducting of these studies briefly covered in the following sections of this report.

4.1.1. Study of kinetic instabilities.

For the study of electromagnetic waves in plasma with the possible development of microinstabilities a special system of high-frequency magnetic probes was created. Magnetic probe consists of three orthogonal coils embedded with 10 mm in diameter, each of which registers its corresponding component of the magnetic field of the excited wave: the radial, azimuthal and longitudinal (parallel to the axis of the GDT device). Coils through respective paths are electrically connected with the channels of synchronous waveform recorder. The frequency range of the magnetic probes and registration paths lying in $0.1 \div 10$ MHz. The probes were fixed inside the vacuum chamber near the plasma edge at 30 cm from the axis of the GDT device. Six of them were installed on the same line

along the axis, overlapping one half of the movement region of hot ions. Magnetic probes were installed not equidistant, the distances between them were chosen to use the optimal method of correlation analysis of wavelength oscillations propagating along the magnetic field. Also, five probes were placed at equidistant azimuthal angles in the plane perpendicular to the axis of the device that allows analyzing the azimuthal structure of the excited electromagnetic oscillations.

Measurements showed that at total energy accumulated by the injection of hot atomic deuterium ions over $1100 \div 1300$ J oscillations with a narrow frequency range, the maximum of which accounted for 1.15 MHz detected on probes. In this case, the cyclotron frequency of the deuteron in the vacuum field on the axis in the central plane was $\Omega_{ci} = 2.7$ MHz. Oscillations are generated as "bunches" of varying duration, the amplitude in this case was limited and did not depend on the energy (or relative pressure) of hot ions in the range from ≈ 1100 J to maximum ≈ 1900 J.

Correlation analysis of observed electromagnetic oscillations revealed their following properties:

1. The longitudinal oscillation wavelength coincides with the estimate one for the Alfvén wave.
2. The excited wave has elliptical polarization and the direction of rotation of the polarization vector coincides with the direction of rotation of the ions.
3. The wave propagates from the center of the trap towards the mirror.
4. In the spatial oscillation spectrum the mode with azimuthal wave number $m = 1$ dominates.

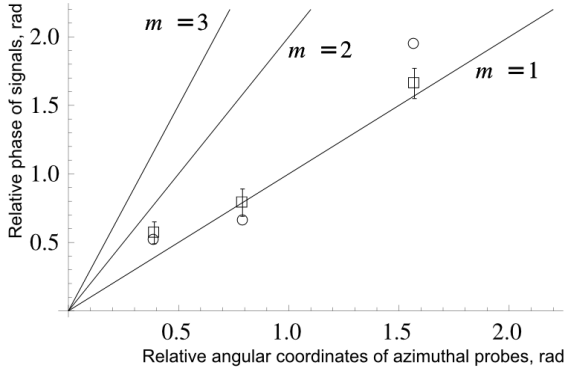


Fig. 4.1.1. The dependence of the relative phase of the signals at the frequency 1.15 MHz from relative angle coordinate of azimuthal probe.

Figure 4.1.1 gives reason for the last statement. It shows the relative phase of the oscillations with the frequency 1.15 MHz from the relative angular coordinates of the corresponding azimuthal probes. It can be seen that the measured values of the phases are close to the line corresponding to the azimuthal wave number $m = 1$.

Mentioned features allow one to conclude that the Alfvén wave is observed, and we have to deal with the

Alfvén ion-cyclotron instability. This type of instability leads to the generation of waves with circular polarization and $\omega < \Omega_{ci}$. Recall that the Alfvén wave propagates along the magnetic field lines.

Preliminary results of an experimental study of micro-instabilities listed above motivated in-depth theoretical analysis of the problem. The analysis took into account the main features of the experiment at GDT:

1. Oblique injection of neutral beams;
2. Close to the real distribution function of the velocity of hot ions;
3. Real spatial inhomogeneity of the magnetic field and plasma.

Brief description of the theoretical analysis is given in [I.S.Chernoshtanov, Yu.A.Tsidulko, "Alfvén ion-cyclotron instability in a mirror trap with skew injection of neutral beams", accepted for publication in the Journal of Fusion Science and Technology]. The main results are as follows conclusions:

1. The generation of an electromagnetic wave is performed by a group of ions with longitudinal velocities exceeding the average longitudinal velocity of the particles of injected atomic beams $|v_{||res}| \geq |v_{||inj}|$.
2. Accounting of transverse inhomogeneity leads to an increase in the threshold values relative pressure of plasma at which the development of the instability begins.

The task of the next step of the experimental research was to test the main conclusions of the analysis. The range of the longitudinal velocity of ions that can interact with the wave was determined from the cyclotron resonance:

$$\omega - \Omega_{ci} = k_{||} v_{||res}, \quad (4.1.1)$$

where ω - wave frequency, Ω_{ci} - cyclotron frequency for of hot ions, corresponding to the magnetic field in the plasma in the central plane of the GDT, where the generation of wave, $k_{||}$ - a projection of the wave vector in the direction of the magnetic field, $v_{||res}$ - longitudinal velocity of the ions in resonance with the wave.

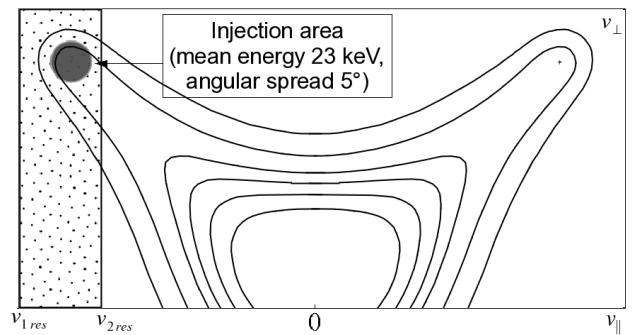


Fig. 4.1.2. The isolines of the distribution function, the area of birth of hot ions, boundary of the loss cone and the area of resonance particles in the plane $v_{||} - v_{\perp}$.

The wave frequency - directly measured value, k_{\parallel} - calculated based on the results of the correlation analysis of the data from the magnetic probes located along the axis of the setup. Thus to evaluate a range of the longitudinal velocity of the resonant ions (4.1.1) we need to know Ω_{ci} . To calculate the cyclotron frequency it's necessary to obtain the value of the magnetic field inside the plasma, taking into account its diamagnetism. In our case it was done the two limiting estimates. In the first case Ω_{ci} was calculated for the vacuum magnetic field in the central plane of the GDT, the magnitude of which was $B_0 = 0.3$ T. Also Ω_{ci} calculation was carried out to the central plane with the maximum value of the parameter β (the transverse plasma pressure to the magnetic field pressure ratio) at the time of the instability development. This value is obtained by direct measurement of the magnetic field inside the plasma by means of a beam-spectroscopic diagnostics, based on the dynamic Stark effect. Measurements are made turning point of hot ions, the value of β , corresponding to the "threshold" of the instability, was $\beta = 0.28$.

Thus, from (4.1.1) two values $v_{\parallel res1}$ and $v_{\parallel res2}$, obtained the minimum and maximum possible values of the longitudinal velocity of the resonant ions. The result is illustrated in Figure 4.1.2, which shows the contours of the distribution function of hot ions in the plane $v_{\parallel} - v_{\perp}$.

The scope of birth of hot ions by trapping of the atomic beams is indicated by the circle. The area with the lowest and highest possible rates of longitudinal resonant velocity of ions is limited by the vertical lines and shaded with dotted texture. It can be seen that the resonant interaction with the wave is only possible for a relatively small group of particles lying in a fairly narrow region of phase space near the region of birth of hot ions due to ionization of injected atoms. Small deceleration or ion scattering to the region far from the boundary of the loss cone enough to remove particles from the region of resonant interaction with the wave.

The main results of 2012 on study of Alfvén ion-cyclotron instability are listed below:

1. The type of instability is identified - Alfvén ion-cyclotron with $\omega \leq \Omega_{ci}$;
2. Found that a group of ions with energies close to the maximum and the angular spread close to the angular spread of the injected neutral beams is in resonance with the wave. During braking and scattering particles leave the resonance region without reaching the loss cone;
3. It is shown that the critical value of β , corresponding to the threshold of the instability development, increases by increasing of the gyroradius of hot ions up to values comparable with the characteristic plasma radius ($\rho_{\perp inj} \rightarrow r_p$).

In 2013 it is planned to complete this cycle of research. The work plan for 2013 includes the following tasks:

1. Clarification of the range width of the longitudinal velocity of the resonant ions;

2. Accurate measurement of the dependence of the β threshold on $r_p/\rho_{\perp inj}$;
3. Experiments with simultaneous injection of beams of D_0 and H_0 . Measurement of β thresholds on the concentration ratio of hot ions with different masses.

To solve these and other problems an additional channel of beam-spectroscopic diagnostics, based on the dynamic Stark effect, will be used. The new measurement channel is fully prepared to work at the time of writing, it allows to measure radial profiles of the magnetic field inside the plasma column in the GDT central plane with high precision in the modes with high β values.

4.1.2. State of work on additional ECR plasma heating in the GDT device.

Energy lifetime of hot ions in GDT is mainly determined by their Coulomb deceleration due to interaction with the electrons and the electron temperature is proportional to the degree of 3/2:

$$\tau_{ei} = \frac{3}{4\sqrt{2\pi}} \cdot \frac{m_i}{\sqrt{m_e}} \frac{T_e^{3/2}}{z^2 \cdot \Lambda \cdot e^4 \cdot n},$$

where m, z - mass and charge of hot ions, m_e, e, n, T_e - mass, charge, density and temperature of the electrons, Λ - Coulomb logarithm. This fact means that the electron temperature is the most important parameter that determines the confinement time of hot ions and the effectiveness of the designed neutron source based on GDT.

The use of an additional electron cyclotron (ECR) heating is one way to increase the electron temperature. To implement the additional heating in GDT the creation of the ECR heating on the basis of two gyrotrons ($f = 54.5$ GHz, $P = 450$ kW) was proposed. The total power of the microwave radiation generated by the two modules of the gyrotron ($2 \times 450 = 900$ kW), is comparable with the power of plasma heating due to the deceleration of hot ions in it (≈ 1000 kW).

Preliminary calculations show that the use of such a system of microwave heating will allow reaching a significant increase in the electron temperature up to 350 eV instead of 250 eV at present. According to the results of numerical simulations, the neutron source based on GDT with the electron temperature $T_e > 300$ eV is quite competitive when compared with the corresponding systems based on accelerators.

ECR heating system design for GDT, as well as the results of the numerical simulation of plasma heating are described in detail in section 4.1 of the report for the Institute of Nuclear Physics SB RAS in 2011. This report briefly lists the main results of 2012 in this direction and the state of work at the time of writing the report.

In 2012 work on the preparation of the experiment on the ECR heating on the GDT was completed. All the elements required for line formation and transport of beams of microwave radiation was obtained from production in the IAP RAS and ZAO "Gikom" (Nizhny Novgorod).

Additional components required for mounting and alignment of waveguides elements manufactured and assembled in the GDT as well as conical elements of the vacuum chamber with ports for injection of microwave radiation into the plasma and movable valves with pneumatic drive to protect the quartz input windows from covering by titanium film during titaniation of inner surface of the vacuum chamber before operating pulses. All the work on the installation and calibration of microwave radiation beam transport lines from the two gyrotron modules to the GDT device completed.

After the completion of installation and calibration of waveguide lines their "hot" test was carried out. Using calorimetry it is shown that in the region of plasma radiation power is at least 80% of the power generated by gyrotrons, which is in good agreement with the results of preliminary electrodynamic calculations.

High-voltage power sources of gyrotrons with 70 kV voltage, current up to 25 A, voltage stability - not more than 1.5% assembled, established and prepared to work. System of control and monitoring of gyrotron parameters, including electronics and software, was assembled, tested and ready for operation.

At the time of writing one of two channels of the ECR heating is fully prepared to work. The first series of experiments on the microwave heating of the plasma on the GDT started. There are works on the preparation and launch of the second channel.

4.1.3. The status of work on the preparation of the experiment with the injection of the electron beam in GDT.

The first series of experiments on the injection of electron beam in GDT was carried out in 2011. The results of these experiments are described in detail in the report of Institute of Nuclear Physics SB RAS for 2011, they motivated the development of a new version of an electron gun for a new series of experiments, which is planned for 2013.

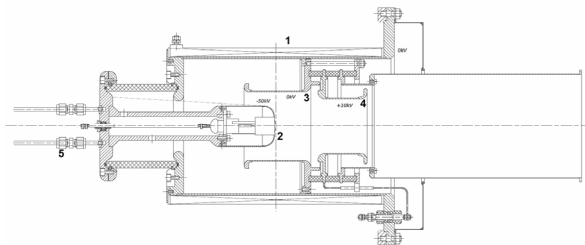


Fig. 4.1.3. Construction of a new version of the electron gun for the experiments with the injection of the electron beam in GDT: 1 – coil, 2 - hot cathode, 3 - anode, 4 - electrode to suppress the flow of ions from the trap, 5 - cooling water tubes.

The design of the new version of the electron gun for experiments with the electron beam injection in GDT is explained by figure 4.1.3. The device is constructed based on the following parameters of the electron beam:

- Electrons energy - 50 keV;
- Beam current - 20 A;
- Pulse duration - 1 ms.

The estimated angular divergence of the beam allows its adiabatic compression during transportation along the magnetic field to the degree of $K > 60$.

Work on the production of electron gun and high-voltage power source to be completed in the first half of 2013. Experiments on further plasma heating using electron beam scheduled for 3 - 4 quarters of 2013.

4.1.4. Experiments with offset of atomic beams axial lines relative to the axis of plasma symmetry.

In 2012 a series of experiments with a small (≈ 5 cm) displacement of axial lines of atomic beams relative to the axis of plasma symmetry in order to transmit the plasma column an additional momentum of different signs depending on beams aiming geometry. The result was that in the case of a transfer of angular momentum in the direction of the natural rotation of the plasma through $E \times B$ drift in the radial electric and magnetic fields plasma confinement is improved significantly. The radial electric field appears due to the radial drop of electron temperature and corresponding to that drop of ambipolar plasma potential gradient. In this mode, the maximum achieved to date, the value of the electron temperature $T_e > 250$ eV.

Figure 4.1.4 shows the result of a measurement of the electron temperature in this mode.

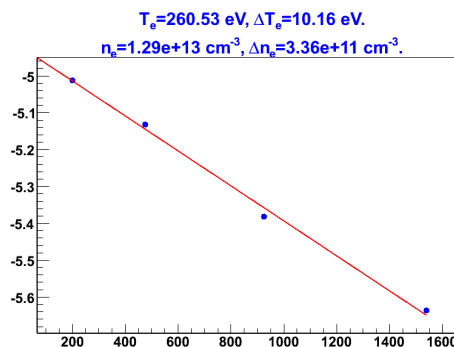


Fig. 4.1.4. The maximum temperature of the electrons obtained in the experiment with offset axial lines of atomic beams relative to the axis of plasma symmetry: is measured on the axis in central plane at the moment of atomic injection end.

4.1.5. Measurements of the heat flux density at the mirror plane.

In 2012 the direct measurements of the heat flux density in a GDT mirror plane were also carried out. It is shown that this parameter had a maximum value of $Q = 0,25 \text{ GW/m}^2$ at the end of the the atomic injection heating pulse and did not achieving steady state values. Numerical modeling of the plasma flows through the mirror shows that in the case of the steady state conditions when the power of the atomic beams $5 \div 10 \text{ MW}$ is possible to obtain heat flux density up to 1 GW/m^2 at the mirror. These results demonstrate that on the basis of GDT the creation of stand for studying the interaction of "plasma-surface", capable to realize a full-scale heat flux density in plasma boundary layer of next generation ITER-like tokamaks, is possible.

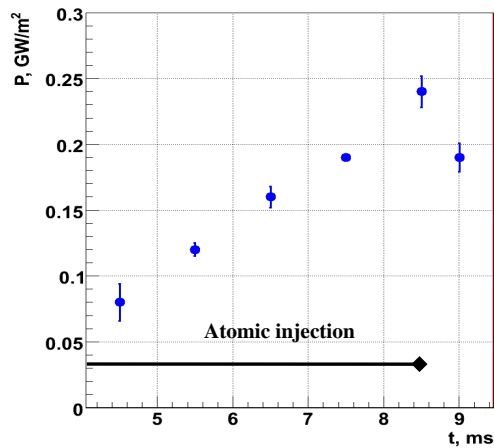


Fig. 4.1.5. The reconstructed from measurements time evolution of thermal power density in the GDT mirror for the plasma gas dynamic regime.

In Figure 4.1.5 shows the calculated from measurements time evolution of thermal power density in the GDT mirror for the plasma gas dynamic regime. We see that at the end of atomic injection (8.5 ms scale in the figure) heat flux density reaches 0.25 GW/m^2 . Thus closest to the linearly increasing pulse shape indicates that for neutral beam injection duration of 5 ms the stationary state is not reached.

4.2. GOL-3 FACILITY

4.2.1. Description and main operation modes of the facility.

The GOL-3 facility is a unique engineering-and-physical complex, which was designed for study of the physics of fast collective plasma heating with a high-power electron beam and the physics of high-temperature plasma confinement in a multiple-mirror open trap. The processes that determine plasma behavior in the trap are characterized with the decisive role of collective and non-linear effects. The scientific program for the year 2012 included several independent lines of research. One of them was the study of generation of sub-terahertz electromagnetic radiation in the vicinity of the double plasma frequency. This radiation arises at strong Langmuir turbulence, which accompanies relaxation of a high-current relativistic electron beam in plasma. Another research direction includes experiments by a new GOL-3 program, in which a long-pulse electron beam of moderate power was injected into plasma. The main results of these works are presented below in this section. Besides, the GOL-3 facility was involved in the research of the physics and technology of collective plasma heating with a high-power electron beam, as well as the influence of high-power plasma flows on constructional materials. In 2012, simultaneously with the experiments by the scientific programs, the development of the experimental base continued.

The appearance of the facility is shown in Fig. 4.2.1. The main solenoid consists of 103 independently fed coils and has a total length of about 12 m. In a standard multiple-mirror configuration, a magnetic field has 52 corrugation periods (cells of the multiple-mirror system) with a field of 4.8 T in the maxima, 3.2 T in the minima, and a cell length of 22 cm. The mirror ratio of the corrugation trap is 1.5, i.e. the facility operates in the "medium-corrugation" mode. The solenoid ends with single magnetic mirrors with a field of 8 – 9 T. The exit unit of the facility consists of an initial plasma source and an expander with the end beam collector. In the expander area, the magnetic field decreases smoothly to 0.05 T, so that the specific energy density on surface decreased to a value allowing application of metals as receiving surfaces.

A typical scenario of experiment in a standard GOL-3 configuration is as follows. A few gas-puff valves in a metal vacuum chamber $\varnothing 10$ cm placed inside a solenoid create a desired longitudinal distribution of the density of hydrogen or deuterium. Then a special longitudinal discharge creates an initial plasma of a length-averaged density varying in the range of $(1 - 30) \times 10^{20} \text{ m}^{-3}$ and a temperature of ~ 2 eV. After that, a relativistic electron beam generated by U-2 accelerator is injected into the plasma. The beam has the following parameters: the electron energy is 0.5 - 0.8 MeV; the current is 20 - 25 kA; the base duration is 8 - 12 μs ; the energy content is up to 120 kJ; the beam diameter is 4.1 cm (this is a figure for a 3.2 T magnetic field, corresponding to the minima of the corrugated field). Such a beam is formed in a slit relativistic



Fig. 4.2.1. Photo of the GOL-3 facility.

diode, and then the magnetic system of the accelerator compresses and converts it into a circular beam. Under collective heating and in optimal regimes, the plasma can reach an ion temperature of the order of 2÷3 keV (in the hottest part of the plasma column). Due to the multiple-mirror confinement scheme (corrugated magnetic field), the hot plasma can be confined for a much longer time than in a simple solenoidal trap.

In 2012, a series of experiments were carried out for the first time in a radically new mode of injection of electron beam of energy of ~ 80 keV, power of up to 10 MW and duration over 100 μs into a multiple-mirror trap. The technology for generation of such electron beams, which are suitable for injection into a plasma trap, i.e. resistant to a high-power plasma flow out of the trap, had been refined on a special stand in a few years.

4.2.2. Terahertz radiation at relaxation of relativistic electron beam.

Investigation of the generation mechanisms and peculiarities of electromagnetic spectrum of emission from plasma under strong Langmuir turbulence, which occurs at intense relaxation of electron beam in the plasma, is one of important fundamental problems of the plasma physics. Besides, it is one of the main problems of astrophysical observations, since the radio emission of astronomical plasma objects such as the Sun is of plasma nature and these phenomena are defined by processes similar to those occurring under turbulent plasma heating in open magnetic systems.

In 2012, the GOL-3 facility remained involved in experiments on generation of subterahertz electromagnetic radiation at relaxation of a relativistic electron beam in plasma. A detailed examination of the evolution of the emission spectrum showed it to depend on the plasma density. So, during injection of the electron beam, see Fig.4.2.2, the generation band shifts with time towards higher frequencies. This fact may be due to the increase in the plasma density during injection of the beam into the plasma, which is confirmed by measurements of average plasma density by interferometry (Fig. 4.2.3).

This fact made it possible to find a mode of GOL-3 operation in which relaxation of a relativistic electron beam in a plasma is accompanied by electromagnetic emission near 0.5 THz, see Fig. 4.2.4.

Since the observed emission is associated with the presence of Langmuir turbulence in the plasma area occupied by the electron beam, the total energy registered with subterahertz radiation detectors can be identified with the electric field value in this area.

4.2.3. Motivation for injection of long-pulse electron beam into multiple-mirror trap.

In 2012, the GOL-3 operation mode was changed, which meant switching to a new system of generation and injection of an electron beam into plasma. These experi-

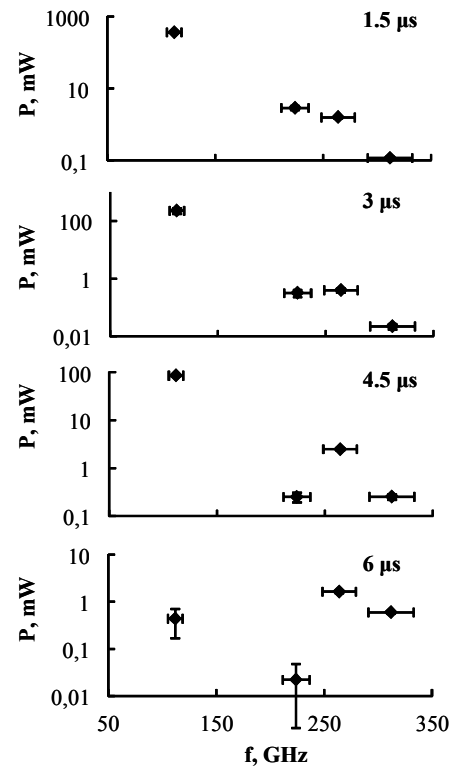


Fig. 4.2.2. Spectra of plasma electromagnetic emission for different times after the beginning of the electron beam injection.

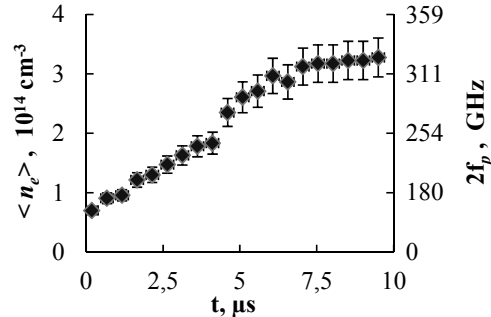


Fig. 4.2.3. Evolution of plasma density from CO_2 interferometry. The right-hand scale corresponds to values of average plasma density recalculated to the double plasma frequency.

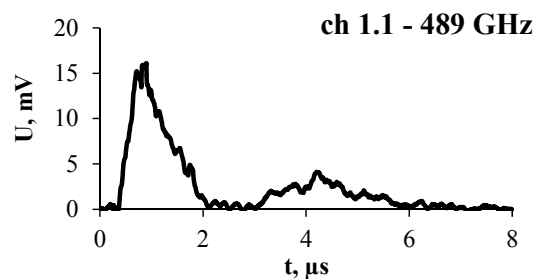


Fig. 4.2.4. Emission dynamics in the 489 GHz spectral channel at relativistic electron beam relaxation in GOL-3.

ments are to demonstrate the possibility of injecting a long-duration electron beam into plasma. The physical program of the research includes both experiments to achieve a quasi-stationary state of plasma in the GOL-3 facility and works to clarify some assumptions to be used in the physical design of a new-generation open trap.

This line of research implies a principal ability of work with stationary injection of electron beam, and therefore it was necessary to create an electron beam source of a moderate power, about 10 MW, capable to operate in an incoming plasma flow. The long-pulse electron beam injection gives a possibility of using other conventional methods of plasma heating, such as neutral injection and RF heating.

Analysis of possible technical solutions showed that the requirements imposed can be met with a scheme of generation in multi-aperture electron-optical system (EOS) with a plasma cathode. This generation scheme has additional features of the presence of a rather strong longitudinal magnetic field, which affects the operation and parameters of the plasma generator, and the necessity for magnetic compression of the electron beam at least 100 times relative to the current density, for the trap to provide an acceptable ratio of the beam electron density to the plasma density.

4.2.4. Source of long-pulse electron beam with plasma emitter.

The scheme of the injector is shown in Fig. 4.2.5. High-voltage electrode (1) of stainless steel is mounted on

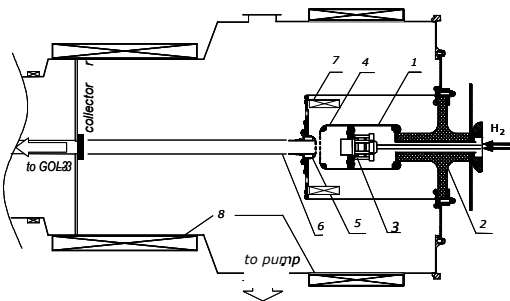


Fig. 4.2.5. Diagram of the beam generator in the expander tank of the GOL-3 facility.



Fig. 4.2.6. General view of the EOS electrodes. Left: cathode; right: anode.

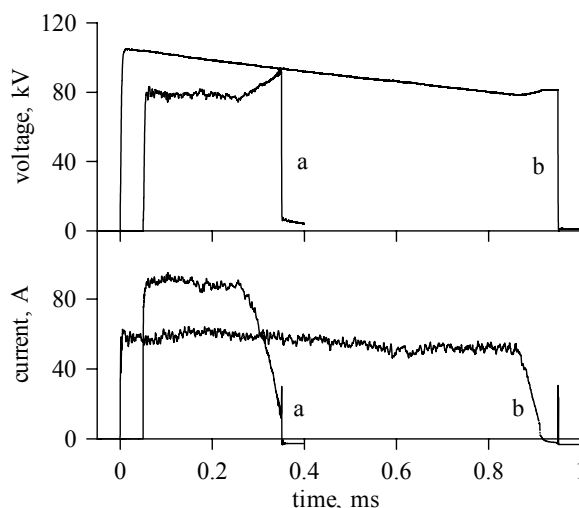


Fig. 4.2.7. Typical waveforms of the beam obtained at work with the collector at a current of ~ 90 A (a) and a maximum duration of ~ 0.9 ms (b).

Plexiglas bushing (2) for a working voltage of up to 150 kV. The beam electrons are extracted from a plasma produced by a pulsed arc discharge in hydrogen. Cold-cathode arc generator (3) is located within the high-voltage electrode. A cylindrical arc channel is made of a set of copper washers, which are insulated from each other. Stabilization of discharge in the arc channel is provided by a magnetic field of ~ 0.1 T, the field is generated by a proprietary small coil.

Emission plasma expander (4) works as a hollow arc discharge anode. At its end there is a molybdenum insert with 241 circular emission apertures (see Fig. 4.2.6). The apertures are arranged in a hexagonal order. The extraction electrode, which also is the anode of diode (5), is grounded and also has 241 openings. Accelerated electrons are transported through drift tube (6) to the metal collector (in the series of test experiments) or to the plasma chamber of GOL-3. A magnetic field (10 - 100 mT) in the vicinity of the injector and drift tube is created by inner vacuum coil (7) of the injector and external coils on the end tank (8).

The power and control electronics of the arc discharge generator are mounted in a Faraday cage, located near the beam source and being under an accelerating potential. An acceleration voltage pulse is generated by a high-voltage capacitor bank and two spark gap switches: the primary and crowbar ones (the latter also serves as protection at the diode breakdowns).

The source was placed in the end expansion tank of GOL-3 and replaced the output beam collector that was used in previous experiments with the relativistic electron beam from the U-2 generator. Typical waveforms of shots in preparatory experiments, where the beam was dumped to the metal collector at 1 m from the diode, are shown in Fig. 4.2.7. Note that the pulse duration was preset in these experiments, and beam generation was stopped when the plasma source was switched off.

4.2.5. Injection of long-pulse electron beam into GOL-3.

The distance from the injector diode to the first input magnetic mirror was about 2 m; the expansion tank was about 1 m in diameter. For reduction of the effect of volume charge, the beam was passed to the magnetic mirror via a metal drift tube of 0.1 m in diameter

The magnetic field in the drift channel from the injector to the first inlet magnetic mirror grew fairly slowly, which allows one to consider the beam compression process in an adiabatic approximation. While the beam was injected, deuterium was puffed into the chamber. The gas puffing was carried out using a pulsed valve located eight meters from the source. Variation in the initial pressure and beam delay relative to the gas puffing ensured a desired distribution of gas density along the facility. The delay varied in the range of 50 - 200 ms. The solid curve in Fig. 4.2.8 shows the distribution of the gas in the chamber of the facility for a typical delay of 50 ms. The configuration and size of the magnetic field were also varied. The field in the source was changed from 10 to 20 mT, and the average field of the solenoid was altered from 0.35 T to 2 T, which corresponds to a range of mirror ratios from 20 to 200.

The injected electron beam had the following parameters: an energy of 70 - 100 keV, a beam current of 15 - 100 A, an injected beam energy of up to 1 kJ, a pulse duration of 300 ms, and a beam power of up to 10 MW. The initial density of the emission current was up to 20 A/cm². After passing through the chamber of GOL-3, the beam arrived to a tantalum collector 12 m from the beam source.

The electron beam generated plasma in the facility from the deuterium puffed. The regular plasma generation system of GOL-3 turned out to be incompatible with the first version of the new electron beam generator because of the strong gas-and-plasma flow that was produced towards the diode and resulted in a breakdown of the latter.

The gas is ionized in the beam cross-section while the beam is transported through the facility. The plasma density dynamics at an observation point is defined by the balance of the processes of local ionization of the gas puffed, gas inlet from the area free of the beam and the plasma flow along the magnetic field. The beam occupied only a small portion of the vacuum chamber, and thus the recombination processes influenced largely the time of plasma confinement. It is planned in future to change from gas puffing to plasma created in advance with a special generator, which is under development now.

The total current flowing in the plasma chamber was measured with Rogowski coils at 8 different positions along the length. The amplitude and shape of currents measured at various points were almost identical, which attests to the fact that in these experiments, there was no current leak across the magnetic field. In most cases, the amplitude of measured net current was 30 - 50% of the injected beam current. The beam current may be (as in the

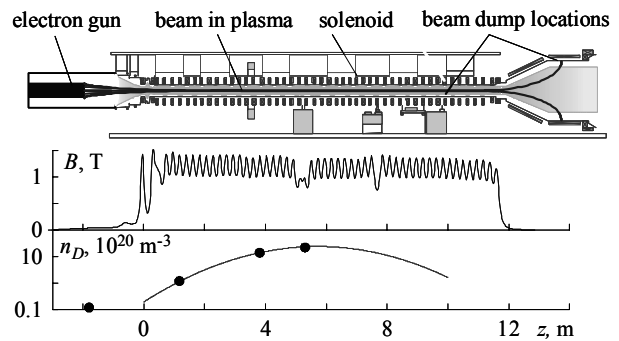


Fig. 4.2.8. Top: diagram of the experiment. Middle: typical distribution of magnetic field along the length of the facility. Bottom: typical initial distribution of deuterium concentration along the length of the facility.

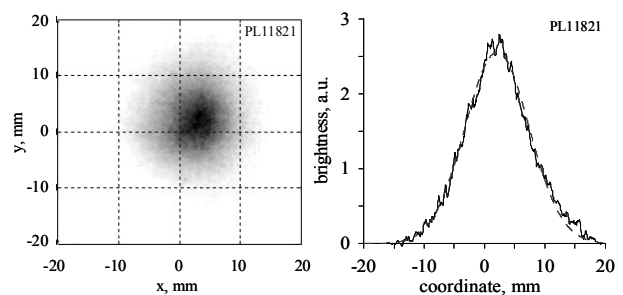


Fig. 4.2.9. Beam imprint on the collector (at 12 m from the source), made with a pinhole camera. The mean of B is 1.24 T. The dotted line shows a Gaussian-profile approximation.

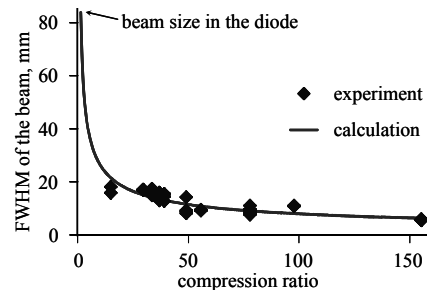


Fig. 4.2.10. Beam transverse size vs. compression factor. Dots: experimentally-obtained transverse dimensions of the beam. Solid line: calculated curve.

case of a relativistic electron beam) partially neutralized by the return plasma current. However, the discrepancy between the beam current and the current flowing through the plasma chamber can also be explained by reflection of some electrons from the entry magnetic mirror.

Beam stability during its transport was tested in experiments with fast X-ray pinhole camera. Fig. 4.2.9 shows a typical X-ray image of the beam on the tantalum collector. The beam imprint size is in a reasonable agreement with the expected value calculated in an assumption of adiabatic motion of the beam in the magnetic field (see Fig. 4.2.10).

Data from an array of Mirnov coils and a speed video camera denote rapid rotation of magnetic disturbances in the middle part of the plasma chamber. However, such small-scale movements in the central part of the chamber remained at a safe level and did not lead to a beam dump on the vacuum chamber wall.

4.2.6. Plasma heating.

Beam injection into deuterium leads to its ionization, and then heating of the resulting plasma. Fig. 4.2.11 presents typical diagnostic signals for a beam shot with an injection power of 1.7 MW. The start of injection is followed by a transition period of plasma formation in the trap. Depending on parameters, this phase lasts for 15 - 30 μ s, and then a quasi-steady state sets. Diamagnetic signals remain almost constant both in time and along the length of the facility. The current along the axis of the plasma chamber also varies only slightly. The power of bremsstrahlung from the collector corresponds to the beam current, from which one can conclude that the degree of beam relaxation stays almost unchanged during a shot.

In these experiments, we also used special microwave diagnostics that detects emission at a double plasma frequency. This emission is a reliable indicator of strong Langmuir turbulence induced by the beam at its relaxation in the plasma. The radiation signal is lasting for a significant part of the shot (Fig. 4.2.11).

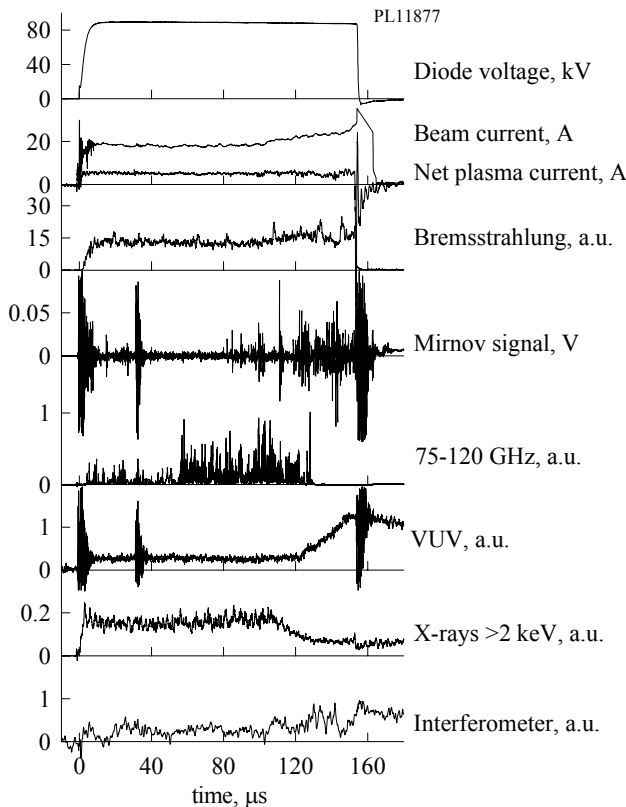


Fig. 4.2.11. Typical waveforms for a beam of a power of 1.7 MW ($n_e \sim (0.5 - 0.9) \times 10^{20} \text{ m}^{-3}$; $\langle B \rangle = 1.24 \text{ T}$.)

Closer to the end of the beam injection, the VUV radiation from the plasma area begins increasing, which is apparently due to the local density growth, which in turn leads to reduced beam-plasma interaction and decreasing intensity of detected electromagnetic radiation (as the frequency of the radiation varies as the square root of plasma density). We also observed soft X-ray radiation from the plasma, associated with formation of fast electrons. The lifetime of such electrons in the trap is up to 1 ms, which is confirmed by the fact that the soft X-ray emission from the plasma remains for this time after the end of beam injection (Fig. 4.2.12).

Data obtained from the Thomson scattering also suggest collective relaxation of the beam as the recorded energy distribution of plasma electrons deviates from the equilibrium distribution. However, at the Maxwell approximation of the core (low-energy part) of the measured distribution, the electron temperature in the center of the beam-plasma column (depending on the mode) is in the range of 20 to 100 eV. Registered via the Thomson scattering, the plasma density in the beam cross-section amounts to $10^{19} - 10^{20} \text{ m}^{-3}$, and the radial density profile is constant. Note that a typical signal of diamagnetism of beam-heated plasma (the radial profile data taken into account) gives an average energy of an electron-ion pair of 100 - 150 eV. Several diagnostics allowing estimation of the ion temperature show that the major part of plasma energy is still contained in fast electrons.

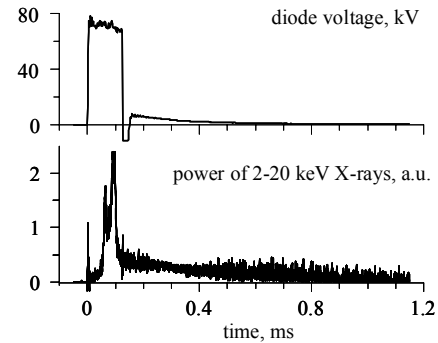


Fig. 4.2.12. Waveforms of the accelerating voltage (top) and soft X-rays in the energy range of 2 - 20 keV (bottom).

4.2.7. Microwave radiation at relaxation of weakly relativistic electron beam.

One of the major demonstrations of interaction of prolonged beam with the plasma was the direct observation of intense generation of electromagnetic radiation in the range of 50 - 200 GHz, which is an indirect indication of energy transfer from the electron beam to the plasma in a turbulent way (see Fig. 4.2.13). The strong irregularity of the detector signals is another evidence of possible formation of dynamic dips in the plasma density (plasma cavities), which follow the Zakharov mechanism, during the development of Langmuir turbulence in the plasma.

Operation with such electron beam makes it possible to obtain experimental observations of emission of electromagnetic radiation for a fairly wide range of the guiding magnetic field of the solenoid, which is equivalent to changing the level of the electron beam compression. In the first experiments on changing the guiding magnetic field it was found that its growth is accompanied by an effective increase in the level of emission of electromagnetic radiation from the plasma. So, for example, at a guiding magnetic field of 0.7 T the power of radiation on the detector is $\sim 8 \mu\text{W}$, while for a field of 1.24 T this

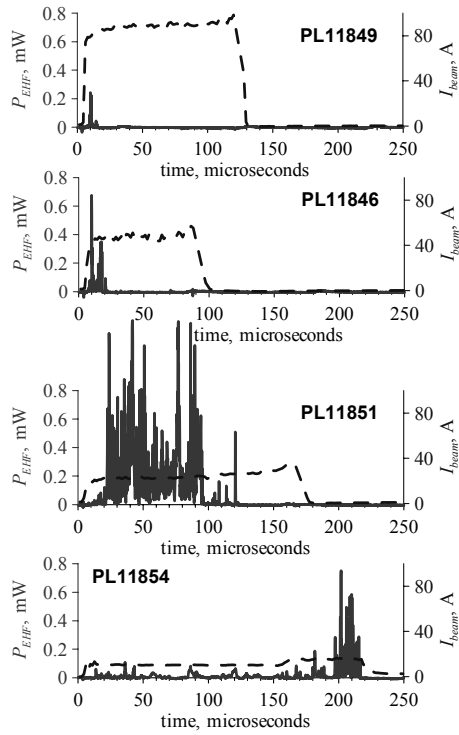


Fig. 4.2.13. Detected power of emission of electromagnetic radiation in the range of 75 - 120 GHz (solid line) for different values of the electron beam current (dashed curve).

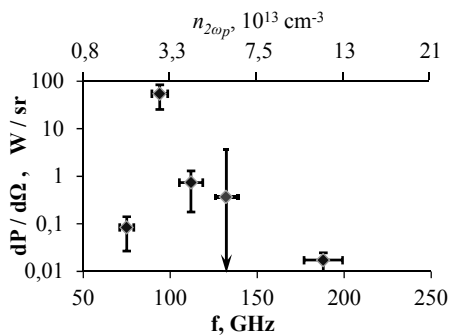


Fig. 4.2.14. Distribution of the power of electromagnetic radiation from the plasma, averaged over the spectral channels of the frequency-selective four-channel quasi-optical system for experiment conditions corresponding to the maximum emission ability of plasma in the given frequency range (the total electron beam current is $25 \pm 3 \text{ A}$; the magnetic field value is 1.24 T).

value is 0.25 mW, and the mode of operation for electron beam generation remains unchanged.

It is important to note that the magnitude and duration of the current of the beam injected into the plasma directly influences both the level of electromagnetic radiation in the microwave range and the time of generation of radiation from the plasma (see Fig. 4.2.13). In particular, it was found that for a magnetic field of 1.24 T at the observation point, the local maximum of the detected power of electromagnetic radiation is observed at a beam current of $\sim 25 \text{ A}$ and is $\sim 4 \text{ mW}$ on the detector. When recalculated to the experimental geometry, the corresponding specific output power of radiation equals $\sim 0.9 \text{ kW/cm}^3$ under an assumption of isotropic distribution. As a result, evaluating the length of the emitting area of the plasma as $\sim 1 \text{ m}$, we obtain an estimate of the total radiation power from the plasma of $\sim 10 \text{ kW}$, which corresponds to approximately 0.5% of the total power of the electron beam.

Thus, a systematic analysis of experimental data on heating of a plasma with the density $n_e = 10^{19} - 10^{20} \text{ m}^{-3}$ in the magnetic field $B = 0.26 - 1.8 \text{ T}$ was performed in 2012 with an electron beam of an energy of 50 - 90 keV, a beam current density of 10 - 180 A/cm^2 and duration of up to 0.1 ms. This analysis revealed dependencies in the formation and evolution of electromagnetic radiation generation during injection of an electron beam in plasma.

From the results of diagnostics of plasma density by the Thomson scattering it was found that interaction of a submillisecond electron beam with a cold plasma is accompanied by formation of a plasma with a density of $3 \times 10^{19} \text{ m}^{-3}$, which corresponds to the plasma frequency $f_p \approx 49 \text{ GHz}$. Since the detection system applied uses detector sections with a transitional input waveguide window that defines a cut-off in the frequency sensitivity band of detectors for 70 GHz or less, it was impossible to observe radiation in the vicinity of the first harmonic of the plasma frequency.

Spectral studies of the microwave radiation in the vicinity of the double plasma frequency revealed a narrow peak in the electromagnetic radiation spectrum in the vicinity of $f \approx 94 \text{ GHz}$, with the width $\Delta f \leq 15 \text{ GHz}$, see Fig. 4.2.14. At a magnetic field of 1.24 T and electron beam current of $\sim 25 \text{ A}$, the power of microwave radiation in the local maximum is $\sim 10 \text{ kW}$.

4.2.8. Summary of the GOL-3 results.

The GOL-3 facility remains involved in experiments aimed at the creation of a physics knowledge base required for construction of an open-trap fusion reactor. The quality of information obtained is improved due to both implementation of new diagnostics techniques and conduction of problem-oriented experiments. New technologies of plasma heating, which will improve plasma parameters, are being developed. Applied research was also conducted in various directions. Further plans include the improvement of the electron beam source and creation of a new source of initial plasma and neutral beam injection system.

4.3. PLASMA THEORY

4.3.1. *Alfven ion-cyclotron instability*

The Alfven ion-cyclotron instability conditions in gas-dynamic trap with sloshing ions are studied in the works Yu.A. Tsidulko, I.S. Chernoshtanov, in proc. of XXXVIV International conf. on plasma physics and CTS, Zvenigorod, (2012) and I.S. Chernoshtanov, Yu.A. Tsidulko, In Proc. of 9th International Conference on Open Magnetic Systems for Plasma confinement, Tsukuba, Japan, August 27-31, (2012).

The AIC instability excitation is resulted from inverse population of resonant ions, which have longitudinal velocity satisfying resonant condition $v_{||res} \approx (\omega - \Omega_{ci})/k$. The total contribution of resonant particles can be destabilizing only in the sloshing ion injection area $v_{||inj} \approx v_{||res}$, which results in the experimentally verified relation of the wave length with injection longitudinal velocity and frequency. The stability threshold is strongly depends on injection details, in particular angle and energy dispersion. The distribution “tail”, arising because of drag and scattering, gives the main contribution into the plasma density and pressure. The threshold weakly depends on the details of the tail area, only integral contributions of the tail is important.

Another taken into account peculiarity of the problem is possibility of the wave dissipation in the plasma periphery, which can significantly enhance the stability threshold.

The used approximation of the distribution function allows to take into account the distribution function details in the injection area and to make analytical continuation of the dispersion relation in z, r, ω and k complex planes. The last is necessary for searching absolute instability threshold and the wave stop points in WKB method.

According to preliminary data (experimental studying is in progress) the main results of the theory are in agreement with the experimental results (P.A. Bagryanskiy, M.S. Korzhavina, V.V. Prikhodko and K.V. Zaytsev, In Proc. of 9th International Conference on Open Magnetic Systems for plasma confinement, Tsukuba, Japan, August 27-31, (2012)).

4.3.2. *Development of the theory of electron cyclotron heating*

Propagation of an extraordinary electromagnetic wave in the vicinity of electron cyclotron resonance surface in an open linear trap is studied analytically, taking into account inhomogeneity of the magnetic field in paraxial approximation. Ray trajectories are derived from a reduced dispersion equation that makes it possible to avoid the difficulty associated with a transition from large propagation angles to the case of strictly

longitudinal propagation. Ray trajectories have been found in analytic form. An analysis of these trajectories has demonstrated that the inhomogeneity of both the magnetic field strength and the field direction can qualitatively change the picture of wave propagation and significantly affect the efficiency of electron cyclotron heating of a plasma in a linear magnetic trap. A criterion for the resonance point on the axis of the trap to be an attractor for the ray trajectories has been found.

As an example, the results of general theory are applied to the electron cyclotron resonance heating experiment which is under preparation on the Gas Dynamic Trap in the Budker Institute of Nuclear Physics.

4.3.3. *Theory of electromagnetic emission generated in a turbulent plasma*

The power of second harmonic electromagnetic emission is calculated for the case when strong plasma turbulence is excited by a powerful electron beam in a magnetized plasma. It is shown that the simple analytical model of strong plasma turbulence with the assumption of a constant pump power is able to explain experimentally observed bursts of electromagnetic radiation as a consequence of separate collapse events. It is also found that the electromagnetic emission power calculated for three-wave interaction processes occurring in the long-wavelength part of turbulent spectrum is in order-of-magnitude agreement with experimental results.

The generation of terahertz electromagnetic radiation due to the coalescence of upper-hybrid waves in the long-wavelength region of strong plasma turbulence driven by a high-current relativistic electron beam in a magnetized plasma is investigated. It is shown that the power density of electromagnetic emission at the second harmonic of plasma frequency in the terahertz range for these laboratory experiments can reach the level of 1MW/cm³ with 1% conversion efficiency of beam energy losses to electromagnetic emission.

4.3.4. *Two-dimensional simulations of nonlinear beam-plasma*

Nonlinear interaction of a low density electron beam with an uniform plasma is studied using two-dimensional particle-in-cell simulations. We focus on formation of coherent phase space structures in the case, when a wide two-dimensional wave spectrum is driven unstable, and we also study how nonlinear evolution of these structures is affected by the external magnetic field. In the case of isotropic plasma, nonlinear buildup of filamentation modes due to the combined effects of two-stream and oblique instabilities is found to exist and growth mechanisms of secondary instabilities destroying the Bernstein-Green-Kruskal-type nonlinear wave are identified. In the weak magnetic field, the energy of beam-excited plasma waves at the nonlinear stage of beam-plasma interaction goes predominantly to the short-

wavelength upper-hybrid waves propagating parallel to the magnetic field, whereas in the strong magnetic field, the spectral energy is transferred to the electrostatic whistlers with oblique propagation.

4.3.5. Optimization of the reactor based on the open trap

Further development of the program of mirror traps in BINP needs analysis of its perspectives, in particular, of the end-product of the program, the fusion reactor, that can be constructed. Significant progress in plasma parameters of open traps in recent years is in conjunction with deviation of their regimes from ambipolar confinement, so that most of previous projects of tandem-mirror reactors do not apply. Multi-mirror and gas-dynamic traps confine dense plasmas in sufficiently long systems. Based on applicable confinement formulas, an approximate mathematical model of burning-plasma reactor is developed. The plasma composition is simulated self-consistently, in accordance with the chosen fuel cycle and the fuel burn-out. The reactor length was used as the optimized function, as the costs of linear reactor grow with its length. The model allowed to determine particulars of the magnetic and other subsystems, that will be developed and tested in future experiments. Estimates show, that the gas-dynamic multiple-mirror systems can be designed to be hundreds of meters (DT-cycle) or up to 3 km long (DD-cycle). However, the plasma radius of such reactors can be very small, of the order of ten centimeters. Such geometry causes significant difference of mirror reactors from toroidal ones: an order of magnitude lower minimal power, lower heat- and neutron loads on the first wall. This would relax requirements to construction materials and operation costs of the reactor.

4.4. BEAM INJECTORS OF HYDROGEN ATOMS AND IONS

4.4.1. Beam Injectors of Hydrogen Atoms

Diagnostic neutral beam injector of hydrogen atoms has been developed for Wendelstein 7-X stellarator, which is currently under construction in Germany. Ion source of the injector forms a beam with a current up to 8.5 A and an energy of 60 keV. Duration of the beam pulse is up to 10 seconds with a different mode of modulation.

4.4.2. Development of powerful continuous injector of beam of fast hydrogen atoms

Works under the project of powerful continuous injector of beam of fast hydrogen atoms with 500-1000 keV energy on the basis of negative ions are continued. The project is based on separate formation and acceleration of negative ion beam. Detailed designing of the basic elements of an injector was completed. Prototype of a source of negative ions of hydrogen is assembled. Experimental test stand for study of formation of intense hydrogen negative ion beam with energy of 120 keV in the ion source was under preparation. The test stand is provided with modern electro-technical and vacuum equipment.

4.5. INSTALLATION GDMT-T

4.5.1 Conceptual design of the GDMT-T facility.

A concept of a new-generation open trap for confinement of plasma with thermonuclear parameters was developed based on new results on plasma confinement in axisymmetric open traps obtained on the BINP plasma facilities GOL-3 and GDL. This installation got a name of GDMT (gas-dynamic multiple-mirror trap). It is a magnetic bottle with multiple-mirror end sections. A system for high-power neutral injection forms a population of sloshing fast ions (Fig. 4.5.1). Plasma confinement in the superconducting multiple-mirror end sections is realized due to stimulation of scattering of ions leaving the trap, because electron beams injected from the ends of the facility excite plasma oscillations.

Construction of a new-generation installation necessitates solution to a series of complex engineering and physical problems. That is why the work will be divided into several stages of creation and testing of some critical elements and systems of the future installation. The first step is to create the GDMT-T facility, which is a multiple-mirror end section of the GDMT installation with the output expansion tank and electron beam generator. In addition to scientific problems that are directly associated with the development of the new open trap for fusion research, this installation can be an effective and popular stand for experiments on the interaction of high-power plasma flows with surface and testing elements of plasma dumps of fusion facilities.

GDMT-T is schematically shown in Fig. 4.5.2. The central part of the installation is a superconducting solenoid, which is a prototype of the end section of GDMT. The central solenoid is connected to the expansion tank with the electron beam generator and the test chamber with samples to study. One of the diagnostic intervals of the central solenoid hosts a system for generation of steady-state plasma flow on the basis of helical microwave dis-

charge at a frequency of 915 MHz. The system generates a plasma with density of up to 10^{20} m^{-3} and a temperature of 1-10 eV, which enables a plasma flow with a power density of up to 10 MW/m^2 and a particle flux density of 10^{24} m^2 on a sample of an area of 7 cm^2 . Additional repetitively pulsed plasma heating with electron beam injection (100 keV, up to 100 A) results in a hundred-fold increase in the power density on the target during the injection (1-5 ms). This allows one to simulate the effect of plasma on divertor plates of reactor-class tokamak in operating with pulse-periodic load (ELM modes). Pulse-periodic loads can otherwise be generated with a gyrotron system of electron-cyclotron heating of plasma.

4.5.2. Superconducting magnetic system.

The magnetic system of the installation consists of three identical superconducting solenoids with a length of 1.6 m and an aperture of 160 mm. Additional warm coils are used for generation of relatively weak magnetic fields in the area of the electron beam generator. The structure of the solenoid is based on BINP developments in the field of superconducting elements for sources of synchrotron radiation. In particular, modern approaches and achievements in the field of cryogenic technology can reduce heat leakage to a cryostat and drastically decrease liquid helium consumption.

Possible configurations of magnetic field in GDMT-T are shown in Fig. 4.5.2. Since these solenoids are planned to be used as end sections of the GDMT facility, the solenoids can generate both a corrugated field and a quasi-uniform one. Each solenoid consists of two coils: the external one, creating a constant magnetic field, and the inner one, consisting of seven sub-sections with opposing connection of adjacent subsections. This allows generation of a multiple-mirror magnetic field.

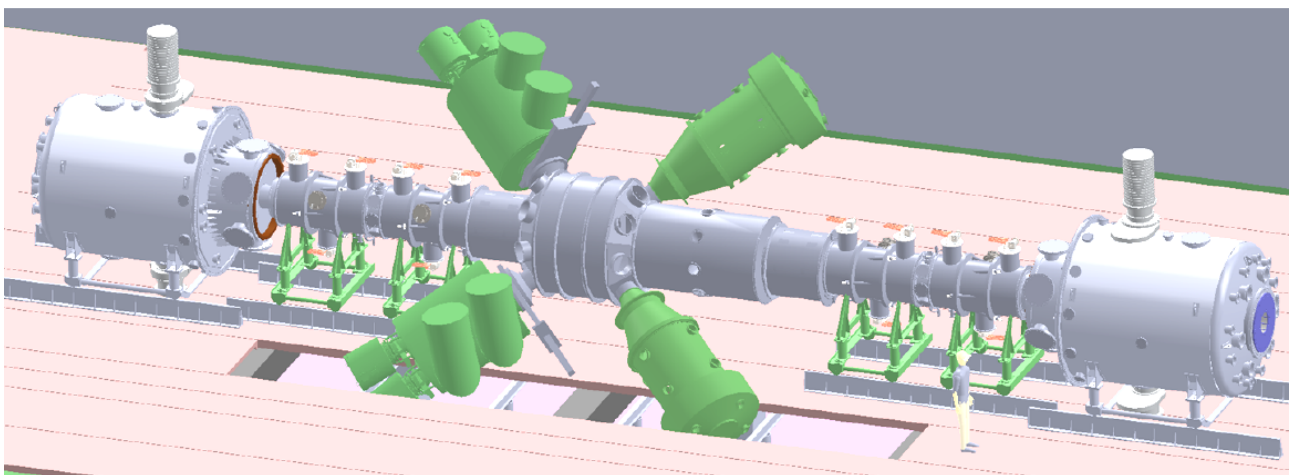


Fig. 4.5.1. GDMT installation.

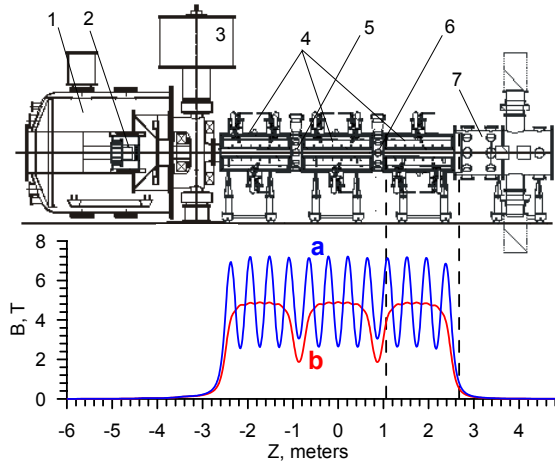


Fig. 4.5.2. Top: scheme of GDMT-T. 1 - the expansion tank; 2 - the electron beam generator; 3 - the cryopump; 4 - the superconducting solenoids, 5 - diagnostics interval I with the steady-state plasma system; 6 - diagnostics interval II (targets and the ECR heating system); 7 - the test chamber. Bottom: possible configurations of magnetic field of the installation. a - a multiple-mirror configuration, b - a quasi-homogeneous magnetic field configuration.

When both (internal and external) coils are switched on, the solenoid creates a multiple-mirror magnetic field with a maximum field of 7.2 T and a mirror ratio of 2.6. A configuration with quasi-uniform field, which is achieved with only the external coil switched, is more preferable for experiments on interaction of plasma with surface. In this case, varying the current in the coil of the third (output) solenoid, one can regulate the magnetic field and thus the power density on the target.

4.5.3. Production of steady-state plasma flow.

RF heating of plasma is widely used for generation of steady low-pressure discharges. The GDMT-T installation assumes generation of plasma flow with a helical discharge, which occurs when fast helical waves are excited in a magnetized plasma with collisional damping. A magnetron with an operating frequency of 915 MHz can serve as a microwave power source. These magnetrons, widely used in the industry, have high efficiency, high output power (up to 100 kW) and a relatively low cost. Simulation of absorption of microwaves in the plasma shows that at the selected operating frequency, the system can be used for generation of plasma flows at magnetic fields of up to 2-5 T and a plasma density of up to 10^{20} m^{-3} .

A scheme of possible mounting of a helicon antenna is shown in Fig. 4.5.3. Because of the high plasma density and high magnetic field, the characteristic wavelength in the plasma is several centimeters, which hinders the use of antennas of traditional configurations (helicon, saddle, of the Nagoya type, etc.).

A double half-turn antenna seems to be more promising. Such antenna excites a symmetric helicon mode $m = +1$ (m is the azimuthal wave number, and the plus sign

means that the wave rotates in the same direction as the magnetized electrons of the plasma do). Microwave power is transmitted to the antenna through a coaxial input with a bore for cooling fluid.

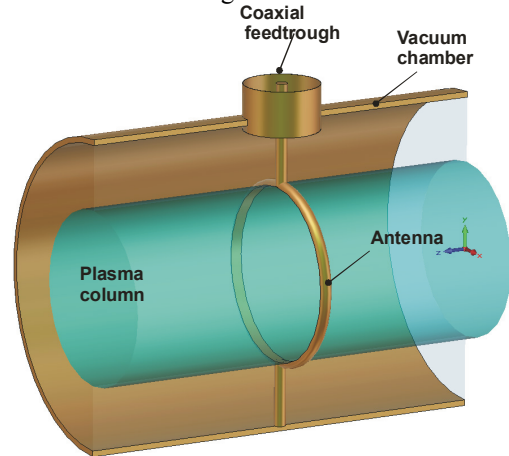


Fig. 4.5.3. Antenna unit for plasma generation.

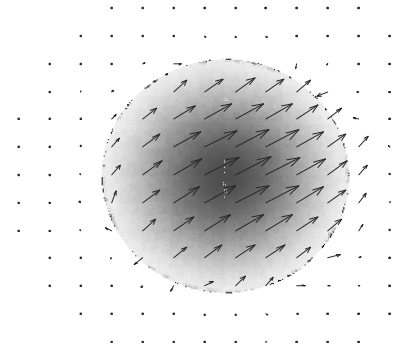


Fig. 4.5.4. Electric field configuration (arrows) and microwave power absorption in plasma due to collisions (fill) for the mode $m = +1$ in the GDMT-T facility.

The field structure and dispersion characteristics of various oscillation modes were numerically simulated for the actual geometry of the GDMT installation at different plasma parameters. In these calculations, plasma was modeled as an anisotropic continuum with a complex dielectric tensor, i.e. the vacuum chamber was a circular waveguide partially filled with a gyrotropic medium. The transverse structure of the electric field and the amount of power absorbed for the mode $m = +1$ is shown in Fig. 4.5.4. In a 2 T magnetic field, which corresponds to the field in the antenna area, the oscillation wavelength for the given mode is 2.5 cm and the length of collision absorption is about two meters, which is comparable with the length of the GDMT-T installation.

It should be noted that these calculations do not take into account the effects of excitation of slow long-wave surface oscillations (the Trivelpiece-Gould modes). These oscillations can also be excited in a helicon discharge. In this case, the length of absorption of the Trivelpiece-Gould modes is a few centimeters, which greatly increases the overall efficiency of plasma heating.

4.5.4. Electron beam generator:

For experimental simulation of pulsed loads on the plasma dumps of the ITER tokamak divertor, the targets must be exposed to plasma flows with a power density of 0.5-4 MJ/m² per pulse of 0.3-0.6 ms, i.e. the system of plasma heating shall provide an energy deposition to the plasma of a power of about 1 MW per millisecond pulse with a relative pulse duration of 100-1000. Such flows can be created in several ways, in particular by means of neutral injection or electron-cyclotron plasma heating with gyrotrons.

Pulsed plasma heating was provided mainly with an electron beam injected into the plasma through one end of the installation. This choice was determined by the acquired experience in creation of electron-beam generators with similar parameters on the GOL-3 facility and the importance of further development of this technology for the GDMT installation.

The electron beam generator is a multiple-aperture vacuum diode with arc plasma emitter. The energy of electrons in the beam is taken to be 100 keV, which is optimal from the point of view of achieving small angular spread, efficiency of beam-plasma interaction and simplicity of the power system. For decrease in the density of particle flux from the plasma, the generator shall be placed in a low magnetic field. In this case, the possible beam compression in the magnetic field is limited with the angular spread of electrons in the beam and amounts $B_{\max}/B_0 \sim 200$, which determines the magnetic field magnitude in the 0.03-0.04 T beam generator. Then the equivalent current of ions from the plasma in the beam generator is reduced to a value of 0.1 A/cm². It should be noted that the ion current value is considerably higher than the steady work limit, 20 mA/cm², determined on GDMT in experiments with diodes with incandescent emitters.

At this degree of compression, the electron current density required for influencing the plasma dumps is 5 mA/cm², i.e. the diode shall work in an inefficient mode, the main power spent on acceleration of the counter ion flux. One can overcome this problem via increasing the local density of electron current through beam filamentation and use of more rapid modulation.

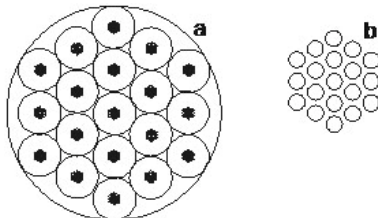


Fig. 4.5.5. Geometry of unit cells in the electron beam generator.

Below is described a diode structure chosen from these considerations. A planar diode of 50 cm in diameter consists of 361 holes combined in 19 groups hexagonally-located within an aperture of 34 cm in diameter (Fig. 4.5.5a). Each group of 2 cm in diameter is powered from

its own arc plasma source and consists of 19 holes, which are the unit cells of the accelerating diode (Fig. 4.5.5b). A unit cell consists of a cathode hole of 3 mm in diameter and an anode opening of 3.6 mm in diameter, with a spacing of 15 mm.

This arrangement of the holes results in the maximum local density of electron current if elementary beams are arranged sufficiently uniformly on the diode surface, with a minimum number of arc units required. It should be noted that experiments on GOL-3 have shown the beam filamentation to disappear after compression in the magnetic field and a beam in a strong field to have a homogeneous structure.

A further increase in the current density can be achieved via fast beam modulation. Preliminary experiments showed that this modulation with a relative pulse duration of ten and a frequency of 10 kHz can be obtained through control of the current of the arc plasma generator.

Increase in the beam current density has an additional advantage of amplified efficiency of the beam-plasma interaction. This interaction shifts the spectrum of the electron beam towards lower energies, which is preferable for experiments on test of components of plasma dumps. The ratio of beam electron concentration to the plasma electron concentration is a critical parameter that determines the efficiency of the beam-plasma interaction. This ratio shall exceed a value of 10^{-3} . With these beam parameters, the beam current density significantly exceeds this limit, which allows efficient transfer of energy from beam electrons to plasma thermoelectrons.

4.5.5. Conclusion.

Implementation of the GDMT-T project will enable creation of a BINP up-to-date stand for research on the plasma-surface interaction. Such stand is required both for implementation of the ITER project and for development of a reactor based on an open trap. Within this project, technical solutions for a reactor-type plasma installation will be tested and physical aspects of plasma confinement in a magnetic field and interaction of high-power electron beams with plasma will be investigated.

A physical project of the installation and main technological components has been developed so far and the design documentation for components of the installation is being prepared. Experiments on the new plant will start in 2015.

4.6. RESEARCH ON GENERATION OF MILLIMETER WAVE RADIATION ON THE ELMI INSTALLATION

4.6.1. Introduction.

Within a research on radiation generation in a single-channel planar free-electron maser (FEM) with two-dimensional distributed feedback, which was performed earlier on the ELMI installation, there was demonstrated

generation of 4 millimeter wave radiation with a power of about 10 MW and duration of 300 ns in single-mode operation at the frequency of one of hybrid Bragg cavity eigenmodes. These results formed the basis for the development of two-step generator of submillimeter wave radiation using a planar FEM consisting of two channels with strip relativistic electron beams (REB). A 4 mm wave radiation in the first (low-frequency) channel shall be generated similarly to generation in the single-channel FEM. In this case, the generated 4 mm wave radiation shall be sent via waveguides to the second (RF) channel of the generator. In this channel, the 4 mm wave radiation will be a pump mode for generation of THz radiation using the second strip beam.

Before the experiments on the two-step generation of terahertz radiation, we carried out experiments on simultaneous generation of 4 mm wave radiation in the two channels of the planar FEM. The purpose of this research was to determine the possibility of exchanging electromagnetic radiation fluxes between the cavities of these two channels to achieve matching of electromagnetic waves in the channels under the conditions of two-dimensional distributed feedback.

4.6.2. Arrangement of the experiment.

Experiments on the generation of 4 mm wave radiation were performed in the two-channel FEM, a scheme of which is given in Fig 4.6.1. The electrodynamic system of each of the two identical channels of the maser was a planar hybrid resonator with a gap between the wall planes of 0.95 cm and a total length of 72 cm. There is a two-dimensional Bragg reflector on the beam entry to the resonator and a one-dimensional reflector at the exit. These reflectors are connected via a segment of a regular waveguide with a 0.95x8.5 cm section and a length of 32 cm. The entry reflector is formed of two Bragg gratings, which are plane-parallel copper plates with two-dimensional surface corrugation in the form of staggered square grooves (Fig. 4.6.1). The surface corrugation period is 4 mm in both directions; the corrugation depth is 170 microns; the length of the corrugated surface is 20 cm. "Cold" electrodynamic measurements have shown the staggered-cut-surface Bragg gratings to have selective properties close to those of gratings with ideal two-dimensional sinusoidal corrugation. Similarly to the case of single-channel FEM, for the purpose of suppression of spurious modes trapped between the walls of the resonator that is closed at the ends, these ends are equipped with corner scatters of transverse wave flows arising in the reflector. Since the main increase in the amplitude of the electromagnetic wave pumped by the electron beam in the resonator occurs after the two-dimensional mirror, the energy loss in the generator associated with the above scattering on the non-regular side surfaces are sufficiently small. The exit reflector consisted of two one-dimensional Bragg gratings with corrugation in the form of parallel rectangular grooves with a period of 2 mm and a depth of 70 m (Fig. 4.6.1). The length of the corrugated surface is 20 cm.

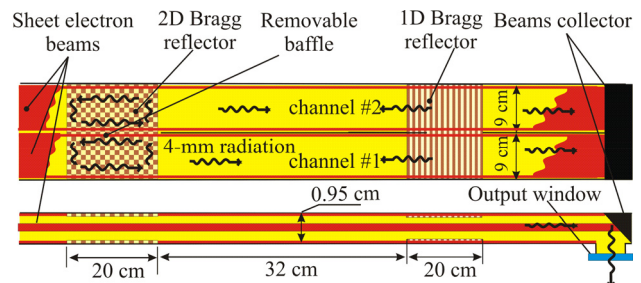


Fig. 4.6.1. Scheme of experiments on generation of millimeter wave radiation in the two-channel FEM.

In the first series of experiments, the FEM channels were separated with a metal bar throughout their length. Even with this separation, there was electrodynamic coupling between the FEM channels in the experiment, because of the scattering of radiation fluxes near the dumps for absorption of electron beams. On the inclined surface of these dumps, the radiation fluxes from the channels were bent for extraction into the atmosphere. There was an option of removing a portion of the bar in the area of the two-dimensional Bragg reflector in order to provide synchronization of radiation generation via combination of transverse radiation fluxes in the two channels.

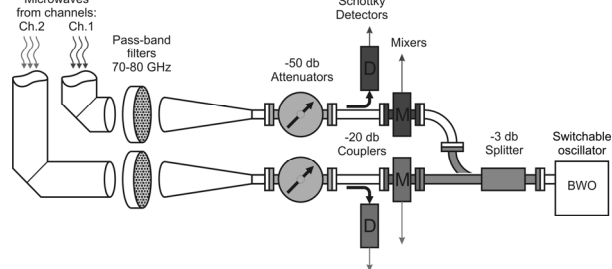


Fig. 4.6.2. Scheme of two-channel heterodyne diagnostics device.

Strip electron beams were generated by two separate cathodes, placed in one common magnetically insulated diode. When beams were passing from the diode to the maser channels, their cross section got compressed in increasing magnetic field. Then the beams were transported through the channels in this guiding magnetic field by a distance of about 1.5 m. At the exit of the channels, the cross-section of the beams gradually increased due to reduction in the magnetic field strength, and then the beams were absorbed by graphite dumps. As noted above, the surface of the dumps was inclined at an angle of 45° to the beam propagation direction in the generation channels. That provided reflection of radiation flux from the channels towards the windows for extraction into the atmosphere. Then, by circular copper waveguides of 9 cm in diameter, the radiation was passed to a noise-immune metallic room, where it was analyzed with the radiation registration system. This system includes detectors "on hot carriers" for registration of behavior of radiation power in the time domain during a generation pulse and a special "TK power/energy meter" calorimeter to measure the total pulse energy. In addition, for measurement of the microwave signal spectrum in four frequency ranges, a

four-channel diagnostics device was fabricated based on waveguide band-pass filters, and for precise spectral measurements we used two-channel heterodyne diagnostics (see a scheme in Fig. 4.6.2.).

4.6.3. Results of research.

In the first series of experiments on generation of radiation in the two-channel FEM, we measured millimeter-wave radiation power vs. undulator magnetic field at several fixed values of guiding magnetic field in the channels of the maser. In these experiments, the maximum voltage across the diode was about 0.8 MV; the beam currents were of a magnitude of 1 to 3 kA; the length of millimeter-wave radiation pulse was up to 0.4 microseconds.

Processing of signals recorded by means of four-channel spectral diagnostics based on waveguide band-pass filters revealed that almost in all shots of this series of experiments, the main portion of FEM microwave radiation power (no less than 70%) is in the spectral range of 74.5 to 75.5 GHz. This interval contains the frequencies of eigenmodes of the hybrid resonator. The rest power is in the frequency interval of 77 to 77.8 GHz, in which a stray coupling of the main TEM mode with mode TM₂ takes place on the one-dimensional corrugation of the exit Bragg reflector. Fig 4.6.3 presents radiation power in the spectral range of 74.5 to 75.5 GHz vs. undulator component of magnetic field at different values of the guiding magnetic field induction. Lines in this figure represent results of theoretical calculations.

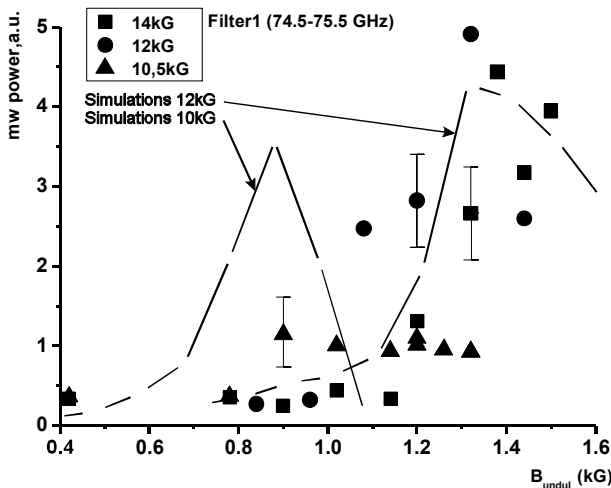


Fig.4.6.3. Mm-wave radiation power in the frequency range of 74.5 to 75.5 GHz vs. undulator field amplitude.

The experiments used a microwave calorimeter for determination of dependences of mm-wave radiation pulse energy on undulator and guiding magnetic fields, which dependences turned out to be similar to those shown in Fig. 4.6.3. A typical value of microwave pulse energy from each FEM channel was 4-6 J, which allowed us to estimate the pulse-duration-average power of the mm-wave radiation, which was - 20-40 MW.

The two-channel heterodyne diagnostics enabled precise measurement of the FEM radiation spectrum in vari-

ous experimental conditions. These measurements have shown that at an arbitrary ratio of the guiding magnetic and undulator fields, in the radiation spectrum, as a rule, there are several lines close to the frequencies of eigenmodes of the resonator. However, if one selects a ratio of the fields and an electron beam energy to meet the resonance condition $\omega - h\nu_{\parallel} = \Omega_b$, where $v_{\parallel} = \beta_{\parallel}c$ is the longitudinal velocity of electron and $\Omega_b = 2\pi\nu_{\parallel}/d_w$ is the frequency of electron bounce oscillations in an undulator magnetic field with a period d_w , a stable single-frequency generation of 4-mm wave radiation is observed in the experiment. Consistency of the electron beam energy near the flat top of voltage across the diode enhances rapid excitation of a single dominant mode in the resonator. Moreover, in such shots, radiation generation in both channels of the FEM occurred at approximately the same frequency and synchronously in the oscillation phase. An example of waveforms of signals registered in one of these shots is shown in Fig. 4.6.4 (a) and Fig. 4.6.4 (b) (enlarged scale).

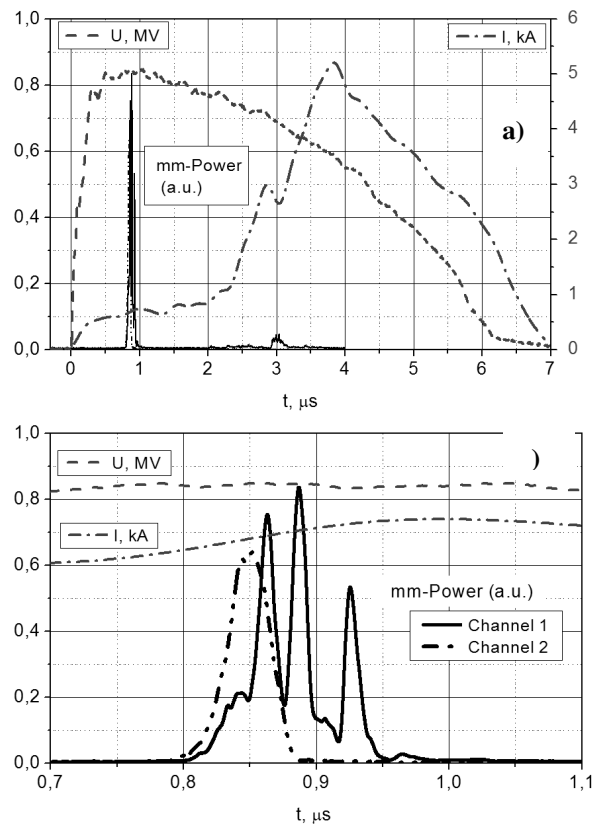


Fig. 4.6.4. Signals of voltage across the diode, current of one of the beams and power of mm-wave radiation in the frequency range of 74-75 GHz in shot # 7671.

The radiation spectrum in this shot shows a stable narrowband generation with a spectral width of ~ 20 MHz at the frequency of one of the modes of the Bragg resonator (Fig.4.6.5). In this case, the typical width of mm-wave radiation pulse was 100 to 200 ns, and the radiation bandwidth was close to the natural width.

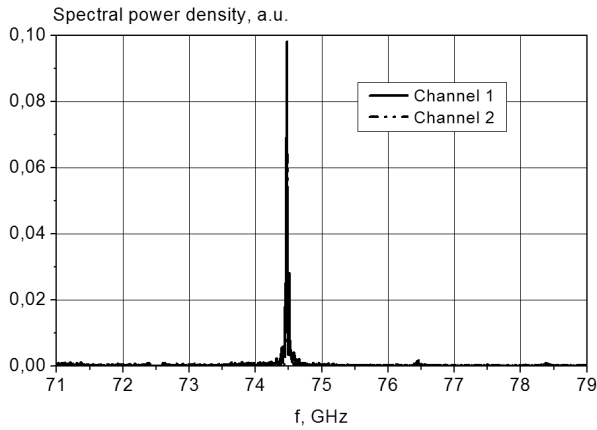


Fig. 4.6.5. Radiation spectrum in shot #7671.

Processing of signals in all shots with single-frequency generation of mm-wave radiation revealed synchronization of electromagnetic waves in both channels of the FEM. Fig. 4.6.6 shows an example of such synchronization of radiation. It presents intermediate frequency signals from mixers that record radiation from the two channels of the FEM. In our view, the synchronism of generation of mm-wave radiation in the two channels of the FEM is provided by the electrodynamic coupling between them due to the scattering of radiation fluxes in the area of the vacuum channels where the radiation fluxes are bent for radiation extraction into the atmosphere.

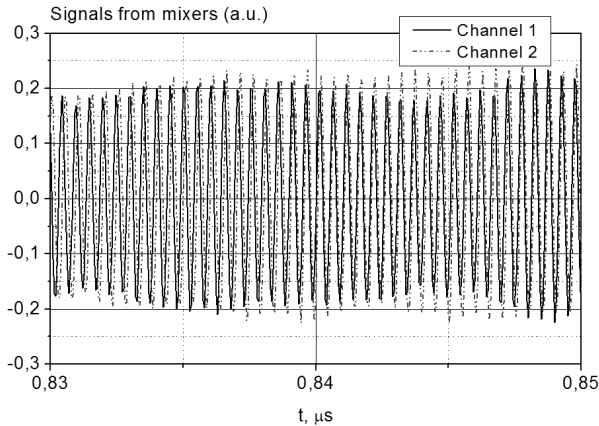


Fig. 4.6.6. Time expanded portion of intermediate-frequency signals received from the mixers used in the measurement of the radiation spectrum in the two channels of the FEM.

4.6.4. Preparation of experiments on two-step generation of terahertz radiation.

To carry out experiments on two-stage generation of THz radiation, we are reconstructing the ELMI facility. A new vacuum chamber with a new system of coils for creation of guiding and undulator fields was designed and fabricated, as well as a new-version electrodynamic system of the maser (for the two-stage scheme of generation). The first test experiments will be carried out in single-pass scattering of millimeter waves. The experimental scheme is shown in Fig. 4.6.7.

In channel № 1, which is a planar FEM with a combined Bragg resonator, a radiation wave with a frequency of about 75 GHz and field structure close to that of TEM wave is generated using the first strip beam. Then the Bragg deflector directs the mm-wave radiation to channel #2, where it is converted inside the planar Bragg converter (Fig. 4.6.7) from the TEM wave to a quasi-critical one, which propagates with a low group velocity towards the second strip beam. Such a wave is a superposition of two plane waves propagating almost perpendicular to the direction of beam motion. Each of them is scattered by the electron beam with frequency conversion from 75 GHz to the range of 600-1000 GHz, depending on the energy of the electrons of the beam, and extracted from the maser by the transport beam line through a window to the atmosphere. Such a scheme was chosen for increasing the coupling of the electrons of the beam with the scattered wave and for reducing the Doppler frequency conversion, which allows one to measure the spectrum of the scattered radiation using the existing diagnostics equipment. Note that in counter scattering of wave on a beam of electrons, the radiation frequency range shifts into the interval of 1.5 - 2 THz, and measurements in this interval require expensive special equipment.

Effectiveness of the two-step generation can be easily improved with integration of an electromagnetic undulator that is a planar Bragg resonator for storing the pump wave. Besides, for mode selection, a planar THz radiation resonator based of modified Bragg reflectors (MBR) will be placed in channel № 2 of the two-stage FEM. The principle of operation of the MBRs is based on the coupling of quasi-critical waves and those propagating along the channel, this coupling realized due to one-dimensional corrugation of the surface of the reflectors. Three-dimensional computer modeling and "cold" measurements have shown the MBRs to provide high selectivity up to the transverse dimensions of the gap in the reflector, which exceed the radiation wavelength by an order of magnitude ($\sim 20 \lambda$). For operation at a frequency of 0.6 THz, we made MBRs with the following parameters: the period of the lateral corrugation of the surface is 0.5 mm, and the corrugation depth is 50 μ m.

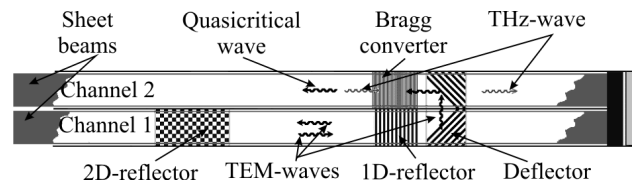


Fig. 4.6.7. Scheme of the electrodynamic system of the two-channel FEM with single-pass scattering of a 4-mm wave into a THz wave.

5.1. VEPP-2000 COMPLEX: WORK WITH ROUND BEAMS AND PLANS ON UPGRADE

5.1.1 Round beams on VEPP-2000

VEPP-2000 working energy range is 0.2–1 GeV, maximal luminosity is $1 \times 10^{32} \text{ cm}^{-2} \text{ s}^{-1}$. The main disadvantage of the complex at the moment is acute shortage of positrons. With given luminosity at the energy 1 GeV particle loss is 6×10^7 , but at the same time the existing system of positrons production can produce 2×10^7 positrons per second only. This means that this system is insufficient taking into account all other transfer coefficients and operational efficiency. All hopes for future for collider VEPP-2000 at BINP are related to injection complex VEPP-5.

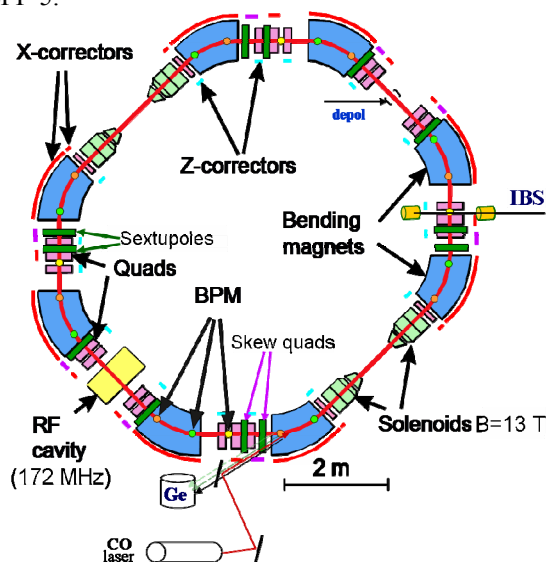


Fig. 5.1.1. Main elements of VEPP-2000 collider.

VEPP-2000 consists of 8 dipole magnets, 24 quadrupoles and 4 superconducting solenoids, which make linear optics of the ring (Fig. 5.1.1). There are numerous corrections: 24 horizontal, 20 vertical, sextupoles, skew-quadrupole corrections provide beam manipulations, control, fine tuning etc. Beam monitoring system includes 16 CCD cameras (2 in each magnet), 4 pickups (1 in each quadrant), current meters and photomultiplier. The complex is equipped with two methods of energy calibration: resonance depolarization (2 Touschek sensors and depolarizer) and back Compton scattering method that is used regularly last year. Collider has two detectors installed: CMD-3 and SND, which are very important instruments for high energy physics as well as for tuning the operation of the accelerator.

VEPP-2000 tuning consists of several stages. The first one is closed orbit correction that includes accumulation of response matrices of closed orbit on variations of quads' gradients, SVD analysis, and calculation of correctors' currents. We need to make 2–3 iterations, each takes

about 10 minutes. Then one should minimize currents in correctors, and we have beam orbit with accuracy of 0.5 mm with respect to the projected orbit. After that we make tuning of the ring optics: accumulation of response matrices in pickups and CCD cameras on variation of dipole correctors, SVD analysis, correcting currents in quadrupoles and solenoids. 3–4 iterations are required (10 minutes each), that is much better than we had in previous experimental season (1 hour per iteration). First of all it is due to installing the new system of CCD cameras in this year. Such progress allowed us to consider this procedure as routine, real tuning of operation can take several hours instead of days in the past. As a result we have smooth beam sizes, projected value of β^* , zero dispersion function outside the achromats. Besides this we correct coupling of betatron oscillation with the aim of 3 families of skew-quadrupoles to the level $v_1 - v_2 < 0.003$.

Fig. 5.1.2 explains the importance of optics correction. During 2010–2011, when this procedure was not so routine, one can see that luminosity remained at low level, after correction the increase is about 4–5 times.

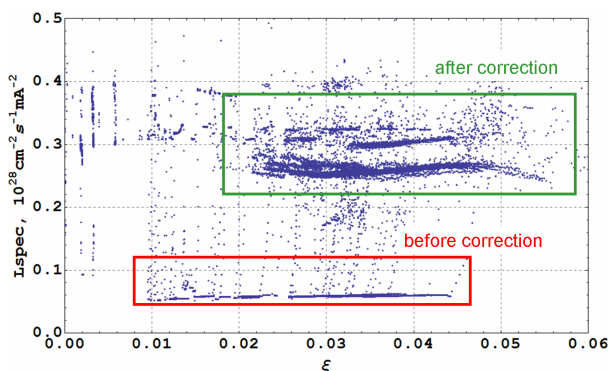


Fig. 5.1.2. Specific luminosity vs ξ parameter at energy 900 MeV.

Together with modernization of beam observation system (4 new CCD servers and 16 fast CCD cameras, Fig. 5.1.3) another control system modernization was carried out (Fig. 5.1.4): the new equipment for VEPP-2000 control room was purchased (Fig. 5.1.5) and the new systems of beam energy calibration with NMR were commissioned. The new system of pickups service that allowed us to measure beams beginning from very small currents is put into operation. The new structure of software – system of logs was realized, which allows one to record all working parameters, analyze and restore successful operating modes. The system repeatedly proved to be in work, and we very actively use it.

Let us shortly describe the history of work in this season. January 2012: tuning VEPP-2000, degassing, operation in 510 MeV range with SND. CMD-3 at the beginning of the year eliminated problems with cryogenic system, in a month they continued normal work.

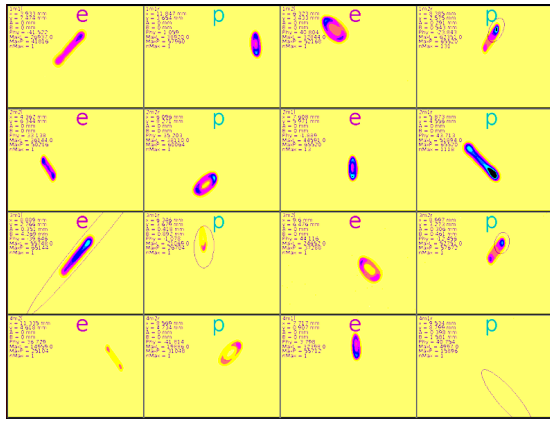


Fig. 5.1.3. Beam from all 16 CCD.

February–march: the laser of Compton backscattering was installed and we performed experiment HIGH 2012 (510-990 MeV). At the beginning we calibrated energy with ϕ -meson at 510 MeV (again with two detectors). But on February 5 there was an accident – current lead of solenoid 1S1 was burned out, the repair took 2 weeks, then we performed degassing and starting operation. Further work went steadily. As it was mentioned our first problem is the lack of positrons. The second difficulty is that at high energies (from 800 MeV) we have to

work in the regime of beam acceleration in VEPP-2000 ring. Injection part (BEP and channels) although is designed for operating at 900 MeV, in real life we can work up to 825 MeV, then beams are injected in VEPP-2000 and further manipulations are performed in the ring. Nevertheless this allowed us to reach 990 MeV, operation of collider is shown in Fig.5.1.6. During the experiment there was accumulated luminosity integral of 13.6 pb^{-1} , Fig.5.1.7.

$$L = 1.061 \times 10^{31} \pm 2.44 \times 10^{30} = 38.18 \text{ nbn}^{-1}/\text{hour}$$

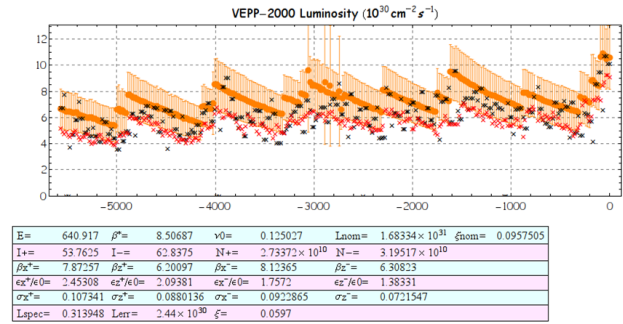


Fig.5.1.6. VEPP-2000 collider regular work.

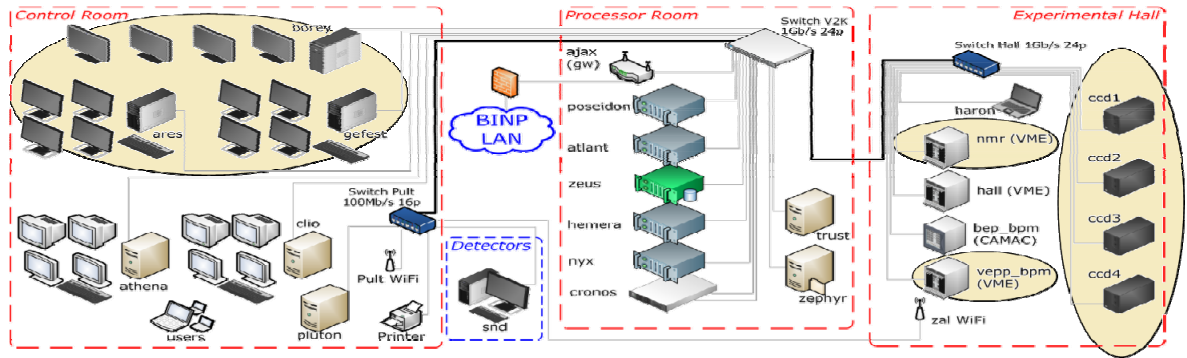


Fig.5.1.4. VEPP-2000 control scheme.



Fig. 5.1.5. VEPP-2000 control room.

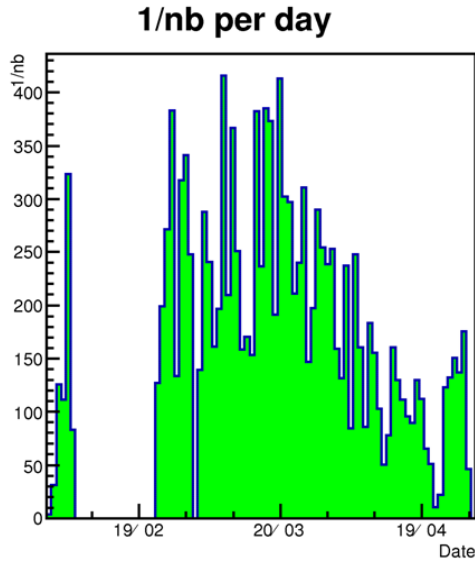


Fig. 5.1.7. Luminosity collected in HIGH 2012 experiment.

At the same time the first test of calibration energy with Compton backscattering was made. Laser beam meets the electron one, and backscattered light is registered with detector (Fig. 5.1.8). And the very first experiments showed us scattering spectrum as in Fig. 5.1.9. There was proposed an explanation based on laser beams interference from several points of interaction region. After that these data were put in the energy calibration formula, the accuracy for the given figure is $E = 993.662 \pm 0.016$ MeV. In this season energy measurement based on CBS method is also an routine operation.

In the summer of 2012 there was installation of additional BPMs in BEP-VEPP-2000 channels, that affected on speed and quality of tuning the injection channels. In September 2012 we started operation, modernization of control system, CCDs, new electronics for pickups installation. October–November: geodesic work, start of operation with round beams, further VEPP-2000 tuning. We

made energy calibration with ϕ and Ω mesons (510 and 390 MeV), 19 points were recorded. Since December 4 up to now: experiment RHO 2012 (energy range from 490 MeV and lower), at the moment we reached 360 MeV, statistics was taken in 32 points, luminosity integral is 4.1 nb^{-1} . Statistical data gathering is shown in Fig, one can see regular growth in spite of energy lowering. The gap in operation is due to NY.

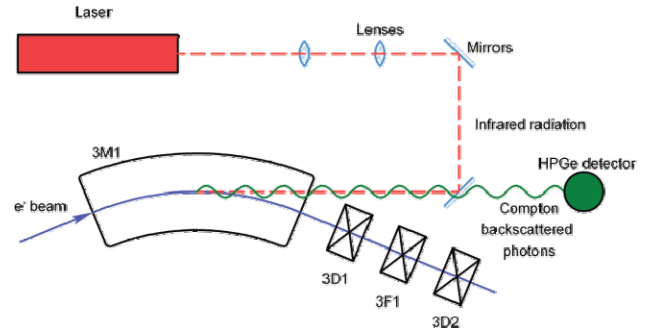


Fig. 5.1.8. CBS method scheme.

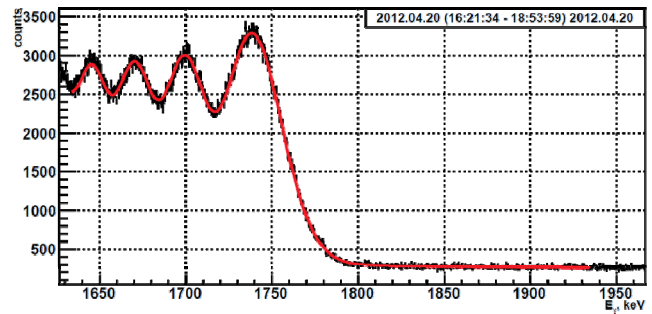


Fig. 5.1.9. Energy calibration.

The feature of VEPP-2000 work at low energies is flip-flop effect – increasing the size of one of the colliding beams and decreasing of another one. But in the case of round colliding beams this effect does not lead to dramatically reduction of luminosity and allows us to work with big enough currents and big specific luminosity. We have stable increasing of accumulated integral in spite of lowering the energy. The beams are presented in Figure 5.1.11 – positron beam is big, electrons are small, but the luminosity is at enough level.

The dependence of collider luminosity on energy is shown in Figure 5.1.12. This is summary picture of all years, two experiments HIGH 2012 and RHO 2012 are added. Starting from the energy 640-650 MeV we have lack in positrons production, and from energy 800 (825) MeV we have to accelerate and decelerate of beams in VEPP-2000 ring for normal operations.

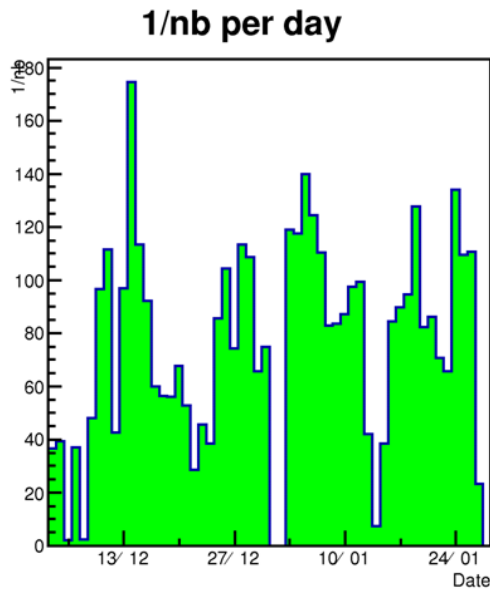


Fig. 5.1.10. Data gathering in RHO 2012 experiment.

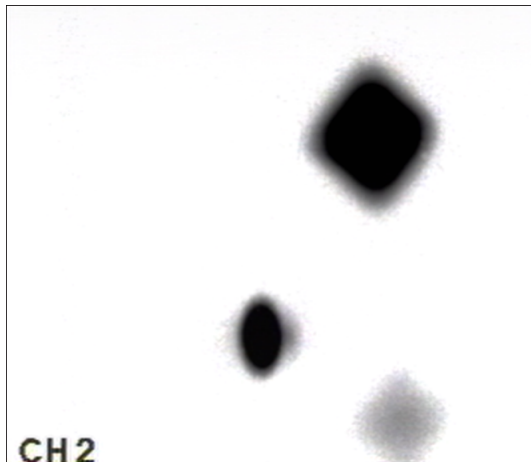


Fig. 5.1.11. Flip-flop effect influence on beam sizes.

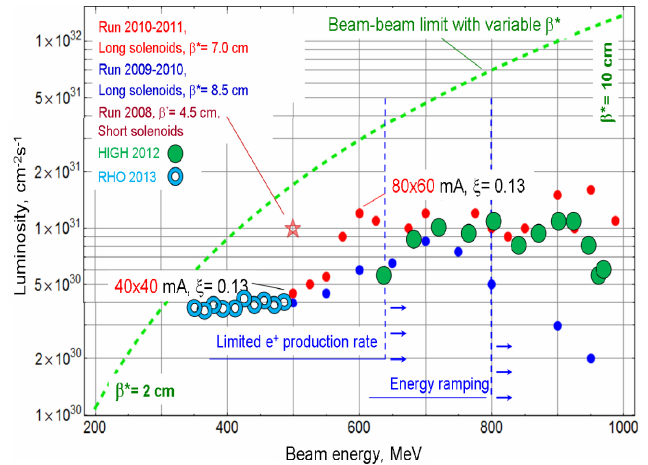


Fig. 5.1.12. Luminosity of VEPP-2000 complex.

5.1.2. Modernization of booster ring BEP and channel K-500.

Modernization of injection part to work at the energy 1 GeV consists of several stages. At first the beams from injection complex VEPP-5 are needed. Secondly, it is necessary to construct and put the K-500 channel into operation. The third point is that we have to upgrade BEP to avoid problems with boost and lowering the beams in VEPP-2000 ring. And of course modernization of BEP-VEPP-2000 channel is required, as it is significantly connected with BEP. The preparation of VEPP-2000 for injection on 1 GeV is also required.

On the K-500 channel at the moment an installation and preliminary geodesic placement of all the magnetic elements is finished, except ones which require dismantling the old injection part we still work with. Laying of feeding cable routes of all elements is complete, power supplies are in active development and production. Vacuum chamber is also complete; system pumping is at the moment carried out. New bending magnet (the last channel element) is almost manufactured. One can see for the Figure 5.1.13 assembled vacuum system, installed quadrupoles, magnets, cables are routed and connected. Further works on turning-on and tuning are assumed.

To upgrade BEP at first the new RF cavity on new energy is needed. The modification of bending magnets is required, and the first one (13th magnet) is modified already and its measurement is carried out. Besides this, modification of quadrupoles is required to increase gradient and to enhance sextupole component to be able to rise beams up to 1 GeV. Modification of aluminum vacuum chamber, new BEP elements such as bump, Ferro probe are needed. The part of these works demands a full stop of the VEPP-2000 complex and BEP dismantling. The new BEP magnet (Fig. 5.1.14) is already placed in the BEP hall, connected, and the first tests showed results as in the Figure 5.1.15. The modification of this magnet appeared not such simple task, insignificant completion was

originally assumed. But during the further work we realized that the magnet has to be more strongly modified for achievement of necessary field level.



Fig. 5.1.13. Tunnel of K-500 channel.



Fig. 5.1.14. New BEP magnet.

Injection channels require manufacturing 8 new magnets, the work is in progress. modification of power supplies is also needed, we assume to use old high-voltage supplies from the old channel. Preparation of VEPP-2000 for injection on 1 GeV is installation of additional inflector plates in the magnets near to RF cavity.

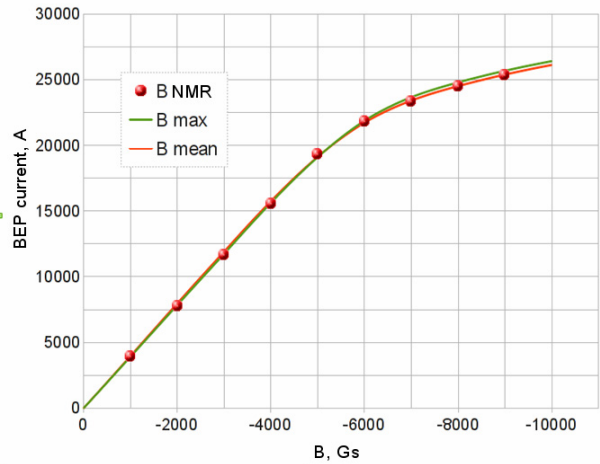


Fig. 5.1.15. Magnetic measurements of modified BEP magnet.

5.1.3 Resonance depolarization on VEPP-2000.

The experiment on energy calibration using resonance depolarization is carried out, preliminary results are shown in Figure 5.1.16 the work took place in a flat beam mode – VEPP-2000 without solenoids and CMD-3. Three runs were made. The first one was a pilot run to simply observe a jump; it was carried out with large amplitude and large depolarizer frequency speed. The jump was at the position predicted by measurement using Compton backscattering method. Following experiments were carried out more accurate with less amplitude and speed of depolarizer. Recorded jumps are almost coincident with each other; movement was at first from right to left, then from left to right. At that the voltage of VEPP-200 RF cavity was different, that in the case of a side resonance would lead to different results It is clearly seen from Figure 5.1.17 a good agreement of measurements with each other as well as with the energy measured in CBS method.

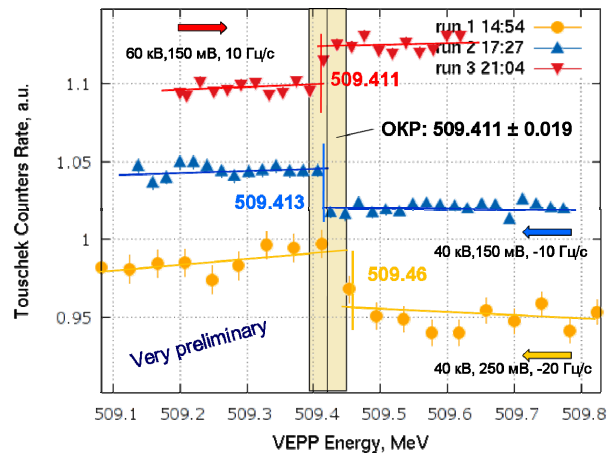


Fig. 5.1.16. Resonance depolarization.

5.2. VEPP-4 ACCELERATOR COMPLEX

Accelerator complex VEPP-4 is a unique installation for experiments with colliding high-energy electron-positron beams. The complex includes injector "Positron", multipurpose storage ring VEPP-3 and electron-positron collider VEPP-4M with the universal magnetic detector KEDR. The main purpose of the VEPP-4M collider is experimental studying of the properties of elementary particles, the parameters of resonances and the cross-sections of electron-positron annihilation processes.

5.2.1. Distribution of working time

In 2012 the planned reconstruction of the KEDR detector was continued, thus, the high-energy physics experiments at the VEPP-4M collider were not carried out. Fig. 5.2.1 shows the time distribution for various aspects of works at the VEPP-4 complex for 2012.

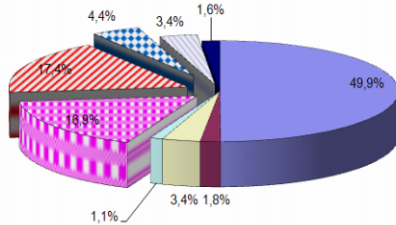


Fig. 5.2.1. Distribution of working time of the VEPP-4 accelerator complex.

As seen from the diagram, this year the complex working hours are distributed mainly between the experiments with synchrotron radiation (16,9 % VEPP-3 + 1,6 % VEPP-4M), and also the DEUTERON experiment at VEPP-3 (17,4 %). Regular maintenance works (1,8 %) are carried out weekly. The accelerator physics experiments at VEPP-4M were performed to adjust the scattered electron registration system and to develop the research on CPT theorem checking. The series of experiments with a beam of high-energy γ -quanta obtained by conversion at the internal target («the output beam») is also continued at VEPP-4M.

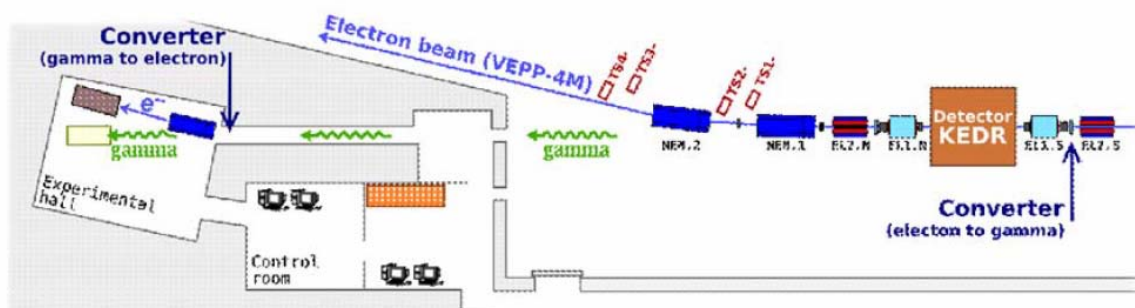


Fig. 5.2.3. The output beam at VEPP-4M.

5.2.2. DEUTERON experiment at VEPP-3.

Measurement of ratio of cross-sections of the elastic electron/positron scattering on a proton allows determination of the contribution of a two-photon exchange to this process. The necessity to take into account the two-photon exchange has been realized due to the contradiction in the results of measurements of proton electromagnetic form-factors.

In 2009 the measurement of R with the accuracy considerably exceeding the accuracy of the known world data is performed at the storage ring VEPP-3. In 2011 the measurement of R in other kinematic area was started (Fig. 5.2.2), this will allow us to double the achieved accuracy. These works were continued in 2012. By 1.04.2012 the planned integral of luminosity - over 100 kilocoulomb - was obtained. Currently the experiment is finished and the collected data are under processing.



Fig.5.2.2. The DEUTERON experiment equipment at VEPP-3.

5.2.3. The output beam at VEPP-4M.

Calibration of various systems of elementary particle detectors for the accelerators being under construction and design requires the beams of γ -quanta and electrons with certain properties. This type of beams are obtained at VEPP-4M via using the electron scattering either on the residual gas or on the tungsten converter specially inserted into the accelerator vacuum chamber. The produced secondary particles get to the equipped experimental hall through the collimator (Fig. 5.2.4). The design parameters of γ -quanta and electron beams are represented in Table 5.2. 1.

Started in 2011, the testing of FARICH prototype for the super $c\text{-}\tau$ factory being under design was continued in March – May 2012. Along with testing of the equipment designed and manufactured in BINP, testing of the detectors provided by PHILIPS company was carried out. Continuation of both experiments is planned for 2013.

Table 5.2.1. Parameters of the output γ -quanta and electron beams

Parameter	electrons	γ -quanta
Energy, GeV	0.1 ÷ 3.0	0.1 ÷ 3.0
$\frac{\sigma_E}{E}$, %	0.5 ÷ 5.0	~ 1
Intensity, Hz	10 ÷ 1000	1000
Coordinate resolution, mm	0.5	-

5.2.4. Scattered electron registration system.

Modernization of the registration system was carried out: new two-co-ordinate Gas Electronic Amplifiers (detectors) were added, the complicated system of energy calibration including two lasers and a BGO-based precise calorimeter was produced and put into operation. The adjustment of the system was performed with the VEPP-4M electron beam at the energy $E = 4$ GeV. These modifications provided a considerable improvement in the accuracy of measurement of the parameters of two-photon events; this is especially important for studying the production of single pseudoscalar resonances.

5.2.5. 7-pole wiggler with a 3T field.

In 2012, at VEPP-4M accelerator the experiments with a new element of magnetic structure – a 7-pole wiggler with a 3T field (Fig. 5.2.4).

Radiation from the wiggler goes through the new SR beamline to the experimental hall where it is supposed to be used for various experiments (Fig. 5.2.5).



Fig.5.2.4. 7-pole wiggler with a 3T field, installed in the northern semi-ring of the VEPP-4M accelerator.



Fig. 5.2.5. Experimental hall and the new SR beamline.

5.2.6. Experiment on CPT-invariance check

Experiment consists in comparison of the energies of electron and positron beams at the VEPP-4M collider using the method of resonant depolarization with the accuracy better than 10^{-9} . To eliminate the systematic errors in energy measurement, the solution of the problem of separating the beams in parasitic interaction points was required. The suggested method allows us to avoid use of the systems of electrostatic separation of the orbits of electrons and positrons. The method is based on affecting the particle radial orbit by RF signal on the second subharmonic of revolution frequency. In this case electron and positron bunches run along the same orbit which is closed every two turns.

Bunches collide at the main interaction point, and at parasitic interaction point are always separated. The system for RF separation is installed in a technical area of VEPP-4M and is tested with electrons (Fig. 5.2.6).

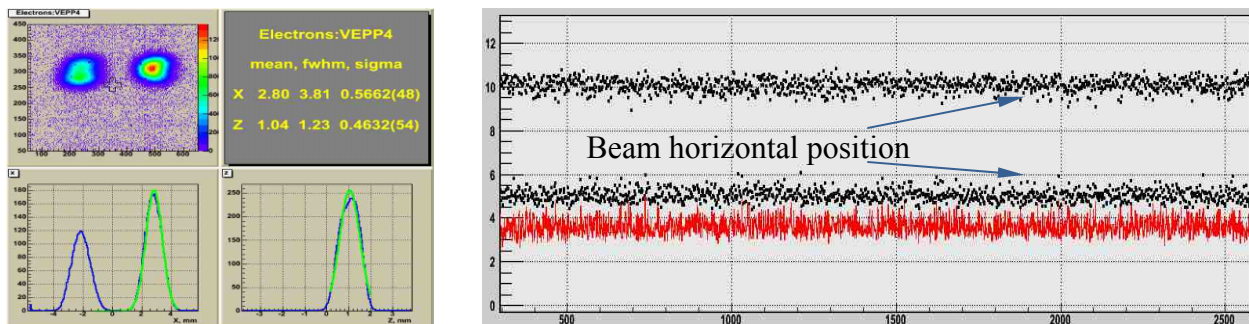


Fig. 5.2.6. Separation of two electron bunches by means of RF-system. On the left – CCD-matrix data, on the right – turn-by-turn diagram of electron beam centre-of-gravity position registered by the multianode PMT.

5.3. INJECTION COMPLEX VEPP - 5

5.3.1. Activity in 2012.

Upgrade of the vacuum system of the Injection complex was completed, and operation of the RF system of the complex was started at maximum design values of RF power of all the klystrons. The old RF loads of the accelerating structures of the linear electron accelerator were replaced with new, more powerful devices. The second acceleration structure of the linear electron accelerator was also replaced. The previous prototype structure at this site had constraints on the average RF power input to the structure. In addition, the new beam diagnostics system was prepared for operation with positrons in the linear positron accelerator. This system includes three extendable phosphor sensors, one of them combined with a Faraday cup. Each sensor has its own digital external-synchronization photometric camera for measurement of transverse distribution of beam intensity. In the linear electron accelerator, phase tuning of RF accelerating fields in the structures was performed, which was necessary for optimal acceleration of bunches. The computer control system of the complex and part of the control software were upgraded. The upgrade of the control system involved replacement of outdated system modules and monitors of the main control computers with new ones and switching to a more recent version of the operat-

ing system LINUX. The Injection complex is now working 24 hours a day in the adjustment regime; the new power supply system of the pulsed flux-concentrator magnet for positron production is being tested; training of the accelerating RF system of the fourth module at the maximum RF power is close to completion; the damping ring of the complex is ready to receive a positron beam.

5.3.2. Studies of wakefield acceleration.

The BINP workshop completed the production of plasma section elements for study of wakefield acceleration. The plasma section is being prepared for vacuum tests in the laboratory. Beams of the storage ring will be used for experiments on plasma wakefield acceleration. An installation for investigation into plasma acceleration is being built in a hall neighboring the storage ring. This installation is an additional transport line for electron and positron beams emitted from the storage ring (see Fig. 5.3.1). In its full version, the installation will include a beam compression system, although at first a simplified version will be commissioned, with uncompressed beams injected into plasma. In this case, one can also observe a significant change in the energy and angular spread of beam due to the development of transverse two-stream instability in plasma.

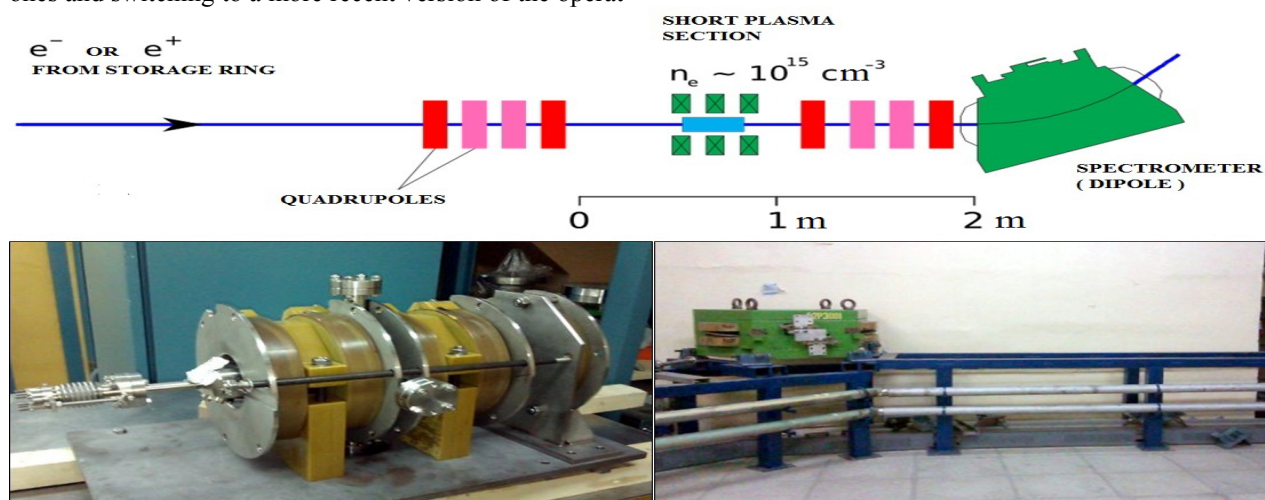


Fig. 5.3.1. The first stage of the experiment on wakefield acceleration in the BINP injection complex (above). Short plasma section (bottom left). Place for the short plasma section on beam extracted from the storage-ring (bottom right).

5.4. ELECTRON-BEAM WELDING

5.4.1. Works carried out in 2012.

Works on refining of the promising electron-beam welders that were developed and manufactured by BINP were continued. These welders are intended for electron-beam technology, first of all (in case of fine-focusing electron beams) for welding and cutting of metals and their alloys, including refractory ones. With other beams, these welders can be applied to high-temperature heating of

materials and melting, including thick layers on substrates.

The electron optical column of the welders can be mounted both outside the operational vacuum chamber and inside it, on a handler.

Currently, 7 electron beam welders are operated at enterprises of the Russia defense industry. Last year BINP assisted these enterprises in maintenance of these plants and provision with expendable materials.

5.4.2. Designing a vacuum system and technology for its production for high-intensity electron-positron colliders.

Below are listed works under ISTC project № 4022 "Development of vacuum system and technology for its production for high-intensity electron-positron colliders" that were continued in 2012.

- A vacuum system of an operational volume of 4 m^3 was fabricated and assembled; a working vacuum of $3 \cdot 10^{-6}$ was attained;

- a power unit with the following elements was manufactured and assembled:

- a 60 kV electron gun with a continuous or modulated current of 100 mA, combined with magnetic optics;
- a 60 kV high-power source;
- cathode-area electronics controlling the welding electron beam current and its modulation;
- power supply system for the magnetic optics;
- locks and alarm system;
- computer control via the CAN bus.

A general view of the electron-beam welder is shown in Fig. 5.4.1. Test startups of the power unit with the computer control were carried out and an electron beam was generated.

For software debugging and welding refining, a four-coordinate system for sample motion was mounted on the existing stand for electron-beam welding (see Fig. 5.4.2).

Some fragments of an aluminum vacuum chamber of a high-intensity electron-positron collider have been welded (see Fig. 5.4.3).



Fig. 5.4.1. Electron-beam welder.



Fig. 5.4.2. Four-drive system with stepper motors.



Fig. 5.4.3. Vacuum chamber fragments welded on the stand for electron beam welding.

5.5. TECHNICAL PROJECT OF LINEAR INDUCTION ACCELERATOR LIA - 20R

The linear induction accelerator LIA-20R being designed at BINP is a unique, no-analogues-in-the-world facility, which provides operation of a promising radiographic complex at VNIITF. The accelerator will generate a high-power high-quality electron beam suitable for radiography with submillimetric spatial resolution and high penetrability. All physical and technical solutions for LIA-20R are aimed at making the phase volume of intense electron beam extremely small. This, in turn, provides an extremely small transverse size of the source of X-ray bremsstrahlung and the highest possible spatial resolution of this technique.

The basic physical parameters of the linear induction accelerator LIA-20R are shown in Table 5.5.1.

Table 5.5.1. Basic physical parameters of LIA-20R.

<i>Parameter</i>	<i>Value</i>
Electron beam energy	20 MeV
Electron beam pulse current	2 kA
Beam current duration	350 ns
Electron beam phase volume (emittance) at the output of the accelerator (not more than)	50 mm·mrad
Pulses per series	2
Adjustable interval between pulses in series	3-10 μ s
Maximum repetition frequency of pulse series	0.1 Hz
Time instability of beam energy over a single pulse	0.5 %

The initial shaping of the electron beam takes place in the Injector, which consists of a high-vacuum diode with a low-temperature dispenser cathode and accelerating section. The electron beam has a maximum energy of 2 MeV at the exit of the Injector. Then 30 short identical accelerating modules and 12 long identical accelerating modules accelerate the beam to an energy of 20 MeV. Such partition of the accelerator into modules and the low value of average acceleration rate are associated with the minimization of transverse beam focusing aberrations in the accelerating/focusing system, which ensures small beam phase volume at the exit of the accelerator. Aberrations caused by non-linear defocusing effects of space charge forces and imaging currents are optimized through the optimal arrangement of the focusing elements and minimization of variations in the transverse beam size in the accelerator. Increase in the beam phase volume due to inaccuracy in alignment of the focusing and accelerating elements is constantly controlled by a special system for on-line geodetic measurements of the accelerator geometry. Results of these measurements are used for position adjustment of the accelerator elements. Operation of all accelerator subsystems in all modes is controlled from the central console through a specialized control system. So, LIA-20R consists of six basic elements: the injector, system of short accelerating modules (30 modules), system of long accelerating modules (12 modules), system for on-line geodetic measurements, control system, and system for on-line measurements and magnetic field correction. The first three elements are localized, while the three latter are evenly distributed throughout the accelerator. A general scheme of the accelerator LIA-20R is shown in Fig. 5.5.1.

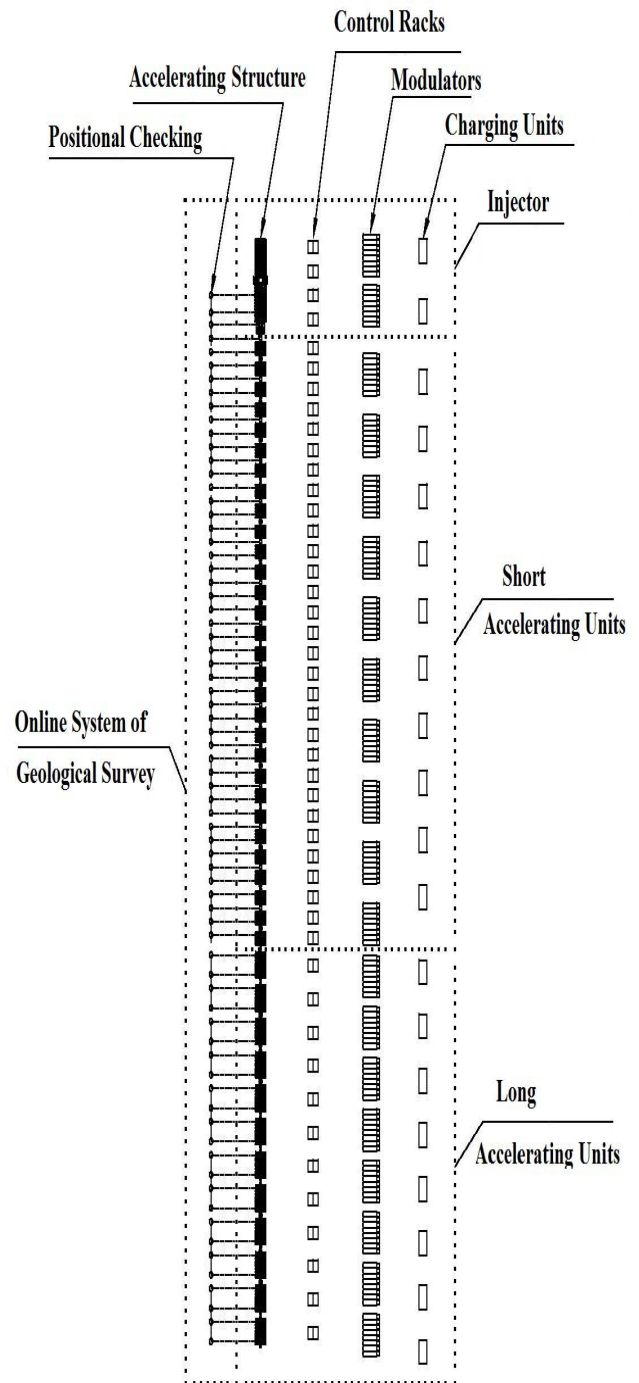


Fig. 5.5.1. General scheme of LIA – 20R.

5.6. QUADRUPOLES FOR NSLS II

In 2009, BINP and the Brookhaven Laboratory concluded a contract for the manufacture of 120 quadrupoles for the main ring of the synchrotron radiation source NSLS II. In 2010, an additional contract for the manufacture of 7 lenses more, of another type, was concluded.

The lenses were of six types, differing mainly in the yoke length and shape of the side spacers (see Fig. 5.6.1 and Fig. 5.6.2).

Lens parameters are presented in Table 5.6.1. Requirements to the field quality were very high. The magnitude of higher harmonics relative to the main field may not exceed $3 \cdot 10^{-4}$ to $5 \cdot 10^{-5}$, depending on the harmonic number.

Table 5.6.1. Parameters of the quadrupoles for NSLS II.

	Unit	Type 9801 and 9802	Type 9804 and 9807	Type 9810 and 9813
Quantity		60	60	7
Aperture radius	mm	33	33	33
Lens yoke length	m	0.217	0.415	0.250
Magnetic field gradient, max	T/m	11.2	20.2	21
Ampere-turns	kA	4.9	9.0	9.4

Below is described the technology for the magnet production. The yoke was stacked of laminations 1 mm thick. There were two poles on each lamination.

The laminations were stamped from low-carbon silicon electrical steel, grade 1200-100 Power Core. The steel was received from ThyssenKrupp in rolls with adhesive coating. The laminations were stamped sequentially with roughing and finishing punches. The roughing punch cut a lamination 6 mm oversize, and the finishing one forged it finish. The finished laminations were stacked into yoke halves and then glued together. In the course of the gluing, the pole gaps were adjusted. Then, the gap was measured at 20 points along the axis of the lens, for each half. The measurements showed that on the completed halves the mean gap value is held within an accuracy of 20 - 40 μm and its uniformity along the axis of the lens, of 10 microns.



Fig. 5.6.1. Types of the BINP lenses for the main ring of the NSLS II synchrotron radiation source.

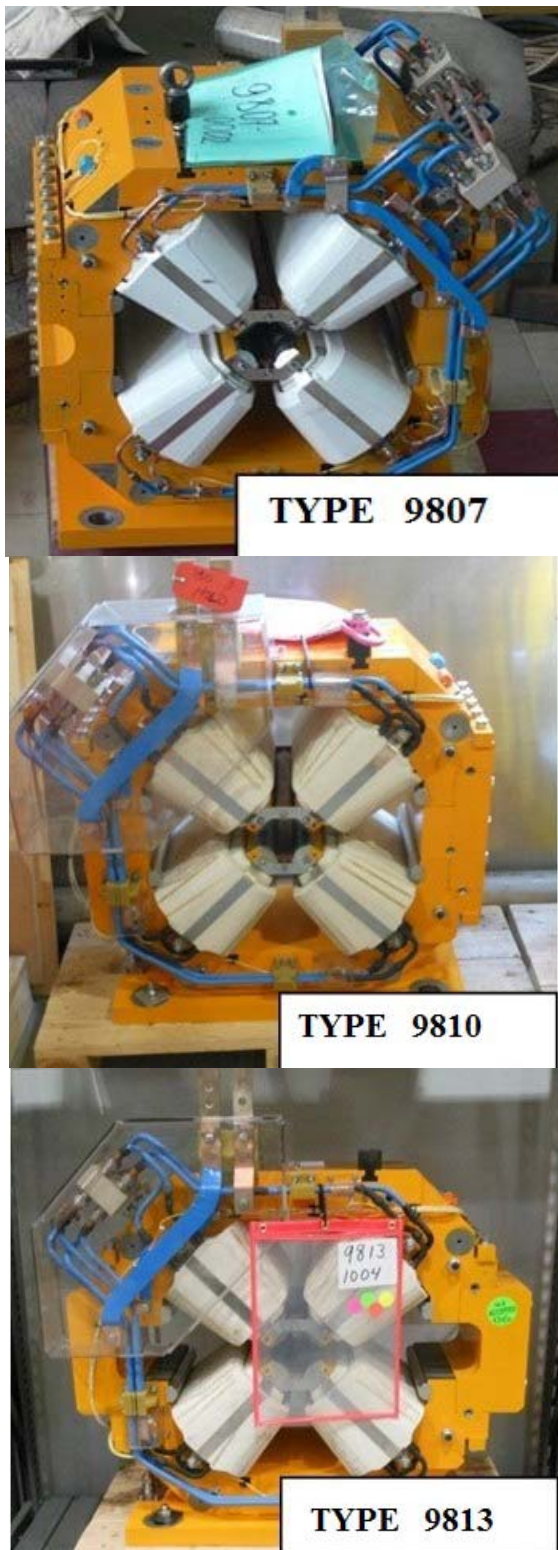


Fig. 5.6.2. Types of the BINP lenses for the main ring of the NSLS II synchrotron radiation source.

Here, the uniformity is taken as the standard deviation from mean. Then a preliminary assembly of the lens was carried out; the first measurements of the magnetic field harmonics were performed; inter-pole inserts and pole overlays were mounted, which helped in fine tuning of

magnetic fields. After the fine tuning of magnetic fields, the lenses were passed to the final stage (installation of the water cooling and supply system, the carrier plate, painting, etc.).

After that, two control measurements of magnetic field harmonics of the lens were performed. Measurements made before and after re-assembly (lens separation into the top and bottom halves for simulation of installation on the accelerator) were to agree with each other and specification requirements.

Amplitudes measured on finished lenses for all harmonics are shown in Fig.5.6.3.

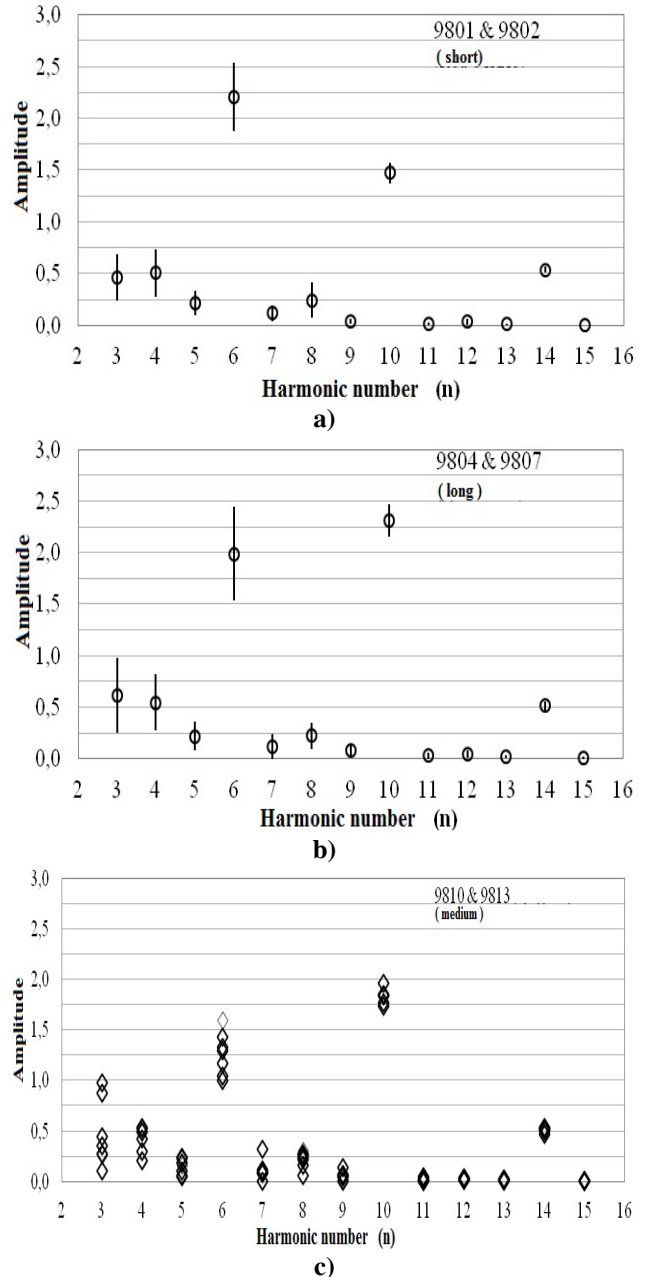


Fig. 5.6.3. Harmonic amplitudes measured in units of 10^{-4} relative to the fundamental harmonic: a) statistics over 60 short lenses, b) statistics over 60 long lenses, and c) measurement of seven medium lenses.

In May 2012, the last of the lenses were dispatched to the Brookhaven Laboratory. BNL experts subjected all the lenses to internal control and found them to be completely compliant with the set parameters. The quality of magnetic fields of our lenses was identified as the best among all the manufacturers of lenses for NSLS II. BNL experts are now assembling the facility.



Fig. 5.6.4. Part of the BINP team near the lenses mounted on the NSLS II ring. April 2012.

5.7. SWITCHED POWER SUPPLY FOR NSLS II BOOSTER INJECTION/EXTRACTION SYSTEM

The beam injection system in the NSLS II Booster applies four kickers with an efficient length of 200 mm. Two kickers (BU3 and BU4) deflect the beam in regimes for single injection or storage. Another two kickers (BU1 and BU2) are used only in the storage regime. The extraction system employs one kicker with a sum efficient length of 800 mm (four sections, each 200 mm long). Table 5.7.1 summarizes the requirements to the power supply system for the extraction/injection kickers, which shall ensure the required parameters of pulsed field in a magnet of a given design at operation of the Booster in various regimes.

The switch-mode power supply systems for injection and extraction are based on a common principle. Immediately under the magnet in the Booster ring, there is a pulse generator (Pulser), which includes a pulse shaping line (PSL), thyatron with trigger unit, and filter elements. When the thyatron is triggered, the Pulser generates a current pulse with set parameters in the magnet buses. In the injection system, there is one pulser per kicker, whereas each kicker in the extraction system is fed from two pulsers. The PSL of each generator is charged from its charger unit with control electronics (PSU). The PSUs of all the six generators are placed in a single rack, which is set in the “service area” of the Booster. The block diagram of the switch-mode power supply is shown in Fig. 5.7.1.

Table 5.7.1. Requirements to the power supply system for the extraction/injection kickers.

Name	Injection		Extraction
	Single injection (BU3, BU4)	Storage regime 2nd pulse (BU3,4 BU1,2)	
Amplitude of current in the magnet buses, A	1.650	1.120/795	2.300
Current amplitude at the modulator output, A	3.300	2.240/1.590	4.600
Magnet section inductance, nH	650		650
Equivalent load inductance, nH	162.5		325
Pulse flat top length, ns	310		310
Pulse rise time, ns	<210		<210
Decay time, ns	<210		-
Load current stability (including fluctuations on the pulse top)	±0.5% (including fluctuations in the pulse tail)		±0.2%
Pulse shaping line impedance, Ohm	5.9		4.4
Maximum charge voltage of the pulse shaping line, kV	20		21
Voltage amplitude on the magnet buses, kV	15		20

Some characteristics of the pulsers are worth noting. The pulsers were designed subject to special requirements to output current stability and pulse top evenness.

The evenness of the top is defined by the accuracy of impedance setting for individual cells of the pulse shaping line. The resulting evenness of the pulse top of the extraction kicker field was within $\pm 0.09\%$. Current stability depends on the temperature derating of parameters of various elements of the generator and instability of voltage drop on the thyatron at current switching. The temperature derating can be tracked and compensated for via changes in the charging voltage. Instability of voltage drop on the thyatron is a stochastic value and generally fits into allowable limits. The measurements revealed that the standard deviation of the extraction kicker from a target value is less than $3 \cdot 10^{-4}$.

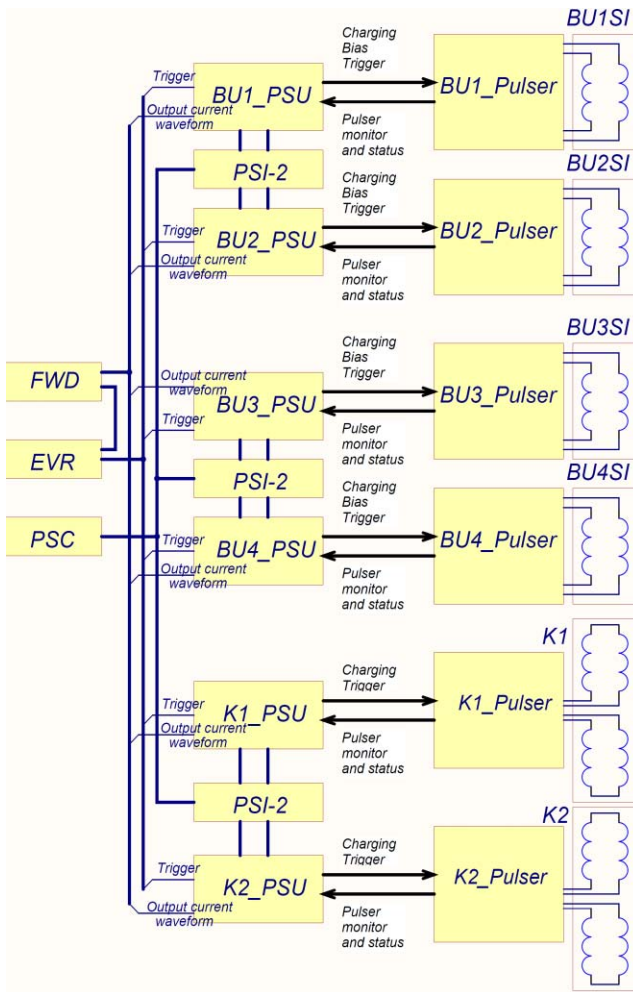


Fig. 5.7.1. Block diagram of the switched-mode power supply for the kickers of the extraction-injection system.

Pulsers of the injection system shall comply with the requirement of minimization of the amplitude of current oscillations in the pulse tail. To this end, a saturable choke was brought into the generator circuit in series with the thyatron. The "diode" properties of the choke reduced the amplitude of oscillations in the tail of the field pulse of the injection kickers to a level of $\pm 0.45\%$. Another distinctive feature of the injection pulsers is the necessity of ensuring required pulse parameters in two different operation modes at different levels of PSL charge. Since ceramic capacitors in the PSL are dependent on voltage, it was necessary to adjust the impedance of the PSL cells to some medium value that would ensure the required pulse parameters in different operating modes. As a result, the evenness of the pulse top of the injection kicker field was $\pm 0.3\%$. Pulse shapes of the injection and extraction kicker fields are shown in Fig. 5.7.2 and Fig. 5.7.3., respectively. Fig. 5.7.4 represents a photo of the pulser with kicker connected in the Booster ring.

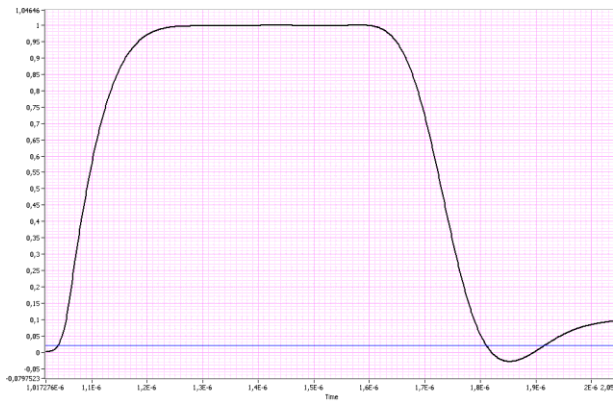


Fig. 5.7.2. Field shape measured on the axis of the extraction kicker; the field amplitude corresponds to 720 G; the time scale is 100 ns/square.

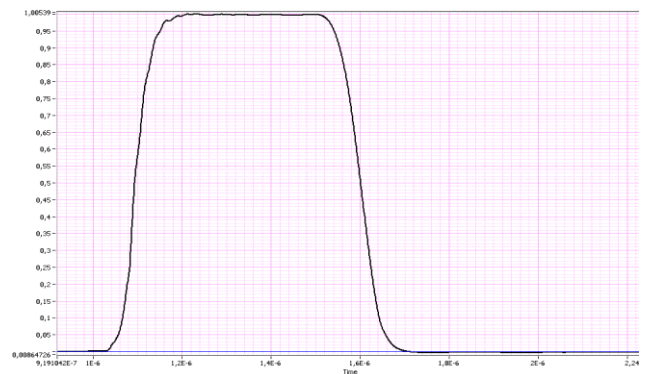


Fig. 5.7.3. Field shape measured on the axis of the injection kicker; the field amplitude corresponds to 510 G; the time scale is 200 ns/square.

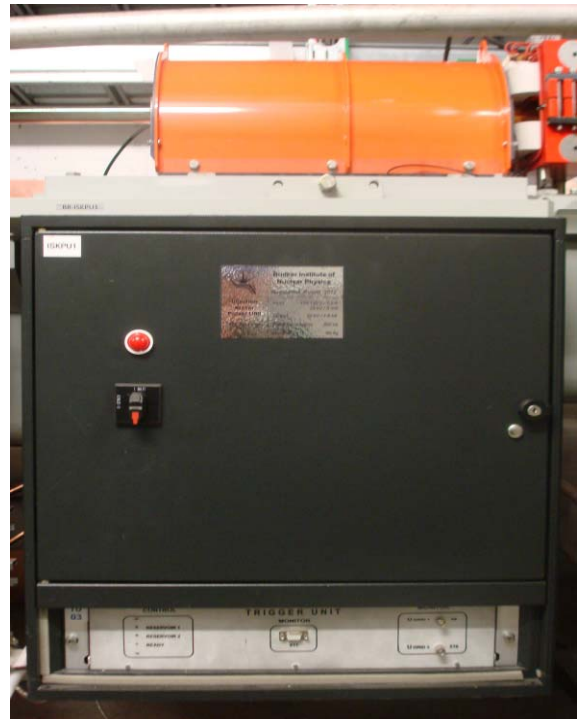


Fig. 5.7.4. Pulser assembled in the NLS II Booster ring.

5.8. CONNECTION MODULE FOR THE EUROPEAN XFEL (DESY)

The European XFEL project was first to propose using high-power multi-beam horizontal-design klystrons as RF power supplies for superconducting sections of accelerator. The horizontal klystron design made it possible to significantly reduce the cost of XFEL tunnel construction, although it significantly complicated the mechanism of connecting and powering the klystrons in the tunnel, because of the limited space in the tunnel and large weights and sizes of the klystrons and pulse transformers.

To solve this problem BINP developed a connection module (Figure 5.8.1).

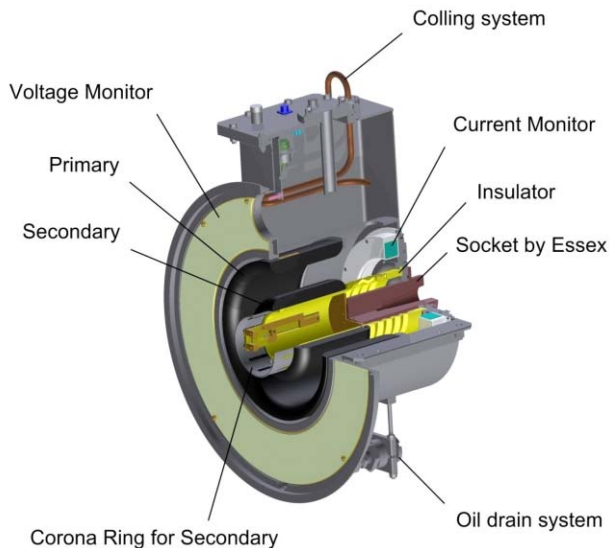


Fig. 5.8.1. 3D view of the connection module.

The following is possible with the original design of the connection module:

- powering horizontal-design klystrons (Toshiba, Thales, CPI) from a pulse transformer through a flexible cable connection;
- stable supply of klystron filament through an isolation filter transformer from a specially developed inverter controlled remotely via the Ethernet protocol;
- pulse measurements of the current and voltage of the klystrons;
- cooling the klystron cathode volumes.

In 2012, BINP delivered 13 connection modules to DESY. Most connection modules have been successfully tested on test stands at DESY (see Fig. 5.8.2).

Under attachment # 27, BINP shall deliver another 27 connection modules in the period from March 2012 to March 2014.

Assembly of the XFEL accelerator is to start in September 2013.

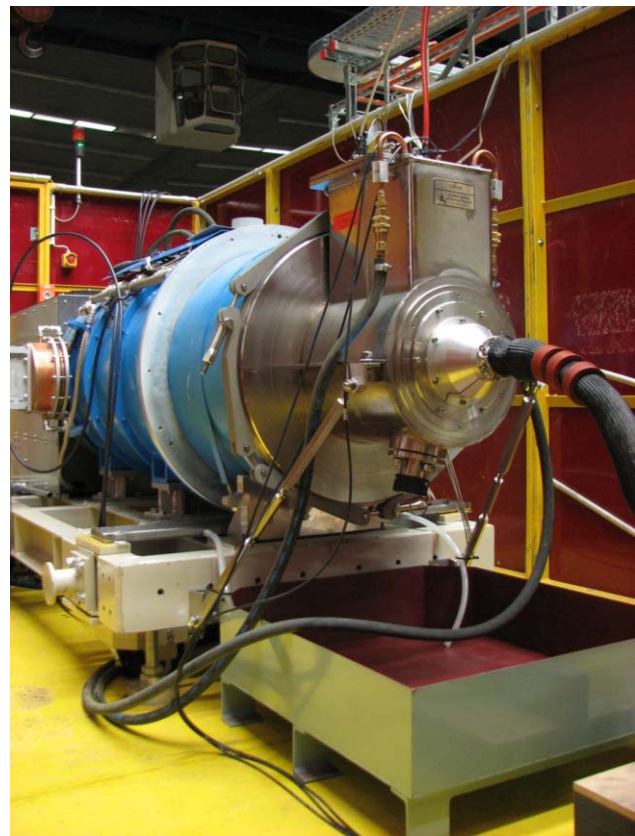


Fig. 5.8.2. Connection module on the test stand at DESY.

5.9 ELECTRON COOLING FACILITY

5.9.1. *Electron cooling facility for the German Synchrotron COSY.*

A fundamentally new 2 MV electron cooler for the German accelerator center COSY was completed and dispatched to Germany in 2012. This electron cooler offers a unique opportunity to experiment with a detector of elementary particles on suppression of effects associated with scattering on target nuclei and emergence of spread of pulses because of fluctuations of ionization losses. In contrast to the 4 MeV cooler on TEVATRON FNAL, the new cooler needed much faster cooling using a strongly magnetized electron beam. This high-voltage cooler is based on the following BINP research and developments:

- 1). an in-vacuum laser compass for high-precision control of straightness of lines of force in a cooling section;
- 2). adjustment of position of coils of cooling section;
- 3). a four-electrode electron gun with controlled beam profile; modulation of different parts of electron beam enables measurement of its position and dimensions.
- 4). an integrated electron beam profilometer;
- 5). a high-power cascade transformer, which provides energy to a high-voltage terminal and creates a solenoidal field along accelerating and decelerating tubes.
- 6). a system of pick-ups to be placed along the perimeter of beam lines and on the ends of cooling section.

The 2 MeV electron cooler includes an accelerator tower for acceleration and deceleration of the electron beam, beam lines for transport of electrons to and from a cooling section and a cooling section, in which energy is transferred from hot ions to a cold electron beam. To ensure electron cooling in the wide energy range from 25 keV to 2 MeV, it was proposed to make a modular electrostatic accelerator. Each new installation is assembled from standardized modules for any given energy.

The cooling system was assembled and tested with beam in 2012. High voltage tests with the high-voltage tank filled with insulating gas have shown the possibility of attaining a voltage of up to 1.5 MV. Experiments with an electron beam at a voltage of 30 kV showed the possibility of obtaining a current of 1A. The current was 0.5 A at a voltage of 1.0 MeV and about 200 mA at the maximum voltage. The assembling and commissioning of the electron cooling installation will start in Germany in early 2013.

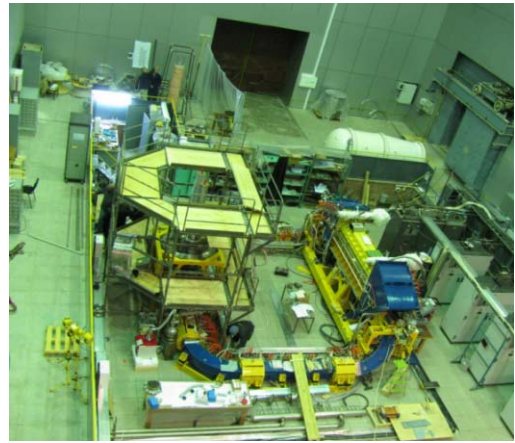


Fig. 5.9.1. Early 2012: assembling and tuning of the electron cooler and control and power supply electronics.



Fig. 5.9.2. End of 2012: loading of cooling section into a truck for transport to Germany.

5.9.2. *Compass for measurement of straightness of line of force.*

To maintain high cooling capacity at high electron beam energy, it is very important to have a small angle deviation between the ion beam and the electron one. So, it was decided to install a laser compass in the cooling section for control of straightness of line of force. The necessity of heating of the cooling section imposes severe restrictions on the design of the compass. We had to give up the lately-used fiber suspension design and return to the first version of gimbal suspension on jewels.

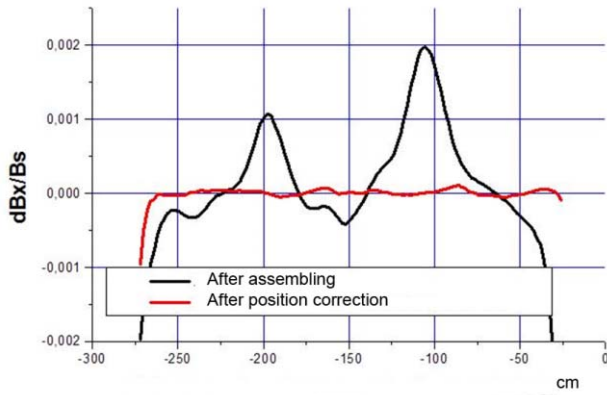


Fig. 5.9.3. Horizontal component of slope of line of force in the cooling section as measured before and after coil position adjustment.

In the tests, friction in the axes turned out to be much higher than expected, and we had to eliminate the hysteresis via a special magnetic cycle during the measurements.

5.9.3. Electron beam profiler.

In first runs with electron beam, we observed severe deterioration of the emission ability of the cathode during abnormal recovery of electron beam. This was accompanied by strong degassing, which necessitated a long training of the cathode for its restoration. This manifested itself in a marked asymmetry of electron beam and a "toothy profile form". The figure shows electron beam profiles at different ratios of voltages across the anode and the gate electrode of the gun.

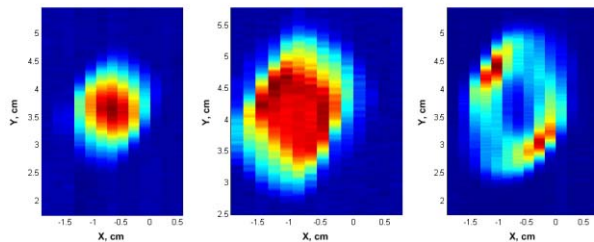


Fig. 5.9.4. Electron beam profiles at various voltages across the electrodes.

One can see that there are areas with good and bad emission of electrons. During the commissioning in Germany, the electron gun and accelerating tube will be cleaned via training at low voltages for prevention of bombardment of the cathode with high energy ions.

Responses of correction coils on the pick-up electrodes were measured in operation with beam. Beam displacements correspond to the calculated values.

The magnetic system of the cooler has six areas of potential "heating" on the way from the gun to the entrance to the cooling solenoid: three 90° bends, a 45° toroid and

2 intervals with nonadiabatic field rise. A beam of a given energy enters the solenoid without "heating" only for certain field values in these areas. So, there arises a problem of control of the "heating".

The "heating" was observed on the pick-up electrodes in scanning of field in the solenoid from 370 to 480 G. The field in the toroids was reduced to 440 G; the beam energy was 150 keV. Accordingly, the number of Larmor electron gyrations along the solenoid length varied from 11 to 14.

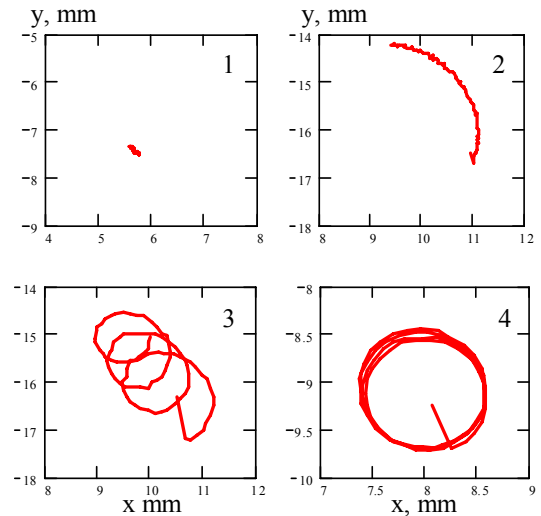


Fig. 5.9.5. Beam center in scanning of the field of the solenoid. 1 – a pick-up at the entry to the 45° toroid; 2 – a pick-up at the entry to the solenoid; 3 – a pick-up at the exit of the solenoid; 4 – a pick-up at the exit of the 45° toroid.

5.9.4. Collector with Wien filter.

A collector was developed for the high-voltage electron cooling facility for COSY. A Wien filter is used for suppression of reverse flow of electrons backscattered from the collector (Fig. 5.9.5).

The idea is to use crossed electric and magnetic fields. As for the main beam, the effect of the shear forces is compensated, and the beam moves without deviation. As for backscattered electrons, the Lorentz force is directed in the opposite direction, and strengthens the effect of the electric field instead of compensating it. Thus the inverse electron flow deflects aside, where it can then be absorbed by a special collection plate. The presence of a longitudinal magnetic field in the Wien filter prevents ingress of electrons reflected from the collector to electrostatic plates that create the electric field, since the secondary beam is displaced due to the drift, which is directed parallel to the plates.

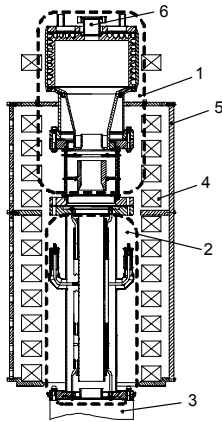


Fig. 5.9.6. Collector unit. 1 – the collector with the suppressor and the electrode in the collector area; 2 – the Wien filter unit; 3 – the accelerating tube; 4 – the longitudinal field coils; 5 – the magnetic shield; 6 – a flange for additional vacuum pumping.

Tests revealed that the effectiveness of such collector depends on the quality of beam passage through the system. The characteristic value of the efficiency is of the order of 10^{-5} at a current of several hundred milliamps (see Fig. 5.9.6).

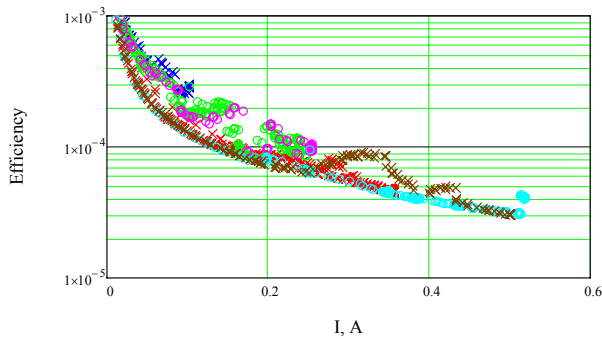


Fig. 5.9.7. Efficiency of the collector vs. electron beam current in different operation modes of the gun and collector.

The values of efficiency of the collector as attained on the facility are approximately an order of magnitude worse than those obtained on the test bench. This may be caused by both inaccuracies in the assembly of the accelerating tubes and the effects of electron scattering on the residual gas. This issue needs further study.

5.10. ACCELERATOR MASS SPECTROMETER

In 2012, over 600 samples were subjected to accelerator mass spectrometry (AMS) analysis. Those included technological samples (for development of sample preparation techniques) and natural ones (bones of animals, coals of burned buildings, remains of organic food on pottery, and bottom sediments of lakes). Fig.5.10. presents a curve of radiocarbon concentration in peat deposits of the river Dem'yanka in Tyumen region. Archaeologists had estimated the age of a substantial portion of the artifacts. The natural samples included both "old" (over 40,000 years) and modern specimens.

Works on the improvement of the components of the AMS complex and the technique of AMS analysis were continued. The reliability and stability of the power supplies of the AMS complex and radio-carbon-cycle analysis of samples were increased. Despite the lack of dedicated funding, the main part of a special stand for experiments on preparation of biomedical samples was constructed.

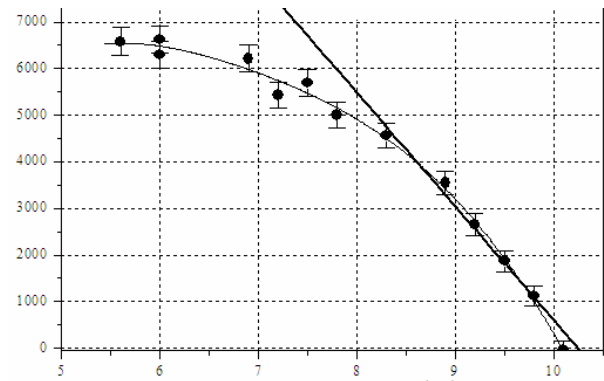


Fig. 5.10.1. Radiocarbon dating of peat deposits vs. height above the water level.

5.11. VACUUM SYSTEMS

5.11.1. Electron clouds.

High-density electron clouds are one of the factors impeding increasing intensity of relativistic beams of positively charged particles. A test operation of the LHC with a design inter-bunch spacing of 25 ns is one of the latest examples. The results revealed that, unlike laboratory experiments, training of a closed cold surface substantially slows down, and low values of secondary emission coefficient cannot be achieved in a predicted time of 1-2 weeks.

Simulation of electron clouds is hindered by, on the one hand, a large number of input parameters (often ill-defined), and, on the other hand, a small number of "output" parameters that can be measured at accelerator installations. The aim of this work is to create an installation for production of electron clouds in laboratory conditions, and research on their interaction with the surface in the presence of a magnetic field.

A scheme of the installation is shown in Fig. 5.11.1. All the main elements – C (thermal cathode), M (modulator), D (diaphragm (grounded)), BM1 (first beam monitor (a cylinder with adjustable potential)), BM2 (second beam monitor with adjustable potential), and S (sample to study (grounded through a current meter)) – are placed in row along the lines of the magnetic field inside the solenoid. Manipulator SM is intended for quick change of samples (S) without letting the atmosphere air in.

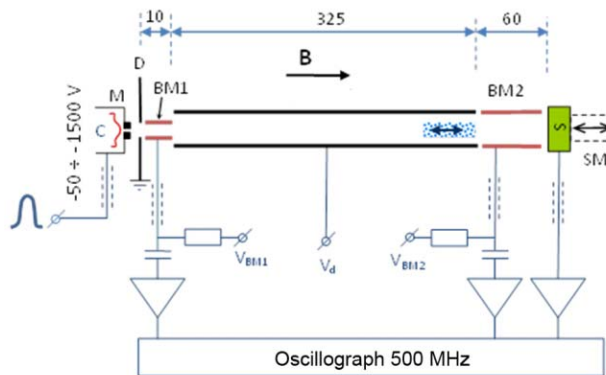


Fig.5.11.1. Structure diagram of the installation.

The installation operates by a pulse measurement technique with a time resolution of 1 ns. Matched coaxial lines are run to the modulator, beam monitors and sample. A voltage pulse applied to the modulator creates a pri-

mary electron beam with a duration of $2 \div 10$ ns. The energy of the primary electrons is defined by the potential of the cathode. Signals from the beam monitors and the sample are amplified, which increases the signal/noise ratio, and then are recorded on an electronic oscillograph with a bandwidth of 500 MHz and a sampling frequency of 5 GHz.

Interaction of initial electrons with the sample results in formation of secondary electrons, which are mainly of low energy, move only along the magnetic field lines, and are restricted by the negative potential of the cathode and the sample surface. Thus, the electrons can leave this structure only through a contact with the sample surface. The time when this happens depends on the coefficient of effective reflection of secondary electrons from the sample surface. Because of difficulties in control of electron flows of energies 1 eV or less, this parameter, which is important for prediction of formation of an electron cloud in accelerators, is extremely hard to determine via direct measurements.

Parameters of the installation are as follows:

- maximum sample diameter: 13 mm;
- primary electron energy: $50 \div 1500$ eV;
- primary electron pulse current: to 0.2 mA;
- pulse duration: $1 \div 10$ ns;
- amplitude of control pulse to the modulator: up to 100 V;
- beam diameter: $1.4 \div 2$ mm;
- maximum magnetic field: 0.04 T (with an option of placement of all the elements in a superconducting solenoid with a magnetic field of up to 13 T);
- potentials on the BM1, BM2, and the drift tube can be set independently;
- parameters of the preamplifiers: the band of $0 \div 1.8$ GHz and a gain of 25.

In 2012, test experiments were conducted at room temperature on samples made of oxygen-free copper, stainless steel, titanium and aluminum alloy 6063.

The first experiments showed that the main obstacle is the fact that a control pulse of the modulator excites a high-frequency electromagnetic field. Nevertheless, when there is no magnetic field, the electron bunch scatters and does not reach the sample. Thus we managed to allow for this magnetic excitation via recording currents with the magnetic field on and off:

$$I = I [\text{"B" on}] - I [\text{"B" off}]$$

That allowed us to increase the sensitivity of the measurements by an order the least and conduct experiments at low current pulses (up to $20 \mu\text{A}$), the relative accuracy of the measurement being better than 10%.

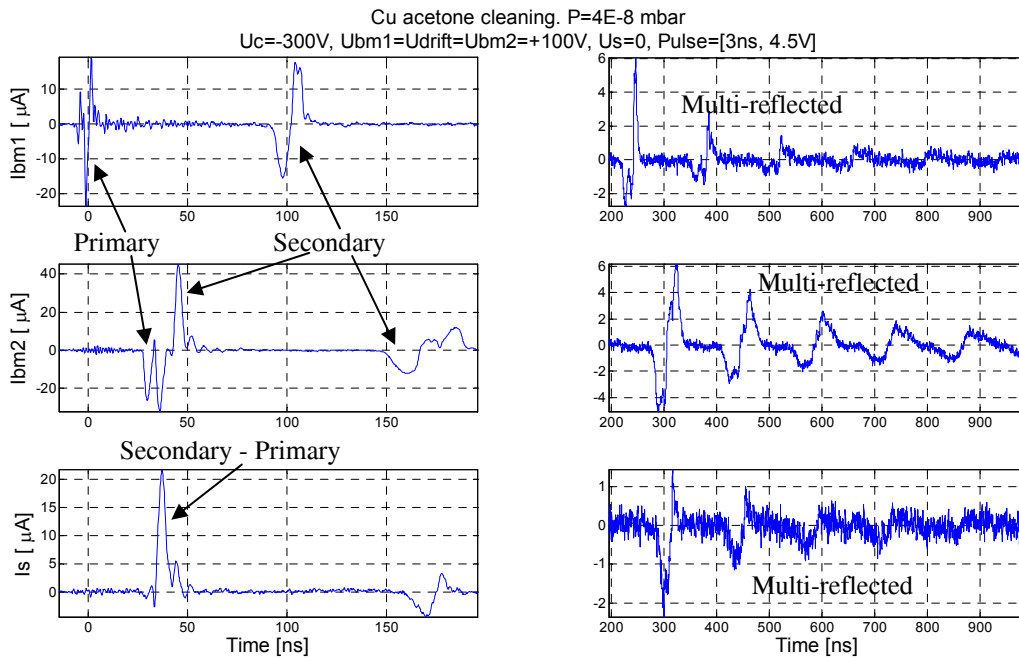


Fig.5.11.2. Signals from beam monitors Ibm1 and Ibm2 and the sample to study (Is).

Fig. 5.11.2. shows typical time dependences of currents from the monitors (Ibm1 and Ibm2) and the sample (Is). The left charts show a passage of primary electrons, their interaction with the sample and the first cycle of passage of secondary electrons from the sample surface to diaphragm D and back. The right-hand graphs show long-time dynamics of the electron cloud, i.e. multiple reflections of electrons from the sample surface, or, which cannot be excluded, capture of electrons in the drift structure because of the electron energy loss in interaction with the space charge.

The experimental data give several ways to compute the coefficient of secondary electron yield (SEY). SEY determination from the following formula turned out to be the least sensitive to noise:

$$SEY = \frac{Q_P + \Delta Q}{Q_P}$$

Here Q_p is the full charge of the primary electrons (an integral of the first negative pulse Ibm2, see Fig. 5.10.2.); ΔQ is an additional charge emitted from the sample due to secondary emission (an integral of the first positive pulse Is, see Fig. 5.10.2.). The measured SEY values as functions of primary electron energy are shown in Fig. 5.10.3 for samples of different materials.

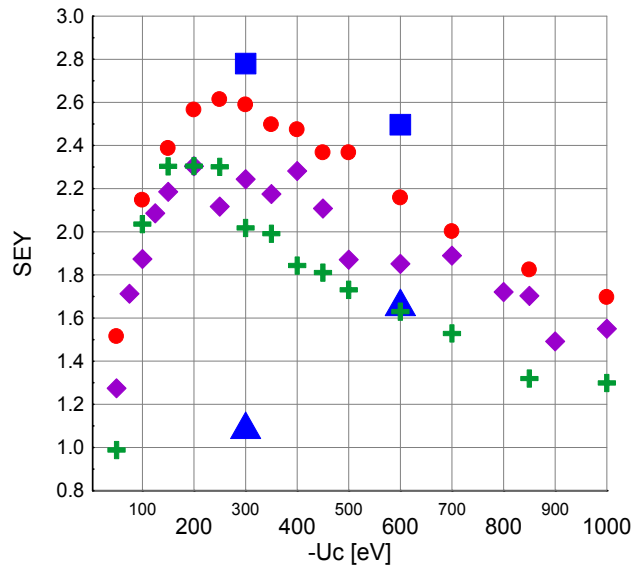


Fig. 5.11.3. $-U_c$ – energy of the primary electrons; “●” – titanium ($U_d=40$ V, $I_p=14$ μ A); “◆” – stainless steel ($U_d=40$ V, $I_p=20$ μ A); “+” – oxygen-free copper ($U_d=40$ V, $I_p=20$ μ A); “■” – aluminum alloy 6063 ($U_d=100$ V, $I_p=140$ μ A); “▲” – aluminum alloy 6063, a sawtooth surface with an opening angle of 30°. U_d is the potential on BM1, BM2 and the drift cylinder; I_p is the amplitude of the primary electron pulse. The pulse duration is 3 ns.

All the samples have a rather large SEY with a characteristic maximum at primary electron energies of $200 \div 400$ eV. The difference from the table values is caused by the presence of oxide films on the surface. A sample with

a sawtooth surface with an opening angle of 30° showed an unexpectedly large suppression of the secondary electron yield (about 2.5 times, while the expected value was 1.5) at $-U_c=300$ V. At $-U_c=600$ V, the suppression ratio decreases to 1.5. The explanation is that the SEY grows in an oblique incidence of primary electrons and the SEY peak shifts significantly towards increase in the energy of primary electrons. Thus the effect of a sawtooth surface capturing the secondary electrons is partially compensated by increase in the SEY.

Fig. 5.11.4. shows SEY vs. extracting field, which is defined by the potential on BM2 relative to the sample. Potentials on BM1 and the drift cylinder were set equal to the potential on BM2.

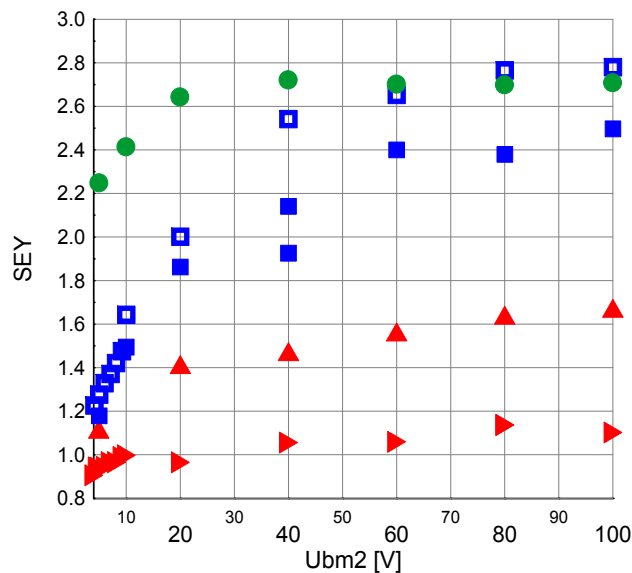


Fig. 5.11.4. Measurement of SEY for samples of aluminum alloy 6063. Ubm2 – potential on beam monitor BM2 [V]. “●” – flat ($-U_c=300$ V, $I_p=22$ μ A); “■” – flat ($-U_c=600$ V, $I_p=120$ μ A); “□” – flat ($-U_c=300$ V, $I_p=120$ μ A); “▲” – sawtooth with an opening angle of 30° ($-U_c=600$ V, $I_p=120$ μ A); “▶” – sawtooth with an opening angle of 30° ($-U_c=300$ V, $I_p=110$ μ A).**

A dependence of the secondary electron yield on the extraction potential means that the space charge returns some electrons to the sample. The cloud density reaches a maximum near the sample surface immediately after the emission of secondary electrons. The maximum density is estimated to be about 10^8 cm^{-3} at a peak current of the primary electrons of 20 μ A and a 3 ns pulse duration. Some of the electrons will slow down due to the interaction with the space charge and be trapped in the drift structure, having no sufficient energy to reach the surface of the sample. Processing of the shape of the current pulse that corresponds to escape of secondary electrons and BM2 (see Fig. 5.11.5.) yields the distribution of secondary electrons along the axis of the structure (solenoid).

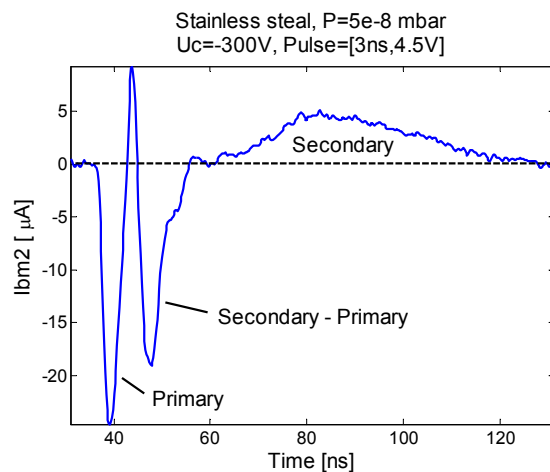


Fig. 5.11.5. BM2 current record, which reflects the entry of primary electrons, interaction with the sample and emission of secondary electrons.

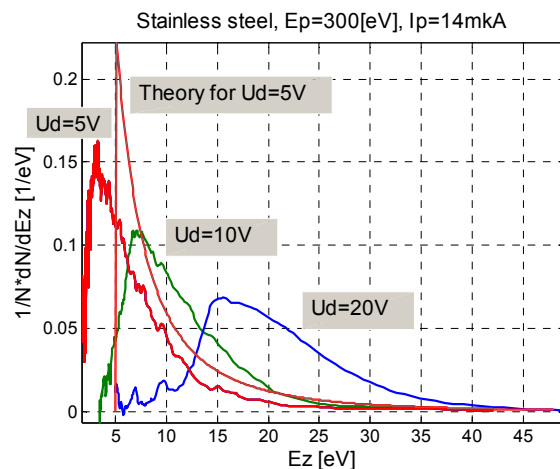


Fig. 5.11.6. Energy distribution of secondary electrons over magnetic field in departure from BM2. Ud is the potential on BM2.

Fig. 5.11.6. presents a theoretical calculation of distribution of secondary electrons over magnetic field in their escape from BM2 and distribution resulting from processing of the experimental data. The distribution is shifted by +5V relative to the potential of the sample. One can see that a large part of the electrons acquires energy less than the potential of the extracting field. Thus, the multiple passages of electrons through the structure (the right-hand graphs in Fig. 5.11.2) can be explained not only by a high coefficient of reflection, but also by the fact that some of the secondary electrons do not have enough energy to reach the surface of the sample.

To make the space charge negligible, it is necessary to reduce its density by about two orders of magnitude (to $\sim 10^6$ cm^{-3}). The peak current of secondary electrons can be reduced to values of about $0.2 \div 1.0$ μ A on a condition that the electromagnetic excitation from the control pulse is completely suppressed. But it allows only a single-

order reduction of the density of the cloud. Further reduction is possible via increase in the beam diameter (up to 5 mm, for example). Both the methods are easy to implement with a photocathode, which is planned to be installed, together with a control semiconductor laser, in 2013.

5.11.2. Vacuum system of the NSLS-II booster.

In 2012, we continued works on the creation of the vacuum system for the NSLS-II synchrotron booster under construction at the Brookhaven National Laboratory, USA.

As was reported in the last report, the residual gas pressure is expected to be 10^{-7} Torr or better after accumulation of an integral current of about 1 A·h. 72 ion pumps (Gamma Vacuum) ensure vacuum with a pumping speed of 45 l/s. The average distance between the pumps is 2.3 meters.

The assembling of the entire vacuum system booster has been completed; vacuum $<10^{-8}$ Torr has been attained, which exceeds the expectations. The manufacture of the chambers of the injection (Fig. 5.11.7) and extraction intervals was most difficult from the technological point of view.



Fig. 5.11.7. Inlet interval (beam injection).

5.11.3. Study of activation and gas-absorbing characteristics of Wafer Module cartridge based on St'707 getter.

Cryogenic pumping can be replaced with "warm" pump systems in different injectors of hydrogen atom beams. Getter pumping is one of such systems. SAES Getters is the most popular and reliable manufacturer of various getters.

To ensure the required characteristics (vacuum not worse than 10^{-5} Torr and hydrogen dose of 10^6 l·Torr at least) we consider the possibility of applying Wafer Mod-

ule based on the St'707 getter in the beam injector. The aim of this work is confirmation of the rated values. Since cesium is used for creation of hydrogen atoms, it is important to understand the influence of cesium atoms on the activation and gas-absorption characteristics of the getter.

The regeneration time, i.e. the time during which the getter emits all absorbed hydrogen, is an important parameter. In our case, the regeneration time is about 32 hours (90% of the released gas). Fig. 5.11.8 shows equilibrium pressure of hydrogen vs. regeneration time.

Dependence of equilibrium pressure on dose (Fig.5.11.9) and on temperature of regeneration (Fig.5.11.10) are another important parameters of a cartridge.

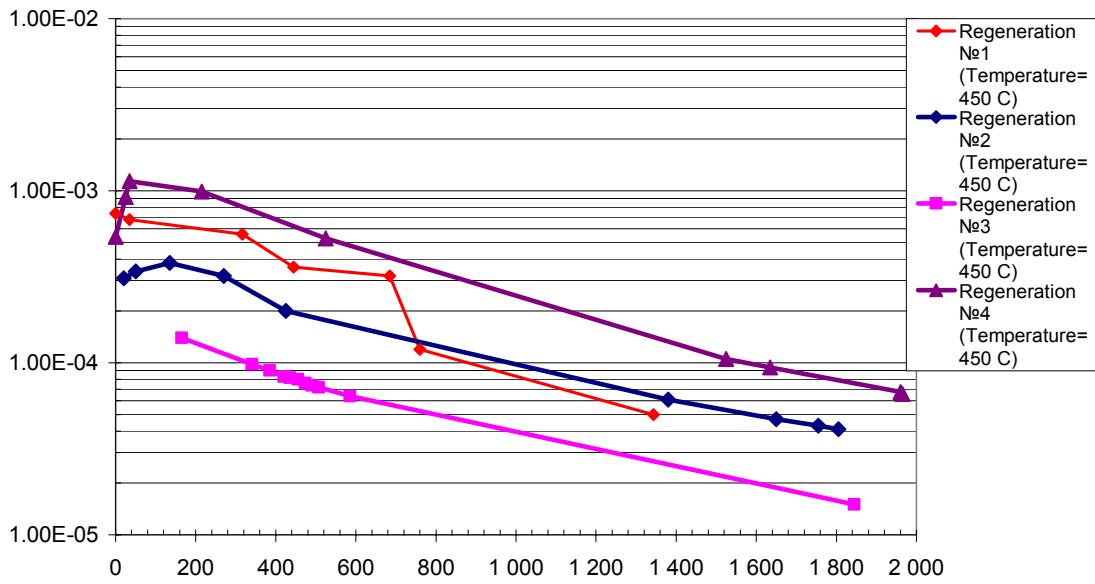


Fig. 5.11.8. Equilibrium pressure of hydrogen getter (Torr) vs. regeneration time (min).

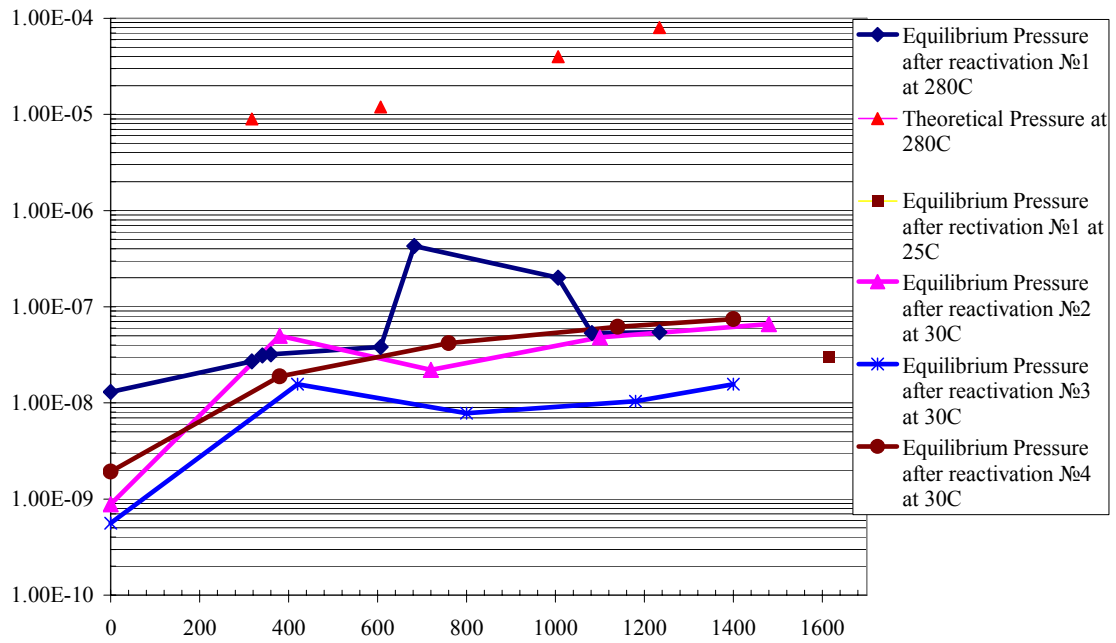


Fig. 5.11.9. Equilibrium pressure (Torr) vs. dose (L*Torr).

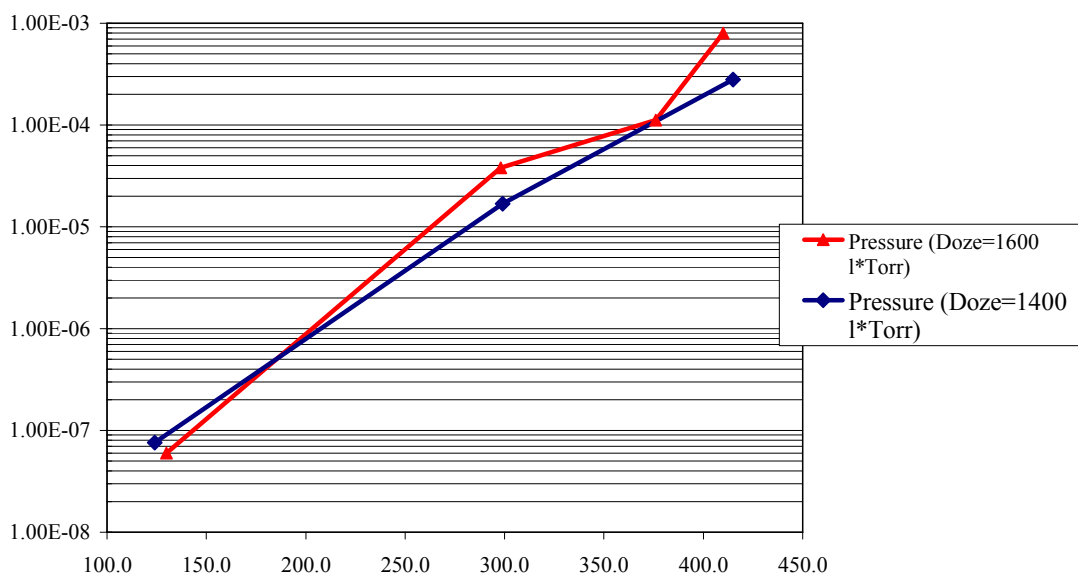


Fig. 5.11.10. Equilibrium pressure (Torr) vs. regeneration temperature (°C).

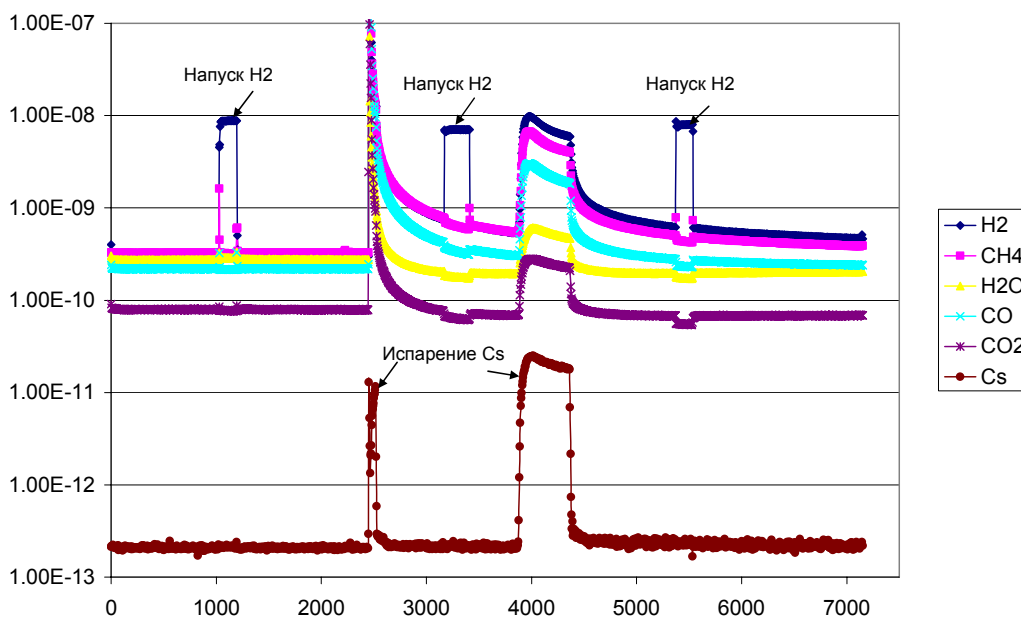


Fig. 5.11.11. Measurement of influence of cesium on getter parameters after activation. About $2 \cdot 10^{19}$ molecules of cesium were sprayed on the getter. Evaporation was going on without pre-degassing of the dispenser.

The rate of hydrogen evacuation from the getter was constant during the activations/regenerations and equaled approximately 1,000 l/s.

Experiments with cesium were conducted using a cesium evaporator (dispenser) made by SAES Getters. Cesium was evaporating after activation of the getter (Fig. 5.11.11) at 400-450 °C during 100 minutes and after regeneration of the getter. We measured the rate of evacua-

tion of hydrogen before and after the evaporation of cesium from the dispenser.

The rate of evacuation of hydrogen from the getter was constant (1,000 l/s), as well as the temperature and time required for regeneration.

6.1. INTRODUCTION

The shared-use Siberian Synchrotron and Terahertz radiation Center (SSTRC) has been operating for more than thirty years on the basis of facilities and laboratories of the Institute of Nuclear Physics SB RAS. The activity of the center includes two directions: with synchrotron and terahertz radiation.

The synchrotron radiation (SR) activity includes works on SR beams from the VEPP-3 and VEPP-4 storage rings, as well as the designing and development of systems for SR generation for Russian and foreign centers.

The other direction, associated with terahertz radiation, includes works with the use of radiation from Novosibirsk free electron laser (FEL) (in the range of 110-240 μm and 40-120 μm), as well as further development of Novosibirsk FEL and participation in international projects on this topic.

Besides that, undergraduate and graduate students are taught and trained at the center.

In 2012, 1590 hours were planned for work on SR beams from VEPP-3 (2028 hours in 2011) (60 hours were lost because of large breakdowns), and 48 hours were allocated for work on VEPP-4 (180 hours in 2011). 10 stations on 7 SR beam extraction lines of the VEPP-3 storage ring and 2 SR stations on VEPP-4 were involved in experiments. Research groups from more than 50 institutes and other organizations carried out works at the stations.

6.2. WORK ON SR BEAMS FROM VEPP-3

6.2.1. Station "Extreme state of matter".

The station is intended for investigation into fast explosion and shock-wave processes. The station is equipped with an explosion chamber and a system for registration of transmitted radiation and small-angle synchrotron radiation scattering.

Participant organizations:

- Lavrentyev Institute of Hydrodynamics, SB RAS, Novosibirsk;
- The Russian Federal Nuclear Center "All-Russian Research Institute of Experimental Physics (VNIIEF)", Sarov;
- The Russian Federal Nuclear Center "All-Russian Research Institute of Technical Physics (VNIITF)", Snezhinsk;
- the Institute of Solid State Chemistry and Mechanochemistry SB RAS, Novosibirsk;
- Budker Institute of Nuclear Physics SB RAS, Novosibirsk.

In 2012, the works at the station were carried out in accordance with plans of the participant institutions and with the financial support from the following projects and contracts:

- SB RAS integration project #65 "Study of large-scale effects in detonation of high explosives", 2012-2014;

- "Study of dynamics of condensation of nanoparticles in detonation of TATB mixtures by small-angle scattering of synchrotron radiation" and the RAS Presidium program "Matter at high energy densities," 2012-2014;

- RFBR 12-01-00177-a "Tomography of mechanical parameters of detonation flow and equation of state of explosion products", 2012-2014 (directed by E.R. Prueel); RFBR 10-08-00859-a "Study of shock wave front in nanoscopic SiO₂ aerogel using synchrotron radiation", 2010-2012 (directed by K.A.Ten); RFBR 11-03-00874-a "Study of the dynamics of condensation of nanoparticles in detonation by small-angle scattering of synchrotron radiation", 2011-2013 (directed by V.M.Titov);

- contract 2/2012 of 16 February 2012 "Study of detonation processes with the use of synchrotron radiation". Customer: Federal State Unitary Enterprise "Russian Federal Nuclear Center - All-Russian Scientific-Research Institute of Experimental Physics" (VNIIEF);

- Contract 6/2012 of 28 May 2012, "SR studies of structure of high explosives and its effect on detonation parameters". Customer: All-Russian Scientific Research Institute of Technical Physics (Russian Federal Nuclear Center - VNIITF).

Some works performed in 2012:

1. SR SAXS measurement in detonation of BTF.

Dynamic experiments with registration of small-angle X-ray scattering (SAXS) followed a measurement scheme described in papers by V.M. Titov, E.R. Prueel, K.A. Tena, L.A. Lukyanchikov, L.A. Merzhievsky, B.P. Tolochko, V.V. Zhulanov, L.I. Shehtman (Experience of using synchrotron radiation for research into detonation processes // *Combustion, Explosion, and Shock Waves*, 2011, v.47, № 6, pp. 3-16. Bibl. 26; Application of introduced nano-diamonds for the study of carbon condensation during detonation of condensed explosives. // *Nuclear Instruments and Methods in Physics Research*, ISSN 0168-9002, Section A, Vol. 603, Issue 1-2, 2009, pp. 102-104; Measurements of SAXS signal during TATB detonation using synchrotron radiation.// *PROCEEDINGS Fourteenth International Detonation Symposium*, 2010, Coeur d'Alene, Idaho, USA. PP. 387 - 391. ONR-351-10-185).

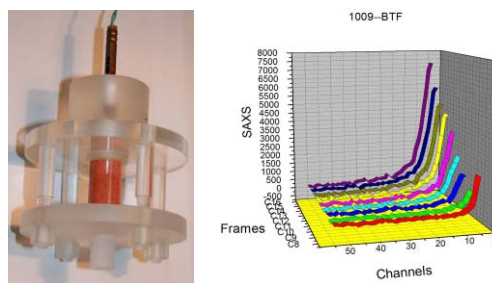


Fig. 6.2.1. General view of the experimental assembly (left). Dynamics of SAXS distribution in the BTF detonation. Frame C11 corresponds to the detonation wave passage. The time interval between frames is 0.5 μs (right).

Pressed charges of BTF were studied. The diameter of the charges was 200 mm; their length was 30 to 32 mm. A charge was placed in an assembly (Fig. 6.2.1), clamped with screws and initiated with an intermediate plasticized-TEN charge.

The SAXS distribution shown in Fig.6.2.1 is intense enough to be processed with the GNOM code.

Below are shown the processed experimental data (Fig. 6.2.2) at the moment of detonation wave passage and 1 μ s later. The volume distributions

$D(R) = \frac{4\pi R^3}{3} \cdot N(R)$, where $N(R)$ is the number of particles with the radius R , are given in the left. A graph of the relative number of particles with the radius R , $\frac{N(R)}{N}$, is

shown in the right. The value N was determined individually for each plot.

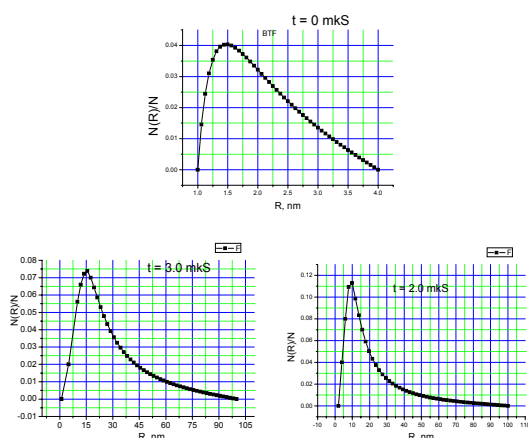


Fig. 6.2.2. Relative distribution of scattering particles in detonation wave passage after the time $t = 0.2$ and 3μ s. The radius of particle in nm is laid in the X axis.

Thus, the dynamic experiments confirm the data in the paper by I.Yu. Mal'kov, L.I. Philatov, V.M. Titov, B.V. Litvinov, A.L. Chuvilin and T.S. Teslenko "Formation of diamond from the carbon liquid phase" // *Combustion, Explosion, and Shock Waves*, 1993, v. 29, № 4, p. 131-134), which studied BTF detonation products remaining in the explosion chamber. In these experiments, the absence of hydrogen in the initial BTF composition may cause two factors of influence on the process of carbon condensation. Firstly, the absence of water vapor in explosion products leads to an increase in the temperature of the products, and hence to a rise in the rate of condensation (formation) of carbon nanoparticles. Secondly, the absence of C-H radicals may fundamentally change the course of condensation. A mathematical simulation of formation of nanodiamonds via collision of carbon atoms shows that carbon nanoparticles of 5 nm in size appear in picoseconds. In dynamic experiments, nanoparticle growth is fixed within microseconds. The presence of in-

termediate C-H radicals is one mechanism explaining the long growth of carbon nanoparticles.

2. Reconstruction of flow parameters; results obtained in detonation of BTF.

The method of reconstructing fields of gas-dynamic characteristics of detonation flow is based on a numerical solution to the gas-dynamic problem in a set corresponding to the experiment. Let us consider the problem of a cylindrically symmetric gas flow. In this case, the equations of continuity and motion in the Euler coordinates are as follows:

$$\begin{aligned} \frac{\partial r \rho u}{\partial r} + \frac{\partial r \rho v}{\partial z} &= \frac{\partial r \rho}{\partial t}, \\ \frac{\partial r \rho u^2}{\partial r} + \frac{\partial r \rho u v}{\partial z} + r \frac{\partial p}{\partial r} &= \frac{\partial r \rho u}{\partial t}, \\ \frac{\partial r \rho v^2}{\partial z} + \frac{\partial r \rho u v}{\partial r} + r \frac{\partial p}{\partial z} &= \frac{\partial r \rho v}{\partial t}, \end{aligned} \quad (6.2.)1$$

where ρ is the density; p is the pressure; u and v are the axial and radial components of the velocity vector \mathbf{v} ; r and z are the radial and axial spatial coordinates; t is the time. Changing to the Lagrange coordinate system, we will solve the problem of gas flow governed by the following equation of state:

$$p(\rho) = p_0 (\rho / \rho_{00})^{G(\rho)}, \quad (6.2.)2$$

(p_0 , ρ_{00} , and $G(\rho)$ are parameters to be determined).

Given the values of the parameters, we calculate the flow field a density distribution in which can be compared with that obtained experimentally. The calculation was performed in an area the right-hand boundary of which was considered to be flat, which corresponds to an assumption of a planar detonation wave propagating in the charge with a constant velocity D . The boundary condition was the inflow of mass and momentum flux ($\rho_0 D$ and $\rho_0 D^2$, respectively). Boundary conditions in the rest border were determined from the solution to the problem of decay of discontinuity between the detonation products and air. The use of the Lagrange coordinates allows a natural way to separate the detonation discontinuity and do the calculations only in an area occupied by the detonation flow. The numerical solution at varying required parameters was found by the Godunov method.

The required parameters were determined via minimizing the functional of standard deviations between the calculated and experimentally obtained X-ray "shadows" of the flow under study in selected nodes of the computation area. The $G(\rho)$ dependence was approximated with a cubic spline. The arising problem of multidimensional minimization was solved by the simplex method as described and implemented in the Gnu Science Library documentation.

The result of the reconstruction is the parametric equation of state of detonation products. It enables reconstructing restoring a number of mechanical parameters of the flow not only in the field of observation of the X-ray shadow, but in the whole space filled with the products of

explosion. Figs. 6.2.3 and 6.2.4 show the results obtained for a benzotrifuroxan (BTF) charge of 20 mm in diameter.

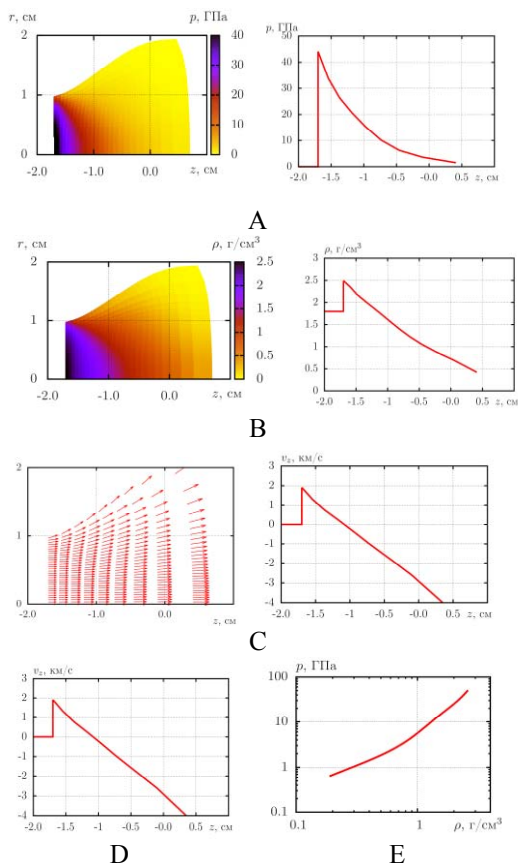


Fig. 6.2.3. Spatial distributions of parameters and their values on the axis in detonation of a cylindrical BTF charge 2 microseconds after initiation. A and E: pressure; B: density; C and E: mass velocity in the detonation front and in the stationary frame of reference; D: adiabat of unloading of detonation products, built along the flowline passing through the axis.

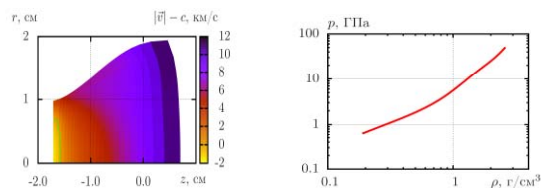


Fig. 6.2.4. Sonic border in detonation of a cylindrical BTF charge 2 microseconds after initiation.

6.2.2. Station "LIGA technology and X-ray lithography"

The station is designed for experiments on X-ray lithography in thick resistive layers with the aim of manufacture of microstructures, including X-ray masks.

Participant organizations:

- Budker Institute of Nuclear Physics SB RAS, Novosibirsk;

- the Institute of Cytology and Genetics SB RAS, Novosibirsk;
- the Institute of Solid State Chemistry and mechanochemistry SB RAS, Novosibirsk;
- the Institute of Automation and Electrometry SB RAS, Novosibirsk;
- Vorozhtsov Institute of Organic Chemistry SB RAS, Novosibirsk;
- The Institute for Automation and Control FEB RAS, Vladivostok.

In 2012, works at the station were carried out with the financial support from the following projects:

- State contract dated October 12, 2011 № 16.513.11.3135 "Development of experimental model of new-generation bio-analytical complex based on micro/nanofluidic systems";
- State Contract dated 29 August 2011 № OK12-R-VK/2011 "X-ray microlithograph";
- RFBR project № 12-02-12071 (years 2012-2014); won the ofi_m competition; title: "Development of methods for high-resolution phase-contrast imaging using X-ray diffraction optics";
- SB RAS and FEB RAS interdisciplinary project № 92 (years 2012-2014) "Material and LIGA technology for production of microfluidic analytical systems to register fluorescence".

Some works carried out at the station

They at the LIGA station on the VEPP-3 storage ring of the Siberian Synchrotron and Terahertz Radiation Center (SSTRC) implemented an X-ray lithographer, a new device for direct formation of microstructures in thick X-ray resist layers, e.g. for manufacture of X-ray masks. Special software applied, a collimated SR beam forms a microstructure pattern of a given topology directly in an active layer of negative resist SU-8 1 mm thick, the substrate moving randomly.

The aim of this work was to modernize the equipment and software of the LIGA station on the SR beam extraction line from the VEPP-3 storage ring for implementation of SR-beam formation of high-aspect structures with micron-scale elements of arbitrary topology.

They at STSRC manufactured and tested a microbeam X-ray lithographer designed for formation of deep microstructures of a given topology with smooth vertical walls. This microbeam X-ray lithographer enables flexible production of X-ray masks for deep X-ray lithography with different experimental topologies: microfluidic modules, grid elements for filtering of terahertz radiation, etc. Samples of deep microstructures of negative resist SU-8 and an X-ray mask with a 20 μm absorbing conductive layer of gold have been manufactured for deep X-ray lithography in the SR spectral range of 1-3 Å.

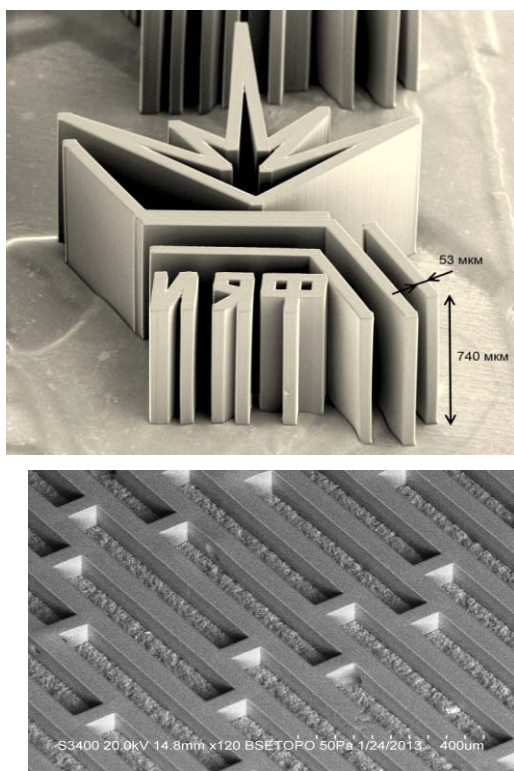


Fig. 6.2.5. Examples of microstructures.

6.2.3. Stations "Anomalous Scattering" and "Precision Diffractometry"

The station "Anomalous Scattering" is intended for research of material structure by methods of X-ray diffraction with high angular resolution using the anomalous scattering effect.

Participant organizations:

- Boreskov Institute of Catalysis SB RAS, Novosibirsk;
- The Institute of Solid State Chemistry and Mechanochemistry SB RAS, Novosibirsk;
- Nikolaev Institute of Inorganic Chemistry SB RAS, Novosibirsk;
- Tomsk State University, Tomsk;
- Tomsk Polytechnic University, Tomsk;
- Rzhanov Institute of Semiconductor Physics SB RAS, Novosibirsk.

The station "Precision diffractometry" is intended for research on material structure by methods of time-resolved X-ray diffraction under conditions of high temperature and reaction media.

Participant organizations:

- Boreskov Institute of Catalysis SB RAS, Novosibirsk;
- The Institute of Solid State Chemistry and Mechanochemistry SB RAS, Novosibirsk;
- Nikolaev Institute of Inorganic Chemistry SB RAS, Novosibirsk;

- Novosibirsk State University, Novosibirsk;
- Tomsk State University, Tomsk;
- Tomsk Polytechnic University, Tomsk.

In 2012, works were carried out at the stations with the financial support from the following projects:

- RFBR project № 11-03-00498-a, "Experimental and theoretical study of mechanism of self-excited oscillations in reactions of catalytic oxidation of methane, ethane and propane on nickel";
- RFBR project № 11-08-00625-a, "Study of mechanisms of formation of nanocrystalline state of superhard coatings produced by plasma-assisted vacuum-arc evaporation of composite cathodes";
- RFBR project № 11-08-98077-r_sibir_a "Kinetics of absorption, migration and spatial localization of hydrogen in metals";
- RFBR project № 12-03-01091-a "Nitrogen-containing carbon nanofibers: mechanisms of catalytic synthesis, properties and applications of resulting nanocomposites."

Some works performed at the stations "Anomalous scattering" and "Precision diffractometry":

1. *Investigation into the phase composition of thin films of mixed hafnium-scandium oxides obtained by the method of chemical vapor deposition (CVD).*

Nikolaev Institute of Organic Chemistry works on the synthesis of new materials for micro- and nanoelectronics. Nowadays, conventional materials cannot be used in nanometer elements of integrated circuits – the gate insulator in field effect transistors (MOSFET devices) becomes too thin, which leads to increasing leakage currents. Therefore, a material with a high dielectric constant is required, a so-called high-k dielectric. Simple and complex oxides were considered as such materials. They would have a minimum mismatch of lattice parameters with a silicon substrate. Recently it was proposed to use mixed oxides of hafnium, which have a high dielectric constant and thermodynamic compatibility with silicon. This work is devoted to the study of thin films of complex oxide of hafnium/scandium, these films produced by chemical vapor deposition.

The research was conducted at the station "Anomalous scattering" in the grazing incidence geometry. The resulting X-ray patterns demonstrate an orthorhombic hafnium oxide structure stabilized with scandium. The change in the unit cell parameter with increasing concentration of scandium is associated with formation of solid solution. Fig.6.2.6. demonstrates how the position of one of the most intense reflections from the material depends on the scandium content in the sample. The graph shows that with scandium concentrations of 9-14 at.%, the lattice parameter does not depend on the concentration, which indicates formation of a variable composition phase close in structure to $\text{Sc}_4\text{Hf}_3\text{O}_{12}$. With the same concentration range, the material has the highest dielectric constant, 42 to 44, and leakage currents do not exceed values of 10^{-8} A/cm². Thus, it can be said that a thin-film dielectric ma-

terial was synthesized. It has a high dielectric constant, chemical and thermal stability and low leakage current. The width of the forbidden band of the films is estimated to fall in the range of 4.5-6 eV, depending on the concentration of scandium.

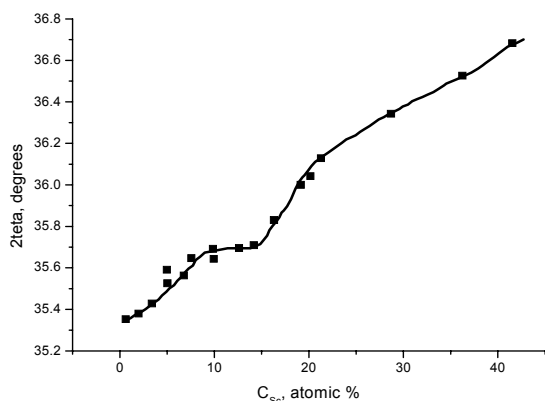


Fig. 6.2.6. Position of the (101) reflection of $\text{HfO}_2\text{-Sc}_2\text{O}_3$ vs. scandium concentration in sample.

2. Investigation into the processes of bulk diffusion of oxygen in complex perovskite-like oxides.

Owing to a wide variety of their properties, complex perovskite-like oxides are attractive materials for various applications. For example, some of perovskite-like oxides exhibit properties of high ionic, electronic and mixed electron-ionic conductivity, which is one of the requirements to materials for solid oxide fuel cell cathodes and membranes with oxygen permselectivity. A distinctive feature of oxides with such structure is the possibility of cationic substitution over a broad range of concentrations, such substitution being one of the main ways to modify properties of material.

This work presents an X-ray method of determination of the chemical diffusion coefficient of oxygen. Its main difference from the other methods, e.g. conductivity relaxation, thermogravimetry, or manometry, is the possibility of direct observation of structural changes in a sample in chemical diffusion of the components.

The experiments were performed with several series of samples, two of which are presented here as examples. Initial samples of $\text{LaFe}_{0.7}\text{Ni}_{0.3}\text{O}_3$ (LFNO calcined at 900°C) and $\text{La}_{0.9}\text{Sr}_{0.1}\text{Fe}_{0.7}\text{Ni}_{0.3}\text{O}_3$ (LSFNO calcined at 1200°C) were synthesized at the Laboratory of deep-oxidation catalysts of the Institute of Catalysis, using an original method of polymerized ester precursors (the Pechini method).

The experiments were carried out in several stages. First, the samples were heated to 900°C in a vacuum ($\sim 10^{-4}$ mbar) at a rate of $10^\circ\text{C}/\text{min}$, diffraction patterns recorded with a collection time of 1 minute per frame. Then the sample was kept in a vacuum chamber for ~ 1 hour. Further, the chamber was filled either with the atmosphere (in case of LFNO) or a gas mixture of

$1\%\text{O}_2+99\%\text{N}_2$ (in case of LSFNO), in which the sample was kept for ~ 1 hour. After that, the chamber was evacuated again, and relaxation was observed within a few hours. At these stages, the exposure time was 3 minutes per frame. Then the sample was cooled to the room temperature in the vacuum at a rate of $10^\circ\text{C}/\text{min}$, and, similarly to the heating stage, diffraction patterns were recorded with a collection time of 1 minute per frame. The detectable range of diffraction angles was $\sim 30 \div 60^\circ$.

For both samples, there is observed a slow lattice expansion in the vacuum (sections 1 and 3 in Fig.6.2.7.), which is caused by a change in the oxygen stoichiometry. These relaxation curves are well described by the following equation:

$$\ln\left(1 - \frac{\Delta\omega_t}{\Delta\omega_\infty}\right) = \ln\left(\frac{6}{\pi^2}\right) - \frac{\pi^2 Dt}{R^2}, \quad (6.2.)3$$

where $\Delta\omega_t$ and $\Delta\omega_\infty$ are changes in the mass of the sample in the time t and when the equilibrium state is reached, respectively; D is the chemical diffusion coefficient; R is the radius of spherical particle; t is the time. These curves allow one to determine the value of the reduced diffusion coefficient D/R^2 . For LFNO and LSFNO its value was $(1.97 \pm 0.01) \cdot 10^{-5} \text{ s}^{-1}$ and $(1.67 \pm 0.03) \cdot 10^{-5} \text{ s}^{-1}$, respectively. The calculations were done on interval 3 in the curve of the dependence of cell volume on time. A sharper slope can be seen at the beginning of dependence 2 in Fig. 6.2.7, which may indicate a more rapid process with the "tail" registered. From the equation it is clear that the diffusion coefficient varies significantly depending on the value of R . One can estimate the diffusion coefficient, basing on $R = 100 \text{ nm}$, corresponding to the mean radius of particles in samples, obtained by electron microscopy. For LFNO and LSFNO, it is $\sim 2 \cdot 10^{-15} \text{ cm}^2 \cdot \text{s}^{-1}$ and $\sim 1.5 \cdot 10^{-15} \text{ cm}^2 \cdot \text{s}^{-1}$, respectively.

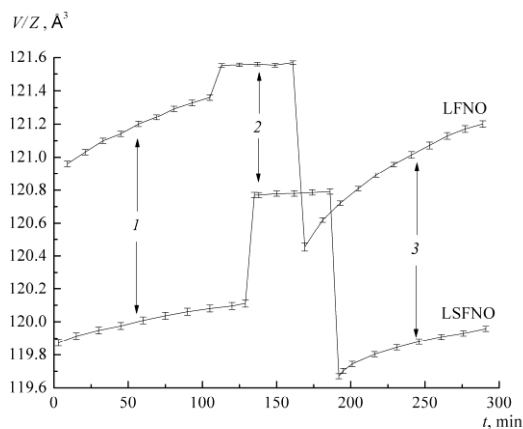


Fig. 6.2.7. Volume per formula unit vs. time for LFNO and LSFNO during the experiment at a temperature of 900°C . 1: keeping in the vacuum after heating; 2: filling with the atmosphere (LFNO) or the gas mixture of $1\%\text{O}_2+99\%\text{N}_2$ (LSFNO); 3: evacuation of the chamber after saturation of the samples with oxygen.

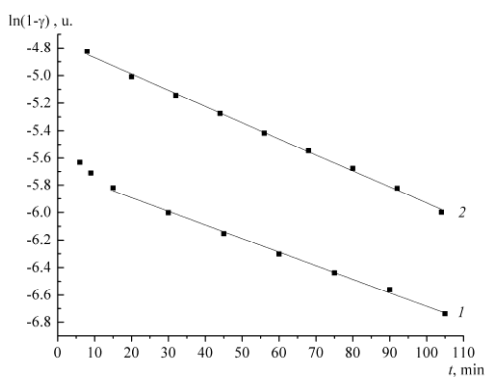


Fig.6.2.8. Time dependence of the parameter γ – ratio of the unit cell volume of the sample after the time t to the equilibrium one – for calculation of the diffusion coefficient by the presented formula. 1: dependence for LSFNO; 2: dependence for LFNO.

The so-estimated diffusion coefficients seem to be largely understated. On the other hand, changes in the volume of the unit cells of the two samples when pressure is applied or released occur in a short time of about 2-3 minutes. This may mean that two processes are running in the system at different rates, and both are associated with changes in the oxygen stoichiometry. The first process, which causes a relatively rapid, within a few minutes, change in the symmetry of the structure and increase or decrease in the volume of the unit cell, is caused by the migration of oxygen in the coordination sphere of nickel cations. In this case, the coefficient of chemical diffusion, estimated by the relaxation method or via conductivity of the LSFNO sample, is of the order of $10^{-7} \text{ cm}^2 \cdot \text{s}^{-1}$ at 700 °C. The second process, which manifests itself in a rather slow change in the unit cell volume, is the exit of the residual oxygen from the coordination sphere of the iron cations. Furthermore, the slow change in the cell volume may be due to the conjugate migration of nickel and iron cations to the surface of particles with appearance of cationic vacancies in the volume, because the chemical diffusion coefficients of the cations, according to the literature, have a similar order of magnitude.

3. Investigation into sorption of ammonia on composites 'salt in porous matrix'.

Composite adsorbents 'salt in porous matrix' (CSPMs) seem to be promising for a variety of adsorption applications, including energy-efficient processes of adsorption heat conversion. Due to the chemical reaction between the salt and adsorbed substance (water, alcohols, ammonia, etc.) vapour, CSPMs have high adsorption capacity and low regeneration temperature, and their sorption characteristics can be regulated pointedly. This allows one to design materials with properties meeting requirements of a particular adsorption process, which improves their effectiveness. Introduction of double salt systems into pores of matrix is an effective tool for synthesis of adsorbents with desired properties. This work is devoted to the investigation into the mechanism of adsorption of ammonia on

a composite adsorbent on the basis of the $(\text{BaCl}_2 + \text{BaBr}_2)$ system in pores of vermiculite, which was pointedly designed for the adsorption refrigeration cycle.

A sample was placed in an XRK-900 chamber, evacuated to a residual pressure of 0.1 mbar, heated to 423 °K during 1 hour, and then cooled to 303 °K. The pressure was monitored with a DM5001E-Y2 type pressure sensor. At the adsorption stage, the chamber was filled with ammonia to a pressure of 4.9 ± 0.1 bar with simultaneous registration of X-ray patterns, to full saturation of the sample. At the desorption stage, the saturated sample was heated in the temperature range of 303 to 433 K at a rate of 5 °C/min. The exposure time was 1 min/frame.

Fig. 6.2.9 presents X-ray patterns of the sample during the adsorption/desorption. During the adsorption, the intensity of the (112) and (211) reflections, related to the solid-salt phase of BaHal_2 , decreases gradually until complete disappearance of the reflections (Fig. 6.2.9a). At the same time there are appearing new reflections, apparently related to the phase of the ammonia complex $\text{BaHal}_2 \cdot n\text{NH}_3$. No rise of intermediate phases was observed. In the process of sorption, reflections related to the phase of the solid solution ammonia complex of $\text{BaHal}_2 \cdot n\text{NH}_3$ are shifted towards larger angles (Fig. 6.2.9a). This indicates a decrease in the parameters of the crystal lattice of the $\text{BaHal}_2 \cdot n\text{NH}_3$ complex in the process of adsorption of ammonia. Indeed, at first the inter-planar distances calculated for the reflections of ammonia complex $\text{BaHal}_2 \cdot n\text{NH}_3$ decrease with time and then cease to vary (Fig.6.2.10a). This behavior of the interplanar distances may be due to the enrichment of the ammonia complex $\text{BaHal}_2 \cdot n\text{NH}_3$ with chloride ions during the sorption process.

When the composite sorbent saturated with ammonia vapor is heated, there is observed a gradual disappearance of reflections relating to the phase $\text{BaHal}_2 \cdot n\text{NH}_3$ and appearance of reflections related to the phase BaHal_2 (Fig. 6.2.9b). No intermediate crystalline phases were found in the thermal decomposition of ammine. In the course of desorption, there was observed a shift of reflections corresponding the phase $\text{BaHal}_2 \cdot n\text{NH}_3$ towards smaller angles. The dependence of the interplanar distance on the temperature is non-linear (Fig. 6.2.10b). This indicates that in addition to the thermal expansion of the sample during the heating there occur changes in the phase of the ammonia complex, leading to an increase in the interplanar distance. Apparently, during the heating and decomposition of the complex $\text{BaHal}_2 \cdot n\text{NH}_3$, depletion of chloride ions happens. Thus, during the formation and decomposition of the ammonia complex, it changes its chemical composition. Since BaBr_2 is characterized by higher attraction to ammonia, at the beginning of the sorption process there arises a complex enriched with bromide ions, which is gradually saturated with chloride ions in the further sorption. In the decomposition of the complex $\text{BaHal}_2 \cdot n\text{NH}_3$, on the contrary, its composition is enriched with bromide ions.

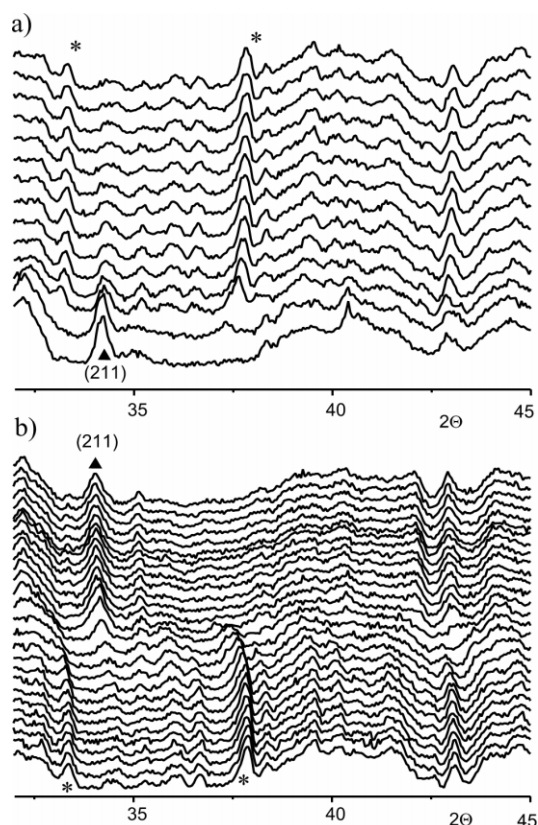


Fig. 6.2.9. *in situ* XFA data for composite BaClBr. a) adsorption; b) desorption; (*) ammonia complex $BaHal_2 \cdot n NH_3$, (▲) solid solution $BaHal_2$.

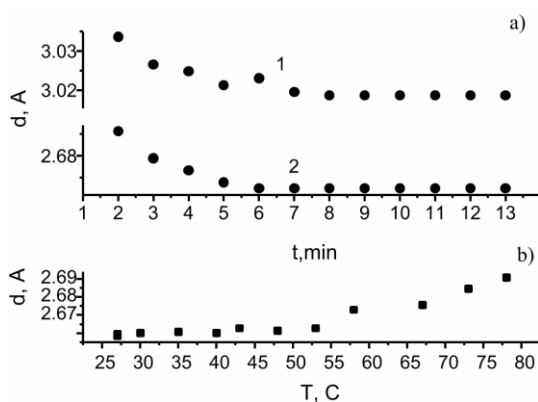


Fig. 6.2.10. Changing interplanar distances of reflections of the ammonia complex: a) adsorption; b) desorption.

6.2.4. Station "X-ray fluorescence analysis".

The station is intended for determination of elemental composition of samples of different origin: geological rocks, biological tissues, aerosols, etc., by X-ray fluorescence analysis using synchrotron radiation (SR XFA). The elemental analysis may be done in both local and scanning modes.

Participant organizations:

- Voevodsky Institute of Chemical Kinetics and

- Combustion SB RAS, Novosibirsk,
- the Central Siberian Botanical Garden SB RAS, Novosibirsk,
- the Institute of Plant and Animal Ecology, UB RAS, Novosibirsk,
- Budker Institute of Nuclear Physics, SB RAS, Novosibirsk.
- the Institute of Internal Medicine SB RAMS, Novosibirsk,
- the Institute of Geology and Mineralogy SB RAS, Novosibirsk,
- Vinogradov Institute of Geochemistry SB RAS, Irkutsk,
- the Institute of Biophysics SB RAS, Krasnoyarsk,
- Sukachev Institute of Forest SB RAS, Krasnoyarsk,
- the Institute of Geology and Geophysics, Chinese Academy of Sciences, Beijing,
- the Institute of Natural Resources, Environment and Cryology Sciences SB RAS, Chita,
- the Institute of Archaeology and Ethnography SB RAS, Novosibirsk,
- Nikolaev Institute of Inorganic Chemistry SB RAS, Novosibirsk.

In 2012, works were carried out at the stations with the financial support from the following projects:

SB RAS basic research program, Research project V.39.2.3. "Investigation into the mechanisms of formation and distribution of aerosols in the atmosphere. Physical and chemical processes of transformation and migration of fine substances in environment objects"; the SB RAS Presidium interdisciplinary integration project #34 "Cyclicity in biogeological sedimentary systems of Central Asia in the absolute time scale of the Holocene: global response of solar-terrestrial relations"; project RFBR #12-05-31324 "Investigation into the distribution of uranium and phosphorus in the sediments of Lake Baikal, oceanic ferromanganese nodules and sediments of the Uzon caldera to identify short-period climatic oscillations (by nuclear-physical methods of analysis)"; RFBR project 10-06-00406-a "Hairs from ancient tombs as an object of interdisciplinary research (study of remains of Xiongnu culture representatives)"; SB RAS Presidium interdisciplinary integration project # 50 "Reconstruction of annual dynamics of glaciers of Eastern Siberia over last millenniums from bottom sediments of proglacial lakes and terrestrial sections"; Project #6 of the SB RAS program of innovative development of unique scientific instrument making.

Some works carried out at the station:

1. *Study of the diurnal and seasonal variation of the mass concentration and chemical composition of atmospheric aerosols in the continental territory of Western Siberia.*

Examination of the diurnal and seasonal variation of the multi-elemental composition of atmospheric aerosols samples in the settlement of Kluchi and in the city of Novosibirsk, at the center for environmental monitoring, continued in 2012. In summer 2012, when intense fires

were observed on the northern territory of Tomsk and Krasnoyarsk regions, peak of smoke in Novosibirsk was observed visually on 4-8 July and 24 - July 28, which is confirmed by the satellite maps of burning natural forests. Examination of atmospheric aerosol samples in the pre-smoke, smoke and post-smoke periods resulted in a conclusion that a transfer of smoke emission far from the source of combustion has no effect on the elemental composition of the mineral component of the air aerosol. The registered significant increase in the mass concentration of the submicron fraction of the atmospheric aerosol in the smoke-filled periods of 2012 is associated with the high content of organic matter in the atmosphere.

2. Investigation into the role of atmospheric aerosols in the migration of chemical elements in the tissues of living organisms and in the environment

As part of this research, animals' (wool) and human (blood) tissues, vegetation and relevant soils were subjected to multi-element analysis.

The method of correlation analysis proved a relationship between the total concentration of elements in atmospheric aerosols of the Altai Mountains and in the wool of the gray Ukrainian and Galloway cattle and bison brought for acclimatization in this area. The figure graphically displays the relation between the elements in the wool of the Galloway cows and in the atmospheric aerosol of the Altai Mountains.

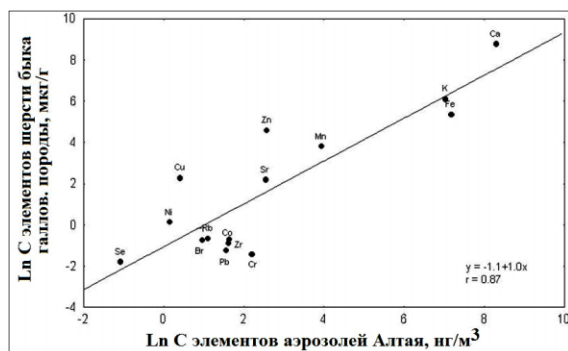


Fig.6.2.11.

Interbreed and interspecific differences in the accumulation of chemical elements were revealed from data on the content of chemical elements in the wool of the cattle. The results lead to the following conclusion: the bigger are genetic differences between herbivores, the bigger are differences in the content of chemical elements.

Collaborative research with the Institute of Internal Medicine SB RAS discovered a relationship of chemical elements with risk factors of chronic noninfectious cardiovascular disease in the population of Novosibirsk. It was shown that certain concentrations of chemical elements create a background for development of cardiovascular risk factors.

3. Investigation into cyclicity in biogeological sedimentation systems of Central Asia in the absolute time scale of the Holocene.

Cores from varve lakes of Central Asia were investigated for creation of time series reflecting the dynamics of biological, lithological, geochemical and physico-

chemical processes of sediment formation in the absolute timeline of last millenniums. The main objects of study were lakes in the south of West Siberia with sediments of annual layers (varves): Lake Shira, Lake Bele, Lake Itkul, and Lake Utyachye. Scanning microanalysis of the sediment samples was performed at the experimental station SR XFA with steps of 100 and 200 microns at excitation energies of 12, 17 and 21 keV. Processing of the profilograms assumed isolation of individual layers and detailed study of their internal structure.

In order to study the elemental composition of core samples of bottom sediments by X-ray fluorescence microanalysis with high spatial resolution, we carried out methodological works to create a one-coordinate scanner with X-ray focusing optics, a polycapillary lens. X-ray optics offers several advantages. Firstly, the minimum focus size can be about 10 microns; second, a gain in the intensity may be about 10^3 - 10^4 as compared with a collimating aperture.

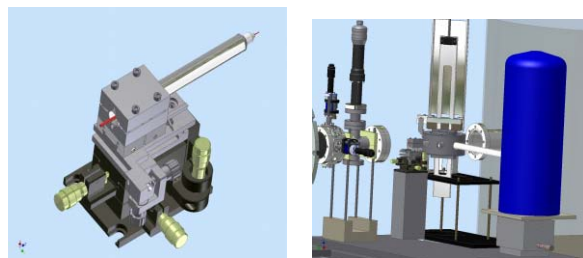


Fig. 6.2.12. X-ray optical module (left). Model of one-dimension X-ray scanner with installed X-ray optical module (right).

4. Modeling of sedimentation process in Lake Sihaylongvan.

Analytical data on the seasonal distribution of trace elements in the annual layers of the past decades, coupled with data of sediment traps, for samples of Lake Sihaylongvan enabled development of a geochemical model of seasonal deposition in systems of carbonate and clastic-organogenous sediments. The experimental data were used for verification of thermodynamic computation of the processes of carbonate sedimentation in complex biogeochemical systems.

Results accumulated for Lake Sihaylongvan allow assuming several sources of sediment and their geochemical indicators. Classification of "clastic" and "organogenous" elements allows one to go to the search of climate-dependent geochemical indicators, the content of which in different layers of sediment will reflect variations of the basic climatic parameters: temperature, amount of atmospheric precipitation, wind speed, etc. Given the analytical characteristics and prevalence of natural elements, we used a time series of Zr content. Zr time series (sediments of Lake Sihaylongvan) in the time interval of 700-2000 AD was processed by the EEMD method (Huang N.E. et al., Reviews of Geophysics, 2008) with insulation of 7 cycles with periods of 4 to 470 years.

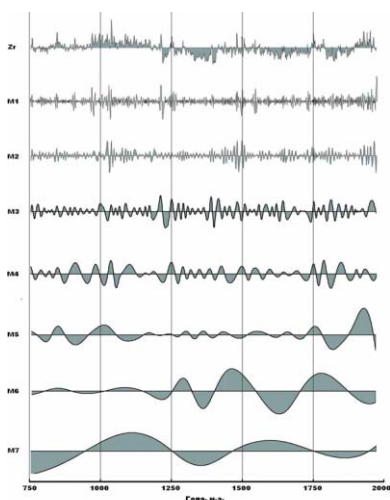


Fig. 6.2.13. An age model obtained through counting of annual layers visually insulated in thin sections of bottom sediments of Lake Sihaylongvan [G.Chu et al., 2009] was applied to the construction of time series. The model was verified with AMS ^{14}C datings.

5. Study of sediments in thermal lakes of Uzon caldera.

In the first stage, sediment cores were scanned layer by layer with excitation energies of 27, 31 and 40 keV and a step of 1mm. Quantitative distributions of elements from K through Te were obtained along the entire profile of the cut.

The application of atomic absorption analysis yielded values of concentrations of various elements at certain points along the scanning profile. The SR XFA data were compared with those obtained by atomic adsorption. Furthermore, layer-by-layer SR XFA scanning enables identification of rapidly oscillating fluctuations in concentrations of elements, which cannot be carried out with other methods. The mere obtaining of distributions of concentrations of these elements in a section of thermal lakes is of great interest, because such work was performed for the first time.

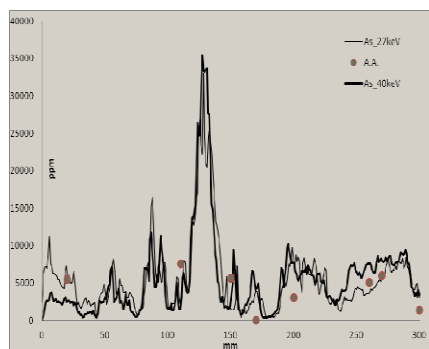


Fig. 6.2.14. Distribution of arsenic in a section of lake Fumarolnoe (the Uzon caldera, Kamchatka), absolute values in ppm for energies of 27 and 40 keV. Dots: absolute values obtained by the method of atomic absorption.

6. Research on remains of Hun people.

Hairs retrieved from ancient burials of Hun people in several Nail-Ula mounds were analyzed by the SR XFA method. The content of about 20 chemical elements in the samples was determined. The content of copper and zinc turned out to be anomalous in all the studied samples.

For understanding the causes, investigations were carried out by methods of high-resolution X-ray computed tomography, scanning electron microscopy and XAFS techniques, which gave additional information about the structure of the hairs.

7. Reconstruction of parameters of deglaciation of glaciers with a step of year to decade through interpretation of mineralogical and geochemical signals from bottom sediments of glacial lakes.

The X-ray fluorescence method with SR as the primary excitation source (SR XRF) was applied to the research on the elemental composition of a core 83 cm long with 1 mm increments from proglacial Lake Gitara, located at the foot of the glacier of Chersky mountain (Baikal Ridge, Baikal region). Concentrations of the following rock-forming and trace elements were determined: K, Ca, Ti, Mn, and Fe, as well as of the following rare and scattered elements: Ni, Cu, Zn, As, Br, Rb, Sr, Y, Zr, Nb, Mo, Ba, La, and Ce. For determination of quantitative concentrations of elements with account of humidity of the cores, samples were taken from chunks; the material was dried; tablets were made and analyzed by the external standard method (Baikal sludge standard BIL-1). Scanning (SR XFA) of three cores obtained during field work in 2012 is also close to completion. This work investigates the content of elements that are markers of physical weathering (Y, Th, Ga, Rb, Zr, Nb and Rb/Sr) and, consequently, increasing flow of clastic material of pelite and fine silt dimensions into the lake.

A distribution of elements along a core describes the following processes associated with accumulation of sediments: leaching of rocks and soils of the drainage basin of the lake, intensity of accumulation of autochthonous material, and intensity of physical wearing-off of silicates and, as a consequence, increasing flow of clastic material of pelite and fine silt dimensions into the lake

8. Creation of spectrometer for X-ray fluorescence analysis of nano-inclusions of trace elements by the method of total external reflectance.

The main goal of this project is the development of X-ray fluorescence analysis (XFA) of liquid samples using the technique of total external reflectance (TIR) to determine ultralow concentrations of rare (heavy) elements and their chemical state.

A pilot TIR XFA spectrometer was made and put into operation at the SR XFA experimental station. Tests showed that scattered light background and signals from the substrate decrease significantly in the TIR operation mode. A Si (111) crystal was used as the substrate.

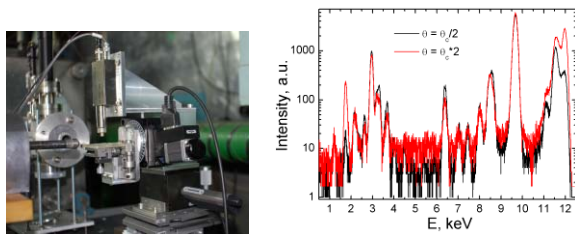


Fig. 6.2.15. TIR XFA spectrometer at the experimental station (left). Detector signal at angles less and greater than the critical one (right).

6.2.5. Station "Hard X-ray diffraction".

The station is intended for diffraction research on the structure of matter at high pressures and temperatures.

Participant organizations:

- the Institute of Geology and mineralogy SB RAS;
- the Institute of Solid State Chemistry and Mechanochemistry SB RAS;
- the Institute of Solid State Chemistry UB RAS;
- the Institute of Inorganic Chemistry SB RAS.

In 2012, works at the station were carried out with the financial support of the following projects:

- RAS (Division of Earth Sciences) program of basic research "Petrology, mineralogy and geochemistry of metamorphic rocks formed at different P-T parameters, fluid regime and geodynamic conditions (by the example of Central Asia)", 2012-2014, RAS order;
- RFBR project 10-05-00483-a "Structural evolution of Ca and Na zeolites and microporous heterosilicate equivalents at high pressures" 2010-1012;
- RFBR project 11-05-01121-a "Dynamics of lattices of microporous minerals in their interaction with aqueous medium at high pressures", 2011-2013;
- RFBR project 12-05-31431-mol-a "Sources of potassium in subducting oceanic lithosphere and its behavior in subduction metamorphism", 2012-2014;
- RFBR project 12-05-00841-a "Conditions of stability of hydrocarbon compounds at high pressures and temperatures and implications for the deep structure of the Earth and planets", 2012-2014.

Some works carried out at the station:

1. Within a research on water inclusion in the structure of silicates at high P-T parameters in connection with the problem of water transport in the Earth's crust, a transition in natural cordierite at a high water pressure of 45-50 kbar was studied. Excessive hydration, which disturbs regular compression (Fig. 6.2.16), is caused by the fact that H₂O molecules gradually occupy positions in the center of 6-fold rings. Anisotropic deformation of structure and reduced compressibility along the **a**-axis at $P > 50$ kbar are associated with the orientation of the hydrogen bonds of H₂O molecule in a 6-fold ring, which bonds prevent compression.

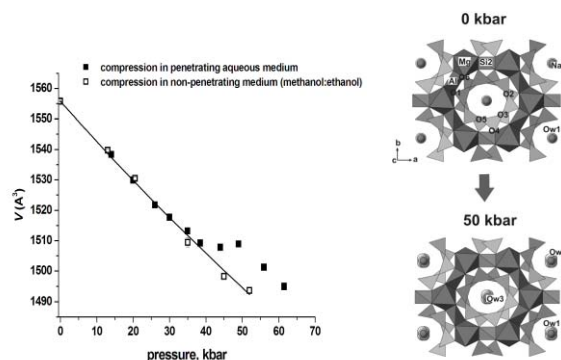


Fig. 6.2.16. Disturbance in regular compression of cordierite in an aqueous medium and a corresponding change in its structure (appearance of new H₂O positions and deformation of the 6-fold ring).

2. Within a research on the equations of state of polycyclic hydrocarbons at high pressures and temperatures in connection with modeling of deep fluids, compressibility curves and temperature dependences of elastic parameters were obtained for naphthalene (Fig. 6.2.17). Here are compressibility parameters of naphthalene with the Wien equation of state for the 298 K isotherm: $V_0 = 361 \text{ \AA}^3$, $K_0 = 9.3 \text{ GPa}$, and $K' = 6.0$.

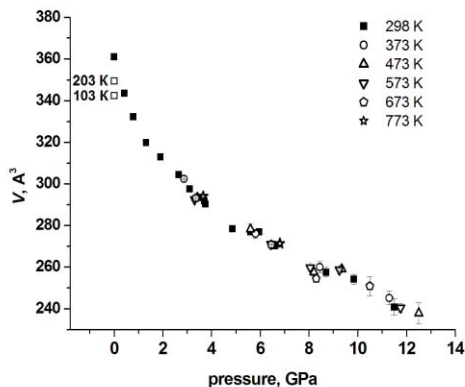


Fig.6.2.17. Pressure dependence of naphthalene C₁₀H₈ unit cell volume (space group $P 21/c$) at 298-773 K (open squares: data of low-temperature measurement at atmospheric pressure).

3. Study of the stages of phase formation under high temperatures during chemical interaction of nickel and cobalt with liquid tin, indium, bismuth and other metals and alloys.

Interaction in a solid-liquid system goes in two main directions. The first is diffusion, through which atoms of one kind penetrate into a layer of the other substance and chemical compounds form in the boundary layer. The second is dissolution of the solid component or reaction product in the liquid component and formation of crystallites either on the boundary between the solid and the liquid phase or in the near-boundary space in the liquid phase.

These processes go simultaneously, but at different speeds. For determination of a process that prevails during the interaction, research is carried out at temperatures 2-5 °C below the temperature of liquid phase formation and at temperatures 2-5 °C above this temperature.

It has been found that in cobalt-tin and cobalt-indium systems, the interaction begins only in the presence of the liquid phase, and in nickel-tin and nickel-indium and system it occurs in the solid phase, too.

6.2.6. Station "X-ray microscopy and tomography".

The station "X-ray microscopy and tomography" is intended for research on the structure of samples with high spatial resolution.

Participant organizations:

- Budker Institute of Nuclear Physics SB RAS, Novosibirsk;
- the Institute of Geology and Mineralogy SB RAS, Novosibirsk;
- Lavrentiev Institute of Hydrodynamics SB RAS, Novosibirsk;
- the Institute of Chemical Kinetics and Combustion SB RAS, Novosibirsk;
- the Institute of Archaeology and Ethnography SB RAS, Novosibirsk;
- the Institute of History of Material Culture, RAS, St. Petersburg.

In 2012, works at the station were carried out with the financial support from the following projects:

1. RFBR grant #09-05-00985-a "Zonal-sectorial structure of diamonds from kimberlite deposits of Yakutia as reflection of evolving conditions of their formation".

2. RFBR grant #12-03-13502-ofi_m_RA "Investigation into the kinetics of physical and chemical processes under the influence of pulsed laser radiation on crystalline condensed systems".

3. SB RAS project 24 "Unknown pages in the history and culture of ancient civilizations in the 1st century BC – 1st century AD (the Han Empire, Parthia, the Roman Empire, and the Empire of the Huns) from the results of interdisciplinary research on archeology findings from "royal" tombs in northern Mongolia".

Works in 2012:

- Examination of defects and micro-inclusions in natural diamonds from kimberlite deposits of Yakutia.
- Obtaining data on the microstructure of high-energy materials by computational X-ray tomography (CXT) with high spatial resolution.
- Quality control of X-ray masks for LIGA technology.
- Examination of archaeological findings by the non-destructive method of CXT.

The unique properties of synchrotron radiation (high intensity, small angular divergence, wide range, and natural polarization) allow one to work at the station in the 3-

crystal topography scheme, which is practically unfeasible with X-ray equipment, because of very long exposures. The spatial resolution of the resulting images is 2-3 microns for a monochromatic radiation with a wavelength of 1.13 Å. We have developed a scheme that provides maximum possible sensitivity to disorientation of crystallographic planes for several arc seconds; see Fig. 6.2.18 (a).

The RT was supplemented with a method based on diffraction of backscattered electrons (DBSE). The research was carried out on the scanning electron microscope "Hitachi S-3400" equipped with the attachment "Oxford Instruments HKL". We apply DBSE to imaging of crystal orientations and microdeformation in diamond samples with a spatial resolution of 5-10 μm. The accuracy of determination of direction of crystallographic axes makes parts of degree and depends largely on the quality of the sample surface. DBSE is applicable to examination of block or multiple crystals of diamond with disorientation of crystallographic planes of a few degrees; see Fig.6.2.18 (b). In this case, RT gives detailed information only about individual units of the crystal, and the full picture can be obtained by the DBSE method.

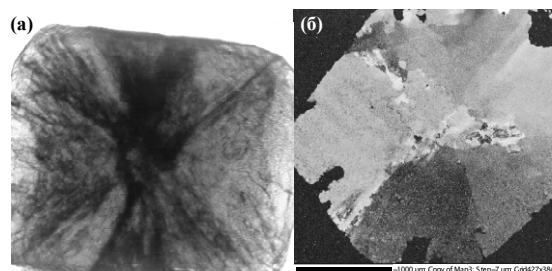


Fig. 6.2.18. Image of diamond crystals obtained using RT (a) and DBSE (b).

To understand how the microstructure of high-energy materials is interrelated with the crystalline structure of the sample, we performed experiments using the methods of X-ray computer tomography and diffraction.

The research was carried out on miniature (with a characteristic dimension of 0.8 mm) samples cut from FTDO/DNP mixture drops crystallized under various temperature conditions. Fig.6.2.19. presents images of tomographic slices of samples of the mixture FTDO/DNP = 75/25. The slices were crystallized at temperatures of +20 °C and -20 °C. The thickness of slice is 2 mm; the spatial resolution is at a level of 3-4 microns.

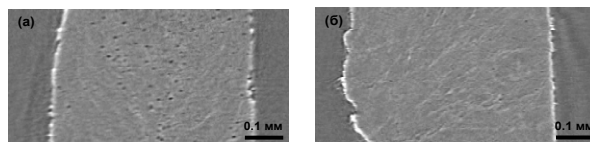


Fig. 6.2.19. Tomographic slice of samples of the mixture FTDO/DNP = 75/25 made at temperatures of -20 °C (a) and 20 °C (b).

The samples differ in concentrations of pores, which are shown black in the figure. Apparently, with rapid crystallization occurring at low temperatures, gas bubbles result from the chemical reaction do not have time to be pushed by growing crystallites on the surface of the sample.

With an addition of 3% nano-size titanium oxide catalyst (Fig. 6.2.20), the pore concentration in the sample stays low and depends on the crystallization temperature. This fact requires further investigation.

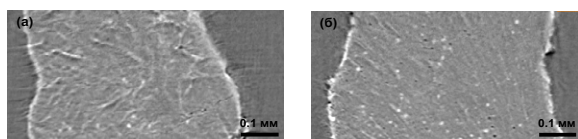


Fig. 6.2.20. Tomographic slice of samples of the FTDO/DNP = 75/25 mixture with an addition of 3% TiO₂, cut at a temperature of -20 °C(a) and 20 °C(b).

The light-colored points in Fig. 6.2.20 are agglomerates of micron-size TiO₂ nanoparticle, which indicates unevenness of distribution of the catalyst in the sample.

In all tomographic slices there are white bands, which are due to the boundaries of crystallites and indirectly indicate the direction of their growth.

From diffraction patterns in Fig. 6.2.21, recorded by the Debye-Scherrer method, one can see that the crystallite growth has a preferential direction, which causes uneven intensity in the diffraction rings.

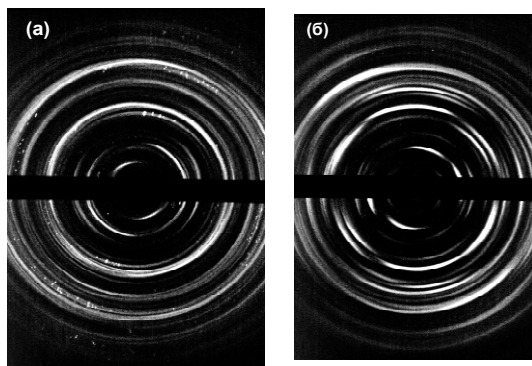


Fig. 6.2.21. Diffraction patterns of the samples of FTDO/DNP = 75/25 (20 °C) (a) and FTDO/DNP = 75/25 with an addition of 3% TiO₂ (20 °C) (b), received in a radiation with the wavelength $\lambda=0.727 \text{ \AA}$.

One can also see from the point reflections on the Debye rings (Fig. 6.2.21 (a)) that rather large crystallites arise in the samples at a temperature of +20 °C without any admixture of TiO₂.

Data on the internal structure of samples of crystallized mixtures are used for control and improvement of the technology of sample preparation and for detection of relation of results of fire tests with sample quality. Similar data were obtained earlier for samples of a molecular compound and a eutectic mixture (FTDO/DNP = 49/51

and 65/35, respectively). These measurements will be continued for mixtures with a FTDO content of up to 90%, with a more detailed analysis of the structure of samples.

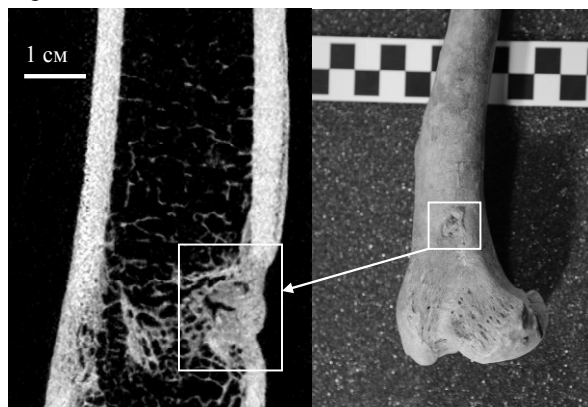


Fig. 6.2.22. Consolidated perforation in the wolf bone that was found on a site of ancient people at the mouth of the Lena River. Tomographic slice (left) and photo of the bone (right).

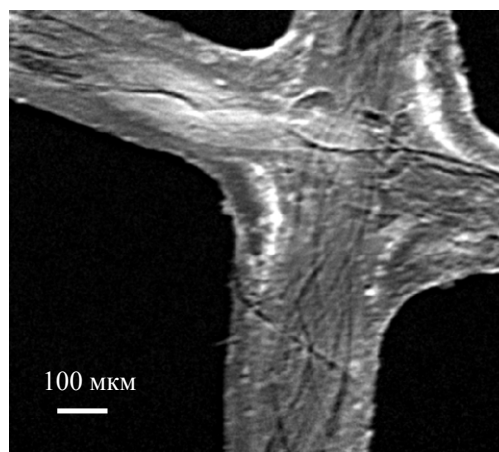


Fig. 6.2.23. Microstructure of fragment of perforated fabric that was found during excavations of burial mounds in northern Mongolia.

Non-destructive analysis carried out at the station "X-ray microscopy and tomography" is very important in the research on interesting archaeological finds that required detailed inner study. Fig.6.2.22 and Fig.6.2.23 present last-year examples of such studies performed at the station.

6.2.7. Station "Diffraction movie".

The station is intended for X-ray diffraction research on the structural and phase transformations in solids in chemical reactions. After the installation of the two-coordinate detector MarCCD, station is also used for diffraction research on single crystals. The 2D detector enables examination of small amounts of material, as well as samples of a pronounced texture.

Participant organizations:

- The Institute of Inorganic Chemistry SB RAS, Novosibirsk,
- Novosibirsk State Technical University, Novosibirsk,
- the Institute of Solid State Chemistry and mechanochemistry SB RAS, Novosibirsk.

Works in 2012:

1. Determination of structural characteristics of bismuth complex.

Bismuth citrate complexes are used in medicine as a basis for anti-ulcer drugs, eg Denol. However, the structure and structural characteristics of the active compound have not been determined, as it exists in solution and undergoes a series of transformations and loses its activity if one tries to produce a crystal.

The size of the complex was estimated from diffraction patterns at small angles.

Transmission patterns of the samples were recorded. The wavelength was 1.516 Å. The cell was made of two mica plates. The solution was placed in the cell and then the plates were compressed to a thickness allowing partial transmission of direct beam. Plot 1 in Fig. 6.2.24 presents a diffraction pattern for the pure solvent. Then, the cell was filled with Deanol solution of initial concentration (plot 3) and diluted four times (plot 2).

The broad peak was processed, and its position (3.82°) turned out to correspond to an interparticle distance of ~ 22 Å, and the width of the peak (3.57°) was found to correspond to a particle of ~ 22 Å in size. Diluting the solution resulted in a simultaneous increase in the interparticle distance and the particle size to 26 Å. This may indicate that some amount of water molecules penetrated into the structure of the complex.

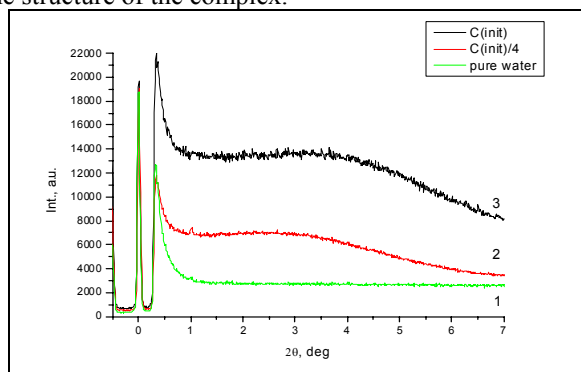


Fig. 6.2.24. Diffraction patterns of pure solvent (1), complex solution of initial concentration (3), and diluted 4 times (2).

2. Research on the structure of calcium phosphate films on surfaces of medical implants

Implants made of titanium and its alloys are widely used in dentistry and orthopedics. Implants of alumina ceramics have been introduced lately. Problems associated with improving the biocompatibility of materials and fixation of a prosthesis in a bone, accelerating the healing processes and increasing the life of implant have been

successfully solved via coating the implant surface with resorbable bioactive hydroxyapatite (HA).

The growth and crystallization of HA film on a porous surface of alumina ceramics and oxidized titanium are practically unstudied. In addition, in structural annealing it is important to ensure minimum temperature in order to reduce thermal stress and prevent destruction of the film. Dehydroxylation of HA at a temperature above 800°C and decomposition of the material are an additional case for reduction of the temperature and time of annealing. The purpose of this paper is *in situ* SR XRD research on the structural transformation in thin calcium phosphate films on the surface of medical implants made of ceramic alumina and oxidized titanium.

Calcium-phosphate films were applied by the method of RF magnetron sputtering. After the sputtering, the samples were placed in a chamber for thermal annealing. The samples were heated during 2.5 hours from the room temperature to 750°C . Diffraction spectra were recorded every 5 minutes. Immediately after the deposition, films 1 μm thick are virtually amorphous; the degree of crystallization does not exceed 20-25%. There are observed only HA-typical spectrum lines corresponding to reflections from crystallographic planes $2\theta = 25.8$ (002), 31.7 (211), and 32.2 (112). Changes in the spectra occur at temperatures of $\sim 400^\circ\text{C}$, and active crystallization of the coating begins at $520 \dots 530^\circ\text{C}$. At 700°C , the structure of the coating gets formed and will not change. There appear practically all the peaks corresponding to the structure of hydroxyapatite. It should be noted that at temperatures of about 400°C , in the diffraction pattern there appears a diffraction peak ($2\theta = 36.5^\circ$), which corresponds to calcium oxide (CaO). The presence of calcium oxide is probably due to the excess of calcium in the films as compared with the stoichiometric one. No peaks of other calcium phosphate compounds resulting from decomposition of HA were found.

The research revealed the following general regularities of formation of HA film structure on a variety of medical implants:

- regardless of the material and substrate surface morphology (porous ceramics, titanium with porous coating, pure titanium, and polished silicon), the main component (over 85%) of the calcium phosphate coating structure applied via RF magnetron sputtering, after annealing at a temperature of 700°C , is hexagonal synthetic hydroxyapatite corresponding to JCPDS-09-432;
- dynamics of structural changes in the film during the annealing process is virtually the same for all the studied substrates;
- the minimum size of the polycrystalline grain amounts to 10-100 nm.

6.2.8. Station "EXAFS spectroscopy".

The station "EXAFS spectroscopy" is intended for recording of X-ray absorption spectra (EXAFS and XANES) of different, usually X-ray amorphous, samples in liquid and solid states. The obtained data enable deter-

mination of the electronic structure and parameters of the near local environment (coordination number and interatomic distances) of ions under study, including samples that do not allow radiographic structural methods. The station is mainly used for research on fine objects: nanomaterials and catalysts. Depending on the applied methods, the volume, surface or near-surface layers are analyzed. The following techniques of spectra recording have been implemented: transmission, X-ray fluorescence, and total external reflectance. Unique methods of sample preparation have been developed for recording spectra of reaction-active compounds and catalysts under inert conditions. Samples can be investigated at temperatures of 77 to 900 K in conditions of a given atmosphere (*in situ*).

Participant organizations:

- the Institute of Catalysis SB RAS (Novosibirsk)
- the Institute of Inorganic Chemistry SB RAS (Novosibirsk)
- the Institute of Chemical Kinetics and Combustion SB RAS (Novosibirsk)
- the Institute of Solid State Chemistry and Mechanochemistry SB RAS (Novosibirsk)
- the Physical-Technical Institute UB RAS
- Topchiev Institute of Petrochemical Synthesis RAS.

In 2012, works at the station were carried out with the financial support from the following projects:

- RFBR grant 12-02-00262-a. "Research on the microstructure and electronic structure of calibrated gold clusters in cucurbit[*n*]urils with application of XAFS spectroscopy";
- RFBR grant 11-03-00219-a. "Inclusion compounds of complexes and clusters of nickel and copper in cavitand cucurbit[8]uril: chemical experiment, spectroscopic analysis, and quantum-chemical modeling";
- RFBR grant 12-03-00131 "Non-equilibrium phase formation in ternary oxide films produced via doping of HfO₂ with rare earth elements";
- RFBR project 11-03-12014-ofi-m-2011 "Multi-functional nano-sized mixed metal-oxide systems based on layered silicates as catalysts for steam reforming of methane, sustainable to sulfur-containing compounds";
- State contract № 16.513.11.3043 "Formation of space-ordered/correlated arrays of semiconductor heterostructures based on germanium and compounds of its isoelectronic series with controllable band gap for promising elements of nano-electronics and nanophotonics";
- Grant 12-03-00306-a "Determination of the structure of active centers of acid-base catalysis on layered niobates produced via exfoliation";
- Grant 12-03-00173-a "Determination of the influence of the structure of quaternary ammonium cation on the catalytic activity of tungsten peroxocomplexes in reactions of oxidation of organic compounds";
- Grant 12-03-90821-mol_rf_nr "EXAFS and XANES research on the composition and structure of supported palladium catalysts produced by various meth-

ods for liquid-phase selective hydrogenation of acetylene to ethylene after exposure to a reaction medium";

- Grant 12-03-01154 "Research on the local structure of active component of bimetallic heterogeneous supported catalysts promising for alternative power engineering and environmental catalysis";
- Grant 11-08-12104-ofi "Method of introduction of carbon nanotubes and nanowires in aluminosilicate matrix to create oxide ceramic filters".

Works in 2012:

1. Hydrogen production systems for portable power units.

Amorphous metal borides have been intensively investigated over the past 20 years because of their unique electronic, magnetic and catalytic properties. Particular attention is paid to cobalt borides as cheap but effective catalysts of selective hydrogenation, hydrodesulfurization, and reduction, as well as hydrolysis of sodium borohydride (NaBH₄) for hydrogen production for portable power units.

The CoCl₂ + NaBH₄ system is the most investigated one. Nevertheless, the nature of the resulting cobalt boride (Co_xB) has not been identified completely yet. Fresh cobalt borides are X-ray amorphous. Diffraction patterns contain a little-information broad line at $2\theta=45\pm 2^\circ$, which can be a superposition of peaks of cobalt borides of different composition (CoB, Co₂B, and Co₃B) and metallic cobalt Co⁰. Structural data on the amorphous phase of the CoB_x system can only be obtained using EXAFS.

EXAFS data have shown that the active phase is an amorphous boride of unknown structure. Its structure does not match any of the known stoichiometric borides. When calcinated, this structure is destroyed, and there arises an inactive metallic cobalt.

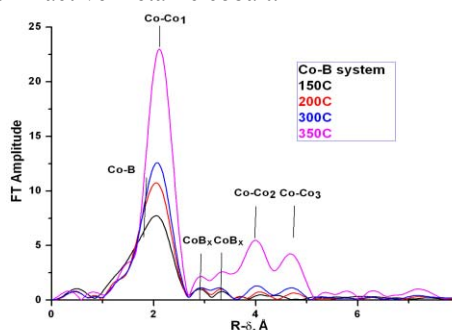


Fig. 6.2.25. Structure of amorphous boride and its transformation to pure metal during crystallization.

These results allow building a provisional model of the structure of the resulting amorphous boride. The idea is that the reduction is accompanied by formation of two-dimensional particles of metallic cobalt of hexagonal structure, which corresponds to bulk crystal structures of metallic cobalt. These nanoparticles of a thickness of one layer of cobalt atoms are crosslinked by boron atoms. Already at a temperature of 200 °C there appear far distances from the metal hexagonal cobalt phase, which are marked as Co-Co₂ and Co-Co₃ in the figures.

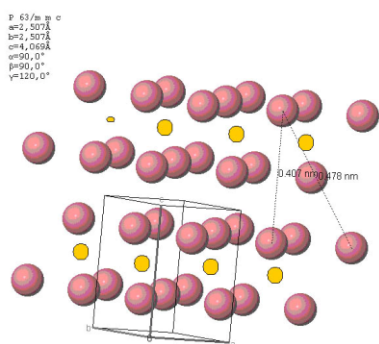


Fig.6.2.26. Model of the structure of amorphous borides.

2. Production of ethylene from acetylene for oil-associated gases.

At present, one of the most pressing problems is the processing of oil-associated gases to products of higher value. In addition to traditional approaches (through intermediate production of synthesis gas), the last decade is associated with the development of a technology based on acetylene extraction from oil-associated gases, followed by liquid-phase catalytic hydrogenation of acetylene to ethylene and oligomerization of the latter with production of components of engine fuels. The key step in the process is selective hydrogenation of acetylene to ethylene.

Pd-Ga and Pd deposited on Al_2O_3 are the most active and selective ingredients in the reaction of liquid-phase hydrogenation of acetylene to ethylene. These properties are associated with the formation of intermetallic compounds of palladium and gallium (Pd_3Ga_7 and PdGa). The increased stability of the catalysts and their selectivity to ethylene are due to the "isolation" of the acetylene adsorption sites, which leads to a change in the character of acetylene fixation to an active site.

The catalytic properties of palladium-gallium catalysts in the liquid-phase reaction of selective hydrogenation of acetylene to ethylene have been studied. Furthermore, the composition and structure of active nuclei in the Pd/ Ga_2O_3 catalyst in dependence on the preparation conditions were studied using EXAFS spectroscopy.

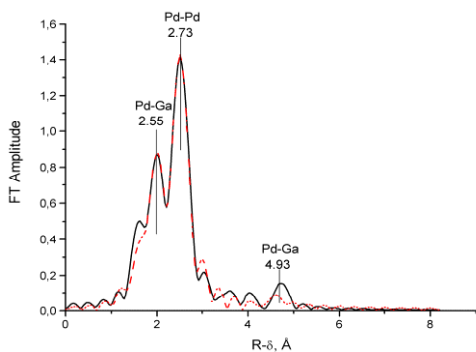


Fig. 6.2.27. Environment of palladium in the Pd/ Ga_2O_3 catalyst reduced in hydrogen at 200 °C.

Since no Pd-Pd distances exceeding 2.82 Å, which are typical to the stoichiometric intermetallic compounds, are observed in the catalysts studied, one can conclude that

no bulk phase of the intermetallic compound arises in this case. However, the presence of a short distance of 2.55 Å, which is modeled via the Pd-Ga distance, may indicate a heterogeneous-composition alloy of palladium with gallium.

According to the data obtained, at the first step of preparation of the catalyst, palladium interacts with gallium oxide and forms mixed oxides.

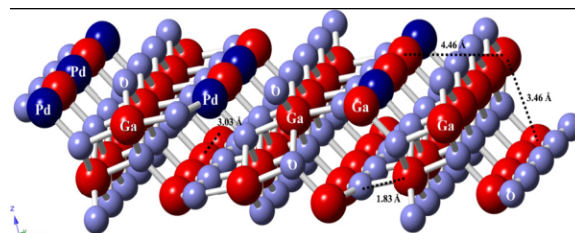


Fig.6.2.28. Model of intercalation of palladium to gallium oxide in application.

When reduced, the resulting metallic palladium activates hydrogen, which reduces not only palladium intercalated with Ga_2O_3 but also gallium to the metallic state. In this system, the corresponding alloy is formed due to the diffusion of atomic gallium from the surface into palladium particles; the metal (Pd) exists only in the nucleus of a particle and the alloy is on the surface. Thus, saturation of the surface of a metallic palladium particle with gallium results in formation of inhomogeneous microalloy in the subsurface area, the metallic palladium nucleus remaining.

One of the problems of the modern materials science is the development of approaches to production of new functional nanomaterials based on the study of fundamental laws – relationship of chemical and phase compositions, structure, and physical and electrical properties of thin films and multilayers. This problem includes production of films of binary oxides, emerging in systems based on hafnium oxide.

The current considerable attention to hafnium oxide films and solid solutions based on them is, first of all, due to the necessity of production of materials with high dielectric constant ("high k ", dielectrics) for technologies of micro- and nano-electronic devices. Hafnium oxide films are very attractive because of the large values of dielectric constant and band gap, as well as thermodynamic stability in contact with silicon.

This, however, applies only to amorphous films. HfO_2 films have a disadvantage of tendency to crystallization, and the crystalline phase has high conductivity. One way of amorphization of the films or decrease in the crystallite size is doping them with rare earth elements, aluminum and silicon.

For binary oxides $\text{HfO}_2\text{-Al}_2\text{O}_3$ it has been shown that alloying of HfO_2 with aluminum causes amorphization of the films at aluminum concentration of ~ 30 at.% [9]. There arise amorphous films of solid solutions instead of mechanical mixtures of respective oxides.

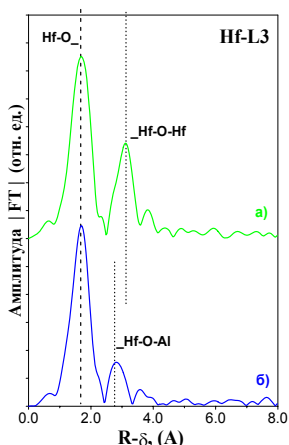


Fig. 6.2.29. Functions of radial distribution of atoms of hafnium local environment for a) HfO_2 and b) $8 (\text{HfO}_2)_x (\text{Al}_2\text{O}_3)_{1-x}$ on silicon.

These results are supported by STM data.

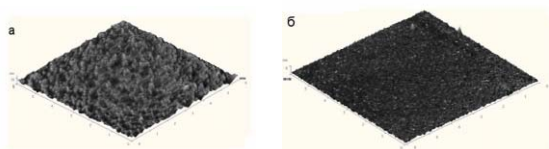


Fig.6.2.30. ACM image of the surface morphology of HfO_2 (a) and $(\text{Al}_2\text{O}_3)_x(\text{HfO}_2)_{1-x}$ films.

The surface morphology of HfO_2 films changes when films are doped with aluminum (Fig.6.2.30). The roughness of the films is 2.4 nm for HfO_2 and 0.65 nm for $(\text{HfO}_2)_{1-x}(\text{Al}_2\text{O}_3)_x$.

6.3. WORKS ON SR BEAMS FROM VEPP-4M

6.3.1. Metrological Station "Space".

In 2012, the station "Space" was involved in the development of research methodologies on the degradation of silicon photodiodes under the influence of EUV and soft X-rays. The first problem to solve was production of SR beams of a given spectral range and a power flow density (PFD) sufficient for observation of degradation of detectors under its influence within a reasonable time (1 to 10 hours). The characteristic values of the energy flow density (EFD) leading to significant degradation of detector equal (depending on the photon energy) 100 mJ/cm^2 to 100 J/cm^2 . As a rule, PFD after a monochromator at the station "Space" makes parts of nanowatt per square centimeter, which is not enough. In this regard, some optical circuits have been developed for isolation of a relatively broad spectrum band with high PFD from a "white" SR beam. The optical system includes a mirror of total external reflectance (TIR) and thin-film X-ray filter. The TIR mirror suppresses high energy photons, while the filter restricts the flow of low-energy photons. Position of the

spectrum cutoff boundary is defined by the material and thickness of the filter, as well by the sputtered material and the angle between the SR beam and TIR mirror. Fig.6.3.1 presents spectral properties of the optical elements and a typical SR range of such a filter system.

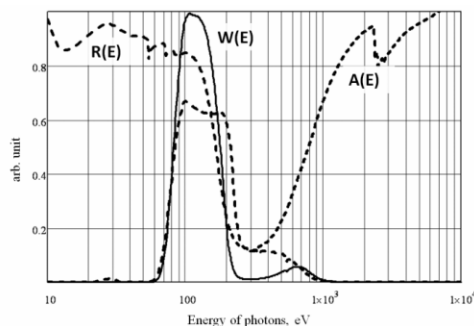


Fig.6.3.1. Spectral properties of the optical elements for quasi-monochromatic radiation in the range of 78-138 eV. $A(E)$ is the absorption factor of the Nb/Zr filter 0.2 micron thick. $R(E)$ is the reflectance of a pair of gold TIR mirrors (the angle between the beam and the mirror surface is $\theta=14^\circ$); $W(E)$ is the resulting SR spectrum after the optical system.

A number of such optical systems have been developed, which enable covering a spectral interval of 50 eV - 3 keV.

We tried to increase the radiation power using optical schemes with only one TIR mirror. From the methodological point of view, the main shortcoming of such schemes is the increased complexity of tuning and the need to arrange "theta-2theta" kinematics schemes inside the vacuum chamber. We also tried a number of schemes including a focusing spherical ($R = 10 \text{ m}$) gold-plated mirror. The focusing allowed us to increase the power density approximately one order of magnitude. The highest-aperture scheme of this type (with a working zone of 0.7 to 1.7 keV) made it possible to attain a PFD of about 40 mW/cm^2 at a storage ring current of 20 mA. Detectors of the FDUK-100UV type (developed by PTI, St.Petersburg) and AXUV-100G type (produced by IRD Inc, USA) have been irradiated in the following three spectral regions: 19.5-45 eV, 78-138 eV, and 700-1 700 eV; the acquired doses amounted to 30, 300 and 8000 mJ/cm^2 , respectively.

The essence of the technique to study radiation hardness of the detectors was to locally irradiate the surface of the detector with a quasimonochromatic SR beam and then compare sensitivity of exposed and unexposed parts. The measurements were carried out via scanning with the detector relative to a monochromatic beam of 0.5 mm.

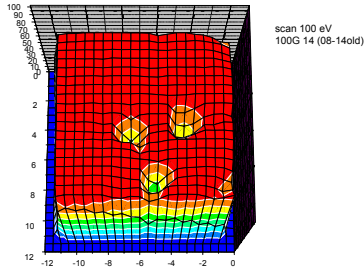


Fig. 6.3.2. Map of the AXUV-100G detector response, which was thrice irradiated with photons with an energy of 10 eV and EFD of 2.7 mJ/cm^2 . There are local places of 10% degradation of the sensitivity of the detector. The measurements were carried out at an energy of 100 eV.

Furthermore, we compared the spectral response of the detector in the irradiated and non-irradiated areas. The measurements were carried out in the spectral range of 90-120 eV (near the Si L-III absorption edge), using the regular two-mirror monochromator of the station "Space". The ratio of the spectral responses (Fig.6.3.3) demonstrates an additional 12 nm dead layer of silicon at the place of irradiation of the detector.

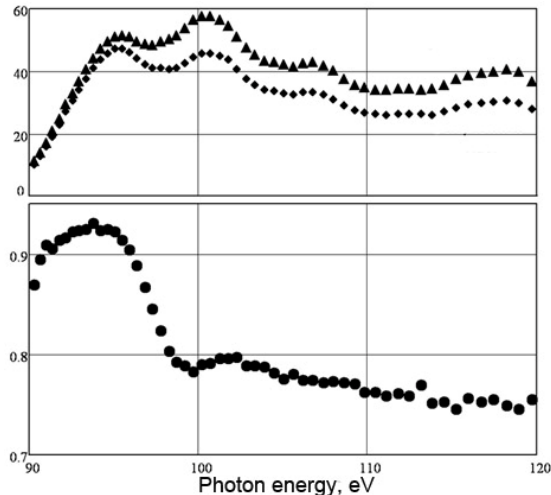


Fig.6.3.3. Top: spectral response of the detector to monochromatic radiation in the non-irradiated (triangles) and irradiated (diamonds) regions. Bottom: ratio of the two above graphs. The sensitivity jump in the vicinity of the L-III edge of silicon allows one to estimate the thickness of the additional dead layer of silicon on the surface of the detector (about 12 nm).

6.3.2. Outcoupling of radiation from 7-pole wiggler into SR bunker on VEPP-4.

The station "Detonation" on the 8th SR beam line of the VEPP-4 storage ring with a 7-pole wiggler (five main poles with a field of 1.4 T and two side ones with half the field) is intended for research on ultrafast processes in

detonation wave and in shock wave front and chemical reactions under extreme conditions. As compared with the station on VEPP-3, this new station has significantly better basic parameters of the experiment, such as intensity and hardness of the SR spectrum, explosion chamber volume, and allowable weight of samples to explode. This enables a significant reduction in the influence of impediment factors typical to small explosive samples and associated with the influence of close surface, front curvature and so on.

This new station will be equipped with the single-coordinate detector DIMEX-3. Its use at the station "Explosion" of the VEPP-3 storage ring proved SR methods using to be promising in research on ultrafast processes.

Fig. 6.3.4 shows the field distribution along the wiggler in bench tests with a maximum achievable current of 1.8 kA; the operating current will be increased up to 2 kA.

The wiggler emission spectrum for a field of 1.3 T, provided that the electron energy equals 4 GeV and the current in the storage ring is 20 mA, is shown in Fig.6.3.5 for a horizontal angle (fan) of 1 mrad (integral over the vertical angle). It also shows the spectrum after beryllium foils (of a total thickness of 12 mm) and after a nickel-plated mirror at an angle of 2 mrad to the SR beam.

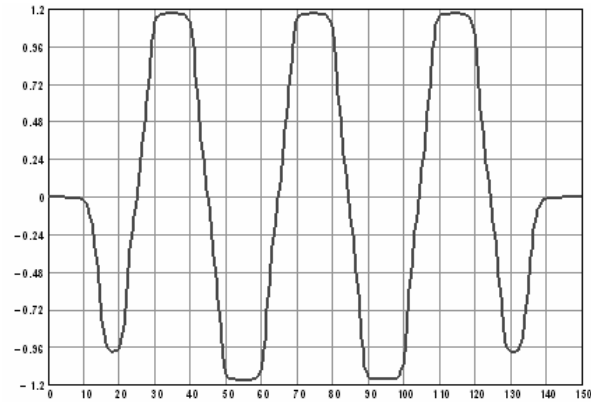


Fig. 6.3.4. Magnetic field distribution (T) vs x-coordinate (cm) at the wiggler center at the main coil current $I_{\text{coil}} = 1.8 \text{ kA}$.

Quick beam chopper with two working edges based on the integrated servodrive SPSH10 ("Servotechnika") and the Kratky collimator are placed in the pumped volume.

An ionization sensor for precise control of the beam vertical position and intensity is placed upstream the pumped volume.

The beam chopper opens the beam for a time of about 60 microseconds, which is enough for an explosive experiment and not enough for formation of a slow ion cloud, distorting the desired signal, in the detector DIMEX. The time-averaged intensity of the beam after the chopper is attenuated more than a hundred times, and this reduces the thermal load on next important element of the beam line, a nickel-coated grazing reflection mirror at an angle of about 2 mrad to the beam. The mirror makes it possible to remove the hard component of the beam (Fig. 6.3.5).

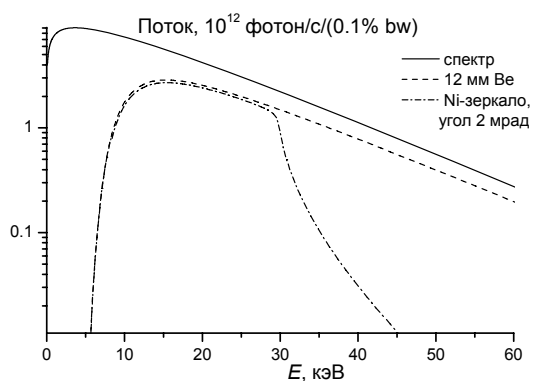


Fig. 6.3.5. SR range (a current of 20 mA, an electron energy of 4 GeV, a 1.3 T field of the main poles of the wiggler, a critical energy of 13.8 keV) from the source, after the Be foils and the nickel-coated mirror (an angle 2 of mrad).

The most voluminous element of the installation, the explosion chamber with mufflers and inputs, is placed after the mirror. The chamber is connected to the system for purging and removal of gaseous products of reaction.

The beam line ends with the recording unit. It is a radiation-protected volume accommodating the following: (a) an automated system of filter change (up to seven filters, plus "pure" beam), which are used for calibration purposes etc., (b) a knife to cut off a direct beam (for SAXS experiments, one automatically controlled degree of freedom), (c) detector DIMEX and a system for its fixation (for both horizontal and vertical positioning) and fine positioning (three automatically controlled degrees of freedom). As compared with the recording unit on VEPP-3, there was added an additional level of automatically controlled adjustment related to rotation about the vertical axis (the yaw angle circuit) and the change of filters was automated.



Fig. 6.3.6. General view of the 8th SR beam line from the 7-pole wiggler of VEPP-4.



Fig. 6.3.7. Synchrotron radiation of the 8th beam line from the 7-pole wiggler in the SR bunker of VEPP-4.

6.4. WORK WITH TERAHERTZ RADIATION BEAMS

6.4.1. Novosibirsk terahertz free electron laser

Novosibirsk free electron laser (FEL) is still the most powerful source of terahertz radiation in the world. The maximum value of average output power at a pulse repetition of 11.2 MHz is 500 W. In 2012, the time of Novosibirsk FEL operation for users was about 1000 hours. With the standard operation for users at a repetition rate of 5.6 MHz, the average radiation power at the stations depended on the radiation wavelength and tuning of the acceleration system and was about 100 W. The FEL radiation is linearly polarized and fully spatially coherent; the wavelength is tunable in the range of 40 - 240 microns; the relative spectral width (FWHM) is less than 1%; the pulse duration (FWHM) is less than 100 ps.

One of the two main objectives of the year 2012 was the organization of regular work at the six user stations. The second task was the preparation for the commissioning of the third stage of Novosibirsk FEL.

6.4.2. Experiments on THz beams

22 groups from 13 research institutions of Novosibirsk, Moscow, and South Korea worked with terahertz beams at the Siberian center of synchrotron and terahertz radiation.

Works on the terahertz beams of Novosibirsk free electron laser largely determine the current world's level in this area. The following activity should be noted:

- pioneering works on the application of THz radiation to nondestructive soft ablation of biological objects, polymers, and mineral clusters, as well as the development of rapid examination of the fractional composition of resulting aerosol particles (the Institute of Chemical Kinetics and Combustion of the Russian Academy of Sciences (SB RAS), the Institute of Cytology and Genetics SB RAS, and Budker Institute of Nuclear Physics SB RAS);
- ultra-fast precision terahertz time-domain spectroscopy of chemical objects (Budker Institute of Nuclear Physics SB RAS and the Institute of Chemical Kinetics and Combustion SB RAS);
- study of the effect of THz radiation on biological objects (DNAs, proteins, cells, and microorganisms) (the Institute of Cytology and Genetics SB RAS and Budker Institute of Nuclear Physics SB RAS);
- study of the interaction of THz radiation with new resonant metamaterials (Novosibirsk State University and Budker Institute of Nuclear Physics SB RAS);
- production of carbon nanotubes and nanohorns using a focused THz radiation beam (Budker Institute of Nuclear Physics SB RAS and the Institute of Inorganic Chemistry SB RAS);
- study of the interaction of THz radiation with materials based on carbon nanotubes (Rzhanov Institute of Semi-

- conductor Physics SB RAS, the Institute of Inorganic Chemistry SB RAS, and Budker INP SB RAS);
- plasmon spectroscopy of surfaces and films using THz radiation (Moscow State University, Novosibirsk State University, and Budker INP SB RAS);
- development of tomography, holography, and metrology with a source of coherent monochromatic THz radiation (Novosibirsk State Technical University, Novosibirsk State University and Budker INP SB RAS);
- development of methods for diagnostics of flames (the Institute of Chemical Kinetics SB RAS and Combustion and Budker INP SB RAS);
- ellipsometric measurements in the THz region of the spectrum (Rzhanov Institute of Semiconductor Physics SB RAS);
- study of combustion of H₂ - O₂ with tuning of THz radiation to the H₂O absorption line (Lavrentyev Institute of Hydrodynamics SB RAS, the Institute of Chemical Kinetics and Combustion SB RAS, and Budker INP SB RAS);
- study of detonation and explosive processes in gas mixtures using THz radiation (Lavrentyev Institute of Hydrodynamics SB RAS, Institute of Chemical Kinetics and Combustion SB RAS, and Budker INP SB RAS);
- speckle photography and speckle interferometry in THz radiation (Novosibirsk State University and Budker INP SB RAS);
- Talbot metrology in the THz range (Novosibirsk State University and Budker INP SB RAS).

Below are listed some works carried out in 2012 and their executors.

1. The effect of THz radiation on the spin state of a photoswitchable polymer complex was studied. Budker INP SB RAS and the International Tomography Centre SB RAS.
2. A unique method of ultrafast high-resolution spectral measurements in the terahertz range was developed. Direct measurements of time dependence of narrow-band terahertz emission from molecules excited with a powerful and relatively short FEL pulse were carried out for the first time. Budker INP SB RAS and the Institute of Chemical Kinetics and Combustion of the SB RAS.
3. Sensing of thin films on metal surfaces by the method of plasmon-polariton spectroscopy was demonstrated. Budker Institute of Nuclear Physics SB RAS and Scientific and Technological Center of Unique Instrumentation (Moscow).
4. A technique of examination of condensed media with a THz attenuated total reflection spectrometer was developed. Budker INP SB RAS and Novosibirsk State university.
5. Properties of semiconductors promising as concerns creation of THz detector arrays were investigated. Budker INP SB RAS and Rzhanov Institute Semiconductor Physics SB RAS.

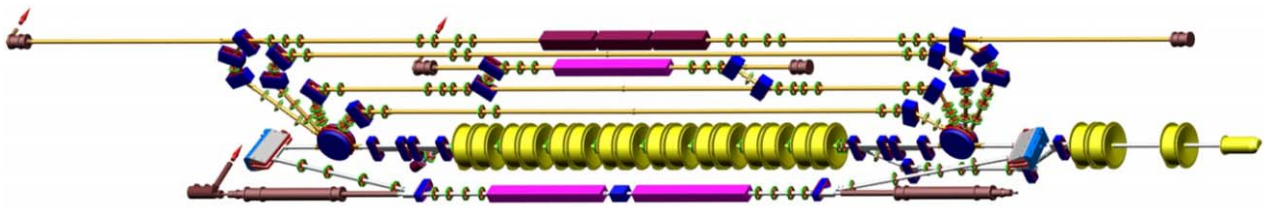


Fig. 6.4.1. General view of the energy recovery linac with free electron lasers installed on the first, second, and fourth tracks. A circulating electron beam was obtained on the third and fourth tracks in 2012.

6.4.3. Upgrade of the FEL and commissioning of the third stage of the energy recovery linac

In 2012, components for upgrade of the RF generator were designed and manufactured. Cables for measurement of voltage phases on the accelerating RF cavities were replaced to air-insulated ones, which increased the absolute measurement accuracy. The upgraded output stage of the RF generator was tested. Parameters of the output circuits were tuned for suppression of self-excitation. An additional high-voltage rectifier was designed for increasing the anode voltage.

The magnetic-vacuum system of the third stage of the FEL is situated on the third and fourth tracks of the energy recover linac (ERL) (see Fig. 6.4.1). It consists of 10 bending magnets and 7 large and 26 small quadrupole magnets. Besides, it includes vacuum chambers with ion pumps, electron beam position monitors, vacuum valves, and units for synchrotron radiation extraction.

In 2012, the mode of fourfold acceleration and fourfold deceleration of electrons in the four-track ERL of the FEL third stage was demonstrated for the first time, with eight different beams observed on the pickup electrodes of the common track at different moments of time (see Fig. 6.4.2). One can see on this oscillogram that beam currents are about the same, which is an evidence of almost full passage of electrons throughout the ERL. More accurate measurements of current in the dump show that over 95% of electrons arrive to the beam dump.

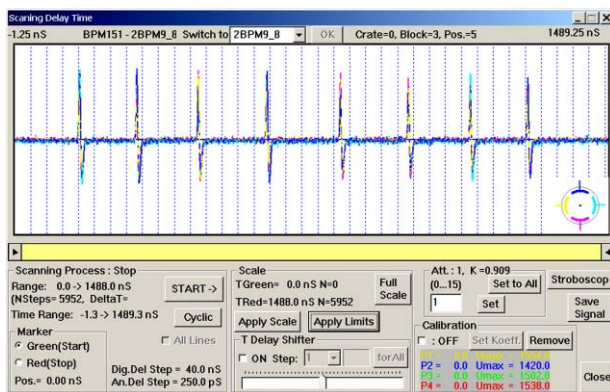


Fig. 6.4.2. Signal from one of the pickup electrodes of the common track.

Transverse beam positions at all pickup stations are shown in Fig. 6.4.3.

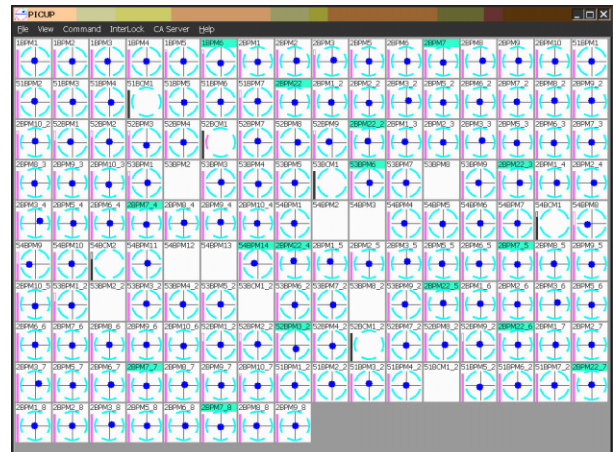


Fig. 6.4.3. Transverse beam positions at all pickup stations.

Thus, the world's first four-track energy recover linac has been constructed and commissioned.

This facility is a proof of the feasibility of the new class of accelerators, i.e. the multi-track energy recovery linacs. These accelerators can be used for generation of subpicosecond X-ray pulses of high brightness with a repetition of tens of megahertz. Ultrashort X-ray pulses are applied to the study of fast processes, for example, chemical reactions and fast phase transitions. Another promising application of this class of accelerators is nuclear physics experiments with internal target.

6.4.4. Assembling undulators for the third stage of the FEL and correcting field in them

The third stage FEL is an optical klystron with a buncher that accommodates a radiator. The FEL uses three identical permanent magnet undulators.

Magnetic blocks are mounted on the top and bottom bases ("jaws") of the undulator (see Fig.6.4.4). The bases, in turn, are held by actuator screws fixed on the frame. Rotating the screws, one can adjust the working gap of the undulator and thus the amplitude of its field.



Fig. 6.4.4. Assembly of one of the three undulators of the third stage.

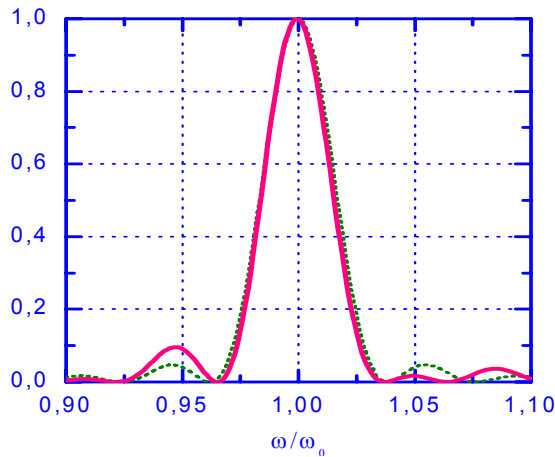


Fig. 6.4.5. Forward spontaneous emission spectrum in the measured field. The dashed line shows the ideal spectrum.

Moving Hall probes along the undulator, we measured magnetic field values. The design of the undulator is such that any of the magnetic units can be replaced for correction of magnetic field. To be sure that the level of field errors is low, we calculated the motion trajectory and the spectrum of forward spontaneous emission (Fig.6.4.5) in the measured field. The deviation from a straight path is much smaller than the transverse size of the eigenmode of the optical resonator (the intensity rms size is about 2 mm). The spectrum broadening and corresponding decrease in the amplitude of spontaneous emission are also small. The field quality in the undulator, therefore, was found to be acceptable.

Besides that, some elements of the optical resonator of the third stage FEL were fabricated and the project of outcoupling of radiation from the third stage FEL was developed.

6.4.5. Results of 2012 and plans for 2013

Main results of 2012:

1. The world's first energy recovery linac with four tracks was commissioned.
2. Experiments using THz radiation at user stations were continued.
3. Development and fabrication of components of the test bench for the RF injector were continued.

Plans for 2013:

1. Mounting of the optical resonator, installation of undulators, and commissioning of the third stage of the FEL.
2. Continuation of the creation of new stations.
3. Further experiments using THz radiation at the user stations of the third stage.

6.5. DEVELOPMENT AND CREATION OF SPECIALIZED SR GENERATORS – SUPERCONDUCTING WIGGLERS

Contract works on the development and production of various superconducting cryogenic magnetic systems for SR generation were continued in 2012.

In August 2012, a trial run of a 63-pole wiggler (Fig.6.5.1) with a period of 51 mm, a magnetic field of 4.0 T and a pole gap of 15.2 mm was carried out at the customer's site. This wiggler is intended for the Australian Synchrotron storage ring (Melbourne). Zero consumption of liquid helium was demonstrated, as well as negative pressure in the helium vessel with helium temperature decreased to 3.5 K. This enabled attaining a magnetic field exceeding the planned 4.2 T. Preparation to the mounting of the wiggler on the Australian Synchrotron storage ring is underway. The final commissioning is scheduled for January 2013.



Fig. 6.5.1. 63-pole 4 T wiggler for the Australian Synchrotron storage ring (Melbourne).

A 15-pole wiggler (Figs.6.5.2 and 6.5.3) with a field of 7.5 T, a magnet gap of 26 mm and a period of 200 mm for the CAMD-LSU storage ring (USA) was assembled in its own cryostat in October of 2012. After a training of the superconducting magnetic system, the required level of magnetic field was achieved. Now assembling of the wiggler in its cryostat is close to completion. A full cycle of tests and dispatch of the wiggler to the customer are scheduled for January 2013. Commissioning of the wiggler on the CAMD-LSU storage ring will take place in March 2013.

The "short" prototype magnetic system for the multi-pole wiggler CATACT (Fig.6.5.4) for the ANKA storage ring (Karlsruhe, Germany) was successfully tested in November 2012. Now a full-length 44-pole wiggler with a period of 48 mm, a magnetic field of 2.5 T and a pole gap of 20 mm is being fabricated.

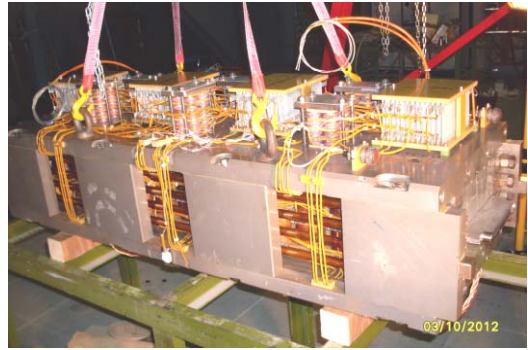


Fig. 6.5.2. Superconducting magnetic system of the 15-pole wiggler with a field of 7.5 T for the CAMD-LSU storage ring (USA).

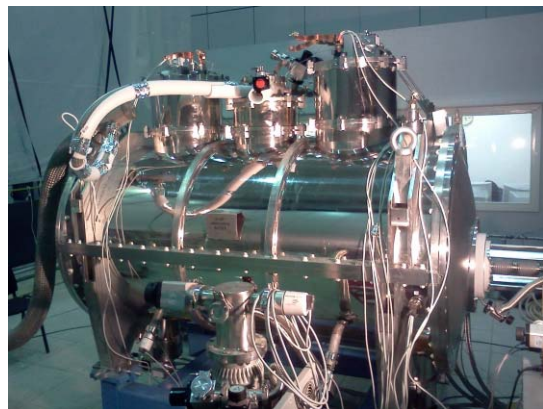


Fig. 6.5.3. 15-pole wiggler with a field of 7.5 T and a period of 200 mm for the CAMD-LSU storage ring (USA).

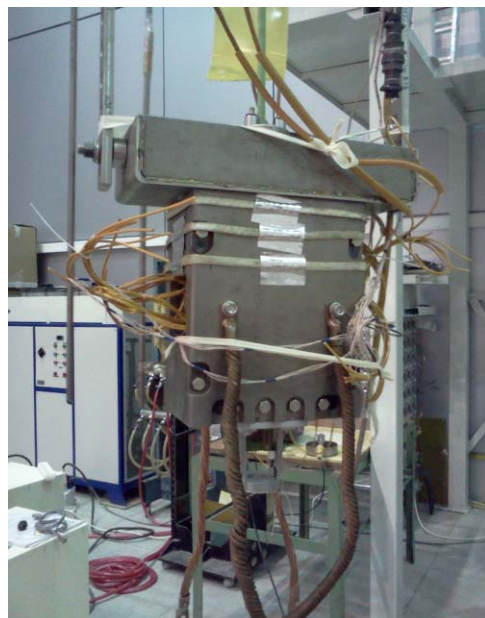


Fig. 6.5.4. Prototype magnetic system of the multi-pole 2.5 T wiggler CATACT for the ANKA storage ring (Karlsruhe, Germany).

Another wiggler (CLIC) with a field of 3 T, a period of 51 mm and a magnetic gap of 18 mm, manufactured for the ANKA storage ring (Karlsruhe, Germany), differs radically in design from all previous wigglers. In this wiggler, cooling to low temperatures is performed not with liquid helium, but by means of chillers, through thermal mechanical contacts (Fig.6.5.5). The magnetic system is thus located in vacuum. A short prototype of such magnet was tested in December 2012. It was cooled to a temperature of 3 K, and the attained magnetic field level was 3.3 T. At the moment, the magnet is being tested in different operation regimes. The commissioning of the full-scale magnet with contact cooling is planned for early 2014.



Fig. 6.5.5. Prototype of the superconducting helium-free wiggler CLIC with a 3 T field for the ANKA storage ring (Karlsruhe, Germany).

The upgrade of already operating wigglers, which was started in 2011, continued in 2012. Contracts on the manufacturing of new cryogenic systems with zero consumption of liquid helium for the wigglers for ELETTRA (Trieste, Italy) and HMI (Berlin) were concluded. Both the contracts are to be completed in the summer of 2013.

Introduction

BINP works in the field of radiophysics and electronics are performed mainly by the Radiophysics laboratories. The laboratories are engaged in the development and research of radio physical systems for accelerators and storage rings of charged particles, facilities for studying the physics of high-temperature plasma and other systems.

These works include development of diverse radio-electronic equipment (power supplies, control and diagnostics systems, computer control systems, RF accelerating systems and sources of RF and microwave energy) and research on behavior of charged particle beams in interaction with accelerating systems and other elements and devices of accelerators and storage rings of charged particles. The main laboratories' results are part of the general results of research and works carried out at the existing complexes: VEPP-4, VEPP-2000, FEL, the injection complex and systems for research on the physics of high-temperature plasma.

Due to their universal character, some developments performed by the laboratories have become a basis for new devices of independent scientific and technological value. Some developments are used at the Institute in research on other topics and performance of contracts with Russian and/or foreign scientific centers (USA, Germany, Switzerland, Japan, China, and South Korea).

It should be noted that 2012 was a very tense year for the staff of the Radiophysics laboratories, because of the large amount of works under contracts with the research center at Jülich Institute (Germany), Brookhaven National Laboratory (USA), KAERI (Korea), TAE (USA) and other partners.

Below are summarized some results of the works carried out in 2012 and guidelines for activities that will continue in 2013 and further.

7.1. POWER SUPPLIES FOR ELECTRO-PHYSICAL INSTALLATIONS

7.1.1. Stabilized current sources.

Development of stabilized current sources for powering various electrophysical installations and their components is one of the main objectives of the Radio Physics Laboratory. Those are, first of all, sources of direct current for powering electromagnets of charged particle storage rings. Depending on application, the output current of such sources makes up amperes to tens of kiloamperes. Correspondingly, the output power is tens of watts to hundreds of kilowatts or megawatts. Current of these power supplies is typically widely variable (up to 60 dB) with high accuracy and stabilization (error of 0.01% or less). Current sources are complex electro-physical devices with computer control, monitoring and testing and with a complex system of locks and internal control devices. The Russian industry produces no analogues.

Works on upgrading power supplies and instrumentation of the physical facilities of the Institute continued.

- In 2012, the long-term work on the modernization of the electronics of precision sources of the "IST" series for powering electromagnets was continued. Such a device for a power of 50kW, 100kW and 200kW has a thyristor regulator and a pulse suppression channel. The sources are governed by integrated controllers (SEAS121), containing a single-channel 20-bit DAC and 8-channel 24-bit ADC. Current is measured using contactless magnetic modulating pickups (DCCTs).
- New-version current sources of the "IST" type with an output current of up to 400 A and power of up to 200 kW enable testing of the electron cooling installation, which was designed and fabricated by BINP for Jülich Research Center, Germany. Thyristor rectifiers of these current sources were manufactured at the Low-Voltage Equipment Plant (NVA, Rasskazovo, Tambov region) and furnished with electronics for current control and stabilization that was developed and manufactured by BINP.
- In 2012, a number of innovative power supplies for electromagnets of the booster accelerator of the NSLS-II synchrotron light source (BNL, USA) were manufactured and successfully commissioned. The booster is capable of operating at a repetition rate of up to 2 Hz, so requirements to the power sources are quite rigid. While meeting high requirements to current stabilization accuracy, the sources shall have good dynamic characteristics. In particular, the time of current rise from minimum to the nominal value must be 0.26 seconds at most for all the power supplies. The total number of developed and manufactured current sources for electromagnets of the booster is more than 50. Table 1 shows the main parameters of these power supplies.
- In 2012, the development and manufacturing of high-precision current sources with an output power of up to 10 kW and a current of up to 1000 A were continued. The sources were made with converters of high (about 20 kHz) frequency. That involved designing and manufacturing of new high-precision four-quadrant power sources of the "RF-500" type (500A/12V), which were delivered under contracts to BNL, the USA (2 items) and KAERI, Korea (4 items).
- Development and full-scale testing of a high-power (an output current of up to 800 A and maximum voltage of up to 400 V) precision source of pulsed current of arbitrary shape were completed. Such sources are needed for powering magnetic systems of synchrotrons and booster accelerators operating with a repetition rate of 2.1 Hertz.

Table 7.1.1. Main parameters of the power supplies for the NSLS-II booster.

Power supply	Q-ty	Max current, A	Max voltage, V	Max power, W
BR-QF	1	157	207	32.496
BR-QD	1	85	49	4.200
BR-QG	1	126	73.2	9.229
BR-SXV	8	18	17.4	2.507
BR-SXH	8	18	17.4	2.507
BR-Corr	32	7	8.8	1.963
DC-septum	1	400	15	6.000

- A substantial amount of high-precision current sources for correctors were produced under contracts. In particular, over 50 current sources of the "MPS-6" type (an output current of up to 6 A), 10 power sources of the "MPS-20" type (an output current of up to 20 A) and 10 2-channel units of the "SR-20-30" type (current stabilizers with magnet coil shunting) were manufactured and put into operation in 2012.
- Over 30 channels of sources for corrective magnets with output currents of up to 3 A were manufactured and put into operation. The sources were delivered to KAERI, Korea and are also used at BINP SB RAS.
- Development and production of a power system for correction magnets for the X-Ray Free Electron Laser Facility (Germany) were started. The system includes about 400 high-precision current sources.
- In 2012, we continued the development and fabrication of individual units of a high-voltage source for the high-power injector of negative ions which is to be produced under a contract with TAE, the USA. Parameters of the high-voltage power supply are as follows: $U(\text{output})=880$ kV; $I(\text{output}) = 10$ A; $T(\text{imp}) = 100$ seconds. The high-voltage power supply consists of eight in-series connected high-voltage rectifiers with an output voltage of 110 kV. The rectifiers are placed in one volume, which is filled with insulating gas. Regulated AC voltage for these rectifiers is produced by high-power voltage invertors (a frequency of 2 kHz and output power of up to 300 kW).
- For the stand of the negative ion source to be produced under the contract with TAE, the USA, we are making a high-voltage power supply for 120 kV and 100 mA. It consists of a high-voltage generator (voltage multiplier) and a regulated voltage inverter of high (20 kHz) frequency.

7.2. SOURCES OF STABILIZED HIGH DIRECT VOLTAGE

The Institute is successfully developing high-voltage sources of direct stabilized current with a wide power range:

- tens of watts, for powering electrostatic devices for deflection or focusing of charged particle beams;
- hundreds of watts to tens of kilowatts, for powering various high-voltage direct-action accelerators;
- hundreds of kilowatts, high-voltage power for ion sources and atom injectors.

High-voltage power supplies have good stability and accuracy of regulation; they are protected from breakdowns and short circuiting.

7.2.1. High-voltage power supplies for atom injectors for diagnostics and plasma heating in plasma devices.

Development and creation of high-power high-voltage power sources for atom injectors for corpuscular diagnostics and plasma heating in experimental plasma devices remains one of the important activities of the laboratory.

7.2.2. High-voltage power supplies for accelerating tubes.

The development, improvement and manufacturing of components and units of high-voltage power sources for electron acceleration tubes were continued in 2012.

- The production of high-voltage power supplies for the FEL and electron-beam welding installations started using elements of cascade generator (push-pull voltage multiplier). The PSs are designed for work with a beam current of 100 mA. The output voltage of the FEL HV power supply is 300 kV, and that of the EBW PS is 60 kV.
- An HV rectifier with an output voltage of up to 60 kV and a high-frequency (20 kHz) semiconductor converter for the EBW installation with power increased up to 60 kW were designed and manufactured.
- A high-power (40 kW) resonant inverter with high conversion frequency (25 kHz) was developed for powering an acceleration tube with a voltage of up to 2 V for the electron cooling facility for the COSY accelerator, Germany.

The creation and acceptance tests of the electron cooling installation developed for Jülich Research Center, Germany were completed in 2012. A "high-voltage tower", producing a regulated stabilized voltage of up to 2 MW with a stability level of the order of 10 ppm is one of the most complicated elements of the installation. The "high-voltage tower" consists of cascaded high-voltage transformers operating at 20 kHz. Additional windings of the transformers are used for creation of regulated current in solenoids distributed along the tower. The "high-voltage tower" is a complex mix of power, control and measurement electronics. It has an electron beam dump for a power of up to 15 kW. For generation of regulated voltage across the dump (1 ... 5 kV), an innovative voltage source was designed and built with a power of up to 15 kW under a HV potential of 2 MV.

7.2.3. *Switching Power Supplies for electromagnets of accelerator complexes.*

Production of various surge current generators was continued in 2012. 75 switching power supplies of the "GID-25" type were produced for beam transport line "K-500". One rack accommodates 8 generators of the "GID-25" type, and automated control units. The power supplies have been prepared for real-load tests.

7.3. DEVELOPMENT OF MEASUREMENT SYSTEMS AND DEVICES FOR AUTOMATION OF PHYSICAL EXPERIMENTS

The laboratory participates in automation of installations, test benches and large physical complexes:

- development and delivery of ready-made systems (control, diagnostics and computer systems) with subsequent participation of the authors in adaptation of the systems;
- development of elements of control and timing of power supply systems with subsequent comprehensive delivery of these systems to accelerators and charged particle storage rings and studies of their influence on the complex as a whole;
- delivery of individual standardized modules (CAMAC, VME, "Cherry" and Euromechanics) to existing or new installations and stands;
- development of new approaches, techniques and, as a result, new devices that enable solving physical experimental problems at a new level;
- modernization of existing automation, control and diagnostics systems on operating physical installations;
- repair and maintenance of several thousand units of electronics and whole systems developed by the laboratory.

Equipment developed and manufactured by BINP is widely used not only at the Russian Academy of Sciences, but also at many scientific organizations in Russia and abroad. Below are presented main results in 2012.

- New electronics were manufactured and launched for 4 pick-ups installed on the VEPP-2000 storage ring. The electronics have high temporal resolution, enabling separate measurement of position of electron and positron beams passing through a pick-up with intervals of ~ 20 ns. The total error of coordinate measurements is about 10-20 microns. The electronics allow turn-by-turn measurement of beam position. A pick-up station is a 1U Euromechanics module with a depth of 200 mm. 15 pick-up stations are planned to be produced based on this development and installed on VEPP-4 (in addition to 3 pick-up stations already installed).
- New version of precision electronics for pick-ups was designed, manufactured and tested on VEPP-3. Parameters of the new electronics are comparable with similar parameters of the penultimate version by Libera Brilliance (Instrumentation Technologies, Slovenia). The beam position measurement error does not exceed a few microns. This electronics cannot measure position of individual bunches, but it enable turn-by-turn measurement for all bunches summed. A pick-up station is a 1U Euromechanics module with a depth of 330 mm. A prototype worked on VEPP-3 for more than six months. 5 additional pick-up stations are planned to be produced based on this development and installed on VEPP-3.
- New electronics for pick-ups for the linear accelerator of the injection complex were developed. An electronics prototype that allows measurement of beam position after each shot was manufactured and tested on the electron linac. The beam position measurement error does not exceed 5-10 microns for electrons and 25-30 microns for positrons. 13 pick-up stations were made. Commissioning of the new electronics is planned for the first half of 2013.
- A new system (12 pick-ups) for beam position measurement has been tested on the cooler for COSY (Germany). This system includes a subsystem for electron beam current modulation and a subsystem for processing signals from the pick-ups. The system enables simultaneous measurement of the position of electron and proton beams with a resolution of a few microns at an electron current amplitude modulation of 0.2-2 mA
- Electronics for the ion beam phase measurement system for the booster NICA were developed under a contract with the JINR. This system complements the RF system of the booster, which is also developed by BINP. The system makes it possible to measure the beam phase relative to the accelerating voltage of the RF system every 10 μ s with an error of no more than 1 degree. Both a prototype and operating version of the electronics were fabricated. The prototype was tested and demonstrated the re-

quired parameters. The operating version will be passed to Dubna and tested on the running JINR nuclotron in March 2013.

- A new system for betatron frequency measurement was designed, manufactured and commissioned (without beam) at BNL. This system has a distinguishing speed of 1 ms. Due to this, up to 300 measurements can be done during energy rise in the booster. The measurement error does not exceed 50-100 ppm. The system makes it possible to measure betatron frequencies even at very low beam currents, down to 100 mA. Its software, running in the EPICS environment, was developed and debugged. Commissioning of the system with beam is scheduled for May and June 2013.
- 40 electronics modules for measuring beam position in beam line K-500 with 'wall current monitors' were fabricated and configured. The modules are placed near the monitors and connected with one coaxial cable for power supply, timing signals and data exchange with the host computer.
- A new NMR magnetometer was designed and fabricated. It has higher performance due to faster processing of NMR signals. The accuracy of measurement of homogeneous fields (with a gradient less than 10^{-4} /cm) does not exceed 1 ppm. The magnetometer has an embedded DAC for field feedback with the power supply of the magnet. 3 magnetometers of new type were fabricated. One device is mounted on VEPP-4 and used for the main field stabilization. 2 magnetometers are installed on VEPP-2000.
- Works on improving the system for SR beam stabilization on VEPP-3 are going on. X-ray attenuation filters were calibrated and replaced.
- Works on improving the quality and operational parameters of the control system of the linear induction accelerator for X-ray radiography (VNIITF Snezhinsk) are going on. This includes upgrade of the subsystem of synchronization and interlocks, aimed at more precise synchronization with experiment.
- Upgrade of the pulsed measurement system of VEPP-2000 started based on earlier-developed high-precision multi-function integrators VsDC2.
- Using the previously created stands and software, we carried out the performance measurement and acceptance testing of pulsed magnets of the injection/extraction system of the NSLS-II booster.
- Magnetic measurements of the quadrupole magnets of the NSLS-II main ring and sextupole and quadrupole magnets of the booster were successfully completed on specially-prepared stands.
- Measurements of the pulse parameters of the BD and BF dipole magnets of the NSLS-II booster were carried out. Relevant equipment and software were provided for this.
- Equipment for measurement of pulsed magnetic fields of the septum and bump magnets of the injection/extraction system of the NSLS-II booster was put into operation at Brookhaven National Laboratory.
- Works on the mounting and commissioning of the thermal control system on the SR beam lines of the wiggler on VEPP-4 started.
- A system for acquisition and control of data from the neutral beam injector of the W7X stellarator (Germany) was designed, manufactured and debugged.
- Development, manufacturing and commissioning of the control system and the data acquisition system for the stand of neutral beam injectors for the "TAE" installation (USA) are going on.
- Development of the new-generation control system and data acquisition system for "TAE-3U" installations (USA) started.
- Operating documentation for the control system and the data acquisition system of the neutral particle injector (NPI) for the T-15 tokamak (Moscow) was developed.
- About 50 different units with the CAN-BUS interface for control systems of electrophysical installations were made, debugged and put into operation. These units are listed in Table 7.3.1. A detailed description of the units is available on the web-site of the laboratory.
- It should be noted that these devices are widely used for completion of contracts. Over the past years, more than half of the produced modules were supplied bundled with various power sources and as part of instrumentation systems under contracts with Russian and foreign partners.

Table 7.3.1. Family of devices with the CAN-BUS interface.

Name	Brief description
CANDAC16	16-channel, 16-bit DAC; 8-bit input and output registers
CANADC40	40-channel, 24-bit ADC (class 0.03%); 8-bit input and output registers
CDAC20	20-bit DAC; 5-channel, 24-bit ADC (class 0.003%); 8-bit input and output registers (VISHNYA and Euromechanics)
CEAC 51	20-bit DAC; 5-channel, 24-bit ADC (class 0.003%); 8-bit input and output registers (Euromechanics 3U)
CAC208	8-channel, 16-bit DAC; 20-channel, 24-bit ADC (class 0.003%); 8-bit input and output registers (VISHNYA and Euromechanics)
CEAC124	4-channel, 16-bit DAC; 12-channel, 24-bit ADC (class 0.003%); 4-bit input and output registers (Euromechanics 3U)
CEAC121	1-channel, 16-bit DAC; 12-channel, 24-bit ADC (class 0.003%); 4-bit input and output registers (Euromechanics 3U); for control of fast sources
CEAD20	20/40-channel, 24-bit ADC (class 0.003%); 4-bit input and output registers (Euromechanics 3U)
CGVI8	8-channel, 16-bit generator of delayed pulses; 8-bit input and output registers
CPKS8	8-channel, 16-bit code-duty factor converter
SLIO24	CANbus interface: 24-bit bidirectional bus, built-in card
CKVCH	Commutator of RF signals 8-1, 2*(4-1) 4*(2-1)
CANIPP	CANbus interface: 2 branches of the BPM type
CANIVA	16-channel vacuum meter (current of ion pump)
CURVV	Universal input/output register (2 input and 4 output registers of 8 bits)
CIR8	Recorder of discrete signals (interrupt register, BSI, input/output registers)
CAC168	8-channel, 16-bit DAC; 16-channel, 24-bit ADC (class 0.03%); input and output registers; built-in card
CAN-DDS	CAN-DDS module: divider of input clock frequency with remotely tunable fractional coefficient
CAN-ADC3212	For closing the feedback loop in the thermal adjustment scheme of RF cavities.
CANGW	Ethernet-CAN/RS485 gateway
VME-CAN	VME-CAN interface
CEDIO_A	Multi-port input/output register
GZI-CAN	4-channel generator of delayed pulses, 80 ns - 10.28 μ s
VSDC2	Module for precision measurement of magnetic fields by the induction method, 2 channels
IVI1811	Time interval meter with a resolution of 0.5 ns
CEGVI8	8-channel, 16-bit generator of delayed pulses, Euromechanics

- Complex testing of electronics for powering and control of the electron gun of the ion coolant for COSY was performed on the running system.
- Works on improving the metrological and operational characteristics of the electronics for magnetic field alignment in the solenoid of the ion coolant (COSY) are going on.
- Under the contract on the NSLS-II booster, the system for interrogation and monitoring of thermal switches and vacuum control system were installed and tested.
- Works on the creation of a control system for the 4-track FEL are going on.
- Tests of the new modulator of the electron gun of the FEL injector were continued. The modulator has the following unique parameters: a pulse duration of 1 ns, an amplitude of 0-120 V at 25 Ohms, and a repetition frequency of 0-90 MHz.
- Work on the introduction of up-to-date intelligent controllers in control systems of physical plants was continued. Another batch of controllers and CAN-Ethernet gateways for various facilities of the Institute was made.
- Works to improve the operational characteristics of the system for weld search and electron beam pointing were continued on the electron beam welding plant, as well as the creation of a modernized version of the system for testing of welding technology.
- Operational testing of the 2-channel high-precision current meter for ionization chambers (a resolution of 2-3 fA) was continued. The device is designed for experiments with synchrotron radiation. A serial meter was developed based on the results.
- A module of generator of time intervals was designed, tested and put into mass production for numerous pulsed systems of beam line K-500.

7.4. DEVELOPMENT OF TAILOR-MADE AND SPECIAL ELECTRONICS

The Institute has developed a lot of tailor-made and special electronics. In particular, the following was made in 2012:

- A commutator for powering of vacuum ion-getter pumps was designed, manufactured and tested. The rated current of the device is 50 A; the voltage is 30 V.
- The development and manufacture of capacitive and ultrasonic hydrostatic sensors was continued. Under a contract with KEK (Japan), fabrication of 20 capacitive hydrostatic sensors was started.
- A prototype semiconductor RF generator was designed, manufactured and successfully tested with an option of amplitude modulation of 4 MHz output voltage for powering the plasma emitter of the ion source of the diagnostics atom injector. The prototype, which ensures an output power of up to 20 kW of 4 MHz RF voltage, was tested in operation in the atomic injector. Fabrication of a generator for a power of up to 40 kW was started.
- For the splicing area of the BINP experimental production, an automatic control system for the new furnace was developed and commissioned.

In 2012, as in previous years, we performed the technical support to previously-manufactured electronic systems and their components in use at facilities of the Institute and beyond.

7.5. RESEARCH RELATED TO MODELING AND SOLVING ELECTROSTATIC AND ELECTRODYNAMIC PROBLEMS OF ACCELERATOR PHYSICS

In 2012, the work on the calculation and designing of elements of accelerators was continued, both for the needs of the Institute and within the framework of international cooperation. This resulted in development and upgrade of computational methods and programs for analysis and designing of elements of accelerator equipment, as well as computer simulation of dynamics of charged particle beams, including the following:

- Under a contract on the creation of a high-power source of neutral particles, the final optimization of magnetic field in a plasma exchange target was carried out; estimates were made for streams of electrons to the chamber walls; the final version of the magnetic system was passed to the design office.
- Under the contract on the creation of a high-voltage installation for electron cooling for COSY, we continued the creation of the electron gun and collector. Stand measurements were carried out; data comparison showed

good agreement between the measured and calculated parameters.

- Works continued on the further development of programs for calculation of electrostatic and magnetic fields and electron and ion guns. As for the UltraSAM set of programs, the work of pre- and post-processors was significantly improved; revealed bugs were removed.

In accordance with the plan of the contract for the development of the prototype injector of high-energy atomic beam on the basis of negative ion source, some numerical simulation was carried out.

1. Within the framework of designing a prototype atomic injector with one "driver", the following was performed:

- calculation and optimization of the magnetic field of the plasma electrode filter;
- calculation and optimization of the bending magnet of the ion-optical system;
- calculation of electric fields in the ion-optical system of the prototype atomic injector with one driver and "single-aperture extraction";
- calculation of trajectories of accelerated negative ions and associated electrons.

2. Similar calculations were performed for the prototype of the high-voltage high-power atom injector with four drivers and a beam current of up to 1.5 A.

3. Calculations of beam passage from the ion source through the bending magnets and accelerator were done for the prototype with four drivers and a beam of 1.5A.

- The development of the Web page of the Radiophysics Laboratory was continued. This web page is to contribute to a more complete and correct use of developments by the laboratory. To this end, in addition to descriptions of various modules, the web page offers some application notes.

7.6. NEW 174 MHZ RF SYSTEM FOR THE BEP STORAGE RING

BINP is creating a new RF system for the BEP storage ring, which is the injector for the VEPP-2000 accelerator complex. The new RF system will allow increasing the energy of particles in the BEP from 0.9 to 1 GeV. The RF system operates at a frequency of 174 MHz (the 13th harmonic of the BEP revolution frequency) and consists of an accelerating cavity, RF power generator and control system.

The coaxial accelerating cavity for a maximum voltage of 120 kV enables tuning of the fundamental and higher modes. The output stage of the RF generator for a maximum power of 20 kW is equipped with a GU-92A tetrode. The pre-stages of the generator are made on transistors. The control system adjusts the amplitude and phase of accelerating voltage and synchronizes the filling of the separatrices of the storage ring.

In 2012, the BINP experimental workshop made the housing and central coaxial inserts of the cavity. A check assembly of the cavity with all the units has been performed, and the first RF measurements of the operating mode have been carried out (Fig. 7.6.1).



Fig. 7.6.1. New BEP cavity during check assembly in the experimental workshop.

The fabrication of the parts of the feeder line connecting the generator to the cavity is close to completion. The cooling system for output stage of the generator is equipped with a bought-in fan. The stage will be fed from an existing generator.

New units of the control system are manufactured and tuned (the control system will use some of the electronics of the old RF system).

7.7. 816 MHZ PASSIVE SINGLE-MODE RF CAVITY

In May 2011, BINP has signed a contract with the National Synchrotron Radiation Center of China in He-fei (National Synchrotron Radiation Laboratory) for the development and manufacture of a 816 MHz single-mode passive RF cavity (Fig. 7.7.1). This cavity will be used in the storage ring for increasing the length of bunches, which enables reduction of the "Touschek effect" and increase in the beam lifetime. The cavity operates at the fourth harmonic of the accelerating RF power. The cavity will be excited directly by the beam. The required voltage level on the cavity is regulated via detuning of the cavity relative to the RF harmonic. The maximum voltage is 80 kV.



Fig. 7.7.1. 816 MHz single-mode passive RF cavity.

By now, the cavity has been assembled with all the units and passed the vacuum tests and measurements of the fundamental mode parameters and the spectrum of high modes. Its dispatch is scheduled for February 2013.

7.8. WORKS WITH THE RF SYSTEM OF THE VEPP-4 STORAGE RING

Currently, the RF system of the VEPP-4 storage ring is arranged as follows. From the RF generator and by a rectangular waveguide, power is supplied to the waveguide splitter, which distributes this power over five cavities.

The output stage of the generator is now equipped with two GU-101A tubes, which enables a power of up to 200 kW. The operating frequency is 181.8 MHz.

For a long time, the storage ring was working at energies of up to 2 GeV. In 2012, increasing the energy of the storage ring up to 4.2 GeV required execution of some works with the RF system of the storage ring for better reliability of the system. The following works were performed:

1) inspection of the high voltage part of the cabinets of the 5 kV and 50 kV bias rectifiers. DC voltage from these rectifiers is applied to the electrodes of the cavities for suppression of the multipactor;

2) inspection and tuning of the RF generator, tuning of the interstage links of the generator, and connection of the generator with the waveguide;

3) inspection of the control system of the RF system;

4) detuning of high modes of the cavity and additional tuning of the output stage of the generator, which enabled increasing the threshold of phase instability of stored beam;

5) a multipactor training in the range of 30 kV to 600 kV was carried out on cavity 2, which was mounted in the storage ring in the fall of 2011. Now a multipactor zone in the region of 50 kV deteriorates the vacuum. This area is quickly trained, but it recovers if the RF power is switched off for 24 hours or more.

The RF system works stably at an overall voltage of up to 2.8 MW on 5 cavities. A power of 80 kW dissipates in the walls of the cavities at such voltage. The RF system ensures a rise in the energy of particles in VEPP-4 up to 4.2 GeV.



Fig. 7.8.1. 181.8 MHz cavity after the rework.

In 2012, experimental workshop 1 completed the rework of the accelerating cavity that had been removed from the VEPP-4 storage ring. The design of the indium vacuum seals of the discs and ports of units was improved; leaks in the welds of these ports were eliminated. Currently, works on preparation to the vacuum heating of this cavity (Fig.7.8.1) are underway outside the VEPP-4 ring.

Experimental workshop 1 continues the refinement of replacement units for the cavities of VEPP-4.

7.9. DEVELOPMENT OF RF SYSTEMS FOR HIGH-POWER INJECTORS OF BEAMS OF NEUTRAL ATOMS FOR PLASMA FACILITIES

7.9.1. RF system of the diagnostic injector of neutral beams of RUDI-X for the "Wandelstein" stellarator.

In 2012, BINP completed the fabrication of a diagnostic injector of beams of neutral atoms for Max Planck Institute for Plasma Physics (Greifswald, Germany). Plasma in the injector is created using an RF discharge. An RF system for powering the plasma emitter was manufactured.

Main parameters of the system are given in Table 7.9.1.

Table 7.9.1. Main parameters of the RF system of the RUDI-X injector.

Operating frequency, MHz	$4 \pm 3.5\%$
Load power, kW	30
Amplitude of RF voltage on the "antenna", kV	0-8
Modulated pulse duration, s	10
Maximum time of "high" power level within a pulse, s	2.5
Anode supply voltage, kV	10
DC voltage on the "antenna", kV	60

A drive oscillator forms a 4 MHz signal at a small power level. A phase-locked loop system tunes the frequency of the drive oscillator within 3.5%, following the resonant frequency of the oscillatory circuit formed by an inductor and ceramic capacitors, placed in the screen of the RF emitter.

A tunable amplifier (TA) amplifies the signal from the drive oscillator, adjusts the output power level and maintains stable amplitude. The signal from the TA output arrives at the pre-amplification transistor stage. The output stage is made on the 4CW50000E metalceramic tetrode made by Eimac (USA) in a shared-cathode circuit. From the output of the stage and via an RF isolating (oil-filled) transformer the RF power is applied to the plasma emitter inductor. The toroidal magnetic circuit is made of amorphous iron. The system is placed in three "Euromechanica" cabinets.

7.9.2. RF system for high-power continuous injector of beams of fast hydrogen atoms.

BINP continues works on the project of injector of beams of 500-1000 keV fast hydrogen atoms on the basis of negative ions. The source of plasma is an RF discharge. An RF system for powering the sources was de-

signed and is being fabricated. Parameters of the RF system are presented in Table 7.9.2.

Table 7.9.2. Main parameters of the first stage of the RF system of the test bench, with a beam current of 1.5 A.

Operating frequency	$4 \pm 3.5\%$ MHz
Load power	40 kW
Operating regime	Continuous
DC voltage on the "antenna" relative to platform	120 kV
Anode supply power	400 kW
Flow of deionized water for cooling the 4CW50.000E tetrode	40 l/min

Elements of the first stage of the RF system of the experimental bench for acceleration of 1.5 A negative hydrogen ion beams to an energy of 120 keV were manufactured. A full-scale anode supply source for the entire system (four channels) was manufactured and assembled. The control rack, one channel of the RF generator and a 120 kV RF isolation transformer (Fig. 7.9.1.) were assembled; their wiring was completed. The system is being refined now.



Fig. 7.9.1. RF isolation transformer.

7.10. CCDTL ACCELERATING STRUCTURES FOR LINAC4, CERN

Together with VNIITF (Russian Federal Nuclear Center - All-Russia Institute of Technical Physics, Snezhinsk), BINP is making 7 accelerating modules for the CCDTL (Coupled Cavity Drift Tube Linac, a linear ac-

celerator with drift tubes and connection cells) for energies of 50 to 104 MeV for the 160 MeV new linear accelerator of H⁻ ions under construction at CERN within the framework of the upgrade of the LHC injection complex.

The fabrication of the housings of the cavities of all the 7 accelerating modules was completed in 2012. Drift tubes were made for 6 modules.

Modules 2 to 6 with drift tubes have been assembled, tuned and subjected to RF measurements on a BINP bench. Modules 2 and 3 have been dispatched to CERN. In the Linac4 tunnels, the CCDTL modules are mounted on rigid support frames made by BINP. Before the dispatch to CERN, module 2 was assembled and adjusted on a frame (Fig. 7.10.1.).

The BINP team has assembled modules 2 and 3 at CERN (Fig. 7.10.2.).



Fig. 7.10.1. Adjustment of module 2 at BINP (with the participation of CERN representatives).



Fig. 7.10.2. BINP team assembling CCDTL module 2 at CERN.

Module 3 was placed on the bench for conduction of "hot" tests (Fig. 7.10.3) at a rated voltage on the module. After 2 weeks of RF training, the rated voltage in the short-pulse mode was achieved (Fig. 7.10.4).

Completion of the works is targeted for 2013.

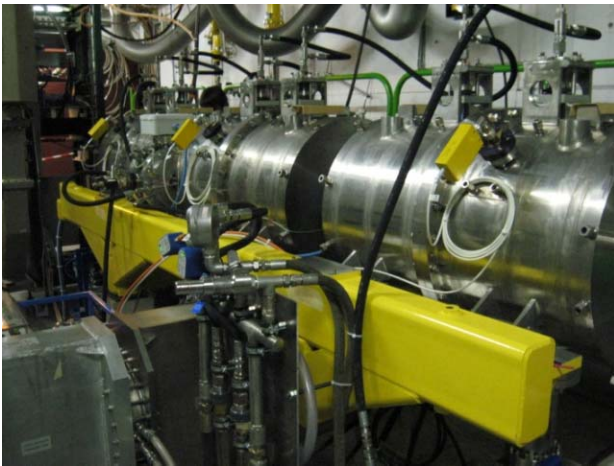


Fig. 7.10.3. Module 3 on the bench for "hot" tests at CERN.

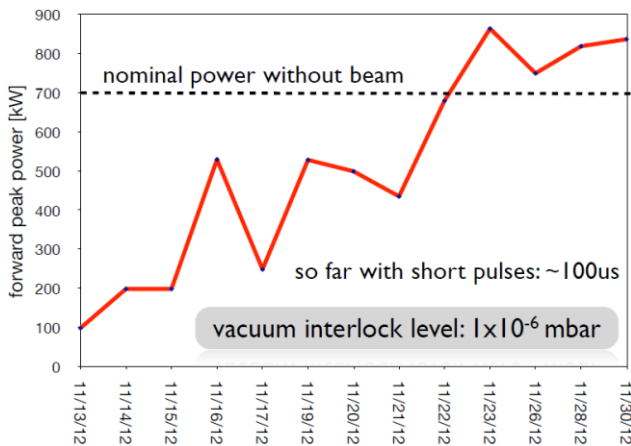


Fig. 7.10.4. First results of "hot" tests of module 3.

7.11. ACCELERATING RF STATIONS OF ION BOOSTER OF NICA-MPD COLLIDER

The booster of the NICA-MPD accelerator complex is designed for acceleration of Au^{32+} ions injected from the linear accelerator with an energy of 2 MeV/nucleon to an energy of 600 MeV/nucleon, as well as for electron cooling of bunches.

The booster is supposed to have two modes of operation: within the NICA project and independently.

For work within the NICA project:

- adiabatic capture into acceleration and acceleration up to 40 MeV/nucleon at the sixth harmonic of the revolution frequency;
- exit to the magnetic field 'table' for electron cooling;
- adiabatic capture and acceleration of cooled beam to an energy of 600 MeV/nucleon at the second harmonic of the revolution frequency;
- two-step bypass of two bunches from the Booster to the Nuclotron.

For independent operation:

- adiabatic capture into acceleration and acceleration to an energy of 600 MeV/nucleon at the fifth harmonic of the revolution frequency;
- slow delivery to the target.

The accelerating system of the booster consists of two identical acceleration stations, each giving a half of a set maximum acceleration voltage of 10 kV. Parameters of the accelerating system of the booster are given in Table 7.11.1.

When a bunch is bypassed from the Booster to the Nuclotron, the accelerating systems of the two accelerators work at the second harmonic of the revolution frequency. The perimeter of the booster is 216 m; the perimeter of the Nuclotron is 251.52 m. Two bunches are bypassed. The accuracy of getting to the center of the separatrix of the Nuclotron is 1 ns.

Table 7.11.1. Parameters of the accelerating system of the booster.

No	Parameter	
1.	Frequency tuning range, MHz (NICA)	0.5 – 2.5
2.	Frequency tuning range, MHz (independent)	0.5—5.5
3.	Harmonic number (NICA)	6/2
4.	Harmonic number (independent)	5
5.	Cavity external diameter, m	< 1.2
6.	Vacuum chamber dimensions, mm	160 x 70 (or Ø160)
7.	Cavity length, m	1.4
8.	Height from the cavity axis to the accelerator floor, mm	1500
8.	Number of cavities	2
9.	Minimum voltage amplitude in the adiabatic capture, V	100
10.	Voltage amplitude in the acceleration, kV	10
11.	Duration of acceleration (NICA), s	~0.3+~1.5=1.8
12.	Duration of acceleration (independent), s	1.5

The control system has a revolution-frequency driving oscillator. It links the frequency of this oscillator with the magnetic field and corrects the frequency in accordance with the beam position monitor. The control system also adjusts the amplitude of the accelerating voltage in accordance with clock signals and a given program. The system of control of the accelerator stations should be integrated into the overall control system of the NICA-MPD accelerator complex. The matching parameters will be determined after additional consultations.

Requirements to vacuum conditions: pressure of $5 \cdot 10^{-11}$ or lower.

The booster operates (NICA) as follows:

- 80 successive acceleration cycles;
- independent operation for about 1 hour.

A cycle of magnetic field change (one acceleration cycle) lasts 4 seconds. During such a cycle, the RF system operates in the areas of field growth, the total duration of which is 2 seconds.

In the offline mode of the booster, the cycles are continuously repeating.

The acceleration cycle is 6 seconds long (1.5 seconds of growth, 3 seconds of shelf, and 1.5 seconds of decay). The time of work with RF power is 1.5 seconds.

The thermal conditions were defined for maintaining an RF amplitude of 10 kV in the areas of magnetic field growth.

Structure.

The accelerating cavities are mounted on frames with four removable feet and equipped with lifting eye bolts. On the bottom of the removable feet there are mounted adjustable supports for accurate alignment. For correct positioning of the cavities in the accelerator, a few fiducials are placed on the accelerating cavities. The accelerating cavities are essentially broadband fixed-frequency inductive-resistive loads of amorphous iron ribbons wound in 44 rings. A ribbon of amorphous iron of 5V-M grade of a thickness of $\sim 30 \mu\text{m}$ and a width of 15 mm is wound in rings of an outer diameter of 500 mm and an inner diameter of 250 mm. The rings are glued together by two and envelope the vacuum chamber from both sides, symmetrically about the ceramic insulator of the accelerating gap (Fig.7.11.1).

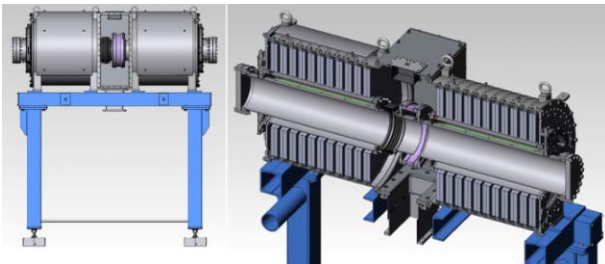


Fig. 7.11.1. Structure of accelerating cavity of the accelerator station of the booster.

There are clearances between the pairs of rings for radial passage of cooling air from the center. Fig. 7.11.2 shows impedance versus frequency in the operating frequency band for a half resonator.

The RF generator module with the anode and screen supply sources is driven on rolls under the cavity, and the accelerating gap is connected to the anode of the tetrodes with short LC chains, which partially compensate the reactive load on the tubes in the operating band. The output amplification stage of the RF generator is a broadband symmetrical double-step one on SU-36B1 tetrodes in a shared-cathode circuit. The RF station is cooled with air with an inlet fan, via a flexible hose. The fan is placed in a separate box with air filters on the out-

side walls. The anode voltage of the tetrode supply is 4 kV; the screen voltage is 1 kV. The tetrodes operate without cut-off in the "A" regime in the most linear portion of the current-voltage characteristic. In these conditions, power released on the anodes is close to the maximum allowable value, but the average power dissipating on the tubes is much less, since the control grid bias unlocks the tubes only for time when an exciting RF signal is applied during an acceleration time of 1.5-1.9 seconds with intervals of 4 - 4.5 seconds. The value of fixed bias on the control grids of the unlocked tubes is selected individually for aligning the currents and preventing the RF ferrite choke of the anode supply from magnetization. Fig.7.11.3. presents RF circuit schematics of the output stage.

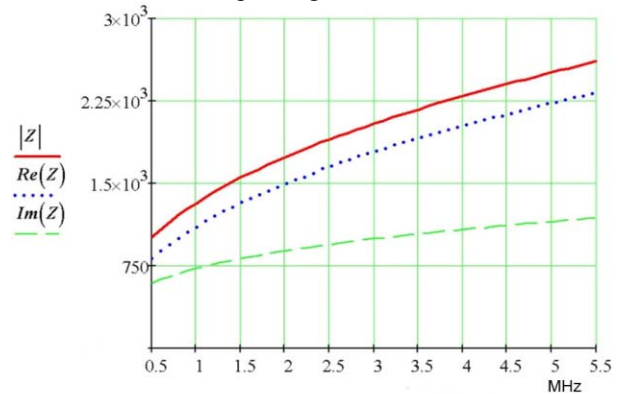


Fig. 7.11.2 Impedance of the half accelerating cavity.

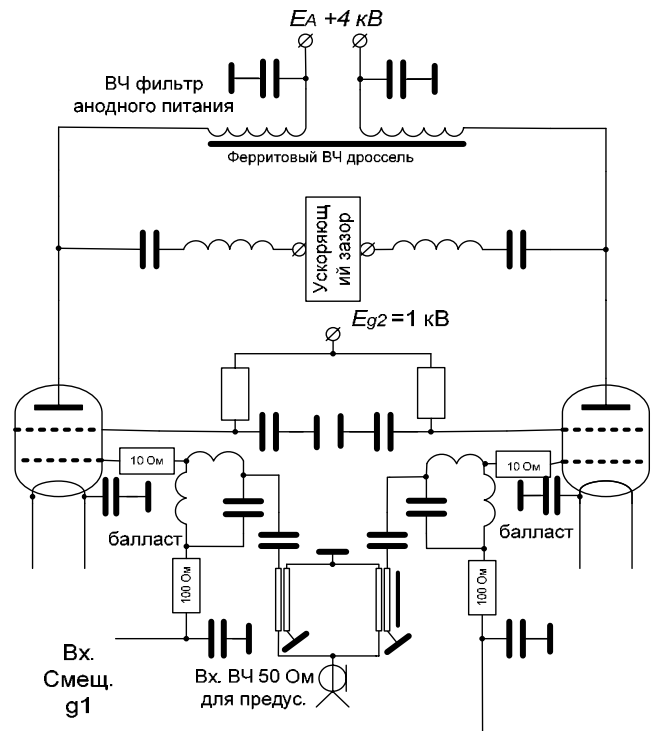


Fig. 7.11.3. Circuit of the high-frequency output stage of the RF generator.

The input signal from the preamplifier is divided equally and is delivered in opposite phase to the control grids via 100-ohm twisted-pair lines on ferrite and with no ferrite.

State of work.

Shipment to the customer is scheduled for the 4th quarter of 2013. Currently, the fabrication of the accelerating cavities and supports for them is close to completion; boards for the input and output circuits of the output stage, transformers and chokes of the power supplies have been made; the manufacture of the housings for the output amplifier and the box of the fan has started; almost all components have been purchased. Fig. 7.11.4. shows the inner segments of the vacuum chamber for the half cavities; Fig. 7.11.5 shows the housing of half cavity with openings for cooling air.



Fig. 7.11.4. Parts and components of the RF cavity in the workshop.



Fig. 7.11.5. Housing of half cavity with openings for cooling air.

7.12. RECONSTRUCTION OF RF SYSTEMS OF THE ELECTRON ACCELERATOR OF THE RESEARCH CENTER KAERI, REPUBLIC OF KOREA

Under a contract between BINP and the research center KAERI, Republic of Korea, the laboratory participated in the restoration of the RF systems of the electron accelerator after a fire in April 2009. The accelerator has two RF systems. The first system operates at a frequency of 176 MHz and has three independent channels with the total power of the RF generators in continuous mode of 200 kW. Two channels of the second RF system operate at a frequency of 352 MHz. The total power of the supply RF generators is 100 kW. The first part of the contract, i.e. the restoration of the first RF system, was fulfilled in 2012.

During 2012, BINP made new power supplies for the RF generator source, including a 9.0 kV anode rectifier with an output power of 600 kW in continuous mode and a control system with a set of control programs. In May - June 2012, a group of experts of the laboratory went to Korea to mount the equipment and prepare the rest for operation of the accelerator. Power supplies for the RF generator were mounted and adjusted; the RF stages of the power amplifiers were tuned; maintenance and preventive works on the accelerating cavities were done. When the whole system was switched on, the required RF voltages on the accelerating cavities were attained, and the electron beam was accelerated to the desired energy. The second RF system will be restored next year, and thus the contract will be completed.

7.13. RF INJECTOR OF MICROTRON-RECUPERATOR

First tests of the RF injector for the microtron-recuperator consisting of a 90 MHz accelerating cavity with built-in grid hot cathode unit were successfully conducted in 2012. The tests were carried out on a specially designed stand.

The tests included RF training of the cavity for creation of a high accelerating gradient. The cavity has been trained to a nominal voltage of 300 kV in continuous mode and to 450 kV in pulsed mode. Good vacuum characteristics of the cavity were achieved. The works were carried out at a pressure below 10^{-6} Pa. After the training, the threshold of radiative emission because of dark currents was elevated from 100 kV to 250 kV. Tests with beam have been carried out.

Bunches with a charge of 1.5 nC and duration adjustable in the range of 0.5-1.5 ns have been output at the exit of the RF injector. The duration varies in dependence on the gating impulse phase relative to the RF phase in the cavity, which is consistent with calculations. The energy of bunches in the tests was set in the interval of 100-250 keV. The minimum bunch repetition frequency, 20 kHz, was chosen with a view of prevention of beam overheating

of the load. The unit of gating impulses, which controls the grid-cathode assembly, went through a test on production of bunches with a nominal repetition rate of 90 MHz (on a similar unit of an RF tube GS-34).

Works on the stand will be continued in 2013. In particular, after the installation of enhanced radiation protection and a 30 kW load for the beam, the beam energy will be increased to a nominal magnitude of 300 keV and the average beam current, to 100 mA. A beam diagnostics system is being created and refined on the stand now. A bending magnet to measure the beam energy and the beam energy spread is being installed. Equipment for measurement of the emittance and other beam characteristics is being prepared for installation.

7.14. RF GUN FOR ACCELERATOR OF VNIIEF

BINP is developing an injector for the accelerator of VNIIEF, Sarov. The main part of the injector is a grid-controlled hot-cathode RF gun on a 100 MHz RF coaxial resonator, which is fed from an RF generator with a power of up to 20 kW. The average current of the RF injector is 40 mA and higher; the energy of electrons is 50 to 100 keV. If compared with static guns, RF guns have an advantage of immeasurably larger life time of cathodes at high average beam current, because their cathodes are not bombarded by accelerated ions of the residual gas, ionized by the electron beam. A similar hot-cathode RF gun, created by BINP for the microtron-recuperator, is under testing on the bench now.

7.15. UPGRADE OF THE RF SYSTEM OF THE FEL MICROTRON

Works on the upgrade of the RF generators of the FEL microtron were continued. GU101A tubes were gradually replaced with TN781 ones made by THALES. Power supplies for generators on the TN781 tubes were optimized with the aim of increasing the output power of the generators.

8.1. ACCELERATOR SUPPLIES

Since 1983 the ILU accelerators are supplied abroad where they are used for researches and are working in the industrial lines. Some of these machines are working round the clock for years. The reliability and technical level of these machines is confirmed by the new supplies.

2 converters with collimators for X-rays generation were designed and produced according the contract with the Korean firm EB-TECH Co., Ltd. The converters are purposed for 2 electron accelerators with beam power up to 10 kW and electron energy range of 5 – 7.5 MeV. The presence of the controlled collimators was stipulated by the customer from the very beginning. The collimators are absorbing the radiation generated by the converter's target on the broadsides.

The adjustment works started on the ILU-10 machine mounted in the Park for Nuclear Technologies, town of Kurchatov, Kazakhstan.

The works on the ILU-14 machine delivered and mounted in the Federal Medical Biophysical Center named by Burnazyan, Moscow, were continued during the year of 2012.

In 2012 2 ILU-10 machines were mounted, tuned and put into work in the company SFM-Pharm, Biotech-nopark, town of Koltsovo, Novosibirsk region. Fig. 8.1.1 shows the ILU-10 machine in Koltsovo – the vacuum tank with the resonator and RF generators. The beam extraction device and the underbeam conveyor are shown in Fig. 8.1.2.

The contract for design, manufacturing, mounting and adjustment of the ILU-8 machine for radiation treatment of cables was signed with public corporation OKB KP, Mytischki, Moscow region.

8.2. DEVELOPMENT OF NEW POWERFUL ELECTRON ACCELERATORS

8.2.1. Development of the beam scanning system with independent power supply.

In the ILU machines the powerful electron beam is extracted into atmosphere through the beam window covered with titanium foil. To prevent the local overheating and foil breaking the electron beam is scanned along the window. The beam extraction and scanning system is the essential accelerator's part – the accelerator will not work without this system.

The ILU accelerators are the pulse machines, pulse duration is about 0.5 ms, pulse repetition rate – up to 50 Hz.

The development of the new beam scanning system for ILU-10 machine was carried out during the year of 2012. The system was designed for electron energy up to 5 MeV and pulse beam current up to 400-500 mA. During the beam pulse (0.5 ms) the beam scanning system ought to generate the current pulse having the form and amplitude sufficient for electron beam turning and its scanning

along the beam window in such a manner that the absorbed dose nonuniformity should be minimal.

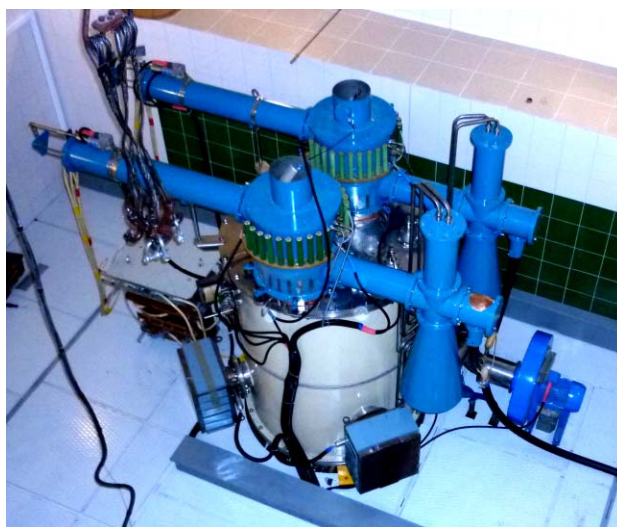


Fig. 8.1.1. ILU-10 machine in Koltsovo – the vacuum tank with the resonator and RF generators.



Рис. 8.2.1. The underbeam conveyor and ILU-10 standard trigonal beam extraction device, Koltsovo, Novosibirsk region.



Fig. 8.2.2. Modernized beam extraction device with the new beam scanning system and the underbeam conveyor, ILU-10 machine, Kurchatov, Kazakhstan

The new magnetic system was designed, the beam passage through the extraction device was simulated, the new power supply and control system for magnet feeding was developed.

The magnet system scanning coils are placed around the neck of the extraction device in the atmosphere, and the magnetic field propagates into the beam channel (where the high vacuum is maintained) through the thin stainless steel walls. At the pulse duration of 0.5 ms the stainless steel walls sufficiently alter the magnetic field created by the scanning coils. The pulse magnetic field formation in the beam channel was simulated considering the influence of the walls.

The beam extraction device design was developed for this new system. Fig. 8.2.1 shows the standard trigonal beam extraction device of the ILU-10 machine, and Fig. 8.2.2 shows the extraction device of the new design installed in the Park for Nuclear Technologies, town of Kurchatov, Kazakhstan. Unlike the standard beam extraction device (that has one Panofsky lens) the new device has 2 Panofsky lenses for beam bending before passing the window foil. These 2 lenses are installed one over another (their yellow windings are seen in Fig. 8.2.2).

The beam scanning system with power supply independent on accelerator pulse was manufactured, mounted checked and adjusted. This system is supplied with the ILU-10 machine installed in the Park for Nuclear Technologies, town of Kurchatov, Kazakhstan.

Beam scanning system parameters:

Magnetic field – up to 0.1 Tl;

Scanning coils current – up to ± 250 A;

Charging voltage in the scanning coils feeding circuit – up to 700 V.

The beam scanning system permits to correct the form of scanning current to achieve the good absorbed dose uniformity along the beam window.

8.2.2. Development of the control system for ILU machines powerful pulse modulators.

The RF generators of the powerful (up to 100 kW) ILU-14 machine with energy up to 10 MeV and pulse beam current up to 600 mA are fed by pulse power supply units (modulators), see Fig. 8.2.3. The RF generators are using the powerful triodes type GI-50A.

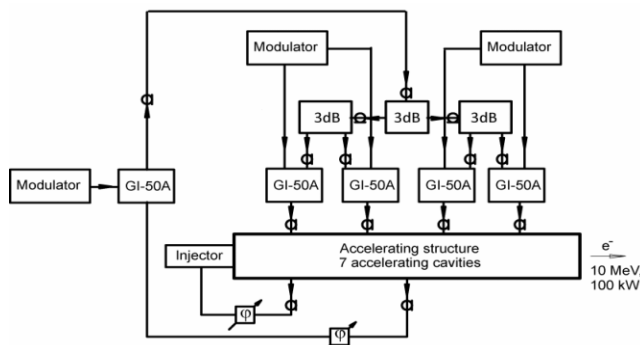


Fig. 8.2.3. ILU-14 block diagram.

To optimize the feeding electric net loading the control system was developed for driving the 3 ILU modulators. The periods for energy storage in the inductive reactors in these 3 modulators were shifted in time. The generation of the powerful pulsed for RF generators feeding is done synchronously by all 3 modulators. The work on this power supply and control system was continuing in the year of 2012.

The development of the new equipment for the ILU machines was carried out according to the BINP Plan for the Research Work within the framework of the State Program.

8.3. NEW RADIATION TECHNOLOGIES DEVELOPMENT

Radiation-thermal hardening of the bore bits was carried out, the resulting abrasion resistance increase in 2 times, it means its lifetime also increased in 2 times. Fig. 8.3.1 shows the bore bit section, the hardened zone is darker.

The work was performed in collaboration with Institute of Theoretical and Applied Mechanics, Siberian Branch of Russian Academy of Science.



Fig. 8.3.1. Bore bit section, the hardened zone is darker.

The study of electron beam treatment on optical cables was carried out in collaboration with Institute for Automation and Electrometry, Siberian Branch of Russian Academy of Science. The radiation creates the defects that can become the active centers for lasing, and this effect can be used for transmission laser amplification.

The development of the radiation-thermal ferrite synthesis process was carried out in collaboration with Tomsk Polytechnical University.

The mixed feed electron beam treatment was carried out in collaboration with the Institute of Experimental Veterinary for Siberia and Far East, Siberian Branch of Russian Agricultural Academy, to prolong the keeping time for the products delivered to the Northern Territories of Russia.

The irradiation influence on samples made of various polymers (polyethylene, fluorocarbon polymer, polymethylmethacrylate, etc.) was carried out to study the changes in strength properties (plasto-elastic deformations). The work was performed in collaboration with the Institute of Hydrodynamics, Siberian Branch of Russian Academy of Science, to set the data for deformation analysis models.

The irradiation influence on samples made of specially prepared nylon films with various impregnations was carried out to create the blood vessels prosthetics. The work was performed in collaboration with the Institute of Chemical Biology and Fundamental Medicine, Siberian Branch of Russian Academy of Science. The first prosthetics were successfully implanted in mice. The final goal – the growth of the body's own tissues on these prosthetics.

The radiation-induced epoxide resin condensation was studied.

The process of the electron beam methylmethacrylate polymerization in oil solution was elaborated in collaboration with the Institute of Solid State Chemistry and Mechanochemistry, Siberian Branch of Russian Academy of Science.

The possibilities of electron beam treatment for the heavy hydrocarbon compounds (including tar oil and pitch) were studied in collaboration with the Institute of Solid State Chemistry and Mechanochemistry, Siberian Branch of Russian Academy of Science.

The electron beam treatment of the silver stearate and the silver salts solutions was carried out in collaboration with the Institute of Solid State Chemistry and Mechanochemistry, Siberian Branch of Russian Academy of Science, to obtain the silver nanoparticles.

The chemical reactions mechanisms in the encapsulated systems based on the nanostructured oxides formed by the mechanochemical and radiation thermal processes were studied aiming the formation of materials with the set functional properties. The work was carried out in collaboration with the Institute of Solid State Chemistry and Mechanochemistry, Siberian Branch of Russian Academy of Science, within the framework of the SB RAS Integration Project.

9.1. THE CURRENT STATUS ON BNCT

9.1.1. Introduction.

Presently, Boron Neutron Capture Therapy (BNCT) is considered to be a promising method for the selective treatment of malignant tumours. The results of clinical tests, which were carried out using nuclear reactors as neutron sources, showed the possibility of treating brain glioblastoma and metastasizing melanoma incurable by other methods. The broad implementation of the BNCT in clinics requires compact inexpensive sources of epithermal neutrons. At the BINP the source of epithermal neutrons based on 2 MeV Vacuum Insulation Tandem Accelerator (VITA) and neutron generation through ${}^7\text{Li}(p,n){}^7\text{Be}$ reaction were proposed and realized. Although the accelerator is designed to obtain a 5 mA proton beam, but in the experiments carried out in 2008-11 we usually got the proton beam currents of hundreds of microamperes, and occasionally for a short time - a few milliamps. Such a current was enough to demonstrate the generation of neutrons and monochromatic gamma-quanta, to carry out initial *in vitro* investigations, but it is clearly not sufficient for the thorough BNCT research and other applications. The main goal of our work in 2012 was to increase the current of the proton beam and improve the stability of the accelerator.

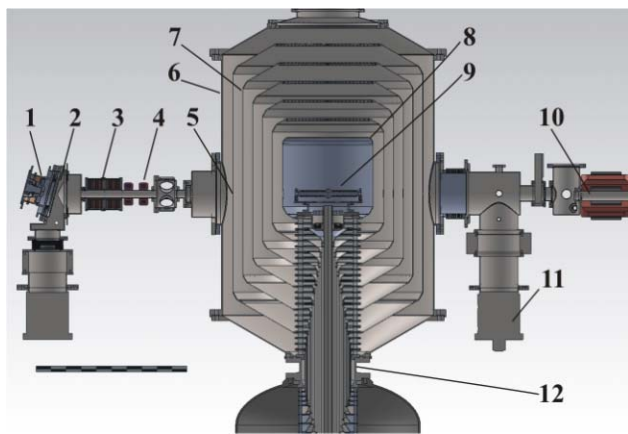


Fig. 9.1.1: High-current vacuum insulation tandem accelerator. 1 – H^- ion source, 2 – diaphragm, 3 – magnetic lenses, 4 – corrector, 5 – a temporary location of the beam detector, 6 – accelerator, 7 – electrodes, 8 – high voltage electrode, 9 – stripper, 10 – high energy beam transport, 11 – turbo molecular pumps, 12 – insulator.

General view of the accelerator is shown in Fig. 9.1.1. Negative hydrogen ions are injected and accelerated up to 1 MeV by potential applied to the electrodes, then H^- turn into protons in the charge-exchange target and at last the protons are accelerated up to 2 MeV by the same potential. Pumping of the gaseous charge-exchange target is carried out by cryogenic and turbomolecular pumps through the blinds. The potential of the high-voltage and

five intermediate electrodes is supplied by a high-voltage source through the insulator which has a resistive divider.

9.1.2. Dark currents.

The accelerator has a high electric field in the electrode gap - about 25 kV/cm, and a large total area of the electrodes - tens of square meters. In such a system in the electrode gap dark currents of different nature must inevitably occur, which may have a significant impact on the potential distribution along the accelerating channel.

When training the accelerator, at the time of voltage increasing, a dark current is recorded. It is associated with the appearance of micro-discharges, accompanied by desorption of adsorbed gases on the surface of the electrodes. Usually within an hour of training the value of the dark current decreases from the typical values of 100 - 300 μA to ten microamperes and then to few microamperes.

In a series of experiments in order to increase the H-beam current the apertures of electrodes were increased from 20 to 58 mm, except for the high-voltage electrode, in which the diameter of the hole was still 20 mm. This change resulted in frequent registration of dark current of high intensity – up to 3 - 4 mA. Flowing of such a current compared to the standard training mode led to a nearly 100-times increase in radiation. The latter fact assumed high energy of electrons which is possible when the current flows not in the gap between adjacent electrodes but, for example, between the case of vacuum tank and the high-voltage electrode. This assumption was confirmed by measuring the X-ray spectrum by BGO-spectrometer: the maximum of the spectrum was shifted from 120 to 400 keV. It was found that when the aperture of the channel increases, the electric field on the sharp edge of the cathode part of diaphragm mountings increases by 20% - up to 51 kV/cm, which leads to increased emission of electrons directly into the acceleration channel. To prevent the occurrence of this phenomenon the aperture of the channel has been reduced and sharp edges of diaphragm mountings has been rounded. This study shows the danger of exceeding the electric field strength of 50 kV/cm. Earlier in we found that the 70 kV/cm electric field leads to dramatic increase of field emission current in the high-voltage gap.

9.1.3. Beam injection.

Negative ion beam with energy of 21 keV and current of 5 mA is created by surface-plasma source with Penning discharge and hollow cathode. After turning at an angle of 15 degrees the peripheral part of the beam is cut off by 28mm cone diaphragm and the rest center of the beam enters into the transport channel. Then the divergent beam is focused by two magnetic lenses and can be shifted by two correctors for subsequent precise input into the accelerator. Tandem accelerator with vacuum insulation is characterized not only by a high rate of acceleration, but also by

a strong entry electrostatic lens between the cover of the accelerator and the first accelerating electrode. To study the influence of the lens and to optimize H⁻ beam injection the 22-channel detector has been produced and installed at the entrance of the accelerator. Beam detector is mounted directly on the first electrode of the accelerator. Using the detector we have measured the dependence of the relative maximum beam current density on the focusing magnetic lenses current. It has been determined that the best agreement with the numerical calculation is achieved by assuming the full compensation of the space charge in the transport channel and setting the transverse ion temperature equal to 1 eV at the plasma boundary of the ion source. This study described in detail in resulted in better focusing of the beam required for acceleration of the beam without significant losses.

9.1.4. Charge-exchange target.

To increase the current flow a new charge-exchange target has been made. It is designed as a cooled tube having length of 400 mm and internal diameter of 16 mm, with argon gas valve in the middle. Previously we used a tube with diameter of 10 mm.

Negative ion beam with energy of 21 keV was injected into the accelerator with the high-voltage electrode potential of 800 kV. When there was no gas supply in the charge-exchange target the Faraday cylinder at the exit of the accelerator registered negative current. This current was the current of negative hydrogen ions, which were first accelerated and then decelerated. When the charge-exchange target is filled with argon it exchanges negative hydrogen ions into protons. When the thickness of the target is $0.29 \cdot 10^{16} \text{ cm}^{-2}$ the number of appeared protons is comparable to the number of negative hydrogen ions and detected current becomes equal to zero. Registration of the moment of the current transition from negative to positive with changing argon pressure has become a useful direct diagnostics of charge-exchange target thickness. Also the thickness of the target is indirectly characterized by the residual gas pressure, because the experimentally measured dependence of the residual pressure on the amount of supplied argon is linear in operating range of parameters. With a further target density increase there is a growth of output current and its saturation. When injected H⁻ current is around hundreds of microamps the dependence measured experimentally is in good agreement with the calculated one (Fig. 9.1. 2).

9.1.5. Modification of the insulator.

The insulator of the tandem accelerator consists of 24 glass sections, which are sealed to the electrodes using indium. Inside the vacuum part of the insulator there is a resistive divider, providing uniform distribution of potential between the electrodes of the accelerator. The insulator having such a construction requires regular maintenance followed by obligatory keeping in rest the collected

insulator for a month until the working thickness of indium seals will be achieved in sections. Modification of the electrodes of the insulator was performed, allowing the use of rubber seals and significantly reducing the time spent on maintenance. It is planned to create a new insulator, having no resistive divider in the vacuum part, which will increase the technical inspection periods up to several years.

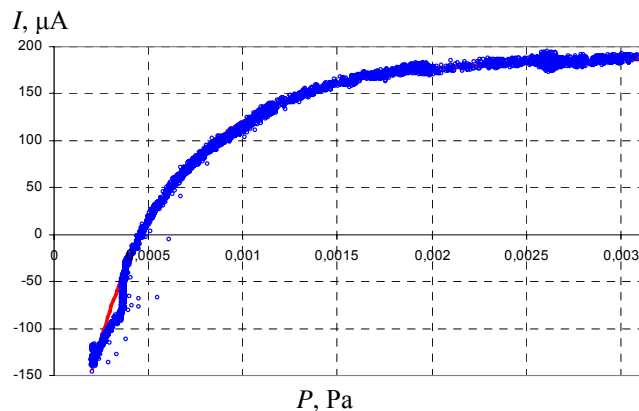


Fig. 9.1. 2: Measured and calculated (solid line) dependence of the detected output current of the accelerator on the residual gas pressure.

9.1.6. Dark matter.

A new method is proposed for the generation of monoenergetic neutrons of any energy. Generation of neutrons is carried out using a proton beam obtained from an accelerator and a neutron producing target. The method is based on the use of threshold reaction of neutron generation and the use of a thin neutron producing layer. Monoenergetic neutron beam is formed of neutrons emitted in the direction opposite to the direction of the protons. Neutron energy is clearly determined by the energy of the protons and the angle of emission. Monochromaticity of the beam is determined by the energy of the protons, the solid angle and the thickness of the neutron producing layer.

The implementation of the proposed method is considered in details for 77 keV neutrons using the reaction ${}^7\text{Li}(p,n){}^7\text{Be}$. It is shown that a beam of 77 keV neutrons is best suited for measuring the quench factor of liquid argon used as a sensitive material for a dark matter detector. It is defined the plan of works on the facility for calibration of the dark matter detector.

The above described ideas were checked for infringement, then united in a single conception and sent as an application "Method of producing a beam of monoenergetic neutrons, device for its realization and method of calibrating the dark matter detector using the resulting beam of monoenergetic neutrons" for registration of intellectual property rights.

9.1.7. Results and prospects.

The above-described investigations allowed us to move to a long stable operation with a much higher average current - 1.5 - 2 mA instead of previously achieved 0.1 - 0.7 mA. This current provides the possibility of measuring neutron spectrum by the time-of-flight technique, carrying out *in vitro* and *in vivo* studies and developing other techniques for BNCT. Numerical simulation is used to optimize beam forming unit for epithermal neutrons and, in addition to the standard mode with a 2.5 MeV proton beam, there are determined 2 more acceptable modes: i) at the near-threshold energy of 1.95 MeV, which is characterized by low activation of the lithium target and the facility, and ii) orthogonal at 2.5 MeV, characterized by high therapeutic dose - up to 3 Sv/min @ 10 mA. Discovered modes allow changing in the design of installation for hospitals, which can make it more attractive.

Also on the facility it is possible and it is planned to carry out the investigations of i) testing the method of fast detection of explosives and narcotics by resonance absorption of monochromatic gamma rays, ii) measuring the cross section and the spectrum of α -particles from neutronless thermonuclear reaction $^{11}\text{B}(p,\alpha)2\alpha$, iii) dating of rock formation (apatite) by inducing the fission of ura-

nium nuclei which it contains, iv) forming monochromatic beams of epithermal neutrons for calibration of dark matter detector.

This work is carried out as part of the research project II.13.3.7 "Neutron source for neutron therapy of cancer based on a tandem electrostatic accelerator" the fundamental research program of the SB RAS on the physics and technology of charged particle accelerators. Partial support for the work is ensured by the government contracts № 16.518.11.7038 and № 14.518.11.7039, interdisciplinary integration projects of fundamental research of SB RAS № 52 "Carcinogenesis of gliomas and reparation of the human brain" and № 134 "Implementation of size effects in the original nanobiocomposites with a controlled complex of magnetic-, neutron-, gamma-, X-, photo-, radiation-sensitive and highly biospecific properties to new quality level of low- or non-invasive radiation diagnosis and treatment", and the RFBR grant 12-02-31402 "Obtaining of monoenergetic neutrons for calibration of the dark matter detector".

9.2. X-RAY DETECTORS FOR MEDICINE AND EXAMINATION OF PEOPLE

9.2.1. Low Dose digital Radiographic Device (LDRD) "Siberia".

The development of linear detector for digital fluorography with parameters optimal for this type of X-ray examination was completed early in 2012. As compared with a similar detector, D1536, which has been fabricated by BINP since 2010, the new detector D2048 has higher spatial resolution (2.5 lp/mm vs 2.0 lp/mm) and larger entrance window (426 mm vs of 400 mm). Furthermore, the D2048 detector is more manufacturable. With the newly-developed software, this detector can be used as part of a radiographic installation. The technology of manufacturing and the new software of the new detector were purchased by a Chinese company under contract № RU/E-11034. Works under this contract were completed in late 2012.



Fig. 9.2. 1 D2048 detector.

A pilot detector was fabricated and used in test measurements. Characteristics of the detector (spatial resolution, contrast sensitivity, DQE, irradiation doses, etc.) derived from the measurements are fully consistent with the design calculations.

9.2.2. System for Radiographic Control (SRC) "Sibscan" for people examination.

In 2012, a new technology for the manufacture of linear detector for SRC was developed and implemented. As compared with the D768 detector, which had been developed and manufactured by BINP, the new D512 detector allows more than 2 times reducing the irradiation doses during examination. The D512 detector is much easier in manufacturing than the D768 detector. New software was developed for application of the D512 detector as part of SRC installation. SRC installations equipped with the D512 detector have been installed at several Russian



Fig. 9.2. 2 X-ray image of lungs made with the D2048 detector.

airports. BINP has organized small-scale production of the D512 detectors.

Characteristics of the D512 detector and those of a scintillation detector of similar destination were compared in detail. The latter detector has been made at the Institute of Applied Physics (Novosibirsk) with the use of lumino-phor {Gd₂O₂S:Tb} and a scintillator {CsJ:Tl}, the light detected with photodiodes. It was found, that the spatial resolution and contrast sensitivity of both detectors to be approximately equal. The scintillation detector is more manufacturable than the gaseous D512 detector, but has a lower efficiency of gamma-ray detection and worse radiation resistance, which leads to a shorter lifetime.

In total for 2012 the following quantity of detectors has been made and delivered consumers: five D1536 detectors, one D2048 detector, four D768 detectors, and twelve D572 detectors.

BIBLIOGRAPHY

List of publications

[1] Aad G., ATLAS Collab., Anisenkov A., Beloborodova O., Bobrovnikov V.S., Bogdanchikov A., Kazanin V.F., Kolachev G.M., Korol A., Malyshev V., Maslennikov A.L., Orlov I., Peleganchuk S.V., Shamov A.G., Skovpen K., Soukharev A., Talyshev A., Tikhonov Y.A., Zaytsev A., et al. A search for t anti t resonances with the ATLAS detector in 2.05 fb^{-1} of proton-proton collisions at $\sqrt{s} = 7 \text{ TeV}$. // Eur. Phys. J. C. - 2012. - V.72, N7. - p.2083 (23 p.).

[2] Aad G., ATLAS Collab., Anisenkov A., Beloborodova O., Bobrovnikov V.S., Bogdanchikov A., Kazanin V.F., Kolachev G.M., Korol A., Malyshev V., Maslennikov A.L., Maximov D.A., Orlov I., Peleganchuk S.V., Shamov A.G., Skovpen K., Soukharev A., Talyshev A., Tikhonov Y.A., Zaytsev A., et al. Electron performance measurements with the ATLAS detector using the 2010 LHC proton-proton collision data. // Eur. Phys. J. C. - 2012. - V.72, N3. - p.1909 (46 p.).

[3] Aaij R., LHCb Collab., Bobrov A., Bondar A., Eidelman S., Krokovny P., Poluektov A., Shekhtman L., et al. Measurement of charged particle multiplicities in pp collisions at $\sqrt{s} = 7 \text{ TeV}$ in the forward region. // Eur. Phys. J. C. - 2012. - V.72, N4. - p.1947 (14 p.).

[4] Aaij R., LHCb Collab., Bobrov A., Bondar A., Eidelman S., Krokovny P., Poluektov A., Shekhtman L., et al. Measurement of Υ production in pp collisions at $\sqrt{s} = 7 \text{ TeV}$. // Eur. Phys. J. C. - 2012. - V.72, N6. - p.2025 (12 p.).

[5] Aaij R., LHCb Collab., Bobrov A., Bondar A., Eidelman S., Krokovny P., Poluektov A., Shekhtman L., et al. Measurement of $\psi(2S)$ meson production in pp collisions at $\sqrt{s} = 7 \text{ TeV}$. // Eur. Phys. J. C. - 2012. - V.72, N8. - p.2100 (12 p.).

[6] Aaij R., LHCb Collab., Bobrov A., Bondar A., Eidelman S., Krokovny P., Kudryavtsev V., Poluektov A., Shekhtman L., Vorobyev V., et al. Measurement of relative branching fractions of B decays to $\psi(2S)$ and J/ψ mesons. // Eur. Phys. J. C. - 2012. - V.72, N8. - p.2118 (9p.).

[7] Aad G., ATLAS Collab., Anisenkov A., Beloborodova O., Bobrovnikov V.S., Bogdanchikov A., Kazanin V.F., Kolachev G.M., Korol A., Malyshev V., Maslennikov A.L., Maximov D.A., Orlov I., Peleganchuk S.V., Shamov A.G., Skovpen K., Soukharev A., Talyshev A., Tikhonov Y.A., Zaytsev A., et al. Measurement of t anti t production with a veto on additional central jet activity in pp collisions at $\sqrt{s} = 7 \text{ TeV}$ using the ATLAS detector. // Eur. Phys. J. C. - 2012. - V.72, N6. - p.2043 (24 p.).

[8] Aad G., ATLAS Collab., Anisenkov A., Beloborodova O., Bobrovnikov V.S., Bogdanchikov A., Kazanin V.F., Kolachev G.M., Korol A., Malyshev V., Maslennikov A.L., Orlov I., Peleganchuk S.V., Shamov A.G., Skovpen K., Soukharev A., Talyshev A., Tikhonov Y.A., Zaytsev A., et al. Measurement of τ polarization in $W \rightarrow \tau \nu$ decays with the ATLAS detector in pp collisions at $\sqrt{s} = 7 \text{ TeV}$. // Eur. Phys. J. C. - 2012. - V.72, N7. - p.2062 (21 p.).

[9] Aad G., ATLAS Collab., Anisenkov A., Beloborodova O., Bobrovnikov V.S., Bogdanchikov A., Kazanin V.F., Kolachev G.M., Korol A., Malyshev V., Maslennikov A.L., Maximov D.A., Orlov I., Peleganchuk S.V., Shamov A.G., Skovpen K., Soukharev A., Talyshev A., Tikhonov Y.A., Zaytsev A., et al. Measurement of the polarisation of W bosons produced with large transverse momentum in pp collisions at $\sqrt{s} = 7 \text{ TeV}$ with the ATLAS experiment. // Eur. Phys. J. C. - 2012. - V.72, N5. - p.2001 (30 p.).

[10] Aad G., ATLAS Collab., Anisenkov A., Beloborodova O., Bobrovnikov V.S., Bogdanchikov A., Kazanin V.F., Kolachev G.M., Korol A., Malyshev V., Maslennikov A.L., Maximov D.A., Orlov I., Peleganchuk S.V., Shamov A.G., Skovpen K., Soukharev A., Talyshev A., Tikhonov Y.A., Zaytsev A., et al. Measurement of the top quark mass with the template method in the t anti $t \rightarrow \text{lepton} + \text{jets}$ channel using ATLAS data. // Eur. Phys. J. C. - 2012. - V.72, N6. - p.2046 (30 p.).

[11] Aad G., ATLAS Collab., Anisenkov A., Beloborodova O., Bobrovnikov V.S., Bogdanchikov A., Kazanin V.F., Kolachev G.M., Korol A., Malyshev V., Maslennikov A.L., Maximov D.A., Orlov I., Peleganchuk S.V., Shamov A.G., Skovpen K., Soukharev A., Talyshev A., Tikhonov Y.A., Zaytsev A., et al. Measurement of the charge asymmetry in top quark pair production in pp collisions at $\sqrt{s} = 7 \text{ TeV}$ using the ATLAS. // Eur. Phys. J. C. - 2012. - V.72, N6. - p.2039 (27 p.).

[12] Aaij R., LHCb Collab., Bobrov A., Bondar A., Eidelman S., Krokovny P., Poluektov A., Shekhtman L., et al. Opposite-side flavour tagging of B mesons at the LHCb experiment. // Eur. Phys. J. C. - 2012. - V.72, N6. - p.2022 (16 p.).

[13] Aad G., ATLAS Collab., Beloborodova O., Bobrovnikov V.S., Bogdanchikov A., Kazanin V.F., Kolachev G.M., Korol A., Malyshev V., Maslennikov A.L., Maximov D.A., Orlov I., Peleganchuk S.V., Shamov A.G., Skovpen K., Soukharev A., Talyshev A., Tikhonov Y.A., Zaytsev A., et al. Performance of missing transverse momentum reconstruction in proton-proton collisions at $\sqrt{s} = 7 \text{ TeV}$ with ATLAS. // Eur. Phys. J. C. - 2012. - V.72, N1. - p.1844 (35 p.).

- [14] Aad G., ATLAS Collab., Beloborodova O., Bobrovnikov V.S., Bogdanchikov A., Kazanin V.F., Kolachev G.M., Korol A., Malyshev V., Maslennikov A.L., Maximov D.A., Orlov I., Peleganchuk S.V., Schamov A.G., Skovpen K., Soukharev A., Talyshev A., Tikhonov Y.A., Zaytsev A., et al. Performance of the ATLAS trigger system in 2010. // *Eur. Phys. J. C.* - 2012. - V.72, N1. - p.1849 (61 p.).
- [15] Aad G., ATLAS Collab., Anisenkov A., Beloborodova O., Bobrovnikov V.S., Bogdanchikov A., Kazanin V.F., Kolachev G.M., Korol A., Malyshev V., Maslennikov A.L., Maximov D.A., Orlov I., Peleganchuk S.V., Shamov A.G., Skovpen K., Soukharev A., Talyshev A., Tikhonov Y.A., Zaytsev A., et al. Rapidity gap cross sections measured with the ATLAS detector in pp collisions at $\sqrt{s} = 7$ TeV. // *Eur. Phys. J. C.* - 2012. - V.72, N3. - p.1926 (31 p.).
- [16] ATLAS Collab., Anisenkov A., Beloborodova O., Bobrovnikov V.S., Bogdanchikov A., Kazanin V.F., Kolachev G.M., Korol A., Malyshev V., Maslennikov A.L., Maximov D.A., Orlov I., Peleganchuk S.V., Shamov A.G., Skovpen K., Soukharev A., Talyshev A., Tikhonov Y.A., Zaytsev A., et al. Search for a fermiophobic Higgs boson in the diphoton decay channel with the ATLAS detector. // *Eur. Phys. J. C.* - 2012. - V.72, N9. - p.2157 (18 p.).
- [17] Aad G., ATLAS Collab., Anisenkov A., Beloborodova O., Bobrovnikov V.S., Bogdanchikov A., Kazanin V.F., Kolachev G.M., Korol A., Malyshev V., Maslennikov A.L., Maximov D.A., Orlov I., Peleganchuk S.V., Shamov A.G., Skovpen K., Soukharev A., Talyshev A., Tikhonov Y.A., Zaytsev A., et al. Search for anomaly-mediated supersymmetry breaking with the ATLAS detector based on a disappearing-track signature in pp collisions at $\sqrt{s} = 7$ TeV. // *Eur. Phys. J. C.* - 2012. - V.72, N4. - p.1993 (20 p.).
- [18] Aad G., ATLAS Collab., Anisenkov A., Beloborodova O., Bobrovnikov V.S., Bogdanchikov A., Kazanin V.F., Kolachev G.M., Korol A., Malyshev V., Maslennikov A.L., Maximov D.A., Orlov I., Peleganchuk S.V., Shamov A.G., Skovpen K., Soukharev A., Talyshev A., Tikhonov Y.A., Zaytsev A., et al. Search for decays of stopped, long-lived particles from 7 TeV pp collisions with the ATLAS detector. // *Eur. Phys. J. C.* - 2012. - V.72, N4. - p.1965(21 p).
- [19] Aad G., ATLAS Collab., Anisenkov A., Beloborodova O., Bobrovnikov V.S., Bogdanchikov A., Kazanin V.F., Kolachev G.M., Korol A., Malyshev V., Maslennikov A.L., Maximov D.A., Orlov I., Peleganchuk S.V., Shamov A.G., Skovpen K., Soukharev A., Talyshev A., Tikhonov Y.A., Zaytsev A., et al. Search for heavy neutrinos and right-handed W bosons in events with two leptons and jets in pp collisions at $\sqrt{s} = 7$ TeV with the ATLAS detector. // *Eur. Phys. J. C.* - 2012. - V.72, N7. - p.2056 (22 p.).
- [20] Aad G., ATLAS Collab., Anisenkov A., Beloborodova O., Bobrovnikov V.S., Bogdanchikov A., Kazanin V.F., Kolachev G.M., Korol A., Malyshev V., Maslennikov A.L., Maximov D.A., Orlov I., Peleganchuk S.V., Shamov A.G., Skovpen K., Soukharev A., Talyshev A., Tikhonov Y.A., Zaytsev A., et al. Search for lepton flavour violation in the e mu continuum with the ATLAS detector in $\sqrt{s} = 7$ TeV pp collisions at the LHC. // *Eur. Phys. J. C.* - 2012. - V.72, N6. - p.2040 (19 p.).
- [21] ATLAS Collab., Anisenkov A., Beloborodova O., Bobrovnikov V.S., Bogdanchikov A., Kazanin V.F., Kolachev G.M., Korol A., Malyshev V., Maslennikov A.L., Maximov D.A., Orlov I., Peleganchuk S.V., Shamov A.G., Skovpen K., Soukharev A., Talyshev A., Tikhonov Y.A., Zaytsev A., et al. Search for second generation scalar leptoquarks in pp collisions at $\sqrt{s} = 7$ TeV with the ATLAS detector. // *Eur. Phys. J. C.* - 2012. - V.72, N9. - p.2151 (26 p.).
- [22] Abelev B., ALICE Collab., Pestov Y., et al. Transverse sphericity of primary charged particles in minimum bias proton-proton collisions at $\sqrt{s}=0.9, 2.76$ and 7 TeV. // *Eur. Phys. J. C.* - 2012. - V.72, N9. - p.2124 (16 p.).
- [23] Ivanyushenkov Y., Abliz M., Boerste K., Buffington T., Doose C., Fuerst J., Hasse Q., Kasa M., Kim S.H., Kustom R.L., Lev V., Mezentsev N.A., Moog E.R., Skidopoulos D., Syrovatin V., Tsukanov V., Trakhtenberg E.M., Vasserman I.B., Xu J. Development of a planar superconducting undulator for the advanced photon source. // *IEEE T. Appl. Supercon.* - 2012. - V.22, N3. - p.4100804-1-4.
- [24] Muehle C., Gurov D., Khavin N., Kolokolnikov Yu., Moritz G., Utkin A., Vobly P., Will Ch., Winkler M. Radiation resistant prototype dipole for the first stage of super-FRS. // *IEEE T. Appl. Supercon.* - 2012. - V.22, N3. - p.4003304-1-4.
- [25] Acosta G., Avilov M., Bermudez J., Blinov V.E., Logatchev P., Shiyankov S., Tecchio L.B., Udup E., Zaitsev V. A safety device for the neutron converter of the SPIRAL2 project. // *Nucl. Instrum. Meth. A.* - 2012. - V.684. - p.1-6.
- [26] Pinfeld J., Maslennikov A., Soukharev A., Talyshev A., Tikhonov Yu., et al. Evaluation of the local hadronic calibration with combined beam-test data for the endcap and forward calorimeters of ATLAS in the pseudorapidity region $2.5 < \eta < 4.0$. // *Nucl. Instrum. Meth. A.* - 2012. - V.693. - p.74-97.
- [27] Glatte A., Bedareva T., Grekhov A., Maslennikov A., Peleganchuk S., Pivovarov S., Snopkov R., Starostin A., Talyshev A., Tikhonov Y., et al. Liquid argon calorimeter performance at high rates. // *Nucl. Instrum. Meth. A.* - 2012. - V.669. - p.47-65.
- [28] Zhmurikov E.I., Savchenko I.V., Stankus S.V., Yatsuk O.S., Tecchio L.B. Measurements of the thermophysical properties of graphite composites for a

neutron target converter. // Nucl. Instrum. Meth. A. - 2012. - V.674. - p.79-84.

[29] Tuszewski M., Smirnov A., Thompson M.C., Akhmetov T., Ivanov A., Voskoboinikov R., et al. A new high performance field reversed configuration operating regime in the C-2 device. // Physics of Plasmas. - 2012. - V.19, N5. - p.056108-1-8.

[30] Shalashov A.G., Gospodchikov E.D., Smolyakova O.B., Bagryansky P.A., Malygin V.I., Thumm M. Auxiliary ECR heating system for the gas dynamic trap. // Physics of Plasmas. - 2012. - V.19, N5. - p.052503-1-8.

[31] Lotov K.V. Controlled self-modulation of high energy beams in a plasma. // Physics of Plasmas. - 2012. - V.18, N3. - p.024501-1.

[32] Bagulov D.S., Kotelnikov I.A. Electron cyclotron resonance near the axis of the gas-dynamic trap. // Physics of Plasmas. - 2012. - V.19, N8. - p.082502-1-8.

[33] Tsidulko Yu.A., Helsabeck T.J., O'Neil T.M. Particle fluxes through the separatrix in the trapped particle diocotron mode. // Physics of Plasmas. - 2012. - N8. - p.084505-1-4.

[34] Caldwell A., Lotov K. Plasma wakefield acceleration with a modulated proton bunch. // Physics of Plasmas. - 2012. - V.18, N10. - p.103101-1-9.

[35] Aad G., ATLAS Collab., Anisenkov A., Beloborodova O., Bobrovnikov V.S., Bogdanchikov A., Kazanin V.F., Kolachev G.M., Korol A., Malyshev V., Maslennikov A.L., Maximov D.A., Orlov I., Peleganchuk S.V., Schamov A.G., Skovpen K., Soukharev A., Talyshev A., Tikhonov Y.A., et al. A measurement of the ratio of the W and Z cross sections with exactly one associated jet in pp collisions at $\sqrt{s}=7$ TeV with ATLAS. // Phys. Lett. B. - 2012. - V.708, N3/5. - p.221-240.

[36] Aaij R., LHCb Collab., Bobrov A., Bondar A., Eidelman S., Krokovny P., Kudryavtsev V., Poluektov A., Shekhtman L., Vorobyev V., et al. A model-independent Dalitz plot analysis of $B^{\pm} \rightarrow DK^{\pm}$ with $D \rightarrow K_S^0 h^+ h^-$ ($h = \pi, K$) decays and constraints on the CKM angle γ . // Phys. Lett. B. - 2012. - V.718, N1. - p.43-55.

[37] Aad G., ATLAS Collab., Anisenkov A., Beloborodova O., Bobrovnikov V.S., Bogdanchikov A., Kazanin V.F., Kolachev G.M., Korol A., Malyshev V., Maslennikov A.L., Maximov D.A., Orlov I., Peleganchuk S.V., Schamov A.G., Skovpen K., Soukharev A., Talyshev A., Tikhonov Y.A., Zaytsev A., et al. Combined search for Standard Model Higgs boson using up to 4.9 fb^{-1} of pp collision data at $\sqrt{s}=7$ TeV with the ATLAS detector at the LHC. // Phys. Lett. B. - 2012. - V.710, N1. - p.49-66.

[38] Aad G., ATLAS Collab., Anisenkov A., Beloborodova O., Bobrovnikov V.S., Bogdanchikov A., Kazanin V.F., Kolachev G.M., Korol A., Malyshev V., Maslennikov A.L., Maximov D.A., Orlov I., Peleganchuk

S.V., Schamov A.G., Skovpen K., Soukharev A., Talyshev A., Tikhonov Y.A., Zaytsev A., et al. Erratum to: "Search for first generation scalar leptoquarks in pp collisions at $\sqrt{s}=7$ TeV with the ATLAS detector". // [Phys. Lett. B 709 (2012) 158]. // Phys. Lett. B. - 2012. - V.711, N5. - p.442-455.

[39] Aad G., ATLAS Collab., Anisenkov A., Beloborodova O., Bobrovnikov V.S., Bogdanchikov A., Kazanin V.F., Kolachev G.M., Korol A., Malyshev V., Maslennikov A.L., Maximov D.A., Orlov I., Peleganchuk S.V., Schamov A.G., Skovpen K., Soukharev A., Talyshev A., Tikhonov Y.A., Zaytsev A., et al. Evidence for the associated production of a W boson and a top quark in ATLAS at $\sqrt{s}=7$ TeV. // Phys. Lett. B. - 2012. - V.716, N1. - p.142-159.

[40] Aaij R., LHCb Collab., Bobrov A., Bondar A., Eidelman S., Poluektov A., Shekhtman L., et al. First observation of the decay $B_s^0 \rightarrow K^{*0} \bar{K}^{*0}$. // Phys. Lett. B. - 2012. - V.709, N1/2. - p.50-58.

[41] Khriplovich I.B. Gravitational four-fermion interaction on the Planck scale. // Phys. Lett. B. - 2012. - V.709, N3. - p.111-113.

[42] Pestov Y., ALICE Collab., et al. Hadronic decomposition of two particle angular correlations in Pb-Pb collisions at $\sqrt{s_{NN}}=2.76$ TeV. // Phys. Lett. B. - 2012. - V.708, N3/5. - p.249-264.

[43] Pestov Y., ALICE Collab., et al. Heavy flavour decay muon production at forward rapidity in proton-proton collisions at $\sqrt{s}=7$ TeV. // Phys. Lett. B. - 2012. - V.708, N3/5. - p.265-275.

[44] Pestov Y., ALICE Collab., et al. J/ψ production as a function of charged particle multiplicity in pp collisions at $\sqrt{s}=7$ TeV. // Phys. Lett. B. - 2012. - V.712, N3. - p.165-175.

[45] Pestov Y., ALICE Collab., et al. K_S^0/K^0 correlations in pp collisions at $\sqrt{s}=7$ TeV from the LHC ALICE experiment. // Phys. Lett. B. - 2012. - V.717, N1/3. - p.151-161.

[46] Pestov Y., ALICE Collab., et al. Light vector meson production in pp collisions at $\sqrt{s}=7$ TeV. // Phys. Lett. B. - 2012. - V.710, N4/5. - p.557-568.

[47] Aaij R., LHCb Collab., Bobrov A., Eidelman S., Poluektov A., Shekhtman L., et al. Measurement of b-hadron masses. // Phys. Lett. B. - 2012. - V.708, N3/5. - p.241-248.

[48] Aad G., ATLAS Collab., Beloborodova O., Bobrovnikov V.S., Bogdanchikov A., Kazanin V.F., Kolachev G.M., Korol A., Malyshev V., Maslennikov A.L., Maximov D.A., Orlov I., Peleganchuk S.V., Schamov A.G., Skovpen K., Soukharev A., Talyshev A., Tikhonov Y.A., et al. Measurement of cross-section for b-jets produced in association with a Z boson at $\sqrt{s}=7$

TeV with the ATLAS detector. // Phys. Lett. B. - 2012. - V.706, N4/5. - p.295-313.

[49] Anashin V.V., Aulchenko V.M., Baldin E.M., Barladyan A.K., Barnyakov A.Yu., Barnyakov M.Yu., Baru S.E., Basok I.Yu., Beloborodova O.L., Blinov A.E., Blinov V.E., Bobrov A.V., Bobrovnikov V.S., Bogomyagkov A.V., Bondar A.E., Buzykaev A.R., Eidelman S.I., Grigoriev D.N., Glukhovchenko Yu.M., Gulevich V.V., Gusev D.V., Karnaev S.E., Karpov G.V., Karpov S.V., Kharlamova T.A., Kiselev V.A., Kolmogorov V.V., Kononov S.A., Kotov K.Yu., Kravchenko E.A., Kulikov V.F., Kurkin G.Ya., Kuper E.A., Levichev E.B., Maksimov D.A., Malyshev V.M., Maslennikov A.L., Medvedko A.S., Meshkov O.I., Mishnev S.I., Morozov I.I., Muchnoi N.Y., Neufeld V.V., Nikitin S.A., Nikolaev I.B., Okunev I.N., Onuchin A.P., Oreshkin S.B., Orlov I.O., Osipov A.A., Peleganchuk S.V., Pivovarov S.G., Piminov P.A., Petrov V.V., Poluektov A.O., Prisekin V.G., Ruban A.A., Sandyrev V.K., Savinov G.A., Shamov A.G., Shatilov D., Shwartz B.A., Simonov E.A., Sinyatkin S.V., Skrinsky A.N., Smalyuk V.V., Sokolov A.V., Soukharev A.M., Starostina E.V., Talyshev A.A., Tayursky V.A., Telnov V.I., Tikhonov Yu.A., Todyshev K.Yu., Tumaikin G.M., Usov Yu.V., Vorobiov A.I., Yushkov A.N., Zhilich V.N., Zhulakov V.V., Zhuravlev A.N. (KEDR Collab.). Measurement of main parameters of the $\psi(2S)$ resonance. // Phys. Lett. B. - 2012. - V.711, N3/4. - p.280-291. [<http://arxiv.org/pdf/1109.4215v2.pdf>].

[50] Anashin V.V., Aulchenko V.M., Baldin E.M., Barladyan A.K., Barnyakov A.Yu., Barnyakov M.Yu., Baru S.E., Basok I.Yu., Beloborodova O.L., Blinov A.E., Blinov V.E., Bobrov A.V., Bobrovnikov V.S., Bogomyagkov A.V., Bondar A.E., Buzykaev A.R., Eidelman S.I., Grigoriev D.N., Glukhovchenko Yu.M., Gulevich V.V., Gusev D.V., Karnaev S.E., Karpov G.V., Karpov S.V., Kharlamova T.A., Kiselev V.A., Kolmogorov V.V., Kononov S.A., Kotov K.Yu., Kravchenko E.A., Kulikov V.F., Kurkin G.Ya., Kuper E.A., Levichev E.B., Maksimov D.A., Malyshev V.M., Maslennikov A.L., Medvedko A.S., Meshkov O.I., Mishnev S.I., Morozov I.I., Muchnoi N.Y., Neufeld V.V., Nikitin S.A., Nikolaev I.B., Okunev I.N., Onuchin A.P., Oreshkin S.B., Orlov I.O., Osipov A.A., Peleganchuk S.V., Pivovarov S.G., Piminov P.A., Petrov V.V., Poluektov A.O., Prisekin V.G., Ruban A.A., Sandyrev V.K., Savinov G.A., Shamov A.G., Shatilov D., Shwartz B.A., Simonov E.A., Sinyatkin S.V., Skrinsky A.N., Smalyuk V.V., Sokolov A.V., Soukharev A.M., Starostina E.V., Talyshev A.A., Tayursky V.A., Telnov V.I., Tikhonov Yu.A., Todyshev K.Yu., Tumaikin G.M., Usov Yu.V., Vorobiov A.I., Yushkov A.N., Zhilich V.N., Zhulakov V.V., Zhuravlev A.N. (KEDR Collab.). Measurement of $\psi(3770)$ parameters. // Phys. Lett. B. - 2012. - V.711, N3/4. - p.292-300. [[arXiv:1109.4205](http://arxiv.org/abs/1109.4205) [hep-ex]].

[51] Aaij R., LHCb Collab., Bobrov A., Bondar A., Eidelman S., Poluektov A., Shekhtman L., et al.

Measurement of the $B_s^0 - \bar{B}_s^0$ oscillation frequency Δm_s in $B_s^0 \rightarrow D_s^- 3\pi$ decays. // Phys. Lett. B. - 2012. - V.709, N3. - p.177-184.

[52] Aaij R., LHCb Collab., Bobrov A., Bondar A., Eidelman S., Krokovny P., Kudryavtsev V., Poluektov A., Shekhtman L., Vorobyev V., et al. Measurement of the $B_s^0 \rightarrow J/\psi K_S^0$ branching fraction. // Phys. Lett. B. - 2012. - V.713, N3. - p.172-179.

[53] Aad G., ATLAS Collab., Beloborodova O., Bobrovnikov V.S., Bogdanchikov A., Kazanin V.F., Kolachev G.M., Korol A., Malyshev V., Maslennikov A.L., Maximov D.A., Orlov I., Peleganchuk S.V., Schamov A.G., Skovpen K., Soukharev A., Talyshev A., Tikhonov Y.A., Zaytsev A., et al. Measurement of the centrality dependence of the charged particle pseudorapidity distribution in lead-lead collisions at $\sqrt{s_{NN}}=2.76$ TeV with the ATLAS detector. // Phys. Lett. B. - 2012. - V.710, N3. - p.363-382.

[54] Aaij R., LHCb Collab., Bobrov A., Bondar A., Eidelman S., Poluektov A., Shekhtman L., et al. Measurement of the CP violating phase ϕ_s in anti $B_s^0 \rightarrow J/\psi f^0(980)$. // Phys. Lett. B. - 2012. - V.707, N5. - p.497-505.

[55] Aaij R., LHCb Collab., Bobrov A., Bondar A., Eidelman S., Kudryavtsev V., Poluektov A., Shekhtman L., et al. Measurement of the CP-violating phase ϕ_3 in anti $B_s^0 \rightarrow J/\psi \pi^+\pi^-$ decays. // Phys. Lett. B. - 2012. - V.713, N4/5. - p.378-386.

[56] Aad G., ATLAS Collab., Beloborodova O., Bobrovnikov V.S., Bogdanchikov A., Kazanin V.F., Kolachev G.M., Korol A., Malyshev V., Maslennikov A.L., Maximov D.A., Orlov I., Peleganchuk S.V., Schamov A.G., Skovpen K., Soukharev A., Talyshev A., Tikhonov Y.A., Zaytsev A., et al. Measurement of the cross section for the production of a W boson in association with b-jets in pp collisions at $\sqrt{s}=7$ TeV with the ATLAS detector. // Phys. Lett. B. - 2012. - V.707, N5. - p.418-437.

[57] Aaij R., LHCb Collab., Bobrov A., Bondar A., Eidelman S., Poluektov A., Shekhtman L., et al. Measurement of the cross section ratio $\sigma_{\chi_{c2}}/\sigma_{\chi_{c1}}$ for prompt χ_c production at $\sqrt{s}=7$ TeV. // Phys. Lett. B. - 2012. - V.714, N2/5. - p.215-223.

[58] Aaij R., LHCb Collab., Bobrov A., Bondar A., Eidelman S., Krokovny P., Kudryavtsev V., Poluektov A., Shekhtman L., Vorobyev V., et al. Measurement of the $D_s^+ - D_s^-$ production asymmetry in 7 TeV pp collisions. // Phys. Lett. B. - 2012. - V.713, N3. - p.186-195.

[59] Aaij R., LHCb Collab., Bobrov A., Bondar A., Eidelman S., Poluektov A., Shekhtman L., et al. Measurement of the effective $B_s^0 \rightarrow K^+ K^-$ lifetime. // Phys. Lett. B. - 2012. - V.707, N3/4. - p.349.

[60] Aaij R., LHCb Collab., Bobrov A., Bondar A., Eidelman S., Krokovny P., Kudryavtsev V., Poluektov A., Shekhtman L., Vorobyev V., et al. Measurement of the effective $B_s^0 \rightarrow K^+ K^-$ lifetime. // Phys. Lett. B. - 2012. - V.716, N2. - p.393-400.

[61] Aaij R., LHCb Collab., Bobrov A., Bondar A., Eidelman S., Krokovny P., Kudryavtsev V., Poluektov A., Shekhtman L., Vorobyev V., et al. Measurement of the effective $B_s^0 \rightarrow K^+ K^-$ lifetime. // Phys. Lett. B. - 2012. - V.716, N3/5. - p.393-400.

[62] Aaij R., LHCb Collab., Bobrov A., Bondar A., Eidelman S., Krokovny P., Kudryavtsev V., Poluektov A., Shekhtman L., Vorobyev V., et al. Measurement of the polarization amplitudes and triple product asymmetries in the $B_s^0 \rightarrow \varphi\varphi$ decay. // Phys. Lett. B. - 2012. - V.713, N4/5. - p.369-377.

[63] Aad G., ATLAS Collab., Beloborodova O., Bobrovnikov V.S., Bogdanchikov A., Kazanin V.F., Kolachev G.M., Korol A., Malyshev V., Maslennikov A.L., Maximov D.A., Orlov I., Peleganchuk S.V., Schamov A.G., Skovpen K., Soukharev A., Talyshev A., Tikhonov Y.A., et al. Measurement of the pseudorapidity and transverse momentum dependence of the elliptic flow of charged particles in lead-lead collisions at $\sqrt{s_{NN}}=2.76$ TeV with the ATLAS detector. // Phys. Lett. B. - 2012. - V.707, N3/4. - p.330-348.

[64] Aad G., ATLAS Collab., Anisenkov A., Beloborodova O., Bobrovnikov V.S., Bogdanchikov A., Kazanin V.F., Kolachev G.M., Korol A., Malyshev V., Maslennikov A.L., Maximov D.A., Orlov I., Peleganchuk S.V., Schamov A.G., Skovpen K., Soukharev A., Talyshev A., Tikhonov Y.A., Zaytsev A., et al. Measurement of the t-channel single top-quark production cross section in pp collisions at $\sqrt{s}=7$ TeV with the ATLAS detector. // Phys. Lett. B. - 2012. - V.717, N4/5. - p.330-350.

[65] Aad G., ATLAS Collab., Anisenkov A., Beloborodova O., Bobrovnikov V.S., Bogdanchikov A., Kazanin V.F., Kolachev G.M., Korol A., Malyshev V., Maslennikov A.L., Maximov D.A., Orlov I., Peleganchuk S.V., Schamov A.G., Skovpen K., Soukharev A., Talyshev A., Tikhonov Y.A., Zaytsev A., et al. Measurement of the top quark pair cross section with ATLAS in pp collisions at $\sqrt{s}=7$ TeV using final states with an electron or a muon and a hadronically decaying tau lepton. // Phys. Lett. B. - 2012. - V.717, N1/3. - p.89-108.

[66] Aad G., ATLAS Collab., Beloborodova O., Bobrovnikov V.S., Bogdanchikov A., Kazanin V.F., Kolachev G.M., Korol A., Malyshev V., Maslennikov A.L., Maximov D.A., Orlov I., Peleganchuk S.V., Schamov A.G., Skovpen K., Soukharev A., Talyshev A., Tikhonov Y.A., Zaytsev A., et al. Measurement of the top quark pair production cross section in pp collisions at

$\sqrt{s}=7$ TeV in dilepton final states with ATLAS. // Phys. Lett. B. - 2012. - V.707, N5. - p.459-477.

[67] Aad G., ATLAS Collab., Beloborodova O., Bobrovnikov V.S., Bogdanchikov A., Kazanin V.F., Kolachev G.M., Korol A., Malyshev V., Maslennikov A.L., Maximov D.A., Orlov I., Peleganchuk S.V., Schamov A.G., Skovpen K., Soukharev A., Talyshev A., Tikhonov Y.A., Zaytsev A., et al. Measurement of the top quark pair production cross-section with ATLAS in the single lepton channel. // Phys. Lett. B. - 2012. - V.711, N3/4. - p.244-263.

[68] Aad G., ATLAS Collab., Beloborodova O., Bobrovnikov V.S., Bogdanchikov A., Kazanin V.F., Kolachev G.M., Korol A., Malyshev V., Maslennikov A.L., Maximov D.A., Orlov I., Peleganchuk S.V., Schamov A.G., Skovpen K., Soukharev A., Talyshev A., Tikhonov Y.A., et al. Measurement of the $W \rightarrow \text{tau nu/sub tau/}$ cross section in pp collisions at $\sqrt{s}=7$ TeV with the ATLAS experiment. // Phys. Lett. B. - 2012. - V.706, N4/5. - p.276-294.

[69] Aad G., ATLAS Collab., Anisenkov A., Beloborodova O., Bobrovnikov V.S., Bogdanchikov A., Kazanin V.F., Kolachev G.M., Korol A., Malyshev V., Maslennikov A.L., Maximov D.A., Orlov I., Peleganchuk S.V., Schamov A.G., Skovpen K., Soukharev A., Talyshev A., Tikhonov Y.A., Zaytsev A., et al. Measurement of the WW cross section in $\sqrt{s}=7$ TeV pp collisions with the ATLAS detector and limits on anomalous gauge couplings. // Phys. Lett. B. - 2012. - V.712, N4/5. - p.289-308.

[70] Aad G., ATLAS Collab., Anisenkov A., Beloborodova O., Bobrovnikov V.S., Bogdanchikov A., Kazanin V.F., Kolachev G.M., Korol A., Malyshev V., Maslennikov A.L., Maximov D.A., Orlov I., Peleganchuk S.V., Schamov A.G., Skovpen K., Soukharev A., Talyshev A., Tikhonov Y.A., Zaytsev A., et al. Measurement of the W+Z production cross section and limits on anomalous triple gauge couplings in proton-proton collisions at $\sqrt{s}=7$ TeV with the ATLAS detector. // Phys. Lett. B. - 2012. - V.709, N4/5. - p.341-357.

[71] Aad G., ATLAS Collab., Anisenkov A., Beloborodova O., Bobrovnikov V.S., Bogdanchikov A., Kazanin V.F., Kolachev G.M., Korol A., Malyshev V., Maslennikov A.L., Maximov D.A., Orlov I., Peleganchuk S.V., Schamov A.G., Skovpen K., Soukharev A., Talyshev A., Tikhonov Y.A., Zaytsev A., et al. Measurement of $W\gamma$ and $Z\gamma$ production cross sections in pp collisions at $\sqrt{s}=7$ TeV and limits on anomalous triple gauge couplings with the ATLAS detector. // Phys. Lett. B. - 2012. - V.717, N1/3. - p.49-69.

[72] Aad G., ATLAS Collab., Beloborodova O., Bobrovnikov V.S., Bogdanchikov A., Kazanin V.F., Kolachev G.M., Korol A., Malyshev V., Maslennikov A.L., Maximov D.A., Orlov I., Peleganchuk S.V.,

Schamov A.G., Skovpen K., Soukharev A., Talyshev A., Tikhonov Y.A., et al. Measurements of the electron and muon inclusive cross-sections in proton-proton collisions at $\sqrt{s}=7$ TeV with the ATLAS detector. // Phys. Lett. B. - 2012. - V.707, N5. - p.438-458.

[73] Pestov Y., ALICE Collab., et al. Multi-strange baryon production in pp collisions at $\sqrt{s}=7$ TeV with ALICE. // Phys. Lett. B. - 2012. - V.712, N4/5. - p.309-318.

[74] Pestov Y., ALICE Collab., et al. Neutral pion and eta meson production in proton-proton collisions at $\sqrt{s}=0.9$ TeV and $\sqrt{s}=7$ TeV. // Phys. Lett. B. - 2012. - V.717, N1/3. - p.162-172.

[75] Aad G., ATLAS Collab., Anisenkov A., Beloborodova O., Bobrovnikov V.S., Bogdanchikov A., Kazanin V.F., Kolachev G.M., Korol A., Malyshev V., Maslennikov A.L., Maximov D.A., Orlov I., Peleganchuk S.V., Schamov A.G., Skovpen K., Soukharev A., Talyshev A., Tikhonov Y.A., Zaytsev A., et al. Observation of a new particle in the search for the Standard Model Higgs boson with the ATLAS detector at the LHC. // Phys. Lett. B. - 2012. - V.716, N1. - p.1-29.

[76] Aaij R., LHCb Collab., Bobrov A., Bondar A., Eidelman S., Kudryavtsev V., Poluektov A., et al. Observation of CP violation in $B^+ \rightarrow DK^+$ decays. // Phys. Lett. B. - 2012. - V.712, N3. - p.203-212.

[77] Aaij R., LHCb Collab., Bobrov A., Bondar A., Eidelman S., Poluektov A., Shekhtman L., et al. Observation of J/ψ pair production in pp collisions at $\sqrt{s}=7$ TeV. // Phys. Lett. B. - 2012. - V.707, N1. - p.52-59.

[78] Ablikim M., BESSIII Collab., Achasov M.N., Muchnoi N.Yu., Nikolaev I.B., et al. Precision measurement of the branching fractions of $J/\psi \rightarrow \pi^+\pi^-\pi^0$ and $\psi' \rightarrow \pi^+\pi^-\pi^0$. // Phys. Lett. B. - 2012. - V.710, N4/5. - p.584-599. [arXiv:1202.2048 [hep-ex].

[79] Aad G., ATLAS Collab., Beloborodova O., Bobrovnikov V.S., Bogdanchikov A., Kazanin V.F., Kolachev G.M., Korol A., Malyshev V., Maslennikov A.L., Maximov D.A., Orlov I., Peleganchuk S.V., Schamov A.G., Skovpen K., Soukharev A., Talyshev A., Tikhonov Y.A., Zaytsev A., et al. Searches for supersymmetry with the ATLAS detector using final states with two leptons and missing transverse momentum in $\sqrt{s}=7$ TeV proton-proton collisions. // Phys. Lett. B. - 2012. - V.709, N3. - p.137-157.

[80] Aad G., ATLAS Collab., Beloborodova O., Bobrovnikov V.S., Bogdanchikov A., Kazanin V.F., Kolachev G.M., Korol A., Malyshev V., Maslennikov A.L., Maximov D.A., Orlov I., Peleganchuk S.V., Schamov A.G., Skovpen K., Soukharev A., Talyshev A., Tikhonov Y.A., et al. Search for a heavy Standard Model Higgs boson in the channel $H \rightarrow ZZ \rightarrow l+l-q \text{ anti } q$ using

the ATLAS detector. // Phys. Lett. B. - 2012. - V.707, N1. - p.27 - 45. - Bibliogr. : 52 ref.

[81] Aad G., ATLAS Collab., Anisenkov A., Beloborodova O., Bobrovnikov V.S., Bogdanchikov A., Kazanin V.F., Kolachev G.M., Korol A., Malyshev V., Maslennikov A.L., Maximov D.A., Orlov I., Peleganchuk S.V., Schamov A.G., Skovpen K., Soukharev A., Talyshev A., Tikhonov Y.A., Zaytsev A., et al. Search for a Standard Model Higgs boson in the $H \rightarrow ZZ \rightarrow l^+ l^- \nu \bar{\nu}$ decay channel using 4.7 fb^{-1} of $\sqrt{s}=7$ TeV data with the ATLAS detector. // Phys. Lett. B. - 2012. - V.717, N1/3. - p.29-48.

[82] Aad G., ATLAS Collab., Anisenkov A., Beloborodova O., Bobrovnikov V.S., Bogdanchikov A., Kazanin V.F., Kolachev G.M., Korol A., Malyshev V., Maslennikov A.L., Maximov D.A., Orlov I., Peleganchuk S.V., Schamov A.G., Skovpen K., Soukharev A., Talyshev A., Tikhonov Y.A., Zaytsev A., et al. Search for contact interactions in dilepton events from pp collisions at $\sqrt{s}=7$ TeV with the ATLAS detector. // Phys. Lett. B. - 2012. - V.712, N1/2. - p.40-58.

[83] Aad G., ATLAS Collab., Beloborodova O., Bobrovnikov V.S., Bogdanchikov A., Kazanin V.F., Kolachev G.M., Korol A., Malyshev V., Maslennikov A.L., Maximov D.A., Orlov I., Peleganchuk S.V., Schamov A.G., Skovpen K., Soukharev A., Talyshev A., Tikhonov Y.A., et al. Search for diphoton events with large missing transverse momentum in 1 fb^{-1} of 7 TeV proton-proton collision data with the ATLAS detector. // Phys. Lett. B. - 2012. - V.710, N4/5. - p.519-537.

[84] Aad G., ATLAS Collab., Beloborodova O., Bobrovnikov V.S., Bogdanchikov A., Kazanin V.F., Kolachev G.M., Korol A., Malyshev V., Maslennikov A.L., Maximov D.A., Orlov I., Peleganchuk S.V., Schamov A.G., Skovpen K., Soukharev A., Talyshev A., Tikhonov Y.A., Zaytsev A., et al. Search for displaced vertices arising from decays of new heavy particles in 7 TeV pp collisions at ATLAS. // Phys. Lett. B. - 2012. - V.707, N5. - p.478-496.

[85] Aad G., ATLAS Collab., Anisenkov A., Beloborodova O., Bobrovnikov V.S., Bogdanchikov A., Kazanin V.F., Kolachev G.M., Korol A., Malyshev V., Maslennikov A.L., Maximov D.A., Orlov I., Peleganchuk S.V., Schamov A.G., Skovpen K., Soukharev A., Talyshev A., Tikhonov Y.A., Zaytsev A., et al. Search for events with large missing transverse momentum, jets, and at least two tau leptons in 7 TeV proton-proton collision data with the ATLAS detector. // Phys. Lett. B. - 2012. - V.714, N2/5. - p.180-196.

[86] Aad G., ATLAS Collab., Anisenkov A., Beloborodova O., Bobrovnikov V.S., Bogdanchikov A., Kazanin V.F., Kolachev G.M., Korol A., Malyshev V., Maslennikov A.L., Maximov D.A., Orlov I., Peleganchuk S.V., Schamov A.G., Skovpen K., Soukharev A., Talyshev A., Tikhonov Y.A., Zaytsev A., et al. Search for extra dimensions using diphoton events in 7 TeV proton-

proton collisions with the ATLAS detector. // Phys. Lett. B. - 2012. - V.710, N4/5. - p.538-556.

[87] Akimov A.V., ATLAS Collab., Anisenkov A., Beloborodova O., Bobrovnikov V.S., Bogdanchikov A., Kazanin V.F., Kolachev G.M., Korol A., Malyshev V., Maslennikov A.L., Maximov D.A., Orlov I., Peleganchuk S.V., Schamov A.G., Skovpen K., Soukharev A., Talyshev A., Tikhonov Y.A., Zaytsev A., et al. Search for FCNC single-top-quark production at $\sqrt{s}=7$ TeV with the ATLAS detector. // Phys. Lett. B. - 2012. - V.712, N4/5. - p.351-369.

[88] Aad G., ATLAS Collab., Anisenkov A., Beloborodova O., Bobrovnikov V.S., Bogdanchikov A., Kazanin V.F., Kolachev G.M., Korol A., Malyshev V., Maslennikov A.L., Maximov D.A., Orlov I., Peleganchuk S.V., Schamov A.G., Skovpen K., Soukharev A., Talyshev A., Tikhonov Y.A., Zaytsev A., et al. Search for first generation scalar leptoquarks in pp collisions at $\sqrt{s}=7$ TeV with the ATLAS detector. // Phys. Lett. B. - 2012. - V.709, N3. - p.158-176.

[89] Aad G., ATLAS Collab., Anisenkov A., Beloborodova O., Bobrovnikov V.S., Bogdanchikov A., Kazanin V.F., Kolachev G.M., Korol A., Malyshev V., Maslennikov A.L., Maximov D.A., Orlov I., Peleganchuk S.V., Schamov A.G., Skovpen K., Soukharev A., Talyshev A., Tikhonov Y.A., Zaytsev A., et al. Search for heavy vector-like quarks coupling to light quarks in proton-proton collisions at $\sqrt{s}=7$ TeV with the ATLAS detector. // Phys. Lett. B. - 2012. - V.712, N1/2. - p.22-39.

[90] Aad G., ATLAS Collab., Anisenkov A., Beloborodova O., Bobrovnikov V.S., Bogdanchikov A., Kazanin V.F., Kolachev G.M., Korol A., Malyshev V., Maslennikov A.L., Maximov D.A., Orlov I., Peleganchuk S.V., Schamov A.G., Skovpen K., Soukharev A., Talyshev A., Tikhonov Y.A., Zaytsev A., et al. Search for new particles decaying to ZZ using final states with leptons and jets with the ATLAS detector in $\sqrt{s}=7$ TeV proton-proton collisions. // Phys. Lett. B. - 2012. - V.712, N4/5. - p.331-350.

[91] Aad G., ATLAS Collab., Beloborodova O., Bobrovnikov V.S., Bogdanchikov A., Kazanin V.F., Kolachev G.M., Korol A., Malyshev V., Maslennikov A.L., Maximov D.A., Orlov I., Peleganchuk S.V., Schamov A.G., Skovpen K., Soukharev A., Talyshev A., Tikhonov Y.A., et al. Search for new physics in the dijet mass distribution using 1 fb^{-1} of pp collision data at $\sqrt{s}=7$ TeV collected by the ATLAS detector. // Phys. Lett. B. - 2012. - V.708, N1/2. - p.37-54.

[92] Aad G., ATLAS Collab., Anisenkov A., Beloborodova O., Bobrovnikov V.S., Bogdanchikov A., Kazanin V.F., Kolachev G.M., Korol A., Malyshev V., Maslennikov A.L., Maximov D.A., Orlov I., Peleganchuk S.V., Schamov A.G., Skovpen K., Soukharev A.,

Talyshev A., Tikhonov Y.A., Zaytsev A., et al. Search for scalar top quark pair production in natural gauge mediated supersymmetry models with the ATLAS detector in pp collisions at $\sqrt{s}=7$ TeV. // Phys. Lett. B. - 2012. - V.715, N1/3. - p.44-60.

[93] Aad G., ATLAS Collab., Beloborodova O., Bobrovnikov V.S., Bogdanchikov A., Kazanin V.F., Kolachev G.M., Korol A., Malyshev V., Maslennikov A.L., Maximov D.A., Orlov I., Peleganchuk S.V., Schamov A.G., Skovpen K., Soukharev A., Talyshev A., Tikhonov Y.A., et al. Search for squarks and gluinos using final states with jets and missing transverse momentum with the ATLAS detector in $\sqrt{s}=7$ TeV proton-proton collisions. // Phys. Lett. B. - 2012. - V.710, N1. - p.67-85.

[94] Aad G., ATLAS Collab., Anisenkov A., Beloborodova O., Bobrovnikov V.S., Bogdanchikov A., Kazanin V.F., Kolachev G.M., Korol A., Malyshev V., Maslennikov A.L., Maximov D.A., Orlov I., Peleganchuk S.V., Schamov A.G., Skovpen K., Soukharev A., Talyshev A., Tikhonov Y.A., Zaytsev A., et al. Search for Standard Model Higgs boson in the mass range 200 - 600 GeV in the $H \rightarrow ZZ \rightarrow l+l- q \text{ anti } q$ decay channel with the ATLAS detector. // Phys. Lett. B. - 2012. - V.717, N1/3. - p.70-88.

[95] Aad G., ATLAS Collab., Beloborodova O., Bobrovnikov V.S., Bogdanchikov A., Kazanin V.F., Kolachev G.M., Korol A., Malyshev V., Maslennikov A.L., Maximov D.A., Orlov I., Peleganchuk S.V., Schamov A.G., Skovpen K., Soukharev A., Talyshev A., Tikhonov Y.A., Zaytsev A., et al. Search for strong gravity signatures in same-sign dimuon final states using the ATLAS detector at the LHC. // Phys. Lett. B. - 2012. - V.709, N4/5. - p.322-340.

[96] Aad G., ATLAS Collab., Anisenkov A., Beloborodova O., Bobrovnikov V.S., Bogdanchikov A., Kazanin V.F., Kolachev G.M., Korol A., Malyshev V., Maslennikov A.L., Maximov D.A., Orlov I., Peleganchuk S.V., Schamov A.G., Skovpen K., Soukharev A., Talyshev A., Tikhonov Y.A., Zaytsev A., et al. Search for supersymmetry with jets, missing transverse momentum and at least one hadronically decaying tau lepton in proton-proton collisions at $\sqrt{s}=7$ TeV with the ATLAS detector. // Phys. Lett. B. - 2012. - V.714, N2/5. - p.197-214.

[97] Aad G., ATLAS Collab., Anisenkov A., Beloborodova O., Bobrovnikov V.S., Bogdanchikov A., Kazanin V.F., Kolachev G.M., Korol A., Malyshev V., Maslennikov A.L., Maximov D.A., Orlov I., Peleganchuk S.V., Schamov A.G., Skovpen K., Soukharev A., Talyshev A., Tikhonov Y.A., Zaytsev A., et al. Search for TeV-scale gravity signatures in final states with leptons and jets with the ATLAS detector at $\sqrt{s}=7$ TeV. // Phys. Lett. B. - 2012. - V.716, N1. - p.122-141.

- [98] Aad G., ATLAS Collab., Anisenkov A., Beloborodova O., Bobrovnikov V.S., Bogdanchikov A., Kazanin V.F., Kolachev G.M., Korol A., Malyshev V., Maslennikov A.L., Maximov D.A., Orlov I., Peleganchuk S.V., Schamov A.G., Skovpen K., Soukharev A., Talyshev A., Tikhonov Y.A., Zaytsev A., et al. Search for the decay $B_s^0 \rightarrow \mu^+ \mu^-$ with the ATLAS detector. // Phys. Lett. B. - 2012. - V.713, N4/5. - p.387-407.
- [99] Aaij R., LHCb Collab., Bobrov A., Bondar A., Eidelman S., Poluektov A., Shekhtman L., et al. Search for the rare decays $B_s^0 \rightarrow \mu^+ \mu^-$ and $B^0 \rightarrow \mu^+ \mu^-$. // Phys. Lett. B. - 2012. - V.708, N1/2. - p.55-67.
- [100] Aad G., ATLAS Collab., Anisenkov A., Beloborodova O., Bobrovnikov V.S., Bogdanchikov A., Kazanin V.F., Kolachev G.M., Korol A., Malyshev V., Maslennikov A.L., Maximov D.A., Orlov I., Peleganchuk S.V., Schamov A.G., Skovpen K., Soukharev A., Talyshev A., Tikhonov Y.A., Zaytsev A., et al. Search for the Standard Model Higgs boson in the decay channel $H \rightarrow ZZ(*) \rightarrow 4l$ with 4.8 fb^{-1} of pp collision data at $\sqrt{s} = 7 \text{ TeV}$ with ATLAS. // Phys. Lett. B. - 2012. - V.710, N3. - p.383 - 402.
- [101] Aad G., ATLAS Collab., Anisenkov A., Beloborodova O., Bobrovnikov V.S., Bogdanchikov A., Kazanin V.F., Kolachev G.M., Korol A., Malyshev V., Maslennikov A.L., Maximov D.A., Orlov I., Peleganchuk S.V., Schamov A.G., Skovpen K., Soukharev A., Talyshev A., Tikhonov Y.A., Zaytsev A., et al. Search for the Standard Model Higgs boson in the $H \rightarrow WW(*) \rightarrow l \nu l \nu$ decay mode with 4.7 fb^{-1} of ATLAS data at $\sqrt{s} = 7 \text{ TeV}$. // Phys. Lett. B. - 2012. - V.716, N1. - p.62-81.
- [102] Piazza A.Di, Milstein A.I. Angular distribution of high-energy e^+e^- photoproduction close to the end of the spectrum at large momentum transfer. // Phys. Rev. A. - 2012. - V.85, N4. - p.042107-1-6.
- [103] Lee R.N., Milshtein A.I., Strakhovenko V.M. Charge asymmetry in the differential cross section of high-energy e^+e^- photoproduction in the field of a heavy atom. // Phys. Rev. A. - 2012. - V.85, N4. - p.042104-1-11.
- [104] Lee R.N., Milstein A.I., Terekhov I.S. Quasilocalized states in a electron-electron interaction in graphene. // Phys. Rev. B. - 2012. - V.86, N3. - p.035425-1-9.
- [105] Aad G., ATLAS Collab., Anisenkov A., Beloborodova O., Bobrovnikov V.S., Bogdanchikov A., Kazanin V.F., Kolachev G.M., Korol A., Malyshev V., Maslennikov A.L., Maximov D.A., Orlov I., Peleganchuk S.V., Shamov A.G., Skovpen K., Soukharev A., Talyshev A., Tikhonov Y.A., Zaytsev A., et al. Measurement of the azimuthal anisotropy for charged particle production in $\sqrt{s}_{NN} = 2.76 \text{ TeV}$ lead-lead collisions with the ATLAS detector. // Phys. Rev. C. - 2012. - V.86, N1. - p.014907-1-41.
- [106] Lees J.P., BABAR Collab., Blinov V.E., Buzykaev A.R., Druzhinin V.P., Golubev V.B., Kravchenko E.A., Onuchin A.P., Serednyakov S.I., Skovpen Yu.I., Solodov E.P., Todyshev K.Yu., Yushkov A.N. Amplitude analysis and measurement of the time-dependent CP asymmetry of $B^0 \rightarrow K_s^0 K_s^0 K_s^0$ decays. // Phys. Rev. D. - 2012. - V.85, N5. - p.054023-1-21.
- [107] Lees J.P., BABAR Collab., Blinov V.E., Buzykaev A.R., Druzhinin V.P., Golubev V.B., Kravchenko E.A., Onuchin A.P., Serednyakov S.I., Skovpen Yu.I., Solodov E.P., Todyshev K.Yu., Yushkov A.N., et al. B^0 meson decays to $\rho^0 K^{*0}$, $f_0 K^{*0}$ and $\rho^0 K^{*+}$, including higher K^* resonances. // Phys. Rev. D. - 2012. - V.85, N7. - p.072005-1-16.
- [108] Aihara H., Belle Collab., Arinstein K., Aulchenko V., Bondar A., Eidelman S., Epifanov D., Gabyshev N., Garmash A., Krovovny P., Kuzmin A., Matvienko D., Poluektov A., Shwartz B., Vinokurova A., Vorobyev V., Zhilich V., Zhulanov V., et al. First measurement of ϕ_3 with a model-independent dalitz plot analysis of $B^{\pm} B^{\mp} \rightarrow D K^{\pm}$, $D \rightarrow K_s^0 \pi^+ \pi^-$ decay. // Phys. Rev. D. - 2012. - V.85, N11. - p.112014-1-17.
- [109] Lees J.P., BABAR Collab., Blinov V.E., Buzykaev A.R., Druzhinin V.P., Golubev V.B., Kravchenko E.A., Onuchin A.P., Serednyakov S.I., Skovpen Yu.I., Solodov E.P., Todyshev K.Yu., Yushkov A.N., et al. Initial-state radiation measurement of the $e^+e^- \rightarrow \pi^+ \pi^- \pi^+ \pi^-$ cross section. // Phys. Rev. D. - 2012. - V.85, N11. - p.112009-1-17.
- [110] Aad G., ATLAS Collab., Beloborodova O., Bobrovnikov V.S., Bogdanchikov A., Kazanin V.F., Kolachev G.M., Korol A., Malyshev V., Maslennikov A.L., Maximov D.A., Orlov I., Peleganchuk S.V., Shamov A.G., Skovpen K., Soukharev A., Talyshev A., Tikhonov Y.A., Zaytsev A., et al. K_s^0 and Lambda production in pp interactions at $\sqrt{s} = 0.9$ and 7 TeV measured with the ATLAS detector at the LHC. // Phys. Rev. D. - 2012. - V.85, N1. - p.012001-1-28.
- [111] Aaij R., LHCb Collab., Bobrov A., Bondar A., Eidelman S., Poluektov A., Shekhtman L., et al. Measurement of b hadron production fractions in 7 TeV pp collisions. // Phys. Rev. D. - 2012. - V.85, N3. - p.032008-1-16.
- [112] Aad G., ATLAS Collab., Beloborodova O., Bobrovnikov V.S., Bogdanchikov A., Kazanin V.F., Kolachev G.M., Korol A., Malyshev V., Maslennikov A.L., Maximov D.A., Orlov I., Peleganchuk S.V., Shamov A.G., Skovpen K., Soukharev A., Talyshev A., Tikhonov Y.A., Zaytsev A., et al. Measurement of D^{*+} meson production in jets from pp collisions at $\sqrt{s} = 7 \text{ TeV}$ with the ATLAS detector. // Phys. Rev. D. - 2012. - V.85, N5. - p.052005-1-22.
- [113] Aad G., ATLAS Collab., Beloborodova O., Bobrovnikov V.S., Bogdanchikov A., Kazanin V.F., Kolachev G.M., Korol A., Malyshev V., Maslennikov

- A.L., Maximov D.A., Orlov I., Peleganchuk S.V., Shamov A.G., Skovpen K., Soukharev A., Talyshev A., Tikhonov Y.A., Zaytsev A., et al. Measurement of the inclusive W^+ - and Z/γ^* cross sections in the e and μ decay channels in pp collisions at $\sqrt{s} = 7$ TeV with the ATLAS detector. // *Phys. Rev. D.* - 2012. - V.85, N7. - p.072004-1-39.
- [114] Aad G., ATLAS Collab., Beloborodova O., Bobrovnikov V.S., Bogdanchikov A., Kazanin V.F., Kolachev G.M., Korol A., Malyshev V., Maslennikov A.L., Maximov D.A., Orlov I., Peleganchuk S.V., Shamov A.G., Skovpen K., Soukharev A., Talyshev A., Tikhonov Y.A., Zaytsev A., et al. Measurement of the isolated diphoton cross section in pp collisions at $\sqrt{s} = 7$ TeV with the ATLAS detector. // *Phys. Rev. D.* - 2012. - V.85, N1. - p.012003-1-28.
- [115] Aad G., ATLAS Collab., Beloborodova O., Bobrovnikov V.S., Bogdanchikov A., Kazanin V.F., Kolachev G.M., Korol A., Malyshev V., Maslennikov A.L., Maximov D.A., Orlov I., Peleganchuk S.V., Shamov A.G., Skovpen K., Soukharev A., Talyshev A., Tikhonov Y.A., Zaytsev A., et al. Measurement of the production cross section for Z/γ^* in association with jets in pp collisions at $\sqrt{s} = 7$ TeV with the ATLAS detector. // *Phys. Rev. D.* - 2012. - V.85, N3. - p.032009-1-42.
- [116] Aad G., ATLAS Collab., Anisenkov A., Beloborodova O., Bobrovnikov V.S., Bogdanchikov A., Kazanin V.F., Kolachev G.M., Korol A., Malyshev V., Maslennikov A.L., Maximov D.A., Orlov I., Peleganchuk S.V., Shamov A.G., Skovpen K., Soukharev A., Talyshev A., Tikhonov Y.A., Zaytsev A., et al. Measurement of the production cross section of an isolated photon associated with jets in proton-proton collisions at $\sqrt{s} = 7$ TeV with the ATLAS detector. // *Phys. Rev. D.* - 2012. - V.85, N9. - p.092014-1-30.
- [117] Aaij R., LHCb Collab., Bobrov A., Bondar A., Eidelman S., Poluektov A., Shekhtman L., et al. Measurement of the ratio of branching fractions $B(B^0 \rightarrow K^{*0} \gamma) / (B(B_s^0 \rightarrow \phi \gamma))$. // *Phys. Rev. D.* - 2012. - V.85, N11. - p.112013-1-8.
- [118] Lees J.P., BABAR Collab., Blinov V.E., Buzykaev A.R., Druzhinin V.P., Golubev V.B., Kravchenko E.A., Onuchin A.P., Serednyakov S.I., Skovpen Yu.I., Solodov E.P., Todyshev K.Yu., Yushkov A.N., et al. Measurement of the semileptonic branching fraction of the B_s meson. // *Phys. Rev. D.* - 2012. - V.85, N1. - p.011101-1-9.
- [119] Aad G., ATLAS Collab., Beloborodova O., Bobrovnikov V.S., Bogdanchikov A., Kazanin V.F., Kolachev G.M., Korol A., Malyshev V., Maslennikov A.L., Maximov D.A., Orlov I., Peleganchuk S.V., Shamov A.G., Skovpen K., Soukharev A., Talyshev A., Tikhonov Y.A., Zaytsev A., et al. Measurement of the transverse momentum distribution of W bosons in pp collisions at $\sqrt{s} = 7$ TeV with the ATLAS detector. // *Phys. Rev. D.* - 2012. - V.85, N1. - p.012005-1-30.
- [120] Rohrken M., Belle Collab., Aulchenko V., Bondar A., Gabyshev N., Garmash A., Krokovny P., Poluektov A., Shwartz B., Vorobyev V., Zhilich V., Zhulanov V., et al. Measurements of branching fractions and time-dependent CP violating asymmetries in $B^0 \rightarrow D^{(*)\pm} D^{\mp}$ decays. // *Phys. Rev. D.* - 2012. - V.85, N9. - p.091106-1-7.
- [121] Aaij R., LHCb Collab., Bobrov A., Bondar A., Eidelman S., Kudryavtsev V., Poluektov A., Shekhtman L., Vorobyev V., et al. Measurements of the branching fractions and CP asymmetries of $B^+ \rightarrow J/\psi \pi^+$ and $B^+ \rightarrow \psi(2S) \pi^+$ decays. // *Phys. Rev. D.* - 2012. - V.85, N9. - p.091105-1-8.
- [122] Lees J.P., BABAR Collab., Blinov V.E., Buzykaev A.R., Druzhinin V.P., Golubev V.B., Kravchenko E.A., Onuchin A.P., Serednyakov S.I., Solodov E.P., Todyshev K.Yu., Yushkov A.N., et al. Observation and study of the baryonic B -meson decays $B \rightarrow D/\text{sub } (*) / p \text{ anti } p(\pi)(\pi)$. // *Phys. Rev. D.* - 2012. - V.85, N9. - p.092017-1-21.
- [123] Aaij R., LHCb Collab., Bobrov A., Bondar A., Eidelman S., Krokovny P., Poluektov A., Shekhtman L., et al. Searches for Majorana neutrinos in B^- decays. // *Phys. Rev. D.* - 2012. - V.85, N11. - p.112004-1-13.
- [124] Ablikim M., BESSIII Collab., Achasov M.N., Muchnoi N.Yu., Nikolaev I.B., et al. Search for a light exotic particle in J/ψ radiative decays. // *Phys. Rev. D.* - 2012. - V.85, N9. - p.092012-1-7. [arXiv:1111.2112 [hep-ex].
- [125] Aad G., ATLAS Collab., Beloborodova O., Bobrovnikov V.S., Bogdanchikov A., Kazanin V.F., Kolachev G.M., Korol A., Malyshev V., Maslennikov A.L., Maximov D.A., Orlov I., Peleganchuk S.V., Shamov A.G., Skovpen K., Soukharev A., Talyshev A., Tikhonov Y.A., Zaytsev A., et al. Search for anomalous production of prompt like-sign muon pairs and constraints on physics beyond the standard model with the ATLAS detector. // *Phys. Rev. D.* - 2012. - V.85, N3. - p.032004-1-23.
- [126] Lees J.P., BABAR Collab., Blinov V.E., Buzykaev A.R., Druzhinin V.P., Golubev V.B., Kravchenko E.A., Onuchin A.P., Serednyakov S.I., Skovpen Yu.I., Solodov E.P., Todyshev K.Yu., Yushkov A.N., et al. Search for anti $B \rightarrow \text{Lambda}^+ / \text{sub } c / \text{Xl- anti nu / sub l / decays in events with a full reconstructed B meson. // Phys. Rev. D. - 2012. - V.85, N1. - p.011102-1-8.$
- [127] Lees J.P., BABAR Collab., Blinov V.E., Buzykaev A.R., Druzhinin V.P., Golubev V.B., Kravchenko E.A., Onuchin A.P., Serednyakov S.I., Skovpen Yu.I., Solodov E.P., Todyshev K.Yu., Yushkov A.N., et al. Search for CP violation in the $\tau^- \rightarrow \pi^- K^0 / \text{sub } s / (\geq 0 \pi^0) \text{nu / sub } \tau /$. // *Phys. Rev. D.* - 2012. - V.85, N3. - p.031102-1-8.

- [128] Shen C.P., Belle Collab., Arinstein K., Eidelman S., Gabyshev N., Garmash A., Krokovny P., Zhilich V., Zhulanov V., et al. Search for double charmonium decays of the P-wave spin-triplet bottomonium states. // Phys. Rev. D. - 2012. - V.85, N7. - p.071102-1-7.
- [129] Aad G., ATLAS Collab., Beloborodova O., Bobrovnikov V.S., Bogdanchikov A., Kazanin V.F., Kolachev G.M., Korol A., Malyshev V., Maslennikov A.L., Maximov D.A., Orlov I., Peleganchuk S.V., Shamov A.G., Skovpen K., Soukharev A., Talyshev A., Tikhonov Y.A., Zaytsev A., et al. Search for excited leptons in proton-proton collisions at $\sqrt{s} = 7$ TeV with the ATLAS detector. // Phys. Rev. D. - 2012. - V.85, N7. - p.072003-1-23.
- [130] Lees J.P., BABAR Collab., Blinov V.E., Buzykaev A.R., Druzhinin V.P., Golubev V.B., Kravchenko E.A., Onuchin A.P., Serednyakov S.I., Skovpen Yu.I., Solodov E.P., Todyshev K.Yu., Yushkov A.N., et al. Search for lepton-number violating processes in $B^+ \rightarrow h^- l^+ l^+$ decays. // Phys. Rev. D. - 2012. - V.85, N7. - p.071103-1-8.
- [131] Aad G., ATLAS Collab., Anisenkov A., Beloborodova O., Bobrovnikov V.S., Bogdanchikov A., Kazanin V.F., Kolachev G.M., Korol A., Malyshev V., Maslennikov A.L., Maximov D.A., Orlov I., Peleganchuk S.V., Shamov A.G., Skovpen K., Soukharev A., Talyshev A., Tikhonov Y.A., Zaytsev A., et al. Search for resonant WZ production in the $WZ \rightarrow l \nu l'$ channel in $\sqrt{s} = 7$ TeV pp collisions with the ATLAS detector. // Phys. Rev. D. - 2012. - V.85, N11. - p.112012-1-21.
- [132] Aad G., ATLAS Collab., Beloborodova O., Bobrovnikov V.S., Bogdanchikov A., Kazanin V.F., Kolachev G.M., Korol A., Malyshev V., Maslennikov A.L., Maximov D.A., Orlov I., Peleganchuk S.V., Shamov A.G., Skovpen K., Soukharev A., Talyshev A., Tikhonov Y.A., Zaytsev A., et al. Search for supersymmetry in final states with jets, missing transverse momentum and one isolated lepton in $\sqrt{s} = 7$ TeV pp collisions using 1 fb^{-1} of ATLAS data. // Phys. Rev. D. - 2012. - V.85, N1. - p.012006-1-30.
- [133] Aad G., ATLAS Collab., Anisenkov A., Beloborodova O., Bobrovnikov V.S., Bogdanchikov A., Kazanin V.F., Kolachev G.M., Korol A., Malyshev V., Maslennikov A.L., Maximov D.A., Orlov I., Peleganchuk S.V., Shamov A.G., Skovpen K., Soukharev A., Talyshev A., Tikhonov Y.A., Zaytsev A., et al. Search for supersymmetry in pp collisions at $\sqrt{s} = 7$ TeV in final states with missing transverse momentum and b-jets with the ATLAS detector. // Phys. Rev. D. - 2012. - V.85, N11. - p.112006-1-29.
- [134] Lees J.P., BABAR Collab., Blinov V.E., Buzykaev A.R., Druzhinin V.P., Golubev V.B., Kravchenko E.A., Onuchin A.P., Serednyakov S.I., Solodov E.P., Todyshev K.Yu., Yushkov A.N., et al. Search for the decay $D^0 \rightarrow \gamma\gamma$ and measurement of the branching fraction for $D^0 \rightarrow \pi^0\pi^0$. // Phys. Rev. D. - 2012. - V.85, N9. - p.091107-1-8.
- [135] Aaij R., LHCb Collab., Filippov S., Gushchin E., Kravchuk L., Mazurov A., Bobrov A., Bondar A., Eidelman S., Poluektov A., Shekhtman L., Vorobyev V., et al. Search for the X(4140) state in $B^+ \rightarrow J/\psi\phi K^+$ decays. // Phys. Rev. D. - 2012. - V.85, N9. - p.091103-1-7.
- [136] Lees J.P., BABAR Collab., Blinov V.E., Buzykaev A.R., Druzhinin V.P., Golubev V.B., Kravchenko E.A., Onuchin A.P., Serednyakov S.I., Skovpen Yu.I., Solodov E.P., Todyshev K.Yu., Yushkov A.N., et al. Search for the $Z/\text{sub } 1/(4050)^+$ and $Z/\text{sub } 2/(4250)^+$ states in anti $B^0 \rightarrow \text{Chi}/\text{sub } c1/K\text{-}\pi^+$ and $B^+ \rightarrow \text{Chi}/\text{sub } c1/K^0/\text{sub } s/\pi^+$. // Phys. Rev. D. - 2012. - V.85, N5. - p.052003-1-12.
- [137] Higuchi T., Belle Collab., Aulchenko V., Bondar A., Eidelman S., Epifanov D., Gabyshev N., Garmash A., Krokovny P., Kuzmin A., Matvienko D., Shebalin V., Shwartz B., Usov Y., Vinokurova A., Vorobyev V., Zhilich V., Zhulanov V., et al. Search for time-dependent CPT violation in hadronic and semileptonic B decays. // Phys. Rev. D. - 2012. - V.85, N7. - p.071105-1-7.
- [138] Lees J.P., BABAR Collab., Blinov V.E., Buzykaev A.R., Druzhinin V.P., Golubev V.B., Kravchenko E.A., Onuchin A.P., Serednyakov S.I., Solodov E.P., Todyshev K.Yu., Yushkov A.N., et al. Study of CP violation in Dalitz-plot analyses of $B^0 \rightarrow K+K^0/\text{sub } s/$, $B^+ \rightarrow K+K^0/\text{sub } s/$, and $B^+ \rightarrow K^0/\text{sub } s/ K^+$. // Phys. Rev. D. - 2012. - V.85, N11. - p.112010-1-31.
- [139] Aad G., ATLAS Collab., Anisenkov A., Beloborodova O., Bobrovnikov V.S., Bogdanchikov A., Kazanin V.F., Kolachev G.M., Korol A., Malyshev V., Maslennikov A.L., Maximov D.A., Orlov I., Peleganchuk S.V., Shamov A.G., Skovpen K., Soukharev A., Talyshev A., Tikhonov Y.A., Zaytsev A., et al. Study of jets produced in association with a W boson in pp collisions at $\sqrt{s} = 7$ TeV with the ATLAS detector. // Phys. Rev. D. - 2012. - V.85, N9. - p.092002-1-40.
- [140] Ablikim M., BESSIII Collab., Achasov M.N., Muchnoi N.Yu., Nikolaev I.B., et al. Two-photon widths of the $\text{Chi}/\text{sub } c0,2/$ states and helicity analysis for $\text{Chi}/\text{sub } c2/ \rightarrow \text{gamma gamma}$. // Phys. Rev. D. - 2012. - V.85, N11. - p.112008-1-10. [arXiv:1205.4284 [hep-ex]].
- [141] Aaij R., LHCb Collab., Bobrov A., Bondar A., Eidelman S., Poluektov A., Shekhtman L., et al. Determination of the sign of the decay width difference in the B_s^0 system. // Phys. Rev. Lett. - 2012. - V.108, N24. - p.241801-1-7.
- [142] Aad G., ATLAS Collab., Anisenkov A., Beloborodova O., Bobrovnikov V.S., Bogdanchikov A., Kazanin V.F., Kolachev G.M., Korol A., Malyshev V., Maslennikov A.L., Maximov D.A., Orlov I., Peleganchuk S.V., Shamov A.G., Skovpen K., Soukharev A., Talyshev A., Tikhonov Y.A., Zaytsev A., et al. Determination of the strange-quark density of the proton from ATLAS

measurements of the $W \rightarrow l \nu$ and $Z \rightarrow ll$ cross sections. // Phys. Rev. Lett. - 2012. - V.109, N1. - p.012001-1-17.

[143] Aaij R., LHCb Collab., Bobrov A., Bondar A., Eidelman S., Poluektov A., Shekhtman L., et al. Differential branching fraction and angular analysis of the decay $B^0 \rightarrow K^{*0} \mu^+ \mu^-$. // Phys. Rev. Lett. - 2012. - V.108, N18. - p.181806-1-8 [

[144] Ko B.R., Belle Collab., Aulchenko V., Bondar A., Eidelman S., Gabyshev N., Garmash A., Krokovny P., Kuzmin A., Matvienko D., Poluektov A., Shebalin V., Shwartz B., Sibidanov A., Vinokurova A., Vorobyev V., Zhilich V., Zhulanov V., et al. Erratum: Evidence for CP violation in the decay $D^+ \rightarrow K_s^0 \pi^+$. [Phys. Rev. Lett. 109, 021601 (2012)]. // Phys. Rev. Lett. - 2012. - V.109, N11. - p.119903-1-2.

[145] Lees J.P., BABAR Collab., Blinov V.E., Buzykaev A.R., Druzhinin V.P., Golubev V.B., Kravchenko E.A., Onuchin A.P., Serednyakov S.I., Skovpen Yu.I., Solodov E.P., Todyshev K.Yu., Yushkov A.N., et al. Evidence for an excess of anti $B \rightarrow D^{(*)} \tau$ anti ν_τ decays. // Phys. Rev. Lett. - 2012. - V.109, N10. - p.101802-1-8.

[146] Ko B.R., Belle Collab., Aulchenko V., Bondar A., Eidelman S., Gabyshev N., Garmash A., Krokovny P., Kuzmin A., Matvienko D., Poluektov A., Shebalin V., Shwartz B., Vinokurova A., Vorobyev V., Zhilich V., Zhulanov V., et al. Evidence for CP violation in the decay $D^+ \rightarrow K_s^0 \pi^+$. // Phys. Rev. Lett. - 2012. - V.109, N2. - p.021601-1-6.

[147] Aaij R., LHCb Collab., Bobrov A., Bondar A., Eidelman S., Poluektov A., Shekhtman L., et al. Evidence for CP violation in time-integrated $D^0 \rightarrow h^- h^+$ decay rates. // Phys. Rev. Lett. - 2012. - V.108, N11. - p.111602-1-8.

[148] Hoi C.-T., Belle Collab., Bondar A., Eidelman S., Gabyshev N., Matvienko D., Shebalin V., Zhilich V., et al. Evidence for direct CP violation in $B^\pm \rightarrow \eta h^\pm$ and observation of $B^0 \eta K^0$. // Phys. Rev. Lett. - 2012. - V.108, N3. - p.031801-1-6.

[149] Tuszewski M., TAE Team, Akhmetov T., Ivanov A., Voskoboinikov R., et al. Field reversed configuration confinement enhancement through edge biasing and neutral beam injection. // Phys. Rev. Lett. - 2012. - V.108, N25. - p.255008-1-5.

[150] Aaij R., LHCb Collab., Bobrov A., Bondar A., Eidelman S., Krokovny P., Kudryavtsev V., Poluektov A., Shekhtman L., Vorobyev V., et al. First evidence of direct CP violation in charmless two-body decays of B_s mesons. // Phys. Rev. Lett. - 2012. - V.108, N20. - p.201601-1-8.

[151] Li J., Belle Collab., Arinstein K., Aulchenko V., Eidelman S., Garmash A., Krokovny P., Kuzmin A., Matvienko D., Shebalin V., Usov Y., Vorobyev V., Zhilich V., et al. First observation of $B_s^0 \rightarrow J/\psi \eta$ and B_s^0

$\rightarrow J/\psi \eta'$. // Phys. Rev. Lett. - 2012. - V.108, N18. - p.181808-1-5.

[152] Ablikim M., BESSIII Collab., Achasov M.N., Muchnoi N.Yu., Nikolaev I.B., et al. First observation of $\eta(1405)$ decays into $f_0(980) \pi^0$. // Phys. Rev. Lett. - 2012. - V.108, N18. - p.182001-1-6. [arXiv:1201.2737 [hep-ex].

[153] Aaij R., LHCb Collab., Bobrov A., Bondar A., Eidelman S., Krokovny P., Kudryavtsev V., Poluektov A., Shekhtman L., Vorobyev V., et al. First observation of the decay $B_c^+ \rightarrow J/\psi \pi^+ \pi^- \pi^+$. // Phys. Rev. Lett. - 2012. - V.108, N25. - p.251802-1-7.

[154] Aaij R., LHCb Collab., Bobrov A., Bondar A., Eidelman S., Poluektov A., Shekhtman L., et al. First observation of the decays anti $B^0 \rightarrow D^+ K^- \pi^+ \pi^-$ and $B^- \rightarrow D^0 K^- \pi^+ \pi^-$. // Phys. Rev. Lett. - 2012. - V.108, N16. - p.161801-1-8.

[155] Ablikim M., BESSIII Collab., Achasov M.N., Muchnoi N.Yu., Nikolaev I.B., et al. First observation of the M1 transition $\psi(3686) \rightarrow \gamma \eta_c(2S)$. // Phys. Rev. Lett. - 2012. - V.108, N3. - p.042003-1-7. [arXiv:1205.5103 [hep-ex].

[156] Adachi I., Belle Collab., Arinstein K., Bondar A., Eidelman S., Epifanov D., Gabyshev N., Garmash A., Kuzmin A., Matvienko D., Poluektov A., Shebalin V., Shwartz B., Vinokurova A., Zhilich V., et al. First observation of the P-wave spin-singlet bottomonium states $h_b(1P)$ and $h_b(2P)$. // Phys. Rev. Lett. - 2012. - V.108, N3. - p.032001-1-6.

[157] Abelev B., ALICE Collab., Pestov Y., et al. J/ψ polarization in pp collisions at $\sqrt{s}=7$ TeV. // Phys. Rev. Lett. - 2012. - V.108, N8. - p.082001-1-0.

[158] Abelev B., ALICE Collab., Pestov Y., et al. J/ψ suppression at forward rapidity in Pb-Pb collisions at $\sqrt{s_{NN}}=2.76$ TeV. // Phys. Rev. Lett. - 2012. - V.109, N7. - p.072301-1-11.

[159] Aaij R., LHCb Collab., Bobrov A., Bondar A., Eidelman S., Krokovny P., Kudryavtsev V., Poluektov A., Shekhtman L., Vorobyev V., et al. Measurement of the anti B_s^0 effective lifetime in the $J/\psi f_0(980)$ final state. // Phys. Rev. Lett. - 2012. - V.109, N15. - p.152002-1-8.

[160] Aaij R., LHCb Collab., Bobrov A., Bondar A., Eidelman S., Shekhtman L., et al. Measurement of the CP-violating phase ϕ_s in the decay $B_s^0 \rightarrow J/\psi \phi$. // Phys. Rev. Lett. - 2012. - V.108, N10. - p.101803-1-8.

[161] Sato Y., Belle Collab., Aulchenko V., Bondar A., Eidelman S., Epifanov D., Gabyshev N., Krokovny P., Kuzmin A., Poluektov A., Shwartz B., Zhilich V., Zhulanov V., et al. Measurement of the CP-violation parameter $\sin 2\phi^1$ with a new tagging method at the $Y(5S)$ resonance. // Phys. Rev. Lett. - 2012. - V.108, N17. - p.171801-1-6.

- [162] Aad G., ATLAS Collab., Beloborodova O., Bobrovnikov V.S., Kazanin V.F., Kolachev G.M., Korol A., Malyshev V., Maslennikov A.L., Maximov D.A., Orlov I., Peleganchuk S.V., Schamov A.G., Skovpen K., Soukharev A., Talyshev A., Tikhonov Y.A., Zaytsev A., et al. Measurement of the ZZ production cross section and limits on anomalous neutral triple gauge couplings in proton-proton collisions at. // Phys. Rev. Lett. - 2012. - V.108, N4. - p.041804-1-18.
- [163] Ablikim M., BESSIII Collab., Achasov M.N., Nikolaev I.B., Muchnoi N.Yu., et al. Measurements of the mass and width of the η_c using the decay $\psi(3686) \rightarrow \gamma \eta_c$. // Phys. Rev. Lett. - 2012. - V.108, N22. - p.222002-1-7. arXiv:1111.0398 [hep-ex].
- [164] Aad G., ATLAS Collab., Anisenkov A., Beloborodova O., Bobrovnikov V.S., Bogdanchikov A., Kazanin V.F., Kolachev G.M., Korol A., Malyshev V., Maslennikov A.L., Maximov D.A., Orlov I., Peleganchuk S.V., Skovpen K., Soukharev A., Talyshev A., Tikhonov Y.A., Zaytsev A., et al. Observation of a new χ_b state in radiative transitions to $\Upsilon(1S)$ and $\Upsilon(2S)$ at ATLAS. // Phys. Rev. Lett. - 2012. - V.108, N15. - p.152001-1-17.
- [165] Aaij R., LHCb Collab., Bobrov A., Bondar A., Eidelman S., Poluektov A., Shekhtman L., et al. Observation of anti $B_s^0 \rightarrow J/\psi f_2'(1525)$ in $J/\psi K^+ K^-$ final states. // Phys. Rev. Lett. - 2012. - V.108, N15. - p.151801-1-7.
- [166] Aaij R., LHCb Collab., Bobrov A., Bondar A., Eidelman S., Krokovny P., Kudryavtsev V., Poluektov A., Shekhtman L., Vorobyev V., et al. Observation of $B^0 \rightarrow \text{anti } D^0 K^+ K^-$ and evidence for $B_s^0 \rightarrow \text{anti } D^0 K^+ K^-$. // Phys. Rev. Lett. - 2012. - V.109, N13. - p.131801-1-8.
- [167] Liu Z.Q., Belle Collab., Aulchenko V., Bondar A., Eidelman S., Epifanov D., Gabyshev N., Garmash A., Krokovny P., Kuzmin A., Matvienko D., Shebalin V., Shwartz B., Vinokurova A., Vorobyev V., Zhilich V., Zhulanov V., et al. Observation of new resonant structures in $\gamma\gamma \rightarrow \omega\phi$, $\phi\phi$, and $\omega\omega$. // Phys. Rev. Lett. - 2012. - V.108, N23. - p.232001-1-7.
- [168] Aad G., ATLAS Collab., Anisenkov A., Beloborodova O., Bobrovnikov V.S., Bogdanchikov A., Kazanin V.F., Kolachev G.M., Korol A., Malyshev V., Maslennikov A.L., Maximov D.A., Orlov I., Peleganchuk S.V., Shamov A.G., Skovpen K., Soukharev A., Talyshev A., Tikhonov Y.A., Zaytsev A., et al. Observation of spin correlation in t anti t events from pp collisions at $\sqrt{s}=7$ TeV using the ATLAS detector. // Phys. Rev. Lett. - 2012. - V.108, N21. - p.212001-1-19.
- [169] Bondar A., Garmash A., Arinstein K., Epifanov D., Gabyshev N., Kuzmin A., Matvienko D., Poluektov A., Shebalin V., Shwartz B., Vinokurova A., Zhilich V., Zhulanov V., Zyukova O., Belle Collab., et al. Observation of two charged bottomonium-like resonances in $\Upsilon(5S)$ decays. // Phys. Rev. Lett. - 2012. - V.108, N12. - p.122001-1-6.
- [170] Adachi I., Belle Collab., Aulchenko V., Bondar A., Eidelman S., Epifanov D., Gabyshev N., Garmash A., Krokovny P., Kuzmin A., Matvienko D., Poluektov A., Shebalin V., Shwartz B., Vinokurova A., Vorobyev V., Zhilich V., Zyukova O., et al. Precise measurement of the CP violation parameter $\sin 2\phi^1$ in $B^0 \rightarrow (c \text{ anti } c) K^0$ decays. // Phys. Rev. Lett. - 2012. - V.108, N17. - p.171802-1-6.
- [171] Abelev B., ALICE Collab., Pestov Y., et al. Production of muons from heavy flavor decays at forward rapidity in pp and Pb-Pb collisions at $\sqrt{s_{NN}}=2.76$ TeV. // Phys. Rev. Lett. - 2012. - V.109, N11. - p.112301-1-11.
- [172] Aad G., ATLAS Collab., Anisenkov A., Beloborodova O., Bobrovnikov V.S., Bogdanchikov A., Kazanin V.F., Kolachev G.M., Korol A., Malyshev V., Maslennikov A.L., Maximov D.A., Orlov I., Peleganchuk S.V., Shamov A.G., Skovpen K., Soukharev A., Talyshev A., Tikhonov Y.A., Zaytsev A., et al. Search for a light Higgs boson decaying to long-lived weakly interacting particles in proton-proton collisions at $\sqrt{s}=7$ TeV with the ATLAS detector. // Phys. Rev. Lett. - 2012. - V.108, N25. - p.251801-1-18.
- [173] Staric M., Belle Collab., Arinstein K., Eidelman S., Gabyshev N., Shebalin V., Shwartz B., Zhilich V., Zhulanov V., et al. Search for CP violation in D meson decays to $\phi\pi^+$. // Phys. Rev. Lett. - 2012. - V.108, N7. - p.071801-1-6.
- [174] Aad G., ATLAS Collab., Anisenkov A., Beloborodova O., Bobrovnikov V.S., Bogdanchikov A., Kazanin V.F., Kolachev G.M., Korol A., Malyshev V., Maslennikov A.L., Maximov D.A., Orlov I., Peleganchuk S.V., Shamov A.G., Skovpen K., Soukharev A., Talyshev A., Tikhonov Y.A., Zaytsev A., et al. Search for down-type fourth generation quarks with the ATLAS detector in events with one lepton and hadronically decaying W bosons. // Phys. Rev. Lett. - 2012. - V.109, N3. - p.032001-1-19.
- [175] Aad G., ATLAS Collab., Anisenkov A., Beloborodova O., Bobrovnikov V.S., Bogdanchikov A., Kazanin V.F., Kolachev G.M., Korol A., Malyshev V., Maslennikov A.L., Maximov D.A., Orlov I., Peleganchuk S.V., Shamov A.G., Skovpen K., Soukharev A., Talyshev A., Tikhonov Y.A., Zaytsev A., et al. Search for gluinos in events with two same-sign leptons, jets, and missing transverse momentum with the ATLAS detector in pp collisions at $\sqrt{s}=7$ TeV. // Phys. Rev. Lett. - 2012. - V.108, N24. - p.241802-1-19.
- [176] Aaij R., LHCb Collab., Bobrov A., Bondar A., Eidelman S., Poluektov A., Shekhtman L., et al. Search for lepton number violating decays $B^+ \rightarrow \pi^- \pi^+ \pi^+$ and $B^+ \rightarrow K^- \mu^+ \mu^+$. // Phys. Rev. Lett. - 2012. - V.108, N10. - p.101601.
- [177] Lees J.P., BABAR Collab., Blinov V.E., Buzykaev A.R., Druzhinin V.P., Golubev V.B., Kravchenko E.A., Onuchin A.P., Serednyakov S.I.,

Skovpen Yu.I., Solodov E.P., Todyshev K.Yu., Yushkov A.N., et al. Search for low-mass dark-sector Higgs bosons. // Phys. Rev. Lett. - 2012. - V.108, N21. - p.211801-1-7.

[178] Aad G., ATLAS Collab., Beloborodova O., Bobrovnikov V.S., Bogdanchikov A., Kazanin V.F., Kolachev G.M., Korol A., Malyshev V., Maslennikov A.L., Maximov D.A., Orlov I., Peleganchuk S.V., Schamov A.G., Skovpen K., Soukharev A., Talyshev A., Tikhonov Y.A., Zaytsev A., et al. Search for new phenomena in t anti t events with large missing transverse momentum in proton-proton collisions at $\sqrt{s} = 7$ TeV with the ATLAS detector. // Phys. Rev. Lett. - 2012. - V.108, N4. - p.041805-1-18.

[179] Aad G., ATLAS Collab., Anisenkov A., Beloborodova O., Bobrovnikov V.S., Bogdanchikov A., Kazanin V.F., Kolachev G.M., Korol A., Malyshev V., Maslennikov A.L., Maximov D.A., Orlov I., Peleganchuk S.V., Shamov A.G., Skovpen K., Soukharev A., Talyshev A., Tikhonov Y.A., Zaytsev A., et al. Search for pair production of a heavy up-type quark decaying to a W boson and a b quark in the lepton + jets channel with the ATLAS detector. // Phys. Rev. Lett. - 2012. - V.108, N26. - p.261802-1-18.

[180] Aad G., ATLAS Collab., Anisenkov A., Beloborodova O., Bobrovnikov V.S., Bogdanchikov A., Kazanin V.F., Kolachev G.M., Korol A., Malyshev V., Maslennikov A.L., Orlov I., Peleganchuk S.V., Shamov A.G., Skovpen K., Soukharev A., Talyshev A., Tikhonov Y.A., Zaytsev A., et al. Search for pair production of a new b' quark that decays into a Z boson and a bottom quark with the ATLAS detector. // Phys. Rev. Lett. - 2012. - V.109, N7. - p.071801-1-19.

[181] Aad G., ATLAS Collab., Anisenkov A., Beloborodova O., Bobrovnikov V.S., Bogdanchikov A., Kazanin V.F., Kolachev G.M., Korol A., Malyshev V., Maslennikov A.L., Maximov D.A., Orlov I., Peleganchuk S.V., Shamov A.G., Skovpen K., Soukharev A., Talyshev A., Tikhonov Y.A., Zaytsev A., et al. Search for production of resonant states in the photon-jet mass distribution using pp collisions at $\sqrt{s} = 7$ TeV collected by the ATLAS detector. // Phys. Rev. Lett. - 2012. - V.108, N21. - p.211802-1-18.

[182] Aad G., ATLAS Collab., Anisenkov A., Beloborodova O., Bobrovnikov V.S., Bogdanchikov A., Kazanin V.F., Kolachev G.M., Korol A., Malyshev V., Maslennikov A.L., Maximov D.A., Orlov I., Peleganchuk S.V., Shamov A.G., Skovpen K., Soukharev A., Talyshev A., Tikhonov Y.A., Zaytsev A., et al. Search for scalar bottom quark pair production with the ATLAS detector in pp collisions at $\sqrt{s} = 7$ TeV. // Phys. Rev. Lett. - 2012. - V.108, N18. - p.181802-1-18.

[183] Aad G., ATLAS Collab., Anisenkov A., Beloborodova O., Bobrovnikov V.S., Bogdanchikov A., Kazanin V.F., Kolachev G.M., Korol A., Malyshev V., Maslennikov A.L., Orlov I., Peleganchuk S.V., Shamov

A.G., Skovpen K., Soukharev A., Talyshev A., Tikhonov Y.A., Zaytsev A., et al. Search for supersymmetry in events with three leptons and missing transverse momentum in $\sqrt{s} = 7$ TeV pp collisions with the ATLAS detector. // Phys. Rev. Lett. - 2012. - V.108, N26. - p.261804-1-18.

[184] Aad G., ATLAS Collab., Anisenkov A., Beloborodova O., Bobrovnikov V.S., Bogdanchikov A., Kazanin V.F., Kolachev G.M., Korol A., Malyshev V., Maslennikov A.L., Orlov I., Peleganchuk S.V., Shamov A.G., Skovpen K., Soukharev A., Talyshev A., Tikhonov Y.A., Zaytsev A., et al. Search for t b resonances in proton-proton collisions at $\sqrt{s} = 7$ TeV with ATLAS detector. // Phys. Rev. Lett. - 2012. - V.109, N8. - p.081801-1-19.

[185] Aad G., ATLAS Collab., Anisenkov A., Beloborodova O., Bobrovnikov V.S., Bogdanchikov A., Kazanin V.F., Kolachev G.M., Korol A., Malyshev V., Maslennikov A.L., Maximov D.A., Orlov I., Peleganchuk S.V., Skovpen K., Soukharev A., Talyshev A., Tikhonov Y.A., Zaytsev A., et al. Search for the Higgs boson in the $H \rightarrow WW(*) \rightarrow l^+ \text{ nu } l^- \text{ anti nu}$ decay channel in pp collisions at $\sqrt{s} = 7$ TeV with the ATLAS detector. // Phys. Rev. Lett. - 2012. - V.108, N11. - p.111802-1-19.

[186] Aad G., ATLAS Collab., Anisenkov A., Beloborodova O., Bobrovnikov V.S., Bogdanchikov A., Kazanin V.F., Kolachev G.M., Korol A., Malyshev V., Maslennikov A.L., Maximov D.A., Orlov I., Peleganchuk S.V., Skovpen K., Soukharev A., Talyshev A., Tikhonov Y.A., Zaytsev A., et al. Search for the standard model Higgs boson in the diphoton decay channel with 4.9 fb⁻¹ of pp collision data at $\sqrt{s} = 7$ TeV with ATLAS. // Phys. Rev. Lett. - 2012. - V.108, N11. - p.111803-1-19.

[187] Ablikim M., BESSIII Collab., Achasov M.N., Muchnoi N.Yu., Nikolaev I.B., et al. Spin-parity analysis of p anti p mass threshold structure in J/ψ and ψ (3686) radiative decays. // Phys. Rev. Lett. - 2012. - V.108, N11. - p.112003-1-6. [arXiv:1112.0942 [hep-ex].

[188] Aaij R., LHCb Collab., Bobrov A., Bondar A., Eidelman S., Krokovny P., Kudryavtsev V., Poluektov A., Shekhtman L., Vorobyev V., et al. Strong constraints on the rare decays $B_s^0 \rightarrow \mu^+ \mu^-$ and $B^0 \rightarrow \mu^+ \mu^-$. // Phys. Rev. Lett. - 2012. - V.108, N23. - p.231801-1-8.

[189] Arzhannikov A.V., Timofeev I.V. Generation of powerful terahertz emission in a beam-driven strong plasma turbulence. // Plasma Physics and Controlled Fusion. - 2012. - V.54, N10. - p.105004 (6 p.).

[190] Reusch J.A., Anderson J.K., Belykh V., Eilerman S., Liu D., Fiksel G., Polosatkin S. Calibration of an advanced neutral particle analyzer for the Madison Symmetric Torus reversed-field pinch. // Rev. Sci. Instrum. - 2012. - V.83, N10. - p.10D704-1-3.

[191] Deichuli P., Davydenko V., Belov V., Gorbovsky A., Dranichnikov A., Ivanov A., Sorokin A.,

- Mishagin V., Abdrashitov A., Kolmogorov V., Kondakov A. Commissioning of heating neutral beams for COMPASS-D tokamak. // *Rev. Sci. Instrum.* - 2012. - V.83, N2, Pt.2. - p.02B114 (3 p.).
- [192] Kondrashev S., Dickerson C., Levand A., Ostroumov P.N., Pardo R.C., Savard G., Vondrasek R., Alessi J., Beebe E., Pikin A., Kuznetsov G.I., Batazova M.A. Development of electron beam ion source charge breeder for rare isotopes at Californium Rare Isotope Breeder Upgrade. // *Rev. Sci. Instrum.* - 2012. - V.83, N2, Pt.2. - p.02A902 (3 p.).
- [193] Hampel U., Bartling Y., Hoppe D., Kuksanov N., Fadeev S., Salimov R. Feasibility study for mega-electron-volt electron beam tomography. // *Rev. Sci. Instrum.* - 2012. - V.83, N9. - p.093707-1-7.
- [194] Dreier H., Bagryansky P., Baumgarten N., Beil W., Lambert H.T., Lehnen M., Lizunov A., Solomakhin A. First results from the modular multi-channel dispersion interferometer at the TEXTOR tokamak. // *Rev. Sci. Instrum.* - 2012. - V.82, N6. - p.063509-1-4.
- [195] Izotov I.V., Razin S.V., Sidorov A.V., Skalyga V.A., Zorin V.G., Bagryansky P.A., Beklemishev A.D., Prikhodko V.V. Influence of the shear flow on electron cyclotron resonance plasma confinement in an axisymmetric magnetic mirror trap of the electron cyclotron resonance ion source. // *Rev. Sci. Instrum.* - 2012. - V.82, N2, Pt.2. - p.02A318 (3p.).
- [196] Pikin A., Alessi J., Beebe E., Kponou A., Okamura M., Raparia D., Ritter J., Tan Y., Kuznetsov G. Ion optics of RHIC electron beam ion source. // *Rev. Sci. Instrum.* - 2012. - V.83, N2. - p.02A504-1-3.
- [197] Korepanov S., Smirnov A., Clary R., Dettrick S., Deichuli P., Kondakov A., Murakhtin S. Modulated active charge exchange fast ion diagnostic for the C-2 field-reversed configuration experiment. // *Rev. Sci. Instrum.* - 2012. - V.83, N10. - p.10D720-1-3.
- [198] Lizunov A.A., Den Hartog D.J., Donin A.S., Ivanov A.A., Prikhodko V.V. Note: Multi point measurement of [B] in the gas-dynamic trap with a spectral motional Stark effect diagnostic. // *Rev. Sci. Instrum.* - 2012. - V.82, N8. - p.086105-1-3.
- [199] Dudnikov V., Dudnikov A. Radio frequency discharge with control of plasma potential distribution. // *Rev. Sci. Instrum.* - 2012. - V.83, N2, Pt.2. - p.02A720 (3p.).
- [200] Knyazev B.A., An W., Bluhm H. Stark spectroscopy of a probe lithium beam excited with two dye lasers as a technique to study a high-power ion-beam diode. // *Rev. Sci. Instrum.* - 2012. - V.83, N3. - p.033101-1-9.
- [201] Listopad A., Coenen J., Davydenko V., Ivanov A., Mishagin V., Savkin V., Schweer B., Shulzhenko G., Uhlemann R. Use of the focusing multi-slit ion optical system at Russian Diagnostic Injector (RUDI). // *Rev. Sci. Instrum.* - 2012. - V.83, N2, Pt.2. - p.02B707 (3 p.).
- [202] Rastigeev S.A., Frolov A.R., Goncharov A.D., Klyuev V.F., Konstantinov E.S., Kutnykova L.A., Parkhomchuk V.V., Petrozhitskii A.V. Development of the BINP AMS complex at CCU SB RAS. // *Problems of Atomic Science and Technology.* - 2012. - Vol.79, N3. - p.188-190.
- [203] Lotov K.V., Maslov V.I., Onishchenko I.N., Svistun O.M. Homogeneous focusing of electron bunch sequence by plasma wakefield. // *Problems of Atomic Science and Technology. Ser.: Nuclear Physics Investigations.* - 2012. - Vol.3, N3. - p.159-163.
- [204] Biryuchevsky Yu.A., Gorniker E.I., Kendjebulatov E.K., Krutikhin S.A., Kurkin G.Ya., Petrov V.M., Pilan A.M. Status of 174 MHz RF system for BEP. // *BAHT. Ser. Ядер.-физ. исследования.* - 2012. - N3. - p.49-52.
- [205] Gurov S.M., Akimov A.V., Anchugov O.V., Batrakov A.M., Belikov O.V., Bekhtenev E.A., Burenkov D.B., Cheblakov P.B., Cherepanov V.P., Chernyakin A.D., Cheskidov V.G., Churkin I.N., Elkaer A., Erokhin A.I., Fliller R., Gorchakov K.M., Gurov D.S., Ganetis G., Hseuh H., Karnaev S.E., Karpov G.V., Kiselev V.A., Kobets V.V., Konstantinov V.M., Kolmogorov V.V., Korepanov A.A., Kuper E.A., Kuzminykh V.S., Levichev E.B., De Long J., Mamkin V.R., Medvedko A.S., Meshkov O.I., Nefedov N.B., Neyfeld V.V., Okunev I.N., Petrov V.V., Petrichenkov M.V., Philipchenko A.V., Polyansky A.V., Pureskin D.N., Rakhimov A.R., Ruvinskiy S.I., Schegolev L.M., Semenov A.M., Senkov D.V., Serebnyakov S.S., Shaftan T.V., Sharma S., Shichkov D.S., Singh O., Shiyankov S.V., Shvedov D.A., Sinyatkin S.V., Smaluk V.V., Sukhanov A.V., Tian Y., Utkin A.V., Willeke F., Yaminov K.R., Yong H. Status of NSLS-II booster. // *Problems of Atomic Science and Technology.* 2012. - N4(80). - p.3-6.
- [206] Chernyak V.L. Mass spectrum in SQCD and problems with the seiberg duality. Another scenario. // *JETP.* 2012. - Vol.114. - p.61-79. [*JETP.* - 2012. - V.141, N1. - p.71-89.].
- [207] Dolgov A.M., Khriplovich I.B., Rudenko A.S. Difference between radiative transition rates in atoms and antiatoms. // *JETP Letters.* - 2012. - V.96, N7/8. - p.467-469.
- [208] Khriplovich I.B., Rudenko A.S. Can CP violation be observed in heavy-ion collisions? // *Ядерная физика.* - 2012. - V.75, N9. - p.1209-1211.
- [209] Koop I.A., Shatunov Yu.M., Nedorezov V.G. Electron-ion Collider in the center for antiproton and ion researches (FAIR) (ELISE project). // *Nucl. Energy.* - 2012. - Vol.112, N2. - p.91-98.
- [210] Authors: colleagues. Memory of Eduard Pavlovich Kruglyakov (22.10.1934 - 6.11.2012). // *VANT. Ser.: Thermonuclear Fusion.* - 2012. - N4. - p.103-105.
- [211] Soldatkina E.I., Bagryansky P.A., Zaytsev K.V., Ivanov A.A., Lizunov A.A., Lozhkina A.N., Maksimov

- V.V., Prikhodko V.V., Solomakhin A.L., Savkin V.Ya., Trunev Yu.A., Shulzhenko G.I. First experiments on electron beam injection into the gas dynamic trap. // VANT. Ser.: Thermonuclear Fusion. - 2012. - N4. - p.14-22.
- [212] Anikeev A.V., Bagryansky P.A., Donin A.S., Zaitsev K.V., Korzhavina M.S., Lizunov A.A., Loshkina A.N., Maksimov V.V., Prikhodko V.V., Soldatkina E.I., Solomakhin A.L. Experiments on ambipolar confinement of plasma in GDT. // VANT. Series: Thermonuclear Fusion. - 2012. - N4. - p.3-13.
- [213] Golubenko Yu.I., Kogut D.A., Kuksanov N.K., Nemytov P.I., Chakin I.K. Information measuring tracking of ELV accelerators and concomitant technological equipment. // Problems of Atomic Science and Technology. Series: Nuclear Physics Investigations. - 2012. - N3 (79). - p.211-214.
- [214] Kuksanov N.K., Fadeev S.N., Golubenko Yu.I., Kogut D.A., Korchagin A.I., Lavruhin A.V., Nemytov P.I., Salimov R.A., Domarov E.V. Development of the model range and improve performance accelerators ELV. // XXII Intern. Workshop on Charged Particle Accelerators. // VANT. Nuclear Physics Researches Series. - 2012. - N3. - p.15-18.
- [215] A.A. Vorobjev, E.M. Ivanov, A.G. Krivshich, G.A. Ryabov, V.M. Samsonov, D.M. Seliverstov, Yu.N. Gavrish, V.G. Mudrolyubov, A.P. Stokach, V.A. Vostrikov, E.B. Levichev, Yu.A. Tihonov, V.M. Vinogradov, S.V. Gerasimov, A.M. Granov, R.A. Shalek, N.N. Yalynych. Proton Therapy center of the B.P. Konstantinov Petersburg Nuclear Physics Institute. // VANT. Nuclear Physics Researches Series. - 2012. - N4(80). - p.146-150.
- [216] Listopad A.A., Davydenko V.I., Ivanov A.A., Mishagin V.V., Ulemann R., Shveer B. Multislit four-electrode ion-optical system for fast atomical diagnostic beam formation. // Novosibirsk, Vestnik NSU. Ser. Physics. - 2012. - V.7, N2. - p.15-24.
- [217] Baldin E.M., Blinov V.E., Zaitsev A.S., Korol A.A., Logashenko I.B., Sukharev A.M., Talyshev A.A., Tikhonov Yu.A. Super charm-tau factory: computing requirements. // Novosibirsk, Vestnik NSU. Ser. Physics. - 2012. - Vol.7, N1, p.94-99.
- [218] Arzhannikov A.V., Ginzburg N.S., Zaslavskiy V.Yu., Zotova I.V., Kalinin P.V., Kuznetsov S.A., Malkin A.M., Peskov N.Yu., Sergeev A.S., Sinitsky S.L., Stepanov V.D., Thumm M. Development of the two-stage planar FEM for the terahertz band on the basis of the ELMI accelerator. // Novosibirsk, Vestnik NSU. Ser. Physics. - 2012. - Vol.7, N1. - p.5-14 (in Russian).
- [219] Kozak V.R., Cooper E.A., Vinokurov N.A., Serednyakov S.S., Tararyshkin S.V., Tribendis A.G., Selivanov P.A. Control system of Novosibirsk free electron laser. // Vestnik NGU. Ser. Physics. - 2012. - Vol.7, N3. - p.24-33 (in Russian).
- [220] Burdin P.N., Devyataikina T.A., Kazantseva E.S., T.V. Rubitskaya, Skarbo B.A., Starostenko A.A., Tsyganov A.S.. Improvement of quadrupole magnets field quality in serial production. // Novosibirsk, Vestnik NSU. - 2012. - N3, Vol.7. - p.34-43.
- [221] Arakcheev A.S. and Lotov K.V. Analytical Model of brittle destruction based on hypothesis of scale similarity. // Journal of Experimental and Theoretical Physics. - 2012. - Vol.115, N2. - P.242-248. [JETP. - 2012. - Vol.142, N2(8). - p.271-278].
- [222] Nikitin S.A., Nikolaev I.B. Calculation of the intensity of Toushek electrons in the VEPP-4M storage ring // JETP. - 2012. - V.142, N1(7). - p.44-55. [http://www.jetp.ac.ru/cgi-bin/dn/r_142_44.pdf].
- [223] Khalizeva M. Electron cooler for protons. // Science in Siberia. - 2012. - N4. - p.32-34 (in Russian).
- [224] Tikhonov Yu.A. Search for the origin of everything. // Science First Hand. - 2012. - N3(45). - p.6-13.
- [225] Parkhomchuk V.V. History of the electron cooling. // SCIENCE First Hand, 2012. - N4. - p.46-57 (in Russian).
- [226] Blinov V.E. The new cosmology for the old Universe. // SCIENCE from First Hand. - 2012. - N1(43). - p.16-19 (in Russian).
- [227] Shiltsev V.D., Nesterenko I.N. " Fortune I see in you or Venus...". // SCIENCE First Hand. - 2012. - N3(45). - C.60-73 (in Russian).
- [228] Arzhannikov A.V., Ginzburg N.S., Zaslavskii V.Yu., Kalinin P.V., Malkin A.M., Peskov N.Yu., Sergeev A.S., Sinitsky S.L., and Tumm M. Experimental testing of short-wave variable frequency Bragg reflectors based on coupling of propagating and quasi critical waves. // Technical Physics Letters. - 2012. - Vol.38, N7. - p.600-603. [JTP Letters. - 2012. - Vol.38, N13. - p.8-16].
- [229] Parkhomchuk V.V. Open questions in electron cooling. // Physics of Particles and Nuclei Letters. - 2012. - Vol.9, N4-5. - p.527-536 (in Russian).
- [230] Akhmanova E.V., Ivanov A.V., Kobets A.G., Kokurkin M.P., Lysov N.Yu., Meshkov I.N., Pashin M.M., Pivin R.V., Rudakov A.Yu., Smirnov A.V., Topilin N.D., Numanova Yu.A., Filippov A.A., Shabunov A.V., Yakovenko S.L. Project of high-voltage electron cooling system for NICA collider. // PEPAN Letters. - 2012. - Vol.9, N4/5. - p.597-603.
- [231] Vostrikov V.A., Kiselev V.A., Levichev E.B., Parkhomchuk V.V., Reva V.B., Sinyatkin S.V. The project of a synchrotron with electron cooling for cancer therapy. // PEPAN Letters. - 2012. - V.9, N4/5. - P.700-705.
- [232] Пархомчук В.В., Растигеев С.А. Селекция ионов в ускорительном масс-спектрометре ИЯФ СО РАН. // Письма в ЭЧАЯ. - 2012. - Т.9, N4/5. - С.666-671.

- [233] Пархомчук В.В., Петрожицкий А.В., Растигеев С.А. Тонкоплочный детектор для регистрации ионов на ускорительном масс-спектрометре. // Письма в ЭЧАЯ. - 2012. - Т.9, N4/5. - С.729-734.
- [234] V.Yu. Ivanov, V.A. Pustovarov, A. Kikas, T. Kaambre, I. Kuusik, M. Kirm, E. I. Zinin. Vacuum ultraviolet and X-ray emission spectroscopy of anion and cation excitons in oxide crystals // Journal of Surface Investigation. X-ray, Synchrotron and Neutron Techniques. - 2012. - N2. - p.5-10.
- [235] Goldenberg B.G., Petrova E.V., Pindyurin V.F., Kozlov A.S. Studies of the effect of synchrotron radiation on the thermophysical parameters of PMMA X-ray resist. // The Journal of Surface Investigation. X-ray, Synchrotron and Neutron Techniques. - 2012. - N1. - p.14-20 (in Russian).
- [236] Kotelnikov A.I., Selivanov A.N., Fedotov M.G. CCD detector for experiments with high temporal resolution on SR beams. // The Journal of Surface Investigation. X-ray, Synchrotron and Neutron Techniques - 2012. - N5. - p.25-30 (in Russian).
- [237] Korneev V.N., Shlektarev V.A., Zabelin A.V., Aulchenko V.M., Tolochko B.P., Ariskin N.I., Lanina N.F., Vazina A.A. X-ray stations based on cylindrical zoom lenses for nanostructure research using synchrotron radiation. // The Journal of Surface Investigation. X-ray, Synchrotron and Neutron Techniques. - 2012. - N10. - p.71-87 (in Russian).
- [238] Volkov A.A., Lev V.H., Mezentsev N.A., Miginskaya E.G., Syrovatin V.M., Khrushchev S.V., Tsukanov V.M., Shkaruba V.A. Superconducting 119-pole wiggler with a field of 2.1 T and a period of 30 mm for the the ALBA storage ring. // The Journal of Surface Investigation. X-ray, Synchrotron and Neutron Techniques. - 2012. - N5. - p.3-12 (in Russian).
- [239] Legkodymov A.A., Mashkovtsev M.R., Nikolenko A.D., Pindyurin V.F., Lyakh V.V., Avakian S.V., Voronin N.A. Comparative validation of secondary electron multipliers in ultrasoft X-rays. // The Journal of Surface Investigation. X-ray, Synchrotron and Neutron Techniques. - 2012. - N5. - p.31-34 (in Russian).
- [240] Nikolenko A.D., Avakian S.V., Afanasiev I.M., Voronin N.A., Kovalenko N.V., Legkodymov A.A., Lyakh V.V., Pindyurin V.F. "Space" station. Application of synchrotron radiation from the VEPP-4 storage ring to meteorological measurements in the VUV and soft X-ray ranges. // The Journal of Surface Investigation. X-ray, Synchrotron and Neutron Techniques. - 2012. - N5. - p.13-19 (in Russian).
- [241] Ivanov A.A., Aleinik V.I., Ivanenko S.V., Kvashnin A.N., Puryga E.A., Rovenskikh A.F., Sulyaev Yu.S., and Khilchenko A.D. An adaptive γ -ray spectrometer with a high event processing rate. // Instruments and Experimental Techniques. - 2012. - Vol.55, N1. - p.1-10. [Instruments and Experimental Techniques. - 2012. - N1. - p.5-15].
- [242] Raschenko V.V. A ГИД 25 bipolar pulse generator for energizing elements of the K500 beam transportation channel. // Instruments and Experimental Techniques. - 2012. - Vol.55, N1. - p.49-55. [Instruments and Experimental Techniques. - 2012. - N1. - p.56-63].
- [243] Burmasov V.S., Bobilev V.B., Ivanova A.A., Ivanenko S.V., Kasatov A.A., Kasatov D.A., Kruglyakov E.P., Kuklin K.N., Popov S.S., Postupaev V.V., Puryga E.A., Rovenskikh A.F., Sklyarov V.F. Infrared interferometer for investigation of subthermonuclear plasma in multimirror trap GOL-3. // Instruments and Experimental Techniques. - 2012, Vol.55, N2, p.259-262. [Instruments and Experimental Techniques. - 2012. - N2. - p.120-123].
- [244] Akimov A.V., Logatchov P.V., Korepanov A.A., Averin F.V., Savinova O.V., Mamaev G.L., Mamaev S.L. Magnetic cores made of an amorphous tape for the induction accelerator. // Instruments and Experimental Techniques. - 2012. - N2. - p.129-134 (in Russian).
- [245] Puryga E.A., Khilchenko A.D., Kvashnin A.N., Zubarev P.V., Ivanova A.A., and Ivanenko S.V. An ADC12500 multifunction fast recorder. // ISSN 0020_4412, Instruments and Experimental Techniques. - 2012. - Vol.55, N3. - p.368-376.
- [246] Akimov A.V., Akimov V.E., Bak P.A., Bochkov V.D., Vechroeva L.T., Korepanov A.A., Logatchov P.V., Panov A.N., Starostenko D.A., Shilin O.V. System of pulse power for linear induction accelerator LIU-2. // Instruments and Experimental Techniques. - 2012. - N2. - p.77-83.
- [247] Blinov V.E., Prisekin V.G. Investigation of a cathode aging and field emission threshold for cathode wires in drift chambers. // PTE. - 2012. - N4. - p.14-25.
- [248] Epstein L.B., Yudin Yu.V. Processing of the signals from the Liquid-Xenon Calorimeter of the CMD-3 Detector for timing measurements. // PTE. - 2012. - N5. - p.43-53 (in Russian).
- [249] Groshev V.R., Kazanin V.F., Ottmar A.V., Fedotov M.G., Tsyganov A.S. Applications of digital image recorders in beam diagnostics systems. // Instruments and Experimental Techniques. - 2012. - Vol. 55, N1. - C.38-43. [PTE. - 2012. - N1. - p.44-49].
- [250] Barkov L.M., Vinokurov N.A., Kovalchuk M.V., Korchuganov V.N., Kruglyakov E.P., Levichev E.B., Mezentsev N.A., Meshkov I.N., Parkhomchuk V.V., Skrinsky A.N., Khriplovich I.B., Shatunov Yu.M. Jubilee article. [Gennady Kulipanov (to the 70th jubilee)]. // UFN. - 2012. - v.182, N2. - p.231-232 (in Russian).
- [251] Arzhannikov A.V., Burdakov A.V., Vyacheslavov L.N., Ivanov I.A., Ivantsivsky M.V., Kasatov A.A., Kuznetsov S.A., Makarov M.A., Mekler K.I., Polosatkin S.V., Postupaev V.V., Popov S.S., Sinitsky S.L., Sklyarov V.F., Thumm M.K.A. Diagnostic system for studying generation of subterahertz radiation during beam-plasma interaction in the GOL-3 facility. // Plasma Physics Reports. - 2012. - Vol.38, N6. - p.450-

459. [Plasma Physics Reports. - 2012. - Vol.38, N6. - C.496-505.
- [252] Sudnikov A.V., Burdakov A.V., Ivanov I.A., Makarov M.A., Mekler K.I., Rovenskikh A.F., Polosatkin S.V., Postupaev V.V., Sinitzky S.L., Sorokina N.V., and Sulyaev Yu.S. Study of plasma rotation in the GOL-3 Facility. // Plasma Physics Reports. - 2012. - Vol.38, N9. - p.718-728. [Plasma Physics Reports. - 2012. - Vol.38, N9. - p.779-791].
- [253] Skovorodin D.I., Beklemishev A.D. Plasma outflow from a corrugated trap in the kinetic regime. // Plasma Physics Reports. - 2012. - Vol.38, N3, p. 202-206.
- [254] Kotelnikov I.A. Braginskii and Balescu kinetic coefficients for electrons in Lorentzian plasma. // Plasma Physics Reports. - 2012. - Vol.38, N8. - p.608-619. [Plasma Physics Reports. - 2012. - Vol.38, N8. - C.665-676].
- [255] Vyacheslavov L.N., Ivantsivsky M.V., Meshkov O.I., Popov S.S., Smalyuk V.V. Methods of optical diagnostics of the electron-positron beams and plasma interaction with a high-current electron beam. // PEPAN Letters. - 2012. - T.43, N2. - C.451-499.
- [256] Smaluk V.V. The overview of the collective beam instabilities in the electron-positron storage rings. // PEPAN Letters. - 2012. - V.43, N2. - P.401-450.
- [257] Kozlov M.G., Reznichenko A.V., Fadin V.S. Impact factor for gluon production in multi-Regge kinematics in the next-to-leading order. // Physics of Atomic Nuclei, July 2012. - Volume 75, Issue 7. - p.850-865. [Physics of Atomic Nuclei. - 2012. - Vol.75, N7. - p.905-920].
- [258] Kozlov M.G., Reznichenko A.V., Fadin V.S. Check of the gluon-reggeization condition in the next-to-leading order: Gluon part. // Physics of Atomic Nuclei, April 2012. - Volume 75, Issue 4. - p.493-506. [Physics of Atomic Nuclei. - 2012. - Vol.75, N4. - p.529-542].
- [259] Fedotov A.P., Trunova V.A., Zvereva V.V., Maksimovskaya V.V., Melgunov M.S. Reconstruction of glacier fluctuation (East Siberia, Russia) during the last 160 years based on high resolution geochemical proxies from proglacial lake bottom sediments of the Baikalsky Ridge. // Intern. Journal of Environmental Studies. - 2012. - V.69, N5. - p.806-815.
- [260] Voevoda M.I., Kruchinina M.V., Peltek S.E., Kurylowich S.A., Kruchinin V.N., Spesivtsev E.V., Rykhlitsky S.V., Volodin V.A., Generalov V.M., Gerasimov V.V., Knyazev B.A. Optical methods of blood analysis in staging of diffuse liver pathology. // Archives of Internal Medicine. - 2012. - N4 (6). - p.46-54 (in Russian).
- [261] Kubarev V.V., Makashev E.V., Palagin K.S., Serednyakov S.S., Fedotov M.G. Terahertz power meters and imaging systems of Novosibirsk free electron laser. // NSTU Bulletin. - 2012. - N4 (49). - p.76-79 (in Russian).
- [262] Vinokurov N.A., Vlasenko M.G., Gerasimov V.V., Demjanenko M.A., Esaev D.G., Knyazev B.A., Kulipanov G.N., Nikitin A.K., Cherkassky V.S., Choporova Yu.Yu. High-power terahertz free electron laser: metrological aspects. // NSTU Bulletin. - 2012. - N4 (49). - p.63-71 (in Russian).
- [263] Kubarev V.V., Vinokurov N.A., Kolobanov E.I., Kulipanov G.N., Matveenko A.N., Salikova T.V., Serednyakov S.S., Sheglov M.A. Fourier spectroscopy of water vapor in the 40-meter optical beam transport line of Novosibirsk free electron laser. // NSTU Bulletin. - 2012. - N4 (49). - p.72-75 (in Russian).
- [264] Peltek S.E., Moshkin M.P., Gerlinskaya L.A., Goryachkovskaya T.N., Bannikova S.V., Podkolodnaya O.A., Popik V.M., Kolchanov N.A. SPF vivarium: science and technology complex for nanobiosafety research. // Nanotechnology. Ecology. Production. - 2012. - N15. - p.30-33 (in Russian).
- [265] Markova Yu.N., Kerber E.V., Anchoutina E.A., Zarubina O.V., Maksimovskaya V.V., Zolotarev K.V. Standard sediment samples in assessment of X-ray analysis methods using synchrotron radiation // Standard samples. - 2012. - N2. - p.52-58 (in Russian).
- [266] Stankus S.V., Yatsuk O.S., Zhmurikov E.I., Tecchio L. The thermal extension of the artificial graphite in the 293-1650 K temperature range. // Thermal Physics and Aeromechanics. - 2012. - Vol.19, N5(77) . - p.637-642.
- [267] Thumm M.K.A., Arzhannikov A.V., Astrelin V.T., Burdakov A.V., Ginzburg N.S., Ivanov I.A., Kalinin P.V., Kuznetsov S.A., Makarov M.A., Mekler K.I., Paulish A.G., Peskov N.Yu., Polosatkin S.V., Popov S.A., Postupaev V.V., Rovenskikh A.F., Sergeev A.S., Sinitzky S.L., Sklyarov V.F., Stepanov V.D., Vyacheslavov L.N., Zaslavsky V.Yu. Generation of high power THz waves in relativistic electron beam plasma and two-sheet-beam FEM. // Terahertz Science and Technology. - 2012. - Vol.5, N1. - p.18-39.
- [268] Eilerman S., Anderson J.K., Reusch J.A., Liu D., Fiksel G., Polosatkin S. and Belykh V. Time-resolved ion energy distribution measurements using an advanced neutral particle analyzer on the MST reversed-field pinch. // Rev. Sci. Instrum. -2012. - Vol.83. - 10D302; doi: 10.1063/1.4728312.
- [269] Arzhannikov A.V., Ginzburg N.S., Kalinin P.V., Malkin A.M., Peskov N.Yu., Sergeev A.S., Sinitzky S.L., Thumm M., Zaslavsky V.Yu. Short-wavelength tunable Bragg reflectors based on coupling of propagating and cutoff waves: modeling and experimental studies. // Applied Physics Letters. - 2012. - Vol.101, Iss.8. - Paper 083507.
- [270] Ginzburg N.S., Peskov N.Yu., Sergeev A.S., Zaslavsky V.Yu., Arzhannikov A.V., Kalinin P.V., Sinitzky S.L., Thumm M. High selective two-dimensional Bragg resonators of planar geometry: theoretical,

computational and experimental study. // Journal of Applied Physics. - 2012. - Vol.112. - 114504.

[271] Astrelin V.T., Burdakov A.V., Vshivkov V.A., Snytnikov A.V. Investigation of collective processes in multi-mirror trap. // Book: Numerical methods, algorithms and hardware and software tools for parallel simulation of natural processes /Editor: V.G. Khoroshevsky. - Novosibirsk: SB RAS. - 2012. - p.97-105 (354 p.) (in Russian).

[272] Sinitzky S.L., Arzhannikov A.V. Powerful pulsed beams. // Textbook. - NGU, Novosibirsk. - 2012. - 140 p. (in Russian).

[273] Khriplovich I.B. and Rudenko A.S. Cosmology constrains gravitational four-fermion interaction. // JCAP11 (2012) 040.

[274] Dmitriev V.F., Flambaum V.V. Decays of fourth generation bound states. // International Journal of Modern Physics A. - 2012. - Vol. 27. - 1250179.

[275] Fadin V.S. and Lipatov L.N. BFKL equation for the adjoint representation of the gauge group in the next-to-leading approximation at $N=4$ SUSY. // Phys. Lett. B. - 2012. - V.706. - p.470-476.

[276] Fadin V.S., Fiore R., Grabovsky A.V. and Papa A. Connection between complete and Möbius forms of gauge invariant operators. // Nucl. Phys. B. - 2012. - V.856. - p.111-124.

[277] Fadin V.S., Fiore R. and Papa A. Difference between standard and quasi-conformal BFKL kernels. // Nucl. Phys. B. - 2012. - Vol.865. - p.67-82.

[278] Lee R.N. DRA method: Powerful tool for the calculation of the loop integrals. // Journal of Physics: Conference Series. - 2012. - Vol.368. - 012050.

[279] Lee R.N. Smirnov A.V. and Smirnov. V.A. Master Integrals for four-loop massless propagators up to transcendentality weight twelve. // Nucl. Phys. B. - 2012. - Vol.856. - p.95-110. [arXiv: 1108.0732].

[280] Lee R.N. and Smirnov V.A. The dimensional recurrence and analyticity method for multicomponent master Integrals: using unitarity cuts to construct homogeneous solutions. // JHEP. - 2012. - Vol 1212. - Vol.104. [arXiv:1209.0339].

[281] Salnikov S.G. Spin-dependent part of $\bar{p}d$ interaction cross section and Nijmegen potential. // Nuclear Physics A. - 2012. - Vol.874. - p.98-107.

[282] Grozin A.G. Massless two-loop self-energy diagram: Historical review. // J. Mod. Phys. A. - 2012. - Vol.27. - 1230018 (22p.). [arXiv:1206.2572v3 [hep-ph]].

[283] Grozin A.G. Höschele M., Hoff J., Steinhauser M. Simultaneous decoupling of bottom and charm quarks. // Proceedings of Science (LL2012) 032 (10 p.) (<http://pos.sissa.it/cgi-bin/reader/conf.cgi?confid=151>) [arXiv:1205.6001 [hep-ph]].

[284] Lee R.N. Milstein A.I., Terekhov I.S. // Quasilocalized states in a model of electron-electron

interaction in grapheme. // Phys. Rev. B. - 2012. - Vol.86. - 035425.

[285] Katkov V.M. Production of a pair by a polarized photon in a uniform constant electromagnetic field. // JETP. - 2012. - Vol 114, N2. - p.226-233. [JETP. - 2012. - Vol.141, N2. - p.258-266].

[286] Andrew Feldman, Andrei A. Pomeransky. Charged black rings in supergravity with a single non-zero gauge field. // JHEP. - 2012. - Vol.1207. - p.141.

[287] Zhiron O.V., Shepelyansky D.L. Wigner crystal in snaked nanochannels: outlook. // Physica B. - 2012. - Vol.407. - p.1909-1911.

[288] Baru S.E. System of x-ray examination «Sibskan M1» - the product of new generation intended for examination of a body of the person. // Collection «Innovation 2012». Publishing house «Novosibirsk - prestige», Novosibirsk. - 2012. - p.104 (in Russian).

[289] Kalmykov V.V., Ukraintsev Yu.G. Siberian examination scanner. // Airports. Progressive technologies. 2012. - N1 (54). - p.13-16 (in Russian).

[290] Slezko S.M., Ukraintsev Yu.G. Decision on maintenance of complex safety of the airports. // Airports. Progressive technologies. 2012. - N3 (56). - p.17-19 (in Russian).

[291] Kalmykov V.V., Slezko S.M., Ukraintsev Yu.G. Maintenance of transport safety on objects of an infrastructure of the airport. // World and safety. - 2012. - N4. - p.22-24 (in Russian).

[292] Voronin K.A., Ukraintsev Yu.G. Model of effective system of examination at the airport. // World and safety. - 2012. - N2. - p.38-40 (in Russian).

[293] Bondar A., Buzulutskov A., Dolgov A., Grebenuk A., Peleganchuk S., Porosev V., Shekhtman L., Shemyakina E., Sokolov A. Study of infrared scintillations in gaseous and liquid argon. Part II: light yield and possible applications. // Journal of Instrumentation. - 2012. - N7. - P06014.

[294] Aulchenko V.M., Bondar A.E., Dolgov A.M., Kudryavtsev V.N., Nikolenko D.M., Papishev P.A., Prueel E.R., Rachek I.A., Shekhtman L.I., Ten K.A., Titov V.M., Tolochko V.P., Zhilich V.N., Zhulanov V.V. GEM-based detectors for SR imaging and particle tracking. // Journal of Instrumentation. - 2012. - N7. - C03021.

[295] Parkhomchuk V.V., Rastigeev S.A. Ion selection in accelerator mass spectrometer at the Budker Institute of Nuclear Physics. // Physics of Particles and Nuclei Letters. - 2012. - Vol.9, N4-5. - p.406-409.

[296] Parkhomchuk V.V., Petrozhitskii A.V., and Rastigeev S.A. Thin film detector for ion registration in accelerator mass spectrometers. // Physics of Particles and Nuclei Letters. - 2012. - Vol.9, N4-5. - p.448-451.

- [297] Buzulutskov A. Advances in cryogenic avalanche detectors (review). // J. of Instrumentation. - 2012. - V.7. - Paper C02025. P.1-56.
- [298] Bondar A., Buzulutskov A., Dolgov A., Grebenuk A., Shemyakina E., Sokolov A. Study of infrared scintillations in gaseous and liquid argon. Part I: methodology and time measurements. // J. of Instrumentation. - 2012. - V.7. - Paper P06015. P.1-17.
- [299] D. Akimov, I. Aleksandrov, V. Belov, V. Belyaev, A. Bolozdinya, A. Buzulutskov et al. // Hardware system to measure the response of liquid xenon for low energy recoil nuclei at the reactor IRT MEPhI. // Nuclear Physics and Engineering. - 2012. - V.3, N6. - p.490-495.
- [300] Aaij R., LHCb Collab., Bobrov A., Bondar A., Eidelman S., Krokovny P., Kudryavtsev V., Poluektov A., Shekhtman L., Vorobyev V., et al. Observation of excited Λ_b baryons. // Phys. Rev. Lett. - 2012. - V.109. - p.172003.
- [301] Aaij R., LHCb Collab., Bobrov A., Bondar A., Eidelman S., Krokovny P., Kudryavtsev V., Poluektov A., Shekhtman L., Vorobyev V., et al. Measurements of B_c^+ production and mass with $B_c^+ \rightarrow J/\psi \pi^+$ decay. // Phys. Rev. Lett. - 2012. - V.109. - p.232001.
- [302] Chang M.C., Belle Collab., Bondar A., Eidelman S., Garmash A., Krokovny P., Usov Y., Vorobyev V., Zhilich V., Zhulanov V., et al. Measurement of $B^0 \rightarrow J/\psi \eta'$ and constraint on the $\eta - \eta'$ mixing angle. // Phys. Rev. D. - 2012. - V. 85. - p.091102.
- [303] Beringer J., Eidelman S., et al. (Particle Data Group). Review of Particle Physics. // Phys. Rev. D. - 2012. - Vol.86. - 010001.
- [304] Negishi K., Belle Collab., Bondar A., Eidelman S., Gabyshev N., Krokovny P., Matvienko D., Shebalin V., Shwartz B., Vorobyev V., Zhilich V., Zhulanov V., et al. Search for the decay $B^0 \rightarrow D K^{*0}$ followed by $D \rightarrow K^- \pi^+$. // Phys. Rev. D. - 2012. - Vol.86. - p.011101(R).
- [305] Kim J.H., Belle Collab., Aulchenko V., Bondar A., Eidelman S., Gabyshev N., Krokovny P., Kuzmin A., Shwartz B., Vorobyev V., Zhilich V., Zhulanov V., et al. Search for $B \rightarrow \phi \pi$ decays. // Phys. Rev. D. - 2012. - Vol.86. - p.031101(R).
- [306] Shen C-P., Belle Collab., A., Eidelman S., Gabyshev N., Krokovny P., Kuzmin A., Shebalin V., Shwartz B., Usov Y., Zhilich V., Zhulanov V., et al. First observation of exclusive $\Upsilon(1S)$ and $\Upsilon(2S)$ decay into light hadrons. // Phys. Rev. D. - 2012. - Vol.86. - p.031102(R).
- [307] Hsu C.-L., Belle Collab., Arinstein K., Aulchenko V., Bondar A., Eidelman S., Epifanov D., Gabyshev N., Krokovny P., Kuzmin A., Shwartz B., Usov Y., Vorobyev V., Zhilich V., Zhulanov V., et al. Search for B^0 decays to invisible final states at Belle. // Phys. Rev. D. - 2012. - Vol.86. - p.032002.
- [308] Zhang C.C., Belle Collab., Eidelman S., Gabyshev N., Krokovny P., Kuzmin A., Matvienko D., Shebalin V., Shwartz B., Vinokurova A., Vorobyev V., Zhulanov V., et al. First study of $\eta_c(1S)$, $\eta(1760)$ and $X(1835)$ production via $\eta' \pi^+ \pi^-$ final states in two-photon collisions. // Phys. Rev. D. 2012. - Vol.86. - p.052002.
- [309] Aaij R., LHCb Collab., Bobrov A., Bondar A., Eidelman S., Krokovny P., Kudryavtsev V., Poluektov A., Shekhtman L., Vorobyev V., et al. Analysis of the resonant components in $B_s \rightarrow J/\psi \pi^+ \pi^-$. Phys. Rev. D. 2012. - Vol.86. - p.052006.
- [310] Aaij R., LHCb Collab., Bobrov A., Bondar A., Eidelman S., Krokovny P., Kudryavtsev V., Poluektov A., Shekhtman L., Vorobyev V., et al. Measurement of the $B_s^0 \rightarrow J/\psi \bar{K}^{*0}$ branching fraction and angular amplitudes. // Phys. Rev. D. - 2012. Vol.86. - p.071102.
- [311] Kronenbitter B., Belle Collab., Arinstein K., Bondar A., Eidelman S., Gabyshev N., Krokovny P., Usov Y., Vorobyev V., Zhilich V., Zhulanov V., et al. First observation of CP violation and improved measurement of the branching fraction and polarization of $B^0 \rightarrow D^{*+} D^{*-}$ decays. // Phys. Rev. D. - 2012. - Vol.86. - p.071103.
- [312] Stypula J., Belle Collab., Bondar A., Eidelman S., Gabyshev N., Krokovny P., Kuzmin A., Usov Y., Vorobyev V., Zhilich V., Zhulanov V., et al. Evidence for $B^- \rightarrow D_s^+ K^- \Gamma^- \bar{\nu}_l$ and search for $B^- \rightarrow D_s^{*+} K^- \Gamma^- \bar{\nu}_l$. // Phys. Rev. D. - 2012. - Vol.86. - p.072007.
- [313] Uehara S., Belle Collab., Bondar A., Eidelman S., Epifanov D., Gabyshev N., Krokovny P., Kuzmin A., Matvienko D., Shwartz B., Vinokurova A., Vorobyev V., Zhilich V., Zhulanov V. et al. Measurement of $\gamma \gamma^* \rightarrow \pi^0$ transition form factor at Belle. // Phys. Rev. D. - 2012. - Vol.86. - p.092007.
- [314] Dalseno J., Belle Collab., Aulchenko V., Eidelman S., Gabyshev N., Garmash A., Krokovny P., Matvienko D., Shebalin V., Usov Y., Zhilich V., Zhulanov V., et al. Measurement of branching fraction and first evidence of CP violation in $B^0 \rightarrow a_1^+(1260) \pi^{\mp}$ decays. // Phys. Rev. D. - 2012. - Vol.86. - p.092012.
- [315] Aaij R., LHCb Collab., Bobrov A., Bondar A., Eidelman S., Krokovny P., Kudryavtsev V., Poluektov A., Shekhtman L., Vorobyev V., et al. First observation of the decays $B_s \rightarrow D_s K \pi \pi$ and $B_s \rightarrow D_{s1}(2536) \pi$. // Phys. Rev. D. 2012. - Vol.86. - p.112005.
- [316] Aaij R., LHCb Collab., Bobrov A., Bondar A., Eidelman S., Kudryavtsev V., Poluektov A., Shekhtman L., et al. Measurement of the ratio of prompt χ_c to J/ψ production in pp collisions at $\sqrt{s}=7$ TeV. // Phys. Lett. B - 2012. - Vol.718. - p.431.
- [317] Aaij R., LHCb Collab., Bobrov A., Bondar A., Eidelman S., Poluektov A., Shekhtman L., et al. Absolute luminosity measurements with the LHCb detector at the LHC. // JINST. 2012. - Vol.7. - P01010.

[318] Eidelman S.I. and Shwartz B.A. Interactions of particles and radiation with matter. // In Grupen, Claus (ed.) et al.: Handbook of particle detection and imaging. - 2012. - Vol.1, p.3-23.

[319] Bodenstern, ..., Eidelman S., et al. Confronting electron-positron annihilation into hadrons with QCD: an operator product expansion analysis. // JHEP. - 2012. - Vol.1201. - p.039.

[320] Aaij R., LHCb Collab., Bobrov A., Bondar A., Eidelman S., Krokovny P., Poluektov A., Shekhtman L., et al. Measurement of the B^{\pm} production cross section in pp collisions at $\sqrt{s}=7$ TeV. // JHEP. - 2012. - Vol.1204. - 093.

[321] Aaij R., LHCb Collab., Bobrov A., Bondar A., Eidelman S., Krokovny P., Poluektov A., Shekhtman L., et al. Measurement of mixing and CP violation parameters in two-body charm decays. // JHEP. - 2012. - Vol.1204. - 129.

[322] Aaij R., LHCb Collab., Bobrov A., Bondar A., Eidelman S., Krokovny P., Kudryavtsev V., Poluektov A., Shekhtman L., et al. Inclusive W and Z production in the forward region $\sqrt{s}=7$ TeV. // JHEP. - 2012. - Vol.1206. - p.058.

[323] Aaij R., LHCb Collab., Bobrov A., Bondar A., Eidelman S., Krokovny P., Kudryavtsev V., Poluektov A., Shekhtman L., et al. Measurements of the branching fractions of the decays $B_s^0 \rightarrow B_s^{\mp} K^{\pm}$ and $B_s^0 \rightarrow D_s^- \pi^+$. // JHEP. 2012. - Vol.1206. - p.115.

[324] Aaij R., LHCb Collab., Bobrov A., Bondar A., Eidelman S., Krokovny P., Kudryavtsev V., Poluektov A., Shekhtman L., et al. Observation of double charm production involving open charm pp collisions at $\sqrt{s}=7$ TeV. // JHEP. 2012. - Vol.1206. - p.141.

[325] Aaij R., LHCb Collab., Bobrov A., Bondar A., Eidelman S., Krokovny P., Kudryavtsev V., Poluektov A., Shekhtman L., Vorobyev V., et al. Measurement of the isospin asymmetry in $B \rightarrow K^{(*)} \mu^+ \mu^-$ decays. // JHEP. - 2012. - Vol.1207. - p.133.

[326] Aaij R., LHCb Collab., Bobrov A., Bondar A., Eidelman S., Krokovny P., Kudryavtsev V., Poluektov A., Shekhtman L., et al. Measurement of b-hadron branching fractions for two-body decays into charmless charged hadrons. // JHEP. - 2012. - Vol.1210. - 037.

[327] Aaij R., LHCb Collab., Bobrov A., Bondar A., Eidelman S., Krokovny P., Kudryavtsev V., Poluektov A., Shekhtman L., Vorobyev V., et al. Study of D_{sJ} decays to $D^+ K_S$ and $D^0 K^+$ final states in pp collisions. // JHEP. 2012. - Vol.1210. - p.151.

[328] Aaij R., LHCb Collab., Bobrov A., Bondar A., Eidelman S., Krokovny P., Kudryavtsev V., Poluektov A., Shekhtman L., Vorobyev V., et al. Measurement of the fraction of $\Upsilon(1S)$ originating from $\chi_b(1P)$ decays in

pp collisions at $\sqrt{s}=7$ TeV. // JHEP. 2012. - Vol.1211. - p.031.

[329] Aaij R., LHCb Collab., Bobrov A., Bondar A., Eidelman S., Krokovny P., Kudryavtsev V., Poluektov A., Shekhtman L., Vorobyev V., et al. First observation of the decay $B^+ \rightarrow \pi^+ \mu^+ \mu^-$. // JHEP. - 2012. - Vol.1212. - p.125.

[330] Aaij R., LHCb Collab., Bobrov A., Bondar A., Eidelman S., Krokovny P., Poluektov A., Shekhtman L., et al. Observation of $X(3872)$ production in pp collisions $\sqrt{s}=7$ TeV. // Eur. Phys. J. C. - 2012. - Vol.72. - p.1972.

[331] Aaij R., LHCb Collab., Bobrov A., Bondar A., Eidelman S., Krokovny P., Kudryavtsev V., Poluektov A., Shekhtman L., Vorobyev V., et al. Measurement of prompt hadron production ratios in pp collisions at $\sqrt{s}=7$ TeV. // Eur. Phys. J. C. - 2012. - Vol.72. - p.2168.

[332] Brodzicka J., Belle Collab., Eidelman S., et al. Physics Achievements from the Belle Experiment. // PTEP. - 2012. - Vol.2012. - p.04D001.

[333] R.R. Akhmetshin, A.V. Anisyonkov, S.A. Anokhin, V.M. Aulchenko, V.S. Banzarov, L.M. Barkov, N.S. Bashtovoy, D.E. Berkaev, A.E. Bondar, A.V. Bragin, S.I. Eidelman, D.A. Epifanov, L.B. Epshteyn, G.V. Fedotov, S.E. Gayazov, A.A. Grebenuk, D.N. Grigoriev, E.M. Gromov, F.V. Ignatov, S.V. Karpov, V.F. Kazanin, B.I. Khazin, I.A. Koop, A.N. Kozyrev, A.S. Kuzmin, A.E. Kuzmenko, I.B. Logashenko, A.P. Lysenko, P.A. Lukin, K.Yu. Mikhailov, Yu.N. Pestov, E.A. Perevedentsev, S. Pirogov, S.G. Pivovarov, A.S. Popov, Yu.S. Popov, S.I. Redin, Yu.A. Rogovsky, A.A. Ruban, N.M. Ryskulov, A.E. Ryzhenkov, V.E. Shebalin, D.N. Shemyakin, B.A. Shwartz, D.B. Shwartz, A.L. Sibidanov, P.Yu. Shatunov, Yu.M. Shatunov, I.G. Snopkov, E.P. Solodov, V.M. Titov, A.A. Talyshev, A.I. Vorobiov, Yu.V. Yudin, A.S. Zaytsev (CMD-3 Collab.). First results from the CMD-3 detector at the VEPP-2000 Collider. // Nucl. Phys. B. Proc. Suppl. - 2012. - Vol.225-227. - p.43-47.

[334] R.R. Akhmetshin, A.V. Anisyonkov, S.A. Anokhin, V.M. Aulchenko, V.S. Banzarov, L.M. Barkov, N.S. Bashtovoy, D.E. Berkaev, A.E. Bondar, A.V. Bragin, S.I. Eidelman, D.A. Epifanov, L.B. Epshteyn, G.V. Fedotov, S.E. Gayazov, A.A. Grebenuk, D.N. Grigoriev, E.M. Gromov, F.V. Ignatov, S.V. Karpov, V.F. Kazanin, B.I. Khazin, I.A. Koop, A.N. Kozyrev, A.S. Kuzmin, A.E. Kuzmenko, I.B. Logashenko, A.P. Lysenko, P.A. Lukin, K.Yu. Mikhailov, Yu.N. Pestov, E.A. Perevedentsev, S. Pirogov, S.G. Pivovarov, A.S. Popov, Yu.S. Popov, S.I. Redin, Yu.A. Rogovsky, A.A. Ruban, N.M. Ryskulov, A.E. Ryzhenkov, V.E. Shebalin, D.N. Shemyakin, B.A. Shwartz, D.B. Shwartz, A.L. Sibidanov, P.Yu. Shatunov, Yu.M. Shatunov, I.G. Snopkov, E.P. Solodov, V.M. Titov, A.A. Talyshev, A.I. Vorobiov, Yu.V. Yudin, A.S. Zaytsev (CMD-3 Collab.). Current status of the luminosity measurement with the

CMD-3 detector at the VEPP-2000 e^+e^- collider. // Nucl. Phys. Proc. Suppl. - 2012. - Vol.225-227. - p.69-71.

[335] S. Eidelman. Investigation of meson properties with the Belle detector. // EPJ Web of Conferences. - 2012. - Vol.37. - 01001.

[336] R.R. Akhmetshin, A.V. Anisyonkov, S.A. Anokhin, V.M. Aulchenko, V.S. Banzarov, L.M. Barkov, N.S. Bashtovoy, D.E. Berkaev, A.E. Bondar, A.V. Bragin, S.I. Eidelman, D.A. Epifanov, L.B. Epshteyn, G.V. Fedotovich, S.E. Gayazov, A.A. Grebenuk, D.N. Grigoriev, E.M. Gromov, F.V. Ignatov, S.V. Karpov, V.F. Kazanin, B.I. Khazin, I.A. Koop, A.N. Kozyrev, A.S. Kuzmin, A.E. Kuzmenko, I.B. Logashenko, A.P. Lysenko, P.A. Lukin, K.Yu. Mikhailov, Yu.N. Pestov, E.A. Perevedentsev, S. Pirogov, S.G. Pivovarov, A.S. Popov, Yu.S. Popov, S.I. Redin, Yu.A. Rogovsky, A.A. Ruban, N.M. Ryskulov, A.E. Ryzhenenkov, V.E. Shebalin, D.N. Shemyakin, B.A. Shwartz, D.B. Shwartz, A.L. Sibidanov, P.Yu. Shatunov, Yu.M. Shatunov, I.G. Snopkov, E.P. Solodov, V.M. Titov, A.A. Talyshev, A.I. Vorobiov, Yu.V. Yudina, A.S. Zaytsev (CMD-3 Collab.). Results from the e^+e^- colliders in Novosibirsk. // EPJ Web of Conferences. - 2012. - Vol.37. - 01009.

[337] V.V. Anashin, V.M. Aulchenko, E.M. Baldin, A.K. Barladyan, A.Yu. Barnyakov, M.Yu. Barnyakov, S.E. Baru, I.Yu. Basok, O.L. Beloborodova, A.E. Blinov, V.E. Blinov, A.V. Bobrov, V.S. Bobrovnikov, A.V. Bogomyagkov, A.E. Bondar, A.R. Buzykaev, S.I. Eidelman, D.N. Grigoriev, Yu.M. Glukhovchenko, V.V. Gulevich, D.V. Gusev, S.E. Karneev, G.V. Karpov, S.V. Karpov, T.A. Kharlamova, V.A. Kiselev, V.V. Kolmogorov, S.A. Kononov, K.Yu. Kotov, E.A. Kravchenko, V.F. Kulikov, G.Ya. Kurkin, E.A. Kuper, E.B. Levichev, D.A. Maksimov, V.M. Malyshev, A.L. Maslennikov, A.S. Medvedko, O.I. Meshkov, S.I. Mishnev, I.I. Morozov, N.Yu. Muchnoi, V.V. Neufeld, S.A. Nikitin, I.B. Nikolaev, I.N. Okunev, A.P. Onuchin, S.B. Oreshkin, I.O. Orlov, A.A. Osipov, S.V. Peleganchuk, S.G. Pivovarov, P.A. Piminov, V.V. Petrov, A.O. Poluektov, V.G. Prisekin, A.A. Ruban, V.K. Sandryev, G.A. Savinov, A.G. Shamov, D.N. Shatilov, B.A. Shwartz, E.A. Simonov, S.V. Sinyatkin, A.N. Skrinsky, V.V. Smaluk, A.V. Sokolov, A.M. Sukharev, E.V. Starostina, A.A. Talyshev, V.A. Tayursky, V.I. Telnov, Yu.A. Tikhonov, K.Yu. Todyshev, G.M. Tumaikin, Yu.V. Usov, A.I. Vorobiov, A.N. Yushkov, V.N. Zhilich, V.V. Zhulanov, A.N. Zhuravlev (KEDR Collab.). Recent results from the KEDR detector. // EPJ Web of Conferences. - 2012. - Vol.37. - 09014.

[338] Grishnyaev E.S., Polosatkin S.V. Estimation of yield of titanium neutron-generating target. // Atomic Energy. - 2012. - Vol.113, N.5. - p.276-280.

[339] Achasov M.N., Barnyakov A.Yu., Beloborodov K.I., Berdugin A.V., Berkaev D.E., Bogdanchikov A.G., Borisov A.A., Botov A.A., Bukin D.A., Dimova T.V., Druzhinin V.P., Golubev V.B., Grevtsov K.A., Kardapoltsev L.V., Kharlamov A.G., Koop I.A., Korol

A.A., Koshuba S.V., Kovrizhin D.P., Lysenko A.P., Martin K.A., Nesterenko I.N., Obrazovsky A.E., Pakhtusova E.V., Perevedentsev E.A., Rogovsky Yu.A., Romanov A.L., Serednyakov S.I., Shatunov Yu.M., Shatunov P.Yu., Shtol D.A., Silagadze Z.K., Skovpen K.Yu., Skrinsky A.N., Surin I.K., Tikhonov Yu.A., Usov Yu.V., Vasilyev A.V., Zemlyansky I.M. First results of SND experiments at VEPP-2000. // Nucl. Phys. B. Proc. Suppl. - 2012. - Vol. 225-227. - p.48-51.

[340] Achasov M.N., Barnyakov A.Yu., Beloborodov K.I., Berdugin A.V., Berkaev D.E., Bogdanchikov A.G., Borisov A.A., Botov A.A., Bukin D.A., Dimova T.V., Druzhinin V.P., Golubev V.B., Grevtsov K.A., Kardapoltsev L.V., Kharlamov A.G., Koop I.A., Korol A.A., Koshuba S.V., Kovrizhin D.P., Lysenko A.P., Martin K.A., Nesterenko I.N., Obrazovsky A.E., Pakhtusova E.V., Perevedentsev E.A., Rogovsky Yu.A., Romanov A.L., Serednyakov S.I., Shatunov Yu.M., Shatunov P.Yu., Shtol D.A., Silagadze Z.K., Skovpen K.Yu., Skrinsky A.N., Surin I.K., Tikhonov Yu.A., Usov Yu.V., Vasilyev A.V., Zemlyansky I.M. First results on the nucleon form factors from SND. // Nucl. Phys. B. Proc. Suppl. - 2012. - Vol. 225-227. - p.201-204.

[341] Achasov M.N., Aulchenko V.M., Barnyakov A.Yu., Beloborodov K.I., Berdugin A.V., Bogdanchikov A.G., Botov A.A., Bukin D.A., Golubev V.B., Grevtsov K.I., Dimova T.V., Druzhinin V.P., Kardapoltsev L.V., Kharlamov A.G., Kovrizhin D.P., A.A.Korol, Koshuba S.V., Kravchenko E.A., Martin K.A., Obrazovsky A.E., Onuchin A.P., Pakhtusova E.V., Serednyakov S.I., Shatunov Yu.M., Shtol D.A., Shukaev A.N., Silagadze Z.K., Skovpen K.Yu., Skrinsky A.N., Surin I.K., Tikhonov Yu.A., Usov Yu.V., Vasiljev A.V., Vesenev V.M. Spherical Neutral Detector for experiments at VEPP-2000 e^+e^- collider. // Nucl. Phys. B. Proc. Suppl. - 2012. - Vol.225-227. - p.66-68.

[342] Achasov M.N., Barnyakov A.Yu., Beloborodov K.I., Berdugin A.V., Berkaev D.E., Bogdanchikov A.G., Botov A.A., Bukin D.A., Vasiljev A.V., Golubev V.B., Grevtsov K.I., Dimova T.V., Druzhinin V.P., Kardapoltsev L.V., Kovrizhin D.P., Koop I.A., Korol A.A., Koshuba S.V., Kravchenko E.A., Martin K.A., Obrazovsky A.E., Otboev A.V., Pakhtusova E.V., Romanov A.L., Serednyakov S.I., Silagadze Z.K., Skovpen K.Yu., Skrinsky A.N., Surin I.K., Tikhonov Yu.A., Kharlamov A.G., Shatunov P.Yu., Shatunov Yu.M., Shtol D.A., Shwartz D.B., Zharinov Yu.M. First results of Spherical neutral detector (SND) experiments at VEPP-2000. // Progress in Particle and Nuclear Physics. - 2012. - Vol. 67. - p.594-598.

[343] Bashkirtsev A.G., Ivanov A.A., Kasatov D.A., et al. X-rays induced by high-voltage components of the tandem accelerator with vacuum insulation. // Medical Physics. - 2012. - N2. - p.5-11.

[344] Aleynik V.I., Kuznetsov A.S., Sorokin I.N., Taskaev S.Yu., Tiunov M.A., Schudlo I.M. Calibration of the charge-exchange target of the tandem accelerator with

vacuum insulation. // Vestnik NSTU, Novosibirsk, 2012 (in press).

[345] Vadim Byvaltsev, Vladimir Kanygin, Eugeny Belykh, Sergey Taskaev. Prospects in Boron Neutron Capture Therapy of Brain Tumors. // World Neurosurgery. 2012. - Vol.78, Issues 1-2. - p.8-9.rr

[346] Timofeev I.V.. Second harmonic electromagnetic emission of a turbulent magnetized plasma driven by a powerful electron beam. // Physics of Plasmas. - 2012. - Vol.19. - p.044501.

[347] Timofeev I.V. Two-dimensional simulations of nonlinear beam-plasma interaction in isotropic and magnetized plasmas. // Physics of Plasmas. - 2012. - Vol.19. - p.042108.rr

[348] Borodin A.V., Esaulkov M.N., Kuritsyn I.I., Kotelnikov I.A., Shkurinov A.P. On the role of photoionization in generation of terahertz radiation in the plasma of optical breakdown. // JOSA B. - 2012. - Vol.29, Iss. 8. - p.1911-1919.

[349] Kotelnikov I.A., Romé M. Electron cyclotron resonance near the axis of a quadrupole linear trap. // Phys. Plasmas. - 2012. - Vol.19, N12. - p.122509 [<http://dx.doi.org/10.1063/1.4772772><<http://link.aip.org/link/doi/10.1063/1.4772772>>].

[350] Waksman J., Anderson J.K., Nornberg M.D., Parke E., Reusch J.A., Liu D., Fiksel G., Davydenko V.I., Ivanov A.A., Stupishin N., Deichuli P.P., and Sakakita H. Neutral beam heating of a RFP plasma in MST. // Physics of Plasmas. 2012. - Vol.19. - p.122505.

[351] Ivanov A., Davydenko V. Diagnostic neutral beams for plasma studies in magnetic fusion devices. // In book: Fusion Physics /edited by Mitsuru Kikuchi, Karl Lackner, Minh Kuang Tran. - International Atomic Energy Agency, Vienna, 2012, p.435-438.

[352] Beklemishev A., Anikeev A., Burdakov A., Ivanov A., Ivanov I., Postupaev V., and Sinitsky S. GDT-based neutron source with multiple-mirror end plugs. // AIP Conf. Proc. - 2012. - 1442. - p.147-152.

[353] Beklemishev A.D., Burdakov A.V., Ivanov A.A., Kruglyakov E.P. Magnetic mirrors: history, results and future prospects. // Problems of Atomic Science and Technology, Series: Plasma Physics. - 2012. - Vol.6. - p.8-12.

[354] Lotov K.V. Optimum angle for side injection of electrons into linear plasma wakefields. // J. Plasma Phys. - 2012. - Vol.78, N4. - P.455-459.

[355] Pukhov A., Tuckmantel T., Kumar N., Upadhyay A., Lotov K., Khudik V., Siemon C., Shvets G., Muggli P., and Caldwell A. Principles of self-modulated proton driven plasma wake field acceleration. // AIP Conf. Proc. - 2012. - Vol.1507. - p.103-110.

[356] Hidding B., Rosenzweig J.B., Xi Y., O'Shea B., Andonian G., Schiller D., Barber S., Williams O., Pretzler G., Konigstein T., Kleeschulte F., Hogan M.J.,

Litos M., Corde C., White W.W., Muggli P., Bruhwiler D.L., and Lotov K. Beyond injection: Trojan horse underdense photocathode plasma wakefield acceleration. // AIP Conf. Proc. - 2012. - Vol.1507. - p.570-575.

[357] Yurov D.V., Anikeev A.V., Bagryansky P.A., Brednikhin S.A., Frolov S.A., Lezhnin S.I., and Prikhodko V.V. Parameters optimization in a hybrid system with a gas dynamic trap based neutron source. // Fusion Engineering and Design. - 2012. - Vol.87. - p.1684-1692.

[358] M.N. Achasov, V.M. Aulchenko, A.Yu. Barnyakov, K.I. Beloborodov, A.V. Berdyugin, D.E. Berkaev, A.G. Bogdanchikov, A.A. Borisov, A.A. Botov, D.A. Bukin T.V. Dimova, V.P. Druzhinin, V.B. Golubev, K.I. Grevtsov, L.V. Kardapoltsev, A.S. Kasaev, A.G. Kharlamov, A.N. Kirpotin, I.A. Koop, A.A. Korol, S.V. Koshuba, D.P. Kovrizhin, E.A. Kravchenko, K.A. Martin, A.E. Obrazovsky, A.P. Onuchin, A.V. Otboev, E.V. Pakhtusova, Yu.A. Rogovsky, S.I. Serebnyakov, Yu.M. Shatunov, D.A. Shtol, D.B. Shwartz, Z.K. Silagadze, K.Yu. Skovpen, A.N. Skrinsky, I.K. Surin, Yu.A. Tikhonov, Yu.V. Usov, A.V. Vasiljev. Recent results from SND experiment at VEPP-2000 collider. // Eur. Phys J. (Web Conf.). - 2012. - Vol.37. - p.09020.

[359] Berkaev D., Kirpotin A., Koop I., Lysenko A., Nesterenko I., Otboev A., Perevedentsev E., Rogovsky Yu., Romanov A., Shatunov P., Shatunov Yu., Shwartz D., Skrinsky A., Zemlyansky I. VEPP-2000 operation with round beams in the energy range from 1 GeV to 2 GeV. // Nucl. Phys. Proc. Suppl. - 2012. - Vol.225-227. - 303-308.

[360] M.N. Achasov, A.Yu. Barnyakov, K.I. Beloborodov, A.V. Berdyugin, D.E. Berkaev, A.G. Bogdanchikov, A.A. Botov, D.A. Bukin, A.V. Vasiljev, V.B. Golubev T.V. Dimova, V.P. Druzhinin, I.M. Zemlyansky, L.V. Kardapoltsev, D.P. Kovrizhin, I.A. Koop, A.A. Korol, S.V. Koshuba, K.A. Martin, A.E. Obrazovsky, E.V. Pakhtusova, Yu.A. Rogovsky, A.L. Romanov, S.I. Serebnyakov, Z.K. Silagadze, K.Yu. Skovpen, A.N. Skrinsky, I.K. Surin, Yu.A. Tikhonov, Yu.V. Usov, A.G. Kharlamov, P.Yu. Shatunov, Yu.M. Shatunov, D.B. Shvarts, D.A. Shtol. Measurement of the cross section for the $e^+e^- \rightarrow \omega\pi^0 \rightarrow \pi^0\pi^0\gamma$ process in the energy range of 1.1 - 1.9-GeV. Published in JETP Lett. 94 (2012) 2.

[361] Aad G., ATLAS Collab., Anisenkov A., Beloborodova O., Bobrovnikov V.S., Bogdanchikov A., Kazanin V.F., Kolachev G.M., Korol A., Malyshev V., Maslennikov A.L., Maximov D.A., Orlov I., Peleganchuk S.V., Schamov A.G., Skovpen K., Soukharev A., Talyshev A., Tikhonov Y.A., Zaytsev A., et al. Search for the Higgs boson in the $H \rightarrow WW \rightarrow l\nu jj$ decay channel at $\sqrt{s}=7$ TeV with the ATLAS detector. // Phys. Lett. B. - 2012. - V.718. - p.391-410.

[362] Aad G., ATLAS Collab., Anisenkov A., Beloborodova O., Bobrovnikov V.S., Bogdanchikov A.,

Kazanin V.F., Kolachev G.M., Korol A., Malyshev V., Maslennikov A.L., Maximov D.A., Orlov I., Peleganchuk S.V., Schamov A.G., Skovpen K., Soukharev A., Talyshev A., Tikhonov Y.A., Zaytsev A., et al. Search for the Standard Model Higgs boson produced in association with a vector boson and decaying to a b-quark pair with the ATLAS detector. // Phys. Lett. B. - 2012. - V.718. - p.369-390.

[363] ATLAS Collab., Anisenkov A., Beloborodova O., Bobrovnikov V.S., Bogdanchikov A., Kazanin V.F., Kolachev G.M., Korol A., Malyshev V., Maslennikov A.L., Maximov D.A., Orlov I., Peleganchuk S.V., Shamov A.G., Skovpen K., Soukharev A., Talyshev A., Tikhonov Y.A., Zaytsev A., et al. Measurement of WZ Production in proton-proton collisions at $\sqrt{s} = 7$ TeV with the ATLAS detector. // Eur. Phys. J. C. - 2012. - V.72. - p.2173 (27 p.).

[364] ATLAS Collab., Anisenkov A., Beloborodova O., Bobrovnikov V.S., Bogdanchikov A., Kazanin V.F., Kolachev G.M., Korol A., Malyshev V., Maslennikov A.L., Maximov D.A., Orlov I., Peleganchuk S.V., Shamov A.G., Skovpen K., Soukharev A., Talyshev A., Tikhonov Y.A., Zaytsev A., et al. Search for top and bottom squarks from gluino pair production in final states with missing transverse energy and at least three b-jets with the ATLAS detector. // Eur. Phys. J. C. - 2012. - V.72. - p.2174 (22 p.).

[365] ATLAS Collab., Anisenkov A., Beloborodova O., Bobrovnikov V.S., Bogdanchikov A., Kazanin V.F., Kolachev G.M., Korol A., Malyshev V., Maslennikov A.L., Maximov D.A., Orlov I., Peleganchuk S.V., Shamov A.G., Skovpen K., Soukharev A., Talyshev A., Tikhonov Y.A., Zaytsev A., et al. Measurement of event shapes at large momentum transfer with the ATLAS detector in pp collisions at $\sqrt{s} = 7$ TeV. // Eur. Phys. J. C. - 2012. - V.72. - p.2211 (25 p.).

[366] ATLAS Collab., Anisenkov A., Beloborodova O., Bobrovnikov V.S., Bogdanchikov A., Kazanin V.F., Kolachev G.M., Korol A., Malyshev V., Maslennikov A.L., Maximov D.A., Orlov I., Peleganchuk S.V., Shamov A.G., Skovpen K., Soukharev A., Talyshev A., Tikhonov Y.A., Zaytsev A., et al. Search for supersymmetry in events with large missing transverse momentum, jets, and at least one tau lepton in 7 TeV proton-proton collision data with the ATLAS Detector. // Eur. Phys. J. C. - 2012. - V.72. - p.2215 (25 p.).

[367] ATLAS Collab., Anisenkov A., Beloborodova O., Bobrovnikov V.S., Bogdanchikov A., Kazanin V.F., Kolachev G.M., Korol A., Malyshev V., Maslennikov A.L., Maximov D.A., Orlov I., Peleganchuk S.V., Shamov A.G., Skovpen K., Soukharev A., Talyshev A., Tikhonov Y.A., Zaytsev A., et al. Search for light scalar top quark pair production in final states with two leptons with the ATLAS detector in $\sqrt{s} = 7$ TeV proton-proton collisions. // Eur. Phys. J. C. - 2012. - V.72. - p.2237 (21 p.).

[368] ATLAS Collab., Anisenkov A., Beloborodova O., Bobrovnikov V.S., Bogdanchikov A., Kazanin V.F., Kolachev G.M., Korol A., Malyshev V., Maslennikov A.L., Maximov D.A., Orlov I., Peleganchuk S.V., Shamov A.G., Skovpen K., Soukharev A., Talyshev A., Tikhonov Y.A., Zaytsev A., et al. ATLAS search for a heavy gauge boson decaying to a charged lepton and a neutrino in pp collisions at $\sqrt{s} = 7$ TeV. // Eur. Phys. J. C. - 2012. - V.72. - p.2241 (25 p.).

[369] ATLAS Collab., Anisenkov A., Beloborodova O., Bobrovnikov V.S., Bogdanchikov A., Kazanin V.F., Kolachev G.M., Korol A., Malyshev V., Maslennikov A.L., Maximov D.A., Orlov I., Peleganchuk S.V., Shamov A.G., Skovpen K., Soukharev A., Talyshev A., Tikhonov Y.A., Zaytsev A., et al. Search for doubly-charged Higgs bosons in like-sign dilepton final states at $\sqrt{s} = 7$ TeV with the ATLAS detector. // Eur. Phys. J. C. - 2012. - V.72. - p.2244 (19 p.).

[370] Aad G., ATLAS Collab., Anisenkov A., Beloborodova O., Bobrovnikov V.S., Bogdanchikov A., Kazanin V.F., Kolachev G.M., Korol A., Malyshev V., Maslennikov A.L., Orlov I., Peleganchuk S.V., Shamov A.G., Skovpen K., Soukharev A., Talyshev A., Tikhonov Y.A., Zaytsev A., et al. Search for magnetic monopoles in $\sqrt{s} = 7$ TeV pp collisions with the ATLAS detector. // Phys. Rev. Lett. - 2012. - V.109. - p.261803-1-18.

[371] Aad G., ATLAS Collab., Anisenkov A., Beloborodova O., Bobrovnikov V.S., Bogdanchikov A., Kazanin V.F., Kolachev G.M., Korol A., Malyshev V., Maslennikov A.L., Maximov D.A., Orlov I., Peleganchuk S.V., Shamov A.G., Skovpen K., Soukharev A., Talyshev A., Tikhonov Y.A., Zaytsev A., et al. Search for a supersymmetric partner to the top quark in final states with jets and missing transverse momentum at $\sqrt{s} = 7$ TeV with the ATLAS. // Phys. Rev. Lett. - 2012. - V.109. - p.211802.

[372] Aad G., ATLAS Collab., Anisenkov A., Beloborodova O., Bobrovnikov V.S., Bogdanchikov A., Kazanin V.F., Kolachev G.M., Korol A., Malyshev V., Maslennikov A.L., Maximov D.A., Orlov I., Peleganchuk S.V., Shamov A.G., Skovpen K., Soukharev A., Talyshev A., Tikhonov Y.A., Zaytsev A., et al. Search for direct top squark pair production in final states with one isolated lepton, jets, and missing transverse momentum in $\sqrt{s} = 7$ TeV pp collisions using 4.7 fb⁻¹ of ATLAS data. // Phys. Rev. Lett. - 2012. - V.109. - p.211803.

[373] Aad G., ATLAS Collab., Beloborodova O., Bobrovnikov V.S., Bogdanchikov A., Kazanin V.F., Kolachev G.M., Korol A., Malyshev V., Maslennikov A.L., Maximov D.A., Orlov I., Peleganchuk S.V., Shamov A.G., Skovpen K., Soukharev A., Talyshev A., Tikhonov Y.A., Zaytsev A., et al. Measurement of inclusive jet and dijet production in pp collisions at $\sqrt{s} = 7$ TeV using the ATLAS detector. // Phys. Rev. D. - 2012. - V.86. - p.014022.

[374] Aad G., ATLAS Collab., Beloborodova O., Bobrovnikov V.S., Bogdanchikov A., Kazanin V.F., Kolachev G.M., Korol A., Malyshev V., Maslennikov A.L., Maximov D.A., Orlov I., Peleganchuk S.V., Shamov A.G., Skovpen K., Soukharev A., Talyshev A., Tikhonov Y.A., Zaytsev A., et al. Search for pair-produced heavy quarks decaying to Wq in the two-lepton channel at ATLAS at $\sqrt{s} = 7$ TeV. // Phys. Rev. D. - 2012. - V.86. - p.012007.

[375] Aad G., ATLAS Collab., Anisenkov A., Beloborodova O., Bobrovnikov V.S., Bogdanchikov A., Kazanin V.F., Kolachev G.M., Korol A., Malyshev V., Maslennikov A.L., Maximov D.A., Orlov I., Peleganchuk S.V., Schamov A.G., Skovpen K., Soukharev A., Talyshev A., Tikhonov Y.A., Zaytsev A., et al. Measurement of the azimuthal ordering of charged hadrons with the ATLAS detector. // Phys. Rev. D. - 2012. - V.86. - p.052005.

[376] Aad G., ATLAS Collab., Anisenkov A., Beloborodova O., Bobrovnikov V.S., Bogdanchikov A., Kazanin V.F., Kolachev G.M., Korol A., Malyshev V., Maslennikov A.L., Maximov D.A., Orlov I., Peleganchuk S.V., Schamov A.G., Skovpen K., Soukharev A., Talyshev A., Tikhonov Y.A., Zaytsev A., et al. ATLAS measurements of the properties of jets for boosted particle searches. // Phys. Rev. D. - 2012. - V.86. - p.072006.

[377] Aad G., ATLAS Collab., Anisenkov A., Beloborodova O., Bobrovnikov V.S., Bogdanchikov A., Kazanin V.F., Kolachev G.M., Korol A., Malyshev V., Maslennikov A.L., Maximov D.A., Orlov I., Peleganchuk S.V., Schamov A.G., Skovpen K., Soukharev A., Talyshev A., Tikhonov Y.A., Zaytsev A., et al. Underlying event characteristics and their dependence on jet size of charged-particle jet events in pp collisions at $\sqrt{s} = 7$ TeV with the ATLAS detector. // Phys. Rev. D. - 2012. - V.86. - p.072004.

[378] Aad G., ATLAS Collab., Anisenkov A., Beloborodova O., Bobrovnikov V.S., Bogdanchikov A., Kazanin V.F., Kolachev G.M., Korol A., Malyshev V., Maslennikov A.L., Maximov D.A., Orlov I., Peleganchuk S.V., Shamov A.G., Skovpen K., Soukharev A., Talyshev A., Tikhonov Y.A., Zaytsev A., et al. Further search for supersymmetry at $\sqrt{s} = 7$ TeV in final states with jets, missing transverse momentum and isolated leptons with the ATLAS detector. // Phys. Rev. D. - 2012. - V.86. - p.092002.

[379] Aad G., ATLAS Collab., Anisenkov A., Beloborodova O., Bobrovnikov V.S., Bogdanchikov A., Kazanin V.F., Kolachev G.M., Korol A., Malyshev V., Maslennikov A.L., Maximov D.A., Orlov I., Peleganchuk S.V., Shamov A.G., Skovpen K., Soukharev A., Talyshev A., Tikhonov Y.A., Zaytsev A., et al. Search for top-jet resonances in the lepton+jets channel of $tt + \text{jets}$ events with the ATLAS detector in 4.7 fb^{-1} of pp collisions at $\sqrt{s} = 7$ TeV. // Phys. Rev. D. - 2012. - V.86. - p.091103.

[380] Aad G., ATLAS Collab., Anisenkov A., Beloborodova O., Bobrovnikov V.S., Bogdanchikov A., Kazanin V.F., Kolachev G.M., Korol A., Malyshev V., Maslennikov A.L., Maximov D.A., Orlov I., Peleganchuk S.V., Schamov A.G., Skovpen K., Soukharev A., Talyshev A., Tikhonov Y.A., Zaytsev A., et al. Measurement of the cross section for top-quark pair production in pp collisions at $\sqrt{s} = 7$ TeV with the ATLAS detector using final states with two high-pT leptons. // JHEP. - 2012. - Vol 1205. - p. 059.

[381] Aad G., ATLAS Collab., Anisenkov A., Beloborodova O., Bobrovnikov V.S., Bogdanchikov A., Kazanin V.F., Kolachev G.M., Korol A., Malyshev V., Maslennikov A.L., Maximov D.A., Orlov I., Peleganchuk S.V., Schamov A.G., Skovpen K., Soukharev A., Talyshev A., Tikhonov Y.A., Zaytsev A., et al. Search for same-sign top quark production and fourth-generation down-type quarks in pp collisions at $\sqrt{s} = 7$ TeV with the ATLAS detector. // JHEP. - 2012. - Vol 1204. - p.069.

[382] Aad G., ATLAS Collab., Anisenkov A., Beloborodova O., Bobrovnikov V.S., Bogdanchikov A., Kazanin V.F., Kolachev G.M., Korol A., Malyshev V., Maslennikov A.L., Maximov D.A., Orlov I., Peleganchuk S.V., Schamov A.G., Skovpen K., Soukharev A., Talyshev A., Tikhonov Y.A., Zaytsev A., et al. Forward-backward correlations and charged-particle azimuthal distributions in pp interactions using the ATLAS detector. // JHEP. - 2012. - Vol 1207. - p.019.

[383] Aad G., ATLAS Collab., Anisenkov A., Beloborodova O., Bobrovnikov V.S., Bogdanchikov A., Kazanin V.F., Kolachev G.M., Korol A., Malyshev V., Maslennikov A.L., Maximov D.A., Orlov I., Peleganchuk S.V., Schamov A.G., Skovpen K., Soukharev A., Talyshev A., Tikhonov Y.A., Zaytsev A., et al. Measurement of inclusive two-particle angular correlations in pp collisions with the ATLAS detector at the LHC. // JHEP. - 2012. - Vol 1205. - p.157.

[384] Aad G., ATLAS Collab., Anisenkov A., Beloborodova O., Bobrovnikov V.S., Bogdanchikov A., Kazanin V.F., Kolachev G.M., Korol A., Malyshev V., Maslennikov A.L., Maximov D.A., Orlov I., Peleganchuk S.V., Schamov A.G., Skovpen K., Soukharev A., Talyshev A., Tikhonov Y.A., Zaytsev A., et al. Jet mass and substructure of inclusive jets in $\sqrt{s} = 7$ TeV pp collisions with the ATLAS experiment. // JHEP. - 2012. - Vol 1205. - p.128.

[385] Aad G., ATLAS Collab., Anisenkov A., Beloborodova O., Bobrovnikov V.S., Bogdanchikov A., Kazanin V.F., Kolachev G.M., Korol A., Malyshev V., Maslennikov A.L., Maximov D.A., Orlov I., Peleganchuk S.V., Schamov A.G., Skovpen K., Soukharev A., Talyshev A., Tikhonov Y.A., Zaytsev A., et al. Search for charged Higgs bosons decaying via $H^+ \rightarrow \text{tau} + \nu$ in $t\bar{t}$ events using 4.6 fb^{-1} of pp collision data at $\sqrt{s} = 7$ TeV with the ATLAS detector. // JHEP. - 2012. - Vol 1206. - p.039.

[386] Aad G., ATLAS Collab., Anisenkov A., Beloborodova O., Bobrovnikov V.S., Bogdanchikov A., Kazanin V.F., Kolachev G.M., Korol A., Malyshev V., Maslennikov A.L., Maximov D.A., Orlov I., Peleganchuk S.V., Schamov A.G., Skovpen K., Soukharev A., Talyshev A., Tikhonov Y.A., Zaytsev A., et al. Measurement of W boson polarization in top quark decays with the ATLAS detector. // JHEP. - 2012. - Vol.1206. - p.088.

[387] Aad G., ATLAS Collab., Anisenkov A., Beloborodova O., Bobrovnikov V.S., Bogdanchikov A., Kazanin V.F., Kolachev G.M., Korol A., Malyshev V., Maslennikov A.L., Maximov D.A., Orlov I., Peleganchuk S.V., Schamov A.G., Skovpen K., Soukharev A., Talyshev A., Tikhonov Y.A., Zaytsev A., et al. A search for flavour changing neutral currents in top-quark decays in pp collision data collected with the ATLAS detector at $\sqrt{s} = 7$ TeV. // JHEP. - 2012. - Vol 1206. - p.139.

[388] Aad G., ATLAS Collab., Anisenkov A., Beloborodova O., Bobrovnikov V.S., Bogdanchikov A., Kazanin V.F., Kolachev G.M., Korol A., Malyshev V., Maslennikov A.L., Maximov D.A., Orlov I., Peleganchuk S.V., Schamov A.G., Skovpen K., Soukharev A., Talyshev A., Tikhonov Y.A., Zaytsev A., et al. Hunt for new phenomena using large jet multiplicities and missing transverse momentum with ATLAS in 4.7fb^{-1} of $\sqrt{s} = 7$ TeV proton-proton collisions. // JHEP. - 2012. - Vol.1207. - p.167.

[389] Aad G., ATLAS Collab., Anisenkov A., Beloborodova O., Bobrovnikov V.S., Bogdanchikov A., Kazanin V.F., Kolachev G.M., Korol A., Malyshev V., Maslennikov A.L., Maximov D.A., Orlov I., Peleganchuk S.V., Schamov A.G., Skovpen K., Soukharev A., Talyshev A., Tikhonov Y.A., Zaytsev A., et al. Search for the Standard Model Higgs boson in the H to $\tau^+ \tau^-$ decay mode in $\sqrt{s} = 7$ TeV pp collisions with ATLAS. // JHEP. - 2012. - Vol 1209. - p.070.

[390] Aad G., ATLAS Collab., Anisenkov A., Beloborodova O., Bobrovnikov V.S., Bogdanchikov A., Kazanin V.F., Kolachev G.M., Korol A., Malyshev V., Maslennikov A.L., Maximov D.A., Orlov I., Peleganchuk S.V., Schamov A.G., Skovpen K., Soukharev A., Talyshev A., Tikhonov Y.A., Zaytsev A., et al. A search for $t\bar{t}$ resonances in lepton+jets events with highly boosted top quarks collected in pp collisions at $\sqrt{s} = 7$ TeV with the ATLAS detector. // JHEP. - 2012. - Vol.1209. - p. 041.

[391] Aad G., ATLAS Collab., Anisenkov A., Beloborodova O., Bobrovnikov V.S., Bogdanchikov A., Kazanin V.F., Kolachev G.M., Korol A., Malyshev V., Maslennikov A.L., Maximov D.A., Orlov I., Peleganchuk S.V., Schamov A.G., Skovpen K., Soukharev A., Talyshev A., Tikhonov Y.A., Zaytsev A., et al. Measurements of the pseudorapidity dependence of the total transverse energy in proton-proton collisions at $\sqrt{s} = 7$ TeV with ATLAS. // JHEP11. - 2012. - p.033.

[392] Aad G., ATLAS Collab., Anisenkov A., Beloborodova O., Bobrovnikov V.S., Bogdanchikov A., Kazanin V.F., Kolachev G.M., Korol A., Malyshev V., Maslennikov A.L., Maximov D.A., Orlov I., Peleganchuk S.V., Schamov A.G., Skovpen K., Soukharev A., Talyshev A., Tikhonov Y.A., Zaytsev A., et al. Search for a heavy top-quark partner in final states with two leptons with the ATLAS detector at the LHC. // JHEP11. - 2012. - p.094.

[393] Aad G., ATLAS Collab., Anisenkov A., Beloborodova O., Bobrovnikov V.S., Bogdanchikov A., Kazanin V.F., Kolachev G.M., Korol A., Malyshev V., Maslennikov A.L., Maximov D.A., Orlov I., Peleganchuk S.V., Schamov A.G., Skovpen K., Soukharev A., Talyshev A., Tikhonov Y.A., Zaytsev A., et al. Search for high-mass resonances decaying to dilepton final states in pp collisions at $\sqrt{s} = 7$ TeV with the ATLAS detector. // JHEP11. - 2012. - p.138.

[394] Aad G., ATLAS Collab., Anisenkov A., Beloborodova O., Bobrovnikov V.S., Bogdanchikov A., Kazanin V.F., Kolachev G.M., Korol A., Malyshev V., Maslennikov A.L., Maximov D.A., Orlov I., Peleganchuk S.V., Schamov A.G., Skovpen K., Soukharev A., Talyshev A., Tikhonov Y.A., Zaytsev A., et al. Search for anomalous production of prompt like-sign lepton pairs at $\sqrt{s} = 7$ TeV with the ATLAS detector. // JHEP12. - 2012. - p.007.

[395] Aad G., ATLAS Collab., Anisenkov A., Beloborodova O., Bobrovnikov V.S., Bogdanchikov A., Kazanin V.F., Kolachev G.M., Korol A., Malyshev V., Maslennikov A.L., Maximov D.A., Orlov I., Peleganchuk S.V., Schamov A.G., Skovpen K., Soukharev A., Talyshev A., Tikhonov Y.A., Zaytsev A., et al. Time dependent angular analysis of the decay $B_s \rightarrow J/\psi \phi$ and extraction of $\Delta\Gamma_s$ and the CP-violating weak phase ϕ_s by ATLAS. // JHEP12. - 2012. - p.072.

[396] Aad G., ATLAS Collab., Anisenkov A., Beloborodova O., Bobrovnikov V.S., Bogdanchikov A., Kazanin V.F., Kolachev G.M., Korol A., Malyshev V., Maslennikov A.L., Maximov D.A., Orlov I., Peleganchuk S.V., Schamov A.G., Skovpen K., Soukharev A., Talyshev A., Tikhonov Y.A., Zaytsev A., et al. Search for pair production of massive particles decaying into three quarks with the ATLAS detector in $\sqrt{s} = 7$ TeV pp collisions at the LHC. // JHEP12. - 2012. - p. 086.

[397] Aad G., ATLAS Collab., Anisenkov A., Beloborodova O., Bobrovnikov V.S., Bogdanchikov A., Kazanin V.F., Kolachev G.M., Korol A., Malyshev V., Maslennikov A.L., Maximov D.A., Orlov I., Peleganchuk S.V., Schamov A.G., Skovpen K., Soukharev A., Talyshev A., Tikhonov Y.A., Zaytsev A., et al. Search for R-parity-violating supersymmetry in events with four or more leptons in $\sqrt{s} = 7$ TeV pp collisions with the ATLAS detector. // JHEP12. - 2012. - p.124.

[398] Aad G., ATLAS Collab., Anisenkov A., Beloborodova O., Bobrovnikov V.S., Bogdanchikov A., Kazanin V.F., Kolachev G.M., Korol A., Malyshev V.,

- Maslennikov A.L., Maximov D.A., Orlov I., Peleganchuk S.V., Schamov A.G., Skovpen K., Soukharev A., Talyshv A., Tikhonov Y.A., Zaytsev A., et al. A measurement of the material in the ATLAS inner detector using secondary hadronic interactions. // JINST. - 2012. - Vol.7. - P01013.
- [399] Aad G., ATLAS Collab., Anisenkov A., Beloborodova O., Bobrovnikov V.S., Bogdanchikov A., Kazanin V.F., Kolachev G.M., Korol A., Malyshev V., Maslennikov A.L., Maximov D.A., Orlov I., Peleganchuk S.V., Schamov A.G., Skovpen K., Soukharev A., Talyshv A., Tikhonov Y.A., Zaytsev A., et al. Measurement of the b-hadron production cross section using decays to $D^*\mu X$ final states in pp collisions at $\sqrt{s} = 7$ TeV with the ATLAS detector. // Nucl. Phys. B. - 2012. - Vol. 864. - p.341-381.
- [400] Gramolin A.V., Arrington J., Barkov L.M., Dmitriev V.F., Gauzshtein V.V., Golovin R.A., Holt R.J., Kaminsky V.V., Lazarenko B.A., Mishnev S.I., Muchnoi N.Yu., Neufeld V.V., Nikolenko D.M., Rachek I.A., Sadykov R.Sh., Shestakov Yu.V., Stibunov V.N., Toporkov D.K., de Vries H., Zevakov S.A., Zhilich V.N. Measurement of the two-photon exchange contribution in elastic ep scattering at VEPP-3. // Nuclear Physics B (Proc. Suppl.). - 2012. - Vol.225-227. - p.216-220. [arXiv:1112.5369 [nucl-ex].
- [401] Gauzshtein V.V., Dusaev R.R., Zevakov S.A., Loginov A.Yu., Nikolenko D.M., Rachek I.A., Sidorov A.A., Stibunov V.N., Toporkov D.K., Fiks A.I., Shestakov Yu.V. Investigation of tensor analyzing power in the reaction of photoproduction of pi-minus mesons on a deuteron. // Academy news. Physics - 2012 - V.55, N11/2. - p.5-10 (in Russian).
- [402] Ruktuev A.A., Golkovski M.G., Kuksanov N.K., Bataev I.A., Zhuravina T.V., Veselov S.V., Bataev V.A., Bataev A.A.. Metallographic features of Ti – Ta – Nb coats, fused deposited on the titanium substrate by extracted in atmosphere electron beam with 1.4 MeV electrons energy. // Electrotechnica & Electronica E+E. - 2012 (Published by The Union of Electronics, Electrical Engineering and Telecommunications, Bulgaria). - Vol.47, N5-6. - p.223-228.
- [403] Bataev I.A., Bataev A.A., Golkovski M.G., Tepliukh A.M., Burov V.G., Veselov S.V. Non-vacuum electron-beam boriding of low-carbon steel. // Surface & Coatings Technology. - 2012. - Vol.207. - p.245-253.
- [404] Bataev I.A., Golkovsky M.G., Zhuravina T.V., Ruktuev A.A., Samoylenko V.V. Corrosion resistance of Ti-Ta layers, formed by out-of-vacuum electron-beam deposition of a powder mixture onto the CP titanium plates. // Polzunovsky Vestnik. - 2012. - N3/1. - p.80-84. <http://elibrary.ru/item.asp?id=18372507> (in Russian).
- [405] Poletika I.M., Krylov T.A., Ivanov Yu.F., Golkovsky M.V., Kitler V.D., Teresov A.D., Makarov S.A. Formation of hardening of nanostructured coatings by electron-beam processing. // Physical Chemistry of Surfaces and Protection of Materials. - 2012. - Vol.48, N2. - p.201-212 (in Russian).
- [406] Tolochko B.P., Antokhin E.I., Yukhin Yu.M., Eliseev V.S., Golkovsky M.G., Lyakhov N.Z. A method for producing ultrafine bismuth powder. // Patent RU 2426625 C1, application: 2010117096/02 of 29.04.2010.
- [407] Golkovsky M.G., Chakin I.K., Prozorenko P.S., Bataev A.A., Bataev V.A., Zhuravina T.V. Method of anticorrosive coat at titanic goods. // Positive decision for Patent application № 2010128692/02(040721), application date 09.07.2010.
- [408] Babailov S.P., Goryunova A.V., Dudnikov A.V. Magnitrezonansnye termosensornye reagenty na osnove paramagnitnykh trisdiiizobutil-ditiofosfatnykh kompleksov evropia (iii) s 2.2-bipiridilom dlya kontrolya temperatury v rastvorah. // Journal of Structural Chemistry – in press.
- [409] Г.Б. Bekhtenev E.A., Karpov G.V. Automated stand for measurements of electrostatic beam position parameters. // Vestnik NSU. Novosibirsk. Ser.: Physics. - 2012. - Vol.7, N4. - p.49.
- [410] Smaluk V., Sukhanov D., Oreshonok V., Cherepanov V., and Kiselev V. Feedback for suppression of single-bunch transverse instability in electron-positron storage rings. // Journal of Instrumentation. - Jan 2012, Vol. 7. - P01007.
- [411] Volk I., Hansen S., Johnson T., Jostlein H., Kiper T., Shiltsev V., Chupyr A., Kondaurov M., Medvedko A., Parkhomchuk V., Singatulin S., Stetler L., Van Beek J., Fratta D., Roberts J., Wang H. Hydrostatic level sensors as high precision ground motion instrumentation for Tevatron and other energy frontier accelerators. // Journal of Instrumentation (JINST). - 2012. - Vol.7. - P01004.
- [412] Belikov O.V., Veremeenko V.F., Kozak V.R., Medvedko A.S., Kuper E.A. CEAC controllers family for control of power supplies of accelerator facilities. // Novosibirsk. Vestnik NSU. Ser.: Physics, 2012. - Vol.7, N4. - p.43-48.
- [413] Abakumova E., Anashin V., Balewski K., Boespflug R., Gusev G., Levichev E., Krasnov A., Kuzminykh V., Nagorny B., Pupkov Yu., Semenov A., Smaluk V., Tischer M., Wedekind H.-P., Zapfe K., Zhukov A., Zolotarev K. Performance of the vacuum system for the PETRA III damping wiggler section. // Vacuum. - February 2012. - Vo.86, Issue 7. - p.822-826.
- [414] Abakumova E., Ahasov M., Dong H., Qu H., Krasnov A., Kosarev A., Muchnoi N., Pyata E., Xiao Q., Mo X., Wang Y., Zhukov A. Vacuum chamber for the measurement system of the beam energy. // Physics Procedia, The 18th International Vacuum Congress (IVC-18). - 2012. - Vol.32. - p..753-756.
- [415] Anashin V., Bozhko Y., Belova L., Boeckmann T., Kholopov M., Konstantinov V., Petersen B., Pivovarov S., Pyata E., Sellmann D., Wang X.L., Zhimov A., Zolotov A. Test stands for testing serial XFEL

accelerator modules. // *Advances in Cryogenic Engineering*, Vols 57A and 57B. Book Series: AIP Conference Proceedings, Volume: 1434, Pages: 1100-1107 DOI: 10.1063/1.4707030, Published: 2012.

[416] Valishev A., Alexahin Yu., Lebedev V., Shatilov D. Simulation of beam-beam effects and Tevatron experience. // *JINST (Proc. of EPAC08, Genoa, Italy)*. - 2012. - Vol.7. - P12002. [<http://accelconf.web.cern.ch/AccelConf/e08/papers/thym01.pdf>].

[417] Ablikim M., BESIII Collab., Achasov M.N., Muchnoi N., Nikolaev I., et al. Precision measurements of branching fractions for $\psi \rightarrow \pi^0 J/\psi$ and $\eta J/\psi$. // *Phys. Rev. D*. - 2012. - Vol.86. - p.092008. [arXiv:1210.3746 [hep-ex]].

[418] Ablikim M., BESIII Collab., Achasov M.N., Muchnoi N., Nikolaev I., et al. Study of $\psi(3686) \rightarrow \pi^0 h_c$, $h_c \rightarrow \gamma \eta_c$ via η_c exclusive decays. // *Phys. Rev. D*. - 2012. - Vol.86. - p.092009. [arXiv:1209.4963 [hep-ex]].

[419] M.N. Achasov, V.E. Blinov, Xiao Cai, Cheng-Dong Fu, ..., N.Yu. Muchnoi, I.B. Nikolaev, A.G. Shamov, K.Yu. Todyshev, et al. A scenario for high accuracy tau mass measurement at BEPC-II. // *Chin. Phys. C*. - 2012. - Vol.36. - p.573-577. [<http://inspirehep.net/record/1182384>].

[420] Ablikim M., BESIII Collab., Achasov M.N., Muchnoi N., Nikolaev I., et al. Measurement of χ_{cJ} decaying into $p \bar{n}$ and $p \bar{n} \pi^- \pi^0$. // *Phys. Rev. D*. - 2012. - Vol.86. - p.052011. [arXiv:1208.3721 [hep-ex]].

[421] Ablikim M., BESIII Collab., Achasov M.N., Muchnoi N., Nikolaev I., et al. Experimental study of ψ' decays to $K^+ K^- \pi^0$ and $K^+ K^- \eta$. // *Phys. Rev. D*. - 2012. - Vol.86. - p.072011. [arXiv:1208.2320 [hep-ex]].

[422] Ablikim M., BESIII Collab., Achasov M.N., Muchnoi N., Nikolaev I., et al. Observation of $e^+ e^- \rightarrow \eta J/\psi$ at center-of-mass energy $\sqrt{s} = 4.009$ GeV. // *Phys. Rev. D*. - 2012. - Vol.86. - p.071101. [arXiv:1208.1857 [hep-ex]].

[423] Ablikim M., BESIII Collab., Achasov M.N., Muchnoi N., Nikolaev I., et al. Observation of χ_{cJ} decays to $\Lambda \bar{\Lambda} \pi^+ \pi^-$. // *Phys. Rev. D*. - 2012. - Vol.86. - p.052004. [arXiv:1207.5646 [hep-ex]].

[424] Ablikim M., BESIII Collab., Achasov M.N., Muchnoi N., Nikolaev I., et al. Determination of the number of J/ψ events with $J/\psi \rightarrow$ inclusive decays. // *Chin. Phys. C*. - 2012. - Vol.36. - p.915-925.

[425] Ablikim M., BESIII Collab., Achasov M.N., Muchnoi N., Nikolaev I., et al. First observation of the isospin violating decay $J/\psi \rightarrow \Lambda \bar{\Sigma}^0 + c.c.$ // *Phys. Rev. D*. - 2012. - Vol.86. - p.032008. [arXiv:1207.1201 [hep-ex]].

[426] Ablikim M., BESIII Collab., Achasov M.N., Muchnoi N., Nikolaev I., et al. Study of $J/\psi \rightarrow p \bar{p}$ and

$J/\psi \rightarrow n \bar{n}$. // *Phys. Rev. D*. - 2012. - Vol.86. - p.032014. [arXiv:1205.1036 [hep-ex]].

[427] Ablikim M., BESIII Collab., Achasov M.N., Muchnoi N., Nikolaev I., et al. Evidence for the direct two-photon transition from $\psi(3686)$ to J/ψ . // *Phys. Rev. Lett.* - 2012. - Vol.109. - p. 172002. [arXiv:1204.0246 [hep-ex]].

[428] Vostrikov V.A., Kiselev V.A., Levichev E.B., Parkhomchuk V.V., Reva V.B., Sinyatkin S. A project for synchrotron with electron cooling for cancer therapy. // *Phys. Part. Nucl. Lett.* - 2012. - Vol.9. - p.429-432.

Conference presentations

[429] Knyazev B.A. Experiments in terahertz optics: a review of new results at Novosibirsk free electron laser. // 20th Intern. Conf. on Advanced Laser Technologies ALT'12, 2 - 6 Sept., 2012, Thun, Switzerland: Book of Abstracts - Thun: Inst. of Applied Laser, 2012. - p.143-144.

[430] Astrelin V.T., Burdakov A.V., Kandaurov I.V., Karpov I.E., Trunev Yu.A. Conceptual design and numerical simulation of long-pulsed 1-kA electron beam source for open magnetic traps. // 3rd Intern. Congress on Radiation Physics and Chemistry of Condensed Matter, High Current Electronics and Modification of Materials with Particle Beams and Plasma Flows, Tomsk, 2012: Abstracts. - Tomsk: Inst. of High Current Electronics SB RAS, 2012. - p.64-165.

[431] Polosatkin S.V., Burdakov A.V., Grishnyaev E.S., Konstantinov S.G., Shoshin A.A. Freak structures on the surface of copper target irradiated by ion beam. // 3rd Intern. Congress on Radiation Physics and Chemistry of Condensed Matter, High Current Electronics and Modification of Materials with Particle Beams and Plasma Flows, Tomsk, 2012: Abstracts. - Tomsk, 2012. - p.397.

[432] Kandaurov I.V., Astrelin V.T., Avrorov A.P., Burdakov A.V., Bykov P.V., Derevyankin G.E., Ivanov A.A., Ivanov I.A., Kurkuchekov V.V., Polosatkin S.V., Rovenskikh A.F., Trunev Yu.A. High power (10 MW), long pulse multiaperture electron beam injector with plasma emitter designed for beam-plasma experiments. // 3rd Intern. Congress on Radiation Physics and Chemistry of Condensed Matter, High Current Electronics and Modification of Materials with Particle Beams and Plasma Flows, Tomsk, 2012: Abstracts. - Tomsk: Inst. of High Current Electronics SB RAS, 2012. - p.169.

[433] Zhmurikov E.I., Stankus S.V., Yatsuk O.S., Tecchio L.B. Thermal expansion of artificial graphites in the temperature range of 293-1650K. // 3rd Intern. Congress on Radiation Physics and Chemistry of Condensed Matter, High Current Electronics and Modification of Materials with Particle Beams and Plasma Flows, Tomsk, 2012: Abstracts. - Tomsk, 2012. - p.326-327.

- [434] Kubarev V.V. Detailed observation of modulation instability on THz NovoFEL [Electronic resource]. // IRMMW-THz 2012: 37th Intern. Conf. on Infrared, Millimeter and Terahertz Waves, University of Wollongong, Australia, Sept. 23 - 28, 2012. - S.I, 2012.
- [435] Ginzburg N.S., Peskov N.Yu., Sergeev A.S., Zaslavsky V.Yu., Arzhannikov A.V., Kalinin P.V., Sinitsky S.L., Thumm M. Generation of powerful spatial coherent radiation in masers and lasers with two-dimensional distributed feedback [Electronic resource]. // IRMMW-THz 2012: 37th Intern. Conf. on Infrared, Millimeter and Terahertz Waves, University of Wollongong, Australia, Sept. 23 - 28, 2012. - S.I, 2012.
- [436] Kulipanov G.N. High power NovoFEL: developments and new results. // IRMMW-THz 2012: 37th Intern. Conf. on Infrared, Millimeter and Terahertz Waves, University of Wollongong, Australia, Sept. 23 - 28, 2012. - S.I, 2012.
- [437] Eom K.H., Peltek S.E., Popik V.M., Jeong Y.U., Kwon O.S., Park W.Y., Lee W.S., So J.H., Park G.S. Irradiative damage characterization of a lysozyme during high-power THz ablation using MALDI-TOF mass spectrometry [Electronic resource]. // IRMMW-THz 2012: 37th Intern. Conf. on Infrared, Millimeter and Terahertz Waves, University of Wollongong, Australia, Sept. 23 - 28, 2012. - S.I, 2012.
- [438] Knyazev B.A., Choporova Yu.Yu., Gerasimov V.V., Vlasenko M.G., Pavelyev V.S., Volodkin B.O., Agafonov A.N., Tukmakov K.N., Kaveev A.K., Kropotov G.I., Tsygankova E.V., Stupak M.F., Palchikova I.G. Study of diffractive optical elements using high-power radiation of Novosibirsk terahertz free electron laser [Electronic resource]. // IRMMW-THz 2012: 37th Intern. Conf. on Infrared, Millimeter and Terahertz Waves, University of Wollongong, Australia, Sept. 23 - 28, 2012. - S.I, 2012.
- [439] Gerasimov V.V., Cherkassky V.S., Knyazev B.A., Kotelnikov I.A., Mitina N.A., Nikitin A.K., Zhizhin G.N. Study of surface plasmons travelling along straight and curved metal-dielectric interfaces: experiment and theory [Electronic resource]. // IRMMW-THz 2012: 37th Intern. Conf. on Infrared, Millimeter and Terahertz Waves, University of Wollongong, Australia, Sept. 23 - 28, 2012. - S.I, 2012. Report Tue-A4-4.
- [440] Sinitsky S.L., Arzhannikov A.V., Kalinin P.V., Kuznetsov S.A., Stepanov V.D., Ginzburg N.S., Peskov N.Yu., Sergeev A.S., Zaslavsky V.Yu., Thumm M. Synchronous generation of powerful 4-mm radiation in a two-channel planar FEM [Electronic resource]. // IRMMW-THz 2012: 37th Intern. Conf. on Infrared, Millimeter and Terahertz Waves, University of Wollongong, Australia, Sept. 23 - 28, 2012. - S.I, 2012.
- [441] Kubarev V.V., Chesnokov E.N., Koshlyakov P.V. Ultrafast high-resolution THz time-domain spectroscopy [Electronic resource]. // IRMMW-THz 2012: 37th Intern. Conf. on Infrared, Millimeter and Terahertz Waves, University of Wollongong, Australia, Sept. 23 - 28, 2012. - S.I, 2012.
- [442] Thumm M.K.A., Arzhannikov A.V., Astrelin V.T., Burdakov A.V., Ginzburg N.S., Ivanov I.A., Kalinin P.V., Kuznetsov S.A., Makarov M.A., Mekler K.I., Paulish A.G., Peskov N.Yu., Polosatkin S.V., Popov S.A., Postupaev V.V., Rovenskikh A.F., Sergeev A.S., Sinitsky S.L., Sklyarov V.F., Stepanov V.D., Vyacheslavov L.N., Zaslavsky V.Yu. Sub-terahertz emission by magnetized plasma at two-stream instability of REB and by two-channel planar FEM with combined electrodynamic system. // Proc. of the 4th Intern. Workshop on Far-Infrared Technologies (IW-FIRT 2012), March 7 - 9, 2012, University of Fukui, Japan. - Fukui: Univ. of Fukui, 2012. - p.7-17.
- [443] Tolochko B., Zhogin I., Kulipanov G., Aulchenko V., Ten K., Titov V. New possibility of XFEL for shock compression and detonation investigation. // Science at FELs. SRI 2012 Satellite Meeting, 15 - 18 July, 2012, DESY in Hamburg, Germany: Conference Programme, Useful information and Book abstr. - Hamburg: DESY, 2012. - Poster number: 37.
- [444] Miginsky S., Park S., Lee K., Jang Kyu-Ha, Jeong Yo.Uk, Vinokurov N. Activities in World Class Institute Center in KAERI. // XIX National Conference on Synchrotron Radiation: All-Russia Youth Conference "Synchrotron radiation application", 25 - 28 June 2012, Novosibirsk: Book of Abstracts. - Novosibirsk: Budker Institute of Nuclear Physics SB RAS, 2012. - p.12.
- [445] Pustovarov V.A., Kortov V.S., Zinin E.I. Low temperature luminescence of nanostructured alfa-Al₂O₃ crystals in spectral region of 140-900 nm under VUV and soft X-ray excitations. // XIX National Conference on Synchrotron Radiation: All-Russia Youth Conference "Synchrotron radiation application", 25 - 28 June 2012, Novosibirsk: Book of Abstracts. - Novosibirsk: Budker Institute of Nuclear Physics SB RAS, 2012. - p.25.
- [446] Knyazev B.A., Cherkassky V.S., Choporova Yu.Yu., Gerasimov V.V., Kotelnikov I.A., Nikitin A.K., Vlasenko M.G. Optical experiments at NovoFEL facility. // XIX National Conference on Synchrotron Radiation: All-Russia Youth Conference "Synchrotron radiation application", 25 - 28 June 2012, Novosibirsk: Book of Abstracts. - Novosibirsk: Budker Institute of Nuclear Physics SB RAS, 2012 - p.13-14.
- [447] Veber S.L., Maryunina K.Yu., Sheglov M.A., Kubarev V.V., Ovcharenko V.I., Bagryanskaya E.G. The influence of intense THz radiation on spin state of photo-switchable complex CU(HFACO)₂ L^{PR}. // XIX National Conference on Synchrotron Radiation: All-Russia Youth Conference "Synchrotron radiation application", 25 - 28 June 2012, Novosibirsk: Book of Abstracts. - Novosibirsk: Budker Institute of Nuclear Physics SB RAS, 2012. - p.17.
- [448] Legkodymov A.A., Kondratiev V.I., Mashkovtsev M.R., Bryanskaya A.V., Peltek S.E.,

Altapova V.R., Simon R. Analysis of chemical elements of microbial communities using correlation between optical and X-ray images. // XIX National Conference on Synchrotron Radiation: All-Russia Youth Conference "Synchrotron radiation application", 25 - 28 June 2012, Novosibirsk: Book of Abstracts. - Novosibirsk: Budker Institute of Nuclear Physics SB RAS, 2012. - p.99-100 (in Russian).

[449] Dar'in A.V., Kalugin I.A., Rakshun Ya.V., Maksimovskaya V.V., Ivo Zizak. Geochemistry of the annual cycle of sedimentation in the lake Shira (Khakassia) via scanning X-ray microanalysis with a spatial resolution of 20 - 200 microns on SR beams of the VEPP-3 and BESSI-II storage rings. // XIX National Conference on Synchrotron Radiation: All-Russia Youth Conference "Synchrotron radiation application", 25 - 28 June 2012, Novosibirsk: Book of Abstracts. - Novosibirsk: Budker Institute of Nuclear Physics SB RAS, 2012. - p.76-77 (in Russian).

[450] Popova A.A., Sobachkin A.V., Nazarov I.V., Yakovlev V.I., Loginova M.V., Sitnikov A.A., Sharafutdinov M.R., Lyakhov N.Z. Dynamic diffractometry of phase transformations during high-temperature synthesis in powder mechanically-activated systems at 3D ignition. // XIX National Conference on Synchrotron Radiation: All-Russia Youth Conference "Synchrotron radiation application", 25 - 28 June 2012, Novosibirsk: Book of Abstracts. - Novosibirsk: Budker Institute of Nuclear Physics SB RAS, 2012. - p.59-60 (in Russian).

[451] Timchenko N.A., Aumalikova M.N., Goldenberg B.G., Litvin S.V., Yurchenko V.I. Production of regular structures of polymeric membranes by polymerization of a monomer on a pore-forming matrix. // XIX National Conference on Synchrotron Radiation: All-Russia Youth Conference "Synchrotron radiation application", 25 - 28 June 2012, Novosibirsk: book of abstracts. - Novosibirsk: Budker Institute of Nuclear Physics SB RAS, 2012. - p.95-95 (in Russian).

[452] Rakshun Ya.V., Chernov V.A., Kosov A.V., Mezentsev N.A., Sorokoletov D.S. Micron-accuracy SR beam position measurement with a sensor based on total internal reflection mirrors. // XIX National Conference on Synchrotron Radiation: All-Russia Youth Conference "Synchrotron radiation application", 25 - 28 June 2012, Novosibirsk: Book of Abstracts. - Novosibirsk: Budker Institute of Nuclear Physics SB RAS, 2012. - p.101-109 (in Russian).

[453] Fedotov M.G., Sharafutdinov M.R. SR-beam small-angle scattering study of ultrafine silver produced via shock-wave synthesis in cryogenic conditions. // XIX National Conference on Synchrotron Radiation: All-Russia Youth Conference "Synchrotron radiation application", 25 - 28 June 2012, Novosibirsk: Book of Abstracts. - Novosibirsk: Budker Institute of Nuclear Physics SB RAS, 2012. - p.57-58 (in Russian).

[454] Demidova E.V., Goryachkovskaya T.N., Malup T.K., Bannikov S.V., Popik V.M., Semenov A.I., Peltek S.E. Investigation of non-thermal effects of terahertz radiation on gene-sensitive cells of E.coli/pKatg-gfp and E.coli/ pCopA-gfp. // XIX National Conference on Synchrotron Radiation: All-Russia Youth Conference "Synchrotron radiation application", 25 - 28 June 2012, Novosibirsk: Book of Abstracts. - Novosibirsk: Budker Institute of Nuclear Physics SB RAS, 2012. - p.114-115 (in Russian).

[455] Derevjanko D.I., Shelkovnikov V.V., Goldenberg B.G. Investigation of the properties of hybrid photopolymer material for recording of diffraction microstructures. // XIX National Conference on Synchrotron Radiation: All-Russia Youth Conference "Synchrotron radiation application", 25 - 28 June 2012, Novosibirsk: Book of Abstracts. - Novosibirsk: Budker Institute of Nuclear Physics SB RAS, 2012. - p.124 (in Russian).

[456] Sobachkin A.V., Popova A.A., Makarova A.A., Yakovlev V.I., Loginova M.V., Sitnikov A.A., Tolochko B.P., Lyakhov N.Z. Complex for high-frequency induction heating of mechanically activated powder formulations for dynamic-diffraction study of SHS reactive systems. // XIX National Conference on Synchrotron Radiation: All-Russia Youth Conference "Synchrotron radiation application", 25 - 28 June 2012, Novosibirsk: Book of Abstracts. - Novosibirsk: Budker Institute of Nuclear Physics SB RAS, 2012. - p.91-92 (in Russian).

[457] Reznikova E.F., Goldenberg B.G., Kondratiev V.I., Kulipanov G.N., Korol'kov V.P., Nasyrov R.K. LIGA technology for synthesis of three-dimensional diffraction-refraction intraocular lenses. // XIX National Conference on Synchrotron Radiation: All-Russia Youth Conference "Synchrotron radiation application", 25 - 28 June 2012, Novosibirsk: Book of Abstracts. - Novosibirsk: Budker Institute of Nuclear Physics SB RAS, 2012. - p.90-91 (in Russian).

[458] Reznikova E.F., Goldenberg B.G., Kondratiev V.I., Kulipanov G.N., Korol'kov V.P., Nasyrov R.K. LIGA technology for synthesis of three-dimensional diffraction-refraction intraocular lenses. // XIX National Conference on Synchrotron Radiation: All-Russia Youth Conference "Synchrotron radiation application", 25 - 28 June 2012, Novosibirsk: Book of Abstracts. - Novosibirsk: Budker Institute of Nuclear Physics SB RAS, 2012. - p.98-99.

[459] Vasilieva A.A., Gruzinov A.Yu., Zabelin A.V., Ilyin K.D., Simonova M.A., Podpryatov S.S., Legkodymov A.A., Sigaeva M.V., Simitsyna A.A., Vazina A.A. Methodological aspects of study of biological tissues by methods of SAXS/WAXS diffraction and X-ray fluorescence analysis using synchrotron radiation. // XIX National Conference on Synchrotron Radiation: All-Russia Youth Conference "Synchrotron radiation application", 25 - 28 June 2012,

Novosibirsk: Book of Abstracts. - Novosibirsk: Budker Institute of Nuclear Physics SB RAS, 2012. - p.48 (in Russian).

[460] Skuridin G.M., Chankina O.V., Kutsenogyi K.P., Legkodymov A.A., Kreimer V.K. Microelement composition of the tissues of sea buckthorn (*Hippophae rhamnoides* L.). // XIX National Conference on Synchrotron Radiation: All-Russia Youth Conference "Synchrotron radiation application", 25 - 28 June 2012, Novosibirsk: Book of Abstracts. - Novosibirsk: Budker Institute of Nuclear Physics SB RAS, 2012. - p.68 (in Russian).

[461] Aulchenko V.M., Zhulanov V.V., Ten K.A., Tolochko B.P., Shekhtman L.I. Multi-line silicon microstrip detector for radiation of explosive processes on an SR beam. // XIX National Conference on Synchrotron Radiation: All-Russia Youth Conference "Synchrotron radiation application", 25 - 28 June 2012, Novosibirsk: book of abstracts. - Novosibirsk: Budker Institute of Nuclear Physics SB RAS, 2012. - p.48 (in Russian).

[462] Fedotov M.G. Simulation of tunable multispectral X-ray SR detector with time separation of bands. // XIX National Conference on Synchrotron Radiation: All-Russia Youth Conference "Synchrotron radiation application", 25 - 28 June 2012, Novosibirsk: book of abstracts. - Novosibirsk: Budker Institute of Nuclear Physics SB RAS, 2012. - p.87 (in Russian).

[463] Rakshun Ya.V., Dar'in A.V., Sorokoletov D.S., Kholopov M.A. Upgrade of SR XFA station for development of the method of two-dimensional scanning microanalysis. // XIX National Conference on Synchrotron Radiation: All-Russia Youth Conference "Synchrotron radiation application", 25 - 28 June 2012, Novosibirsk: Book of Abstracts. - Novosibirsk: Budker Institute of Nuclear Physics SB RAS, 2012. - p.102 (in Russian).

[464] Goldenberg B.G., Reznikova E.F., Lemzyakov A.G. Upgrade of the SR station "LIGA" on the VEPP-3 storage ring for direct formation of deep microstructures. // XIX National Conference on Synchrotron Radiation: All-Russia Youth Conference "Synchrotron radiation application", 25 - 28 June 2012, Novosibirsk: book of abstracts. - Novosibirsk: Budker Institute of Nuclear Physics SB RAS, 2012. - p. 95 (in Russian).

[465] Vazina A.A., Kulipanov G.N. Molecular and nanostructural features of biological tissues in different functional states. // XIX National Conference on Synchrotron Radiation: All-Russia Youth Conference "Synchrotron radiation application", 25 - 28 June 2012, Novosibirsk: Book of Abstracts. - Novosibirsk: Budker Institute of Nuclear Physics SB RAS, 2012. - p.47 (in Russian).

[466] Shevchenko O.A., Arbuzov V.S., Vinokurov N.A., Vlasenko M.G., Vobly P.D., Volkov V.N., Getmanov Ya.V., Gorniker E.I., Deichuli O.I.,

Dement'ev E.N., Dovzhenko B.A., Kondakov A.A., Knyazev B.A., Kozak V.R., Kozyrev E.V., Kolobanov E.I., Kubarev V.V., Kulipanov G.N., Cooper E.A., Kuptsov I.V., Kurkin G.Ya., Medvedev L.E., Myronenko L.A., Ovchar V.K., Persov B.Z., Pilan A.M., Popik V.M., Repkov V.V., Salikova T.V., Sedlyarov I.K., Serdobintsev G.V., Serednyakov S.S., Skorokhod D.A., Skrinsky N.A., Sozinov G.I., Tararyshkin S.V., Cheskidov V.G. Chernov K.N., Sheglov M.A. Novosibirsk free electron laser, current status and prospects for development. // XIX National Conference on Synchrotron Radiation: All-Russia Youth Conference "Synchrotron radiation application", 25 - 28 June 2012, Novosibirsk: Book of Abstracts. - Novosibirsk: Budker Institute of Nuclear Physics SB RAS, 2012. - p.12 (in Russian).

[467] Zhogin I.L., Zhulanov V.V., Titov V.M. On an algorithm of determination of photon coordinates in the X-ray detector OD-3M. // XIX National Conference on Synchrotron Radiation: All-Russia Youth Conference "Synchrotron radiation application", 25 - 28 June 2012, Novosibirsk: Book of Abstracts. - Novosibirsk: Budker Institute of Nuclear Physics SB RAS, 2012. - p.78 (in Russian).

[468] Vasiliev A.A., Palchikov E.I., Kubarev V.V., Chesnokov E.N., Koshlyakov P.V., Dolgikh A.V., Krasnikov I.Yu., Pruel E.R., Ten K.A. On works on the study of stationary and non-stationary waves of combustion of hydrogen-oxygen mixture at Novosibirsk terahertz free electron laser. // XIX National Conference on Synchrotron Radiation: All-Russia Youth Conference "Synchrotron radiation application", 25 - 28 June 2012, Novosibirsk: Book of Abstracts. - Novosibirsk: Budker Institute of Nuclear Physics SB RAS, 2012. - p.97-98 (in Russian).

[469] Nikolenko A.D., Gorlovoi A.V., Ivlyushkin D.V., Legkodymov A.A., Lyakh V.V., Mashkovtsev M.R., Pindyurin V.F., Shadrin N.S. Development of hardware and methodological support for metrological works in soft X-rays and VUV radiation using synchrotron radiation at SCTSR. // XIX National Conference on Synchrotron Radiation: All-Russia Youth Conference "Synchrotron radiation application", 25 - 28 June 2012, Novosibirsk: Book of Abstracts. - Novosibirsk: Budker Institute of Nuclear Physics SB RAS, 2012. - p.94 (in Russian).

[470] Gentshev A.N., Goldenberg B.G., Lemzyakov A.G., Kondratiev V.I., Zelinsky A.G. X-ray masks for terahertz optics. // XIX National Conference on Synchrotron Radiation: All-Russia Youth Conference "Synchrotron radiation application", 25 - 28 June 2012, Novosibirsk: Book of Abstracts. - Novosibirsk: Budker Institute of Nuclear Physics SB RAS, 2012. - p.92 (in Russian).

[471] Gentshev A.N., Kondratiev V.I., Zelinsky A.G. X-ray masks based on graphite epoxide. // XIX National Conference on Synchrotron Radiation: All-Russia Youth

Conference "Synchrotron radiation application", 25 - 28 June 2012, Novosibirsk: book of abstracts. - Novosibirsk: Budker Institute of Nuclear Physics SB RAS, 2012. - p.89-90 (in Russian).

[472] Gentshev A.N., Goldenberg B.G., Kondratiev V.I., Lemzyakov A.G., Pindyurin V.F. X-ray masks with X-ray-resist masking layer. // XIX National Conference on Synchrotron Radiation: All-Russia Youth Conference "Synchrotron radiation application", 25 - 28 June 2012, Novosibirsk: book of abstracts. - Novosibirsk: Budker Institute of Nuclear Physics SB RAS, 2012. - p.89 (in Russian).

[473] Kubarev V.V., Chesnokov E.N., Koshlyakov P.V. Ultrafast high-resolution time-domain spectroscopy at Novosibirsk terahertz free electron laser. // XIX National Conference on Synchrotron Radiation: All-Russia Youth Conference "Synchrotron radiation application", 25 - 28 June 2012, Novosibirsk: Book of Abstracts. - Novosibirsk: Budker Institute of Nuclear Physics SB RAS, 2012. - p.21 (in Russian).

[474] Mashkovtsev M.R., Nikolenko A.D., Kondratiev V.I., Vasilenko V.S., Legkodymov A.A. Freely-suspended X-ray film filters with windows transparent in the range of 15 - 2000 eV. // XIX National Conference on Synchrotron Radiation: All-Russia Youth Conference "Synchrotron radiation application", 25 - 28 June 2012, Novosibirsk: Book of Abstracts. - Novosibirsk: Budker Institute of Nuclear Physics SB RAS, 2012. - p.97 (in Russian).

[475] Reznikova E.F., Kondratiev V.I., Goldenberg B.G. Wettability of LIGA polymers in microfluidic biochemical modules. // XIX National Conference on Synchrotron Radiation: All-Russia Youth Conference "Synchrotron radiation application", 25 - 28 June 2012, Novosibirsk: Book of Abstracts. - Novosibirsk: Budker Institute of Nuclear Physics SB RAS, 2012. - p.100-101 (in Russian).

[476] Palchikov E.I., Dolgikh A.V., Kondratiev V.I., Matrosov A.D. Mutlizonal digital X-ray diagnostics of explosive processes on the basis of ImagePlate detectors separated by an absorber. // XIX National Conference on Synchrotron Radiation: All-Russia Youth Conference "Synchrotron radiation application", 25 - 28 June 2012, Novosibirsk: Book of Abstracts. - Novosibirsk: Budker Institute of Nuclear Physics SB RAS, 2012. - p. 56-57 (in Russian).

[477] Korneev V.N., Shlektarev V.A., Zabelin A.V., Lanina N.F., Aulchenko V.M., Tolochko B.P., Ariskin N.I., Vazina A.A. Status of the stations on the basis of X-ray optical zoom lenses for study of biological nanostructures and experimental results using synchrotron radiation. // XIX National Conference on Synchrotron Radiation: All-Russia Youth Conference "Synchrotron radiation application", 25 - 28 June 2012, Novosibirsk: Book of Abstracts. - Novosibirsk: Budker Institute of Nuclear Physics SB RAS, 2012. - p.81 (in Russian).

[478] Ten K.A., Prueel E.R., Luk'yanchikov L.A., Efremov B.P., Bespalov E.V., Tolochko B.P., Zhulanov V.V., Shekhtman L.I. Shock compression of nanostructured SiO₂ aerogel. // XIX National Conference on Synchrotron Radiation: All-Russia Youth Conference "Synchrotron radiation application", 25 - 28 June 2012, Novosibirsk: Book of Abstracts. - Novosibirsk: Budker Institute of Nuclear Physics SB RAS, 2012. - p.105 (in Russian).

[479] Shadrin N.S., Nikolenko A.D. SR beam monitor based on photoemission for the metrological station "Space". // XIX National Conference on Synchrotron Radiation: All-Russia Youth Conference "Synchrotron radiation application", 25 - 28 June 2012, Novosibirsk: Book of Abstracts. - Novosibirsk: Budker Institute of Nuclear Physics SB RAS, 2012. - p.100 (in Russian).

[480] Gerasimov V.V., Knyazev B.A., Kotelnikov I.A., Mitina N.A., Nikitin A.K., Zhizhin G.N. Characteristics of surface plasmons propagating along a metal-insulator-air boundary. // XIX National Conference on Synchrotron Radiation: All-Russia Youth Conference "Synchrotron radiation application", 25 - 28 June 2012, Novosibirsk: Book of Abstracts. - Novosibirsk: Budker Institute of Nuclear Physics SB RAS, 2012. - p.79 (in Russian).

[481] Markova Yu.N., Kerber E.V., Maksimovskaya V.V., Zolotarev K.V. Elemental composition of bottom sediments of lakes as an indicator of climatic conditions during their formation. // XIX National Conference on Synchrotron Radiation: All-Russia Youth Conference "Synchrotron radiation application", 25 - 28 June 2012, Novosibirsk: Book of Abstracts. - Novosibirsk: Budker Institute of Nuclear Physics SB RAS, 2012. - p. 67 (in Russian).

[482] Azarov I.A., Shvets V.A., Prokopiev V.Yu., Doolin S.A., Choporova Yu.Yu., Rykhlytskii S.V., Knyazev B.A. Ellipsometry in the terahertz frequency range using a free electron laser. // XIX National Conference on Synchrotron Radiation: All-Russia Youth Conference "Synchrotron radiation application", 25 - 28 June 2012, Novosibirsk: book of abstracts. - Novosibirsk: Budker Institute of Nuclear Physics SB RAS, 2012. - p. 85 (in Russian).

[483] Gusev I.A., Senkov D.V., Erokhin A.I., Kolmogorov V.V., Medvedko A.S., Potapov S.I., Pureskin D.N. 3-channel current source with channel output current up to 180 A and output voltage up to 180 V [Electronic resource]. // XXIII Russian Particle Accelerator Conference: RuPAC'2012, Sept. 24 - 28, 2012, Saint-Petersburg, Russia: Proc. - Saint-Petersburg, 2012. - p.509.

[484] Bezuglov V., Bryazgin A., Factorovich B., Kokin E., Radchenko V., Shtarklev E., Vlasov A. Beam extraction for industrial electron accelerator ILU-14 [Electronic resource]. // XXIII Russian Particle Accelerator Conference: RuPAC'2012, Sept. 24 - 28, 2012, Saint-Petersburg, Russia: Proc. - Saint-Petersburg, 2012. - p.161.

[485] Bekhtenev E.A., Cherepanov V.P., Karpov G.V., Reva V.B., Shubin E.I., Skorobogatov D.N. Beam position monitor system for 2 MeV electron cooler for COSY [Electronic resource]. // XXIII Russian Particle Accelerator Conference: RUPAC2012, Sept. 24 - 28, 2012, Saint-Petersburg, Russia: Proc. - Saint-Petersburg, 2012. - p.608. WEPPD028.

[486] Shevchenko O.A., Arbuzov V.S., Chernov K.N., Demytyev E.N., Dovzhenko B.A., Getmanov Ya.V., Gorniker E.I., Knyazev B.A., Kolobanov E.I., Kondakov A.A., Kozak V.R., Kozyrev E.V., Kubarev V.V., Kulipanov G.N., Kuper E.A., Kuptsov I.V., Kurkin G.Ya., Medvedev L.E., Mironenko L.A., Ovchar V.K., Persov B.Z., Pilan A.M., Popik V.M., Repkov V.V., Salikova T.V., Scheglov M.A., Sedlyarov I.K., Serdobintsev G.V., Serednyakov S.S., Skrinsky A.N., Tararyshkin S.V., Tcheskidov V.G., Vinokurov N.A., Vlasenko M.G., Vobly P.D., Volkov V.N. Budker INP free electron laser facility - current status and future prospects [Electronic resource]. // XXIII Russian Particle Accelerator Conference: RuPAC'2012, Sept. 24 - 28, 2012, Saint-Petersburg, Russia: Proc. - S.I, 2012. - p.136.

[487] Kuznetsov A., Aleynik V., Sorokin I., Taskaev S., Tiunov M., Shudlo I. Calibration testing of the stripping target of the vacuum insulated tandem accelerator [Electronic resource]. // XXIII Russian Particle Accelerator Conference: RuPAC'2012, Sept. 24 - 28, 2012, Saint-Petersburg, Russia: Proc. - Saint-Petersburg, 2012. - p.560-562.

[488] Chernousov Yu., Ivannikov V., Shebolaev I., Levichev E., Pavlov V. Characteristics of the model of linear accelerator based on parallel coupled accelerating structure with beam loading [Electronic resource]. // XXIII Russian Particle Accelerator Conference: RuPAC'2012, Sept. 24 - 28, 2012, Saint-Petersburg, Russia: Proc. - Saint-Petersburg, 2012. - p.164.

[489] Yaminov K.R., Belikov O.V., Medvedko A.S., Kolmogorov V.V., Erokhin A.I., Singatulin S.R., Karnaev S.E., Cheblakov P.B. Correcting magnet power supplies for the NSLS-II booster [Electronic resource]. // XXIII Russian Particle Accelerator Conference: RuPAC'2012, Sept. 24 - 28, 2012, Saint-Petersburg, Russia: Proc. - Saint-Petersburg, 2012. - p.500.

[490] Levichev E. e+e- collider VEPP-4M: status and prospects [Electronic resource]. // XXIII Russian Particle Accelerator Conference: RuPAC'2012, Sept. 24 - 28, 2012, Saint-Petersburg, Russia: Proc. - Saint-Petersburg, 2012. - p.20.

[491] Gambaryan V., Starostenko A. Fast kicker [Electronic resource]. // XXIII Russian Particle Accelerator Conference: RuPAC'2012, Sept. 24 - 28, 2012, Saint-Petersburg, Russia: Proc. - S.I, 2012. - p.483.

[492] Bekhtenev E.A., Cherepanov V.P., Karpov G.V., Styuf A.S. Fast tune measurement system [Electronic resource]. // XXIII Russian Particle Accelerator Conference: RuPAC'2012, Sept. 24 - 28, 2012, Saint-

Petersburg, Russia: Proc. - Saint-Petersburg, 2012. - p.611.

[493] Volkov V.N., Arbuzov V.S., Gorniker E.I., Kolobanov E.I., Krutikhin C.A., Kuptsov I.V., Kurkin G.Ya., Osipov V.N., Petrov V.M., Pilan A.M., Sedlyarov I.K., Scheglov M.A., Vinokurov N.A. First test results of RF gun for the race-track microtron recuperator of BINP SB RAS [Electronic resource]. // XXIII Russian Particle Accelerator Conference: RuPAC'2012, Sept. 24 - 28, 2012, Saint-Petersburg, Russia: Proc. - Saint-Petersburg, 2012. - p.424.

[494] Bryzgunov M., Bublely A., Goncharov A., Panasyuk V., Parkhomchuk V., Reva V., Skorobogatov D., Deitrich J., Kamerzhiev V. High voltage electron cooler [Electronic resource]. // XXIII Russian Particle Accelerator Conference: RuPAC'2012, Sept. 24 - 28, 2012, Saint-Petersburg, Russia: Proc. - Saint-Petersburg, 2012. - p.38. TUXCH01.

[495] Kuksanov N.K., Golubenko Y.I., Nemytov P.I., Salimov R.A., Fadeev S.N., Lavrukhin A.V., Korchagin A.I., Kogut D.S., Semenov A.V. High voltage ELV accelerators for industrial application (family of accelerators and tendency of development)[Electronic resource]. // XXIII Russian Particle Accelerator Conference: RuPAC'2012, Sept. 24 - 28, 2012, Saint-Petersburg, Russia: Proc. - Saint-Petersburg, 2012. - p.227.

[496] Gusev I.A., Medvedko A.S., Protopopov A.Yu., Pureskin D.N., Senkov D.V. High-voltage source with output voltage up to 110 kV with output current up to 100 mA [Electronic resource]. // XXIII Russian Particle Accelerator Conference: RuPAC'2012, Sept. 24 - 28, 2012, Saint-Petersburg, Russia: Proc. - Saint-Petersburg, 2012. - p.506.

[497] Chekavinskiy V.A., Bekhtenev E.A., Gusev I.A., Kondaurov M.N., Kozak V.R., Kuper E.A., Mamkin V.R., Medvedko A.S., Pureskin D.N., Skorobogatov D.N. High voltage terminal in COSY electron cooler [Electronic resource]. // XXIII Russian Particle Accelerator Conference: RuPAC'2012, Sept. 24 - 28, 2012, Saint-Petersburg, Russia: Proc. - Saint-Petersburg, 2012. - p.503.

[498] Starostenko A.A., Burdin P., Devyataikina T., Kazantseva E.S., Rybitskaya T.V., Skarbo B.A., Tsyganov A.S. Improvement of quadrupole magnets field quality in serial production [Electronic resource]. // XXIII Russian Particle Accelerator Conference: RuPAC'2012, Sept. 24 - 28, 2012, Saint-Petersburg, Russia: Proc. - Saint-Petersburg, 2012. - p.486.

[499] Kuksanov N.K., Fadeev S.N., Kogut D.A. Improving of uniformity of the electron-beam treatment of materials by ELV accelerators [Electronic resource]. // XXIII Russian Particle Accelerator Conference: RuPAC'2012, Sept. 24 - 28, 2012, Saint-Petersburg, Russia: Proc. - Saint-Petersburg, 2012. - p.557.

[500] Bragin A.V., Khrushev S.V., Mezentsev N.A., Miginskaya E.G., Poletaev I.V., Shkaruba V.A., Syrovatin V.M., Tsukanov V.M., Volkov A.A., Zolotarev K.V. Indirect cooled superconductive wiggler magnet [Electronic resource]. // XXIII Russian Particle Accelerator Conference: RuPAC'2012, Sept. 24 - 28, 2012, Saint-Petersburg, Russia: Proc. - Saint-Petersburg, 2012. - p.140.

[501] Chernousov Yu., Ivannikov V., Shebolaev I., Barnyakov A., Levichev A., Pavlov V. Localisation of the RF breakdown in the parallel coupled accelerating structure [Electronic resource]. // XXIII Russian Particle Accelerator Conference: RuPAC'2012, Sept. 24 - 28, 2012, Saint-Petersburg, Russia: Proc. - Saint-Petersburg, 2012. - p.281.

[502] Getmanov Ya.V., Shevchenko O.A., Vinokurov N.A. Longitudinal stability of ERL with two accelerating RF structures. // XXIII Russian Particle Accelerator Conference: RuPAC'2012, Sept. 24 - 28, 2012, Saint-Petersburg, Russia: Proc. - Saint-Petersburg, 2012. - p.575.

[503] Bryzgunov M., Bubley A., Panasyuk V., Parkhomchuk V., Polukhin V., Reva V. Low energy cooler for NICA booster [Electronic resource]. // XXIII Russian Particle Accelerator Conference: RuPAC'2012, Sept. 24 - 28, 2012, Saint-Petersburg, Russia: Proc. - Saint-Petersburg, 2012. - p.391. TUPPB034.

[504] Kulipanov G.N., Getmanov Ya.V., Shevchenko O.A., Skrinsky A.N., Vinokurov N.A., Kovalchuk M.V., Korchuganov V.N. MARS: fourth generation X-ray light source based on multiturn energy-recovery linac [Electronic resource]. // XXIII Russian Particle Accelerator Conference: RuPAC'2012, Sept. 24 - 28, 2012, Saint-Petersburg, Russia: Proc. - Saint-Petersburg, 2012. - p.123.

[505] Astrelina K., Petrenko A. Measurement of beam parameters in the VEPP-5 damping ring using betatron oscillations decoherence [Electronic resource]. // XXIII Russian Particle Accelerator Conference: RuPAC'2012, Sept. 24 - 28, 2012, Saint-Petersburg, Russia: Proc. - Saint-Petersburg, 2012. - p.385.

[506] Batrakov A., Pavlenko A., Chichkov D., Vagin P. Multimode digital integrators for precise magnetic measurements [Electronic resource]. // XXIII Russian Particle Accelerator Conference: RuPAC'2012, Sept. 24 - 28, 2012, Saint-Petersburg, Russia: Proc. - Saint-Petersburg, 2012. - p.617.

[507] Karpov G.V., Styuf A.S. New beam position monitor electronics for VEPP-5 preinjector [Electronic resource]. // XXIII Russian Particle Accelerator Conference: RUPAC2012, Sept. 24 - 28, 2012, Saint-Petersburg, Russia: Proc. - S.I, 2012. - p.614. [www.jacow.org, WEPD030].

[508] Tsyganov A., Batrakov A., Kazantseva E., Pavlenko A., Rybitskaya T., Skarbo B., Shichkov D., Starostenko A., Vobly P. Nonlinear shunting as method

of magnetic field correction in quadrupole lenses [Electronic resource]. // XXIII Russian Particle Accelerator Conference: RuPAC'2012, Sept. 24 - 28, 2012, Saint-Petersburg, Russia: Proc. - Saint-Petersburg, 2012. - p.492. [http://accelconf.web.cern.ch/].

[509] Makarov A., Aleynik V., Kuznetsov A., Sorokin I., Taskaev S., Tiunov M., Bashkirtsev A., Shchudlo I. Optimization of the negative hydrogen ion beam injection into the tandem accelerator with vacuum insulation [Electronic resource]. // XXIII Russian Particle Accelerator Conference: RuPAC'2012, Sept. 24 - 28, 2012, Saint-Petersburg, Russia: Proc. - S.I, 2012. - p.623-625.

[510] Rybitskaya T.V., Kazantseva E.S., Skarbo B.A., Starostenko A.A., Tsyganov A.S. Quadrupole harmonics tuning by nose pieces [Electronic resource]. // XXIII Russian Particle Accelerator Conference: RuPAC'2012, Sept. 24 - 28, 2012, Saint-Petersburg, Russia: Proc. - Saint-Petersburg, 2012. - p.489. [http://accelconf.web.cern.ch/].

[511] Barnyakov A., Levichev A., Pavlov V., Chernousov Yu., Ivannikov V., Shebolaev I. RF antenna lead [Electronic resource]. // XXIII Russian Particle Accelerator Conference: RuPAC'2012, Sept. 24 - 28, 2012, Saint-Petersburg, Russia: Proc. - Saint-Petersburg, 2012. - p.284.

[512] Dudnikov A. Simplified beam line with space charge compensation of low energy ion beam [Electronic resource]. // XXIII Russian Particle Accelerator Conference: RuPAC'2012, Sept. 24 - 28, 2012, Saint-Petersburg, Russia: Proc. - Saint-Petersburg, 2012. - p.388.

[513] Tsuganov A., Batrakov A., Kazantseva E., Pavlenko A., Rybitskaya T., Skarbo B., Shichkov D., Starostenko A., Vobly P. Stand for precise measurements of magnetic lenses field quality [Electronic resource]. // XXIII Russian Particle Accelerator Conference: RuPAC'2012, Sept. 24 - 28, 2012, Saint-Petersburg, Russia: Proc. - Saint-Petersburg, 2012. - p.495. [http://accelconf.web.cern.ch/].

[514] Berkaev D., Borisov A., Garinov Yu., Kirpotin A., Koop I., Lysenko A., Nesterenko I., Otboev A., Perevedentsev E., Rogovsky Yu., Romanov A., Shatunov P., Shwartz D., Skrinsky A., Shatunov Yu. Status of electron-positron collider VEPP-2000 [Electronic resource]. // XXIII Russian Particle Accelerator Conference: RuPAC'2012, Sept. 24 - 28, 2012, Saint-Petersburg, Russia: Proc. - Saint-Petersburg, 2012. - p.15-19.

[515] Eliseev A.V., Kozlov O.S., Meshkov I.N., Sidorin A.V., Smirnov A.V., Trubnikov G.V., Katayama T., Volkov V.N., Kenzhebulatov E.K., Kurkin G.Y., Petrov V.M. Storage, acceleration and short bunched beam formation of $/sab\ 197/AU/sab\ +79/$ ions in the NICA collider [Electronic resource]. // XXIII Russian Particle Accelerator Conference: RuPAC'2012, Sept. 24 -

28, 2012, Saint-Petersburg, Russia: Proc. - Saint-Petersburg, 2012. - p.30.

[516] Skorobogatov D., Bryzgunov M., Goncharov A., Gusev I., Kondaurov M., Kozak V., Medvedko A., Parkhomchuk V., Pureskin D., Putmakov A., Reva V., Senkov D. The power supply system for the accelerating column of the 2 MeV electron cooler for COSY [Electronic resource]. // XXIII Russian Particle Accelerator Conference: RuPAC'2012, Sept. 24 - 28, 2012, Saint-Petersburg, Russia: Proc. - Saint-Petersburg, 2012. - p.512. [WEPPC032].

[517] Repkov V.V., Kuper E.A., Protopopov A.U., Zharikov A.A. The system for control of an electron beam welding machines [Electronic resource]. // XXIII Russian Particle Accelerator Conference: RuPAC'2012, Sept. 24 - 28, 2012, Saint-Petersburg, Russia: Proc. - S.I, 2012. - p.620.

[518] Kuper E.A., Kozak V.R., Mamkin V.R., Ovchar V.K., Repkov V.V., Serednyakov S.S., Tararyshkin S.V., Zverev D.A. The system of power supplies, control and modulation of electron gun for free electron laser [Electronic resource]. // XXIII Russian Particle Accelerator Conference: RuPAC'2012, Sept. 24 - 28, 2012, Saint-Petersburg, Russia: Proc. - Saint-Petersburg, 2012. - p.427.

[519] Taskaev S., Aleynik V., Bayanov B., Kuznetsov A., Makarov A., Sorokin I., Tiunov M., Bashkirtsev A., Schudlo I., Kamkin M., Kasatov D. Vita based neutron source - status and prospects [Electronic resource]. // XXIII All Russian Particle Accelerator Conference: RuPAC'2012, Sept. 24 - 28, 2012, Saint-Petersburg, Russia: Proc. - Saint-Petersburg, 2012. - p.230-232.

[520] Sorokin I., Bashkirtsev A., Ivanov A., Kasatov D., Kuznetsov V.A., Taskaev S., Chudaev V. X-ray radiation high-voltage elements of the tandem accelerator with vacuum insulation [Electronic resource]. // XXIII Russian Particle Accelerator Conference: RuPAC'2012, Sept. 24 - 28, 2012, Saint-Petersburg, Russia: Proc. - Saint-Petersburg, 2012. - p.299-301.

[521] Arzhannikov A.V., Burdakov A.V., Burmasov V.S., Ivanov I.A., Ivantsivsky M.V., Kuznetsov S.A., Mekler K.I., Popov S.S., Polosatkin S.V., Postupaev V.V., Rovenskikh A.F., Sinitsky S.L., Sklyarov V.F., Tumm M.K.A. Generation of subTHz-radiation experiments on plasma heating in the solenoid by a powerful relativistic electron beam. // XXXIX Intern. (Zvenigorod) Conference on Plasma Physics and Controlled Fusion, 6 - 10 February, 2012, Zvenigorod. - M: "PLAZMAIOFAN", 2012. - p.63.

[522] Chernoshtanov I.S., Tsidulko Yu.A. Alfven ion-cyclotron instability in a mirror trap with skew injection of neutral beams. // XXXIX Intern. (Zvenigorod) Conference on Plasma Physics and Controlled Fusion, 6 - 10 February, 2012, Zvenigorod. - M: "PLAZMAIOFAN", 2012. - p.56.

[523] Belykh V.V., Polosatkin S.V., Davydenko V.I., Ivanov A.A., Kapitonov V.A., Mishagin V.V., Voskoboinikov R.V., Tiunov M.A., Liu D., Clary R., Fiksel G. Neutral particle analyzer for the study of populations of fast ions in plasma. // XXXIX Intern. (Zvenigorod) Conference on Plasma Physics and Controlled Fusion, 6 - 10 February, 2012, Zvenigorod. - M: "PLAZMAIOFAN", 2012. - p.60.

[524] Beklemishev A.D. Helicoidal system for axial plasma confinement or acceleration. // XXXIX Intern. (Zvenigorod) Conference on Plasma Physics and Controlled Fusion, 6 - 10 February, 2012, Zvenigorod. - M: "PLAZMAIOFAN", 2012. - p.31.

[525] Ivantsivsky M.V., Arzhannikov A.V., Astrelin V.T., Burdakov A.V., Burmasov V.S., Vyacheslavov L.N., Popov S.S., Ivanov I.A., Kasatov A.A., Makarov M.A., Mekler K.I., Polosatkin S.V., Postupaev V.V., Rovenskikh A.F., Sinitsky S.L., Sudnikov A.V., Sulyaev Yu.S., Sklyarov V.F. The study of fast density fluctuations at the electron beam injection into the plasma of multimirror trap GOL-3. // XXXIX Intern. (Zvenigorod) Conference on Plasma Physics and Controlled Fusion, 6 - 10 February, 2012, Zvenigorod. - M: "PLAZMAIOFAN", 2012. - p.35.

[526] Belov V.P., Ivanov A.A., Kapitonov V.A., Prokhorov I.A., Sorokin A.V., Tkachev A.A. Ion-optical system of the hydrogen diagnostic neutral beam for W7-X stellarator. // XXXIX Intern. (Zvenigorod) Conference on Plasma Physics and Controlled Fusion, 6 - 10 February, 2012, Zvenigorod. - M: "PLAZMAIOFAN", 2012. - p.40.

[527] Bagryansky P.A., Zaytsev K.V., Korzhavina M.S., Prikhodko V.V. Magnetic measurements at GDT device. // XXXIX Intern. (Zvenigorod) Conference on Plasma Physics and Controlled Fusion, 6 - 10 February, 2012, Zvenigorod. - M: "PLAZMAIOFAN", 2012. - p.32.

[528] Popov S.S., Burdakov A.V., Ivanov A.A., Kotelnikov I.A. Non-resonant photon storage device to neutralize the powerful negative ion beams. // XXXIX Intern. (Zvenigorod) Conference on Plasma Physics and Controlled Fusion, 6 - 10 February, 2012, Zvenigorod. - M: "PLAZMAIOFAN", 2012. - p.232.

[529] Burdakov A.V., Avrorov A.P., Arzhannikov A.V., Astrelin V.T., Batkin V.I., Beklemishev A.D., Belykh V.V., Burmasov V.S., Vyacheslavov L.N., Gavrilenko D.E., Grishnyaev E.S., Derevyankin G.E., Ivanenko V.G., Ivanov A.A., Ivanov I.A., Ivantsivsky M.V., Kalinin P.V., Kandaurov I.V., Kuznetsov S.A., Kuklin K.N., Kurkuchekov V.V., Makarov M.A., Mekler K.I., Polosatkin S.V., Popov S.S., Postupaev V.V., Rovenskikh A.F., Sinitsky S.L., Stepanov V.D., Sudnikov A.V., Sulyaev Yu.S., Sklyarov V.F., Sorokina N.V., Trunev Yu.A., Shoshin A.A. Perspectives of an axially symmetrical multimirror trap. // XXXIX Intern. (Zvenigorod) Conference on Plasma Physics and

Controlled Fusion, 6 - 10 February, 2012, Zvenigorod. - M: "PLAZMAIOFAN", 2012. - p.29

[530] Arzhannikov A.V., Kotelnikov I.A. Plasma oscillations at the pumping of Langmuir turbulence by a high-current electron beam as a laboratory source of powerful electromagnetic radiation of the terahertz frequency range. // XXXIX Intern. (Zvenigorod) Conference on Plasma Physics and Controlled Fusion, 6 - 10 February, 2012, Zvenigorod. - M: "PLAZMAIOFAN", 2012. - p.221.

[531] Anikeev A.V., Bagryansky P.A., Brednikhin S.A., Lezhnin S.I., Prikhodko V.V., Frolov S.A., Yurov D.V. Plasma neutron source based on gas dynamic trap device for nuclear power plants. // XXXIX Intern. (Zvenigorod) Conference on Plasma Physics and Controlled Fusion, 6 - 10 February, 2012, Zvenigorod. - M: "PLAZMAIOFAN", 2012. - p.30.

[532] Astrelin V.T., Burdakov A.V., Kandaurov I.V., Karpov I.E. Design of millisecond electron beam injector based on the plasma emitter for the plasma heating in linear traps. // XXXIX Intern. (Zvenigorod) Conference on Plasma Physics and Controlled Fusion, 6 - 10 February, 2012, Zvenigorod. - M: "PLAZMAIOFAN", 2012. - p.230.

[533] Maksimov V.V., Ivanov A.A., Pinzhenin E.I., Pchelyakov O.P., Tishkovsky E.G., Chistyukhin I.B. Registration of the particle flow profile by the obscure chamber based on the diode array at the GDT. // XXXIX Intern. (Zvenigorod) Conference on Plasma Physics and Controlled Fusion, 6 - 10 February, 2012, Zvenigorod. - M: "PLAZMAIOFAN", 2012. - p.59.

[534] Vyacheslavov L.N., Ivantsivsky M.V., Kasatov A.A., Popov S.S., Puryga E.A. Thomson scattering system for measuring the fast density dynamics in the experiments at the GOL-3 device. // XXXIX Intern. (Zvenigorod) Conference on Plasma Physics and Controlled Fusion, 6 - 10 February, 2012, Zvenigorod. - M: "PLAZMAIOFAN", 2012. - p.33.

[535] Bagryansky P.A., Amirov V.Kh., Kovalenko Yu.V., Savkin V.Ya., Thumm M., Yakovlev D.V. ECR heating system for GDT device. // XXXIX Intern. (Zvenigorod) Conference on Plasma Physics and Controlled Fusion, 6 - 10 February, 2012, Zvenigorod. - M: "PLAZMAIOFAN", 2012. - p.64.

[536] Bagulov D.S., Kotelnikov I.A. Theory of multiphoton and tunnel Ionization in a bichromatic field. // XXXIX Intern. (Zvenigorod) Conference on Plasma Physics and Controlled Fusion, 6 - 10 February, 2012, Zvenigorod. - M: "PLAZMAIOFAN", 2012. - p.258.

[537] Starokozhev S.A. Tomographic diagnostic of the plasma in heating beams of the GDL installation. // XXXIX Intern. (Zvenigorod) Conference on Plasma Physics and Controlled Fusion, 6 - 10 February, 2012, Zvenigorod. - M: "PLAZMAIOFAN", 2012. - p.55.

[538] Anikeev A.V., Bagryansky P.A., Donin A.S., Zaytsev K.V., Kovalenko Yu.V., Korzhavina M.S.,

Lizunov A.A., Pushkareva A.N., Maksimov V.V., Pinzhenin E.I., Prikhodko V.V., Soldatkina E.I., Solomakhin A.L., Savkin V.Ya. Improvement of longitudinal plasma confinement and electrons auxiliary heating in the gas dynamic trap. // XXXIX Intern. (Zvenigorod) Conference on Plasma Physics and Controlled Fusion, 6 - 10 February, 2012, Zvenigorod. - M: "PLAZMAIOFAN", 2012. - p.34.

[539] Kurkuchekov V.V., Astrelin V.T., Kandaurov I.V., Trunev Yu.A. The formation of an intense electron beam in a multiaperture diode with a plasma emitter and its transportation through the magnetic mirror. // XXXIX Intern. (Zvenigorod) Conference on Plasma Physics and Controlled Fusion, 6 - 10 February, 2012, Zvenigorod. - M: "PLAZMAIOFAN", 2012. - p.266.

[540] Astrelin V.T., Karpov I.E. Formation of Langmuir layer in diodes with plasma electrodes. // XXXIX Intern. (Zvenigorod) Conference on Plasma Physics and Controlled Fusion, 6 - 10 February, 2012, Zvenigorod. - M: "PLAZMAIOFAN", 2012. - p.257.

[541] Logachev P.V. LIA-2 as a results of new approach in linear induction accelerators design. // Zababakhin Scientific Talks: XI Intern. Conf., Snezhinsk, 16 - 20 April 2012: Abstracts. - Snezhinsk: VNIITF, 2012. - p.140.

[542] Nikitin O.A., Stolbikov M.Yu., Akhmetov A.R., Bazarov P.S., Zhelezkin D.A., Khrenkov S.D., Kargin A.A., Shubin K.S., Syskov D.V., Akimov A.V., Bak Batazova M.A., Batrakov A.M., Belikov O.V., Boimelstein Yu.M., Bolkhovityanov D.Yu., Eliseev A.A., Emanov F.A., Fatkin G.A., Korepanov A.A., Kosarev A.N., Kulenko Ya.V., Kuznetsov G.I., Logachev P.V., Nikolaev I.V., Ottmar A.V., Pachkov A.A., Panov A.N., Pavlov O.A., Pureskin D.N., Ruvinsky E.S., Starostenko D.A., Suvorov S.O., Tokarev Yu.F., Torshin A.P., Tur S.V. A measurement of the electron beam parameters in the injector LIU-2. // Zababakhin Scientific Talks: XI Intern. Conf., Snezhinsk, 16 - 20 April 2012: Abstracts. - Snezhinsk: VNIITF, 2012. - p.168-169.

[543] Akimov A.V., Bak P.A., Batazova M.A., Batrakov A.M., Belikov O.V., Boimelstein Yu.M., Bolkhovityanov D.Yu., Eliseev A.A., Emanov F.A., Fatkin G.A., Korepanov A.A., Kosarev A.N., Kulenko Ya.V., Kuznetsov G.I., Logachev P.V., Nikolaev I.V., Ottmar A.V., Pachkov A.A., Panov A.N., Pavlov O.A., Pureskin D.N., Ruvinsky E.S., Starostenko D.A., Suvorov S.O., Tokarev Yu.F., Torshin A.P., Tur S.V., Nikitin O.A., Stolbikov M.Yu., Akhmetov A.R., Bazarov P.S., Zhelezkin D.A., Khrenkov S.D., Kargin A.A., Shubin K.S., Syskov D.V. A realization of the new approach of a linear induction accelerators development. // Zababakhin Scientific Talks: XI Intern. Conf., Snezhinsk, 16 - 20 April 2012: Abstracts. - Snezhinsk: VNIITF, 2012. - p.139.

[544] Anikeev A.V., Bagryansky P.A., Brednikhin S.A., Lezhnin S.I., Pribaturin N.A., Prikhodko V.V., Frolov S.A., Tsidulko Yu.A., Yurov D.V. Simulation of neutron-

physical processes in a hybrid system with a neutron source based on open plasma trap. // Zababakhin Scientific Talks: XI Intern. Conf., Snezhinsk, 16 - 20 April 2012: Abstracts. - Snezhinsk: VNIITF, 2012. - p.142.

[545] Tolochko B.P., Zhogin I.L., Mezentsev N.A., Levichev E.B., Kulipanov G.N., Aulchenko V.M., Ten K.A. New opportunities in diagnostics of detonation processes at the experimental SR station of the 100-pole superconducting wiggler of the VEPP-4 storage ring. // Zababakhin Scientific Talks: XI Intern. Conf., Snezhinsk, 16 - 20 April 2012: Abstracts. - Snezhinsk: VNIITF, 2012. - p.71.

[546] Beklemishev A.D., Burdakov A.V., Ivanov A.A., Ivanov I.A., Postupaev V.V., Sinitsky S.L. An open trap of the new generation in the BINP. // Zababakhin Scientific Talks: XI Intern. Conf., Snezhinsk, 16 - 20 April 2012: Abstracts. - Snezhinsk: VNIITF, 2012. - p.141.

[547] Nikitin O.A., Stolbikov M.Yu., Akhmetov A.R., Bazarov P.S., Zhelezkin D.A., Khrenkov S.D., Kargin A.A., Shubin K.S., Syskov D.V., Akimov A.V., Bak Batazova M.A., Batrakov A.M., Belikov O.V., Boimelstein Yu.M., Bolkhovityanov D.Yu., Eliseev A.A., Emanov F.A., Fatkin G.A., Korepanov A.A., Kosarev A.N., Kulenko Ya.V., Kuznetsov G.I., Logachev P.V., Nikolaev I.V., Ottmar A.V., Pachkov A.A., Panov A.N., Pavlov O.A., Pureskin D.N., Ruvinsky E.S., Starostenko D.A., Suvorov S.O., Tokarev Yu.F., Torshin A.P., Tur S.V. The X-ray experiments preparation and implementation on the injector LIU-2. // Zababakhin Scientific Talks: XI Intern. Conf., Snezhinsk, 16 - 20 April 2012: Abstracts. - Snezhinsk: VNIITF, 2012. - p.169-170.

[548] Akimov A.V. A high-voltage pulse power supply of LIU-2 // Zababakhin Scientific Talks: XI Intern. Conf., Snezhinsk, 16 - 20 April 2012: Abstracts. - Snezhinsk: VNIITF, 2012. - p.168.

[549] Brodnikov A.F., Cherepanov V.Ya. Definition of the valid temperature of boiling of water by means of constant point of sodium. // Interexpo Geo-Siberia-12. 8th International Specialized Exhibition and Scientific Congress "Customized Instrumentation, Metrology, Thermophysics, Micro Process Engineering, and Nanotechnologies", 10 - 20 April 2012, Novosibirsk, Conf. Proceedings (2 Volume). - Novosibirsk. - 2012. - p.174-177.

[550] Verkhoglyad A.G., Gerasimov V.V., Zavjalova M.A., Knyazev B.A., Makarov S.N., Stupak M.F. Concept of near-field scanning attachment to terahertz frustrated total internal reflection spectrometer. // Optics-and-Information Measuring and Laser Technologies and Systems: Anniversary selected works of TDI SIE SB RAS / ed. By Yu.V.Chuguy. - Novosibirsk: GEO, 2012. - p.409-427. (introduction by Kulipanov G.N. - p.3-6) (in Russian).

[551] Vedernikov V.M., Dutov P.M., Kokarev A.I., Kirjanov V.P., Knyazev B.A., Kulipanov G.N., Nikitin V.G., Palchikova V.G., Sametov A.R., Stupak M.F., Chuguy Yu.V., Chukanov V.V. Synthesis of transmissive diffractive elements for free electron laser. // Optics-and-Information Measuring and Laser Technologies and Systems: Anniversary selected works of TDI SIE SB RAS / ed. By Yu.V.Chuguy. - Novosibirsk: GEO, 2012. - p.360-374. (introduction by Kulipanov GN - p.3-6) (in Russian).

[552] Lotov K.V., Maslov V.I., Onischenko I.N., Yarovaya I.P. Transformer ratio for nonlinear plasma wakefield excitation by a ramped train of electron bunches with a linearly increasing intensity. // X Conference on High Energy Physics, Nuclear Physics, and Particle Accelerators, 27 February - 2 March 2012, Kharkov: abstracts. - Kharkov: NSC KIPT, 2012. - p.87.

[553] Burdakov A.V., Ivanov I.A., Kuklin K.N., Polosatkin S.V., Postupaev V.V., Shoshin A.A. Surface modification and droplet formation of tungsten under hot plasma irradiation at the GOL-3. // 20th Intern. Conference on Plasma Surface Interactions in Controlled Fusion Devices, May 21 - 25, 2012, Eurogress Aachen, Germany, P2-011. [https://www.congressa.de/PSI2012/files/abstracts/P2-011_Burdakov_PSI2012.pdf].

[554] Kandaurov I.V., Kurkuchekov V.V., Trunev Yu.A. The formation of an intense electron beam in a multiaperture source with plasma emitter and its transportation in a magnetic mirror configuration. // Proc. of the 4th Intern. Kreindel Workshop "Plasma Emission Electronics", 25 - 30 June, 2012", Ulan-Ude. - Publishing house: BSC SB RAS, Ulan-Ude. - 2012. - p.67-73.

[555] Astrelin V.T., Karpov I.E. Numerical simulation of the diode with plasma boundaries using emission characteristics of the cathode and anode plasma. // Proc. of the Intern. 4th Kreindel Workshop "Plasma Emission Electronics", Ulan-Ude, Russia, 25 - 30 June 2012. - Publishing house: BSC SB RAS, Ulan-Ude. - 2012. - p.74-80.

[556] Grigoriev S.V., Astrelin V.T., Kandaurov I.V., Koval N.N., Kozyrev A.V., Moskvina P.V., Teresov A.D. Investigation of the generation and transport of submillisecond electron beam formed in a diode with a plasma cathode with a grid-stabilized plasma boundary and plasma anode with an open mobile boundary. // Proc. of the Intern. 4th Kreindel Workshop "Plasma Emission Electronics", Ulan-Ude, Russia, 25 - 30 June 2012. - Publishing house: BSC SB RAS, Ulan-Ude. - 2012. - p.81-87.

[557] Astrelinn V.T., Karpov I.E. The potential distribution in a planar diode with a plasma cathode and anode plasma flow. // Proc. of the Intern. 4th Kreindel Workshop "Plasma Emission Electronics", Ulan-Ude, Russia, 25-30 June 2012. Publishing house: BSC SB RAS, Ulan-Ude. - 2012. - p.88-90.

[558] Arzhannikov A.V., Burdakov A.V., Kalinin P.V., Kuznetsov S.A., Makarov M.A., Ivanov I.A., Mekler K.I., Kandaurov I.V., Kurkuchekov V.V., Popov A.A., Postupaev V.V., Rovenskikh A.F., Sinitsky S.L., Sklyarov V.F., Stepanov V.D., Sulyaev Yu.S., Thumm M.K.A., Timofeev I.V., Vyacheslavov L.N. Experimental and theoretical investigations of emission of high power mm-wave and THz-radiation from magnetized plasma at two-stream instability of high current electron beams. // 24th Joint Russian-German Meeting on ECRH and Gyrotrons, June 11 - 15, 2012, Nizhny Novgorod, Russia.

[559] Thumm, M., Arzhannikov A.V., Kalinin P.V., Kuznetsov S.A., Sinitsky S.L., Stepanov V.D., Ginzburg N.S., Peskov N.Yu., Sergeev A.S., Zaslavsky V.Yu.. Coherent radiation from two-channel planar FEM with 2D distributed feedback. // 24th Joint Russian-German Meeting on ECRH and Gyrotrons, June 11 - 15, 2012, Nizhny Novgorod, Russia.

[560] Arzhannikov A.V., Timofeev I.V. Theoretical considerations on powerful terahertz emission from strongly turbulent plasmas driven by a relativistic electron beam. // 2nd Intern. Conference "Terahertz and Microwave radiation: Generation, Detection and Applications" (TERA-2012), 20 - 22 June 2012, Moscow. [<http://tera2012.phys.msu.ru>].

[561] Postupaev V.V., Burdakov A.V., Ivanov I.A., Mekler K.I., Rovenskikh A.F., Polosatkin S.V., Sinitsky S.L., Sorokina N.V., Sudnikov A.V.. Study of plasma rotation in GOL-3 multiple-mirror trap. // 39th EPS Conference and 16th Int. Congress on Plasma Physics, Stockholm, Sweden, 2 - 6 July 2012. [<http://ocs.ciemat.es/EPS2012PAP/pdf/P1.074.pdf>].

[562] Burdakov A.V., Avrorov A.P., Arzhannikov A.V., Astrelin V.T., Batkin V.I., Beklemishev A.D., Burmasov V.S., Bykov P.V., Derevyankin G.E., Ivanov I.A., Ivantsivsky M.V., Kandaurov I.V., Kasatov A.A., Kurkuchekov V.V., Kuklin K.N., Mekler K.I., Polosatkin S.V., Popov S.S., Postupaev V.V., Rovenskikh A.F., Shoshin A.A., Sinitsky S.L., Sklyarov V.F., Stepanov V.D., Sudnikov A.V., Sulyaev Yu.S., Timofeev I.V., Trunev Yu.A., and Vyacheslavov L.N. First experiments on injection of high-power long pulse electron beam in multiple-mirror trap GOL-3. // 39th EPS Conference and 16th Int. Congress on Plasma Physics, Stockholm, Sweden, 2 - 6 July 2012. [<http://ocs.ciemat.es/epsicpp2012pap/pdf/PD2.004.pdf>].

[563] Arzhannikov A.V., Burdakov A.V., Burmasov V.S., Ivanov I.A., Ivantsivsky M.V., Kotelnikov I.A., Kuznetsov S.A., Mekler K.I., Popov S.S., Polosatkin S.V., Postupaev V.V., Rovenskikh A.F., Sinitsky S.L., Sklyarov V.F., Timofeev I.V., Thumm M.K.A. Sub-mm wave emission at beam-plasma interaction in a multimirror trap. // 39th EPS Conference and 16th Int. Congress on Plasma Physics, Stockholm, Sweden, 2 - 6 July 2012, [<http://ocs.ciemat.es/epsicpp2012pap/pdf/P5.182.pdf>].

[564] Polosatkin S., Astrelin V., Bazylev B., Beklemishev A., Burdakov A., Gavrilenko D., Huber A., Ivanov A., Ivanov I., Kalinin P., Kandaurov I., Kreter A., Landman I., Postupaev V., Sinitsky S., Shoshin A., Trunev Yu., Thumm M., Unterberg B. GDMT-T: superconducting linear device for PMI studies. // Abstracts of 9th Intern. Conf. on Open Magnetic Systems for Plasma Confinement, Tsukuba, Japan, 27 - 31 August 2012. [<http://www.prc.tsukuba.ac.jp/OS2012/abstract-download/>].

[565] Burdakov A.V., Avrorov A.P., Arzhannikov A.V., Astrelin V.T., Batkin V.I., Beklemishev A.D., Burmasov V.S., Bykov P.V., Derevyankin G.E., Ivanenko V.G., Ivanov I.A., Ivantsivsky M.V., Kandaurov I.V., Kasatov A.A., Kuznetsov S.A., Kurkuchekov V.V., Kuklin K.N., Mekler K.I., Polosatkin S.V., Popov S.S., Postupaev V.V., Rovenskikh A.F., Sinitsky S.L., Stepanov V.D., Sudnikov A.V., Sulyaev Yu.S., Timofeev I.V., Trunev A.Yu., Sklyarov V.F., Sorokina N.V., Shoshin A.A., and Vyacheslavov L.N. Development of extended heating pulse operation mode at GOL-3. // Abstracts of 9th Intern. Conf. on Open Magnetic Systems for Plasma Confinement, Tsukuba, Japan, 27 - 31 August 2012. [<http://www.prc.tsukuba.ac.jp/OS2012/abstract-download/>].

[566] Arzhannikov A.V., Burdakov A.V., Burmasov V.S., Kalinin P.V., Kuznetsov S.A., Makarov M.A., Ivanov I.A., Mekler K.I., Popov A.A., Postupaev V.V., Rovenskikh A.F., Sinitsky S.L., Sklyarov V.F., Stepanov V.D., Timofeev I.V., Thumm M.K.A., Vyacheslavov L.N. Experimental and theoretical investigations of high power sub-millimeter wave emission at two-stream instability of high current REB. // Abstracts of 9th Intern. Conf. on Open Magnetic Systems for Plasma Confinement, Tsukuba, Japan, 27 - 31 August 2012, [<http://www.prc.tsukuba.ac.jp/OS2012/abstract-download/>].

[567] Beklemishev A., Anikeev A., Astrelin V., Bagryansky P., Burdakov A., Davydenko V., Gavrilenko D., Ivanov A., Ivanov I., Ivantsivsky M., Kandaurov I., Polosatkin S., Postupaev V., Sinitsky S., A. Shoshin, Timofeev I., Tsidulko Yu. Novosibirsk project of gas-dynamic multiple-mirror trap. // Abstracts of 9th Intern. Conf. on Open Magnetic Systems for Plasma Confinement, Tsukuba, Japan, 27 - 31 August 2012. [<http://www.prc.tsukuba.ac.jp/OS2012/abstract-download/>].

[568] Burdakov A.V., Ivanov A.A., Kruglyakov E.P., Beklemishev A.D. Axially symmetric magnetic mirrors: history of development and future prospects. // Abstracts of 9th Intern. Conf. on Open Magnetic Systems for Plasma Confinement, Tsukuba, Japan, 27 - 31 August 2012. [<http://www.prc.tsukuba.ac.jp/OS2012/abstract-download/>].

[569] Burdakov A.V., Arzhannikov A.V., Burmasov V.S., Ivanov I.A., Ivantsivsky M.V., Kandaurov I.V.,

Kasatov A.A., Kuznetsov S.A., Kurkuchekov V.V., Kuklin K.N., Mekler K.I., Polosatkin S.V., Popov S.S., Postupaev V.V., Rovenskikh A.F., Sklyarov V.F., Sudnikov A.V., Thumm M.K.A., Trunev Yu.A. and Vyacheslavov L.N. Microwave generation during 100 keV electron beam relaxation in GOL-3. // Abstracts of 9th Intern. Conf. on Open Magnetic Systems for Plasma Confinement, Tsukuba, Japan, 27 - 31 August 2012. [<http://www.prc.tsukuba.ac.jp/OS2012/abstract-download/>].

[570] Ivanov A.A., Akhmetov T.D., Beklemishev A.D., Burdakov A.V., Davydenko V.I., Lizunov A.A., Lozhkina A.N., Maximov V.V., Mishagin V.V., Myskin O.K., Prikhodko V.V., Soldatkina E.I., Savkin V.Ya., Shulzhenko G.I., Solomakhin A.L., Tiunov M.A., Trunev Yu.A., Voskoboynikov R.V., Zaytsev K.V. Auxiliary electron heating and plasma control in GDT device with electron beam: the results of initial experiments. // Abstracts of 9th Intern. Conf. on Open Magnetic Systems for Plasma Confinement, Tsukuba, Japan, 27 - 31 August 2012, P-18. [<http://www.prc.tsukuba.ac.jp/OS2012/abstract-download/>].

[571] Kurkuchekov V.V., Astrelin V.T., Avrorov A.P., Burdakov A.V., Bykov P.V., Davydenko V.I., Derevyankin G.E., Ivanov A.A., Kandaurov I.V., Rovenskikh A.F., Trunev Yu.A. and Yarovoy V.A. Novel injector of intense long pulse electron beam for linear plasma devices. // Abstracts of 9th Intern. Conf. on Open Magnetic Systems for Plasma Confinement, Tsukuba, Japan, 27 - 31 August 2012, P-19. [<http://www.prc.tsukuba.ac.jp/OS2012/abstract-download/>].

[572] Sudnikov A.V., Burdakov A.V., Gavrilenko D.E., Kandaurov I.V., Kurkuchekov V.V., Mekler K.I., Rovenskikh A.F., Polosatkin S.V., Postupaev V.V., and Trunev Yu.A. MHD Activity in GOL-3 during injection of long-pulse electron beam. // Abstracts of 9th Intern. Conf. on Open Magnetic Systems for Plasma Confinement, Tsukuba, Japan, 27 - 31 August 2012. [<http://www.prc.tsukuba.ac.jp/OS2012/abstract-download/>].

[573] Huber A., Burdakov A., Zlobinski M., Wirtz M., Linke J., Mertens Ph., Philipps V., Pintsuk G., Schweer B., Sergienko G., Shoshin A., Samm U., Unterberg B. Investigation of the impact on tungsten of transient heat loads induced by laser irradiation, electron beams and plasma guns. // Abstracts of 9th Intern. Conf. on Open Magnetic Systems for Plasma Confinement, Tsukuba, Japan, 2012, O/PMIF-9.

[574] Shoshin A.A., Burdakov A.V., Dobrovolskaya O.A., Grishnyaev E.S., Ivanov I.A., Kuklin K.N., Polosatkin S.V., Postupaev V.V., Sinitsky S.L., Vasilyev A.A. Study of materials erosion and modification after hot plasma irradiation in exit unit of multimirror trap GOL-3. // Abstracts of 9th Intern. Conf. on Open Magnetic Systems for Plasma Confinement, Tsukuba, Japan, 2012, P/PMIF-7.

[575] Trunev Yu.A., Astrelin V.T., Avrorov A.P., Burdakov A.V., Bykov P.V., Davydenko V.I., Derevyankin G.E., Ivanov A.A., Ivanov I.A., Kandaurov I.V., Kurkuchekov V.V., Mekler K.I., Polosatkin S.V., Postupaev V.V., Rovenskikh A.F., and Yarovoy V.A. Multiaperture electron gun with plasma cathode for injection of electron beam into open plasma trap. // Book of Abstracts of 4th Euro-Asian Pulsed Power Conference and 19th Intern. Conference on High-Power Particle Beams (EAPPC 2012/BEAMS 2012), September 30 - October 4, 2012, Karlsruhe, Germany. - p.109.

[576] Grigoryev S.V., Astrelin V.T., Koval N.N., Moskvina P.V., Teresov A.D. Investigation of the generation and transport of submillisecond electron beam formed in a diode with a grid plasma cathode and plasma anode with moveable open boundary. // Book of Abstracts of 4th Euro-Asian Pulsed Power Conference and 19th International Conference on High-Power Particle Beams (EAPPC 2012/BEAMS 2012), September 30 - October 4, 2012, Karlsruhe, Germany. - p.114.

[577] Stepanov V., Arzhannikov A., Kalinin P., Sinitsky S., Kuznetsov S., Ginzburg N., Peskov N., Sergeev A., Zaslavsky V., Thumm M. Experimental study of two-channel planar FEM with 2D distributed feedback. // Book of Abstracts of 4th Euro-Asian Pulsed Power Conference and 19th Intern. Conference on High-Power Particle Beams (EAPPC 2012/BEAMS 2012), September 30 - October 4, 2012, Karlsruhe, Germany. - p.121.

[578] Arzhannikov A.V., Burdakov A.V., Burmasov V.S., Kalinin P.V., Kuznetsov S.A., Makarov M.A., Ivanov I.A., Mekler K.I., Popov S.S., Postupaev V.V., Rovenskikh A.F., Sinitsky S.L., Sklyarov V.F., Stepanov V.D., Timofeev I.V., Thumm M.K., Vyacheslavov L.N. Experimental and theoretical investigations of high power sub-millimeter wave emission from plasma turbulence pumped by high current REB. // Book of Abstracts of 4th Euro-Asian Pulsed Power Conference and 19th Intern. Conference on High-Power Particle Beams (EAPPC 2012/BEAMS 2012), September 30 - October 4, 2012, Karlsruhe, Germany. - p.126.

[579] Burdakov A.V., Avrorov A.P., Arzhannikov A.V., Astrelin V.T., Batkin V.I., Beklemishev A.D., Burmasov V.S., Bykov P.V., Vyacheslavov L.N., Derevyankin G.E., Ivanenko V.G., Ivanov I.A., Ivantsivsky M.V., Kandaurov I.V., Kasatov A.A., Kuznetsov S.A., Kurkuchekov V.V., Kuklin K.N., Mekler K.I., Polosatkin S.V., Popov S.S., Postupaev V.V., Rovenskikh A.F., Sinitsky S.L., Stepanov V.D., Sudnikov A.V., Sulyaev Yu.S., Timofeev I.V., Sklyarov V.F., Sorokina N.V., Shoshin A.A. Experiments on GOL-3 Multiple Mirror Trap for Fusion Program. // Proc. of 24rd IAEA Fusion Energy Conference, San Diego, USA, 8-13 October, 2012, EX/P3-29.

[580] Kruglyakov Eh.P., Burdakov A.V., Ivanov A.A. Fusion Prospects of axisymmetric magnetic mirror systems. // Proc. of 24rd IAEA Fusion Energy

Conference, San Diego, USA, 8 - 13 October, 2012, OV/P-07.

[581] Fadin V.S. Kernel of the BFKL equation for the adjoint representation in the next-to-leading order. // Intern. Workshop "Hadron Structure and QCD: from LOW to HIGH energies". - July 4 - July 8, 2012, Gatchina, Russia.

[582] Fadin V.S. Presented talk: On radiative corrections to electron-proton scattering. // Olympus Symposium "Experimental and theoretical aspects of the proton form factors", July 9 - 11, 2012, Gatchina, Russia.

[583] Fadin V.S. Presented talk: NLO BFKL kernel for the adjoint representation of the gauge group. // Intern. Workshop "Diffraction 2012", September 11 - 15, Puerto del Camen, Lanzarote, Spain.

[584] Fadin V.S. Presented talk: Kernels of the BFKL equation in the next-to-leading order. // Workshop "Scattering Amplitudes and the Multi-Regge Limit", October 24 - 26, 2012, Madrid, Spain.

[585] Chernyak V.L. Hard two photon processes $\gamma\gamma \rightarrow M_2 M_1$ in QCD. // Invited talk given at the Taipei Intern. Workshop "QCD in Two Photon Processes", 2 - 4 October, 2012, Taipei, Taiwan. [arXiv: 1212.1304 [hep-ph], 2012. - p.1-19 (will be published in proceedings of the Workshop).

[586] Khatsymovsky V.M. On some feature and application of the Faddeev formulation of gravity. // Thesis of Intern. Conference "Quantum Field Theory and Gravity 2012". - July 31 - August 4 2012, Tomsk, Russia - TSPU Bulletin, N13(128). - p.76-80. - 2012. [arXiv: 1212.0978 (2012)].

[587] Sokolov V.V. Chaotic interference versus decoherence: external noise, state mixing and quantum-classical correspondence. // Proc. of the Intern. Conference: Chaos2012, 12 - 15 June, 2012, Athens, Greece. - p.2-5, 2012.

[588] Kharkov Yaroslav A., Sokolov Valentin V. Elastic enhancement factor as a quantum chaos probe. // Intern. Workshop "Quantum Transport and Quantum Effects in Photosynthetic Systems", 20 - 21 September, 2012, Breshia, Italy.

[589] Bapy C.E. Baru S.E. System of examination RCS – a state of affairs and prospects. // Report at the Intern. Scientifically-Practical Conference – An Exhibition «Special Tools not Lethal Action», April, 2012, Moscow, ST and S Ministry of Internal Affairs of the Russian Federation (in Russian).

[590] Baru S.E., Kim D.O. System continuous and selective people and luggage examination for prevention of acts of terrorism. // Report at VII Intern. Scientifically-Practical Conference «Counteraction Means to Terrorist and Criminal Explosions», October, 2012, St-Petersburg. (in Russian).

[591] Baru S.E. Problem's of introduction of innovative workings out INP the Siberian Branch of the Russian

Academy of Science in the field of medicine and safety. // Report at Practical Conference «Academy of Sciences as a Key Resource for New Economy» of Intern. Forum of "Interra", October, 2012, Novosibirsk (in Russian).

[592] Baru S.E., Leonov V.V. Installation of personal examination "Sibskan" // Report on Intern. Scientifically-Practical Congress «Perfection of a Control System, Prevention and Damping Consequences of Emergency Situations of Regions and a Problem of Ability to Live of the Population», October, 25 - 27, 2012, Novosibirsk (in Russian).

[593] Belikov O., Kolmogorov V., Kondaurov M., Kozak V., Medvedko A., Panasyuk V., Reva V. Bypass modules for solenoid shunting of 2 MeV electron cooler for COSY. // XXIII Russian Particle Accelerator Conference, RUPAC 2012, 24 - 28 September, Saint-Petersburg, Russia. WEPPC023.

[594] Reva V.B., Bryzgunov M.I., Panasyuk V.M., Parkhomchuk V.V. High energy electron cooling. // 52nd ICFA Advanced Beam Dynamics Workshop on High-Intensity and High-Brightness Hadron Beams, September 17-21, 2012, Beijing, China. WEO3A01.

[595] Starostenko Alexandr. High-precision magnet production at BINP. // Magnet Production Workshop, April 11-12, 2012, Brookhaven, USA. [http://www.bnl.gov/nsls2/workshops/docs/041212_Magnet_Workshop/default.asp].

[596] Rybitskaya Tatyana. Calculation of magnetic field harmonics. // Magnet Production Workshop, April 11-12, 2012, Brookhaven, USA. [http://www.bnl.gov/nsls2/workshops/docs/041212_Magnet_Workshop/default.asp].

[597] Kazantseva Erica, Skarbo Boris. Magnetic measurement facility. // Magnet Production Workshop, April 11-12, 2012, Brookhaven, USA. [http://www.bnl.gov/nsls2/workshops/docs/041212_Magnet_Workshop/default.asp].

[598] Aleksandr Tsyganov. Quadrupole magnets tuning. // Magnet Production Workshop, April 11-12, 2012, Brookhaven, USA. [http://www.bnl.gov/nsls2/workshops/docs/041212_Magnet_Workshop/default.asp].

[599] Kuznetsov G.I., Batazova M.A., et al. Commissioning of CARIBU EBIS charge breeder sub-systems. // Proc. of HIAT'2012, June 18-21, 2012, Chicago, IL USA, 2012 (WEB02). - p.165-169.

[600] Sokolov A., Bondar A., Buzulutskov A., Dolgov A., Shemyakina E. Study of Geiger-mode APDs performances at cryogenic temperatures. // Poster at Intern. Workshop on New Photon-Detectors (PhotoDet 2012), June 13-15, 2012, Orsay, France, [<http://photodet2012.lal.in2p3.fr>].

[601] Buzulutskov A. Two-phase Cryogenic Avalanche Detectors in Ar for rare-event experiments. // Invited talk at Intern. Workshop "Low Threshold Detectors and Their Application in Neutrino Physics",

Intern. Conference-Session of the Section of Nuclear Physics of PSD RAS, MEPHI, November 16, 2012, Moscow, Russia. [<http://www.icssp.mephi.ru/en>].

[602] Telnov V.I. Restriction on the energy and luminosity of e^+e^- storage rings due to beamstrahlung. // EuCARD LEP-3, CERN June 18, 2011.

[603] Telnov V.I. View on photon colliders at ILC, CLIC, Higgs factory SAPHIRE and super $\gamma\gamma$ factory. // Intern. Workshop on Linear Colliders (LCWS 2012), October 24, 2012, Arlington, US.

[604] Telnov V.I. Photon colliders: summary. // Intern. Workshop on Linear Colliders (LCWS 2012), October 24, 2012, Arlington, US.

[605] Telnov V.I. Limitation on the luminosity of e^+e^- storage rings due to beamstrahlung. // Accelerators for a Higgs factory (HF2012), November 15, 2012, FNAL, US.

[606] Telnov V.I. Limitation on the luminosity of e^+e^- storage rings due to beamstrahlung. // Intern. Workshop LHC on the March, November 21, 2012, Protvino, Russia.

[607] Telnov V.I. Higgs factories. // Intern. Workshop LHC on the March, November 21, 2012, Protvino, Russia.

[608] Bragin A., Levichev E.B., Piminov P.A., Sinyatkin S.V., Strakhovenko V.M., Telnov V.I., Zolotarev K.V. A Multi-TeV linear collider based on CLIC technology. // CLIC Conceptual Design Report, edited by M. Aicheler, P. Burrows, M. Draper, T. Garvey, P. Lebrun, K. Peach, N. Phinney, H. Schmickler, D. Schulte and N. Toge, CERN-2012-007.

[609] Bragin A., Levichev E.B., Piminov P.A., Sinyatkin S.V., Strakhovenko V.M., Telnov V.I., Zolotarev K.V. The CLIC Programme: towards a staged e^+e^- Linear Collider exploring the Terascale. // CLIC Conceptual Design Report, edited by P. Lebrun, L. Linssen, A. Lucaci-Timoce, D. Schulte, F. Simon, S. Stapnes, N. Toge, H. Weerts, J. Wells, CERN-2012-005, arXiv:1209.2543.

[610] Bragin A., Levichev E.B., Piminov P.A., Sinyatkin S.V., Strakhovenko V.M., Telnov V.I., Zolotarev K.V. // Physics and detectors at CLIC. CLIC Conceptual Design Report, edited by L. Linssen, A. Miyamoto, M. Stanitzki, H. Weerts, CERN-2012-003, arXiv:1202.5940, 2012.

[611] V.V. Anashin, V.M. Aulchenko, E.M. Baldin, A.K. Barladyan, A.Yu. Barnyakov, M.Yu. Barnyakov, S.E. Baru, I.Yu. Basok, O.L. Beloborodova, A.E. Blinov, V.E. Blinov, A.V. Bobrov, V.S. Bobrovnikov, A.V. Bogomyagkov, A.E. Bondar, A.R. Buzykaev, S.I. Eidelman, D.N. Grigoriev, Yu.M. Glukhovchenko, V.V. Gulevich, D.V. Gusev, S.E. Karnaev, G.V. Karpov, S.V. Karpov, T.A. Kharlamova, V.A. Kiselev, V.V. Kolmogorov, S.A. Kononov, K.Yu. Kotov, E.A. Kravchenko, V.F. Kulikov, G.Ya. Kurkin, E.A. Kuper,

E.B. Levichev, D.A. Maksimov, V.M. Malyshev, A.L. Maslennikov, A.S. Medvedko, O.I. Meshkov, S.I. Mishnev, I.I. Morozov, N.Yu. Muchnoi, V.V. Neufeld, S.A. Nikitin, I.B. Nikolaev, I.N. Okunev, A.P. Onuchin, S.B. Oreshkin, I.O. Orlov, A.A. Osipov, S.V. Peleganchuk, S.G. Pivovarov, P.A. Piminov, V.V. Petrov, A.O. Poluektov, V.G. Prisekin, A.A. Ruban, V.K. Sandyrev, G.A. Savinov, A.G. Shamov, D.N. Shatilov, B.A. Shwartz, E.A. Simonov, S.V. Sinyatkin, A.N. Skrinsky, V.V. Smaluk, A.V. Sokolov, A.M. Sukharev, E.V. Starostina, A.A. Talyshev, V.A. Tayursky, V.I. Telnov, Yu.A. Tikhonov, K.Yu. Todyshev, G.M. Tumaikin, Yu.V. Usov, A.I. Vorobiov, A.N. Yushkov, V.N. Zhilich, V.V. Zhulanov, A.N. Zhuravlev. Recent results from the KEDR detector. // 12th Intern. Workshop on Meson Production, Properties and Interaction, 31 May - 5 June, 2012, Krakow, Poland.

[612] V.V. Anashin, V.M. Aulchenko, E.M. Baldin, A.K. Barladyan, A.Yu. Barnyakov, M.Yu. Barnyakov, S.E. Baru, I.Yu. Basok, O.L. Beloborodova, A.E. Blinov, V.E. Blinov, A.V. Bobrov, V.S. Bobrovnikov, A.V. Bogomyagkov, A.E. Bondar, A.R. Buzykaev, S.I. Eidelman, D.N. Grigoriev, Yu.M. Glukhovchenko, V.V. Gulevich, D.V. Gusev, S.E. Karnaev, G.V. Karpov, S.V. Karpov, T.A. Kharlamova, V.A. Kiselev, V.V. Kolmogorov, S.A. Kononov, K.Yu. Kotov, E.A. Kravchenko, V.F. Kulikov, G.Ya. Kurkin, E.A. Kuper, E.B. Levichev, D.A. Maksimov, V.M. Malyshev, A.L. Maslennikov, A.S. Medvedko, O.I. Meshkov, S.I. Mishnev, I.I. Morozov, N.Yu. Muchnoi, V.V. Neufeld, S.A. Nikitin, I.B. Nikolaev, I.N. Okunev, A.P. Onuchin, S.B. Oreshkin, I.O. Orlov, A.A. Osipov, S.V. Peleganchuk, S.G. Pivovarov, P.A. Piminov, V.V. Petrov, A.O. Poluektov, V.G. Prisekin, A.A. Ruban, V.K. Sandyrev, G.A. Savinov, A.G. Shamov, D.N. Shatilov, B.A. Shwartz, E.A. Simonov, S.V. Sinyatkin, A.N. Skrinsky, V.V. Smaluk, A.V. Sokolov, A.M. Sukharev, E.V. Starostina, A.A. Talyshev, V.A. Tayursky, V.I. Telnov, Yu.A. Tikhonov, K.Yu. Todyshev, G.M. Tumaikin, Yu.V. Usov, A.I. Vorobiov, A.N. Yushkov, V.N. Zhilich, V.V. Zhulanov, A.N. Zhuravlev. Studies of $\psi(2S)$ and $\psi(3770)$ at KEDR. // 36th Intern. Conference on High Energy Physics, 4 - 11 July, Melbourne, Australia.

[613] Gerigk F., Cuvet Y., Dalocchio A., Favre G., Gentini L., Geisser J.M., Giguat J.M., Mathot S., Polini M., Ramberger S., Riffaud B., Rossi C., Ugena Tirado P., Wegner R., Vretenar M., Naumenko M., Kendjebulatov E., Kryuchkov Ya., Tribendis A. Design and construction of the Linac-4 accelerating structures. // To be published in the Proc. of the 26th Linear Accelerator Conference, September 9-14, 2012, Tel-Aviv, Israel.

[614] Gerigk F., Cuvet Y., Dalocchio A., Favre G., Gentini L., Geisser J.M., Giguat J.M., Mathot S., Polini M., Ramberger S., Riffaud B., Rossi C., Ugena Tirado P., Wegner R., Vretenar M., Naumenko M., Kendjebulatov E., Kryuchkov Ya., Tribendis A. Design and construction of the Linac-4 accelerating structures. // To be published

in the Proc. of the 26th Linear Accelerator Conference, September 9-14, 2012, Tel-Aviv, Israel.

[615] V.V. Anashin, V.M. Aulchenko, E.M. Baldin, A.K. Barladyan, A.Yu. Barnyakov, M.Yu. Barnyakov, S.E. Baru, I.Yu. Basok, O.L. Beloborodova, A.E. Blinov, V.E. Blinov, A.V. Bobrov, V.S. Bobrovnikov, A.V. Bogomyagkov, A.E. Bondar, A.R. Buzykaev, A.I. Vorobiov, Yu.M. Glukhovchenko, D.N. Grigoriev, V.V. Gulevich, D.V. Gusev, V.N. Zhilich, V.V. Zhulanov, A.N. Zhuravlev, E. Karnae, G.V. Karpov, S.V. Karpov, V.A. Kiselev, V.V. Kolmogorov, S.A. Kononov, K.Yu. Kotov, E.A. Kravchenko, V.N. Kudryavtsev, V.F. Kulikov, G.Ya. Kurkin, E.A. Kuper, E.B. Levichev, D.A. Maksimov, V.M. Malyshev, A.L. Maslennikov, A.S. Medvedko, O.I. Meshkov, S.I. Mishnev, I.I. Morozov, N.Yu. Muchnoi, V.V. Neifeld, S.A. Nikitin, I.B. Nikolaev, I.N. Okunev, A.P. Onuchin, S.B. Oreshkin, I.O. Orlov, A.A. Osipov, S.V. Peleganchuk, V.V. Petrov, S.G. Pivovarov, P.A. Piminov, A.O. Poluektov, V.G. Prisekin, A.A. Ruban, G.A. Savinov, V.K. Sandyrev, E.A. Simonov, S.V. Sinyatkin, A.N. Skrinsky, V.V. Smaluk, A.V. Sokolov, E.V. Starostina, A.M. Sukharev, A.A. Talyshev, V.A. Tayursky, V.I. Telnov, Yu.A. Tikhonov, K.Yu. Todyshev, G.M. Tumaikin, Yu.V. Usov, T.A. Kharlamova, A.G. Shamov, D.N. Shatilov, B.A. Shwartz, S.I. Eidelman, A.N. Yushkov. Precision measurement of narrow resonance masses with the KEDR detector. // Talk at the Intern. Conference-Session of the Section of Nuclear Physics of PSD RAS. November 12 - 16, 2012, MEPhI, Moscow.

[616] V.V. Anashin, V.M. Aulchenko, E.M. Baldin, A.K. Barladyan, A.Yu. Barnyakov, M.Yu. Barnyakov, S.E. Baru, I.Yu. Basok, O.L. Beloborodova, A.E. Blinov, V.E. Blinov, A.V. Bobrov, V.S. Bobrovnikov, A.V. Bogomyagkov, A.E. Bondar, A.R. Buzykaev, A.I. Vorobiov, Yu.M. Glukhovchenko, D.N. Grigoriev, V.V. Gulevich, D.V. Gusev, V.N. Zhilich, V.V. Zhulanov, A.N. Zhuravlev, E. Karnae, G.V. Karpov, S.V. Karpov, V.A. Kiselev, V.V. Kolmogorov, S.A. Kononov, K.Yu. Kotov, E.A. Kravchenko, V.N. Kudryavtsev, V.F. Kulikov, G.Ya. Kurkin, E.A. Kuper, E.B. Levichev, D.A. Maksimov, V.M. Malyshev, A.L. Maslennikov, A.S. Medvedko, O.I. Meshkov, S.I. Mishnev, I.I. Morozov, N.Yu. Muchnoi, V.V. Neifeld, S.A. Nikitin, I.B. Nikolaev, I.N. Okunev, A.P. Onuchin, S.B. Oreshkin, I.O. Orlov, A.A. Osipov, S.V. Peleganchuk, V.V. Petrov, S.G. Pivovarov, P.A. Piminov, A.O. Poluektov, V.G. Prisekin, A.A. Ruban, G.A. Savinov, V.K. Sandyrev, E.A. Simonov, S.V. Sinyatkin, A.N. Skrinsky, V.V. Smaluk, A.V. Sokolov, E.V. Starostina, A.M. Sukharev, A.A. Talyshev, V.A. Tayursky, V.I. Telnov, Yu.A. Tikhonov, K.Yu. Todyshev, G.M. Tumaikin, Yu.V. Usov, T.A. Kharlamova, A.G. Shamov, D.N. Shatilov, B.A. Shwartz, S.I. Eidelman, A.N. Yushkov. Results of $\psi(3770)$ parameters measurement at KEDR/VEPP-4M. // Talk at the Intern. Conference-Session of the Section of Nuclear Physics of PSD RAS. November 12 - 16, 2012, MEPhI, Moscow.

[617] V.V. Anashin, V.M. Aulchenko, E.M. Baldin, A.K. Barladyan, A.Yu. Barnyakov, M.Yu. Barnyakov, S.E. Baru, I.Yu. Basok, O.L. Beloborodova, A.E. Blinov, V.E. Blinov, A.V. Bobrov, V.S. Bobrovnikov, A.V. Bogomyagkov, A.E. Bondar, A.R. Buzykaev, A.I. Vorobiov, Yu.M. Glukhovchenko, D.N. Grigoriev, V.V. Gulevich, D.V. Gusev, V.N. Zhilich, V.V. Zhulanov, A.N. Zhuravlev, E. Karnae, G.V. Karpov, S.V. Karpov, V.A. Kiselev, V.V. Kolmogorov, S.A. Kononov, K.Yu. Kotov, E.A. Kravchenko, V.N. Kudryavtsev, V.F. Kulikov, G.Ya. Kurkin, E.A. Kuper, E.B. Levichev, D.A. Maksimov, V.M. Malyshev, A.L. Maslennikov, A.S. Medvedko, O.I. Meshkov, S.I. Mishnev, I.I. Morozov, N.Yu. Muchnoi, V.V. Neifeld, S.A. Nikitin, I.B. Nikolaev, I.N. Okunev, A.P. Onuchin, S.B. Oreshkin, I.O. Orlov, A.A. Osipov, S.V. Peleganchuk, V.V. Petrov, S.G. Pivovarov, P.A. Piminov, A.O. Poluektov, V.G. Prisekin, A.A. Ruban, G.A. Savinov, V.K. Sandyrev, E.A. Simonov, S.V. Sinyatkin, A.N. Skrinsky, V.V. Smaluk, A.V. Sokolov, E.V. Starostina, A.M. Sukharev, A.A. Talyshev, V.A. Tayursky, V.I. Telnov, Yu.A. Tikhonov, K.Yu. Todyshev, G.M. Tumaikin, Yu.V. Usov, T.A. Kharlamova, A.G. Shamov, D.N. Shatilov, B.A. Shwartz, S.I. Eidelman, A.N. Yushkov. Test of lepton universality in J/ψ -meson decays. // Talk at the Intern. Conference-Session of the Section of Nuclear Physics of PSD RAS. November 12 - 16, 2012, MEPhI, Moscow.

[618] Barnyakov A.Yu., Barnyakov M.Yu., Bobrovnikov V.S., Buzykaev A.R., Kononov S.A., Kravchenko E.A., Onuchin A.P. Long-term stability of aerogel Cherenkov counters of the KEDR detector. // Talk at the Intern. Conference-Session of the Section of Nuclear Physics of PSD RAS. November 12 - 16, 2012, MEPhI, Moscow.

[619] Barnyakov A.Yu., Barnyakov M.Yu., Basok I.Yu., Blinov V.E., Bobrovnikov V.S., Borodenko A.A., Buzykaev A.R., Danilyuk A.F., Gulevich V.V., Kononov S.A., Kravchenko E.A., Kuyanov I.A., Onuchin A.P., Ovtin I.V., Talyshev A.A. Test beam experiment with FARICH prototype. // Intern. Workshop on New Photon-Detectors (PhotoDet 2012), June 2012, Orse, France.

[620] Barnyakov A.Yu., Barnyakov M.Yu., Bobrovnikov V.S., Buzykaev A.R., Danilyuk A.F., Degenhardt K., Dorscheid ., Kononov S.A., Kravchenko E.A., Kurepin A., Myulens O., Onuchin A.P., Reshetin A., Talyshev A.A. Usenko E., Finogeev D., Frah T., Tswans B., Shmits A. Beam test of FARICH prototype with PDPC dSiPM readout. // Workshop: Preliminary Results on the Feasibility of Using Digital SiPM (dSiPM) Technology in FARICH, June 2012, CERN, Geneva, Switzerland.

[621] Ivanov A.A., Burdakov A.V., Davydenko V.I. Ion sources and accelerators for a nuclear impurity incorporation and boron - neutron-capture therapy. // IV All-Russian Conference "Physical and Physical-Chemical Foundations of Ion Implantation" (with participation of foreign scientists) and the International Youth

Conference "Radiation-thermal Effects and Processes in Inorganic Materials", October 23 - 26, 2012, Novosibirsk: Book of Abstracts. - Novosibirsk, 2012 - P.100. (It is devoted to memory of the Honored worker of science and engineering of the Russian Federation of Leonid Stepanovich Smirnov).

[622] Trunova V., Fedotov A., Zvereva V., Maksimovskaya V., Melgunov M. Scanning SRXRF analysis in the investigation of the proglacial lake bottom sediments of the Baikalsky Ridge for reconstruction of glacier fluctuation for the last 160 years. // Program and Book of Abstracts of European Conference on X-ray Spectrometry, June 18 -22, 2012, Vienna, Austria. - S.I, 2012. - p.100.

[623] Chernoshтанov I.S., Tsidulko Yu.A. Alf^{ven} ion-cyclotron instability in a mirror trap with skew injection of neutral beams. // Proc. of 9th Intern. Conference on Open Magnetic Systems for Plasma Confinement, August 27-31, 2012, Tsukuba, Japan.

[624] Yurov D.V., Brednikhin S.A., Frolov S.A., Lezhnin S.I., Prikhodko V.V., Tsidulko Yu.A. Recent calculation results for a fission-fusion system with gas dynamic trap neutron source. // Proc. of 9th Intern. Conference on Open Magnetic Systems for Plasma Confinement, August 27-31, 2012, Tsukuba, Japan.

[625] Anderson J.K., Almagri A.F., Den Hartog D.J., Eilerman S., Forest C.B., Koliner J.J., Mirnov V.V., Morton L.A., Nornberg M.D., Parke E., Reusch J.A., Sar J.S., Waksman J., Belykh V., Davydenko V.I., Ivanov A.A., Polosatkin S.V., Tsidulko Y.A., Lin L., Liu D., Fiksel G., Sakakita H., Spong D.A., Titus J. Fast ion confinement and stability in a neutral beam injected reversed field pinch. // 54th Annual Meeting of the APS Division of Plasma Physics. - 2012. - Vol.57, N12.

[626] Romé M., Kotelnikov I. Relativistic thermal equilibria of nonneutral plasmas. // 10th Intern. Workshop on Non-Neutral Plasmas, August 27 - 30, 2012, Greifswald, Germany.

[627] Kotelnikov I.A., Gerasimov V.V., Knyazev B.A. Diffraction of surface wave on conducting rectangular wedge. // 37th Intern. Conference on Infrared, Millimeter and Terahertz Waves (IRMMW-THz 2012), September 23 - 28, 2012, University of Wollongong, Australia. Report Tue-A-4-4.

[628] Eilerman S., Almagri A.F., Anderson J.K., Belykh V.V., Chapman B.E., Davydenko V.I., Den Hartog D.J., Ding W.X., Fiksel G., Forest C.B., Ivanov A.A., Koliner J.J., Kumar S.T.A., Lin L., Liu D., Magee R.M., Mirnov V.V., Nornberg M.D., Polosatkin S.V., Reusch J.A., Sarff J.S., Spong D.A., Stupishin N., Waksman J. Energetic ion generation and confinement in the MST RFP. // 39th EPS Conference on Plasma Physics, 16th Intern. Congress on Plasma Physics, 2 - 6 July, 2012, Stockholm, Sweden. - P2.069.

[629] Ivanov A.A., Abdrashitov G.F., Anashin V.V., Belchenko Yu.I., Burdakov A.V., Davydenko V.I., Deichuli P.P., Dimov G.I., Dranichnikov A.N.,

Kapitonov V.A., Kolmogorov V.V., Kondakov A.A., Sanin A.L., Shikhovtsev I.V., Stupishin N.V., Sorokin A.V., Popov S.S., Tiunov M.A., Voskoboinikov R.V., Belov V.P., Gorbovsky A.I., Kobets V.V., Bindenbauer M., S.Putvinsky, Smirnov A., Seveir L. Development of a negative ion-based neutral beam injector in Novosibirsk. // 3rd Intern. Symposium on Negative Ions, Beams, and Sources, NIBS 2012, 3 - 7 September 2012, Jyväskylä, Finland. - Book of Abstracts. - p.46, O-2 11.

[630] Prokhorov I.A., Abdrashitov G.F., Averbukh I.I., Belov V.P., Davydenko V.I., Ivanov A.A., Kapitonov V.A., Kolmogorov V.V., Kondakov A.A., Shikhovtsev I.V., Sorokin A.V., Tkachev A.A. Ion source for 10 sec diagnostic neutral beam. // Abstracts of 9th Intern. Conf. on Open Magnetic Systems for Plasma Confinement, 27 - 31 August 2012, Tsukuba, Japan. - P-40. [<http://www.prc.tsukuba.ac.jp/OS2012/abstract-download>].

[631] Davydenko V.I., Ivanov A.A., Kotelnikov I., Kreter A., Mishagin V.V., Prokhorov I., Shikhovtsev I.V., Unterberg B. High efficiency helicon plasma source for PMI studies. // Abstracts of Joint Conference of OS2012 and PMIF2012, 27 - 31 August 2012, Tsukuba, Japan. - O-15. [<http://www.prc.tsukuba.ac.jp/OS2012/abstract-download>].

[632] Anikeev A.V., Bagryansky P.A., Brednikhin S.A., Lezhnin S.I., Prikhodko V.V., Frolov S.A., Tsidulko Yu.A., Yurov D.V. Simulation of plasma and neutron processes in the hybrid system with a neutron source based on GDT. // Book of abstracts of Russian Seminar "The Physical and Technical Aspects of the Volume Source of Neutrons for Materials Science, Technology Research and Solving Problems of Nuclear Power", June 4 - 8, 2012, Zvenigorod. - p.18-19.

[633] Bagryansky P.A. The results of experiments in support of the neutron source project based on gas dynamic trap for nuclear power plants. // Book of abstracts of Russian seminar "The physical and technical aspects of the volume source of neutrons for materials science, technology research and solving problems of nuclear power", June 4 - 8, 2012, Zvenigorod. - p.48-49.

[634] Anikeev A.V., Bagryansky P.A., Brednikhin S.A., Lezhnin S.I., Prikhodko V.V., Frolov S.A., Tsidulko Yu.A., Yurov D.V. Plasma neutron source based on gas-dynamic trap for hybrid nuclear plants. Book of abstracts of Russian seminar "The physical and technical aspects of the volume source of neutrons for materials science, technology research and solving problems of nuclear power", June 4 - 8, 2012, Zvenigorod. - p.81-82.

[635] Anikeev A.V. The fusion neutron source as a driver in a sub-critical burner of radioactive wastes. // Humboldt Colloquium «The Role of Fundamental Sciences in Society», USA. - p.18-19.

[636] Barkov L.M., Dmitriev V.F., Dusaev R.R., Gauzshtein V.V., Loginov A.Yu., Mishnev S.I., Nikolenko D.M., Rachek I.A., Sadykov R.S., Shestakov Yu.V., Sidorov A.A., Stibunov V.N., Toporkov D.K.,

Zevakov S.A. Measurement of the exclusive reaction of the negative pion photoproduction on polarized deuterons in the region of the large values of the final proton momenta. // Nucleus 2012: Fundamental problems of nuclear physics, atomic power engineering and nuclear technologies. June 25 - 30, 2012, Voronezh, Russia. - Book of abstract, p.122.

[637] Dusaev R.R., Gauzshtein V.V., Loginov A.Yu., Nikolenko D.M., Rachek I.A., Sadykov R.S., Shestakov Yu.V., Sidorov A.A., Stibunov V.N., Toporkov D.K., Zevakov S.A. Measurement of the tensor analyzing power components of the negative pion photoproduction on deuterons. // Nucleus 2012: Fundamental problems of nuclear physics, atomic power engineering and nuclear technologies. June 25 - 30, 2012, Voronezh, Russia. - Book of abstract, p.127.

[638] Barkov L.M., Dmitriev V.F., Dusaev R.R., Gauzshtein V.V., Loginov A.Yu., Mishnev S.I., Nikolenko D.M., Rachek I.A., Sadykov R.S., Shestakov Yu.V., Sidorov A.A., Stibunov V.N., Toporkov D.K., Zevakov S.A. Measurement of the differential cross section of the negative pion photoproduction on deuteron at large proton momenta // Nucleus 2012: Fundamental problems of nuclear physics, atomic power engineering and nuclear technologies. June 25 - 30, 2012, Voronezh, Russia. - Book of abstract, p.135.

[639] Kuksanov N.K., Fadeev S.N., Golubenko Yu.I., Kogut D.A., Korchagin A.I., Lavrukhin A.V., Nemytov P.I., Salimov R.A., Semenov A.V. ELV-accelerator for industrial application (family of accelerators and tendency of development. // Proc. of 23rd All-Russian Particle Accelerator Conference: RuPAC'2012, Sept. 24 - 28, 2012, Saint-Petersburg, Russia: Proc. - Saint-Petersburg, 2012 (in Russian).

[640] Kuksanov N.K., Fadeev S.N., Kogut D.A. Development of the model range and improve performance accelerators ELV. // Proc of 23rd All-Russian Particle Accelerator Conference: RuPAC'2012, Sept. 24 - 28, 2012, Saint-Petersburg, Russia: Proc. - Saint-Petersburg, 2012 (in Russian).

[641] Shevchenko O.A., Arbuzov V.S., Chernov K.N., Demytyev E.N., Dovzhenko B.A., Getmanov Ya.V., Gorniker E.I., Knyazev B.A., Kolobanov E.I., Kondakov A.A., Kozak V.R., Kozyrev E.V., Kubarev V.V., Kulipanov G.N., Kuper E.A., Kuptsov I.V.Kurkin., G.Ya., Medvedev L.E., Mironenko L.A., Ovchar V.K., Persov B.Z., Pilan A.M., Popik V.M., Repkov V.V., Salikova T.V., Scheglov M.A., Sedlyarov I.K., Serdobintsev G.V., Serednyakov S.S., Skrinsky A.N., Tararyshkin S.V., Tcheskidov V.G., Vinokurov N.A., Vlasenko M.G., Vobly P.D., Volkov V.N. The Novosibirsk Terahertz FEL facility – current status and future prospects. // 34th Intern. Free-Electron Laser (FEL2012), 26 - 31 August, 2012, Nara, Japan.

[642] Kamps T., Anders W., Barday R., Jankowiak A., Knobloch J., Kugeler O., Matveenko A.N., Neumann A., Quast T., Rudolph J., Schubert S.G., Völker J., Kneisel

P., Nietubyc R., Sekutowicz J.K., Smedley J., Teichert J., Volkov V., Will I. Operational experience with the Nb/Pb SRF photoelectron gun. // Intern. Particle Conference (IPAC2012), 20 - 25 May, New Orleans, Louisiana, USA. - p.1518.

[643] Volkov V., Barday R., Kamps T., Knobloch J., Matveenko A.N., Schubert S.G., Völker J., Sekutowicz I.K. The source of emittance dilution and photoemission tunneling effect in photocathode RF guns. // Intern. Particle Conference (IPAC2012), 20 - 25 May, New Orleans, Louisiana, USA. - p.1542.

[644] Volkov V., Barday R., Kamps T., Knobloch J., Matveenko A.N., Neumann A. Interpretation of dark current experimental results in HZB SC RF gun. // Intern. Particle Conference (IPAC2012), 20 - 25 May, New Orleans, Louisiana, USA. - p.1545.

[645] Volkov V., Barday R., Kamps T., Knobloch J., Matveenko A.N. Cathode insert design for SC RF guns Intern. Particle Conference (IPAC2012), 20 - 25 May, New Orleans, Louisiana, USA. - p.1548.

[646] Volkov V. Numerical simulation of dark current and halo particles. // Unwanted Beam Workshop (UBW), 19 - 20 December, 2012, Berlin. [<https://indico.helmholtz-berlin.de/getFile.py/access?contribId=25&sessionId=12&resId=0&materialId=slides&confId=2>].

[647] Belchenko Yu.I., Davydenko V.I., Gorbovsky A.I., Ivanov A.A., Kobets V.V., Konstantinov S.G., Sanin A.L., Schikhovtsev I.V., Tiunov M.A. Multiaperture Negative Ion Source // 3rd Intern. Symp. on Negative Ions, Beams and Sources (NIBS 2012), Sept. 3 - 7, 2012, Jyväskylä, Finland. - Abstracts: Jyväskylä, 2012, p.42.

[648] Belchenko Yu.I., Gorbovsky A.I., Ivanov A.A., Sanin A.L., Savkin V.Ya., Tiunov M.A. Upgrade of CW negative hydrogen ion source. // 3rd Intern. Symp. on Negative Ions, Beams and Sources (NIBS 2012), Sept. 3 - 7, 2012, Jyväskylä, Finland. - Abstr.: Jyväskylä, 2012, p.72.

[649] Taskaev S., Aleynik V., Bashkirtsev A., Kamkin M., Kasatov D., Kuznetsov A., Makarov A., Schudlo I., Sorokin I., Tiunov M. Current progress and future prospects of the VITA based neutron source. // 15th Intern. Congress on Neutron Capture Therapy, Sept. 10 - 14, 2012, Tsukuba, Japan. – Abstracts.: Tsukuba, 2012, p.99.

[650] Volk J., Shiltsev V., Chupyra A., Kondaurov M., Singatulin S., Fratta D., Meulemans A., Potier C., Wang H. Hydrostatic level systems at Fermilab and SURF. // Proc. of 12th Intern. Workshop on Accelerator Alignment (IWAA 12), FNAL, 10 - 14 September 2012, Batavia.

[651] A.L. Gudkov, A.I. Kozlitsin, V.M. Matveev, V.I. Mishachev, N.V. Spinko, V.A. Ushakov, O.V. Anchugov, V.S. Arbuzov, D.E. Berkaev, D.Yu. Bolkhovityanov, S.S. Vasichev, V.F. Veremeenko, B.G. Goldenberg, E.I. Gorniker, B.A. Dovzhenko, S.E. Karnae, B.A. Kiselev, S.A. Krutikhin, V.R. Kozak, G.N. Kulipanov, E.A. Kuper, K.E. Kuper, I.V. Kuptsov,

G.Ya. Kurkin, A.S. Medvedko, A.D. Nikolenko, V.M. Petrov, A.M. Pilan, I.K. Sedlyarov, A.M. Semenov, G.V. Serdobintsev, S.V. Sinyatkin, A.G. Steshov, S.V. Tararyshkin, A.V. Filipchenko, K.N. Chernov, A.D. Chernyakin, I.N. Churkin, D.A. Shvedov, V.D. Yudin, A.G. Valentinov, V.N. Korchuganov, Yu.V. Krylov, D.G. Odintsov, Yu.L. Yupinov. High technology center based on technological synchrotron "Zelenograd": current state and perspectives. // XIX Synchrotron Radiation Conference (SR-2012). 25 - 28 June 2010, Novosibirsk.

[652] Abelleira J., Russenchuck S., ..., Shatilov D., et al. Local chromatic correction scheme and crab-waist collisions for an ultra-low beta at the LHC. // Proc. of IPAC'12, New Orleans, 20 - 25 May, 2012, USA. [<http://accelconf.web.cern.ch/accelconf/IPAC2012/papers/moppc002.pdf>].

[653] Guiducci S., Bacci A., ..., Shatilov D., et al. Baseline design of the SuperB Factory Injection System. // Proc. of IPAC'12, New Orleans, 20 - 25 May, 2012, USA. [<http://accelconf.web.cern.ch/accelconf/IPAC2012/papers/tuppr088.pdf>].

[654] Nagaitsev S., Valishev A., Danilov V., Shatilov D. Beam physics of integrable optics test accelerator at Fermilab. // Proc. of IPAC'12, New Orleans, 20 - 25 May, 2012, USA. [arXiv: 1301.6671 [physics.acc-ph]]. [<http://arxiv.org/abs/1301.6671>].

[655] Nagaitsev S., Valishev A., Danilov V., Shatilov D. Design and simulation of IOTA - a novel concept of integrable optics test accelerator. // Proc. of IPAC'12, New Orleans, 20 - 25 May, 2012, USA. - FERMILAB-CONF-12-247-AD. [arXiv:1301.7032 [physics.acc-ph]]. [<http://arxiv.org/abs/1301.7032>].

[656] Stancari G., Valishev A., Previtali V., Shatilov D. Numerical simulations of transverse beam diffusion enhancement by the use of electron lens in the Tevatron Collider. // Proc. of IPAC'12, New Orleans, 20 - 25 May, 2012, USA. [<http://accelconf.web.cern.ch/accelconf/IPAC2012/papers/tueppb002.pdf>].

[657] Morozov I., Stancari G., Valishev A., Shatilov D. Simulation of hollow electron beam collimation in the Fermilab Tevatron Collider. Proc. of IPAC'12, New Orleans, 20 - 25 May, 2012, USA. [<http://accelconf.web.cern.ch/accelconf/IPAC2012/papers/moeppb008.pdf>].

[658] Nikitin S.A. Status of the Super B project and beam polarization issues. // XX Intern. Symposium on Spin Physics (SPIN6), 17 - 22 Sept., 2012, Dubna. [<http://theor.jinr.ru/~spin2012/talks/s6/Nikitin.pdf>].

[659] Bogomyagkov A.V. BINP tau charm plans and other projects in Turkey/China. // The 5th Intern. Workshop on Charm Physics 9 Charm 2012), May 14 - 17, 2012, Honolulu, Hawaii.

[660] B. Dalena, R. Appleby, A.V. Bogomyagkov, A. Chancé, J. Payet, R. De Maria, B.J. Holzer, A. Faus-Golfe, J. Resta-López, K.M. Hock, M. Korostelev, L.N.S. Thompson, A. Wolski, C. Milardi. Optics and lattice optimizations for the LHC upgrade project. // IPAC12, May 20 - 25, 2012, New Orleans Louisiana, USA.

[661] R. De Maria, S. Fartoukh, A. Bogomyagkov, M. Korostolev. HLLHCv1.0: HL-LHC layout and optics version for 150 mm Nb3Sn triplets and local crab-cavities. // 2nd Joint HiLumi LHC-LARP Annual Meeting, 14 -16 November, 2012, INFN, Frascati.

[662] M. Giovannozzi, R. Appleby, J. Barranco, A. Bogomyagkov, Y. Cai, A. Chance, B. Dalena, R. De Maria, S. Fartoukh, A. Faus-Golfe, K. Hock, Y. Jiao*, M. Korostelev, E. Levichev, Y. Nosochkov, J. Payet, P. Piminov, J. Resta Lopez, L. Rivkin, R. Tomás, M-H. Wang, A. Wolski, Y. Yan, M. Zobov. Particle simulations: status and plans. // 2nd Joint HiLumi LHC-LARP Annual Meeting, 14 -16 November, 2012, INFN, Frascati.

[663] B. Holzer, B. Dalena, A. Bogomyagkov, R. Appleby, A. Faus-Golfe, J. Payet, A. Chance', K. Hock, M. Korostelev, R. de Maria, J. Resta, C. Milardi, L. Thompson, M. Thomas, A. Wolski. HL-LHC optics configuration vs. experiment desiderata. // 2nd Joint HiLumi LHC-LARP Annual Meeting, 14 -16 November, 2012, INFN, Frascati.

[664] A.I. Senchenko, D.E. Berkaev, A.S. Kasaev, I. Koop, V.R. Kozak, A.N. Kyrpotin, A.P. Lysenko, Yu. A. Rogovsky, A.L. Romanov, P.Yu. Shatunov, Y.M. Shatunov, A.S. Stankevich. VEPP-2000 Collider Control System. // Proc. of the 9th Intern. Workshop on Personal Computers and Particle Accelerator Controls, December 4 - 7, 2012, Kolkata, India.

[665] A.I. Senchenko, D.E. Berkaev. VEPP-2000 Logging System. // Proc. of the 9th Intern. Workshop on Personal Computers and Particle Accelerator Controls, December 4 - 7, 2012, Kolkata, India.

Preprints

1. A.V. Bobrov, A.E. Bondar. Background from τ decays in a search for $\tau \rightarrow \mu\gamma$. // Preprint INP 2012-1, 23p. - Novosibirsk, 2012 (in Russian).

2. V.I. Aleinik, A.S. Kuznetsov, I.N. Sorokin, S.Yu. Taskaev, M.A. Tiunov. The registration of high intensity dark current in vacuum insulation tandem accelerator after increasing the aperture of accelerator channel. // Preprint INP 2012-2, 14p. - Novosibirsk, 2012 (in Russian).

3. V.I. Aleinik, A.S. Kuznetsov, I.N. Sorokin, S.Yu. Taskaev, M.A. Tiunov, I.M. Schudlo I.M. Calibration of stripping target in vacuum insulation tandem accelerator. // Preprint INP 2012-4, 15p. - Novosibirsk, 2012 (in Russian). nnn

4. A.A. Listopad, V.I. Davydenko, A.A. Ivanov, V.V. Mishagin, B. Schweer, R. Uhlemann Multislit four-electrode ion-optical system for fast atomical diagnostic beam formation. // Preprint INP 2012-6, 15p. - Novosibirsk, 2012 (in Russian).

5. V.I. Aleinik, A.G. Bashkirtsev, A.S. Kuznetsov, A.N. Makarov, I.N. Sorokin, S.Yu. Taskaev, M.A. Tiunov, I.M. Schudlo. // Optimization of transporting of

hydrogen ion beam in vacuum insulation tandem accelerator. // Preprint INP 2012-7, 12p. - Novosibirsk, 2012 (in Russian).

6. A.G. Bashkirtsev, A.A. Ivanov, D.A. Kasatov, A.S. Kuznetsov, I.N. Sorokin, S.Yu. Taskaev, V.Ya. Chudaev Calculation and experimental accounts of X-ray field generating by high-voltage components of the facility «Accelerator-tandem BNCT». // Preprint INP 2012-8, 18p. - Novosibirsk, 2012 (in Russian).

7. V.M. Aulchenko, M.N. Achasov, A.Yu. Barnyakov, K.I. Beloborodov, A.V. Berdyugin, D.E. Berkaev, B.E. Blinov, A.G. Bogdanchikov, A.A. Borisov, A.A. Botov, A.V. Vasiliev, V.B. Golubev, K.A. Grevtsov, T.V. Dimova, V.P. Druzhinin, I.M. Zemlyansky, L.V. Kardapoltsev, A.S. Kasaev, A.N. Kirpotin, D.P. Kovrizhin, I.A. Koop, A.A. Korol, S.V. Koshuba, E.A. Kravchenko, A.P. Lysenko, K.A. Martin, I.N. Nesterenko, A.E. Obrazovsky, A.P. Onuchin, E.V. Pakhtusova, E.A. Perevedentsev, Yu.A. Rogovsky, A.L. Romanov, S.I. Serednyakov, Z.K. Silagadze, K.Yu. Skovpen, A.N. Skrinsky, I.K. Surin, A.I. Tekutiev, Yu.A. Tikhonov, Yu.V. Usov, A.G. Kharlamov, P.Yu. Shatunov, Yu.M. Shatunov, D.B. Shwartz, D.A. Shtol, A.N. Shukaev. Search of e^+e^- annihilation into neutron-antineutron pair in SND experiment at VEPP-2000 collider. // Preprint INP 2012-14, 27p. - Novosibirsk, 2012 (in Russian).

8. V.G. Barkova, V.Ya. Chudaev, N.S. Shamakina. Attenuation of equivalent dose of direct high-energy bremsstrahlung beam by means of local protective screens // Preprint INP 2012-16, 15p. - Novosibirsk, 2012 (in Russian).

9. Compiled by A.A. Ivanov, V.V. Prikhodko, M.S. Korzhavina, and K.V. Zaytsev. The GDT-based neutron source and related issues (Annotated bibliography), Preprint Budker INP 2012-18, 67p. - Novosibirsk, 2012.

10. V.S. Fadin, R. Fiore, A. Papa. Difference between standard and quasi-conformal BFKL kernels. // Preprint Budker INP 2012-19, 22p. - Novosibirsk, 2012.

11. E.V. Abakumova, V.M. Aulchenko, M.N. Achasov, A.Yu. Barnyakov, K.K.I. Beloborodov, A.V. Berdyugin, D.E. Berkaev, B.E. Blinov, A.G. Bogdanchikov, A.A. Botov, D.A. Bukin, A.V. Vasiliev, V.M. Vesenev, E.A. Vlasenko, V.B. Golubev, K.A. Grevtsov, T.V. Dimova, V.P. Druzhinin, A.A. Zhukov, I.M. Zemlyansky, L.V. Kardapoltsev, A.N. Kirpotin, D.P. Kovrizhin, I.A. Koop, A.A. Korol, S.V. Koshuba, E.A. Kravchenko, A.Yu. Kulpin, A.S. Kupich, A.P. Lysenko, K.A. Martin, I.N. Nesterenko, A.E. Obrazovsky, V.P. Oleinikov, A.P. Onuchin, E.V. Pakhtusova, E.A. Perevedentsev, E.E. Pyata, Yu.A. Rogovsky, A.L. Romanov, S.I. Serednyakov, Z.K. Silagadze, K.Yu. Skovpen, A.N. Skrinsky, I.K. Surin, A.I. Tekutiev, Yu.A. Tikhonov, Yu.V. Usov, A.G. Kharlamov, P.Yu. Shatunov, Yu.M. Shatunov, D.B. Shwartz, D.A. Shtol, A.N. Shukaev. Status of

experiments with the SND detector at the collider VEPP-2000 // Preprint INP 2012-20, 27p. - Novosibirsk, 2012 (in Russian).

12. V.G. Barkova, V.Ya. Chudaev, N.S. Shamakina. Concrete-shield attenuation of the air kerma of bremsstrahlung from thick iron targets at off-normal incidence of bremsstrahlung onto the shield $E_0 = 0.5; 1.0; 2.0; 2.8$ MeV. // Preprint INP 2012-26, 26p. - Novosibirsk, 2012 (in Russian).

13. V.M. Petrov, N.V. Mityanina. Cross feedback networks in synchrotron accelerating RF systems for essential increase of the beam current Preprint INP 2012-27, 41p. - Novosibirsk, 2012 (in Russian).

14. A.M. Batrakov, P.V. Vagin, I.V. Ilyin, A.V. Pavlenko, D.S. Shichkov. Precise multimode digital integrators VsDC2 and VsDC3. // Preprint INP 2012-31, 25p. - Novosibirsk, 2012 (in Russian).

15. S. Bladwell, V.F. Dmitriev, V.V. Flambaum, A. Kozlov. Colour-octet bound states, induced by Higgs mechanism. // arXiv:1212.5416.

16. R.E. Gerasimov, A.V. Grabovsky. Evolution equation for 3-quark Wilson loop operator. // arXiv:1212.1681 [hep-th].

17. Bartels J., Fadin V.S., Lipatov L.N. and Vacca G.P. NLO Corrections to the kernel of the BKP equations. // arXiv:1210.0797 [hep-ph]; to be published in Nucl. Phys. B 867 (2013) 827-854.

18. R.N. Lee. Presenting LiteRed: a tool for the Loop InTEgrals REDuction. // arXiv: 1212.2685.

19. A.G. Grozin. Decoupling in QED and QCD. // arXiv:1212.5144[hep-ph].

20. A.G. Grozin. Quantum Chromodynamics. // arXiv:1205.1815 [hep-ph].

21. A.G. Grozin. Reduce interface. // arXiv:1204.3020 [cs.MS].

22. V.L. Chernyak. Mass spectrum in SQCD with additional fields I. // arXiv: 1205.0410 [hep-th], 2012. - p.1-54.

23. V.L. Chernyak. // Mass spectrum in SQCD with additional fields. II. // arXiv: 1211.1487 [hep-th], 2012, pp. 1-27.

24. V.M. Khatsymovsky. First order representation of the Faddeev formulation of gravity. // arXiv:1201.0806[gr-qc], p.1-9, (2012).

25. Khatsymovsky V.M. Faddeev formulation of gravity in discrete form. // arXiv:1201.0808 [gr-qc], p.1-18, (2012).

26. V.M. Khatsymovsky. On area spectrum in the Faddeev gravity. // arXiv:1206.5509 [gr-qc], p.1-17, (2012).

27. Yaroslav A. Kharkov, Valentin V. Sokolov. Elastic enhancement factor as a quantum chaos probe. //

arXiv:1211.1773v2 [quant-ph]. 8 Nov 2012, published in Phys. Lett. B. 2013, Vol.718, p.1562-1565.

28. Bondar A., Buzulutskov A., Dolgov A., Grebenuk A., Shemyakina E., Sokolov A. Study of infrared scintillations in gaseous and liquid argon. Part I: methodology and time measurements. // E-print: arXiv:1204.0180, 2012.

29. Bondar A., Buzulutskov A., Dolgov A., Grebenuk A., Peleganchuk S., Porosev V., Shekhtman L., Shemyakina E., Sokolov A. Study of infrared scintillations in gaseous and liquid argon. Part II: light yield and possible applications. // E-print: arXiv:1204.0580, 2012.

30. Bondar A., Buzulutskov A., Dolgov A., Grebenuk A., Shemyakina E., Sokolov A., Akimov D., Breskin A. and Thers D. Two-phase Cryogenic Avalanche Detectors with THGEM and hybrid THGEM/GEM multipliers operated in Ar and Ar+N₂. // E-print: arXiv:1210.0649, 2012.

31. Y. Miyazaki, Belle Collab., V. Aulchenko, S. Eidelman, D. Epifanov, N. Gabyshev, A. Garmash, P. Krokovny, A. Kuzmin, D. Matvienko, B. Shwartz, V. Zhulanov, et al. Search for lepton-flavor-violating and lepton-number-violating decay modes. // arXiv:1206.5595.

32. S. Esen, Belle Collab., S. Eidelman, P. Krokovny, B. Shwartz, V. Zhilich, V. Zhulanov, et al. Precise measurement of the branching fractions for $B_s \rightarrow D^{(*)+}_s D^{(*)-}$ and first measurement of the $D^{(*)+}_s D^{(*)-}$ polarization using e⁺e⁻ collisions. // arXiv:1208.0323.

33. R. Aaij, LHCb Collab., A. Bobrov, A. Bondar, S. Eidelman, P. Krokovny, V. Kudryavtsev, A. Poluektov, L. Shekhtman, V. Vorobyev, et al. Differential branching fraction and angular analysis of the $B^+ \rightarrow K^+ \mu^+ \mu^-$ decay. // arXiv:1209.4284.

34. R. Aaij, LHCb Collab., A. Bobrov, A. Bondar, S. Eidelman, P. Krokovny, V. Kudryavtsev, A. Poluektov, L. Shekhtman, V. Vorobyev, et al. First evidence for the annihilation decay mode $B^+ \rightarrow D^+_{s\phi}$. // arXiv:1210.1089.

35. Y.-T. Duh, Belle Collab., V. Aulchenko, A. Bondar, S. Eidelman, P. Krokovny, A. Kuzmin, V. Shebalin, B. Shwartz, A. Vinokurova, V. Zhilich, V. Zhulanov, et al. Measurements of branching fractions and direct CP asymmetries for $B \rightarrow K\pi$, $B \rightarrow \pi\pi$ and $B \rightarrow KK$ decays. // arXiv:1210.1348.

36. R. Aaij, LHCb Collab., A. Bobrov, A. Bondar, S. Eidelman, P. Krokovny, V. Kudryavtsev, A. Poluektov, L. Shekhtman, V. Vorobyev, et al. Evidence for the decay $B^0 \rightarrow J/\psi\omega$ and measurement of the relative branching fractions of B^0_s meson decays to $J/\psi\eta$ and $J/\psi\eta'$. // arXiv:1210.2631.

37. R. Aaij, LHCb Collab., A. Bobrov, A. Bondar, S. Eidelman, P. Krokovny, V. Kudryavtsev, A. Poluektov, L. Shekhtman, V. Vorobyev, et al. Measurement of the CP asymmetry in $B^0 \rightarrow K^{*0} \mu^+ \mu^-$ decays. // arXiv:1210.4492.

38. R. Aaij, LHCb Collab., A. Bobrov, A. Bondar, S. Eidelman, P. Krokovny, V. Kudryavtsev, A. Poluektov, L. Shekhtman, V. Vorobyev, et al. Measurement of the $B^0 - \bar{B}^0$ oscillation frequency Δm_d with the decays $B \rightarrow D^- \pi^+$ and $B^0 \rightarrow J/\psi K^{*0}$. // arXiv:1210.6750.

39. U. Tamponi, Belle Collab., V. Aulchenko, A. Bondar, S. Eidelman, D. Epifanov, P. Krokovny, A. Kuzmin, B. Shwartz, V. Zhilich, V. Zhulanov, et al. Study of the hadronic transitions $\Upsilon(2S) \rightarrow \Upsilon(1S) \eta(\pi^0)$ at Belle. // arXiv:1210.6914.

40. R. Aaij, LHCb Collab., A. Bobrov, A. Bondar, S. Eidelman, P. Krokovny, V. Kudryavtsev, A. Poluektov, L. Shekhtman, V. Vorobyev, et al. Observation of $D^0 - \bar{D}^0$ oscillations. // arXiv:1211.1230.

41. R. Aaij, LHCb Collab., A. Bobrov, A. Bondar, S. Eidelman, P. Krokovny, V. Kudryavtsev, A. Poluektov, L. Shekhtman, V. Vorobyev, et al. First observation of the decay $B^*_{s2}(5840)^0 \rightarrow B^{*+} K^-$ and studies of excited B_s mesons. // arXiv:1211.5994.

42. R. Aaij, LHCb Collab., A. Bobrov, A. Bondar, S. Eidelman, P. Krokovny, V. Kudryavtsev, A. Poluektov, L. Shekhtman, V. Vorobyev, et al. Measurement of the time-dependent CP asymmetry in $B^0 \rightarrow J/\psi K^0_s$ decays. // arXiv:1211.6093.

43. R. Aaij, LHCb Collab., A. Bobrov, A. Bondar, S. Eidelman, P. Krokovny, V. Kudryavtsev, A. Poluektov, L. Shekhtman, V. Vorobyev, et al. Measurement of J/ψ production in pp collisions at $\sqrt{s}=2.76$ TeV. // arXiv:1212.1045.

44. R. Aaij, LHCb Collab., A. Bobrov, A. Bondar, S. Eidelman, P. Krokovny, V. Kudryavtsev, A. Poluektov, L. Shekhtman, V. Vorobyev et al. Measurement of the cross-section for $Z \rightarrow e^+ e^-$ production in pp collisions at $\sqrt{s}=7$ TeV. // arXiv:1212.4620.

45. R. Aaij, LHCb Collab., A. Bobrov, A. Bondar, S. Eidelman, P. Krokovny, V. Kudryavtsev, A. Poluektov, L. Shekhtman, V. Vorobyev et al. Measurement of the forward energy flow in pp collisions at 7 TeV. // arXiv:1212.4755.

46. R. Aaij, LHCb Collab., A. Bobrov, A. Bondar, S. Eidelman, P. Krokovny, V. Kudryavtsev, A. Poluektov, L. Shekhtman, V. Vorobyev et al. Measurement of CP observables in $B^0 \rightarrow D K^{*0}$ with $D \rightarrow K^+ K^-$. // arXiv:1212.5205.

47. B.R. Ko, Belle Collab., K. Arinstein, A. Bondar, S. Eidelman, N. Gabyshev, A. Kuzmin, V. Zhilich et al. Search for CP violation in the decay $D^+ \rightarrow K^0_s K^+$. // arXiv:1212.6112.

48. C. Oswald, Belle Collab., K. Arinstein, A. Bondar, S. Eidelman, N. Gabyshev, P. Krokovny, D. Matvienko, B. Shwartz, V. Zhilich et al. Measurement of the inclusive semileptonic branching fraction $\text{Bf}(B^0_s \rightarrow X^- l^+ \nu)$ at Belle. // arXiv:1212.6400.

49. D. Babusci, ..., P.A. Lukin, A.L. Sibidanov, et al. Precision measurement of $\sigma(e^+e^- \rightarrow \pi^+\pi^-\gamma)/\sigma(e^+e^- \rightarrow$

$\mu+\mu-\gamma$) and determination of the $\pi^+\pi^-$ contribution to the muon anomaly with the KLOE detector. // E-print: arXiv:1212.4524 [hep-ex].

50. A.V. Arzhannikov I.V. Timofeev. Generation of powerful terahertz emission in a beam-driven strong plasma turbulence. // arXiv:1205:4081v1 [physics.plasm-ph].

51. V.I. Telnov. Restriction on the energy and luminosity of e^+e^- storage rings due to beamstrahlung. // arXiv:1203.6563 [physics.acc-ph].

52. Blondel, M. Koratzinos, ..., V. Telnov. LEP3: A high luminosity e^+e^- collider to study the Higgs boson. // arXiv:1208.0504 [physics.acc-ph].

53. K.V. Lotov, G.Z. Lotova, V.I. Lotov, A. Upadhyay, T. Tuckmantel, A. Pukhov, A. Caldwell. Natural noise and external wake field seeding in a proton-driven plasma accelerator. // E-print: arXiv:1204.3444 [physics.plasm-ph].

54. K.V. Lotov, A. Pukhov, A. Caldwell. Effect of plasma inhomogeneity on plasma wakefield acceleration driven by long bunches. // E-print: arXiv:1205.3388 [physics.plasm-ph].

55. R.R. Akhmetshin, A.V. Anisenkov, S.A. Anokhin, V.M. Aulchenko, V.S. Banzarov, L.M. Barkov, N.S. Bashtovoy, D.E. Berkaev, A.E. Bondar, A.V. Bragin, S.I. Eidelman, D.A. Epifanov, L.B. Epshteyn, G.V. Fedotovitch, S.E. Gayazov, A.A. Grebenuk, D.N. Grigoriev, E.M. Gromov, F.V. Ignatov, S.V. Karpov, V.F. Kazanin, B.I. Khazin, I.A. Koop, A.N. Kozyrev, P.P. Krokovny, A.E. Kuzmenko, A.S. Kuzmin, I.B. Logashenko, A.P. Lysenko, P.A. Lukin, K.Yu. Mikhailov, Yu.N. Pestov, E.A. Perevedentsev, S.A. Pirogov, S.G. Pivovarov, A.S. Popov, Yu.S. Popov, S.I. Redin, Yu.A. Rogovsky, A.L. Romanov, A.A. Ruban, N.M. Ryskulov, A.E. Ryzhenkov, V.E. Shebalin, D.N. Shemyakin, B.A. Shwartz, D.B. Shwartz, A.L. Sibidanov, P.Yu. Shatunov, Yu.M. Shatunov, I.G. Snopkov, E.P. Solodov, V.M. Titov, A.A. Talyshev, A.I. Vorobiov, Yu.V. Yudin, A.S. Zaytsev. Study of the process $e^+e^- \rightarrow 3(\pi^+\pi^-)$ in the c.m. energy range 1.5--2.0 GeV with the CMD-3 detector. // E-print: arXiv:1302.0053.

56. E.V. Abakumova, M.N. Achasov, D.E. Berkaev, V.V. Kaminsky, N.Yu. Muchnoi, E.A. Perevedentsev, E.E. Pyata, Yu.M. Shatunov. Backscattering of laser radiation on ultra-relativistic electrons in transverse magnetic field: evidence of photon interference in a MeV scale. Nov 2012, 4 pages. // E-print: arXiv:1211.0103 [physics.acc-ph].

57. B. Wojtsekhowski, D. Nikolenko, I. Rachek. Searching for a new force at VEPP-3. // arXiv:hep-ex/1207.5089.

58. M. Ablikim, BESIII Collab., M.N. Achasov, O. Albayrak, N. Muchnoi, I. Nikolaev, et al. Study of the near-threshold $\omega\phi$ mass enhancement in doubly OZI suppressed $J/\psi \rightarrow \gamma\omega\phi$ decays. // [arXiv:1211.5668 [hep-ex].

59. M. Ablikim, BESIII Collab., M.N. Achasov, O. Albayrak, N. Muchnoi, I. Nikolaev, et al. Measurements of $\psi' \rightarrow \bar{p} K^+ \Sigma^0$ and $\chi_{c1} \rightarrow \bar{p} K^+ \Lambda$. // arXiv:1211.5631 [hep-ex].

60. M. Ablikim, BESIII Collab., M.N. Achasov, N. Muchnoi, I. Nikolaev, et al. Search for η and $\eta' \rightarrow \pi^+ e^- \bar{\nu}_e + \text{c.c.}$ decays in $\psi \rightarrow \phi \rightarrow \eta$ and $\phi \rightarrow \eta'$. // arXiv:1211.3600 [hep-ex].

61. M. Ablikim, BESIII Collab., M.N. Achasov, N.Yu. Muchnoi, I. Nikolaev, et al. Measurements of baryon pair decays of χ_{c1} mesons. // arXiv:1211.2283 [hep-ex].

62. M. Ablikim, BESIII Collab., M.N. Achasov, N. Muchnoi, I. Nikolaev, et al. Observation of η_c decay into $\Sigma^+ \bar{\Sigma}^-$ and $\Xi^- \Xi \bar{\Xi}^+$ final states. // arXiv:1210.2831 [hep-ex].

63. M. Ablikim, BESIII Collab., M.N. Achasov, N. Muchnoi, I. Nikolaev, et al. Search for η and η' invisible decays in $J/\psi \rightarrow \phi\eta$ and $\phi\eta'$. // arXiv:1209.2469 [hep-ex].

64. M. Ablikim, BESIII Collab., M.N. Achasov, N. Muchnoi, I. Nikolaev, et al. Search for hadronic transition $\chi_{c1} \rightarrow \eta_c \pi^+ \pi^-$ and observation of $\chi_{c1} \rightarrow K \bar{K} \pi \pi$. // arXiv:1208.4805 [hep-ex].

65. M. Ablikim, BESIII Collab., M.N. Achasov, O. Albayrak, N. Muchnoi, I. Nikolaev, et al. Evidence for $\eta_c \rightarrow \gamma\gamma$ and measurement of $J/\psi \rightarrow 3\gamma$. // arXiv:1208.1461 [hep-ex].

Thesises reviews

1. SHEKHTMAN L.I. Fast high resolution coordinate gaseous detectors. // 01.04.01 – instruments and methods of experimental physics, Author. papers of thesis for the degree of doctor of phys.-math. science: Novosibirsk, 2008, BINP, SB RAS.

2. KOZAK V.R. Distributed control and measurements systems for BINP accelerator facilities. // 01.04.20 – physics of charged particle beams and accelerator techniques, Author. papers of thesis for the degree of doctor of technical science: Novosibirsk, 2012, BINP, SB RAS.

3. BOGDANCHIKOV A.G. Data acquisition system software of the SND detector. // 01.04.01 - instruments and methods of experimental physics, Author. papers of thesis for the degree of candidate of phys.-math. science: Novosibirsk, 2012, BINP, SB RAS.

4. REZNICHENKO A.V. High energy QCD amplitudes with gluon exchange. // 01.04.02 - theoretical physics, Author. papers of thesis for the degree of candidate of phys.-math. science: Novosibirsk, 2012, BINP, SB RAS.

5. LISTOPAD A.A. Diagnostic atomic injector with multislit system of beam formation. // 01.04.08 - physics of plasma Author. papers of thesis for the degree of

candidate of phys.-math. science: Novosibirsk, 2012, BINP, SB RAS.

6. NIKOLAEV I.B. Measurement of the energy of the beam of the VEPP-4M accelerator by the resonance depolarization method. // 01.04.16 - elementary particle physics, and atomic nuclear physics, Author. papers of thesis for the degree of candidate of phys.-math. science: Novosibirsk, 2012, BINP, SB RAS.

7. SKOVPEN K.Yu. Search for W_R bozon and heavy neutrino with the ATLAS detector. // 01.04.16 - elementary particle physics, and atomic nuclear physics, Author. papers of thesis for the degree of candidate of phys.-math. science: Novosibirsk, 2012, BINP, SB RAS.

8. TODYSHEV K.Yu. Measuring parameters of the $\psi(2S)$ - and $\psi(3770)$ -mesons. // 01.04.16 - elementary particle physics, and atomic nuclear physics, Author. papers of thesis for the degree of candidate of phys.-math. science: Novosibirsk, 2012, BINP, SB RAS.

9. FATKIN G.A. The Structure and hardware of control system for linear induction accelerator of X-ray complex. // 01.04.20 - physics of charged particle beams and accelerator techniques, Author. papers of thesis for the degree of candidate of technical science: Novosibirsk, 2012, BINP, SB RAS.

10. KRASNOV A.A. Study and prediction of residual gases dynamic density in vacuum chambers of modern accelerator-storage ring systems. // 01.04.20 - physics of charged particle beams and accelerator techniques, Author. papers of thesis for the degree of candidate of phys.-math. science: Novosibirsk, 2012, BINP, SB RAS.

11. PETRENKO A.V. Model-independent analysis and calibration of the beam transverse dynamic models in the storage rings. // 01.04.20 – physics of charged particle beams and accelerator techniques, Author. papers of thesis for the degree of candidate of phys.-math. science: Novosibirsk, 2012, BINP, SB RAS.

Participation in conferences

1. XXXIX International (Zvenigorod) Conference on Plasma Physics and Controlled Fusion, 6 - 10 February, 2012, Zvenigorod, Russia.

2. X Conference on High Energy Physics, Nuclear Physics, and Particle Accelerators, 27 February - 2 March 2012, Kharkov.

3. 4th International Workshop on Far-Infrared Technologies (IW-FIRT 2012), March 7 - 9, 2012, University of Fukui, Japan.

4. I KEK Flavor Factory Workshop, March 2012, KEK, Japan.

5. Interexpo Geo-Siberia-12. 8th International Specialized Exhibition and Scientific Congress "Customized Instrumentation, Metrology, Thermophysics, Micro Process Engineering, and Nanotechnologies", 10 - 20 April 2012, Novosibirsk, Russia.

6. Magnet Production Workshop, April 11 - 12, 2012, Brookhaven, USA.

7. Zababakhin Scientific Talks: XI International Conference, 16 - 20 April 2012, Snezhinsk, Russia.

8. International Scientifically-Practical Conference - An Exhibition «Special Tools not Lethal Action», April, 2012, Moscow, Russia.

9. Workshop on Radiative Corrections and MC Generators, April 2012, Frascati, Italy.

10. Workshop on Exotic Hadrons, April 2012, Bonn, Germany.

11. 5th International Workshop on Charm Physics (Charm 2012), May 14 - 17, 2012, Honolulu, Hawaii.

12. 20th International Conference on Plasma Surface Interactions in Controlled Fusion Devices, May 21 - 25, 2012, Eurogress Aachen, Germany.

13. International Particle Conference (IPAC'12), New Orleans, 20 - 25 May, 2012, USA.

14. Workshop on Transition Form Factors, May 2012, Cracow, Poland.

15. 12th International Workshop on Meson Production, Properties and Interaction, 31 May - 5 June, 2012, Krakow, Poland.

16. Russian Seminar "The Physical and Technical Aspects of the Volume Source of Neutrons for Materials Science, Technology Research and Solving Problems of Nuclear Power", June 4 - 8, 2012, Zvenigorod, Russia.

17. 24th Joint Russian-German Meeting on ECRH and Gyrotrons, June 11 - 15, 2012, Nizhny Novgorod, Russia.

18. International Conference: Chaos2012, 12 - 15 June, 2012, Athens, Greece.

19. International Workshop on New Photon-Detectors (PhotoDet 2012), June 13-15, 2012, Orsay, France.

20. HIAT'2012, June 18-21, 2012, Chicago, IL USA.

21. European Conference on X-ray Spectrometry, June 18 -22, 2012, Vienna, Austria.

22. 2nd International Conference "Terahertz and Microwave radiation: Generation, Detection and Applications" (TERA-2012), 20 - 22 June 2012, Moscow, Russia.

23. XIX National Conference on Synchrotron Radiation: All-Russia Youth Conference "Synchrotron radiation application", 25 - 28 June 2012, Novosibirsk, Russia.

24. 4th International Kreindel Workshop "Plasma Emission Electronics, 25 - 30 June, 2012", Ulan-Ude.

25. Nucleus 2012: Fundamental problems of nuclear physics, atomic power engineering and nuclear technologies. June 25 - 30, 2012, Voronezh, Russia.

26. Workshop: Preliminary Results on the Feasibility of Using Digital SiPM (dSiPM) Technology in FARICH, June 2012, CERN, Geneva, Switzerland.

27. Workshop on Analysis Tools for Next Generation Hadron Spectroscopy, June 2012, Camoli, Italy.

28. 39th EPS Conference and 16th International Congress on Plasma Physics, 2 - 6 July, 2012, Stockholm, Sweden.
29. International Workshop "Hadron Structure and QCD: from LOW to HIGH energies", July 4 - July 8, 2012, Gatchina, Russia.
30. 36th International Conference on High Energy Physics, 4 - 11 July, Melbourne, Australia.
31. Olympus Symposium "Experimental and theoretical aspects of the proton form factors", July 9 - 11, 2012, Gatchina, Russia.
32. International Conference "Quantum Field Theory and Gravity 2012", July 31 - August 4 2012, Tomsk, Russia.
33. 34th International. Free-Electron Laser (FEL2012), 26 - 31 August, 2012, Nara, Japan.
34. 10th International Workshop on Non-Neutral Plasmas, August 27 - 30, 2012, Greifswald, Germany.
35. 9th International Conference on Open Magnetic Systems for Plasma Confinement, 27 - 31 August, 2012, Tsukuba, Japan.
36. Joint Conference of OS2012 and PMIF2012, 27 - 31 August 2012, Tsukuba, Japan.
37. 20th International Conference on Advanced Laser Technologies (ALT'12), 2 - 6 September, 2012, Thun, Switzerland.
38. 3rd International Symposium on Negative Ions, Beams, and Sources (NIBS 2012), 3 - 7 September 2012, Jyväskylä, Finland.
39. 26th Linear Accelerator Conference, September 9-14, 2012, Tel-Aviv, Israel.
40. 12th International Workshop on Accelerator Alignment (IWAA 12), FNAL, 10 - 14 September 2012, Batavia.
41. International Workshop "Diffraction 2012", September 11 - 15, Puerto del Camen, Lanzarote, Spain.
42. 52nd ICFA Advanced Beam Dynamics Workshop on High-Intensity and High-Brightness Hadron Beams, September 17 - 21, 2012, Beijing, China.
43. XX International Symposium on Spin Physics (SPIN6), 17 - 22 September, 2012, Dubna, Russia.
44. International Workshop "Quantum Transport and Quantum Effects in Photosynthetic Systems", 20 - 21 September, 2012, Breshia, Italy.
45. 37th International Conference on Infrared, Millimeter and Terahertz Waves, University of Wollongong, September 23 - 28, 2012, Australia.
46. 23rd All-Russian Particle Accelerator Conference (RuPAC'2012), September 24 - 28, 2012, Saint-Petersburg, Russia.
47. XII Workshop on Tau Lepton Physics, September 2012, Nagoya, Japan.
48. 4th Euro-Asian Pulsed Power Conference and 19th International Conference on High-Power Particle Beams (EAPPC 2012/BEAMS 2012), September 30 - October 4, 2012, Karlsruhe, Germany.
49. Taipei International Workshop "QCD in Two Photon Processes, 2 - 4 October, 2012, Taipei, Taiwan.
50. 24rd IAEA Fusion Energy Conference, 8 - 13 October, 2012, San Diego, USA.
51. International Workshop on Linear Colliders (LCWS 2012), October 24, 2012, Arlington, US.
52. Workshop "Scattering Amplitudes and the Multi-Regge Limit", October 24 - 26, 2012, Madrid, Spain.
53. IV All-Russian Conference "Physical and Physical-Chemical Foundations of Ion Implantation" (with participation of foreign scientists) and the International Youth Conference "Radiation-thermal Effects and Processes in Inorganic Materials", October 23 - 26, 2012, Novosibirsk, Russia.
54. International Scientifically-Practical Congress «Perfection of a Control System, Prevention and Damping Consequences of Emergency Situations of Regions and a Problem of Ability to Live of the Population», October, 25 - 27, 2012, Novosibirsk, in Russia.
55. VII International Scientifically-Practical Conference «Counteraction Means to Terrorist and Criminal Explosions», October, 2012, St-Petersburg, Russia.
56. International Scientifically-Practical Congress «Perfection of a Control System, Prevention and Damping Consequences of Emergency Situations of Regions and a Problem of Ability to Live of the Population», October, 25 - 27, 2012, Novosibirsk, Russia.
57. International Conference-Session of the Section of Nuclear Physics of PSD RAS. November 12 - 16, 2012, MEPhI, Moscow, Russia.
58. 2nd Joint HiLumi LHC-LARP Annual Meeting, 14 -16, November, 2012, INFN, Frascati.
59. Accelerators for a Higgs factory (HF2012), November 15, 2012, FNAL, US.
60. International Workshop "Low Threshold Detectors and Their Application in Neutrino Physics", International Conference-Session of the Section of Nuclear Physics of PSD RAS, MEPhI, November 16, 2012, Moscow, Russia.
61. International Workshop LHC on the March, November 21, 2012, Protvino, Russia.
62. Unwanted Beam Workshop (UBW), 19 - 20 December, 2012, Berlin.
63. 3rd International Congress on Radiation Physics and Chemistry of Condensed Matter, High Current Electronics and Modification of Materials with Particle Beams and Plasma Flows, 2012, Tomsk, Russia.
64. 54th Annual Meeting of the APS Division of Plasma Physics, 2012.
65. 9th Intern. Workshop on Personal Computers and Particle Accelerator Controls, December 4 - 7, 2012, Kolkata, India.

List of Collaboration Agreements between the Budker INP and Foreign Laboratories

Name of Laboratory		Title or Field of Collaboration	Dates	Principal Investigators
<i>№</i>	<i>1</i>	<i>2</i>	<i>3</i>	<i>4</i>
1	<i>Daresbury (England)</i>	Generation and utilization of SR.	1977	<i>G. Kulipanov (INP); I. Munro (Daresbury)</i>
2	<i>BESSY (Germany)</i>	Development of the wigglers for BESSY-2.	1993	<i>A. Skrinsky, N. Mezentsev (INP); E. Jaeschke (BESSY)</i>
3	<i>Research Centre Rossendorf (Germany)</i>	Physical foundations of a plasma neutron source.	1994	<i>E. Kruglyakov, A. Ivanov (INP); K. Noack (Germany)</i>
4	<i>Nuclear Centre "Karlsruhe" (Germany)</i>	1. Development of conceptual project and data base for neutron source on the basis of GDT device. 2. Simulation of processes in diverter of ITER device.	1994	<i>E. Kruglyakov, A. Ivanov, A. Burdakov (INP); G. Kessler (Germany)</i>
5	<i>GSI (Germany)</i>	Collaboration in the field of accelerator physics: electron cooling; electron-ion colliders.	1995	<i>Yu. Shatunov, V. Parkhomchuk (INP); H. Eickhoff (GSI)</i>
6	<i>DESY (Germany)</i>	Elementary-particle physics, synchrotron radiation, accelerator physics and technology, electronics and experimental equipment.	1995	<i>A. Skrinsky, G. Kulipanov (INP); A. Vagner, K. Scherff (DESY)</i>
7	<i>CIEMAT (Spain)</i>	Accelerator technology and plasma physics.	2007	<i>E. Levichev (INP), J. Rubio (CIEMAT)</i>
8	<i>CELLS (Spain)</i>	Collaboration in the field of application of new equipment for SR sources.	2008	<i>E. Levichev (INP); Joan Bordas and Orpinell (CELLS)</i>
9	<i>INFN (Italy)</i>	Development of intense source for radioactive ion beams for experiments in nuclear physics	1984	<i>P. Logachev (INP); L. Techio (INFN)</i>
10	<i>University of Milan (Italy)</i>	Theoretical and numerical studies of dynamic chaos in classic and quantum mechanics.	1991	<i>A. Skrinsky, V. Sokolov (INP); T. Montegazza, J. Kasati (Italy)</i>
11	<i>INFN-LNF (Italy)</i>	Development of collider project DAFNE-II	2004	<i>E. Levichev (INP); S. Biscari (INFN-LNF)</i>
12	<i>University of Padua (Italy)</i>	Development of cryogenic detectors for experiments in neutrino physicist.	2008	<i>Yu. Tikhonov, A. Bondar (INP); A. Gudlielmi (Italy)</i>

№	1	2	3	4
13	<i>National Nuclear Center. Park of Nuclear Technology (Kazakhstan)</i>	Development and application of industrial accelerators, generation and utilization of neutron beams, development of SR sources, RF-generators.	2007	<i>G. Kulipanov (INP); K. Kadyrzhanov, A. Kusainov (Kazakhstan)</i>
14	<i>National Nuclear Center. Al-Farabi National University (Kazakhstan)</i>	Creation and development of a multi-purpose research complex of radiation technology and terahertz radiation.	2009	<i>G. Kulipanov (INP); K. Kadyrzhanov, B. Zhumagulov (Kazakhstan)</i>
15	<i>Institute of Morden Physics and Techniques, Lanchzou (China)</i>	Collaboration in the field of accelerator physics: electron cooling.	2000	<i>V. Parkhomchuk (INP); S. Yang (PRC)</i>
16	<i>WOER Company, Shenzhen, (China)</i>	Using of electron accelerator ILU-10, exchanging of personal, information and experimental equipment.	2005	<i>A. Bryazgin (INP); Leo Li (WOER)</i>
17	<i>SINAP Shanghai, (China)</i>	Researching in field of industrial electron accelerators.	2006	<i>A. Bryazgin (INP); Hu Hounku (SINAP)</i>
18	<i>IHEP (China)</i>	Work of Chinese scientists on BINP installations, work of BINP scientists on IHEP installations.	2007	<i>A. Skrinsky (INP); H. Chen (IHEP)</i>
19	<i>Industrial and Technological Center of Cooperation with Russia and Belorussia of Heilongjiang Province (P.R.C) (China)</i>	Exchange of information about BINP-developed devices and the technology and product demand of the Chinese factories.	2009	<i>D. Grigoriev (INP); Zhan Hun-Vei (PRC)</i>
20	<i>POSTECH (Korea)</i>	Creation of beam accelerators, add-on devices, SR experiments.	1992	<i>A. Skrinsky, N. Mezentsev (INP); H. Kim (POSTECH)</i>
21	<i>KAERI (Korea)</i>	Development of FEL and accelerator-recuperator.	1999	<i>N. Vinokurov (INP); B.Ch. Lee (KAERI)</i>
22	<i>BNL, Brookhaven (USA)</i>	1. Measurement of the magnetic muon anomaly. 2. Joint research of RHIC spin.	1991 1993	<i>L. Barkov (INP); J. Bunse (BNL) Yu. Shatunov (INP); S. Ozaki (BNL)</i>
23	<i>ANL, Argonn (USA)</i>	1. Experiments with polarized gas jet target at VEPP-3. 2. SR instrumentation.	1988 1993	<i>L. Barkov (INP); R. Holt (ANL) G. Kulipanov, A. Skrinsky (INP); G. Shenoy (USA)</i>

№	1	2	3	4
24	<i>University of Pittsburgh (USA)</i>	Experiments on VEPP-2M and ϕ -factory.	1989	<i>S. Eidelman, E. Solodov (INP); V. Savinov (USA)</i>
25	<i>University of Duke (USA)</i>	Free electron lasers.	1992	<i>N. Vinokurov (INP); J. Wu (Duke)</i>
26	<i>BNL, Brookhaven (USA)</i>	Collaboration on electron-ion colliders.	1993	<i>V. Parkhomchuk (INP); I. Benzvi (USA)</i>
27	<i>FERMILAB (USA)</i>	Collaboration in the field of accelerator physics: electron cooling; conversion system.	1995	<i>V. Parkhomchuk (INP); O. Finli (FERMILAB)</i>
28	<i>FERMILAB (USA)</i>	Exchange of scientists and engineers for scientific research.	2005	<i>A. Skrinsky (INP); P. Oddone (FERMILAB)</i>
29	<i>SLAC, Stanford (USA)</i>	Obtainment of submicron beams and intensive positron beams, development of B-factory elements, detectors, RF-generators based on magnicons.	1994	<i>A. Skrinsky (INP); Persis Drel (SLAC)</i>
30	<i>Institute of Plasma Physics ASCR (Czech Republic)</i>	Collaboration in the field of plasma physics and plasma diagnostics research.	2008	<i>A. Ivanov (INP); P. Hruška (Czech Republic)</i>
31	<i>CERN (Switzerland)</i>	1. Research and development of the detectors for LHC. 2. Development of the LHC elements.	1992 1996	<i>A. Bondar, Yu. Tikhonov (INP); T. Nakada, P. Yenni (CERN); V. Anashin (INP); L. Evans (CERN)</i>
32	<i>Paul Scherrer Institute (Switzerland)</i>	Collaboration in the field of particle physics.	2009	<i>D. Grigoriev (INP); D. Mecom (Paul Scherrer Institute)</i>
33	<i>CERN (Switzerland)</i>	Research and development of micro-pattern detector technology..	2009	<i>Yu. Tikhonov (INP); S. Bertolucci (CERN)</i>
34	<i>CERN (Switzerland)</i>	Collaboration in the development of the electron-positron colliders with super-high luminosity.	2009	<i>E. Levichev (INP); S. Myers (CERN)</i>
35	<i>RIKEN Spring-8 (Japan)</i>	Collaboration in the field of accelerator physics and synchrotron radiation	1996	<i>G. Kulipanov (INP); H. Kamitsubo (Japan)</i>
36	<i>KEK (Japan)</i>	Research in accelerator physics and allied fields, development of elementary particle detectors.	1995	<i>A. Skrinsky (INP); A. Suzuki (KEK)</i>
37	<i>Center of Plasma Research, Tsukuba (Japan)</i>	Collaboration on Open traps.	2007	<i>A. Ivanov (INP); T. Imai (Japan)</i>

Research Personnel

Members of Russian Academy of Science

Academicians:

Barkov Lev Mitrofanovich

Dikansky Nikolai Sergeevich

Kruglyakov Edward Pavlovich

Kulipanov Gennady Nikolaevich

Skrinsky Alexadr Nikolaevich

Corresponding members:

Bondar Alexandr Evgenievich

Vinokurov Nikolai Alexandrovich

Dimov Gennady Ivanovich

Logachev Pavel Vladimirovich

Parkhomchuk Vasily Vasilievich

Khriplovich Iosif Bentsionovich

Shatunov Yury Michailovich

Director Board

Director:

Skrinsky Alexadr Nikolaevich

Deputy Director (scientific):

Ivanov Alexandr Alexandrovich

Kulipanov Gennady Nikolaevich

Levichev Evgeny Borisovich

Tikhonov Yury Anatolievich

Adviser RAN:

Kruglyakov Edward Pavlovich

Scientific Secretary:

Vasiljev Alexei Vladimirovich

Scientific Council

1. Academician, Chairman
2. Doctor of phys.-math. science, Co-Chairman
3. Academician, Co-Chairman
4. Doctor of phys.-math. science, Co-Chairman
5. Doctor of phys.-math. science, Co-Chairman
6. Candidate of phys.-math. science, Sci. Secretary
7. Candidate of techn. science
8. Doctor of phys.-math. science, Professor
9. Academician
10. Doctor of phys.-math. science
11. Corr. Member RAS
12. Doctor of phys.-math. science
13. Corr. Member RAS
14. Academician

Skrinsky A.N.
Ivanov A.A.
Kulipanov G.N.
Levichev E.B.
Tikhonov Yu.A.
Vasiljev A.V.
Anashin V.V.
Arzhannikov A.V.
Barkov L.M.
Blinov V.E.
Bondar A.E.
Burdakov A.V.
Vinokurov N.A.
Dikansky N.S.

- | | |
|--|---|
| 15. Corr. Member RAS | Dimov G.I. |
| 16. Doctor of phys.-math. science | Druzhinin V.P. |
| 17. Doctor of phys.-math. science | Koop I.A. |
| 18. Academician | <u>Kruglyakov E.P.</u> |
| 19. Doctor of techn. science | Kuper E.A. |
| 20. Corr. Member RAS | Logachev P.V. |
| 21. Candidate of techn. science | Medvedko A.S. |
| 22. Doctor of phys.-math. science | Mezentsev N.A. |
| 23. Corr. Member RAS | Parkhomchuk V.V. |
| 24. Doctor of techn. science, Professor | Salimov R.A. |
| 25. Doctor of phys.-math. science, Professor | Serednyakov S.I. |
| 26. Doctor of phys.-math. science, Professor | Fadin V.S. |
| 27. Doctor of phys.-math. science | Khazin B.I. |
| 28. Corr. Member RAS | Khriplovich I.B. |
| 29. Corr. Member RAS | Shatunov Yu.M. |
| 30. Candidate of techn. science | Shiaynkov S.V. |
| 31. Candidate of phys.-math. Science | Taskaev S.Yu. – Representative
of Trade Union |
| 32. Candidate of phys.-math. science | Shoshin A.A. – Representative
of Council of Young scientists |

Specialized Sections of Scientific Council

Accelerators for Applied Purposes

Kulipanov G.N. (Chrmn.)	Knyazev B.A.	Petrichenkov M.V.
Gorbunov V.A. (Secr.)	Kolmogorov V.V.	Petrov V.M.
Anashin V.V.	Korchagin A.I.	Pindyurin V.F.
Antokhin E.I.	Kuksanov N.K.	Pyata E.E.
Batnikov A.M.	Kuper E.A.	Rakshun Ya.V.
Bondar A.E.	Kuper K.E.	Salimov R.A.
Bryazgin A.A.	Kurkin G.Ya.	Shatunov Yu.M.
Chernyakin A.D.	Levichev E.B.	Shevchenko O.A.
Churkin I.N.	Logachev P.V.	Skaruba V.A.
Dikansky N.S.	Medvedko A.S.	Skrinsky A.N.
Erokhin A.I.	Mezentsev N.A.	Tribendis A.G.
Fadeev S.N.	Mishnev S.I.	Tumaikin G.M.
Goldenberg B.G.	Nemytov P.I.	Vinokurov N.A.
Gurov D.S.	Nikolenko A.D.	Vostrikov V.A.
Ivanov A.A.	Onuchin A.P.	Zolotarev K.V.
Karpov G.V.	Parkhomchuk V.V.	

Plasma Physics and Controlled Fusion Problems

Ivanov A.A. (Chrmn)	Khilchenko A.D.	Sanin A.L.
Kandaurov I.V. (Secr.)	Konstantinov S.G.	Sinitsky S.L.
Anikeev A.V.	Kotelnikov I.A.	Skrinsky A.N.
Akhmetov T.D.	<u>Kruglyakov E.P.</u>	Soldatkina E.I.
Arzhannikov A.V.	Kulipanov G.N.	Solomakhin A.L.
Astrelin V.T.	Kuznetsov A.S.	Sorokin A.V.
Bagryansky P.A.	Lizunov A.A.	Sulyaev Yu.S.
Beklemishev A.D.	Lotov K.V.	Taskaev S.Yu.
Belchenko Yu.I.	Mekler K.I.	Timofeev I.V.
Burdakov A.V.	Murakhtin S.V.	Shiyankov S.V.
Burmasov V.S.	Polosatkin S.V.	Volosov V.I.
Dimov G.I.	Popov S.S.	Vasiljev A.V.
Davydenko V.I.	Postupaev V.V.	Voskoboinikov P.V.
Ivanov I.A.	Prikhodko V.V.	Vyacheslavov L.N.
Kapitonov V.A.		

Colliding Beams

Parkhomchuk V.V. Chrmn)	<u>Kruglyakov E.P.</u>	Salimov R.A.
Petrov V.V. (Secr.)	Kulipanov G.N.	Shatilov D.N.
Anashin V.V.	Kuksanov N.K.	Shatunov P.Yu.
<u>Barkov L.M.</u>	Kuper E.A.	Shatunov Yu.M.
Batratkov A.M.	Kurkin G.Ya.	Shevchenko O.A.
Berkaev D.E.	Levichev E.B.	Shiaynikov S.V.
Blinov V.E.	Logachev P.V.	Simonov E.A.
Bondar A.E.	Medvedko A.S.	Skrinsky A.N.
Bryazgin A.A.	Meshkov O.I.	Solodov E.P.
Dikansky N.S.	Mezentsev N.A.	Starostenko A.A.
Erokhin A.I.	Mishnev S.I.	Shwartz D.B.
Gorbunov V.A.	НИКИТИН С.А.	Tikhonov Yu.A.
Gurov S.M.	Onuchin A.P.	Tumaikin G.M.
Khazin B.I.	Perevedentsev E.A.	Vasiljev A.V.
Kiselev V.A.	Pestrikov D.V.	Vinokurov N.A.
Kolmogorov V.V.	Petrov V.M.	Vobly P.D.
Koop I.A.	Reva V.B.	Zolotarev K.V.
Krasnov A.A.		

Physics of Elementary Particles

Bondar A.E. (Chrmn.)	Khazin B.I.	Pomeransky A.A.
Tayursky V.A. (Secr.)	Khriplovich I.B.	Popov A.S.
Achasov M.N.	Kononov S.A.	Rachek I.A.
Aulchenko V.M.	Koop I.A.	Redin S.I.
<u>Barkov L.M.</u>	Kravchenko E.A.	Ryskulov N.M.
Baru S.E.	Krokovny P.P.	Serednyakov S.I.
Berkaev D.E.	Kuzmin A.S.	Shamov A.G.
Blinov A.E.	Lee R.N.	Shatunov Yu.M.
Blinov V.E.	Levichev E.B.	Shekhtman L.I.
Buzulutskov A.F.	Logachev P.V.	Shwartz B.A.
Chernyak V.L.	Logashenko I.B.	Shwartz D.B.
Dimova T.V.	Lukin P.A.	Silagadze Z.K.
Dmitriev V.F.	Malyshev V.M.	Skovpen Yu.I.
Druzhinin V.P.	Maslennikov A.L.	Skrinsky A.N.
Eidelman S.I.	Milshtein A.I.	Sokolov A.V.
Fadin V.S.	Muchnoi N.Yu.	Sokolov V.V.
Fedotov G.V.	Nikolaev I.B.	Solodov E.P.
Garmash A.Yu.	Nikolenko D.M.	Telnov V.I.
Golubev V.B.	Obrazovsky A.E.	Terekhov I.S.
Grebenyuk A.A.	Onuchin A.P.	Todyshev K.Yu.
Grigoriev D.N.	Pakhtusova E.V.	Tikhonov Yu.A.
Groshev V.R.	Peleganchuk S.V.	Toporkov D.K.
Grozin A.G.	Parkhomchuk V.V.	Vasiljev A.V.
Ignatov F.V.	Pestov Yu.N.	Vorob'ev A.I.
Katkov V.M.	Pivovarov S.G.	Zhilich V.N.
Kharlamov A.G.		

Automation

Tikhonov Yu.A. (Chrmn)	Cheblakov P.V.	Levichev E.B.
Kuper E.A. (Co-Chrmn)	Faktorovich B.P.	Logashenko I.B.
Baldin E.M. (Secr.)	Grozin A.G.	Maximova S.V.
Dubrov S.V. (Secr.)	Kaplin V.I.	Medvedko A.S.
Aleshaev A.N.	Khilchenko A.D.	Nekhanevich E.L.
Amosov S.A.	Kolmogorov V.V.	Shatunov Yu.M.
Aulchenko V.M.	Koop I.A.	Shuvalov B.N.
Banzarov V.Sh.	Korol A.A.	Solodov E.P.
Batrakov A.M.	Kovalenko Yu.V.	Sukharev A.M.
Belov S.D.	Kupchik V.I.	Tararyshkin S.V.
Berkaev D.E.	Kurilin O.Yu.	Tsukanov V.M.
Bolkhovityanov D.Yu.	Kuzin M.V.	Vasiljev A.V.
Buzykaev A.R.	Kvashnin A.N.	

Research Staff and Publications

Abakumova E.V.	413, 414, 56п		557, 562, 564, 565, 567, 571, 575, 576, 579
Abdrakhmanov I.I.		Astrelina K.V.	505
Abdrashitov G.F.	191, 629, 630	Atlukhanov M.G.	
Achasov M.N.	78, 124, 140, 152, 155, 163, 187, 339, 340, 341, 342, 358, 360, 414, 417, 418, 419, 420, 421, 422, 423, 424, 425, 426, 427, 7п, 11п, 56п, 58п, 59п, 60п, 61п, 62п, 63п, 64п, 65п	Aulchenko V.M.	49, 50, 108, 120, 137, 144, 146, 151, 161, 167, 170, 237, 294, 305, 307, 314, 333, 334, 336, 337, 341, 358., 443, 461, 477, 545, 611, 612, 615, 616, 617, 7п, 11п, 31п, 35п, 39п, 55п
Akhmetov T.D.	29, 149, 570	Averbukh I.I.	630
Akhmetshin R.R.	333, 334, 336, 55п	Avilov M.S.	25
Akimov V.E.	246	Avrorov A.P.	432, 529, 562, 565, 571, 575, 579
Akimov A.V.	87, 205, 244, 246, 542, 543, 547, 548		
Aleinik V.I.	241, 487, 509, 519, 649, 2п, 3п, 5п	Babichev E.A.	
Alinovsky N.I.		Bagryansky P.A.	30, 194, 195, 211, 212, 357, 527, 531, 535, 538, 544, 567, 632, 633, 634
Alyakrinskiy O.N.		Bagulov D.S.	32, 536
Amirov V.H.	535	Bak P.A.	246, 542, 543, 547
Anashin V.V.	49, 50, 337, 413, 415, 611, 612, 615, 616, 617, 629	Baldin E.M.	49, 50, 217, 337, 611, 612, 615, 616, 617
Anchugov O.V.	205	Banzarov V.Sh.	333, 334, 336, 55п
Andriyanov A.V.		Barkov L.M.	250, 333, 334, 336, 400, 636, 638, 55п
Anikeev A.V.	212, 352, 357, 531, 538, 544, 567, 632, 634, 635	Barkova V.G.	8п, 12п
Anisenkov A.V.	1, 2, 7, 8, 9, 10, 11, 15, 16, 17, 18, 19, 20, 21, 35, 37, 38, 39, 64, 65, 69, 70, 71, 75, 81, 82, 85, 86, 87, 88, 89, 90, 92, 94, 96, 97, 98, 100, 101, 105, 116, 131, 133, 139, 142, 164, 168, 172, 174, 175, 179, 180, 181, 182, 183, 184, 185, 186, 333, 334, 336, 361, 362, 363, 364, 365, 366, 367, 368, 369, 370, 371, 372, 375, 376, 377, 378, 379, 380, 381, 382, 383, 384, 385, 386, 387, 388, 389, 390, 391, 392, 393, 394, 395, 396, 397, 398, 399, 55п	Barladyan A.K.	49, 50, 337, 611, 612, 615, 616, 617
Anokhin S.A.	333, 334, 336, 55п	Barnyakov A.M.	501, 511
Antokhin E.I.	406	Barnyakov A.Yu.	49, 50, 337, 339, 340, 341, 342, 358, 360, 611, 412, 615, 616, 617, 618, 619, 620, 7п, 11п
Arakcheev A.S.	221	Barnyakov M.Yu.	49, 50, 337, 611, 612, 615, 616, 617, 618, 619, 620
Arbuzov V.S.	466, 486, 493, 641, 651	Baru S.E.	49, 50, 288, 337, 589, 590, 591, 592, 611, 612, 615, 616, 617
Arinstein K.E.	307	Baryshev V.B.	
Arzhannikov A.V.	189, 218, 228, 251, 267, 269, 270, 272, 435, 440, 442, 521, 525, 529, 530, 558, 559, 560, 562, 563, 565, 566, 569, 577, 578, 579, 50п	Basalaev A.V.	
Astrelin V.T.	267, 271, 430, 432, 442, 525, 529, 532, 539, 540, 555, 556,	Bashkirtsev A.G.	343, 509, 519, 520, 649, 5п, 6п
		Bashtovoy N.S.	333, 334, 336, 55п
		Basok I.Yu.	49, 50, 337, 611, 612, 615, 616, 617, 619
		Batazova M.A.	192, 542, 543, 547, 599
		Batkin V.I.	529, 562, 565, 579
		Batrakov A.M.	205, 506, 508, 513, 542, 543, 547, 14п
		Bayanov B.F.	519
		Bedareva T.V.	27
		Bekhtenev E.A.	205, 409, 485, 492, 497

	311, 312, 313, 315, 316, 317, 320, 321, 322, 323, 324, 325, 326, 327, 328, 329, 330, 331, 333, 334, 336, 337, 600, 611, 612, 615, 616, 617, 1п, 28п, 29п, 30п, 33п, 34п, 35п, 36п, 37п, 38п, 39п, 40п, 41п, 42п, 43п, 44п, 45п, 46п, 47п, 48п, 55п		
Bondarenko A.V.			
Borisov A.A.	339, 340, 358, 514, 7п		
Borodenko A.A.	619		
Botov A.A.	339, 340, 341, 342, 358, 360, 7п, 11п		
Bragin A.V.	333, 334, 336, 500, 608, 609, 610, 55п		
Brodnikov A.F.	549		
Bryazgin A.A.	484		
Bryzgunov M.I.	494, 503, 516, 594		
Bublely A.V.	494, 503		
Bukin D.A.	339, 340, 341, 342, 358, 360, 11п		
Burdakov A.V.	251, 252, 267, 271, 352, 353, 430, 431, 432, 442, 521, 525, 528, 529, 532, 546, 553, 558, 561, 562, 563, 564, 565, 566, 567, 568, 569, 570, 571, 572, 573, 574, 575, 578, 579, 580, 621, 629		
Burdin P.N.	498		
Burmasov V.S.	243, 521, 525, 529, 562, 563, 565, 566, 569, 578, 579		
Buzulutskov A.F.	293, 297, 298, 299, 600, 601, 28п, 29п, 30п		
Buzykaev A.R.	49, 50, 106, 107, 109, 118, 122, 126, 127, 130, 134, 136, 138, 145, 177, 611, 612, 615, 616, 617, 618, 619, 620		
Bykov E.V.			
Bykov P.V.	432, 562, 565, 571, 575, 579		
Chakin I.K.	213, 407		
Cheblakov P.B.	205, 489		
Chekavinsky V.A.	497		
Cherepanov V.P.	205, 410, 485, 492		
Cherepkov V.G.			
Chernoshtanov I.S.	522, 623		
Chernov K.N.	466, 486, 641, 651		
Chernyak V.L.	206, 585, 22п, 23п		
Chernyakin A.D.	205, 651		
Cheskidov V.G.	205, 466, 486, 641		
Choporova Yu.Yu.	262, 438, 446, 482, 438, 446, 482		
Chudaev V.Ya.	520, 6п, 8п, 12п		
		Chupyra A.G.	411, 650
		Churkin I.N.	205, 651
		Davidovsky V.G.	
		Davydenko V.I.	191, 201, 216, 350, 351, 523, 567, 570, 571, 575, 621, 625, 628, 629, 630, 631, 647, 4п
		Deichuli O.I.	466
		Deichuli P.P.	191, 197, 350, 629
		Dementiev E.N.	466, 486, 641
		Denisenko R.S.	
		Derbenev A.A.	
		Derevyankin G.E.	432, 529, 562, 565, 571, 575, 579
		Devyataikina T.A.	220, 498
		Dikansky N.S.	
		Dimov G.I.	629
		Dimova T.V.	339, 340, 341, 342, 358, 360, 7п, 11п
		Dmitriev V.F.	274, 400, 636, 638, 15п
		Dobrovolskaya O.A.	574
		Dolgov A.M.	293, 294, 298, 600, 28п, 29п, 30п
		Domarov E.V.	214
		Donin A.S.	198, 212, 538
		Dorokhov D.V.	
		Dovzhenko B.A.	466, 486, 641, 651
		Dranichnikov A.N.	191, 629
		Druzhinin V.P.	106, 107, 109, 118, 122, 126, 127, 130, 134, 136, 138, 145, 177, 339, 340, 341, 342, 358, 360, 7п, 11п
		Dubrovin A.N.	205
		Dudnikov A.V.	199, 408, 512
		Eidelman S.I.	3, 4, 5, 6, 12, 36, 40, 47, 49, 50, 51, 52, 54, 55, 57, 58, 59, 60, 61, 62, 76, 77, 99, 108, 111, 117, 121, 123, 128, 135, 137, 141, 143, 144, 146, 147, 148, 150, 151, 153, 154, 156, 159, 161, 165, 166, 167, 170, 173, 176, 188, 190, 300, 301, 302, 303, 304, 305, 306, 307, 308, 309, 310, 311, 312, 313, 314, 315, 316, 317, 318, 319, 320, 321, 322, 323, 324, 325, 326, 327, 328, 329, 330, 331, 332, 333, 334, 335, 336, 337, 611, 612, 615, 616, 617, 31п, 32п, 33п, 34п, 35п, 36п, 37п, 38п, 39п, 40п, 41п, 42п, 43п, 44п, 45п, 46п, 47п, 48п, 55п
		Eidelman Yu.I.	

Eliseev A.A.	542, 543, 547	Gramolin A.V.	400
Eliseev V.S.	406	Grebenyuk A.A.	293, 298, 333, 334, 336, 28π, 29π, 30π, 55π
Emanov F.A.	542, 543, 547	Grevtsov K.A.	339, 340, 341, 342, 358, 7π, 11π
Emelev I.S.		Grekhov A.N.	27
Epstein L.B.	248, 333, 334, 336, 55π	Grigoriev D.N.	49, 50, 333, 334, 336, 337, 611, 612, 615, 616, 617, 55π
Erokhin A.I.	205, 483, 489	Grishnyaev E.S.	338, 431, 529, 574
Fadeev S.N.	193, 214, 495, 499, 639, 640	Grozin A.G.	282, 283, 19π, 20π, 21π
Fadin V.S.	257, 258, 275, 276, 277, 581, 582, 583, 584, 10π, 17π	Gromov E.M.	333, 334, 336, 55π
Faktorovich B.L.	484	Groshev V.R.	249
Fatkin G.A.	542, 543, 547, 9A	Gubin K.V.	
Fedotov M.G.	236, 261, 453, 462	Gudkov B.A.	
Fedotov G.V.	333, 334, 336, 55π	Gulevich V.V.	49, 50, 337, 611, 612, 615, 616, 617, 619
Feldman A.L.	286	Gurov D.S.	24
Filipchenko A.V.	651	Gurov S.M.	205
Frolov A.R.	202	Gusev G.A.	413
Gabyshev N.I.	108, 120, 128, 137, 144, 146, 148, 156, 161, 169, 170, 173, 304, 305, 306, 307, 308, 311, 312, 313, 314, 31π, 47π, 48π	Gusev D.V.	49, 50, 337, 611, 612, 615, 616, 617
Gavrilenko D.E.	529, 564, 567, 572	Gusev E.A.	
Gambaryan V.V.	491	Gusev I. A.	483, 496, 497, 516
Garmash A.Yu.	108, 120, 128, 137, 144, 146, 151, 169, 170, 302, 314, 31π	Ignatov F.V.	333, 334, 336, 55π
Gafarov M.R.		Iljin I.V.	14π
Gayazov S.E.	333, 334, 336, 55π	Ivanenko S.V.	241, 243, 245
Gentselev A.N.	235, 470, 471, 472	Ivanenko V.G.	529, 565, 579
Gerasimov V.V.	262, 438, 439, 446, 480, 550, 627	Ivanov A.A.	29, 149, 191, 198, 201, 211, 216, 241, 343, 350, 351, 352, 353, 432, 520, 523, 526, 528, 529, 533, 546, 564, 567, 568, 570, 571, 575, 580, 621, 625, 628, 629, 630, 631, 647, 648, 4π, 6π, 9π
Gerasimov R.E.	16π	Ivanov A.V.	230
Getmanov Ya.V.	466, 486, 502, 504, 641	Ivanov Igor A.	352
Glukhov S.A.		Ivanov Ivan A.	251, 252, 267, 432, 442, 521, 525, 529, 546, 553, 558, 561, 562, 563, 564, 565, 566, 567, 569, 574, 575, 578, 579
Glukhovchenko Yu.M.	49, 50, 337, 611, 612, 615, 616, 617	Ivantsivsky M.V.	251, 255, 521, 525, 529, 534, 562, 563, 565, 567, 569, 579
Golkovski M.G.	402, 403, 404, 405, 406, 407	Ivlyushkin D.V.	469
Golovin R.A.	400	Kadyrov R.A.	
Golubev V.B.	106, 107, 109, 118, 122, 126, 127, 130, 134, 136, 138, 145, 177, 339, 340, 341, 342, 358, 360, 7π, 11π	Kalinin P.V.	218, 228, 267, 269, 270, 435, 440, 442, 529, 558, 559, 564, 566, 577, 578
Golubenko Yu.I.	213, 214, 495, 639	Kaminsky V.V.	400, 56π
Goldenberg B.G.	235, 451, 455, 457, 458, 464, 470, 472, 475, 651	Kandaurov I.V.	430, 432, 529, 532, 539, 554, 556, 558, 562, 564, 565, 567, 569, 571, 572, 575, 579
Goncharov A.D.	202, 494, 516		
Gorbovsky A.I.	191, 629, 647, 648		
Gorbunov V.A.			
Gorlovoi A.V.	469		
Gorniker E.I.	204, 466, 486, 493, 641, 651		
Gorchakov K.M.	205		
Grabovsky A.V.	276, 16π		

Kapitonov V.A.	523, 526, 629, 630	446, 466, 480, 482, 486, 550, 551, 627, 641
Kardapoltsev L.V.	339, 340, 341, 342, 358, 360, 7π, 11π	205, 629, 647
Karnaev S.E.	49, 50, 205, 337, 489, 611, 612, 615, 616, 617, 651	213, 214, 495, 499, 639, 640
Karpov G.V.	49, 50, 205, 337, 409, 485, 492, 507, 611, 612, 615, 616, 617	484
Karpov I.E.	430, 532, 540	Kolesnikov E.Yu.
Karpov S.V.	49, 50, 333, 334, 336, 337, 611, 612, 615, 616, 617, 55π	Kolmogorov A.V.
Kas'yanenko P.V.		Kolmogorov V.V.
Kasaev A.S.	358, 7π	49, 50, 191, 205, 337, 483, 489, 593, 611, 612, 615, 616, 617, 629, 630
Kasatov A.A.	243, 251, 525, 534, 562, 565, 569, 579	Kolobanov E.I.
Kasatov D.A.	243, 343, 519, 520, 649, 6π	Kolokolnikov Yu.M.
Katkov V.M.	285	24
Kazanin V.F.	1, 2, 7, 8, 9, 10, 11, 13, 14, 15, 16, 17, 18, 19, 20, 21, 35, 37, 38, 39, 48, 53, 56, 63, 64, 65, 66, 67, 69, 70, 71, 72, 75, 79, 80, 81, 82, 83, 84, 85, 86, 87, 88, 89, 90, 91, 92, 93, 94, 95, 96, 97, 98, 100, 101, 105, 110, 112, 113, 114, 115, 116, 119, 125, 129, 131, 132, 133, 139, 142, 162, 164, 168, 172, 174, 178, 179, 180, 181, 182, 183, 184, 185, 186, 249, 333, 334, 336, 361, 362, 363, 364, 365, 366, 367, 368, 369, 370, 371, 372, 373, 374, 375, 376, 377, 378, 379, 380, 381, 382, 383, 384, 385, 386, 387, 389, 390, 391, 392, 393, 394, 395, 396, 397, 398, 399, 55π	Kondakov A.A.
Kazantseva E.S.	220, 498, 508, 510, 513, 597	191, 197, 466, 486, 629, 630, 641
Kenzhebulatov E.K.	204, 515, 613, 614	Kondaurov M.N.
Kharlamov A.G.	339, 340, 341, 342, 358, 360, 7π, 11π	411, 497, 516, 593, 650
Kharlamova T.A.	49, 50, 337, 611, 612, 615, 616, 617	Kondratjev V.I.
Khatsymovsky V.M.	586, 24π, 25π, 26π	448, 457, 458, 470, 471, 472, 474, 475, 476
Khavin N.G.	24	Kononov S.A.
Khazin B.I.	333, 334, 336, 55π	49, 50, 337, 611, 612, 615, 616, 617, 618, 619, 620
Khilchenko A.D.	241, 534	Konstantinov E.S.
Kholopov M.A.	415, 463	202
Khriplovich I.B.	41, 207, 208, 250, 273	Konstantinov S.G.
Khrushev S.V.	238, 500	431, 647
Kim D.O.	590	Konstantinov V.M.
Kirpotin A.N.	358, 359, 514, 7π, 11π	205, 415
Kiselev V.A.	49, 50, 205, 231, 337, 410, 428, 611, 612, 615, 616, 617, 651	Koop I.A.
Klyuev V.F.	202	209, 333, 334, 336, 339, 340, 342, 358, 359, 360, 514, 7π, 11π, 55π
Knyazev B.A.	200, 260, 262, 429, 438, 439,	Korchagin A.I.
		214, 495, 639
		Korepanov A.A.
		205, 244, 246, 542, 543, 547,
		Korobeinikov M.V.
		Korol A.A.
		1, 2, 7, 8, 9, 10, 11, 13, 14, 15, 16, 17, 18, 19, 20, 21, 35, 37, 38, 39, 48, 53, 56, 63, 64, 65, 66, 67, 68, 69, 70, 71, 72, 75, 79, 80, 81, 82, 83, 84, 85, 86, 87, 88, 89, 90, 91, 92, 93, 94, 95, 96, 97, 98, 100, 101, 105, 110, 112, 113, 114, 115, 116, 119, 125, 129, 131, 132, 133, 139, 142, 162, 164, 168, 172, 174, 175, 178, 179, 180, 181, 182, 183, 184, 185, 186, 217, 339, 340, 341, 342, 358, 360, 361, 362, 363, 364, 365, 366, 367, 368, 369, 370, 371, 372, 373, 374, 375, 376, 377, 378, 379, 380, 381, 382, 383, 384, 385, 386, 387, 389, 390, 391, 392, 393, 394, 395, 396, 397, 398, 399, 7π, 11π
		Korzhevina M.S.
		212, 527, 538, 9π
		Kosarev A.N.
		414
		Koshuba S.V.
		339, 340, 341, 342, 358, 360, 7π, 11π
		Kosov A.V.
		452
		Kotelnikov A.I.
		236

Kotelnikov I.A.	32, 254, 348, 349, 439, 446, 480, 528, 530, 536, 563, 626, 627, 631	Kuper E.A.	49, 50, 205, 219, 337, 412, 466, 486, 497, 517, 518, 611, 612, 615, 616, 617, 641, 651
Kotov K.Yu.	49, 50, 337, 611, 612, 615, 616, 617	Kuper K.E.	651
Kovalenko Yu.V.		Kupich A.S.	11п
Kovrizhin D.P.	339, 340, 341, 342, 358, 360	Kuptsov I.V.	466, 486, 493, 641, 651
Kozak V.R.	219, 412, 466, 486, 497, 516, 518, 593, 641, 651, 2A	Kurkin G.Ya.	49, 50, 204, 337, 466, 486, 493, 515, 611, 612, 615, 616, 617, 641, 651
Kozlov M.G.	257, 258	Kurkuchekov V.V.	432, 529, 539, 554, 558, 562, 565, 569, 571, 572, 575, 579
Kozyrev A.N.	333, 334, 336, 55п	Kuyanov I.A.	
Kozyrev E.V.	466, 486, 641	Kuzmenko A.E.	333, 334, 336, 55п
Krasnov A.A.	413, 414, 10A	Kuzmin A.S.	108, 137, 144, 146, 151, 156, 161, 167, 169, 170, 305, 306, 307, 308, 312, 313, 333, 334, 336, 31п, 35п, 39п, 47п, 55п
Kravchenko E.A.	49, 50, 106, 107, 109, 118, 122, 126, 127, 130, 134, 136, 138, 145, 177, 337, 341, 342, 358, 611, 612, 615, 616, 617, 618, 619, 620, 7п, 11п	Kuzminykh V.S.	205, 413
Krivashin D.S.		Kuznetsov A.S.	344, 487, 509, 519, 649, 2п, 3п, 5п, 6п
Krokovny P.P.	3, 4, 5, 6, 12, 36, 52, 58, 60, 61, 62, 108, 120, 123, 128, 137, 144, 146, 150, 151, 153, 159, 161, 166, 167, 188, 300, 301, 302, 304, 305, 306, 307, 308, 309, 310, 311, 312, 313, 314, 315, 320, 321, 322, 323, 324, 325, 326, 327, 328, 329, 330, 331, 31п, 32п, 33п, 34п, 35п, 36п, 37п, 38п, 39п, 40п, 41п, 42п, 43п, 44п, 45п, 46п, 48п, 55п	Kuznetsov G.I.	192, 196, 542, 543, 547, 599
Kruglyakov E.P.	243, 250, 353, 568, 580	Kuznetsov S.A.	218, 251, 267, 440, 442, 521, 529, 558, 559, 563, 565, 566, 569, 577, 578, 579
Krutikhin S.A.	204, 493, 651	Kvashnin A.N.	241, 245
Krygina A.S.		Lapic R.M.	
Kryuchkov Ya.G.	613, 614	Lavrukhin A.V.	214, 495, 639
Kubarev V.V.	261, 263, 434, 441, 447, 466, 468, 473, 486, 641	Lazarenko B.A.	400
Kudryavtsev V.N.	6, 36, 52, 55, 58, 60, 61, 62, 76, 121, 150, 153, 159, 166, 188, 294, 300, 301, 309, 310, 315, 316, 322, 323, 324, 325, 326, 327, 328, 329, 331, 615, 616, 617, 33п, 34п, 36п, 37п, 38п, 40п, 41п, 42п, 43п, 44п, 45п, 46п	Lebedev N.N.	
Kuklin K.N.	243, 529, 553, 562, 565, 569, 574, 579	Lee R.N.	103, 104, 278, 279, 280, 284, 18п
Kuksanov N.K.	193, 213, 214, 402, 495, 499, 639, 640	Legkodymov A.A.	239, 240, 448, 459, 460, 469, 474
Kulenko Ya.V.	542, 543, 547	Lemzyakov A.G.	464, 470, 472
Kulikov V.F.	49, 50, 337, 611, 612, 615, 616, 617	Leonov V.V.	592
Kulipanov G.N.	262, 263, 436, 443, 457, 458, 465, 466, 486, 504, 545, 551, 641, 651	Lev V.H.	23, 238
		Levichev A.E.	501, 511
		Levichev E.B.	49, 50, 205, 215, 231, 250, 337, 413, 428, 488, 490, 545, 608, 609, 610, 611, 612, 615, 616, 617, 662
		Listopad A.A.	201, 216, 4п, 5A
		Lizunov A.A.	194, 198, 211, 212, 538, 570
		Logachev P.V.	25, 244, 246, 541, 542, 543, 547
		Logashenko I.B.	217, 333, 334, 336, 55п
		Lotov K.V.	31, 34, 203, 221, 354, 355, 356, 552, 53п, 54п
		Lozhkina A.M.	570
		Lukin A.N.	
		Lukin P.A.	333, 334, 336, 49п, 55п
		Lyakh V.V.	239, 240, 469

Lysenko A.P.	333, 334, 336, 339, 340, 359, 514, 7п, 11п, 55п	156, 167, 169, 170, 304, 308, 313, 314, 31п, 48п
Makarov A.N.	509, 519, 649, 5п	Maximov D.A.
Makarov I.G.		2, 7, 9, 10, 11, 13, 14, 15, 16, 17, 18, 19, 20, 21, 35, 37, 38, 39, 48, 49, 50, 53, 56, 63, 64, 65, 66, 67, 68, 69, 70, 71, 72, 75, 79, 80, 81, 82, 83, 84, 85, 86, 87, 88, 89, 90, 91, 92, 93, 94, 95, 96, 97, 98, 100, 101, 105, 110, 112, 113, 114, 115, 116, 119, 125, 129, 131, 132, 133, 139, 142, 162, 164, 168, 172, 174, 175, 178, 179, 181, 182, 185, 186, 337, 361, 362, 363, 364, 365, 366, 367, 368, 369, 370, 371, 372, 373, 374, 375, 376, 377, 378, 379, 380, 381, 382, 383, 384, 385, 386, 387, 388, 389, 390, 391, 392, 393, 394, 395, 396, 397, 398, 399, 611, 612, 615, 616, 617
Makarov M.A.	251, 252, 267, 442, 525, 529, 558, 566, 578	Maximov V.V.
Makeev A.V.		211, 212, 533, 538, 570
Maltseva Yu.I.		Maximovskaya V.V.
Malyshev V.M.	1, 2, 7, 8, 9, 10, 11, 13, 14, 15, 16, 17, 18, 19, 20, 21, 35, 37, 38, 39, 48, 49, 50, 53, 56, 63, 64, 65, 66, 67, 68, 69, 70, 71, 72, 75, 79, 80, 81, 82, 83, 84, 85, 86, 87, 88, 89, 90, 91, 92, 93, 94, 95, 96, 97, 98, 100, 101, 105, 110, 112, 113, 114, 115, 116, 119, 125, 129, 131, 132, 133, 139, 142, 162, 164, 168, 172, 174, 175, 178, 179, 180, 181, 182, 183, 184, 185, 186, 337, 361, 362, 363, 364, 365, 366, 367, 368, 369, 370, 371, 372, 373, 374, 375, 376, 377, 378, 379, 380, 381, 382, 383, 384, 385, 386, 387, 388, 389, 390, 391, 392, 393, 394, 395, 396, 397, 398, 399, 611, 612, 615, 616, 617	259, 265, 449, 481, 622
Mamkin V.R.	205, 497, 518	Medvedev L.E.
Martin K.A.	339, 340, 341, 342, 358, 360, 7п, 11п	466, 486
Martyshev P.V.		Medvedko A.S.
Mashkovtsev M.R.	239, 448, 469, 474, 497	49, 50, 205, 337, 411, 412, 483, 489, 496, 516, 593, 611, 612, 615, 616, 617, 651
Maslennikov A.L.	1, 2, 7, 8, 9, 10, 11, 13, 14, 15, 16, 17, 18, 19, 20, 21, 26, 27, 35, 37, 38, 39, 48, 49, 50, 53, 56, 63, 64, 65, 66, 67, 68, 69, 70, 71, 72, 75, 79, 80, 81, 82, 83, 84, 85, 86, 87, 88, 89, 90, 91, 92, 93, 94, 95, 96, 97, 98, 100, 101, 105, 110, 112, 113, 114, 115, 116, 119, 125, 129, 131, 132, 133, 139, 142, 162, 164, 168, 172, 174, 175, 178, 179, 180, 181, 182, 183, 184, 185, 186, 337, 361, 362, 363, 364, 365, 366, 367, 368, 369, 370, 371, 372, 373, 374, 375, 376, 377, 378, 379, 380, 381, 382, 383, 384, 385, 386, 387, 388, 389, 390, 391, 392, 393, 394, 395, 396, 397, 398, 399, 611, 612, 615, 616, 617	Mekler K.I.
Matveenkov A.N.	263, 642, 643, 644, 645	251, 252, 267, 442, 521, 525, 529, 558, 561, 562, 563, 565, 566, 569, 572, 575, 578, 579
Matvienko D.V.	108, 137, 144, 146, 148, 151,	Meshkov O.I.
		49, 50, 205, 255, 337, 611, 612, 615, 616, 617
		Mezetshev N.A.
		23, 238, 250, 452, 500, 545
		Miginskaya E.G.
		238, 500
		Miginsky S.V.
		444
		Mikhailov K.Yu.
		333, 334, 336, 55п
		Milstein A.I.
		102, 103, 104, 284
		Mironenko L.A.
		466, 486, 641
		Mishagin V.V.
		191, 201, 216, 523, 570, 631, 4п
		Misnev S.I.
		49, 50, 337, 400, 611, 612, 615, 616, 617, 636, 638
		Mitina N.A.
		439, 480
		Mityanina N.V.
		13п
		Morozov I.I.
		49, 50, 337, 611, 612, 615, 616, 617, 657
		Muchnoi N.Yu.
		49, 50, 78, 124, 140, 152, 155, 163, 187, 337, 400, 414, 417, 418, 419, 420, 421, 422, 423, 424, 425, 426, 427, 611, 612, 615, 616, 617, 56п, 58п, 59п, 60п, 61п, 62п, 63п, 64п, 65п
		Murakhtin S.V.
		197
		Murasov A.A.
		Myskin O.K.
		570

Nefedov N.B.	205	Osipov V.N.	617
Nekhaev V.E.		Otboev A.V.	493
Nemytov P.I.	213, 214, 496, 639	Ottmar A.V.	342, 358, 359, 514
Nesterenko I.N.	339, 340, 359, 514, 7п, 11п	Ovchar V.K.	249, 542, 543, 547
Neyfeld V.V.	49, 50, 205, 337, 400, 611, 612, 615, 616, 617	Ovtin I.V.	466, 486, 518, 641
Nikitin S.A.	49, 50, 222, 337, 611, 612, 615, 616, 617, 658	Pachkov A.A.	619
Nikolaev I.B.	49, 50, 78, 124, 140, 152, 155, 163, 187, 222, 337, 417, 418, 419, 420, 421, 422, 423, 424, 425, 426, 427, 611, 612, 615, 616, 617, 58п, 59п, 60п, 61п, 62п, 63п, 64п, 65п, 6A	Pakhutsova E.V.	542, 543, 547
Nikolaev I.V.	542, 543, 547	Panasyuk V.M.	339, 340, 341, 342, 358, 360, 7п, 11п
Nikolenko A.D.	239, 240, 469, 474, 479, 651	Panchenko V.E.	494, 503, 593, 594
Nikolenko D.M.	294, 400, 401, 636, 637, 638, 57п	Panfilov A.D.	
Obrazovsky A.E.	339, 340, 341, 342, 358, 360, 7п, 11п	Panov A.N.	246, 542, 543, 547
Ogurtsov A.B.		Papushev P.A.	294
Okunev I.N.	49, 50, 205, 337, 611, 612, 615, 616, 617	Parkhomchuk V.V.	202, 225, 229, 232, 233, 250, 295, 296, 411, 428, 494, 503, 516, 594
Oleinikov V.P.	11п	Pavlenko A.V.	506, 508, 513, 14п
Onuchin A.P.	49, 50, 106, 107, 109, 118, 122, 126, 127, 130, 134, 136, 138, 145, 177, 337, 341, 358, 611, 612, 615, 616, 617, 618, 619, 620, 7п, 11п	Pavlov O.A.	542, 543, 547
Oreshkin S.B.	49, 50, 337, 611, 612, 615, 616, 617	Pavlov V.M.	488, 501, 511
Oreshonok V.V.	410	Peleganchuk S.V.	1, 2, 7, 8, 9, 10, 11, 13, 14, 15, 16, 17, 18, 19, 20, 21, 27, 35, 37, 38, 39, 48, 49, 50, 53, 56, 63, 64, 65, 66, 67, 68, 69, 70, 71, 72, 75, 79, 80, 81, 82, 83, 84, 85, 86, 87, 88, 89, 90, 91, 92, 93, 94, 95, 96, 97, 98, 100, 101, 105, 110, 110, 112, 113, 114, 115, 116, 119, 125, 131, 132, 133, 139, 142, 162, 164, 168, 172, 174, 175, 178, 179, 180, 181, 182, 183, 184, 185, 186, 293, 337, 361, 362, 363, 364, 365, 366, 367, 368, 369, 370, 371, 372, 373, 374, 375, 376, 377, 378, 379, 380, 381, 382, 383, 384, 385, 386, 387, 388, 389, 390, 391, 392, 393, 394, 395, 396, 397, 398, 399, 611, 612, 615, 616, 617, 29п
Orlov I.O.	1, 2, 7, 8, 9, 10, 13, 14, 15, 16, 17, 18, 19, 20, 21, 35, 37, 38, 39, 48, 49, 50, 53, 56, 63, 64, 65, 66, 67, 68, 69, 70, 71, 72, 75, 79, 80, 81, 82, 83, 84, 85, 86, 87, 88, 89, 90, 91, 92, 93, 94, 95, 96, 97, 98, 100, 101, 105, 110, 112, 113, 114, 115, 116, 119, 125, 131, 132, 133, 139, 142, 162, 164, 168, 172, 174, 175, 178, 179, 180, 181, 182, 183, 184, 185, 186, 337, 361, 362, 363, 364, 365, 366, 367, 368, 369, 370, 371, 372, 373, 374, 375, 376, 377, 378, 379, 380, 381, 382, 383, 384, 385, 386, 387, 388, 389, 390, 391, 392, 393, 394, 395, 396, 397, 398, 399, 611, 612, 615, 616, 617	Perevedentsev E.A.	333, 334, 336, 339, 340, 359, 514, 7п, 11п, 55п, 56п
Osipov A.A.	49, 50, 337, 611, 612, 615, 616,	Persov B.Z.	466, 486, 641
		Pestov Yu.N.	22, 42, 43, 44, 45, 46, 73, 74, 157, 158, 171, 333, 334, 336, 55п
		Pestrikov D.V.	
		Petrenko A.V.	505, 11A
		Petrichenkov M.V.	205
		Petrov V.M.	204, 493, 515, 651, 13п
		Petrov V.V.	49, 50, 205, 337, 611, 612, 615, 616, 617
		Petrova E.V.	235

Petrozhitsky A.V.	202, 233, 296	Protopopov A.Yu.	496, 517
Pilan A.M.	204, 466, 486, 493, 641, 651	Pupkov Yu.A.	413
Piminov P.A.	49, 50, 337, 608, 609, 610, 611, 612, 615, 616, 617, 662	Pureskin D.N.	205, 483, 496, 497, 516, 542, 543, 547
Pindyurin V.F.	235, 239, 240, 497, 472	Putmakov A.A.	516
Pinzhenin E.I.	533, 538	Pyata E.E.	414, 415, 11п, 56п
Pirogov S.A.	333, 334, 336, 338, 55п	Rachek I.A.	294, 400, 401, 636, 637, 638, 57п
Pivovarov I.L.		Radchenko V.M.	484
Pivovarov S.G.	27, 49, 50, 333, 334, 336, 337, 415, 611, 612, 615, 616, 617, 55п	Rakhimov A.R.	205
Podobaev V.S.		Rakshun Ya.V.	449, 452, 463
Poletaev I.V.	500	Raschenko V.V.	242
Polosatkin S.V.	190, 251, 252, 267, 268, 431, 432, 442, 521, 523, 525, 529, 553, 561, 562, 563, 564, 565, 567, 568, 569, 572, 574, 575, 579, 625, 628	Rastigeev S.A.	202, 232, 295
Poluektov A.O.	3, 4, 5, 6, 12, 36, 40, 47, 49, 50, 51, 52, 54, 55, 57, 58, 59, 60, 61, 62, 76, 77, 99, 108, 111, 117, 120, 121, 123, 135, 141, 143, 144, 146, 147, 150, 153, 154, 156, 159, 161, 165, 166, 169, 170, 176, 188, 300, 301, 309, 310, 315, 316, 317, 320, 321, 322, 323, 324, 325, 326, 327, 328, 329, 330, 331, 337, 611, 612, 615, 616, 617, 33п, 34п, 36п, 37п, 38п, 40п, 41п, 42п, 43п, 44п, 45п, 46п	Razorenov V.V.	
Polukhin V.A.	503	Redin S.I.	333, 334, 336, 55п
Polyansky A.V.	205	Repkov V.V.	466, 486, 517, 518, 641
Pomeransky A.A.	286	Reva V.B.	428, 485, 494, 503, 516, 593, 594
Popik V.M.	264, 437, 454, 466, 486, 641	Reznichenko A.V.	257, 258, 4A
Popov A.S.	333, 334, 336, 55п	Reznikova E.F.	457, 458, 464, 475
Popov S.S.	243, 251, 255, 521, 525, 528, 529, 534, 562, 563, 565, 566, 569, 578, 579, 629	Rogovsky Yu.A.	333, 334, 336, 339, 340, 358, 359, 360, 514, 7п, 11п, 55п
Popov Yu.S.	333, 334, 336, 55п	Romanov A.L.	339, 340, 342, 359, 360, 514, , 7п, 11п, 55п
Popova N.I.		Rotov E.A.	
Porosev V.V.	293, 29п	Rovenskih A.F.	241, 243, 252, 267, 432, 442, 521, 525, 529, 558, 561, 562, 563, 565, 566, 569, 571, 572, 575, 578, 579
Postupaev V.V.	243, 251, 252, 267, 352, 442, 521, 525, 529, 546, 553, 558, 561, 562, 563, 564, 565, 566, 567, 569, 572, 574, 575, 578, 579	Ruban A.A.	49, 50, 333, 334, 336, 337, 611, 612, 615, 616, 617, 55п
Potapov S.I.	483	Rudenko A.S.	273
Prikhodko V.V.	195, 198, 211, 212, 357, 527, 531, 538, 544, 570, 624, 632, 634, 9п	Ruvinsky S.I.	205
Prisekin V.G.	49, 50, 247, 337, 611, 612, 615, 616, 617	Rybitskaya T.V.	205, 220, 498, 508, 510, 513, 596
Prokhorov I.A.	526, 630, 631	Ryskulov N.M.	333, 334, 336, 55п
		Ryzhenenkov A.E.	333, 334, 336, 55п
		Sadykov R.Sh.	400, 636, 637, 638
		Salikova T.V.	263, 466, 486, 641
		Salimov R.A.	193, 214, 495, 639
		Salnikov S.G.	281
		Sandyrev V.K.	49, 50, 337, 611, 612, 615, 616, 617
		Sanin A.L.	629, 642, 648
		Savinov G.A.	49, 50, 337, 611, 612, 615, 616, 617
		Savkin V.Ya.	201, 211, 535, 538, 570, 648
		Sazansky V.Ya.	
		Scheglov M.A.	263, 447, 466, 486, 493, 641
		Schegolev L.M.	205

Schudlo I.M.	344, 487, 509, 519, 649, 3π, 5π	159, 160, 165, 166, 176, 188,
Sedlyarov I.K.	466, 486, 493, 641, 651	293, 294, 300, 301, 309, 310,
Selivanov A.N.	236	315, 316, 317, 320, 321, 322,
Selivanov P.A.	219	323, 324, 325, 326, 327, 328,
Semenov A.I.	454	329, 330, 331, 461, 478, 29π,
Semenov A.V.	495, 639	33π, 34π, 36π, 37π, 38π 40π,
Semenov E.P.	205, 413, 651	41π, 42π, 43π, 44π, 45π, 46π,
Semenov Yu.I.		1A
Senchenko A.I.		Shemyakin D.N.
Senkov D.V.	205, 483, 496, 516	333, 334, 336, 55π
Serdobintsev G.V.	466, 486, 641, 651	Shemyakina E.O.
Serednyakov S.I.	106, 107, 109, 118, 122, 126, 127, 130, 134, 136, 138, 145, 177, 205, 339, 340, 341, 342, 358, 360, 7π, 11π	293, 298, 600, 28π, 29π, 30π
Serednyakov S.S.	219, 261, 263, 466, 486, 518, 641	Sheromov M.A.
Shadrin N.S.	469	Shestakov Yu.V.
Shamakina N.S.	8π, 12π	400, 401, 636, 637, 638
Shamov A.G.	1, 2, 7, 8, 9, 10, 11, 13, 14, 15, 16, 17, 18, 19, 20, 21, 35, 37, 38, 39, 48, 49, 50, 53, 56, 63, 64, 65, 66, 67, 68, 69, 70, 71, 72, 75, 79, 80, 81, 82, 83, 84, 85, 86, 87, 88, 89, 90, 91, 92, 93, 94, 95, 96, 97, 98, 100, 101, 105, 110, 112, 113, 114, 115, 116, 119, 125, 129, 131, 132, 133, 139, 142, 162, 168, 172, 174, 175, 178, 179, 180, 181, 182, 183, 184, 337, 361, 362, 363, 364, 365, 366, 367, 368, 369, 370, 371, 372, 373, 374, 375, 376, 377, 378, 379, 380, 381, 382, 383, 384, 385, 386, 387, 388, 389, 390, 391, 392, 393, 394, 395, 396, 397, 398, 399, 419, 611, 612, 615, 616, 617	466, 486, 502, 504, 641
Shatilov D.N.	49, 50, 337, 416, 611, 612, 615, 616, 617, 652, 653, 654, 655, 656, 657	Shichkov D.S.
Shatunov P.Yu.	333, 334, 336, 339, 340, 342, 359, 360, 514, 7π, 11π, 55π	506, 508, 513, 14π
Shatunov Yu.M.	209, 250, 333, 334, 336, 339, 340, 341, 342, 358, 359, 360, 514, 7π, 11π, 55π, 56π	Shikhovtsev I.V.
Shebalin V.E.	137, 144, 146, 148, 151, 156, 167, 169, 170, 173, 304, 306, 308, 314, 333, 334, 336, 35π, 55π	629, 630, 631, 647
Shekhtman L.I.	3, 4, 5, 6, 12, 36, 40, 47, 51, 52, 54, 55, 57, 58, 59, 60, 61, 62, 77, 99, 111, 117, 121, 123, 135, 141, 143, 147, 150, 153, 154,	Shiyankov S.V.
		25, 205
		Shkaruba V.A.
		238, 500
		Shoshin A.A.
		431, 529, 553, 562, 564, 565, 567, 573, 574, 579
		Shtarklev E.A.
		484
		Shtol D.A.
		339, 340, 341, 342, 358, 360, 7π, 11π
		Shubin E.I.
		485
		Shukaev A.N.
		341, 7π, 11π
		Shulzhenko G.I.
		201, 211, 570
		Shvedov D.A.
		205, 651
		Shwartz B.A.
		49, 50, 108, 120, 137, 144, 146, 156, 161, 167, 169, 170, 173, 304, 305, 306, 307, 308, 313, 318, 333, 334, 336, 337, 611, 612, 615, 616, 617, 31π, 32π, 35π, 39π, 48π, 55π
		Shwartz D.B.
		333, 334, 336, 342, 358, 359, 360, 514, 7π, 11π, 55π
		Sidorov A.V.
		195
		Silagadze Z.K.
		339, 340, 341, 342, 358, 360, 7π, 11π
		Simonov E.A.
		49, 50, 337, 611, 612, 615, 616, 617
		Singatulin Sh.R.
		411, 489, 650
		Sinitzky S.L.
		218, 228, 251, 252, 267, 269, 270, 272, 352, 435, 440, 442, 521, 525, 529, 546, 558, 559, 561, 562, 563, 564, 565, 566, 567, 574, 577, 578, 579
		Sinyatkin S.V.
		49, 50, 205, 337, 428, 608, 609, 610, 611, 612, 615, 616, 617, 651
		Skarbo B.A.
		220, 498, 508, 510, 513, 597
		Sklyarov V.F.
		243, 251, 267, 442, 521, 525, 529, 558, 562, 563, 565, 566, 569, 578, 579
		Skorobogatov D.N.
		485, 494, 497, 516
		Skorokhod D.A.
		466

Skovorodin D.I.	253		559, 562, 565, 566, 577, 578, 579
Skovpen K.Yu.	1, 2, 7, 8, 9, 10, 11, 13, 14, 15, 16, 17, 18, 19, 20, 21, 35, 37, 38, 39, 48, 53, 56, 63, 64, 65, 66, 67, 68, 69, 70, 71, 72, 75, 79, 80, 81, 82, 83, 84, 85, 86, 87, 88, 89, 90, 91, 92, 93, 94, 95, 96, 97, 98, 100, 101, 105, 110, 112, 113, 114, 115, 116, 125, 129, 131, 132, 133, 139, 142, 162, 164, 168, 172, 174, 175, 178, 179, 180, 181, 182, 183, 184, 185, 186, 339, 340, 341, 342, 358, 360, 361, 362, 363, 364, 365, 366, 367, 368, 369, 370, 371, 372, 373, 374, 375, 376, 377, 378, 379, 380, 381, 382, 383, 384, 385, 386, 387, 388, 389, 390, 391, 392, 393, 394, 395, 396, 397, 398, 399, 7π, 11π, 7A	Steshov A.G.	651
Skovpen Yu.I.	106, 107, 109, 118, 119, 126, 127, 130, 134, 136, 177	<u>Strakhovenko V.M.</u>	103, 608, 609, 610
Skrinsky A.N.	49, 50, 250, 337, 339, 340, 341, 342, 358, 359, 360, 466, 486, 504, 514, 611, 612, 615, 616, 617, 641, 7π, 11π	Strelnikov N.O.	
Smalyuk V.V.	49, 50, 205, 255, 256, 337, 410, 413, 611, 612, 615, 616, 617	Stupishin N.V.	350, 628, 629
Snopkov G.I.	466	Sudnikov A.V.	252, 529, 561, 562, 565, 569, 572, 579
Snopkov R.G.	27	Sukhanov A.V.	205
Sokolov A.V.	49, 50, 293, 298, 337, 600, 611, 612, 615, 616, 617, 28π, 29π, 30π	Sukhanov D.P.	410
Sokolov V.V.	587, 588, 27π	Sukharev A.M.	1, 2, 7, 8, 9, 10, 11, 13, 14, 15, 16, 17, 18, 19, 20, 21, 26, 35, 37, 38, 39, 48, 49, 50, 53, 56, 63, 64, 65, 66, 67, 68, 69, 70, 71, 72, 75, 79, 80, 81, 82, 83, 84, 85, 86, 87, 88, 89, 90, 91, 92, 93, 94, 95, 96, 97, 98, 100, 101, 105, 110, 112, 113, 114, 115, 116, 125, 129, 131, 132, 133, 139, 142, 162, 164, 168, 172, 174, 175, 178, 179, 180, 181, 182, 183, 184, 185, 186, 217, 337, 361, 362, 363, 364, 365, 366, 367, 368, 369, 370, 371, 372, 373, 374, 375, 376, 377, 378, 379, 380, 381, 382, 383, 384, 385, 386, 387, 388, 389, 390, 391, 392, 393, 394, 395, 396, 397, 398, 399, 611, 612, 615, 616, 617
Soldatov A.E.		Sukhina B.N.	
Solodov E.P.	106, 107, 109, 118, 122, 126, 127, 130, 134, 136, 138, 145, 177, 333, 334, 336, 55π	Sulyaev Yu.S.	241, 252, 525, 529, 558, 562, 565, 579
Solomakhin A.L.	194, 211, 212, 538, 570	Surin I.K.	339, 340, 341, 342, 358, 360, 7π, 11π
Soltatkina E.I.	211, 212, 538, 570	Syrovatin V.M.	23, 238, 500
Sorokin A.V.	191, 526, 629, 630	Talyshev A.A.	1, 2, 7, 8, 9, 10, 11, 13, 14, 15, 16, 17, 18, 19, 20, 21, 26, 27, 35, 37, 38, 39, 48, 49, 50, 53, 56, 63, 64, 65, 66, 67, 68, 69, 70, 71, 72, 75, 79, 80, 81, 82, 83, 84, 85, 86, 87, 88, 89, 90, 91, 92, 93, 94, 95, 96, 97, 98, 100, 101, 105, 110, 112, 113, 114, 115, 116, 119, 125, 129, 131, 132, 133, 139, 142, 162, 164, 168, 172, 174, 175, 178, 179, 180, 181, 182, 183, 184, 185, 186, 217, 333, 334, 336, 337, 361, 362, 363, 364, 365, 366, 367, 368, 369, 370, 371, 372, 373, 374, 375, 376, 377, 378, 379, 380, 381, 382, 383, 384, 385, 386, 387, 388, 389, 390, 391, 392, 393, 394, 395,
Sorokin I.N.	344, 487, 509, 519, 520, 649, 2π, 3π, 5π, 6π		
Sorokina N.V.	252, 529, 561, 565, 579		
Sorokoletov D.S.	452, 463		
Stankevich A.S.			
Starokozhev S.A.	537		
Starostenko A.A.	220, 491, 498, 508, 510, 513, 595		
Starostenko D.A.	246, 542, 543, 547		
Starostina A.S.	27		
Starostina E.V.	49, 50, 337, 611, 612, 615, 616, 617		
Stepanov V.D.	218, 267, 440, 442, 529, 558,		

	396, 397, 398, 399, 611, 612, 615, 616, 617, 619, 620, 55π	Trunев Yu.A.	211, 430, 432, 529, 539, 554, 562, 564, 565, 569, 570, 571, 572, 575
Tararyshkin S.V.	219, 466, 486, 518, 641, 651	Tsukanov V.M.	23, 238, 500
Tarnetsky V.V.		Tsukanova L.A.	205
Taskaev S.Yu.	344, 345, 487, 509, 519, 520, 649, 2π, 3π, 5π, 6π	Tsydulko Yu.A.	33, 522, 544, 567, 623, 624, 625, 632, 634
Tayursky V.A.	49, 50, 337, 611, 612, 615, 616, 617	Tsyganov A.S.	220, 498, 508, 510, 513, 598
Tekutiev A.I.	7π, 11π	Tumaikin G.M.	49, 50, 337, 611, 612, 615, 616, 617
Telnov V.I.	49, 50, 337, 602, 603, 604, 605, 606, 607, 608, 609, 610, 611, 612, 615, 616, 617, 51π, 52π	Ukrainтsev Yu.G.	289, 290, 291, 292
Terekhov A.V.		Usov Yu.V.	49, 50, 137, 151, 302, 306, 307, 311, 312, 314, 337, 339, 340, 341, 358, 360, 611, 612, 615, 616, 617, 7π, 11π
Terekhov I.S.	104, 284	Utkin A.V.	24, 205
Tikhonov Yu.A.	1, 2, 7, 8, 9, 10, 11, 13, 14, 15, 16, 17, 18, 19, 20, 21, 26, 27, 35, 37, 38, 39, 48, 49, 50, 53, 56, 63, 64, 65, 66, 67, 68, 69, 70, 71, 72, 75, 79, 80, 81, 82, 83, 84, 85, 86, 87, 88, 89, 90, 91, 92, 93, 94, 95, 96, 97, 98, 100, 101, 105, 110, 112, 113, 114, 115, 116, 119, 125, 129, 131, 132, 133, 139, 142, 162, 164, 168, 172, 174, 175, 178, 179, 180, 181, 182, 183, 184, 185, 186, 215, 217, 224, 337, 339, 340, 341, 342, 358, 360, 361, 362, 363, 364, 365, 366, 367, 368, 369, 370, 371, 372, 373, 374, 375, 376, 377, 378, 379, 380, 381, 382, 383, 384, 385, 386, 387, 388, 389, 390, 391, 392, 393, 394, 395, 396, 397, 398, 399, 611, 612, 615, 616, 617, 7π, 11π	Vasichev S.S.	651
Tikhonyuk I.I.		Vasiljev A.A.	468, 574
Timofeev I.V.	189, 346, 347, 558, 560, 562, 563, 565, 566, 567, 578, 579, 50π	Vasiljev A.V.	339, 340, 341, 342, 358, 360, 7π, 11π
Titov V.M.	294, 333, 334, 336, 443, 467, 55π	Veremeenko V.F.	412, 651
Tiunov M.A.	344, 487, 509, 519, 523, 570, 629, 647, 648, 649, 2π, 3π, 5π	Vesenev V.M.	341, 11π
Tkachenko V.O.		Vinokurov N.A.	219, 250, 262, 263, 444, 466, 486, 493, 502, 504, 641
Tkachev A.A.	526, 630	Vinokurova A.N.	108, 137, 144, 146, 156, 167, 169, 170, 308, 313, 35π
Todyshev K.Yu.	49, 50, 106, 107, 109, 118, 122, 126, 127, 130, 134, 136, 138, 145, 177, 337, 419, 611, 612, 615, 616, 617, 8A	Vlasenko M.G.	438, 446, 466, 486, 641
Tokarev Yu.F.	542, 543, 547	Vlasov A.Yu.	484
Tolochko B.P.	237, 294, 406, 443, 456, 461, 477, 478, 545	Vobly P.D.	24, 466, 486, 508, 513, 641
Toporkov D.K.	400, 401, 636, 637, 638	Volkov A.A.	238, 500
Tribendis A.G.	219, 613, 614	Volkov V.N.	466, 486, 493, 515, 641, 642, 643, 644, 645, 646
		Volosov V.I.	
		Vorobiov A.I.	49, 50, 333, 334, 336, 337, 611, 612, 615, 616, 617, 33π, 34π, 36π, 37π, 38π, 40π, 41π, 42π, 43π, 44π, 45π, 46π, 55π
		Vorobiov V.S.	6, 36, 52, 58, 60, 61, 62, 108, 120, 121, 135, 137, 144, 146, 150, 151, 153, 159, 166, 167, 170, 188, 300, 301, 302, 304, 305, 307, 308, 309, 310, 311, 312, 313, 315, 325, 327, 328, 329, 331
		Voronin L.A.	
		Voskoboinikov R.V.	29, 149, 523, 570, 629
		Vostrikov V.A.	215, 231, 428
		Vyacheslavov L.N.	251, 255, 267, 442, 525, 529, 534, 558, 562, 565, 566, 569, 578, 579

Yaminov K.R.	205, 489	Zevakov S.A.	400, 401, 636, 637, 638
Yarovoi V.A.	571, 575	Zharikov A.A.	517
Yudin V.D.	651	Zharinov Yu.M.	342, 514
Yudin Yu.V.	248, 55π	Zhilich V.N.	49, 50, 108, 120, 128, 137, 144, 146, 148, 151, 156, 161, 167, 169, 170, 173, 294, 302, 304, 305, 306, 307, 311, 312, 313, 314, 337, 400, 611, 612, 615, 616, 617, 32π, 35π, 39π, 47π, 48π
Yurov D.V.	357, 531, 544, 624, 632, 634	Zhirov O.V.	287
Yushkov A.N.	49, 50, 106, 107, 109, 118, 122, 126, 127, 130, 134, 136, 138, 145, 177, 337, 611, 612, 615, 616, 617	Zhmurikov E.I.	28, 266, 433
Zapryagaev I.A.		Zhukov A.A.	413, 414, 11π
Zavertkin P.S.		Zhulanov V.V.	49, 50, 108, 120, 128, 137, 144, 146, 161, 167, 169, 173, 294, 302, 304, 305, 306, 307, 308, 311, 312, 313, 314, 337, 461, 467, 478, 611, 612, 615, 616, 617, 31π, 32π, 35π, 39π
Zaytsev A.S.	1, 2, 7, 8, 9, 10, 11, 13, 14, 15, 16, 17, 18, 19, 20, 21, 53, 56, 64, 65, 66, 67, 69, 70, 71, 75, 79, 81, 82, 84, 85, 86, 87, 88, 89, 90, 92, 94, 95, 96, 97, 98, 100, 101, 105, 110, 112, 113, 114, 115, 116, 119, 125, 129, 131, 132, 133, 139, 142, 162, 164, 168, 172, 174, 175, 178, 179, 180, 181, 182, 183, 184, 185, 186, 217, 333, 334, 336, 361, 362, 363, 364, 365, 366, 370, 371, 372, 373, 374, 375, 376, 377, 378, 379, 380, 381, 382, 383, 384, 385, 386, 387, 389, 390, 391, 392, 393, 394, 395, 396, 397, 398, 399, 55π	Zhuravlev A.N.	49, 50, 337, 611, 612, 615, 616, 617
Zaytsev K.V.	211, 212, 527, 538, 570, 9π	Zinin E.I.	234, 445
Zaytsev V.N.	25	Zolotarev K.V.	265, 413, 481, 500, 608, 609, 610
Zemlyansky I.M.	339, 340, 359, 360, 7π, 11π	Zorin A.V.	
		Zubarev P.V.	
		Zverev D.A.	518

SIBERIAN BRANCH OF RUSSIAN ACADEMY OF SCIENCES
BUDKER INSTITUTE OF NUCLEAR PHYSICS

ANNUAL REPORT
2012

Cover E.D. Bender

Ответственный за выпуск А.В. Васильев

Работа поступила 14.05. 2013 г.

Сдано в набор 15.06. 2013 г.

Подписано в печать 30.07. 2013 г.

Формат 60x90 1/16 Объем 14,5 печ.л., 11.5 уч.-изд.л.

Тираж 100 экз. Бесплатно. Заказ № 15

Обработано на РС и отпечатано
на ротапринте «ИЯФ им. Г.И. Будкера» СО РАН,
Новосибирск, 630090, пр. Академика Лаврентьева, 11